Small Column Experiments for Continuous Radial Flow Chromatography

A thesis submitted in partial fulfilment

of the requirements for the degree of

Master of Science

in Materials and Process Engineering

by

Sook-Han Yvonne Lee

The University of Waikato

Te Whare Wānanga o Waikato

Hamilton, New Zealand

2010

Abstract

Continuous radial flow chromatography (CRFC) combines radial flow and rotating annular bed chromatography. Solution flows radially from eight fixed ports around the periphery through a rotating annular packed bed towards the axis. Loading, equilibration, elution and reequilibration solutions can be applied simultaneously at different feed ports. Protein is captured on resin in the loading zone and carried around by the annulus to the elution zone to be eluted, making the CRFC a continuous process.

Small axial flow columns experiments were carried out to represent continuous BSA purification in the CRFC for a range of rotation speeds, flow rates, feed concentration, elution buffer concentration, loading sections and elution secions. Quality of the separation was measured based on productivity and height to width ratio.

Best operating conditions for BSA purification in the CRFC include 720 deg/hr rotation speed, 1 mL/min flow rate, 1M elution buffer (NaCl) solution, and either 5 or 1.5 mg/mL feed solution. A wide range of loading sections and elution sections can be allocated. Combinations of these best conditions are restricted by total protein load per chromatography cycle.

Mathematical models solved by finite difference method in Matlab were used to predict CRFC operation under the best conditions. Model accounts for change in solute concentration by convection, film diffusion and uptake into resin. Protein and salt parameters were adjusted to achieve best mached protein peaks. Model simulations agreed well with experimental results. Loading peak width was similar but experimental data showed broader elution peaks. Elution peak height for all simulations was greater while loading peak height were more variable than in the experiments. Peak tailing was observed in both experimental and model data.

Acknowledgements

I would like to thank my supervisor, Dr Mark Lay, and his patience, guidance and support throughout the time of research and writing of this thesis, and for opening my eyes to the world of chromatography. Prof. Janis Swan for giving me the opportunity to embark on this journey. Lisa Li for providing technical support. Secretary of the Department of Engineering, Mary Dalbeth, and Secretaries of the Biological Sciences department, Gloria Edwards and Vicki Smith, for their services. Academic staff, Dr Giridhar Nair, Dr Johan Verbeek, Dr James Carson, Assoc. Prof. Vic Arcus, Dr Ryan Martinus, Prof. Roberta Farrell and Prof Roy Daniel for their dedication and excellent teaching. Dudley Bell, Lynette Baxter and Bruce Patty for the glasshouse jobs which gave me more reasons to be at the university during the weekends. Yoong-Wei Lim for trying to get me thinking like an engineer instead of a biologist. Last but not least, I would like to thank my friends and family for their care and support throughout the years.

Table of Contents

List of Figures

List of Tables

Nomenclature

A_p	Spherical area of a single resin particle (cm^2)
A_{re}	Area in radial direction for an annular segment (cm^2)
A_R	Total spherical area of resin particles (cm^2)
A_z	Area in axial direction (cm^2)
A_θ	Area in angular direction (cm^2)
C_A	Solute A concentration in void fraction of resin bed (mg/mL)
$C_{elution}$	Elution buffer solution concentration (mg/mL)
C_{outA}	Solute A concentration at exit point (mg/mL)
C_{feed}	Concentration of protein feed solution (mg/mL)
C_{RPA}	Average resin pore solute A concentration (mg/mL)
C_{RPA}^*	Resin pore solute A concentration at equilibrium (mg/mL)
C_{RPB}	Resin pore solute B concentration (mg/mL)
C_{RA}	Resin matrix solute A concentration (mg/mL)
C_{RA}^*	Resin matrix solute A concentration at equilibrium (mg/mL)
C_{RAmax}	Resin matrix maximum solute A concentration (mg/mL)
d_p	Resin particle diameter (cm)
d	Annular sections (dimensionless)
D	Total number of annular sections (dimensionless)
D_{Ar}	Dispersion in radial direction (cm^2/s)
D_{Az}	Dispersion in axial direction (cm^2/s)
$D_{A\theta}$	Dispersion in angular direction (cm^2/s)
D_r	Diameter at midpoint of annulus (cm)
H	Annular bed height (cm)
J	Dividing factor for time (dimensionless)
J_A	Mass flux by diffusion into resin ($mg/cm^2.s$)
J_{Az}	Mass flux due to diffusion/dispersion in axial direction ($mg/cm^2.s$)
J_{Ar}	Mass flux due to dispersion in radial direction ($mg/cm^2.s$)
$J_{A\theta}$	Mass flux due to dispersion in angular direction ($mg/cm^2.s$)
k_f	Film diffusion coefficient (cm/s)
k_{A1}	Solute A adsorption rate onto resin matrix (mL/mg.s)
k_{A2}	Solute A desorption rate from matrix (1/s)
K_A	Equilibrium constant for solute A (mL/mg)
K_B	Equilibrium constant for solute B (mL/mg)
L	Axial bed height (cm)
m	Time or angular step (dimensionless)
m_{col}	Time step when output solution collected (dimensionless)
m_{sec1}	Time or angular step when section starts (dimensionless)
m_{sec2}	Time or angular step when section ends (dimensionless)
M	Total time or angular steps (dimensionless)
M_{rev}	Number of time or angular steps per revolution (dimensionless)
M_{run}	Number of time or angular steps per run (dimensionless)
M_{sec}	Number of time or angular steps per section (dimensionless)
n	Stage number (dimensionless)
N	Total number of stages in resin bed (dimensionless)
N_{isw}	Total number of stages in inner sintered wall (dimensionless)

N_{osw}	Total number of stages in outer sintered wall (dimensionless)
N_{steps}	Number of steps per run (dimensionless)
N_a	Total number of angular stages (dimensionless)
N_{max}	Maximum number of stages in annular resin bed (dimensionless)
N_{rev}	Number of revolution per run (dimensionless)
Q_z	Flow-rate through axial column (mL/s)
Q_r	Total flow-rate radial column (mL/s)
Q_e	Flow-rate through an element of radial column (mL/s)
r	Column radius (cm)
r_x	Radius of axial column (cm)
r_1	Outside radius of annular packed bed (cm)
r_2	Inner radius of annular packed bed (cm)
r_p	Resin particle radius (cm)
t	Time (s)
t_{cycle}	Time for one axial run (s)
t_D	Time spent by a section at each feed chamber (s)
t_{run}	Simulation run time (s)
t_{rev}	Time for one revolution (s)
T_{isw}	Inner sintered wall thickness (cm)
T_{osw}	Outer sintered wall thickness (cm)
u	Superficial velocity (cm/s)
v	Interstitial velocity (cm/s)
V_z	Axial stage volume (cm^3)
V_e	Radial element volume (cm^3)
V_R	Total resin volume (cm^3)
V_p	Single resin particle volume (cm^3)
w	Rotation speed of annulus (degrees/s)
z	Axial position (cm)
ε_p	Pore fraction of resin (dimensionless)
ε_R	Void fraction of resin bed (dimensionless)
ε_{isw}	Pore fraction of inner sintered wall (dimensionless)
ε_{osw}	Pore fraction of outer sintered wall (dimensionless)
ϕ	Rotated angle (degrees)
ϕ_p	Angular position (degrees)
π	Mathematical constant (3.142)
θ	Angle of a section of annulus (radians or degrees)
θ_{max}	Total angle of annulus (radians or degrees)

Subscripts

A	Solute A
B	Solute B
isw	Inner sintered wall
osw	Outer sintered wall
z	Axial direction
θ	Angular direction

Chapter 1: Introduction

1.1 Background

Advances in biotechnology have resulted in new developments in large scale production of complex biomolecules. In such processes, isolating and purifying target molecules from complex feedstock or fermentation broths are costly, inevitably involving many steps. Reducing the number of steps and/or processing time makes a process more cost effective, thus increasing efficiency through new techniques is highly desirable.

Chromatography is one of the leading separation and purification methods used in downstream processing of large scale processes. It is extremely useful in bioseparations where the molecules of interest are heat and stress sensitive, such as amino acids, nucleotides, proteins and complex hydrocarbons. Chromatography techniques also have high separation power and are highly versatile.

Chromatography separates one or more molecules from a mixture by manipulating their migration rates through the chromatography media. Migration rates are dependent on molecule size, charge and interaction with specific media. Liquid chromatography has advantages over other chromatography techniques in its simplicity, flexibility and high capacity (Heftmann, Krochta et al. 1972).

In conventional chromatography separation methods, especially when using fine or soft media, scaling up is difficult. This problem is due to effects such as increased back pressures from increasing column height, which in turn results in low throughput, high risk of fouling, lower yield and low resolution. Another disadvantage of conventional chromatography is the inefficient use of separating media. This factor becomes significant in industrial scale processes where cost efficiency is highly important as profit is the main objective.

In developing industrial scale separations, more effective techniques have been investigated. Techniques have been proposed in the past include changes in system configuration to support continuous operation, radial flow and expanded media. Various separations have been successfully performed using radial flow systems. Besides alternative configuration, alternative media such as membranes and monoliths have also been investigated for better chromatography performance and easier scale up.

CRFC is combines two systems; radial flow and rotating annular bed. It operates similarly to rotating annular bed systems except solution flows in the radial direction inwards through the media. In comparison with rotating annular bed systems with axial flow, CRFC has the advantages of lower pressure drop, high throughput and the option of using soft media. It is also easier to pack the CRFC as the fluid distribution system remains intact during the packing process and it can be pump packed (Lay 2005).

1.2 Problem Statement

Mathematical models allow performance predictions of the system under different conditions, increasing the ease of optimization. A model was previously developed for CRFC using the finite difference method. Changes to the model by comparing and matching simulated results to experimental results will produce more accurate predictions.

Single component separation allows clearer observations of the effect of changing various factors. Results from experiments carried out at different flow rates, rotation speed, sample volume, elution buffer volume, sample concentration and elution buffer concentration will be required for a more accurate model.

As industrial chromatography usually involves separation of a number of proteins from a sample mixture or crude feedstock, CRFC experiments should be carried out with feed samples containing various proteins, similar to that used in large scale separations. Mathematical simulation of the CRFC should involve input solution of a mixture of proteins.

Initial and current CRFC prototypes were found to produce low resolution separations due to their small number of feed and exit chambers. A new prototype with increased number of chambers was designed and constructed, and waits to be tested. Producing an improved model allows performance of different CRFC prototypes to be compared and assist in the development of the CRFC system.

1.3 Research Objectives

The objectives of this thesis are:

- To model CRFC using Langmuir isotherm and finite difference method.
- To obtain experimental results for a range of flow rates, rotation speed, feed concentration, elution buffer concentration, feed volume and elution buffer volume.
- To distinguish best conditions for BSA purification in the CRFC
- To match mathematically simulated data to experimental data.

1.4 Thesis Organisation

CRFC is based on two separate systems; radial flow and rotating annular bed chromatography. Various chromatography techniques similar to the CRFC are presented in Chapter 2. Documented applications, discoveries and modelling methods are also discussed in review of these techniques. Axial flow chromatography is briefly explained for comparison to the CRFC. Details of each CRFC prototype such as mechanical problems, design improvements and potential developments will also be covered in Chapter 2.

Models used to predict separation performance in axial flow and radial flow columns are presented in Chapter 3. Models were programmed using Matlab. Simulations were obtained for axial flow column for single protein extraction.

Details of experimental methods carried out are presented in Chapter 4. The experiments were carried out with pure bovine serum albumin (BSA) solution. Small axial flow columns were used with the separation process designed to mimic the continuous operation of the CRFC.

Experimental results and observations are discussed in Chapter 5. Experimental results were compared to simulated results for a range of flow rates, rotation speed, protein feed concentration, elution buffer concentration, feed volume and elution buffer volume.

Conclusions from this research and recommendation for future work will be covered in Chapter 6.

Chapter 1: Introduction

1.1 Background

Advances in biotechnology have resulted in new developments in large scale production of complex biomolecules. In such processes, isolating and purifying target molecules from complex feedstock or fermentation broths are costly, inevitably involving many steps. Reducing the number of steps and/or processing time makes a process more cost effective, thus increasing efficiency through new techniques is highly desirable.

Chromatography is one of the leading separation and purification methods used in downstream processing of large scale processes. It is extremely useful in bioseparations where the molecules of interest are heat and stress sensitive, such as amino acids, nucleotides, proteins and complex hydrocarbons. Chromatography techniques also have high separation power and are highly versatile.

Chromatography separates one or more molecules from a mixture by manipulating their migration rates through the chromatography media. Migration rates are dependent on molecule size, charge and interaction with specific media. Liquid chromatography has advantages over other chromatography techniques in its simplicity, flexibility and high capacity (Heftmann, Krochta et al. 1972).

In conventional chromatography separation methods, especially when using fine or soft media, scaling up is difficult. This problem is due to effects such as increased back pressures from increasing column height, which in turn results in low throughput, high risk of fouling, lower yield and low resolution. Another disadvantage of conventional chromatography is the inefficient use of separating media. This factor becomes significant in industrial scale processes where cost efficiency is highly important as profit is the main objective.

In developing industrial scale separations, more effective techniques have been investigated. Techniques have been proposed in the past include changes in system configuration to support continuous operation, radial flow and expanded media. Various separations have been successfully performed using radial flow systems. Besides alternative configuration, alternative media such as membranes and monoliths have also been investigated for better chromatography performance and easier scale up.

CRFC is combines two systems; radial flow and rotating annular bed. It operates similarly to rotating annular bed systems except solution flows in the radial direction inwards through the media. In comparison with rotating annular bed systems with axial flow, CRFC has the advantages of lower pressure drop, high throughput and the option of using soft media. It is also easier to pack the CRFC as the fluid distribution system remains intact during the packing process and it can be pump packed (Lay 2005).

1.2 Problem Statement

Mathematical models allow performance predictions of the system under different conditions, increasing the ease of optimization. A model was previously developed for CRFC using the finite difference method. Changes to the model by comparing and matching simulated results to experimental results will produce more accurate predictions.

Single component separation allows clearer observations of the effect of changing various factors. Results from experiments carried out at different flow rates, rotation speed, sample volume, elution buffer volume, sample concentration and elution buffer concentration will be required for a more accurate model.

As industrial chromatography usually involves separation of a number of proteins from a sample mixture or crude feedstock, CRFC experiments should be carried out with feed samples containing various proteins, similar to that used in large scale separations. Mathematical simulation of the CRFC should involve input solution of a mixture of proteins.

Initial and current CRFC prototypes were found to produce low resolution separations due to their small number of feed and exit chambers. A new prototype with increased number of chambers was designed and constructed, and waits to be tested. Producing an improved model allows performance of different CRFC prototypes to be compared and assist in the development of the CRFC system.

1.3 Research Objectives

The objectives of this thesis are:

- To model CRFC using Langmuir isotherm and finite difference method.
- To obtain experimental results for a range of flow rates, rotation speed, feed concentration, elution buffer concentration, feed volume and elution buffer volume.
- To distinguish best conditions for BSA purification in the CRFC
- To match mathematically simulated data to experimental data.

1.4 Thesis Organisation

CRFC is based on two separate systems; radial flow and rotating annular bed chromatography. Various chromatography techniques similar to the CRFC are presented in Chapter 2. Documented applications, discoveries and modelling methods are also discussed in review of these techniques. Axial flow chromatography is briefly explained for comparison to the CRFC. Details of each CRFC prototype such as mechanical problems, design improvements and potential developments will also be covered in Chapter 2.

Models used to predict separation performance in axial flow and radial flow columns are presented in Chapter 3. Models were programmed using Matlab. Simulations were obtained for axial flow column for single protein extraction.

Details of experimental methods carried out are presented in Chapter 4. The experiments were carried out with pure bovine serum albumin (BSA) solution. Small axial flow columns were used with the separation process designed to mimic the continuous operation of the CRFC.

Experimental results and observations are discussed in Chapter 5. Experimental results were compared to simulated results for a range of flow rates, rotation speed, protein feed concentration, elution buffer concentration, feed volume and elution buffer volume.

Conclusions from this research and recommendation for future work will be covered in Chapter 6.

Chapter 2: Literature Review

-

2.1 Introduction

In Chapter 2, documented work and findings by various scientists are reviewed. As chromatography is most commonly carried out by axial flow since its early development, conventional methods are first discussed to understand its advantages and limitations. These axial chromatography characteristics build a pathway for the development of alternative chromatography techniques, which includes the CRFC. A major part of this literature review is on the development of CRFC and similar techniques proposed and investigated over the years. Details of various radial flow and annular bed chromatography methods, supports, modes and design are included, along with important factors such as flow geometry, bed height, packing and scale up, and the resulting advantages.

2.2 Axial Flow Chromatography

Conventional chromatography separates molecules by passing a sample solution vertically down the length of an axial column in batch mode. Solutions from each step (equilibration, loading and elution) are applied separately in appropriate sequence. According to Barker and Ganetsos (1988), it is due to this non-continuous process that results in inefficient use of the media as a large part of the media merely acts as a conduit.

Chromatography separation also involves large volumes of chemical solutions and expensive media. In the development of chromatography, various rigid media was designed to accommodate fast flows. These alternative new media were however expensive and has limited derivation. High pressures may be applied to force solution through small, rigid media but results in safety hazards, changes in flow rate and increase in overall cost (Heftmann, Krochta et al. 1972).

2.2.1 Scale up problems

Axial chromatography can be scaled up by increasing bed height and diameter but the increase in bed height causes high back pressure, media compression, fouling and blockade. To counter pressure problems, robust equipment and media will be required. Scaling up of the column will then involve a large diameter and short bed height (Figure 1) with the use of large media particles or macroporous particles. This conventional scale up method risks problems associated with column packing, high cost and increase in floor space requirement.

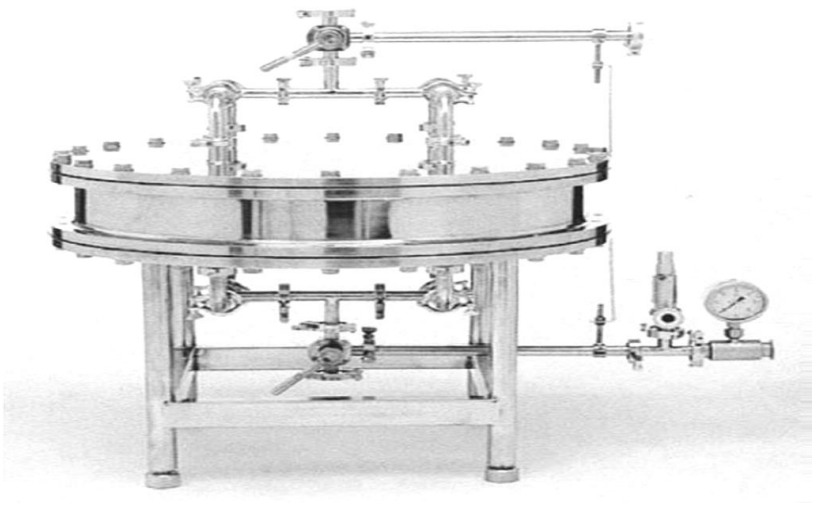

Figure 1. Large scale pancake shaped axial flow column (Gu and Zheng 1999b).

As column diameter is increased, the need for a stronger column with thicker walls and support structures will add to the cost of construction. It will also be more expensive to construct and difficult to pack due to its size. In addition, column diameter can only be scale up to a certain length before efficiency is compromised. Large and macroporous particles may be used to accommodate the increase in pressure with increasing column size but as resolution will be greatly reduced, it will not be applicable to certain processes where high resolution is required.

Many models have been developed to predict performance of axial chromatography**.** Even with optimisation, technical difficulty preventing efficient scale up is common with axial chromatography (Strancar, Barut et al. 1997). When fine or soft supports are used, low flow rates are required. Increase in operation time results in decreased cost efficiency due to low throughput. In dealing with proteins, increase in residence time also increases the risk of denaturation, degradation and aggregation of the target molecule.

Chromatography is a powerful method and widely used in laboratory scale separations but as a technique that is slow and difficult to scale up, it becomes the rate limiting step of many large scale biologically derived products. Continuous radial flow chromatography offers the efficiency and versatility of conventional chromatography along with the possibility of simple linear scale up.

2.3 Radial Flow Chromatography

Major investigations and improvements on liquid chromatography have been mainly for axial flow chromatography. Until now, radial flow chromatography remains a poorly understood technique even with its possible advantages and potential as a more efficient process compared to axial flow chromatography. The first radial flow chromatography system, the chromatofuge (Figure 2) was invented in the 1940s (Hopf 1947). The chromatofuge combines chromatography and centrifugal force for separation.

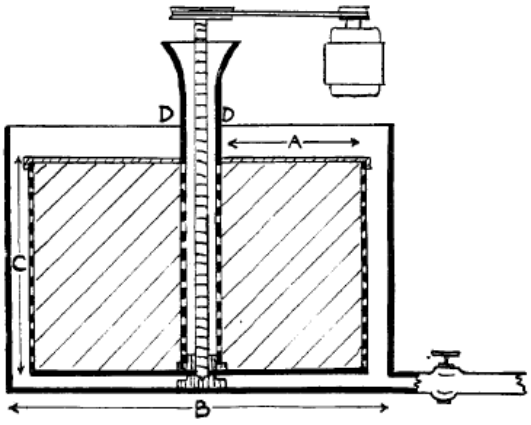

Figure 2. Chromatofuge (Hopf 1947).

Radial flow chromatography differs from conventional axial chromatography in that solution flow radially which allows an increase in the speed of separation. Generally, radial chromatography consists of an annular bed between two concentric cylindrical porous tubes. Flow of solution is directed either inwards from its periphery to the centre or outwards from the centre to the periphery across the radius.

Similar to conventional chromatography, sample is introduced into the chromatographic bed where its components are differentially bound to the media and eluted as it passes through the bed. Effective bed height of a radial flow system is the distance between the inner and outer cylinders while cross sectional area is associated with the surface area of the tube. Short bed depth and large column cross-sectional area enables separations at high flow rates while maintaining low pressure drops (Levison 2003). Linear scale-up involving the increase in flow rate and sample volume by increasing column length is possible as pressure drop do not change with column length.

The basic configurations for radial chromatography include fixed bed, thin layer, spinning disk or bed, and continuous chromatography. Fixed bed, thin layer and spinning disc/bed are operated in batch mode while continuous disc chromatography, which includes the CRFC, is in continuous mode. In terms of separation media, radial flow chromatography can be categorized as membrane, preparative monolithic and packed bed chromatography.

Among the few companies that manufacture radial flow chromatography columns is the filter company Cuno. The column produced consists of a layer of chromatography medium placed on a grid wound around a tube. Solution is flowed through the cartridges and collected through the central tube. The radial flow cartridges used consists of a spirally wound composite matrix (Chen and Hou 1985). This design however resulted in band spreading and in some cases very low resolution.

Another radial chromatography system was designed by Sepragen (Figure 3) (Saxena and Dunn 1989). This radial column design has the advantage which enables the use of soft media. In this column solution flows through the column, across the radius from the outside towards the center. High surface area and relative short bed depth allows high flow rates even with the use of soft media.

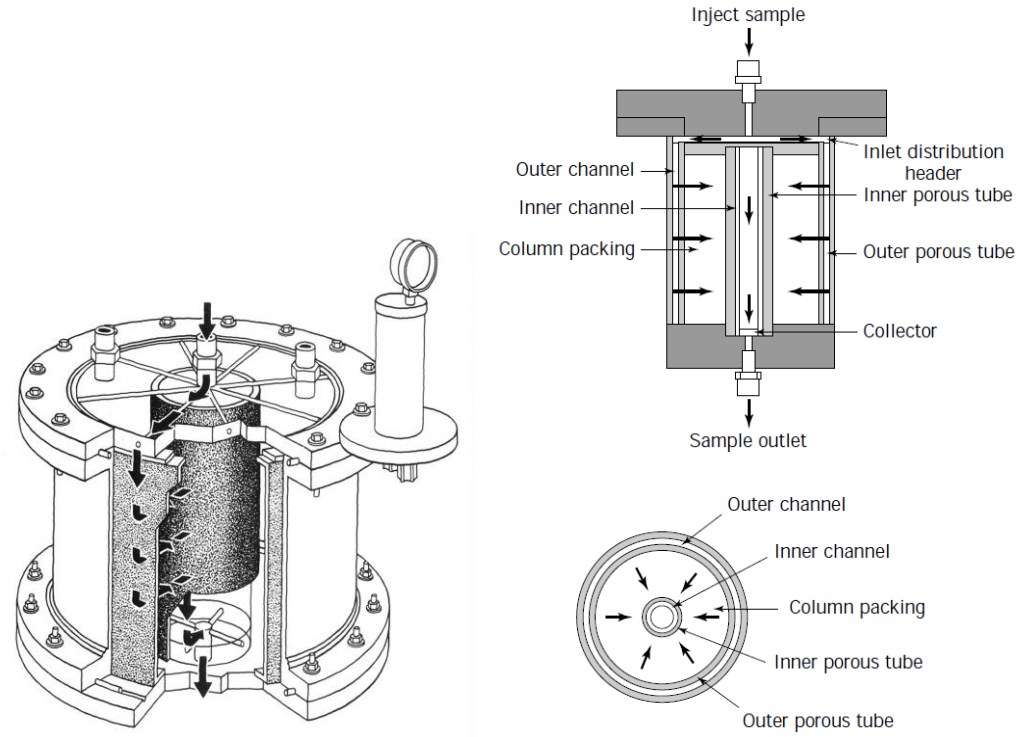

Figure 3. Acrylic Superflo column by Sepragen (Saxena and Dunn 1989).

More research evolved in the 1980s and 1990s. In 1988, Jungbauer carried out a radial ion exchange chromatography scale-up study using ZetaPrep cartridges on monoclonal antibody purification. Huang proved the possibility of linear scale-up of radial flow affinity chromatography on plasma proteins (Huang, Roy et al. 1988). In (1989), Plaigin purified plasma proteins by radial ion exchange and radial affinity chromatography using ZetaPrep and Zetaffinity (Figure 4) cartridges. Hou analyzed the purification of urokinase with zinc-chelated cation exchange radial cartridges (Hou and Zaniewski 1990).

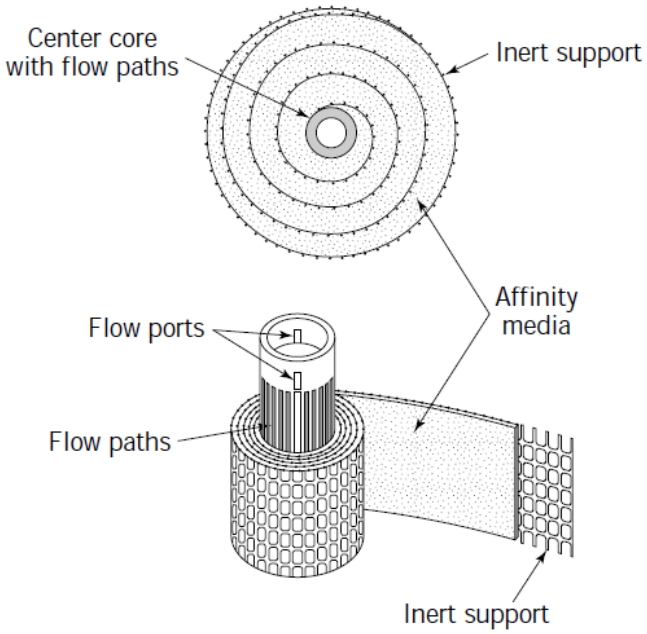

Figure 4. Structure of Zetaffinity cartridge (Gu 1999a).

Ligand utilisation of affinity media is higher in systems with longer flow path as residence time is increased. However, the resulting increase in flow resistance will decrease the flow rate. Liapis presented mass transfer mechanisms and rate steps for the formation and dissociation of the absorbate-ligand complex of various chromatography models to predict performance characteristics of affinity chromatography systems, including radial flow systems. According to Liapis, radial flow systems have lower ligand utilisation and resolution than conventional axial systems with equal radius and length but allow higher flow capacity. During complete saturation, radial flow systems have an advantage of high flow rates over axial flow systems for a given pressure drop (Liapis 1989).

2.3.1 Scale up

As radial flow chromatography allows larger throughputs with low pressure drops, it has the potential for application in industrial processes and use with soft media. Various simulated and experimentally determined performance comparisons between axial flow columns and radial flow columns have continued to be documented but further

understanding is required to successfully incorporate radial flow chromatography in the bioprocess industry.

Authors that studied the performance of radial flow columns in comparison with axial flow column concluded that radial columns are highly suitable for scale-up. However in some cases, comparisons were made between axial column and radial column with different parameters such as different bed heights and different bed volume (Sun, Ge et al. 2000). To properly evaluate the performance difference between axial and radial flow columns, no significant parameter should be mixed.

Recently, Cabanne evaluated the main chromatographic parameters; efficiency, capacity asymmetry and resolution, comparatively between anion exchange radial and axial chromatography of equal bed volume and bed height (Cabanne, Raedts et al. 2007). In this study, the advantages of radial over axial chromatography reported were higher efficiency, higher resolution and lower buffer demand. The height equivalent of a theoretical plate (HETP) decreased by 31% in the radial column, indicating a higher resolution. Higher resolution was also observed by the more symmetrical and narrow peak width in the radial chromatography.

It is assumed that radial flow column produces a more homogeneously packed bed and even sample application which results in a near optimum plug flow effect. Equilibration steps, from storage to equilibration buffer and from elution buffer to equilibration buffer, were reduced by 0.4-0.5 column volumes in the radial chromatography. This reduction in buffer consumption and process time will be highly relevant in large scale processes. Due to similar column parameters (bed height and volume), both columns showed similar retention volume and capacity factor. In radial columns, the inlet surface area is large so protein is applied over a larger surface which functions to prevent protein overload (Cabanne, Raedts et al. 2007).

2.4 Rotating Annular Bed Chromatography

The first annular chromatography was proposed by Martin (1949)**.** It was suggested that the system may compose of a single chromatogram or a circular array of chromatogram tubes. Following the emergence of annular chromatography, various theoretically and experimentally analyses were carried out by different authors.

Solms (1955) continued work on Martin's annular chromatography using a continuous chromatography system of ion exchange medium in a circular array of tubes. Elution agent is continuously supplied at the top of the bed with the liquid collected at different points at the bottom of the bed as the bed rotates on its vertical axis.

Svensson (1955) too designed a similar continuous chromatography system involving the use of a composite column with 36 individual tubes arranged in a circle and rotated around its central axis. Restrictions to annular bed chromatography found in this design were the low quality of the adsorbent and non-uniform flow through each of the chromatograph tubes.

Another alternative system to axial flow chromatography able to produce better resolution and larger throughput is the pressurized annular gas chromatography. Most of the early developments of annular chromatography were used in the separation of gaseous components. In 1959, (Hall and Cole) patented a continuous gas chromatography invention consisting of an annular column which could separate at least one component from a sample mixture. Other patents of continuous annular gas chromatography systems include works by Luft (1962) and Heaton (1963).

Giddings (1962) proved theoretically that annular bed is capable of better resolution and greater throughput than conventional large scale fixed bed gas chromatography. Dinelli (1962) constructed a preparative scale gas chromatography unit with a hundred columns operated continuously by rotating the drum of columns traverse to gas flow. Successful separation of n-heptane and toluene, and n-hexane and acetone indicated that overall efficiency of the system was equivalent to that of a single batch column. Another similar laboratory scale unit was reported to be able to separate isomeric compounds of 3-chloro-2-methyl-propene and 1-chloro-2methyl-propene, α and β pinene, isomers of 1,3-pentadiene, purification of dimethyle-hexa-2,4-diene, and purification of n-hexane (Taramasso and Dinelli 1964).

The first continuous annular chromatography system built for separation of biological components consists of an annulus of media with buffer solution fed into the column through a constant level device (Fox, Calhoun et al. 1969). This system was tested with the separation of myoglobin from haemoglobin in beef heart extracts with Sephadex gels with the fractions collected at their exit points on the annulus. 97% myoglobin

purity was achieved but with an increase of solvent requirement by ten times more than would be required in an axial flow column (Nicholas and Fox 1969).

2.5 Pressurized Continuous Annular Chromatography

Developments in continuous liquid chromatography by Scott (1976) incorporated gas overpressure for pressurized operation and segmenting spacers for gradient elution to liquid rotating annular chromatography. The annular chromatograph built (Figure 5) contains two concentric open cylinders sealed at both ends by flanges, a Teflon flow distributor fit into a port by a double O-ring seal, and six inlet holes through the distributor for feed and eluent streams. Forty-eight spacers at the top and bottom of the annulus maintained constant annular width and segmented the column into different regions for gradient elution without backmixing. The head space pressurized by inert gas functioned as a gas blanket which allowed pressurization up to 25 psig. Two types of separation experiments were carried out; size exclusion separation of blue dextran and $CoCl_2$ using Sephadex G-25, and ion exchange separation of nickel and cobalt using Dowex 50W-X8. Both systems resulted in low resolution separation.

Another pressurized rotating chromatography, a modified system of that used by Scott (1976), with a stationary feed stream and stationary eluent collection devices was analyzed (Canon and Sisson 1978). This sytem has an inlet distributor with four manifolds of eluent entry points which allow gradient elution while capillary tube nozzles evenly distribute the eluents. Two layers of glass beads placed above the resin allow feed band to spread until feed velocity match eluent velocity, at which hydrodynamic spreading stops and initial bandwidth is obtained. Backmixing problem was eliminated by having porous plugs in 180 exit tubes which were soldered to the bed support plate. A device on the side of the column helps maintain liquid level below the surface of the glass beads prevents circumferential mixing in the head space. This system also has the gas overpressure apparatus removed from the rotating annular bed and the entire headspace flooded with eluent.

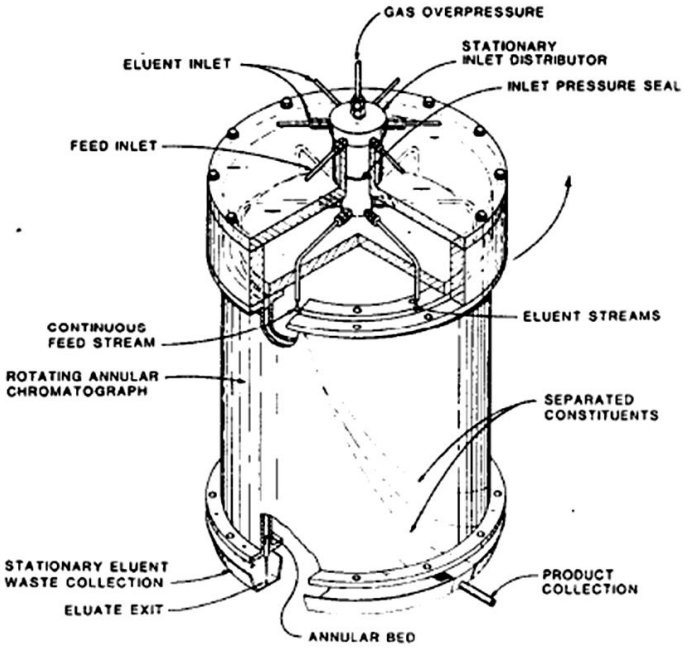

Figure 5. Pressurized annular chromatography (Scott, Spence et al. 1976).

This modified system by Canon and Sisson was tested for the separation of metals. Among the various documented separation experiments are copper, nickel and cobalt; iron and aluminium; zirconium and hafnium; and cobalt and blue dextran (Canon, Begovich et al. 1980; Begovich and Sisson 1981; Begovich, Byers et al. 1983; Begovich and Sisson 1984; Sisson, Begovich et al. 1987).

A valuable advantage of the continuous annular chromatography (CAC) is its suitability for all chromatographic separation techniques and adsorbent known for batch chromatography. CAC research was further carried out with Canon and Sisson's modified system for separating fructose, sucrose and glucose (Howard, Carta et al. 1988; Byers, Sisson et al. 1989), fructose mannitol and sorbitol (Wolfgang, Prior et al. 1995; Bart, Messenböcl et al. 1996), iron and chromium (Carta, DeCarli et al. 1989), and amino acids (Takahashi and Goto 1991; Yonemoto, Kitakawa et al. 1993; Kitakawa, Yamanishi et al. 1995; Kitakawa, Yamanishi et al. 1997). Takahashi's rotating annular chromatograph differs from the more common design by Canon and

Sisson by having the feed supplied to the annulus while eluents enters through rotating nozzles.

Protein separation experiments with P-CAC include the separation of albumin, haemoglobin and cytochrome C (Bloomingburg, Bauer et al. 1991), myoglobin and haemoglobin (Takahashi and Goto 1992), bovine serum albumin and haemoglobin (Bloomingburg and Carta 1994), and desalting of bovine serum albumin (Reissner, Prior et al. 1996).

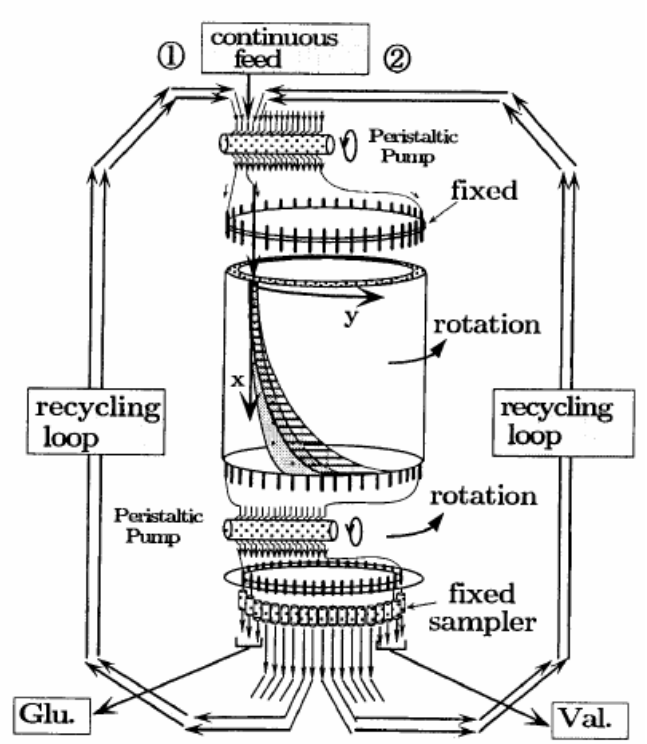

Figure 6. Annular chromatography with partial effluent recycling (Kitakawa, Yamanishi et al. 1997).

In general, annular chromatography consists of a packed bed contained between two concentric cylinders. The cylinders rotate slowly around its axis as a multicomponent mobile phase is pumped continuously into the system through a fixed inlet. As the components move downwards, they are separated according to their affinity to the stationary phase. The rotation the bed results in helical bands of different components

from feed point to exit point (Figure 7). The helical band angle is determined by the component affinity for the stationary phase, flow rate and bed rotation speed. Under stationary conditions, the components separate and leave the system at the same angle, as the feed point (Giovannini and Freitag 2001; Thiele, Falk et al. 2001; Giovannini and Freitag 2002).

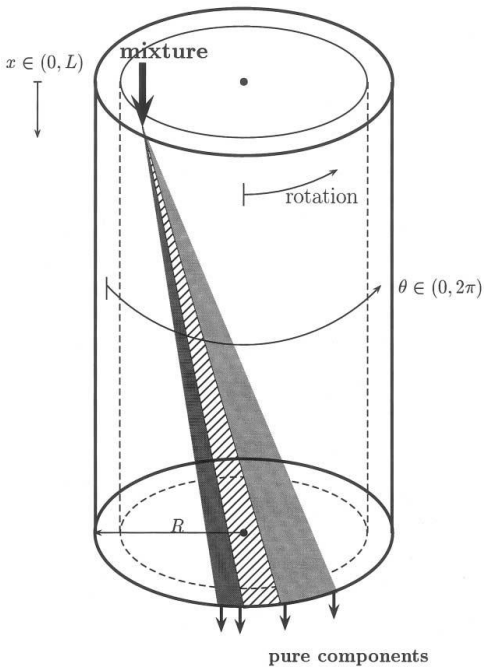

Figure 7. Rotating annular chromatography (Thiele, Falk et al. 2001).

Annular chromatography has several advantages. Firstly, this system enables separation of more than two components in a single step and uses elution method similar to that of a fixed bed system. Process optimisation is easier as it allows the option of step elution and partial recycling (Thiele, Falk et al. 2001). Prior Separation Technology (Austria) started to manufacture commercial CAC systems (Figure 8) first for the separation of metals and then for bioseparations. Various biomolecules has since been isolated from cell culture supernatant.

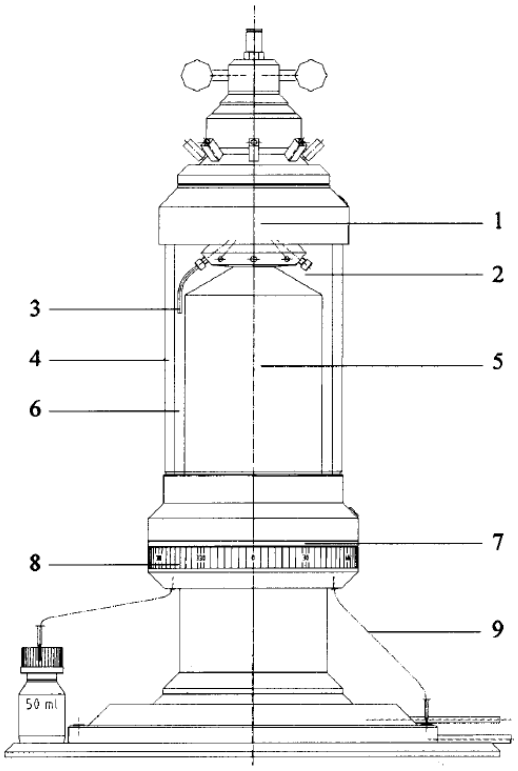

Figure 8. Annular chromatograph from Prior Separation Technology: 1, head; 2, headspace; 3, feed nozzle; 4, outer cylinder; 5, inner cylinder; 6, annulus; 7, stainless steel plate (with 90 exit holes); 8, fixed Teflon slipring (with 90 exit ports); 9, Tygon tubing. (Buchacher, Iberer et al. 2001).

Buchacher (2001) analyzed the resolution, recovery, fouling and productivity of P-CAC in comparison with conventional column chromatography and found protein aggregates could be separated from IgG protein mixture on an industrial scale. Initial regeneration was carried out simultaneously with protein separation but nearly the entire column was needed to completely separate the polymers from the monomer fraction. Even with a successful separation, polymers were eluted along with NaOH which caused protein precipitation which clogged the column. Regeneration was then performed after 5.5 hours of feed supply. By the fourth cycle, fouling occured but could be easily prevented by diluting the sample solution. Maximum feed flow rate, before entering the head space and other parts of the annulus, depends on the feed concentration. Diluted feed allows higher flow rates. A comparison of productivity showed that P-CAC has higher productivity than batch mode axial column separation.

P-CAC (Figure 9) by Prior Separation Technology has also been used in the isolation of recombinant antibody (Giovannini and Freitag 2001) and isolation of plasmid DNA (Giovannini and Freitag 2002) from cell culture supernatant. The performance of a P-CAC was compared to batch and expanded bed chromatography. Separation quality was maintained during the transfer of small batch column protocol to P-CAC by maintaining the dimensionless column loading factor. In the evaluation of P-CAC and batch column performance, the HETP of P-CAC was found to be lower than both analytical and preparative batch columns at low rotation speeds but increases dramatically with increased rotation speeds. Difference in plate height was assumed to be due to an artifact caused by the design of the P-CAC. 90 outlets around the annulus produce an elution angle of 4^0 so at low rotation speeds, the peaks to appear much broader that they are because each fraction is averaged over 4^0. This effect is less pronounced at high speeds as elution occurs over larger number of outlets.

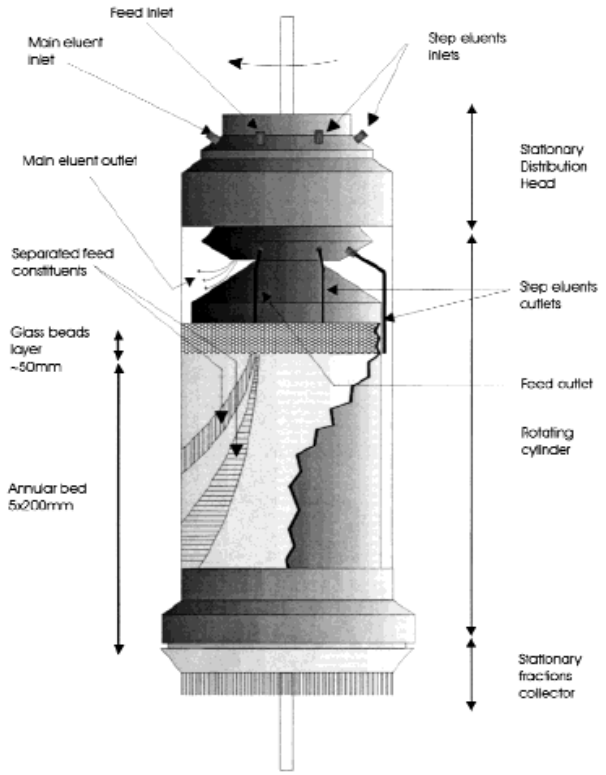

Figure 9. Schematic drawing of the P-CAC system commercialized by Prior Engineering (Austria) (Giovannini and Freitag 2001).

Iberer (2001) compared the P-CAC to conventional packed column in the purification of IgG from protein aggregates and separation of factor IX from vetonectin. Separation efficiency was analyzed by investigating the effects of feed flow rate, eluent flow rate and rotation rate. Reduced extra column band broadening observed in P-CAC was assumed to be due to its lowered height equivalent to theoretical plate value. High feed flow rates was not possible as contamination occurs due to feed entering the headspace. However, it was concluded that P-CAC increases productivity and decreases buffer consumption.

Recombinant protein drugs was isolated from cell culture supernatant in pilot scale at about 144-288L/day using a standard lab-scale P-CAC by Prior Separation Technology (Vogel, Nguyen et al. 2002). In this study, general characterization showed that peak wobbling and peak broadening are the limiting factors for the performance of P-CAC. 3-5 fold increase in purity and 94% yield was achieved with a concentration factor of 30. A conventional batch chromatography protocol was used with adjustments to flow rates and inlet geometry to prevent contact between incompatible buffer and solutions.

P-CAC has also been used in the refolding of proteins. Schlegl was able to continuously refold bovine α-lactalbumin by size exclusion with Superdex 75 PrepGrade medium yielding 41% reactivated monomer, which is an improvement to the batch process where only 30% active monomer was obtained(Schlegl, Iberer et al. 2003). Another documented P-CAC for protein refolding involves the refolding of lysozyme (Lanckriet and Middelberg 2004). It was found that P-CAC produces high refolding yields with an elution profile similar to a batch system. P-CAC behaves similarly to an infinite series of batch size exclusion column system which enables easy optimization and incorporation into downstream processing.

2.6 Continuous Chromatography

Throughout the development of chromatography, batch mode is the most preferred and common process due to its operation simplicity. It is also this reason that industrial scale separations are carried out in batch mode even though continuous chromatography can offer advantages such as increase flexibility, unattended operation, consistent product

quality, reduced recycling requirements and higher efficiency with greater use of the chromatographic media.

In a continuous separation process, all steps are carried out simultaneously. The residence time where biomolecules are in contact with the adsorbant is very short, thus reducing the chances of denaturation, aggregation and degradation of target molecules due to extended period of contact. Column regeneration can also be carried out in a less harsh condition, increasing the lifespan of the media and reducing process time.

Continuous chromatography is achieved by various methods with the stationary phase moving either physically or simulatedly by counter-current, cross-current or co-current flow to the mobile phase (Sussman and Rathore 1975; Barker and Ganetsos 1988). It can be categorised as a moving bed system where relative motion between the stationary and mobile phases results in different retention time and continuous exit of components at different distance from the feed point; paramagnetic pumping system where cyclic operation is achieved by intermittent or sinusoidal flow, or temperature, phase and pressure variations; and electrochromatographic system where adsorption chromatography is combined with electrophoresis resulting in different curve paths for different components.

2.6.1 Moving bed

Continuous chromatography was first reported by Freund in 1957 for the separation of acetylene from acetylene methane mixture and was further researched by Scott in 1958 using gas-liquid chromatography to isolate benzene from coal gas (Scott 2000). In a moving bed system, the stationary phase moves counter-current to the mobile phase causing components with velocity greater than bed velocity will travel in the same direction as the mobile phase while components with velocity less than bed velocity follows the direction of the bed movement. Specific components can then be selectively and continuously separated from a mixture by manipulating the temperature at different sections of the column and by having a number of ports.

2.6.2 Simulated moving bed

A pseudo- moving bed system was developed as an alternative to moving bed system (Barker and Ganetsos 1988). In this system, the column in circular form developed from

the wheel concept where the bed moves continuously in one direction while the mobile phase moves in the opposite direction. The design prevents apertures from opening until they connect with the ports fixed to the column at the periphery during rotation. Components travelling at a rate slower than the "wheel" moves in the same direction as the rotating bed while components travelling at a faster rate will move with the mobile phase in the opposite direction (Figure 10). Due to problems with leaks, this system was not very successful.

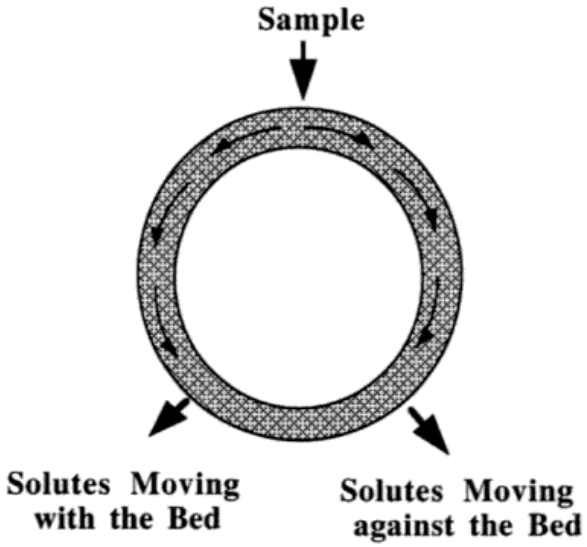

Figure 10. Simulated moving bed column (Scott 2000).

Another simulated moving bed system was proposed by Hurrel (1972) as an extended version of Barker's large circular column which has two advantages. First is in its technical simplicity. Secondly, there is lower solvent requirement due to mobile phase recirculation and conservation of the stationary phase, both of which contributes to reduced cost (Scott 2000).

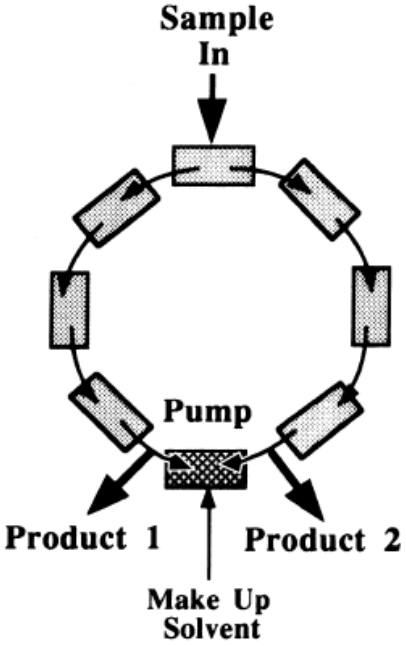

Figure 11. Hurrel's multi column simulated moving bed (Scott 2000).

The Hurrel simulated moving bed system consists of a number of sections joined in the form of a circle by a large rotary disc valve with each section functioning as a short column. The valve upper disc connects to different ports while the lower disc connects to the columns. Construction and operation of the disc valve is simpler than the rotating wheel column by Barker. This system is also leak proof even with high pressures. Most simulated moving bed systems used in preparatory chromatography have been based on the Hurrel's design (Scott 2000).

Pais (1997)continued the analysis of simulated moving bed continuous chromatography by modeling and simulating an operation on a pilot unit, Licosep 12-26 from Separex (France). Purities and recoveries of 95% were obtained in the separation of 1, 1'-bi-2-naphthol enantiomers with 3, 5-dinitrobenzoyl phenylglycine bonded to silica gel stationary phase. In the 1990s, there were more than a hundred simulated moving bed units were operating worldwide but mostly used in chemical processes rather than bioprocesses (Humphrey 1995).

As technology improved, pilot and industrial scale simulated moving bed chromatography became increasingly useful in new biotechnology and pharmaceutical

processes (Hashimoto, Yamada et al. 1989; Kishihara, Horikawa et al. 1989; Ching, Lim et al. 1993; Roger-Marc, Géraldine et al. 1993; Navarro, Caruel et al. 1997).

2.6.3 Continuous chromatography

The first continuous radial flow chromatography system, a rotating annular gas chromatograph (Figure 12) was proposed by Mosier (1963). In the continuous radial system gas is flowed from the axis towards the periphery via the inner annular bed and separated into its components as it passes through the packed bed. Separated components exit the periphery end of the packed bed at different angles depending on the migration rate across the bed. There were two designs of this system but neither was constructed. The first design allows a decrease in gas velocity with increased distance from the axis while the second design maintains constant gas velocity.

A similar system to the continuous radial gas chromatography system by Mosier was proposed by Tuthill (1970). In this system, sample entry and exit points are located at the top of the axis and periphery respectively. There have also been modified versions of the Mosier systems (Figure 13) used in commercial waste gas treatment (LeVan, Carta et al. 1997).

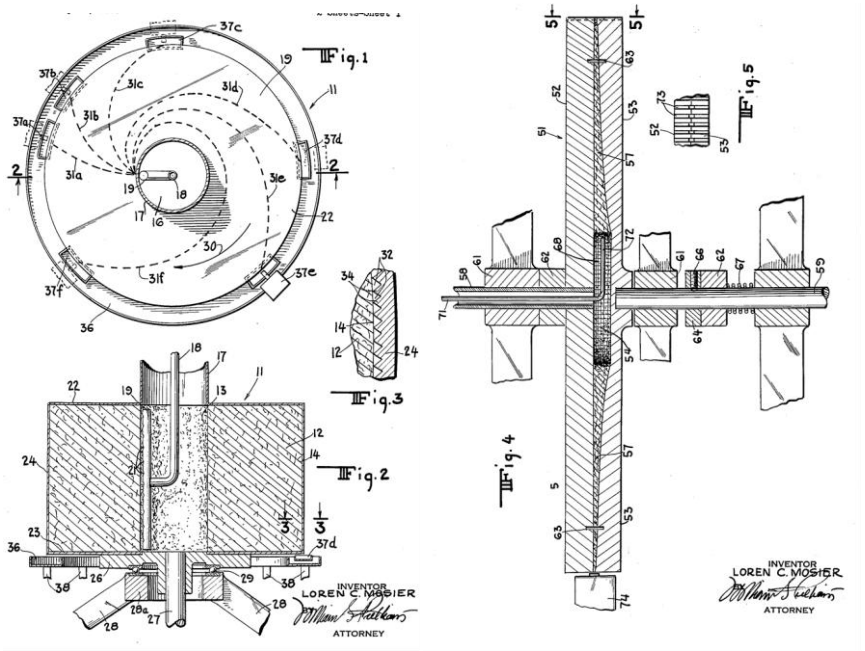

Figure 12. Rotating annular gas chromatography (Mosier 1963).

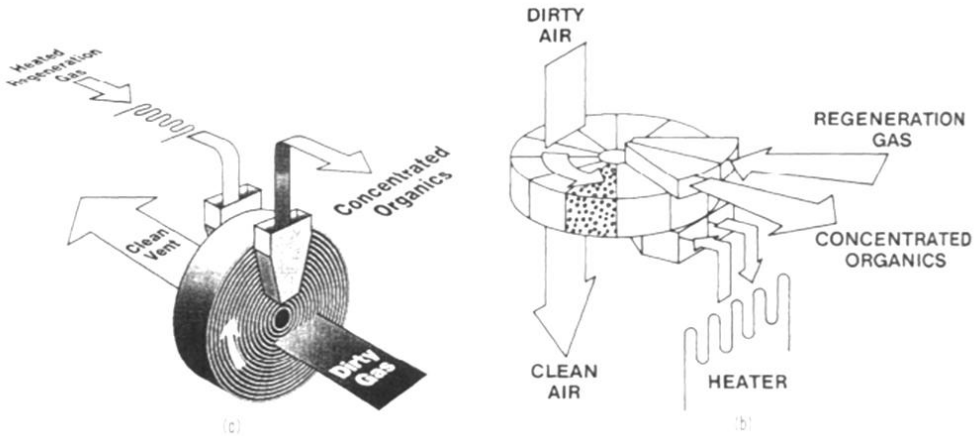

Figure 13. Absorbent wheels for gas separation: horizontal with fixed beds and vertical monolith (LeVan, Carta et al. 1997).

2.7 Continuous Disc Chromatography

The most similar chromatography system to CRFC which was developed to testing stage is the continuous disc chromatography (Sussman 1970; Sussman and Rathore 1975; Sussman 1976). In place of an annular bed, this system functions by having two solvent coated glass discs and spacers (Figure 14). Problems associated with packing are avoided as no bed packing is required.

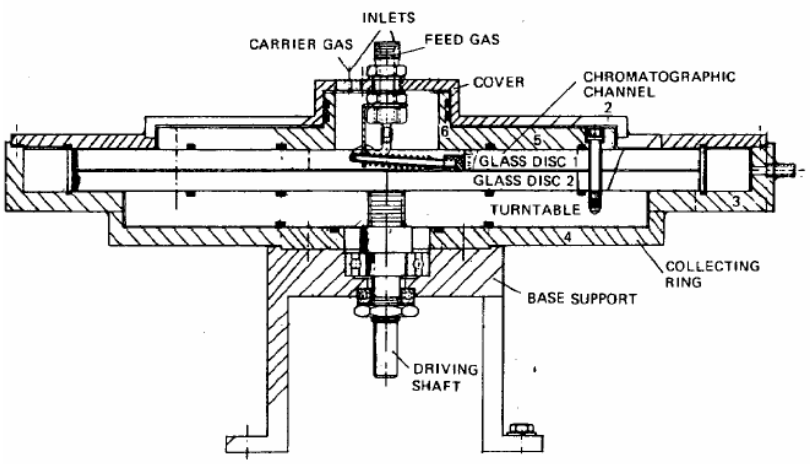

Figure 14. Continuous disc chromatography (Sussman and Rathore 1975).

2.8 Continuous Radial Flow Chromatography

CRFC and continuous disc chromatography is similar only in principle. The differences between these two chromatography systems are in their flow direction, mobile phase, separation molecules, separation media and elution type. Unlike a continuous disc system, CRFC involves a liquid mobile phase, water soluble components, inward flow, step elution and a resin packed bed.

CRFC is a system which combines the advantages of continuous mode, radial flow and a rotating annular bed. In this system, solution flows inwards from the periphery as the resin packed annular bed rotates. In this design, the short bed height prevents large pressure drops which in turn allow greater throughput and the use of soft media. Common problems associated with packed beds are eliminated.

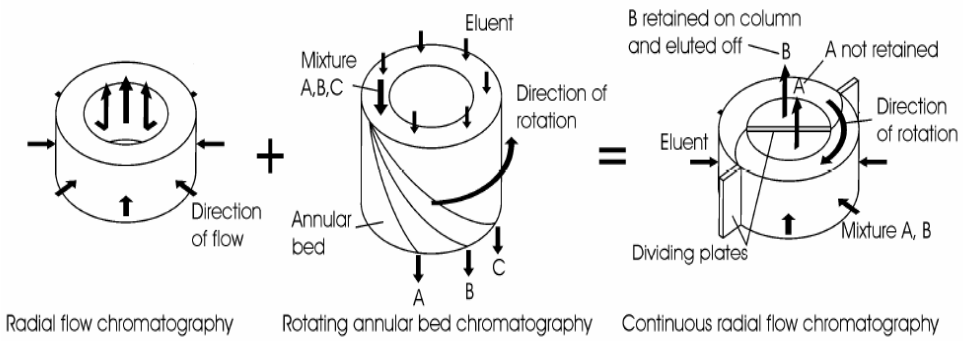

Figure 15. Combination of radial flow and rotating annular bed chromatography to develop the concept of CRFC (Lay, Fee et al. 2006).

2.8.1 First CRFC prototype

The first CRFC prototype (Lay 1998) built was a system with an annular packed bed of I.D. 8.6cm, O.D. 11.6cm and height 12cm contained between two concentric porous cylinders (Figure 16). These inner and outer cylinders are composed of sintered stainless steel sheets. Chromatography media is packed into the annulus through packing ports.

Solution flows radially and cross current to the rotating bed. The annulus is rotated using DC motors connected to a gear attached to the bottom of the annulus. Solution is

pumped into the annulus through the outer feed chambers on the outer periphery of the annulus. Solution then flows across the annular bed in the radial direction and cross current to the rotating bed. After passing through the annular bed, solution exits through the inner chambers.

Feed and exit chambers were divided into two sections, allowing feed solution and elution buffer solution to flow in simultaneously through different sections (Figure 17). When feed solution flows through the chromatography media, target protein binds to the resin. The annulus then rotates, bringing the resin bound proteins to the elution zone where elution buffer passes through the annular bed and elutes the bound proteins.

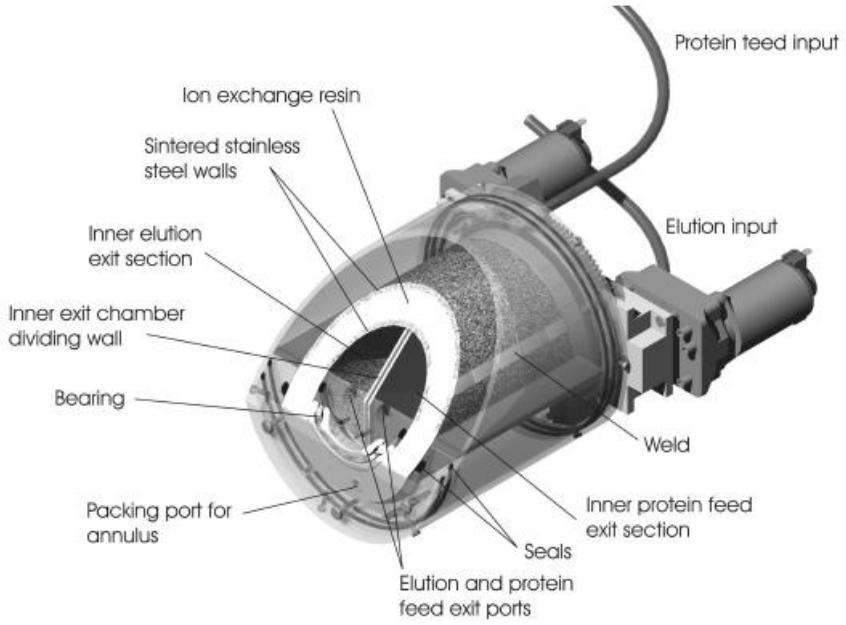

Figure 16. First CRFC prototype (Lay 1998).

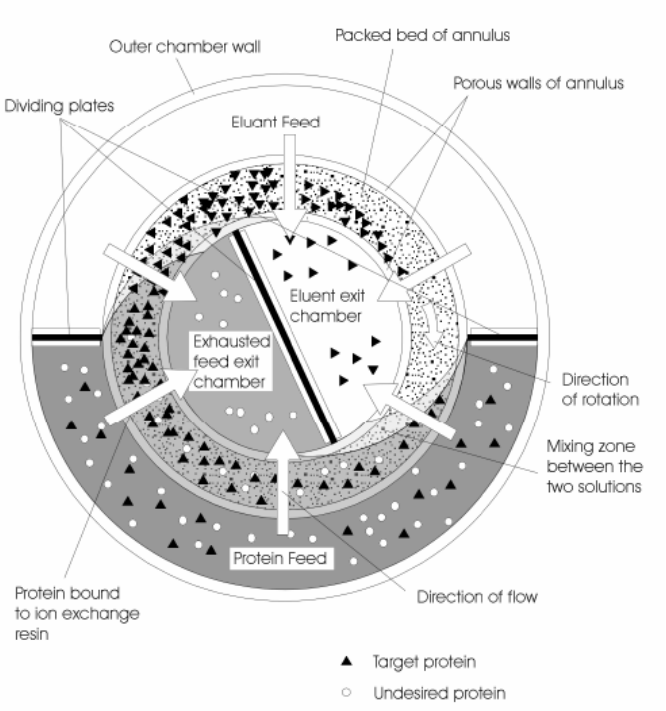

Figure 17. Cross-section of first CRFC prototype (Lay 1998).

Main advantages of this configuration were reduced pressure drop, possibility of multicomponent separations and control simplicity. However, this CRFC prototype had several problems involving the feed and exit chambers, annular bed, and gearing and motors. Large chamber volumes resulted in broad peaks and extended tailing. Short bed depth also caused additional peak broadening effect. Mechanical failures and construction limitations caused cracking, leakage and corrosion in the annulus. Significant amount of solution was required due to the large bed volume. There was also flow obstruction through the walls of the annulus and limited access for unpacking the annulus.

2.8.2 Second CRFC prototype

A second CRFC prototype was designed to minimized or eliminate the problems found in the earlier CRFC system and which research of this thesis is mainly based on. This prototype consists of a top bearing housing, separation module, bottom bearing housing and gear housing; and stand mounted motor which are stacked vertically in alignment with the central axis. The modules slot into each other via keys and pins, and locked in

place with screws. There are various advantages to the modular design and vertical assemble of this CRFC such as easy assembly and possible modification, access to feed and effluent ports, easy purging of air from the system, bearing is better protected, and easy access to separation module (Lay 2005).

Similar to the first prototype, the separation module of the second prototype consists of an annulus, inner chambers and outer chambers. The casing of the annulus where separation media is contained consists of a base welded to two concentric stainless steel cylinders. The removable lid is attached to braces welded onto the cylinders and sealed using o-rings. Separation media can be pump packed into the annulus via the four packing ports located on the lid.

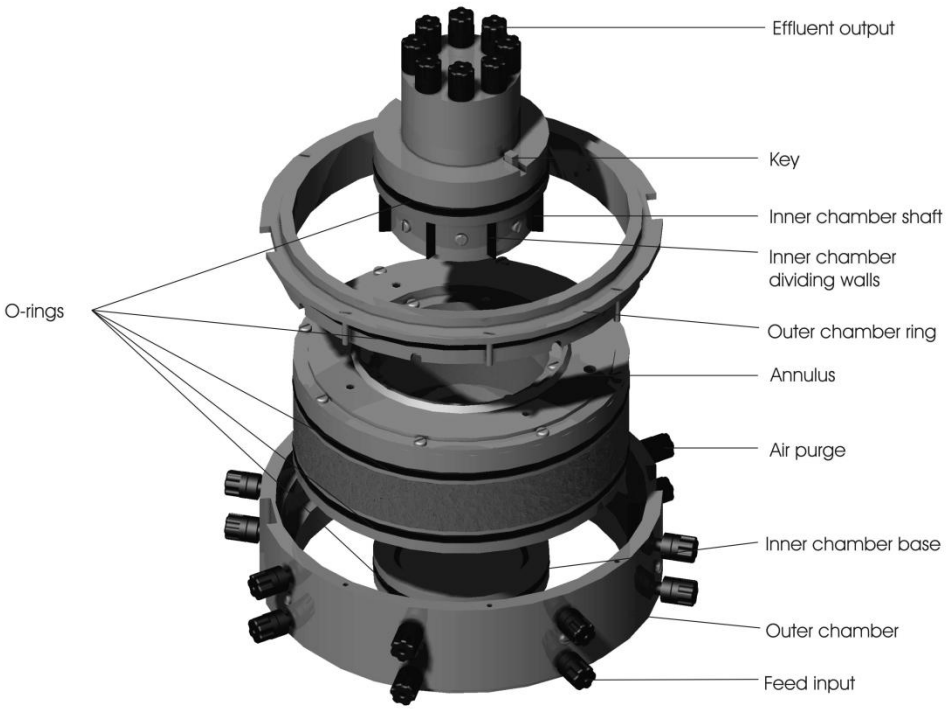

Figure 18. Exploded view of separation module (Lay 2005).

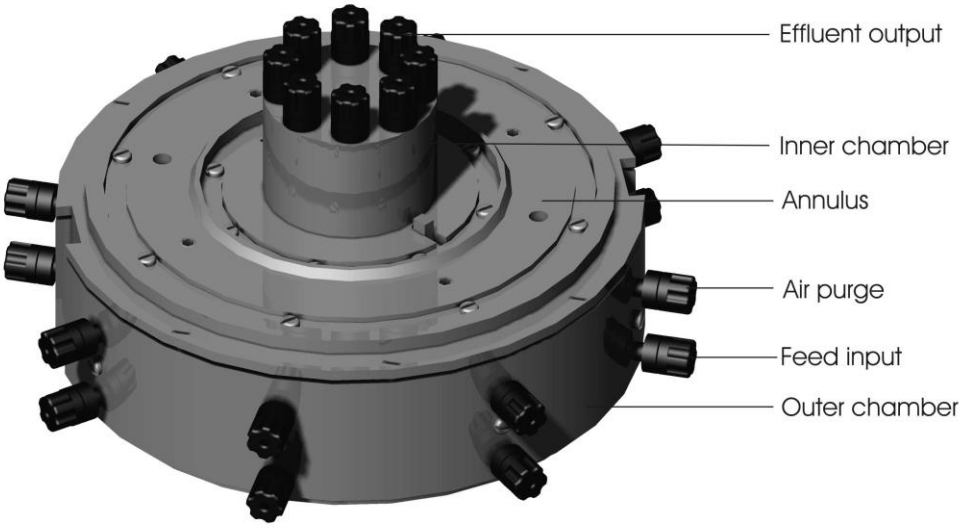

Figure 19. Assembled separation module (Lay 2005).

Eight equal sectioned feed chambers are positioned at the periphery of the annulus, consisting of a chamber wall and outer chamber ring (Figure 18). Exit chamber consisting an inner shaft and base is also divided into eight equal sections. The chambers are connected to the annulus using screws and sealed with O-rings. Rubber seals are used as the divider for the eight chamber sections. Each section is connected to an individual port at any one time, giving the possibility of eight different solutions to be applied simultaneously and collected separately.

Solution applied enters through the outer feed chamber. It then passes through the outer sintered wall, resin packed bed, inner sintered wall and inner exit chamber where solution can be collected from the exit ports.

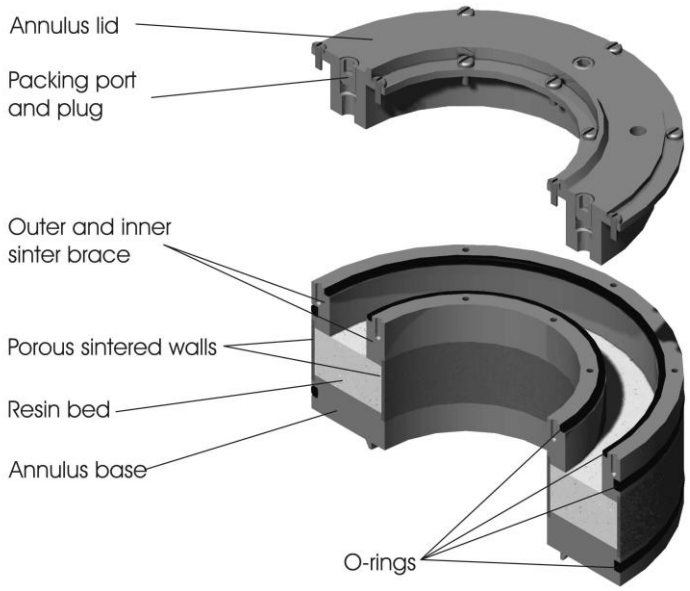

Figure 20. Exploded and sectioned view of annulus. (Lay 2005).

CRFC 2 was designed with several advantages over the previous prototype. It has a lower bed volume and greater bed depth, thus increasing resolution. Overall decrease in bed volume decreases the volume of resin and solutions required. It is also able to operate at lower flow rates and withstand greater pressures. Feed and exit chamber are divided into sections, giving greater separation flexibility through variations in volume of feed solution, buffer solution and elution buffer solution applied.

The CRFC was successfully applied to the continuous extraction of BSA from a stock solution. However, a few problems were encountered. Angular displacement which increases with increasing rotation speeds resulted in broader BSA and NaCl peaks. BSA fouling resulted in increased pressures with each run. A more concentrated NaOH solution was required for regeneration while operation time was reduced due to increased downtime for column regeneration. Channel formation also occurred from the settling of the resin bed.

In the continuous separation of BSA and lactoferrin with the CRFC, it was found that 85% of the BSA could be recovered with 94% purity (Figure 21). BSA separation factor, given as BSA to lactoferrin ratio in the feed stream divided by BSA to lactoferrin ratio in the collection zone was found to be 4.79.

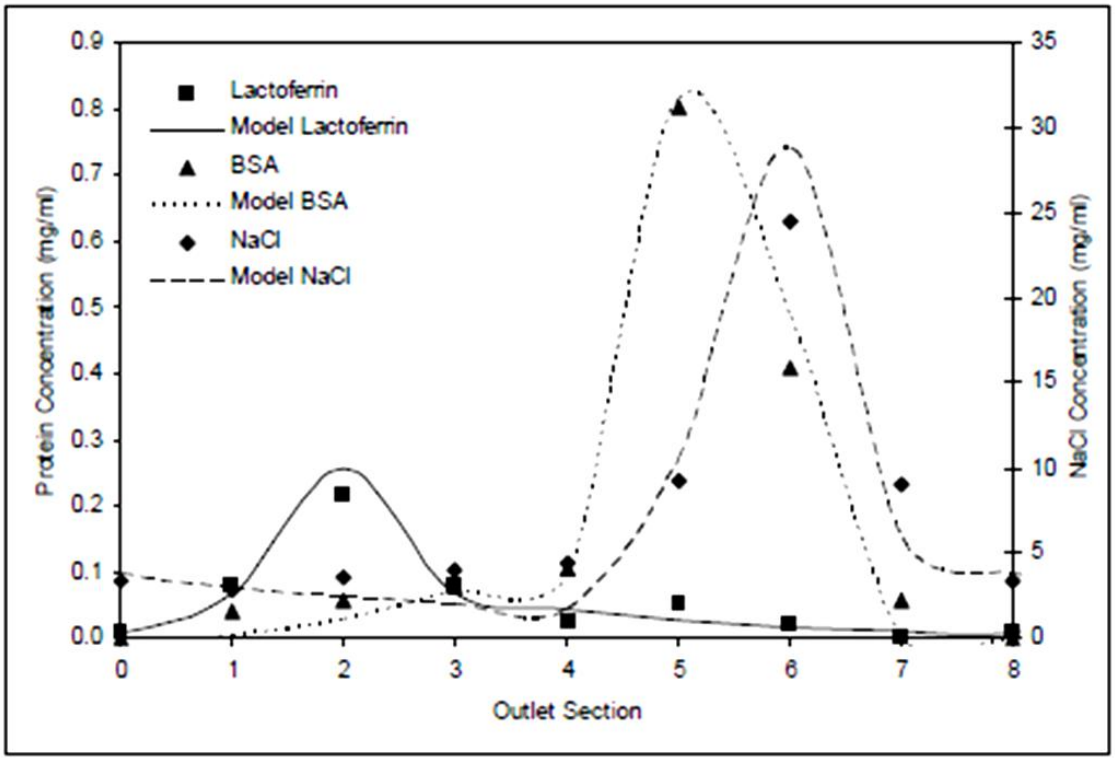

Figure 21. Elution profiles of BSA, lactoferrin and NaCl from the CRFC. Feed was 1.6 mg/mL BSA and 0.53 mg/mL lactoferrin, total flow 40 mL/min, feed flow of 5 mL/min to section 1, elution flow 5mL/min to section 5, and rotation speed 49 min/rev (Lay 2005).

2.9 Modelling

The CRFC combines radial flow and rotating annular bed chromatography into one system. Therefore the CRFC model incorporates general equations developed for both systems. Continuity equation for radial flow chromatography follows

$$\frac{\partial C_A}{\partial t} + \left(\frac{1-\varepsilon_R}{\varepsilon_R}\right)\frac{\partial C_{RA}}{\partial t} = \frac{1}{r}\frac{\partial}{\partial r}\left(r\, D_{Ar}\frac{\partial C_A}{\partial r}\right) - \frac{Q}{\varepsilon_R A_r}\frac{\partial C_A}{\partial r} \qquad (1)$$

where C_A is solute A concentration in the void space, ε_R is the void fraction of the chromatography media, C_{RA} is solute A concentration in the resin, t is time, D_{Ar} is radial dispersion coefficient, Q is flow rate and A_r is area perpendicular to solution flow. (Gu, Tsai et al. 1991; Tsaur and Shallcross 1997)

Continuity equation for rotating annular bed follows

$$w\frac{\partial C_A}{\partial \theta} + w\left(\frac{1-\varepsilon_R}{\varepsilon_R}\right)\frac{\partial C_{RA}}{\partial \theta} = D_{Az}\frac{\partial^2 C_A}{\partial z^2} - \frac{Q}{\varepsilon_R A_z}\frac{\partial C_A}{\partial z} \quad (2)$$

where w is rotation speed, θ is angular position, D_{Az} is axial dispersion coefficient, z is axial position and A_z is area perpendicular to solution flow (Wankat 1977). Equation (2) assumes no change in solute concentration due to angular dispersion. If angular dispersion factor is included, the continuity equation for rotating annular bed would be

$$w\frac{\partial C_A}{\partial \theta} + w\left(\frac{1-\varepsilon_R}{\varepsilon_R}\right)\frac{\partial C_{RA}}{\partial \theta} = D_{Az}\frac{\partial^2 C_A}{\partial z^2} + \frac{D_{A\theta}}{{r_A}^2}\frac{\partial^2 C_A}{\partial \theta^2} - \frac{Q}{\varepsilon_R A_z}\frac{\partial C_A}{\partial z} \quad (3)$$

Where D_{Az} is angular dispersion coefficient and r_A is annular bed radius (Buchacher 2001).

Solute concentration within the void space of the chromatography column also changes due to Eddy dispersion and molecular diffusion. In a liquid chromatography column packed with resin particles, Eddy dipersion is much larger than molecular diffusion. The dispersion coefficient given by Gu (1991) and Thiele (2001), can be simplified to

$$D_A = y_2 2 r_p v \quad (4)$$

where the dispersion coefficient equation is applicable to both radial dispersion and angular dispersion, r_p is the radius of a resin particle, and v is interstitial velocity.

In chromatography with porous media particles, mass transfer also occurs due to film diffusion which involves mass transfer between resin interstices and resin pores, across the stagnant solution surrounding the media particles. It is therefore incorporated into both interstitial and resin pore phase equations. Change in interstitial solute concentration is given by

$$\frac{\partial C_A}{\partial t} = -\frac{3k_{fA}(C_A - C_{RPA})\,(1-\,\varepsilon_R)}{r_p \varepsilon_R} \quad (5)$$

where C_{RPA} is the solute concentration in the resin pores (Kaczmarski, Antos et al. 2001). Change in resin pore solute would then follow equation (5), adjusted to resin

pore volume.

Within the ion exchange resin particle, adsorption onto the matrix can be modeled the Langmuir isotherm. Solute is assumed to be in equilibrium between resin pore solution and resin matrix. Based on the saturation point, solute concentration at equilibrium on the resin matrix in relation to solute concentration in the resin pores is given by

$$C_{RA}{}^{*} = \frac{C_{RAmax}\ K_A C_{RPA}{}^{*}}{1 + K_A C_{RPA}{}^{*}} \tag{6}$$

where C_{RAmax} is the maximum capacity of the resin matrix and K_A is the equilibrium constant for solute A. The Langmuir isotherm equation is also applicable to multicomponent separations as reported by Gu (1991), following

$$C_{Ri}{}^{*} = \frac{K_i C_{RiMax}\ C_{Ri}{}^{*}}{1 + \sum_{j=1}^{Ns} K_j C_{Ri}} \tag{7}$$

where Ns is the number of solutes competing for the matrix binding sites. The Langmuir isotherm equations can be separated into forward and reverse binding equations to give change in solute concentration due to uptake onto the resin matrix.These general equations for the modeling of the CRFC will be further discussed in Chapter 3.

Early works on radial flow chromatography models were carried out by Lapidus and Amundson (1952). Experiments were carried out with a range of flow rate, media particle size and input solute concentration. Various adsorption mechanisms were compared. They reported that KCl adsorption onto Dowex50 was best suited with the linear isotherm and rate determining liquid diffusion mechanism. CuSO4 and HAc adsorption onto Al2O3 was best described with linear isotherm and the rate determining solid diffusion mechanism.

Huang (1988) modeled radial flow chromatography used radial dispersion equation similar to equation (1). However as molecular disperion is assumed to be constant, dispersion equation is written as

$$\frac{D}{r}\frac{\partial}{\partial r}\left(r\,\frac{\partial C_A}{\partial r}\right) \tag{8}$$

where D is equivalent to D_{Ar} in from equation (1).

In the modeling of annular bed chromatography, several authors reported good predictions using the equations introduced earlier in this section. A continuous separation of dilute aqueous mixtures of iron and chromium ions with Dowex 50W-X8 sorbent in the annular chromatograph was modeled (Carta, DeCarli et al. 1989) based on equation (2). Dispersion factors by axial dispersion and film mass transfer resistance was included in the model. The model gave good prediction of the experimental data. Solute uptake was described as linear-solid film diffusion.

DeCarli (1990) also modeled continuous separation of a mixture of amino acids with a cation exchanger in the annular chromatograph. Elution was carried stepwise with different concentrations of NaOH solution. Continuity equations were developed for each of the solutes interacting with the cation exchanger (amino acids and sodium ion) and solved using finite difference method. It was found that the model was able to predict experimental data but with some variance in the edges of the peaks. Experimetnal data was more wide spread than predicted by the model. Fluid phase accumulation in the void space was neglected which resulted in NaOH breakthrough predicted earlier than observed experimentally. The diference in time was corrected by shifting the timeframe of the NaOH profile.

Bloomingburg and Carta (1994) modeled continuous separation of haemoglobin and BSA under conditions for adsorption of only haemoglobin onto the cation exchanger. Uptake equilibrium and kinetics was determined through batch experiments. The model incorporated uptake equilibrium using the Langmuir isotherm which is equivalent to equation (6),

$$\bar{q} = \frac{AC^*}{1 + BC^*} \tag{9}$$

where $\bar{q}$ the average concentration in the resin and C is is the mobilie phase concentration. A and B which are equivalent to $C_{RAmax}.K_A$ and K_A from equation (6) are adjusted to fit

experimental data. Solute concentration was calculated similar to equation (3) without the axial dispersion factor. Model produced reasonably accurate predictions for a range of flow rates, rotation speeds and NaCl concentrations.

2.10 Conclusion

Various chromatography technologies relating to the CRFC have been reviewed in this chapter which includes radial flow systems, annular bed systems and continuous systems. The four main radial flow configurations dicussed include fixed bed, thin layer, spinning disk or bed, and continuous chromatography.

Radial flow columns have several advantages over the more common axial flow columns, such as lower pressure drop and higher possible flow rates. It is highly suited for application with soft media and processes requiring faster separation cycles. This advantage would make the CRFC useful in the separation of biomolecules which have increased probability of degradation or denaturation over time. Continuous annular chromatography is suitable for all chromatographic separation techniques and adsorbent known for batch chromatography. The CRFC uses resin particles as the sorbent but other chromatography media may be applied such as monolithic media.

There are also limitations to radial flow systems due to its short bed depth and increase in fluid velocity through the media bed. Radial flow chromatography incorporates step elution which makes it more suited to large scale processes or initial separation stages where throughput is more important than column resolution.

Several problems were encountered with the first CRFC prototype. Broad and extended peaks were resulted from large feed chamber and short bed depth. The CRFC also faced flow obstruction and unpacking difficulty, and mechanical and construction limitations. The second CRFC was designed and built to solve problems found in the earlier prototype. It has been successfully applied to the extraction of BSA from a stock solution and in the separation of BSA and lactoferrin.

Modelling chromatography protein separations incorporates general equations for mass transfer by convection, dispersion, film diffusion and uptake into the resin. Several authors described models to experimental data comparisons with the liquid radial flow

and continuous annular bed chromatography. These models agreed well with experimental data and can be similarly applied to the CRFC to predict performance under different operational conditions and CRFC configuration.

.

Chapter 3: Modelling

3.1 Introduction

Mathematical modelling for axial flow chromatography and radial flow chromatography is discussed in this chapter. The models used are based on mass transfer by convection, dispersion, film diffusion, adsorption and desorption. Dispersion equations follow the Fick's first law of diffusion. In continuous radial flow, dispersion includes radial and angular dispersion while axial flow includes only axial dispersion. Film diffusion equation is included as the resin particles are porous. Solutes must pass through the stagnant zone surrounding the resin particle to transfer from solution phase to resin pore phase, and vice versa. The Langmuir-Fruendlich isotherm (MLF) is used to model ion exchange (adsorption and desorption) between solution in the resin pores and resin matrix.

The models are solved by Matlab using the finite difference method. In batch mode, concentration changes with axial position and time in an axial flow column. In a batch mode radial flow column, concentration changes with radial position and time. Continuous radial flow chromatography can be modelled in two dimensions as solute concentration with respect to radial position and time, or as a three dimensional model which accounts for radial position, angular position and time. Batch equations are converted to continuous equations following the method by Wankat (1977).

In the simulations carried out, the dispersion factor is omitted. Previous studies have shown that dispersion within the resin bed much less significant than dispersion in the tubings and additional parts of the chromatography system prior and after the chromatographic column such as pH meter, conductivity meter and UV spectrophotometer (Lay 2005). Simulations were restricted to the resin bed for axial flow chromatography. For the CRFC, flow through the resin bed as well as the inner and outer sintered walls were simulated.

3.2 Axial Flow Chromatography

An axial flow model was developed for a small column corresponding to the experimental work carried out on 1mL axial columns. Axial flow model allows more simplified and quick simulations than radial flow model as cross sectional area and fluid velocity do not change with bed height. Parameters of the axial mathematical model and comparative experimental work are set to simulate a section of the CRFC annulus.

3.2.1 Convection

Mass balance of an axial column section due to convection is given by

$$C_A|_{t+\Delta t}\, V_z\, \varepsilon_R = C_A|_t\, V_z\, \varepsilon_R + C_A|_z\, Q_z\, \Delta t - C_A|_{z+\Delta z}\, Q_z \Delta t \quad (10)$$

where C_A is solute A concentration in solution phase with respect to time t and axial position z, V_z is column section volume, ε_R is void fraction of the packed bed, Q_z is solution flow rate and Δt is change in time.

Equation (10) can be simplified to

$$\frac{C_A|_{t+\Delta t} - C_A|_t}{\Delta t} = \frac{z}{V_z\, \varepsilon_R}\left(C_A|_z - C_A|_{z+\Delta z}\right) \quad (11)$$

Volume of an axial column with height Δz and radius r_x is given by

$$V_z = \pi {r_x}^2 \Delta z \quad (12)$$

which is inserted into equation (11) to give

$$\frac{C_A|_{t+\Delta t} - C_A|_t}{\Delta t} = \frac{Q_z}{\pi {r_x}^2 \varepsilon_R} \frac{C_A|_z - C_A|_{z+\Delta z}}{\Delta z} \quad (13)$$

As velocity is

$$u_z = \frac{Q_z}{A_z} \tag{14}$$

and column cross sectional area is

$$A_z = \pi \, {r_x}^2 \tag{15}$$

solution flow rate is calculated as

$$Q_z = u_z \, \pi \, {r_x}^2 \tag{16}$$

When equation (16) is inserted into equation (13) and simplified, the equation becomes

$$\frac{C_A|_{t+\Delta t} \; - \; C_A|_t}{\Delta t} = \frac{u_z}{\varepsilon_R} \frac{C_A|_z \; - \; C_A|_{z+\Delta z}}{\Delta z} \tag{17}$$

As Δt and Δz approach zero, change in solute concentration with respect to time due to convection is then given by

$$\frac{\partial C_A}{\partial t} = \frac{u_z}{\varepsilon_R} \frac{\partial C_A}{\partial z} \tag{18}$$

3.2.2 Dispersion

Change in concentration due to axial dispersion follows the equation

$$C_A|_{t+\Delta t} \, V_z \, \varepsilon_R = C_A|_t \; V_z \, \varepsilon_R \; + J_{Az}|_z \, A_z \, \varepsilon_R \, \Delta t - J_{Az}|_{z+\Delta z} \, A_z \varepsilon_R \Delta t \tag{19}$$

where J_{Az} is flux of solute A through the packed bed void space with respect to axial position z, and can be simplified to

$$\frac{C_A|_{t+\Delta t} - C_A|_t}{\Delta t} = \frac{A_z}{V_z}(J_{Az}|_z - J_{Az}|_{z+\Delta z}) \quad (20)$$

Substituting equation (12) and (15) into equation (20) with further simplification then gives

$$\frac{C_A|_{t+\Delta t} - C_A|_t}{\Delta t} = \frac{J_{Az}|_z - J_{Az}|_{z+\Delta z}}{\Delta z} \quad (21)$$

As Δt and Δz approach zero, equation (21) becomes

$$\frac{\partial C_A}{\partial t} = \frac{\partial J_{Az}}{\partial z} \quad (22)$$

Following Fick's first law,

$$J_{Az} = D_{Az}\frac{\partial C_A}{\partial z} \quad (23)$$

Where D_{Az} is the axial dispersion coefficient given as

$$D_{Az} = y_2 2 r_p v \quad (24)$$

and velocity is

$$v = \frac{Q_z}{A_z} \quad (25)$$

Equation (22) then becomes

$$\frac{\partial C_A}{\partial t} = \frac{\partial}{\partial z}\left(D_{Az}\frac{\partial C_A}{\partial z}\right) \tag{26}$$

The dispersion coefficient for solute A, D_{Az} is dependent on velocity and velocity does not change with bed height of the axial flow column. Change in solute concentration due to axial dispersion with respect to time is then given by

$$\frac{\partial C_A}{\partial t} = D_{Az}\left(\frac{\partial^2 C_A}{\partial z^2}\right) \tag{27}$$

3.2.3 Film diffusion

In the solution flowing past the resin particles, change in solute concentration as solutes enter the resin pores is given by

$$C_A|_{t+\Delta t}\, V_z\, \varepsilon_R \;= C_A|_t V_z\, \varepsilon_R \;- J_A A_R \Delta t \tag{28}$$

where A_R is the total resin spherical surface area and J_A is diffusive flux of solute into the resin. Total resin surface area is given by

$$A_R \;= A_p\left(\frac{V_R}{V_p}\right) \tag{29}$$

where spherical surface area of a single resin particle with particle radius of r_p is

$$A_p \;= 4\pi {r_p}^2 \tag{30}$$

total resin volume is

$$V_R \;= (1 - \varepsilon_R)V_z \tag{31}$$

and volume of a single resin particle is

$$V_p = \frac{4}{3}\pi {r_p}^3 \tag{32}$$

Substituting equation (30), (31) and (32) into equation (29) then gives total resin surface area as

$$A_R = \frac{3V_x}{r_p}(1 - \varepsilon_R) \tag{33}$$

Diffusive flux of solute into the resin is given by

$$J_A = k_{fA}(C_A - C_{RPA}) \tag{34}$$

where k_{fA} is the film diffusion coefficient for solute A and C_{RPA} is the average concentration of solute A within the resin pores. Substituting equation (33) and (34) into equation (28) gives

$$C_A|_{t+\Delta t}\, V_z\, \varepsilon_R = C_A|_t\ V_z\, \varepsilon_R - k_{fA}(C_A - C_{RPA})\left(\frac{3V_z}{r_p}\right)(1 - \varepsilon_R)\, \Delta t \tag{35}$$

which is simplified to

$$\frac{C_A|_{t+\Delta t} - C_A|_t}{\Delta t} = -\frac{3k_{fa}(C_A - C_{RPA})\,(1 - \varepsilon_R)}{r_p \varepsilon_R} \tag{36}$$

As Δt approaches zero, equation (36) becomes

$$\frac{\partial C_A}{\partial t} = -\frac{3k_{fA}(C_A - C_{RPA})\,(1 - \varepsilon_R)}{r_p \varepsilon_R} \tag{37}$$

Volume in the resin pores is different from the volume in the void space. Change in solute concentration due to film diffusion within the resin pores is modelled by multiplying equation (37) with

$$-\frac{\varepsilon_R}{(1-\varepsilon_R)\,\varepsilon_p} \tag{38}$$

where ε_p is the resin pore fraction, thus giving

$$\frac{\partial C_{RPA}}{\partial t} = \frac{3k_{fA}(C_A - C_{RPA})}{r_p\,\varepsilon_p} \tag{39}$$

3.2.4 Adsorption/ desorption

Following the Langmuir isotherm, solute A concentration at equilibrium in the resin pores C_{RPA}* and resin matrix C_{RA}* is related by

$$C_{RA}{}^{*} = \frac{C_{RAmax}\ K_A C_{RPA}{}^{*}}{1 + K_A C_{RPA}{}^{*}} \tag{40}$$

where C_{RAmax} is the maximum capacity of the resin matrix and K_A is the equilibrium constant for solute A. As K_A is dependent on the forward binding rate k_{A1} and reverse binding rate k_{A2} following

$$K_A = \frac{k_{A1}}{k_{A2}} \tag{41}$$

substituting equation (41) into equation (40) gives

$$k_{A2} C_{RA}{}^{*} = k_{A1} C_{RPA}{}^{*}\,(C_{RAmax} - C_{RA}{}^{*}) \tag{42}$$

When the system is not at equilibrium, change in solute A concentration follows

$$C_{RPA}|_{t+\Delta t}\,V_z(1-\varepsilon_R)\varepsilon_p = C_{RPA}|_t\,V_z\,(1-\varepsilon_R)\varepsilon_p - k_{A1}C_{RPA}|_t(C_{RAmax} - C_{RA}|_t)V_z(1-\varepsilon_R)\varepsilon_p\Delta t + k_{A2}C_{RA}|_t V_z\,(1-\varepsilon_R)\varepsilon_p\Delta t \tag{43}$$

Equation (43) can be simplified to

$$\frac{C_{RPA}|_{t+\Delta t} - C_{RPA}|_t}{\Delta t} = -k_{A1} C_{RPA}|_t (C_{RAmax} - C_{RA}|_t) + k_{A2} C_{RA}|_t \quad (44)$$

As Δt approaches zero, equation (44) becomes

$$\frac{\partial C_{RPA}}{\partial t} = -k_{A1} C_{RPA} (C_{RAmax} - C_{RA}) + k_{A2} C_{RA} \quad (45)$$

In the resin matrix where solute concentration increases due to adsorption and decreases due to desorption, equation (45) is multiplied by -1 giving change in solute A concentration as

$$\frac{\partial C_{RA}}{\partial t} = k_{A1} C_{RPA} (C_{RAmax} - C_{RA}) - k_{A2} C_{RA} \quad (46)$$

Equation (46) could be corrected to account for pore volume and resin matrix volume differences to give the actual solute concentration on the matrix. However, as the resin matrix has many binding sites but very small volume, concentration ranges will be very high. For simplicity, concentration changes on the resin matrix will be remain with respect to resin pore volume and noted as such.

Langmuir-Freundlich isotherm can be used for multiple solute mixtures where solute competition for resin matrix occurs. At equilibrium, solute A concentration of a binary mixture follows

$$C_{RA}{}^{*} = \frac{C_{RAmax} K_A C_{RPA}{}^{*}}{1 + K_A C_{RPA} + K_B C_{RPB}} \quad (47)$$

where K_B and C_{RPB} are equilibrium constant and resin pore concentration of solute B respectively. When adsorption and desorption of solute A is not in equilibrium, change in solute A concentration in the presence of a competing solute in resin pore phase follows

$$\frac{\partial C_{RPA}}{\partial t} = \ -k_{A1} C_{RPA}\ (C_{RAmax\ -} C_{RA})\ + k_{A2}(1 + K_B C_{RPB}) C_{RA} \tag{48}$$

In the resin matrix phase, equation for change in solute A concentration follows

$$\frac{\partial C_{RA}}{\partial t} = \ k_{A1} C_{RPA}\ (C_{RAmax\ -} C_{RA}) - k_{A2}(1 + K_B C_{RPB}) C_{RA} \tag{49}$$

Similar to equation (46), change in matrix solute A concentration is with respect to resin pore volume and not actual matrix volume.

3.2.5 Final continuity equation

In solution phase, change in concentration of solute A is due to convection, axial dispersion and film diffusion. Final equation combines equations (18), (27) and (37) to give

$$\frac{\partial C_A}{\partial t} = \ \frac{u_z}{\varepsilon_R}\frac{\partial C_A}{\partial z} + D_{Az}\frac{\partial^2 C_A}{\partial z^2} - \frac{3k_{fA}(C_A - C_{RPA})\,(1 - \ \varepsilon_R)}{r_p \varepsilon_R} \tag{50}$$

Change in solute A concentration in resin pore phase combines film diffusion, adsorption and desorption which combines equations (39) and (45).

$$\frac{\partial C_{RPA}}{\partial t} = \frac{3k_{fA}(C_A - C_{RPA})}{r_p\ \varepsilon_p} - \ k_{A1} C_{RPA}\ (C_{RAmax\ -} C_{RA})\ + k_{A2} C_{RA} \tag{51}$$

Change in solute A concentration on the resin matrix is only due to adsorption and desorption which is equivalent to equation (46).

3.3 Radial Flow Chromatography

In an annular bed with solution flowing radially through the column, change in solute concentration involves changes due to convection, dispersion, film diffusion, adsorption and desorption.

CRFC can operate as a fixed bed or moving bed system. Fixed bed operation is equivalent to conventional batch mode operation with each section following a sequence of steps (loading, wash, elution, reequilibration). For fixed bed operation, solute concentration changes with radial position and time but is constant with angle.

Dispersion from solute concentration differences therefore occurs only in the radial direction.

In a moving bed or continuous mode, the annular bed rotates as solution enters from the feed chamber in the outer periphery. Each section can feed solution independent of each other, allowing all steps to be carried out simultaneously in a single system. Solute concentration changes with both angular position and radial position, and sections responsible for each step (loading, wash, elution, reequilibration). During steady state, solute concentration is independent of time.

3.3.1 Convection

Assuming that solute flow due to convection occurs only in the radial direction and not in the angular direction, change in solute A concentration in solution due to convection is given by

$$C_A|_{t+\Delta t}\, V_e\, \varepsilon_R = C_A|_t\, V_e\, \varepsilon_R + C_A|_r\, Q_e\, \Delta t - C_A|_{r-\Delta r}\, Q_e\, \Delta t \tag{52}$$

V_e is the volume of a section of the annulus given as

$$V_e = \pi r^2 H \frac{\Delta\theta}{\theta_{max}} - \pi(r-\Delta r)^2 H \left(\frac{\Delta\theta}{\theta_{max}}\right) \tag{53}$$

where r is the radius, H is the height, $\Delta\theta$ is the angle of the element and θ_{max} is the total angle of the annular bed. Assuming Δr^2 is negligible as Δr approaches zero, equation (53) can be simplified to

$$V_e = 2\pi r \Delta r H \left(\frac{\Delta\theta}{\theta_{max}}\right) \tag{54}$$

Q_e is flow rate through the element, given as

$$Q_e = Q_r \left(\frac{\Delta\theta}{\theta_{max}}\right) \tag{55}$$

where Q_r is the total flow rate through the annulus. Substituting equation (54) and (55) into equation (52) gives

$$\frac{C_A|_{t+\Delta t} - C_A|_t}{\Delta t} = \frac{Q_e\,(C_A|_r - C_A|_{r-\Delta r})}{2\pi r H \varepsilon_R\,\Delta r} \tag{56}$$

As Δt and Δr approach zero, equation (56) becomes

$$\frac{\partial C_A}{\partial t} = \frac{Q_e}{2\pi r H \varepsilon_R}\frac{\partial C_A}{\partial r} \tag{57}$$

3.3.2 Radial dispersion

When solution moves through the annular packed bed, the change in solute A concentration due to radial dispersion is given by

$$C_A|_{t+\Delta t}\,V_e\,\varepsilon_R = C_A|_t\,V_e\,\varepsilon_R + J_{Ar}|_r\,A_{re}|_r\,\varepsilon_R\,\Delta t - J_{Ar}|_{r-\Delta r}\,A_{re}|_{r-\Delta r}\,\varepsilon_R\,\Delta t \tag{58}$$

where J_{Ar} is the flux of solute A radially through the element and A_{re} is the area of the element. Equation (58) can then be simplified to

$$\frac{C_A|_{t+\Delta t} - C_A|_t}{\Delta t} = \frac{J_{Ar}|_r\,A_{re}|_r - J_{Ar}|_{r-\Delta r}\,A_{re}|_{r-\Delta r}}{V_e} \tag{59}$$

As area of the element at *r* is given by

$$A_{re}|_r = 2\pi r H\left(\frac{\Delta\theta}{\theta_{max}}\right) \tag{60}$$

and surface area of the element at *(r-Δr)* is

$$A_{re}|_{r-\Delta r} = 2\pi(r-\Delta r)H\left(\frac{\Delta\theta}{\theta_{max}}\right) \tag{61}$$

substituting equations (54), (60) and (61) into equation (59) gives

$$\frac{C_A|_{t+\Delta t} - C_A|_t}{\Delta t} = \frac{J_{Ar}|_r\,r - J_{Ar}|_{r-\Delta r}\,(r-\Delta r)}{r\Delta r} \tag{62}$$

As Δt and Δr approach zero, equation (62) becomes

$$\frac{\partial C_A}{\partial t} = \frac{1}{r}\frac{\partial (rJ_{Ar})}{\partial r} \tag{63}$$

Radial dispersion flux by Fick's first law of diffusion is given as (Gu 1991, Tsaur 1997)

$$J_{Ar} = D_{Ar}\frac{dC_A}{dr} \tag{64}$$

Substituting equation (62) into (61) gives

$$\frac{\partial C_A}{\partial t} = \frac{1}{r}\frac{\partial (rD_{Ar}\frac{\partial C_A}{\partial r})}{\partial r} \tag{65}$$

D_{Ar} is radial dispersion coefficient given by

$$D_{Ar} = y_2(2r_p)v \tag{66}$$

where y_2 is a constant of approximately 0.5 and v is interstitial velocity given by

$$v = \frac{Q_r}{2\pi r H \varepsilon_R} \tag{67}$$

Substituting equations (67) into (66) gives

$$D_{Ar} = y_2(2r_p)\frac{Q_r}{2\pi r H \varepsilon_R} \tag{68}$$

Let

$$y = rD_{Ar}\frac{\partial C_A}{\partial r} \tag{69}$$

and y can be derived from the product rule

$$\frac{\partial y}{\partial r} = \frac{\partial e}{\partial r}.f.g + e.\frac{\partial f}{\partial r}.g + e.f.\frac{\partial g}{\partial r} \tag{70}$$

Given that

$$e = r \tag{71}$$

$$f = D_{Ar} \tag{72}$$

and

$$g = \frac{\partial C_A}{\partial r} \tag{73}$$

then equation (70) becomes

$$\frac{\partial y}{\partial r} = D_{Ar} \frac{\partial C_A}{\partial r} + r \frac{\partial D_{Ar}}{\partial r} \frac{\partial C_A}{\partial r} + r D_{Ar} \frac{\partial^2 C_A}{\partial r^2} \tag{74}$$

Substituting equation (68) into (66) gives change in solute A concentration due to radial dispersion as

$$\frac{\partial C_A}{\partial t} = \frac{D_{Ar}}{r} \frac{\partial C_A}{\partial r} + \frac{\partial D_{Ar}}{\partial r} \frac{\partial C_A}{\partial r} + D_{Ar} \frac{\partial^2 C_A}{\partial r^2} \tag{75}$$

3.3.3 Angular dispersion

In batch mode, solute concentration is fixed at all angles so angular dispersion does not apply. In continuous mode however, solute concentration varies with angle of rotation so angular dispersion is included.

Change in solute A concentration due to angular dispersion is given by

$$C_A|_{t+\Delta t} V_e \varepsilon_R = C_A|_t V_e \varepsilon_R + J_{A\theta}|_\theta A_\theta \varepsilon_R \Delta t - J_{A\theta}|_{\theta+\Delta\theta} A_\theta \varepsilon_R \Delta t \tag{76}$$

where $J_{A\theta}$ is the flux of solute A at angle θ and A_θ is the cross sectional area given by

$$A_\theta = \Delta r H \tag{77}$$

Substituting equations (45) and (68) into equation (67) gives

$$C_A|_{t+\Delta t}\ 2\pi r\Delta rH\left(\frac{\Delta\theta}{\theta_{max}}\right)\varepsilon_R = C_A|_t\ 2\pi r\Delta rH\left(\frac{\Delta\theta}{\theta_{max}}\right)\varepsilon_R + J_{A\theta}|_\theta\ \Delta rH\varepsilon_R\Delta t - J_{A\theta}|_{\theta+\Delta\theta}\ \Delta rH\varepsilon_R\Delta t \tag{78}$$

which can be simplified to

$$\frac{C_A|_{t+\Delta t} - C_A|_t}{\Delta t} = \frac{J_{A\theta}|_\theta - J_{A\theta}|_{\theta+\Delta\theta}}{r\Delta\theta} \tag{79}$$

When Δt and Δr approach zero, equation (79) becomes

$$\frac{\partial C_A}{\partial t} = \frac{1}{r}\frac{\partial J_{A\theta}}{\partial\theta} \tag{80}$$

Angular dispersion flux according to Fick's first law is given by

$$J_{A\theta} = D_{A\theta}\ \frac{\partial C_A}{r\partial\theta} \tag{81}$$

Substituting equation (81) into equation (80) gives

$$\frac{\partial C_A}{\partial t} = \frac{1}{r}\frac{\partial\left(D_{A\theta}\ \frac{\partial C_A}{r\partial\theta}\right)}{\partial\theta} \tag{82}$$

Fluid velocity is constant with angular position so $D_{A\theta}$ is also independent of angular position. Equation (82) then becomes

$$\frac{\partial C_A}{\partial t} = \frac{D_{A\theta}}{r^2}\frac{\partial^2 C_A}{\partial\theta^2} \tag{83}$$

3.3.4 Film diffusion

Change in solute A concentration due to film diffusion for radial flow column, as with axial columns follows equation (37) for solution phase and equation (39) for resin pore phase.

3.3.5 Adsorption/ desorption

Adsorption and desorption equations for radial flow chromatography follows equation (45) for pore phase and equation (46) for matrix phase, and equations (48) and (49) for binary mixtures for pore and matrix phase respectively.

3.3.6 Final continuity equation

In batch mode where the annular bed is stationary, angular dispersion factor is not included in the final equation. Change in solute A concentration is due to convection radial dispersion and film diffusion, which combines equations (57), (75) and (37).

$$\frac{\partial C_A}{\partial t} = \frac{Q_e}{2\pi r H \varepsilon_R}\frac{\partial C_A}{\partial r} + \left(\frac{D_{Ar}}{r}\frac{\partial C_A}{\partial r} + \frac{\partial D_{Ar}}{\partial r}\frac{\partial C_A}{\partial r} + D_{Ar}\frac{\partial^2 C_A}{\partial r^2}\right) \qquad (84)$$

$$- \frac{3k_{fA}(C_A - C_{RPA})\,(1 - \varepsilon_R)}{r_p \varepsilon_R}$$

When the annular bed rotates, change of solute A concentration in solution is due to convection, radial dispersion, angular dispersion and film diffusion which is obtained by combining equations (57), (75), (83) and (37).

$$\frac{\partial C_A}{\partial t} = \frac{Q_e}{2\pi r H \varepsilon_R}\frac{\partial C_A}{\partial r} + \left(\frac{D_{Ar}}{r}\frac{\partial C_A}{\partial r} + \frac{\partial D_{Ar}}{\partial r}\frac{\partial C_A}{\partial r} + D_{Ar}\frac{\partial^2 C_A}{\partial r^2}\right) \qquad (85)$$

$$+ \frac{D_{A\theta}}{r^2}\frac{\partial^2 C_A}{\partial \theta^2} - \frac{3k_{fA}(C_A - C_{RPA})\,(1 - \varepsilon_R)}{r_p \varepsilon_R}$$

Final equations for pore phase change in solute A concentration which consists of film diffusion, adsorption and desorption equations combines equations (39) and (45).

$$\frac{dC_{RPA}}{dt} = \frac{3k_{fa}(C_A - C_{RPA})}{r_p\ \varepsilon_p} - k_{A1}C_{RPA}\,(C_{RAmax} - C_{RA}) + k_{A2}C_{RA} \qquad (86)$$

Matrix phase change in solute A concentration is equivalent to equation (46).

3.4 Finite Difference Models

Continuity equations from section 3.2 and 3.3 are solved using the finite difference method and modelled in Matlab. These models can be applied to batch mode, fixed bed or continuous flow chromatography for both axial and radial flow.

3.4.1 Fixed bed Axial Flow

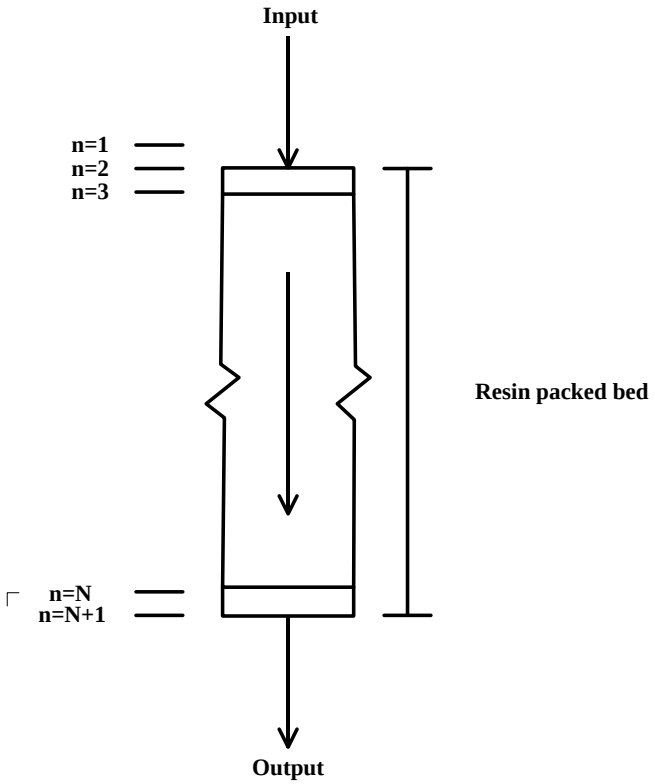

Figure 22. Column stages in an axial flow column.

In axial flow chromatography, the resin bed is divided into N stages following the fluid flow direction along the column axis where each stage simulates a single well mixed stirred tank (Figure 22).

The total number of stages which is rounded to the next integer is given as

$$N = \frac{L}{4d_p} \tag{87}$$

where L is the bed height and d_p is the diameter of a single resin particle. Height of a single stage is given by

$$\Delta z = \frac{L}{N} \tag{88}$$

Cross sectional area (A_x) follows equation (15).

Stage volume is given by

$$V_z = A_z \, \Delta z \tag{89}$$

Interstitial velocity is

$$v = \frac{Q_z}{A_z \, \varepsilon_R} \tag{90}$$

and change in time is

$$\Delta t = \frac{V_z \, \varepsilon_R}{Q_z \, J} \tag{91}$$

where J is the dividing factor, a dimensionless parameter for determining Δt.

Time taken for a single run is given by

$$t_{run} = \sum_{i=1}^{N_{steps}} \frac{V_i}{Q} \tag{92}$$

where N_{steps} is the number of steps in a run and V_i is the volume for ith step. A single run usually consists of the four steps: loading, wash, elution and reequilibration. Total time steps rounde to a whole integer is calculated as

$$M = \frac{t_{run}}{\Delta t} \tag{93}$$

Fixed bed axial flow is modeled in two dimensions of number of stages (n) and time steps (m). The boundary conditions for $1 < n \leq N+1$ and $m = 1$ are set as

$$C_A|_{n,m} = 0, C_{RPA}|_{n,m} = 0, C_{RA}|_{n,m} = 0 \tag{94}$$

An additional stage is included giving a total of N+1 stages to allow input to be set at starting point, n=1.

Solute concentration fed into the column at n=2 changes with time. Assuming that the column has been equilibrated with buffer solution, a typical four step run starts with loading where solution containing solute A is fed into the system. Next a wash step removes any unbound solute and is followed by elution where bound solute A is eluted. Reequilibration step then removes any salts and prepares the column for another chromatography separation.

Concentration of feed solution is set for stage n=1 for each step. As flow rate remains constant for all four steps, the duration of each step can be set based on the volume of input solution (Table 1).

Table 1. Time allocation and input concentration for each step

Step	Volume (mL)	End of step (s)	Step duration (s)	Input solute concentration
Loading	V_1	$t_1 = \frac{V_1}{Q_z}$	$0 < t\|_m \leq t_1$	$C_A\|_{n=1,m} = C_{feed}$ $C_B\|_{n=1,m} = 0$
Wash	V_2	$t_2 = \frac{V_2}{Q_z} + t_1$	$t_1 < t\|_m \leq t_2$	$C_A\|_{n=1,m} = 0$ $C_B\|_{n=1,m} = 0$
Elution	V_3	$t_3 = \frac{V_3}{Q_z} + t_2$	$t_2 < t\|_m \leq t_3$	$C_A\|_{n=1,m} = 0$ $C_B\|_{n=1,m} = C_{elution}$
Reequilibration	V_4	$t_3 = \frac{V_3}{Q_z} + t_2$	$t_3 < t\|_m \leq t_4$	$C_A\|_{n=1,m} = 0$ $C_B\|_{n=1,m} = 0$

Final equation for solute concentration in solution is given as the sum of change in solute concentration due to convection, axial dispersion and film diffusion.

$$C_A|_{n,m} = C_A|_{n,m-1} + \Delta C_{A\ Convection}\ |_{n,m} + \Delta C_{A\ Axial\ \ Dispersion}\ \Big|_{n,m} + \Delta C_{A\ Film\ \ Diffusion}\ \Big|_{n,m} \quad (95)$$

In the resin pores, solute concentration is the total change in concentration due to film diffusion, adsorption and desorption

$$C_{RPA}|_{n,m} = C_{RPA}|_{n,m-1} + \Delta C_{RPA\ Film\ \ Diffusion}\ \Big|_{n,m} + \Delta C_{RPA\ Adsorption\ \ /Desorption}\ \Big|_{n,m} \quad (96)$$

Solute concentration on the matrix is based only on solute exchange between the resin pores and resin matrix

$$C_{RA}|_{n,m} = C_{RA}|_{n,m-1} + \Delta C_{RA\ Adsorption\ \ /Desorption}\ \Big|_{n,m} \quad (97)$$

From the final equations, solute concentration in the void phase of the resin bed, pores of the resin and bound onto the resin matrix for each stage and time step can then be calculated for $1 < n \leq N+1$ and $1 < m \leq M+1$

Convection is follows equation (10)

$$\Delta C_{A\ Convection}\ |_{n,m} = \frac{\left(C_A|_{n-1,m-1} - C_A|_{n,m-1}\right) Q_z \Delta t}{V_z\ \varepsilon_R} \quad (98)$$

Axial dispersion is given by equation (19)

$$\Delta C_{A\ Axial\ \ Dispersion}\ \Big|_{n,m} = \frac{\left(J_{Az}|_{n-1,m-1} - J_{Az}|_{n,m-1}\right) A_z\ \Delta t}{V_z} \quad (99)$$

Flux and dispersion coefficient for solute A is given by equations (23) and (24) respectively while column cross sectional area follows equation (15). Substituting

equations (15), (23) and (24) into equation (101) gives

$$\Delta C_{A\ Axial\ \ Dispersion}\ \Big|_{n,m} = \frac{y_2\ 2r_p\ Q_z\ \Delta t}{V_z\ \varepsilon_R\ \Delta z}\Big(\big(C_A|_{n-1,m-1} - C_A|_{n,m-1}\big) - \big(C_A|_{n,m-1} - C_A|_{n+1,m-1}\big)\Big) \quad (100)$$

Film diffusion follows equation (35), giving change in solute concentration in solution as

$$\Delta C_{A\ Film\ \ Diffusion}\ \Big|_{n,m} = \frac{-3k_{fA}(C_A|_{n,m-1} - C_{RPA}|_{n,m-1})(1 - \varepsilon_R)\ \Delta t}{r_p\ \varepsilon_R} \quad (101)$$

Within the resin pores, change in solute concentration by film diffusion follows equation (37),

$$\Delta C_{RPA\ Film\ \ Diffusion}\ \Big|_{n,m} = \frac{3k_{fA}(C_A|_{n,m-1} - C_{RPA}|_{n,m-1})\Delta t}{r_p\ \varepsilon_p} \quad (102)$$

Solute adsorption and desorption between resin pores and resin matrix follows equation (45) for change in solute concentration in the resin pores

$$\Delta C_{RPA\ Adsorption\ /Desorption}\ \Big|_{n,m} = -k_{A1}C_{RPA}|_{n,m-1}\left(C_{RAmax} - C_{RA}|_{n,m-1}\right) + k_{A2}C_{RA}|_{n,m-1} \quad (103)$$

and equation (46) for change in solute concentration on the resin matrix. Matrix solute concentration changes are not calculated as actual concentration but as mass changes with respect to resin pore volume following

$$\Delta C_{RA\ Adsorption\ /Desorption}\ \Big|_{n,m} = k_{A1}C_{RPA}|_{n,m-1}\left(C_{RAmax} - C_{RA}|_{n,m-1}\right) - k_{A2}C_{RA}|_{n,m-1} \quad (104)$$

In the presence of solute B which competes with solute A for adsorption onto the resin

matrix, change in resin pore solute concentration due to adsorption and desorption follows equation (48).

$$\Delta C_{RPA\ Adsorption\ /Desorption}\Big|_{n,m} = -k_{A1} C_{RPA}|_{n,m-1}(C_{RAmax} - C_{RA}|_{n,m-1}) + k_{A2}(1 + K_B C_{RPB}|_{n,m-1}) C_{RA}|_{n,m-1} \quad (105)$$

and follows equation (49) on the matrix

$$\Delta C_{RA\ Adsorption\ /Desorption}\Big|_{n,m} = k_{A1} C_{RPA}|_{n,m-1}\left(C_{RAmax} - C_{RA}|_{n,m-1}\right) - k_{A2}(1 + K_B C_{RPB}|_{n,m-1}) C_{RA}|_{n,m-1} \quad (106)$$

Substituting equations (98), (100) and (101) into equation (95) gives solute A concentration in solution in the void fraction as

$$C_A|_{n,m} = C_A|_{n,m-1} + \frac{\left(C_A|_{n-1,m-1} - C_A|_{n,m-1}\right) Q_z \Delta t}{V_z\ \varepsilon_R} + \frac{y_2\ 2r_p\ Q_z\ \Delta t}{V_z\ \varepsilon_R\ \Delta z}\left(\left(C_A|_{n-1,m-1} - C_A|_{n,m-1}\right) - \left(C_A|_{n,m-1} - C_A|_{n+1,m-1}\right)\right) - \frac{3k_{fA}(C_A|_{n,m-1} - C_{RPA}|_{n,m-1})(1 - \varepsilon_R)\,\Delta t}{r_p\ \varepsilon_R} \quad (107)$$

For separations where solute B is applied to elute any solute A which are bound to the resin matrix, substituting equations (102) and (105) into equation (96) gives solute A concentration in the resin pores as

$$C_{RPA}|_{n,m} = C_{RPA}|_{n,m-1} + \frac{3k_{fA}\left(C_A|_{n,m-1} - C_{RPA}|_{n,m-1}\right)\Delta t}{r_p\ \varepsilon_p} - k_{A1} C_{RPA}|_{n,m-1}\left(C_{RAmax} - C_{RA}|_{n,m-1}\right) + k_{A2}(1 + K_B C_{RPB}|_{n,m-1}) C_{RA}|_{n,m-1} \quad (108)$$

Substituting equations (106) into equation (97) gives solute A concentration on the resin matrix as

$$C_{RA}|_{n,m} = C_{RA}|_{n,m-1} + k_{A1}C_{RPA}|_{n,m-1}\left(C_{RAmax} - C_{RA}|_{n,m-1}\right) \quad (109)$$

$$-k_{A2}(1 + K_B C_{RPB}|_{n,m-1})C_{RA}|_{n,m-1}$$

In the application of multicomponent solutions, concentrations of other proteins can be similarly calculated from the above equations. The amount of solute bound to the resin matrix, $C_{RA}|_{\mathrm{n,m-1}}$ in the adsorption equations will then be the amount of all solutes bound to the resin matrix. Desorption equations are adjusted to account for competition between all solutes for the matrix, similar to equation (105) and (106).

Different types of protein are assumed to compete with each other for the ion exchanger binding sites. Salt ions will also compete with the proteins for the binding sites. In the calculation for salt ion concentration however, the competition factor is excluded. It is assumed that salt concentration on the resin matrix is unaffected by the presence of proteins and the salt ions are much smaller and present in larger molar concentrations than proteins.

3.4.2 Fixed bed Radial Flow Chromatography

In the CRFC, fluid flows from the outer feed chamber through the outer sintered steel walls, resin bed, inner sintered steels walls and exit through the inner exit chambers. The CRFC model accounts for changes in solute concentration in the annular bed, outer sintered wall and inner sintered wall. As with the axial flow model, the CRFC model is divided into volumetric stages with each stage simulating a well mixed tank.

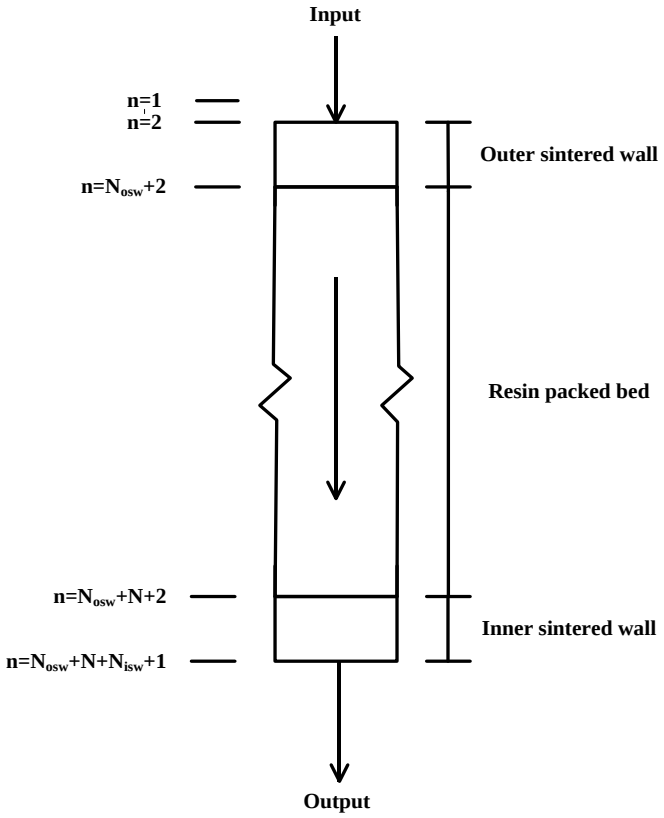

Figure 23. Column stages in the CRFC.

Maximum number of stages in the annular resin bed, rounded to the next integer is given as

$$N_{max} = \frac{r_1 - r_2}{4\, d_p} \tag{110}$$

where r_1 is the outer radius and r_2 is the inner radius of the annulus. Change in radius for a single stage in an annular bed with N number of stages is given by

$$\Delta r = \frac{r_1 - r_2}{N} \tag{111}$$

Number of stages in the outer and inner sintered walls is set as N_{osw} and N_{isw}, giving change in radius of the outer sintered wall as

$$\Delta r_{osw} = \frac{T_{osw}}{N_{osw}} \tag{112}$$

and change in radius of the inner sintered wall as

$$\Delta r_{isw} = \frac{T_{isw}}{N_{isw}} \tag{113}$$

where T_{osw} is thickness of the outer sintered wall and T_{isw} is thickness of the inner sintered wall.

Outer sintered wall, resin bed and inner sintered wall is restricted to stages $1 < n \leq N_{osw}+1$, $N_{osw}+1 < n \leq N_{osw}+N+1$ and $N_{osw}+N+1 < n \leq N_{osw}+N+ N_{isw}+1$ respectively. Radius with respect to stage number in the outer sintered wall is given by

$$r|_n = r_1 + T_{osw} - (n-1)\Delta r_{osw} \tag{114}$$

radius in the resin bed is

$$r|_n = r_1 - (n - N_{osw} - 1)\Delta r \tag{115}$$

and radius in inner sintered wall is

$$r|_n = r_2 - (n - N_{osw} - N - 1)\Delta r_{isw} \tag{116}$$

Volume of a segment of the annulus follows equation (45) which gives stage volume for outer sintered wall as

$$V_e|_n = \pi\left(r|_{n-1}{}^2 - r|_n{}^2\right) H\, \varepsilon_{osw} \tag{117}$$

resin bed as

$$V_e|_n = \pi\left(r|_{n-1}{}^2 - r|_n{}^2\right) H\ \varepsilon_R \tag{118}$$

and inner sintered wall as

$$V_e|_n = \pi\left(r|_{n-1}{}^2 - r|_n{}^2\right) H\ \varepsilon_{isw} \tag{119}$$

Change in time is from one time step to the next is based on the solution residence time through the smallest stage of the annular bed.

$$\Delta t\ =\ \frac{V_e|_{(N_{osw}+N)}\ \varepsilon_R}{Q_r\ J} \tag{120}$$

Time taken for a single run and total number of time steps follows equations (92) and (93) respectively.

Boundary conditions for $1< n \leq N_{osw}+N+ N_{isw} +1$ and $m = 1$ are set as

$$C_A|_{n,m}\ =\ 0, C_{RPA}|_{n,m}\ =\ 0, C_{RA}|_{n,m}\ =\ 0 \tag{121}$$

Concentration of feed solution for stage n=1 is set for each step (loading, wash, elution, reequilibration) is applied according to Table 1.

Outer and inner sintered walls do not contain resin particles and therefore is assumed to not involve film diffusion and adsorption. Solute concentration within the sintered walls is modeled solely based on change in concentration due to convection.

$$C_A|_{n,m}\ =\ C_A|_{n,m-1} + \Delta C_{A\ Convection}\ |_{n,m} \tag{122}$$

Change in concentration due by convection follows equation (48). Therefore change in solute concentration in stages $1 < n \leq N_{osw} +1$ for the outer wall is given by

$$\Delta C_{A\ Convection}\ |_{n,m} = \frac{\left(C_A|_{n-1,m-1}\ - C_A|_{n,m-1}\right) Q_r \Delta t}{V_e|_{\mathrm{n}}\ \varepsilon_{osw}} \tag{123}$$

and in stages $N_{osw}+N +1 < n \leq N_{osw}+N + N_{isw} +1$ for the inner wall as

$$\Delta C_{A\ Convection}\ |_{n,m} = \frac{\left(C_A|_{n-1,m-1} - C_A|_{n,m-1}\right) Q_r \Delta t}{V_e|_{\mathrm{n}}\ \varepsilon_{osw}} \tag{124}$$

Equation (122) is then converted to

$$C_A|_{n,m} = C_A|_{n,m-1} + \frac{\left(C_A|_{n-1,m-1} - C_A|_{n,m-1}\right) Q_r \Delta t}{V_e|_{\mathrm{n}}\ \varepsilon_{osw}} \tag{125}$$

for the outer sintered wall solute concentration and

$$C_A|_{n,m} = C_A|_{n,m-1} + \frac{\left(C_A|_{n-1,m-1} - C_A|_{n,m-1}\right) Q_r \Delta t}{V_e|_{\mathrm{n}}\ \varepsilon_{isw}} \tag{126}$$

for inner sintered wall solute concentration.

In the annular bed consisting of stages $N_{osw}+1 < n \leq N_{osw}+N+1$, final equation for solute concentration in solution is the total change due to convection, radial dispersion and film diffusion.

$$C_A|_{n,m} = C_A|_{n,m-1} + \Delta C_{A\ Convection}\ |_{n,m} + \Delta C_{A\ Radial\ \ dispersion}\ \Big|_{n,m} + \Delta C_{A\ FIlm\ \ diffus\ ion}\Big|_{n,m} \tag{127}$$

In the resin pores, solute concentration is the total change in concentration due to film diffusion, adsorption and desorption which is equivalent to equation (96).

Solute concentration on the matrix is due to solute exchange between the resin pores and resin matrix, given by equation (97).

Change in solute concentration due to convection in the resin bed follows equation (57)

$$\Delta C_{A\ Convection}\ |_{n,m} = \frac{\left(C_A|_{n-1,m-1} - C_A|_{n,m-1}\right) Q_r \Delta t}{V_e|_{\mathrm{n}}\ \varepsilon_R} \tag{128}$$

Change in solute concentration by radial dispersion is given by equation (56)

$$\Delta C_{A\ Radial\ \ dispersion}\ \Big|_{n,m} = \frac{\left(J_{Ar}|_{n-1,m-1}\ A_{re}|_{n-1,m-1} - J_{Ar}|_{n,m-1} A_{re}|_{n,m-1}\ \right)\Delta t}{V_e|_n} \quad (129)$$

Substituting equation (64), (66) and (67) into equation (126) gives

$$\Delta C_{A\ Radial\ \ dispersion}\ \Big|_{n,m} \quad (130)$$
$$= \frac{y_2\ 2r_p\ Q_r\ \Delta t}{V_e|_n\ \varepsilon_R \Delta r}\left(C_A|_{n-1,m-1} -\ 2C_A|_{n,m-1} + C_A|_{n+1,m-1}\right)$$

Film diffusion, adsorption and desorption equations for fixed bed radial flow is equivalent to equations (37), (39), (48) and (49).

Solute A concentration in the void fraction is calculated as

$$C_A|_{n,m}\ =\ C_A|_{n,m-1} + \frac{\left(C_A|_{n-1,m-1} - C_A|_{n,m-1}\right)Q_r \Delta t}{V_e|_{\mathrm{n}}\ \varepsilon_R} \quad (131)$$

$$+ \frac{y_2\ 2r_p\ Q_r\ \Delta t}{V_e|_n\ \varepsilon_R \Delta r}\left(C_A|_{n-1,m-1} -\ 2C_A|_{n,m-1} + C_A|_{n+1,m-1}\right)$$

$$- \frac{3k_{fA}(C_A|_{n,m-1} - C_{RPA}|_{n,m-1})(1 -\ \varepsilon_R)\ \Delta t}{r_p \varepsilon_R}$$

Similar to axial flow chromatography, solute A concentration in the resin pores and resin matrix is given by equations (108) and (109).

3.5 Continuous Mode

The CRFC annular bed can be rotated along its axis, allowing continuous operation where solution from each step is fed independently through different ports. There are two ways of modeling the CRFC in continuous mode. The first method models a thin section of the packed bed in two dimensions of radial position and time. Angular dispersion is assume to be negligible and excluded from the model, or calculated as part of the radial dispersion. The alternative method calculates both angular dispersion and radial dispersion. The resin bed is divided into both radial stages and angular stages, giving solute concentrations with respect to radial position, angular position and time.

3.5.1 Two dimensional CRFC

In the two dimensional model, the thin section is fed solutions following the sequence of steps (loading, wash, elution and reequilibration) at different angles of the annulus as the bed rotates. The sequence of steps is repeated when the annular bed completes a 360° turn. Duration of each step is dependent on the sections allocated for each step and the rotation speed of the annular bed. Elution profiles are obtained as solute concentration with respect to angular position of the exit chamber.

Similar to fixed bed CRFC, the outer sintered wall, resin bed and inner sintered wall are divided into radial stages, represented by N_{osw}, N and N_{isw} respectively. In addition to radial stages, the CRFC is also divided into angular stages N_a.

Stage volume of the annulus follows equation (54), giving stage volume of the outer sintered wall, resin bed and inner sintered wall as equations (117), (118) and (119) respectively. When corrected to the size of a single annular segment stage volume of outer sintered wall is calculated as

$$V_e|_n = \frac{\pi\left(r|_{n-1}{}^2 - r|_n{}^2\right)H\ \varepsilon_{osw}}{N_a} \tag{132}$$

resin bed

$$V_e|_n = \frac{\pi\left(r|_{n-1}{}^2 - r|_n{}^2\right)H\ \varepsilon_R}{N_a} \tag{133}$$

and inner sintered wall

$$V_e|_n = \frac{\pi\left(r|_{n-1}{}^2 - r|_n{}^2\right)H\ \ \varepsilon_{isw}}{N_a} \tag{134}$$

Solution flow rate for each segment is calculated as

$$Q_e = \frac{Q_r}{N_a} \tag{135}$$

Time change between time steps which is based on the residence time through the smallest stage in a segment of the resin bed calculated as

$$\Delta t\ =\ \ \frac{V_e|_{N_{osw}+N}\ \ \varepsilon_R}{Q_e\ J} \tag{136}$$

Change in time can also be calculated based on rotation speed

$$\Delta t\ =\ \ \frac{360}{w\ M_{\ rev}} \tag{137}$$

where rotation speed of the annulus follows

$$w\ =\ \ \frac{360}{t_{rev}} \tag{138}$$

and number of steps per revolution for D number of annular sections with M_{sec} number of steps for each section

$$M_{\ rev}\ = M_{sec}\ D \tag{139}$$

Number of steps per run

$$M_{\ run}\ = M_{\ rev}\ N_{\ rev} \tag{140}$$

where N_{rev} is the number of revolution for the duration of M_{run} time.

Total rotated angle is given by

$$\phi|_m = (m-1)w\,\Delta t \tag{141}$$

where m is the rotation step.

Angular position of the thin segment modeled is given by

$$\phi_p\big|_m = 360\left(0.5 + \alpha\, tan\left(\frac{tan\left(\frac{\phi|_m}{360}\pi + \frac{\pi}{2}\right)}{\pi}\right)\right) \tag{142}$$

In fixed bed operation, solute concentration of the feed solution is allocated based on time as all sections of the annulus simultaneously go through each step. In a rotating bed however, feed solution concentration applied is dependent on angular position as each step is allocated to a number of individual sections.

The CRFC annular bed is divided into eight sections of equal volume, each with individual feed and exit chamber. Input solution for all steps in a complete protein separation run, can be allocated specific number of sections (Table 2).

Table 2. Feed concentrations at *n*=1 with respect to angular position and feed sections.

Step	Feed sections	Feed sections (degrees)	Input solute concentration
Loading	1	$0 < \phi_p\big\|_{\mathrm{m}} \leq 45$	$C_A|_{n=1,m} = C_{feed}$ $C_B|_{n=1,m} = 0$
Wash	2-4	$45 < \phi_p\big\|_{\mathrm{m}} \leq 180$	$C_A|_{n=1,m} = 0$ $C_B|_{n=1,m} = 0$
Elution	5	$180 < \phi_p\big\|_{\mathrm{m}} \leq 225$	$C_A|_{n=1,m} = 0$ $C_B|_{n=1,m} = C_{elution}$
Reequilibration	6-8	$225 < \phi_p\big\|_{\mathrm{m}} \leq 360$	$C_A|_{n=1,m} = 0$ $C_B|_{n=1,m} = 0$

Equations presented for fixed bed operation of CRFC are modified to convert volume and flow rate to correspond to the thin section of the rotating annulus.

For $1 < n \leq N_{osw}+N+ N_{isw} +1$ and $m = 1$, solute concentration is first set to zero

$$C_A|n,m = 0,\ C_{RPA}|n,m = 0,\ C_{RA}|n,m = 0 \tag{143}$$

Change in solute concentration for $1 < m \leq M +1$ in stages $1 < n \leq N_{osw} +1$ for the outer wall is given by

$$C_A|_{n,m} = C_A|_{n,m-1} + \frac{\left(C_A|_{n-1,m-1} - C_A|_{n,m-1}\right)Q_e \Delta t}{V_e|_n\ \varepsilon_{osw}} \tag{144}$$

and $N_{osw}+N +1 < n \leq N_{osw}+N + N_{isw} +1$ for the inner wall as

$$C_A|_{n,m} = C_A|_{n,m-1} + \frac{\left(C_A|_{n-1,m-1} - C_A|_{n,m-1}\right)Q_e \Delta t}{V_e|_n\ \varepsilon_{isw}} \tag{145}$$

In stages $N_{osw}+1 <n \leq N_{osw}+N+1$, solute concentration in solution is given by

$$C_A|_{n,m} = C_A|_{n,m-1} + \frac{\left(C_A|_{n-1,m-1} - C_A|_{n,m-1}\right)Q_e \Delta t}{V_e|_n\ \varepsilon_R} \tag{146}$$

$$+\frac{y_2\ 2r_p\ Q_e\ \Delta t}{V_e|_n\ \varepsilon_R \Delta r}\left(C_A|_{n-1,m-1} - 2C_A|_{n,m-1} + C_A|_{n+1,m-1}\right)$$

$$- \frac{3k_{fA}(C_A|_{n,m-1} - C_{RPA}|_{n,m-1})(1 - \varepsilon_R)\ \Delta t}{r_p \varepsilon_R}$$

Segment volume and flow rate does not affect calculations for change in solute concentration due to film diffusion and ion exchange. Solute concentration in resin pores and resin matrix remains equivalent to equations (108) and (119).

Solution exiting the CRFC is collected through individual output ports connected to each exit chamber. Calculating solute concentration of the smallest stage of the annular bed as the average solute concentration exiting each section gives solute concentration corresponding to the output solution collected. Assuming steady steady is achieved within one revolution of the annulus, solute concentration with respect to angular

position after the first revolution will be constant regardless of time.

Time step per revolution which is rounded to the next positive integer can be calculated as

$$M_{rev} = \frac{t_{rev}}{\Delta t} \tag{147}$$

From equation (139), time steps per section is calculated as

$$M_{sec} = \frac{M_{rev}}{D} \tag{148}$$

Time step at which output solution is collected is given by

$$m_{col} = (N_{rev} - 1)M_{rev} \tag{149}$$

For annular sections $1 \leq d \leq \mathrm{D}$, the start of a section in terms of time steps is given by

$$m_{sec1}|_d = m_{col} + (d-1)\, M_{sec} \tag{150}$$

and the time step at the end of the section is given by

$$m_{sec2}|_d = m_{col} + d\, M_{sec} \tag{151}$$

Average solute concentration exiting each section is calculated as

$$C_{outA}|_d = \frac{\sum_{m=m_{sec1}|_d}^{m=m_{sec2}|_d} C_A|_{(n=Nosw+N+Nisw+1),m}}{M_{sec}} \tag{152}$$

3.5.2 Continuous Axial flow

Verification of the model was carried out on a 1mL DEAE sepharose FF column. The use of a small axial column to simulate a section of the annulus of the CRFC allows the ease of obtaining large amount of experimental data in a shorter amount of time and using smaller amounts of solution. There is also lower risk of problems such as packing difficulty, uneven flow rates and backflow.

Batch axial flow model is converted to a continuous model using equations similar to equations (141)and (142). Amount of time is given by

$$t_x|_m \ = (m-1)\,\Delta t \tag{153}$$

Time at any time step follows

$$t_{xc}|_m \ = \ t_{cycle}\left(0.5 \ + \alpha\, tan\left(\frac{tan\left(\frac{t_x|_m}{t_{cycle}}\pi \ + \ \frac{\pi}{2}\right)}{\pi}\right)\right) \tag{154}$$

where t_{cycle} is the time required for a complete sequence of steps from the start of the loading step until the end of the reequilibration step. Equation (154) allows a single axial flow chromatography run to be repeated continuously.

Results from the continuous axial flow model can be used to represent the CRFC in continuous mode with amount of time in equation (153) equivalent to total rotated angle in equation (141) and specific time in equation (154) equivalent to angular position in equation (142).

Time spent by a single annular section at each feed chamber follows

$$t_D = \ \frac{t_{rev}}{D} \tag{155}$$

such that CRFC operating with a rotating annulus of $w_= 360°/\text{hour}$ and t_{rev}=60 minutes would require 7.5 minutes for a section to pass each feed chamber. Converting the feed concentrations at *n*=1 with respect to angular position and feed sections as allocated to the CRFC according to Table 2 to time allocations for an axial column

would give Table 3.

Table 3. Time allocation representing CRFC in continuous mode

Step	End of step (min)	Step duration (min)	Input solute concentration
Loading	$t_{1=}\ t_D$	$0 < t\|_m \leq t_1$	$C_A\|_{n=1,m} = C_{feed}$ $C_B\|_{n=1,m} = 0$
Wash	$t_{2=}\ 5t_D$	$t_1 < t\|_m \leq t_2$	$C_A\|_{n=1,m} = 0$ $C_B\|_{n=1,m} = 0$
Elution	$t_{3=}\ 6t_D$	$t_2 < t\|_m \leq t_3$	$C_A\|_{n=1,m} = 0$ $C_B\|_{n=1,m} = C_{elution}$
Reequilibration	$t_{4=}\ 8t_D$	$t_3 < t\|_m \leq t_4$	$C_A\|_{n=1,m} = 0$ $C_B\|_{n=1,m} = 0$

3.6 Conclusion

Finite difference method was used to solve the chromatography models in an axial flow column and the CRFC in batch and continuous operation. Simulated data obtained can be used to analyse protein separation in the CRFC and allow model revision for better prediction.

Chapter 4: Methodology

4.1 Introduction

Reagents, equipment and experimental methods used are presented in this chapter.

Experiments were carried out on small axial flow ion exchange columns to mimic continuous separation in the CRFC in a range of loading volumes, elution buffer volumes, protein feed concentration, elution buffer concentration, flow rates and CRFC rotation speeds. Rotation speeds of the CRFC annulus was mimicked by adjusting the duration of each step corresponding to the time spent by an annular section at a single input port.

BSA elution profiles obtained were analyzed and used to validate the mathematical models presented in Chapter 3. Simulated data was compared to experimental data by adjusting parameters to obtain a best fit curve.

4.2 Reagents

The following reagents were used:

- Loading sample:
    - Bovine Serum Albumin (fraction V, low endotoxin; Life Technologies) in equilibration buffer
- Equilibration buffer: Tris-(hydroxymethyl)-aminomethane (AppliChem GmbH) 0.02M, pH7
- Elution buffer: 1M NaCl (University of Waikato) in equilibration buffer
- Regeneration solution: 1M NaOH (AppliChem) and 1M NaCl (University of Waikato)
- Storage solution: 20% V/V Ethanol, analytical grade (Ajax FineChem)
- Bradford reagent (Sigma-Aldrich)

Loading sample, regeneration solution and storage solution were contained in 250mL or 500mL Schott bottles. Equilibration buffer and elution buffer were made up in 2L Schott bottles. Distilled water was used in all solutions.

All solutions except loading sample were degassed with Helium for 5 minutes

immediately after preparation. Equilibration buffer and elution buffer were degassed periodically or as required between experimental runs. In the preparation of BSA feed solution, equilibration buffer was degassed prior to dissolving BSA. Solution pH was achieved by adding 1M hydrochloric acid (AppliChem) dropwise with continuous stirring.

Experiments were carried out at room temperature. Loading sample and Bradford reagent was kept at 4°C when not in use.

4.3 Equipment

The following equipments were used:

- Automated liquid chromatography system: AKTA FPLC (GE Healthcare, Uppsala, Sweden)
- Axial flow column: HiTrap DEAE Fast Flow anion exchange column (GE Healthcare, Uppsala, Sweden) (Appendix A)
- Cyberscan Con 100 (Alphatech Systems, Auckland, New Zealand)
- Inline spectrophotometer (GE Healthcare, Uppsala, Sweden)
- Offline spectrophotometer (GE Healthcare, Uppsala, Sweden)
- pH meter
- Pressure gauge
- Schott bottles, volumetric flasks, measuring cylinders, test tubes, cuvettes, beakers, pipettes, filters, syringes,

4.4 Experimental Methods

4.4.1 AKTA set up

AKTA FPLC (Figure 24) is computer operated using Unicorn software. Experiments are run following the programmed methods (Appendix C). Data from each run is saved in the computer and can be exported. The Unicorn software provides functions such as peak analysis and comparison.

Two different solutions can be supplied at a time to the column through two separate pumps. Both step and gradient change in elution buffer concentration is possible through the control in volume ratio of the solutions which is pumped into a 2 mL mixer. From the mixer, solution is filtered before entering the injection valve.

Sample is supplied from a 50 mL graduated glass syringe (Superloop) which is filled by manually injecting solution through a port in the injection valve using a 10mL syringe. In loading position (Figure 25A), superloop is disconnected from the solution pumps and column. When in inject position (Figure 25B), solution is pumped into the top of the superloop which pushes the plunger downwards, forcing the sample out of the superloop and directed into the column or out as waste.

Solution flowing out of the column passes through the inline UV spectrophotometer and conductivity meter before exiting the system through the outlet valve. Solution from the outlet valve can be directed to the fraction collector or waste container. Tubings (0.5 mm I.D.) connecting the different parts of the system (superloop, valves, column, filter, detectors) are detachable and allows change in fluid pathway through the various valve ports.

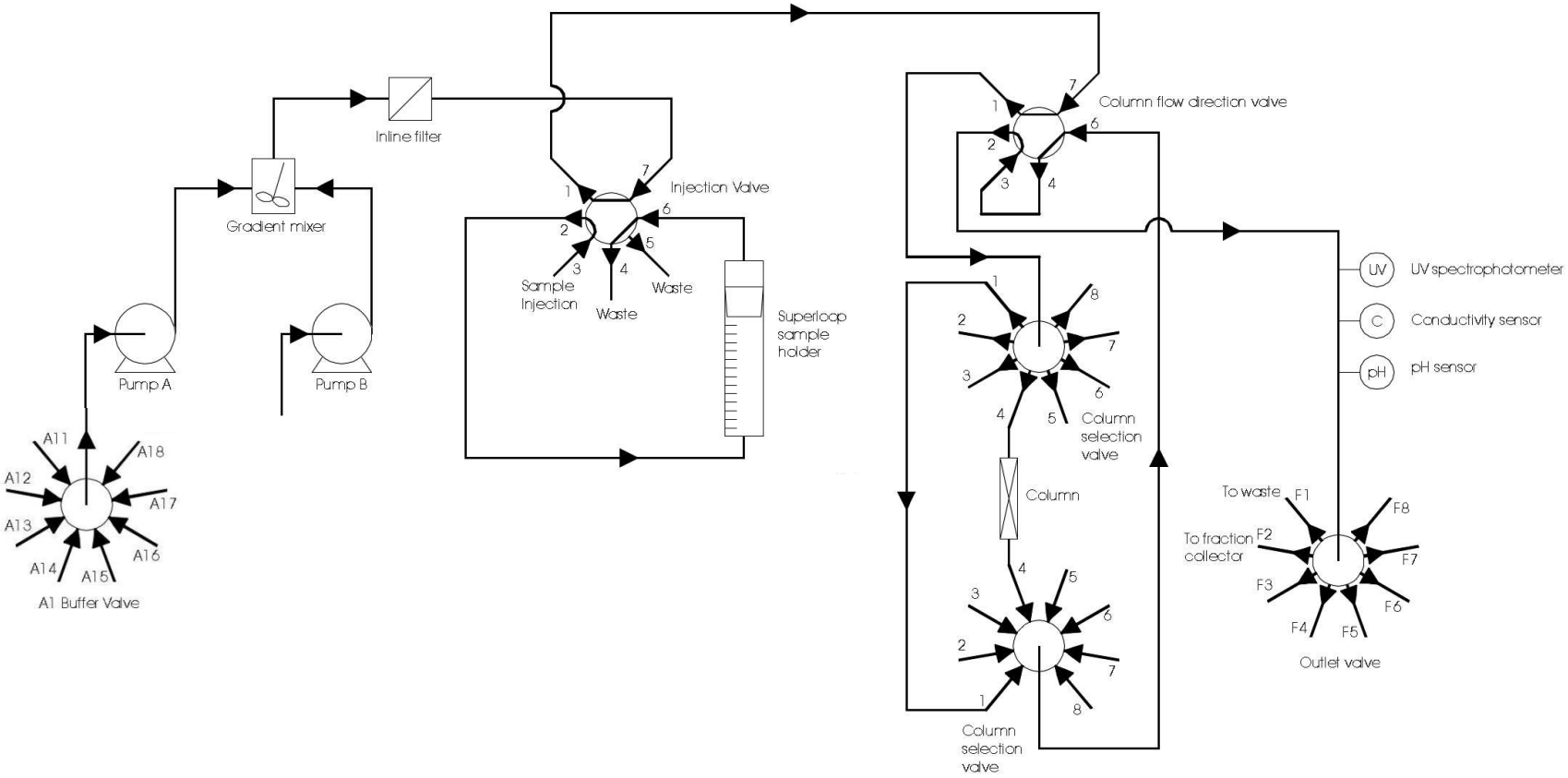

Figure 24. Flow diagram of an AKTA FPLC (adapted from Lay, 2005).

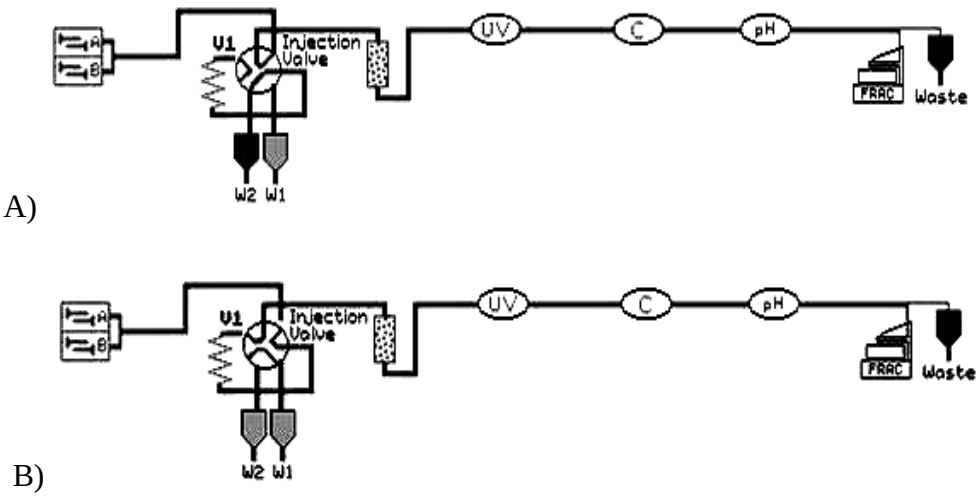

Figure 25. A) Superloop filling when injection valve is in loading position. B) Sample exits superloop when injection valve is in inject position.

4.4.2 Axial Flow Column Experiments

BSA elution experiments were carried out using a 1mL HiTrap DEAE Fast Flow axial column connected to the AKTA FPLC liquid chromatography system (GE Healthcare).

Solutions prepared for each experimental trial were:

- Equilibration buffer: 2L Tris-HCl, pH7
- Loading sample: 250mL or 500mL BSA in equilibration buffer
- Elution buffer: 2L 1M NaCl

Regeneration solution and storage solution were prepared as required.

Methods programmed into AKTA system are listed in Appendix. Each trial consists of three cycles with the following sequence of steps:

1. Column equilibration with equilibration buffer
2. Loading sample application
3. Removal of unbound proteins with equilibration buffer
4. Protein elution with elution buffer

5. Column reequilibration with equilibration buffer
6. Steps (2) to (5) repeated twice

In between trials, the system was prepared by manual control of the AKTA system:

1. Remaining protein in column removed with elution buffer
2. Column reequilibrated with equilibration buffer
3. Loading solution remaining in the superloop removed
4. Superloop filled with loading solution
5. Air in superloop removed
6. Pumps flushed by passing through greater than 20 mL solution volume
7. UV spectrophotometer flushed with equilibration buffer to remove any trapped air

Effluent was measured as absorbance at 280 nm and conductivity. The data was exported to an Excel spreadsheet. Trials were carried out for a range of flow rates, rotation speed, loading protein concentration, elution buffer concentration, loading sample volume and elution buffer volume. Experiments with unexpected results due to the effect of air bubbles, irregular solute concentration of input solution and overpressure in the system were repeated.

When the system was not used for more than 24 hours, the column was regenerated using regeneration buffer, flushed and kept in storage solution.

Loading sample consists of BSA dissolved in Tris-HCl buffer solution at pH 7. The loading sample concentrations used were 1.5, 3 and 5 mg/mL. Elution buffer consists of NaCl in Tris buffer solution. The two elution buffer concentrations used were 1M and 2M NaCl.

Axial flow trials were designed based on three different rotation speed (720, 360 and 180 degrees/hour) in the CRFC. Time per revolution in the CRFC follows

$$t_{rev} = \frac{360}{w}(60) \tag{156}$$

Time spent by each section at a single input port, given by equation (155) is dependent

on the rotation speed of the annulus and the number of annular sections in the CRFC. As the CRFC has eight feed chamber sections, time per section for the different rotation speeds is summarised in Table 4.

Table 4. Time spent by an annular section at an input port.

Rotation speed (degrees/hour)	720	360	180
Time per revolution (min)	30	60	120
Time per section (min)	3.75	7.5	15

The trials were run at flow rates 0.1, 0.21, 0.5 and 1.0 mL/min. Nine trials were allocated a range of loading and elution volumes, set based on number of sections in each step (Table 5). Actual solution input volume is dependent on rotation speed and flow rate.

Experiments were carried out in three continuous cycles per trial and in sets of three trials each time where possible. Additional reequilibration time between trials was allocated.

4.4.3 Comparison between experimental results and model results

Axial flow column experiments were designed to imitate continuous operation in the CRFC. Results from axial flow experiments are representative of the CRFC when the superficial velocity is of similar value. Results from these experiments were compared to the simulation results based on the models presented in Chapter 3.

Fluid velocity through an axial flow column does not change with column length and is equivalent to equation (14). Superficial velocity is also calculated as

$$u = \frac{Q_z}{\pi {r_x}^2} \tag{157}$$

where r_x is the axial column radius.

Table 5. Number of sections allocated to each step.

Trial	Step	Number of sections
1	Loading	1
	Wash	3
	Elution	1
	Reequilibration	3
2	Loading	3
	Wash	2
	Elution	1
	Reequilibration	2
3	Loading	5
	Wash	1
	Elution	1
	Reequilibration	1
4	Loading	1
	Wash	2
	Elution	2
	Reequilibration	3
5	Loading	1
	Wash	2
	Elution	3
	Reequilibration	2
6	Loading	1
	Wash	1
	Elution	5
	Reequilibration	1
7	Loading	2
	Wash	2
	Elution	2
	Reequilibration	2
8	Loading	3
	Wash	1
	Elution	2
	Reequilibration	2
9	Loading	3
	Wash	1
	Elution	3
	Reequilibration	1

In the CRFC, fluid velocity increases with bed depth due to the decrease in volume following direction of flow. Velocity at midpoint through the column is taken as the average superficial velocity in the CRFC, giving the superficial velocity as

$$u = \frac{Q_r}{\pi D_r H} \tag{158}$$

where D_r is the diameter of the column at midpoint of the annulus and H is the column height.

CRFC flow rates can be calculated as

$$Q_r = \pi u D_r H \tag{159}$$

Specifications of the axial column and the CRFC are found in Appendix A. From equations (157) and (159), superficial velocity with respect to flow rate of the experimental trials and corresponding CRFC flow rates were calculated (Table 6).

Table 6. CRFC flow rate corresponding to axial column experiments

Axial flow rate (cm^3/min)	Superficial velocity (cm/min)	CRFC flow rate (cm^3/min)
0.1	0.26	19
0.21	0.55	40
0.5	1.30	95
1.0	2.6	189

Model results were obtained for the complete range of parameters carried out for the experimental trials. For a more accurate comparison, the axial flow model with column dimensions equivalent to the experimental column was used.

4.4.4 Column regeneration

Regeneration solution (1M NaOH and 1M NaCl) was manually injected into the axial flow column using a 10mL syringe. After passing through five column volumes of regeneration solution, the columns were sealed and kept for 16-20 hours at room temperature. Then the column was connected back to the AKTA system with solution flow direction set in reverse. Equilibration buffer solution was passed through the column by manual operation of the AKTA system until absorbance at 280nm and conductivity returned to base value.

4.4.5 Peak area

Pump A was set to supply equilibration buffer. 2 mL of standard BSA solution was injected and passed through the system, bypassing the column. Absorbance was measured at 280nm by the inline UV spectrophotometer. Peak area corresponding to BSA mass of 2, 4, 6, 8 and 10 mg was obtained and exported into Excel. Standard curve of BSA mass to peak area was plotted.

4.4.6 Peak height

A standard curve of protein concentration corresponding to absorbance at 280 detected by the inline spectrophotometer was obtained. BSA solution of concentration ranging from 1 mg/mL to 20 mg/mL was passed through the AKTA system bypassing the column. Peak absorbance for each BSA concentration was measured.

4.4.7 Pumps

Pump A and pump B was checked for accuracy in supplying solution. Fixed volume of distilled water was passed through the AKTA system with the same setup as in the axial column experiments. A fixed volume of distilled water was pumped into the system for a period of time. Solution exiting the system was first collected and measured with a measuring cylinder.

For more accurate determination, the same process was carried out and repeated three times with the exit solution contained in preweighed test tubes. The test tubes were

reweighed and weight of distilled water calculated. Solution supplied from the superloop was similarly measured.

4.4.8 Mass balance

4.4.8.1 Absorbance at 280nm

Protein standards of BSA dissolved in Tris-HCl buffer were prepared. Protein standards between 0.15-1.5 mg/mL were prepared by diluting BSA stock solution with buffer solution. A quartz cuvette containing only buffer solution was used to blank the spectrophotometer at 280nm. The cuvette was emptied and filled with protein standard solution. Absorbance of each protein standard in increasing concentration was taken at 280nm in triplicates.

4.4.8.2 Bradford Assay

100g Coomassie Blue (Sigma Aldrich) was dissolved in 50mL methanol and added to 100mL 85% H3PO4 solution. The solution was diluted to 200mL by adding distilled water and contained in a bottle wrapped in aluminum foil. Final stock solution was stored away from light at 4°C.

Bradford assay reagent was prepared by mixing 1:4 volume to volume ratio of dye stock to distilled water. The diluted dye solution was filtered, kept in an aluminum foil wrapped bottle at 4°C and used for protein assays for up to 4 weeks.

Protein standards of BSA dissolved in Tris-HCl buffer were prepared. Solution concentrations used were between 0.15-1.5 mg/mL. In individual cuvettes, 3mL Bradford assay reagent was added to 0.05mL BSA solution. Each protein concentration assayed was carried out in triplicates. The cuvette was then covered with parafilm and inverted several times to mix the solution, starting from the lowest protein concentration to the highest protein concentration. After 5 minute incubation period, an empty plastic cuvette was used to blank the spectrophotometer and absorbance of each protein standard in increasing concentration was taken at 595nm. The standard assay spectrophotometer reading was repeated for absorbance at 450nm.

The Bradford protein assay was carried out on the chromatography protein feed solution and purified protein solution. Any protein solution with absorbance above the highest

absorbance in the standard assay was diluted before repeating the protein assay. When a protein solution from a new stock solution was assayed, a new calibration curve using the same protein solution was prepared.

Sample protein concentration was determined by absorbance comparison to the standard protein curve.

Chapter 5: Results and Discussion

5.1 Introduction

Results obtained from the small axial flow columns experiments and model simulations are presented in this chapter. The experimental results for a range of different parameters were used to determine the best conditions for the CRFC by analyzing and comparing different trials. Effect of varying different parameters was quantified in terms of peak area and yield. The trials were ranked based on productivity, height to width ratio and overall efficiency.

Selected experimental results were used to verify the finite difference models presented in Chapter 3. Comparison between the actual to predicted results and further modifications to the models will also be discussed.

5.2 Experimental Results

Tris-HCl buffer at pH 7 was used to make BSA sample solution and for column equilibration. BSA has a pI of 4.9-5.1. At pH7, BSA has a negative net charge. When the BSA solution passes through the positively charged DEAE Hitrap FF column media, BSA is adsorbed onto the resin matrix. When elution buffer solution containing NaCl is introduced into the column, BSA is eluted from the column.

BSA purification was carried out under a range of parameters based on continuous operation of the CRFC. Conditions tested include a range of rotation speeds (180, 360 and 720 deg/hr), flow rate (0.1, 0.21, 0.5 and 1.0 mL/min), feed concentration (1.5, 3 and 5 mg/mL), loading volume, elution buffer volume and elution buffer concentration (1 and 2M). Each trial condition was carried out as three cycles repeated continuously.

All experimental results were exported into excel spreadsheets and plotted as absorbance at 280nm with time (Appendix D). Absorbance is converted to BSA concentration using the equation obtained from a standard curve of BSA concentration against absorbance (Appendix B). Area under the peak which corresponds to protein mass is obtained directly from the AKTA system in units of mAU*min.

5.2.1 BSA elution profiles

Experimental trials were compared in terms of peak area and yield with respect to increasing loading sections (1-5 sections), elution section (1-5 sections), rotation speed (180-720 deg/hr), flow rate (0.1-1 mL/min), feed concentration (1.5-5 mg/mL) and elution buffer concentration (1-2M).

Proteins exiting the column were measured in two separate stages; the loading zone and elution zone stages. Loading zone begins from the point of sample injection and ends after the start of elution buffer application. Proteins leaving the column in the loading zone were proteins not adsorbed onto the resin and were counted towards product loss. Elution zone is the period from the start of elution step until the next injection of feed solution. Figure 26 represents a typical elution profile of a single cycle of BSA purification. The first peak corresponds to the amount of BSA lost in the loading zone which exits the column during equilibration step while the second peak corresponds to the purified BSA obtained from the elution zone.

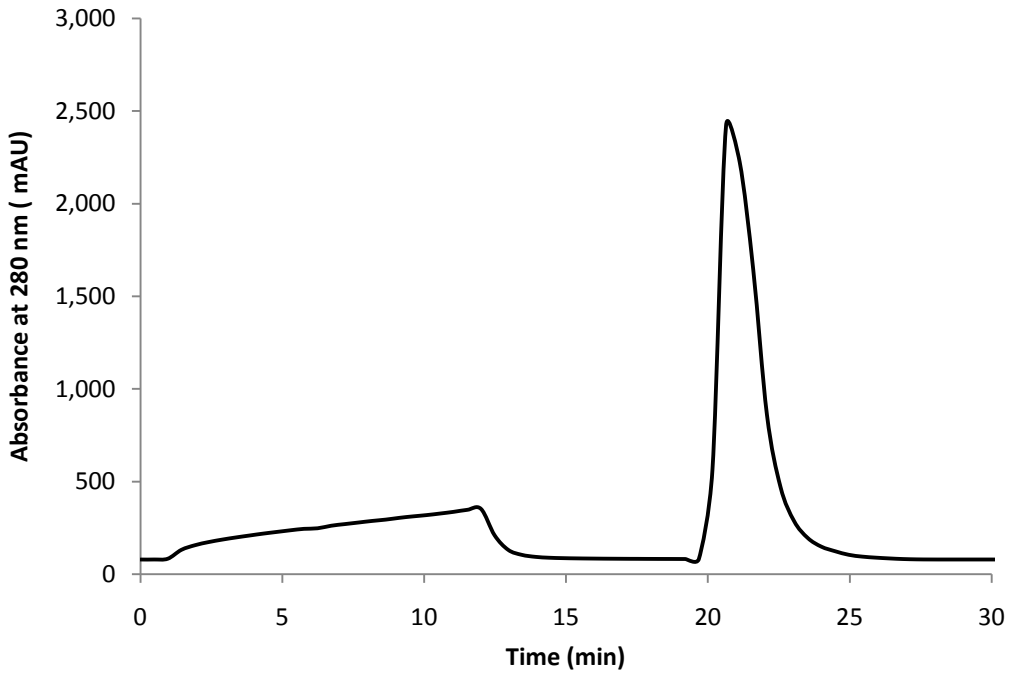

Figure 26. Loading zone and elution zone BSA peaks. First peak is the breakthrough from loading BSA stock solution. Second peak is eluted BSA peak from application of NaCl solution.

Due to insufficient equilibration period, incompletely resolved peaks where baseline absorbance is not achieved between loading zone and elution zone peaks were observed for some trials. In quantifying such peaks (Figure 27), the lowest absorbance value between the two peaks was used as the point of separation. However, peak shoulder and peak tailing which may also be due to insufficient reequilibration, will be counted towards an elution peak.

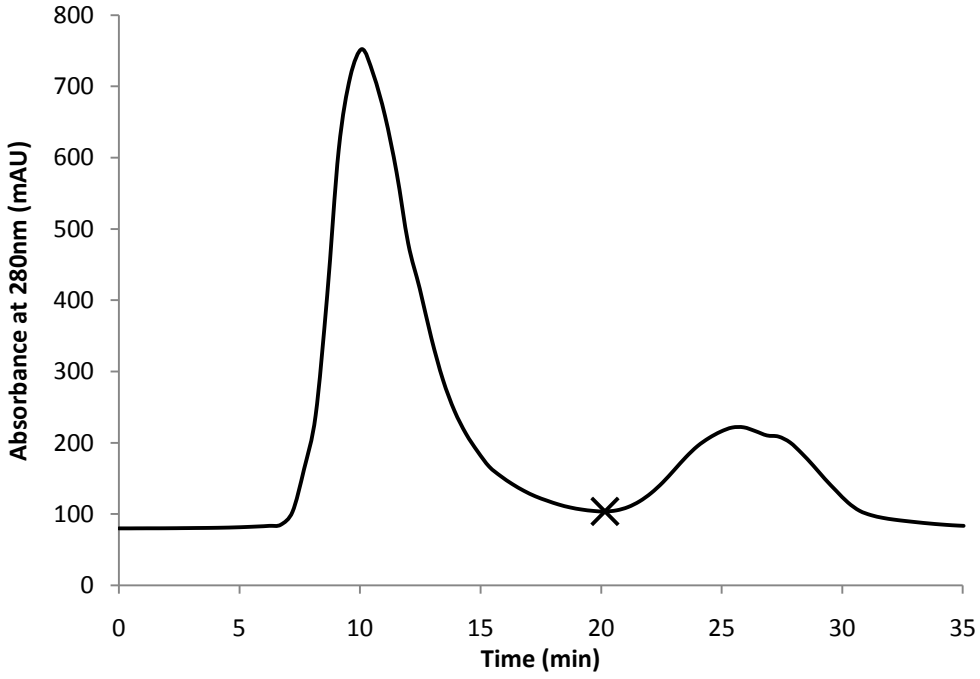

Figure 27. Example of incompletely resolved loading and elution BSA peaks, and allocated point of separation with 3.75 min loading and 18.75 min elution.

An additional peak in the elution zone at retention time greater than the eluted BSA was found in some of the experimental trial results (Figure 28). These constituted to very minute amounts of protein. As the feed solution was made up of pure BSA and the probability of contamination from other sources was low, the secondary peaks observed were suspected to be BSA dimers. Small fractions of BSA dimers are known to be present in commercially produced BSA (Hunter and Carta 2001). As the dimers are more strongly bound to anion exchangers, they elute later than the monomers.

The amount of dimers eluted, if dissociated into monomeric form would have eluted as part of the main elution peak. Therefore, dimers are quantified as part of the elution peak while the width of the elution peak remains the same.

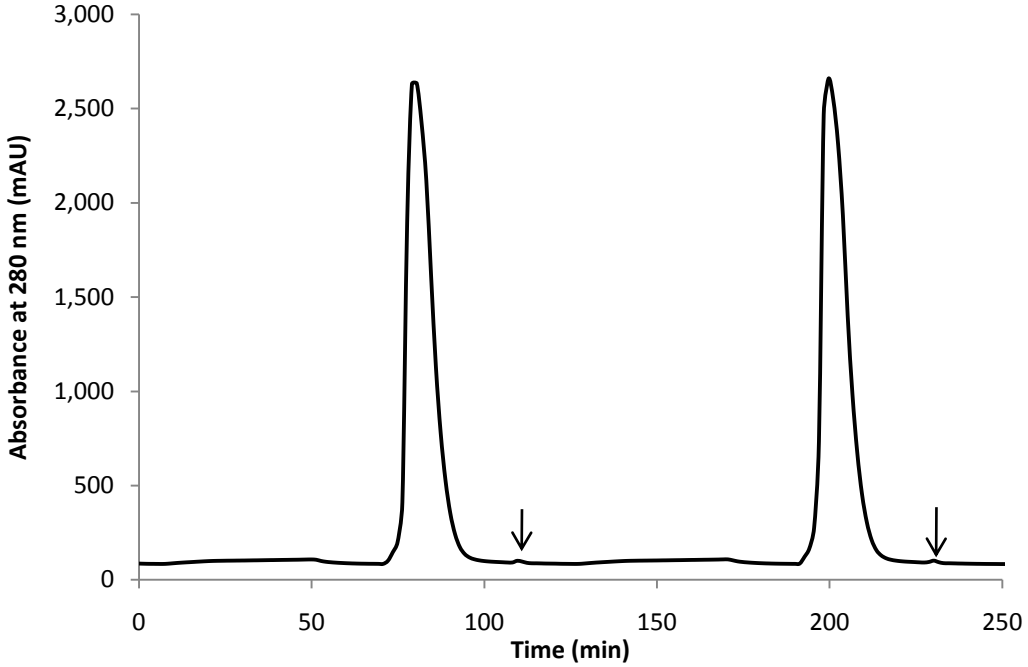

Figure 28. BSA dimer peaks

5.2.2 Peak area

Peak area is measured as area under an absorbance peak to an allocated baseline absorbance of 79 mAU. Actual experimental baseline absorbance is between 79 and 81 mAU. Plots of peak area with respect to loading section, elution sections, rotation speed, flow rate, feed concentration and elution buffer concentration are presented in Appendix E and Appendix F.

5.2.2.1 Loading sections

The CRFC is divided into eight equal sections allowing different solutions to be applied to each section simultaneously. The time spent by a section at a single input port is dependent on the rotation speed of the annulus (Table 4). Nine combinations of number of sections were allocated to loading, equilibration, elution and reequilibration following Table 5. Trials 1, 2 and 3 have loading to elution ratio of 1:1, 3:1 and 5:1 respectively. Trial 3 was not carried out for 180 deg/hr rotation speed at 1.0mL/min flow rate as five sections of loading require 75mL feed solution, an amount which exceeds the capacity of the largest superloop available.

There are eight sections in a single cycle and each section is represented by a specific amount of time. Increasing loading section (time) increases the volume of feed solution applied and therefore the amount of BSA entering the column. As expected, comparison between trials under the same conditions (elution time, rotation speed, feed concentration, elution buffer concentration and flow rate) showed an increase in elution zone peak area with increasing loading section (Appendix E.1).The slope of increasing peak area with increasing loading sections varies with different flow rates. There is greater increment for slow flow rates.

Actual loading volume is also dependent on rotation speed and flow rate. Loading volume is greater for higher flow rates and would be expected to result in greater elution peak area. However, this is not the case as observed by larger peak area when slower flow rates are used.

Figure 29 shows the increase in elution zone peak area with increasing loading sections under conditions of 180 deg/hr rotation speed, 1.5 mg/mL feed concentration and 1M elution buffer concentration for a range of flow rates. All other plots of peak area with increasing loading section showed similar trends (Appendix E.1).

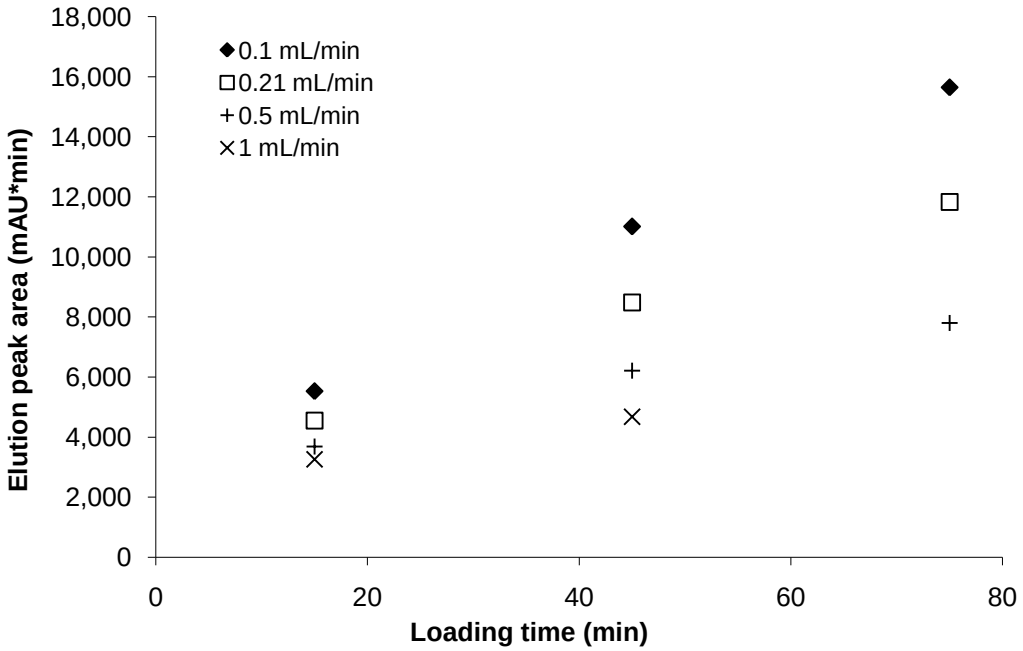

Figure 29. Elution peak area with increasing loading sections under 180 deg/hr rotation speed, 1.5 mg/mL feed concentration and 1M elution buffer concentration.

Peak area in the loading zone which represents the amount of protein loss was found to increase with increasing loading sections (Figure 30 and Appendix F.1). Higher flow rates resulted in larger peak area and greater increase in peak area with increasing loading section. Loading zone peak area matches well with elution zone peak area. Slope of increase in elution zone peak area for slow flow rates such as 0.1 and 0.21mL/min is greater as very small amounts of protein is lost in the loading zone, allowing peak area to increase corresponding to the increase in number of loading sections.

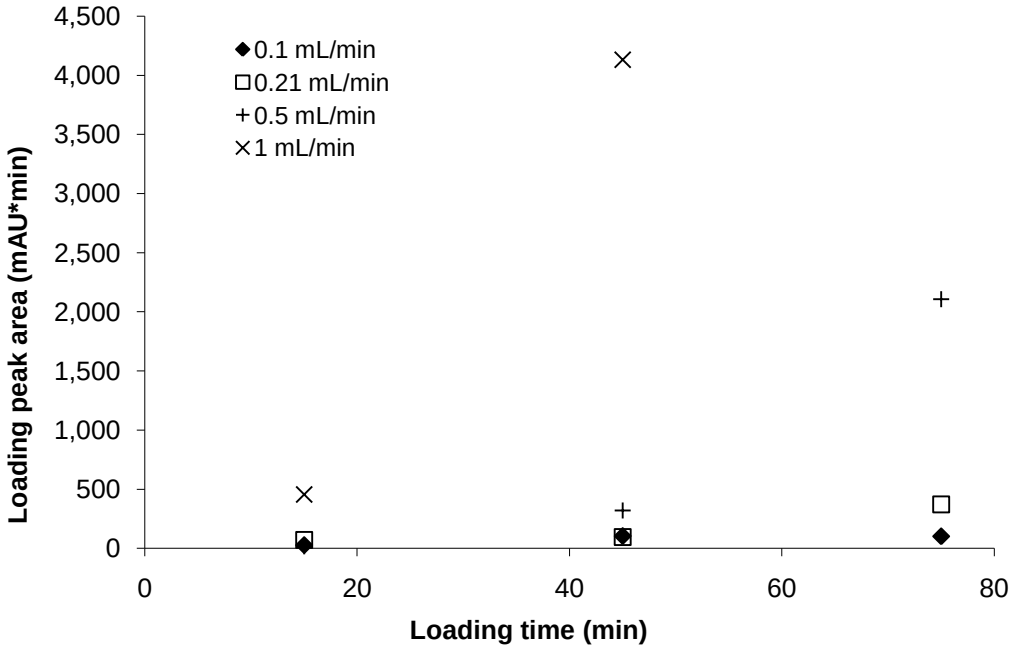

Figure 30. Loading peak area with increasing loading sections under 180 deg/hr rotation speed, 1.5 mg/mL feed concentration and 1M elution buffer concentration.

5.2.2.2 Elution sections

Trials 1, 4, 5 and 6 have elution sections of 1, 2, 3 and 5 respectively while loading amounted to one section each. Similar to observation in the comparison of trials with increasing loading sections, elution zone peak area in the plots of increasing elution section also showed that low flow rates gave larger peak area (Appendix E.2).

Comparing trials with same conditions, elution zone peak area on average does not change much with increasing elution section. Figure 31 compares trials with increasing elution sections under conditions of 180 deg/hr rotation speed, 5 mg/mL feed concentration and 1M elution buffer concentration. Unchanging peak area values with increasing elution sections suggest that one elution section is sufficient for one section of loading.

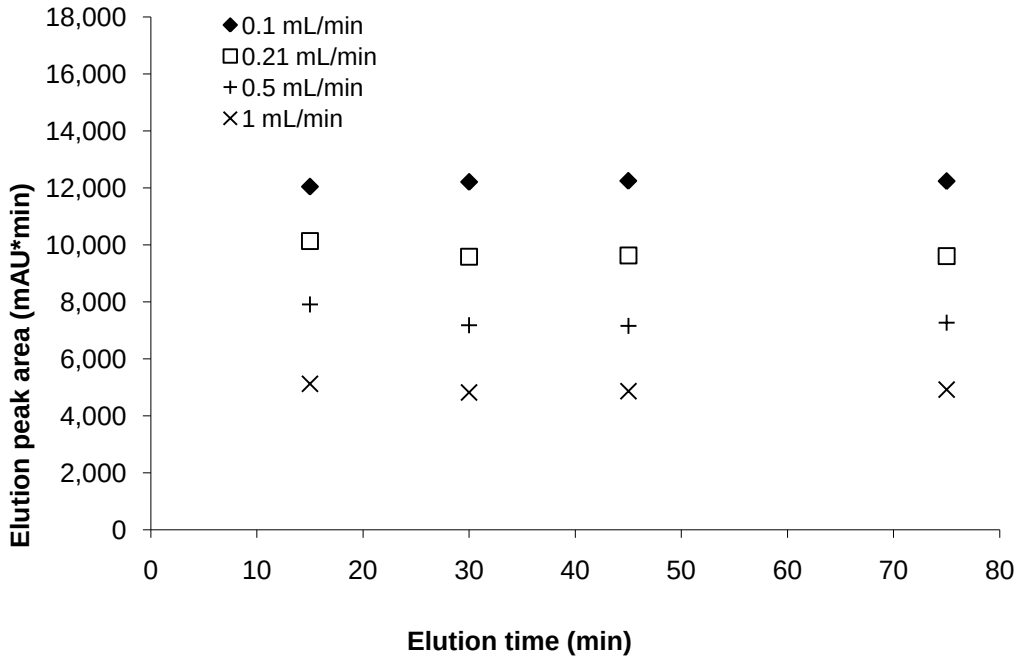

Figure 31. Elution peak area with increasing elution sections under 180 deg/hr rotation speed, 5 mg/mL feed concentration and 1M elution buffer concentration.

Low flow rates of 0.1 and 0.21 mL/min had less consistent elution peak area values than higher flow rates. Peak area for 0.1 mL/min flow rate and 720 deg/hr rotation speed gave the most varied values with increasing number of elution sections (Figure 32).

Loading peak area changes with increasing elution time showed no general trend of increase or decrease (Figure 33 and Appendix F.2). Variability increases towards very high and very low elution times. Peak area at 0.1 mL/min flow rate is most varied and for a number of trial conditions, resulted in drastic increase in peak area at very high elution time.

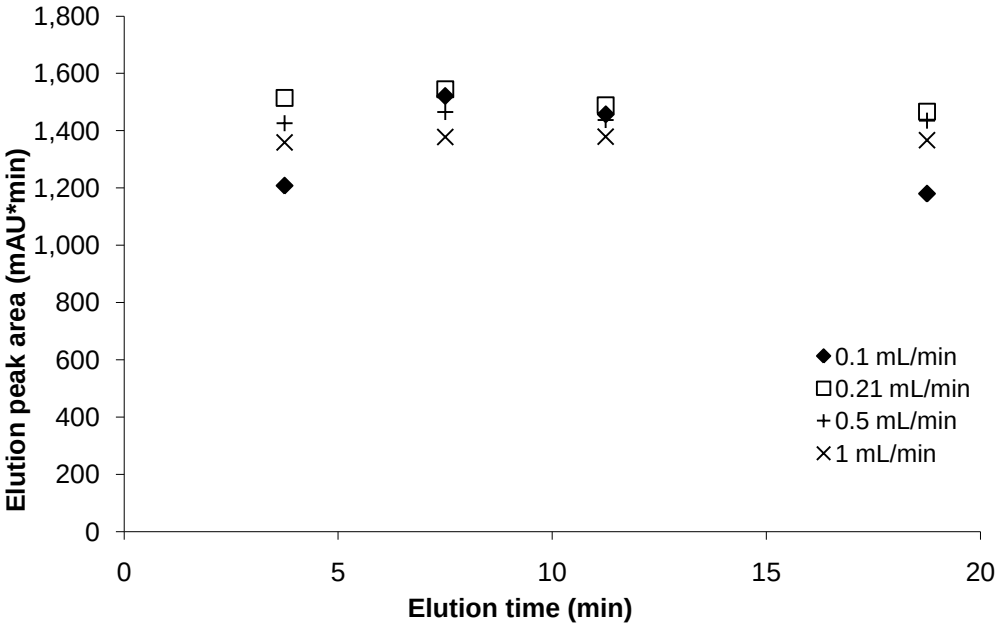

Figure 32. Elution peak area with increasing elution sections under 720 deg/hr rotation speed, 1.5 mg/mL feed concentration and 1M elution buffer concentration.

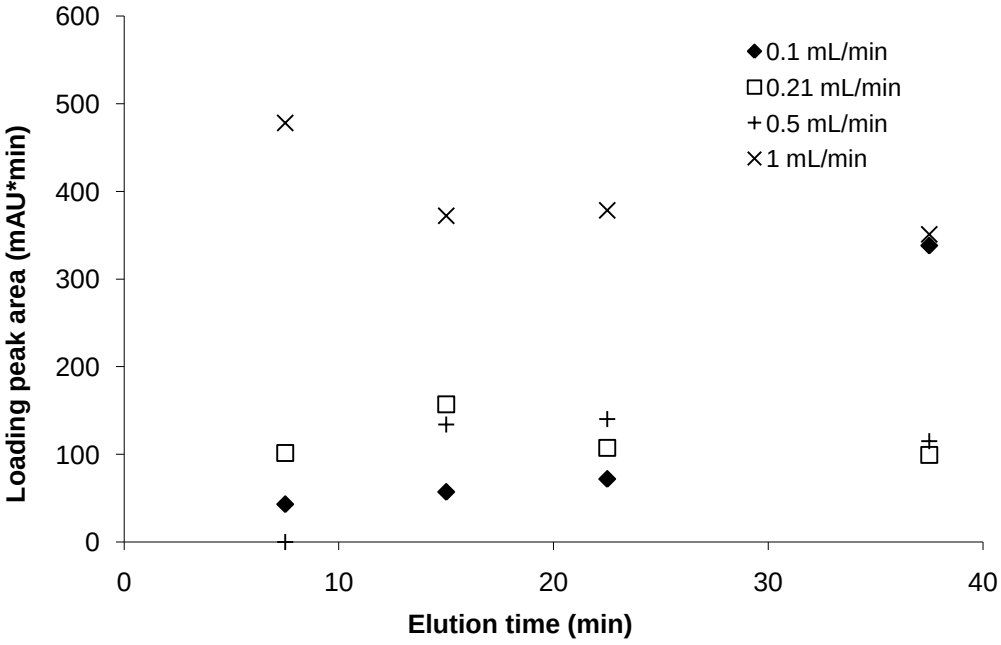

Figure 33. Loading peak area with increasing elution sections under 360 deg/hr rotation speed, 3 mg/mL feed concentration and 1M elution buffer concentration.

5.2.2.3 Rotation speed

Small column axial flow experiments were set up to represent the different rotation speeds that can be run in the CRFC. Rotation speeds of 180, 360 and 720 deg/hr are equivalent to 15, 7.5 and 3.75 minutes spent by a section at a single input port (Table 4). Trials 1-9 which gives a combination of step (loading, equilibration, elution, reequilibration) ratio were carried out for 180, 360 and 720 deg/hr rotation speeds. Trial 3 could not be carried out at 180 deg/hr rotation speed for 1.0 mL/min flow rate due to limited volume (50mL) capacity of the superloop.

Faster rotation speeds would result in less time spent by a section at a single input port, which in turn reduces the volume of solution for each step. Loading time and consequently loading volume would be lower for faster rotation speeds. In comparing trials with increasing rotation speeds without difference in other conditions, elution zone peak area was found to decrease with increasing rotation speeds (Appendix E.3).

Lower flow rates showed greater peak area. Peak area differences between trials of different flow rate diminish with increasing rotation speeds. For trials with greater elution to loading section ratio, 720 deg/hr rotation speeds produced very similar peak area values for all flow rates.

At 720 deg/hr, 0.1mL/min flow rate may result in the smallest peak area. For example, trial 6 which was allocated five elution sections and only one loading section showed that at 720 deg/hr, trials with 0.21-1.0mL/min flow rate have greater peak area with lower flow rate while the trial at 0.1mL/min had unusually low peak area (Figure 34).

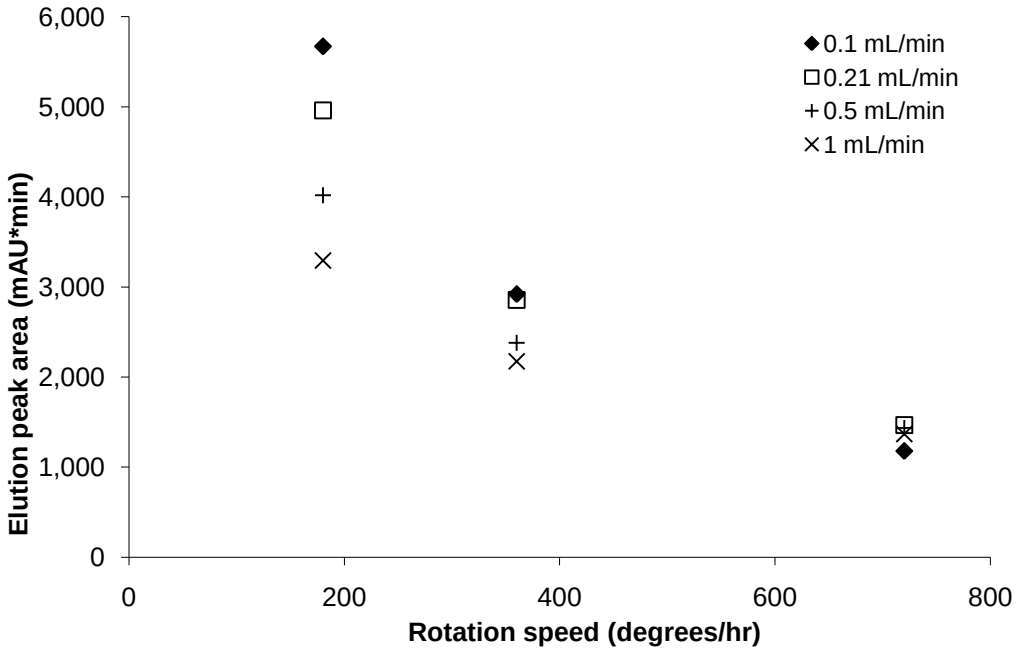

Figure 34. Elution peak area with increasing rotation speed for Trial 6 under 1.5 mg/mL feed concentration and 1M elution buffer concentration.

Loading zone peak area also decreases with increasing rotation speed and is greater for faster flow rates for most conditions (Appendix F.3). A few trials however, showed an increase in peak area with increasing rotation speeds which includes the trials with unusually low elution peak area at 720 deg/hr rotation speed. Trial with increasing loading peak area with increasing rotation speeds such as in Figure 35 have similar conditions of very low flow rates and large elution to loading ratio.

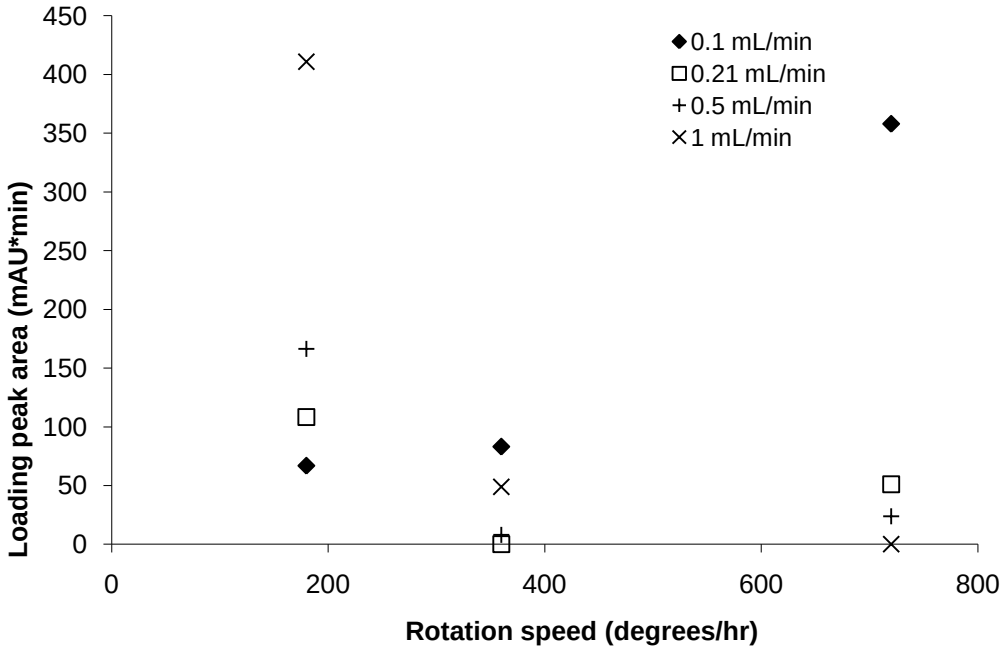

Figure 35. Loading peak area with increasing elution sections for Trial 6 under 1.5 mg/mL feed concentration and 1M elution buffer concentration.

A combination of very low flow rate, short time per section, large number of elution sections and low reequilibration period may have resulted in salt remaining in the column after reequilibration. As salt is not completely removed after one cycle of steps, the next cycle would be affected. Some of the protein entering the column in the following loading step would be immediately eluted.

5.2.2.4 Flow rate

Analysis of peak area with respect to loading section, elution section and rotation speed indicated that peak area is higher with lower flow rates. Plot of elution peak area with increasing flow rate showed that peak area decreased with increasing flow rate (Figure 36 and Appendix E.4), reconfirming earlier observation. These results also supported that peak area decreases with increasing rotation speeds. There were also cases with increasing or unchanging peak area with increasing flow rate (Figure 37). Peak area that did not decrease with increasing flow rates was restricted to trials with 720 deg/hr rotation speed.

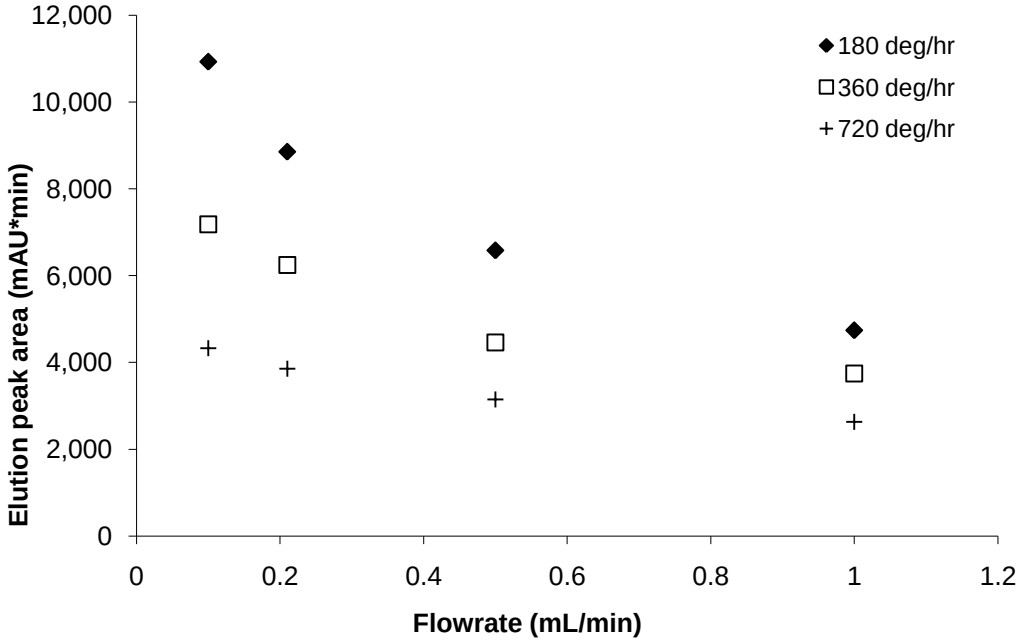

Figure 36. Elution peak area with increasing flow rate for Trial 8 under 1.5 mg/mL feed concentration and 1M elution buffer concentration.

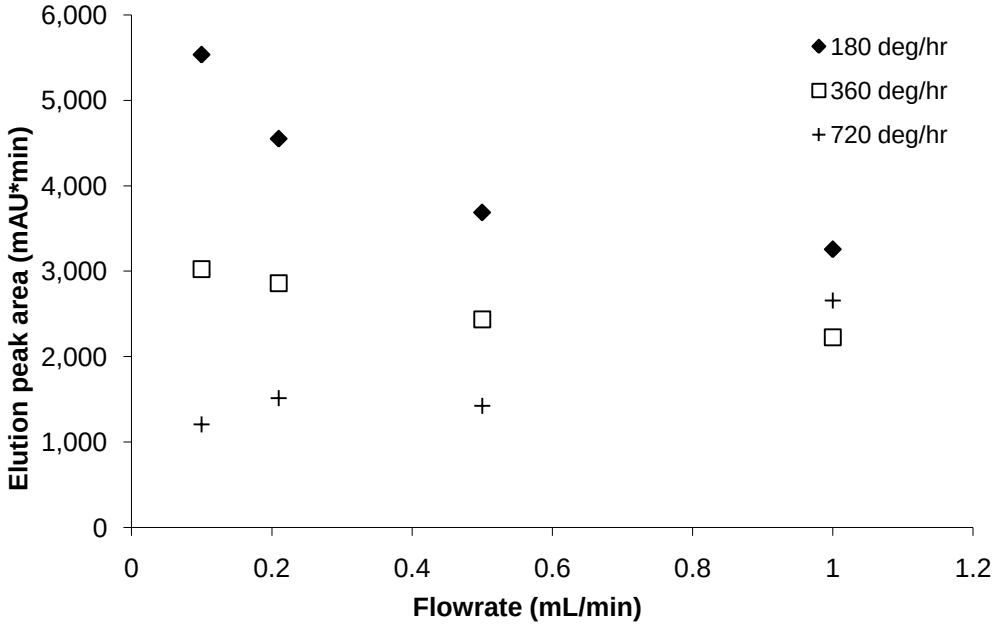

Figure 37. Elution peak area with increasing flow rate for Trial 1 under 1.5 mg/mL feed concentration and 1M elution buffer concentration.

Loading peak area increases with increasing flow rate and is greater for lower rotation speeds (Figure 38 and Appendix F.4). The increase in peak area with flow rate at 180

deg/hr rotation gave the steepest increase in peak area.

Within lower flow rate ranges (0.1- 0.21mL/min), peak area may be higher than expected, especially with fast rotation speeds. Figure 39 is a good example of large peak area at very low flow rates. For both 360 and 720 deg/hr rotation speeds, 0.1 mL/min flow rate prevented successful reequilibration of the column. In addition, five sections of elution buffer were applied but only one section of reequilibration was allocated. The elution buffer concentration is also higher, at 2M.

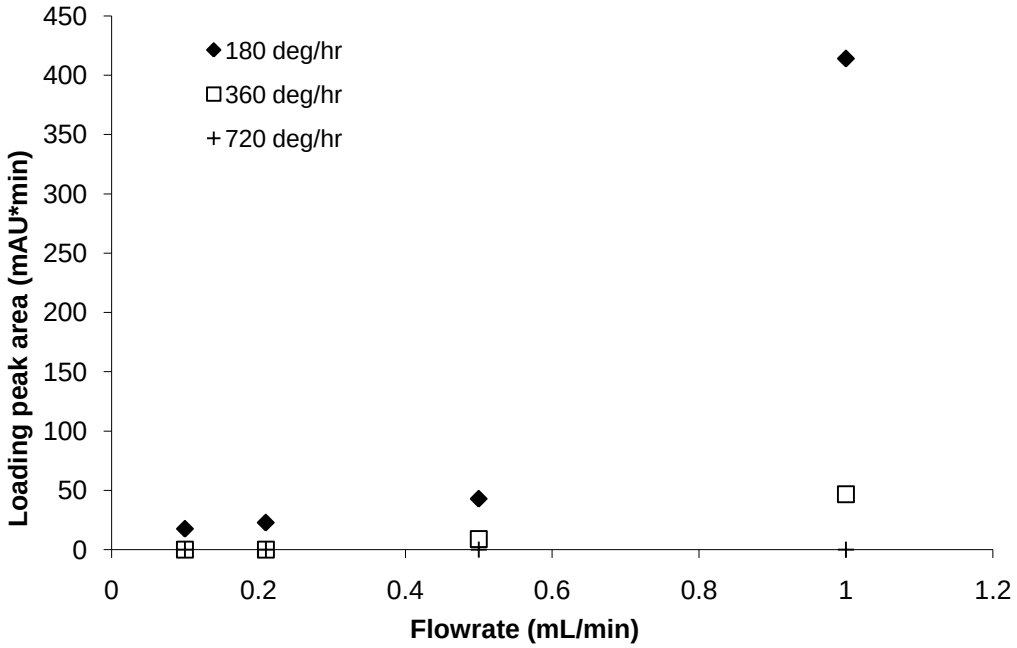

Figure 38. Loading peak area with increasing flow rate for Trial 4 under 1.5 mg/mL feed concentration and 1M elution buffer concentration.

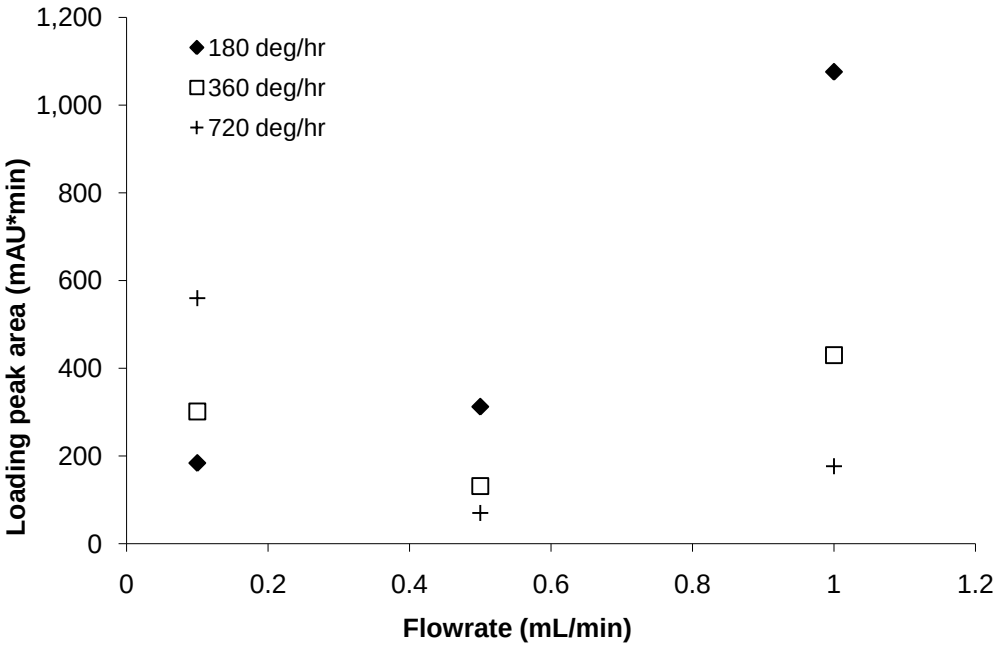

Figure 39. Loading peak area with increasing flow rate for Trial 6 under 1.5 mg/mL feed concentration and 2M elution buffer concentration.

5.2.2.5 Feed concentration

Trials were carried out with feed concentrations of 1.5, 3 and 5 mg/mL at different rotation speeds (180-720 deg/hr), flow rates (0.1-1 mL/min), loading sections (1-5 sections) and elution sections (1-5 sections). However, feed concentration of 3 and 5 mg/mL was not used in combination with 2M elution buffer concentration. Therefore effects of feed concentration will be limited to conditions with 1M elution buffer concentration.

Comparison between trials with the same conditions showed that both elution zone peak area and loading zone peak area increased with increasing feed concentration (Figure 40, Figure 41, Appendix E.5 and Appendix F.5). Peak area is also greater for slower flow rates.

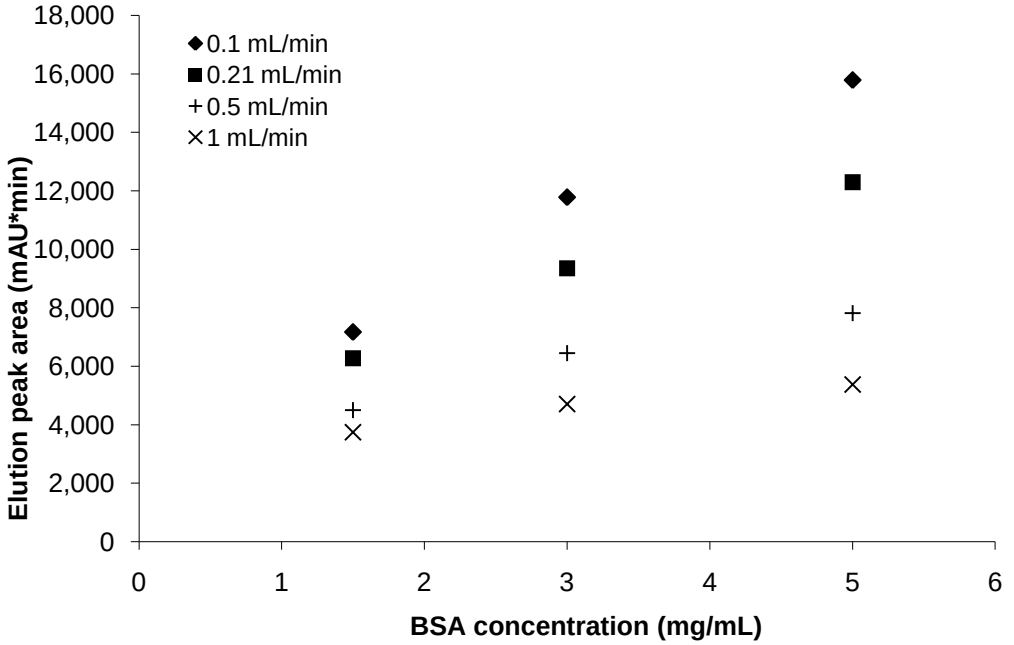

Figure 40. Elution peak area with increasing feed concentraion for Trial 9 under 360 deg/hr rotation speed and 1M elution buffer concentration.

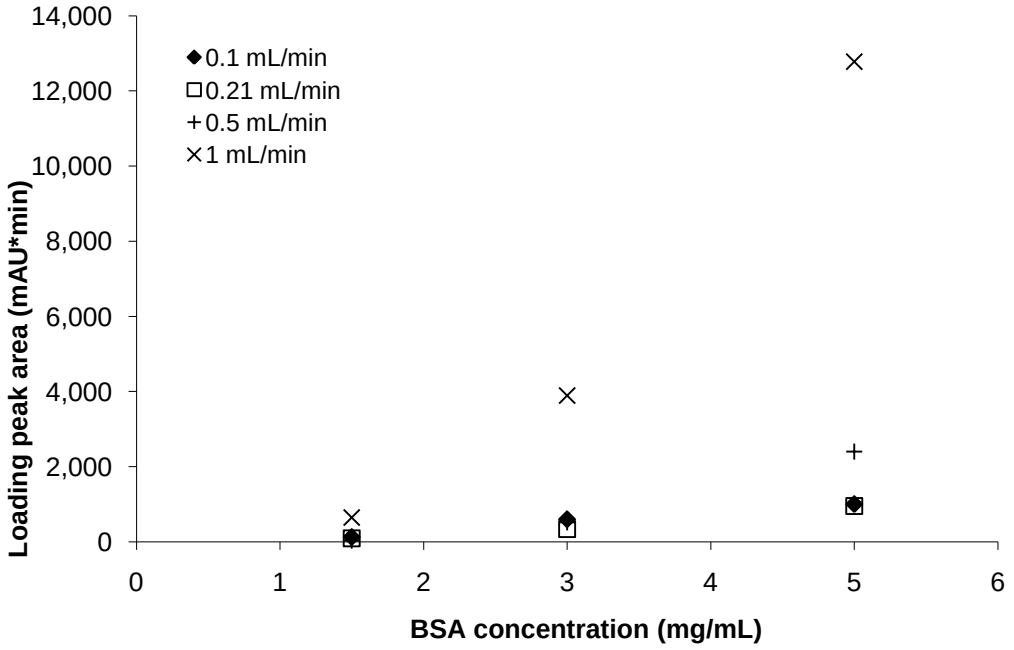

Figure 41. Loading peak area with increasing feed concentration for Trial 9 under 360 deg/hr rotation speeds and 1M elution buffer concentration.

Exceptions where loading peak area was not in increasing order with increasing feed concentration such as observed in Figure 42 was found due to presence of a secondary peak which extends into the loading zone. Each trial is run as three continuously cycles. As the secondary peak is not observed in the loading zone of the first cycle, it was ruled out as protein breakthrough. It is also not due to the presence of BSA dimers as no peak was found after elution in the last cycle.

At very low flow rate of 0.1 mL/min in combination with high rotation speeds, the formation of peak shoulders, peak tailing and secondary peaks is more common. Lower flow rates and faster rotation speeds leads to smaller volumes of input solution. As the trials were run as continuous cycles, salt remaining in the column from insufficient reequilibration will cause premature elution of some of the newly loaded proteins.

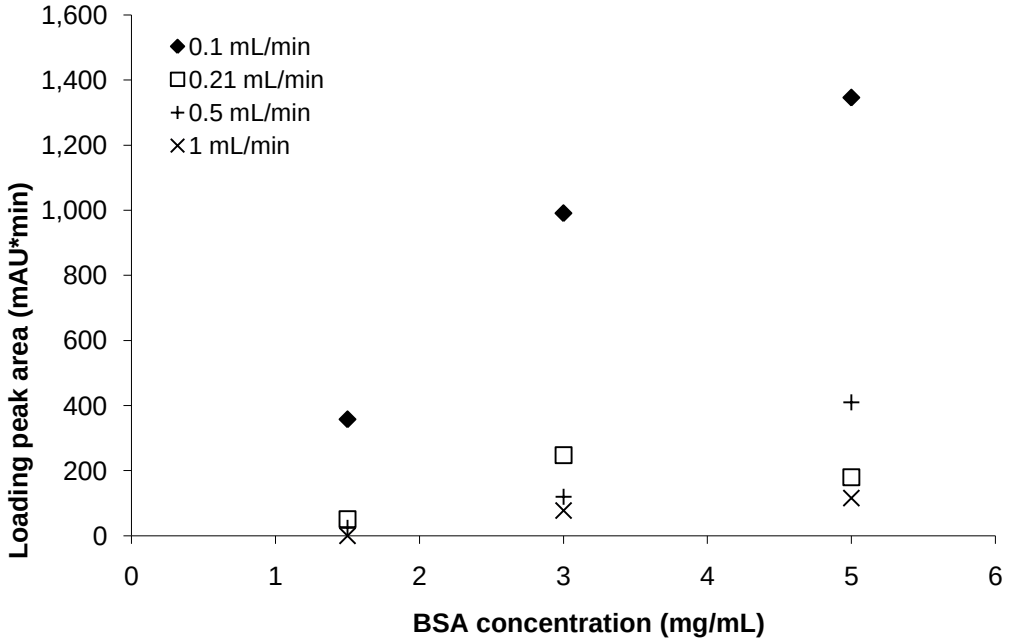

Figure 42. Loading peak area with increasing feed concentration for Trial 6 under 720 deg/hr rotation speeds and 1M elution buffer concentration.

5.2.2.6 Elution buffer concentration

Increasing elution buffer concentration from 1M to 2M resulted in greater peak area in both elution zone and loading zone for most trials (Figure 43, Figure 44, Appendix E.6 and Appendix F.6). At 720 deg/hr rotation speed and 0.1 mL/min flow rate, changes in peak area with elution buffer concentration were most variable. Trials 1-3 which have one elution section each, showed increasing elution peak area and decreasing loading peak area with increased elution buffer concentration. Trials 4-9 have two or more elution sections each and were observed to decrease in elution peak area and increase in loading peak area with elution buffer concentration.

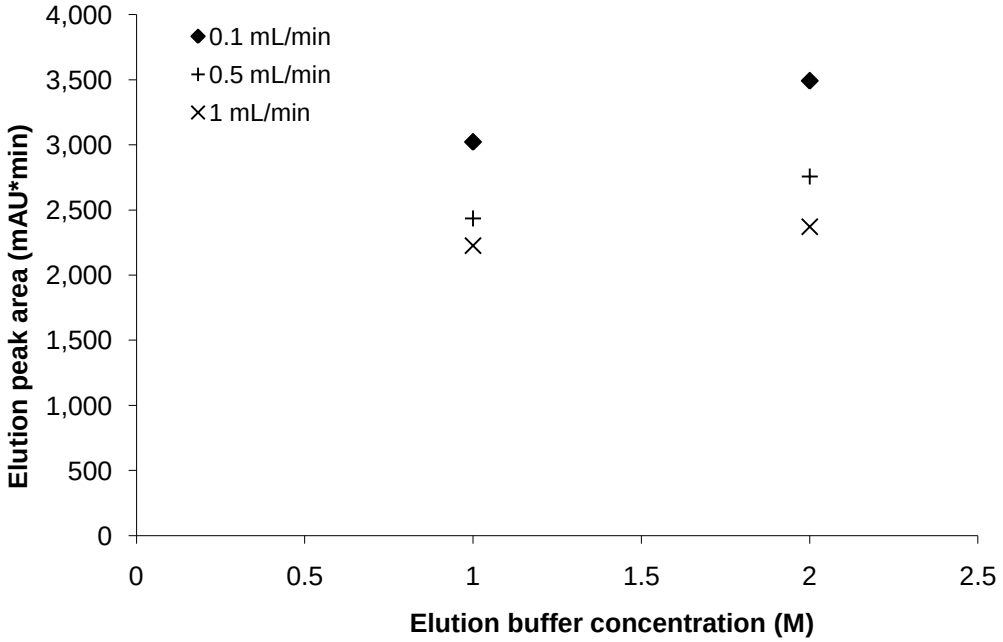

Figure 43. Elution peak area with increasing elution buffer concentration for Trial 1 under 1.5 mg/mL feed concentration and 360 deg/hr rotation speeds.

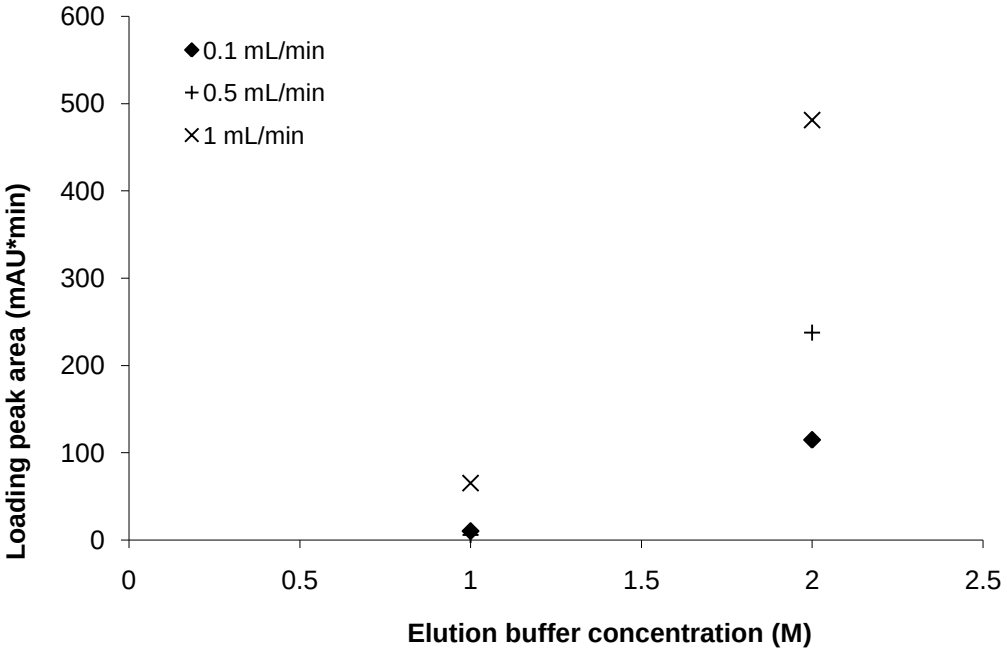

Figure 44. Loading peak area with increasing elution buffer concentration for Trial 1 under 1.5 mg/mL feed concentration and 360 deg/hr rotation speeds.

5.2.3 Yield

Peak area changes under different conditions as discussed earlier showed the effect of increasing loading sections, elution sections, rotation speed, flow rate, feed concentration and elution buffer concentration on the amount of protein captured and protein lost. Although indication of the best conditions can be obtained from peak area analysis, results are based on a single chromatography cycle. Time taken for one complete cycle is dependent on rotation speed, which in turn determines the total protein input for each trial. Yield in terms of mass per hour would be more a suitable comparison between trials as it gives a more relative productivity count.

Mass of protein loaded per cycle is given by

$$m_P = \quad Q\ t_D\ d\ C_{feed} \tag{160}$$

where Q is flow rate, t_D is time per section, d is number of loading sections and C_{feed} is feed concentration. Throughput is calculated as

$$m_{hr} = \frac{m_p w}{360} \qquad (161)$$

where w is the rotation speed.

Peak area from the elution zone and loading zone represents protein captured and loss respectively, and can be represented as percentages of total protein per cycle. For comparative analysis of trials with different rotation speed, yield was obtained as percentage of captured proteins with respect to throughout. The final product would then be quantified as protein mass per hour.

Yield was calculated for all experimental trials carried out (Appendix G.7) and plotted with respect to increasing loading sections, elution sections, rotation speed, flow rate, feed concentration and elution buffer concentration.

5.2.3.1 Loading sections

Yield for trials 1, 2 and 3 were compared to observe the effect of yield changes with increasing loading sections from one section to five sections. Elution sections were equal for all three trials at one section, limiting additional effect from varying elution time and volume. All other conditions were kept the same.

Plots of yield with increasing loading sections are presented in Appendix G.1. Results show that yield increases with increasing loading section with the exception of a few trials carried out at high flow rates and in combination with high feed concentration (Figure 45). At lower feed concentrations, all trials regardless of flow rates indicated that yield increases with increasing loading sections (Figure 46).

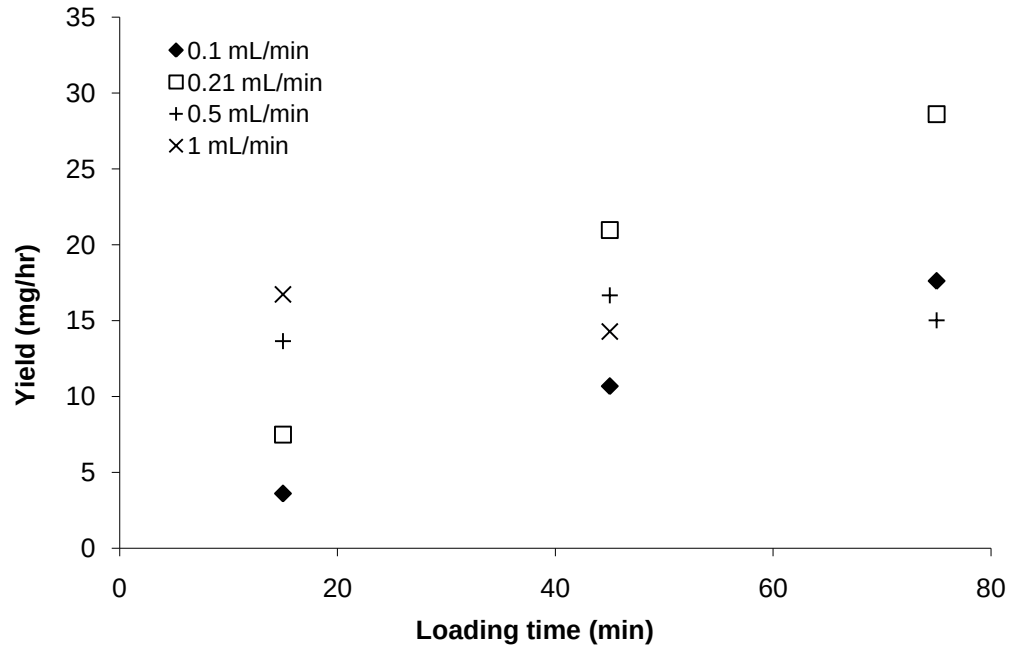

Figure 45. Yield with increasing loading sections under 5 mg/mL feed concentration, 1M elution buffer concentration and 180 deg/hr rotation speeds.

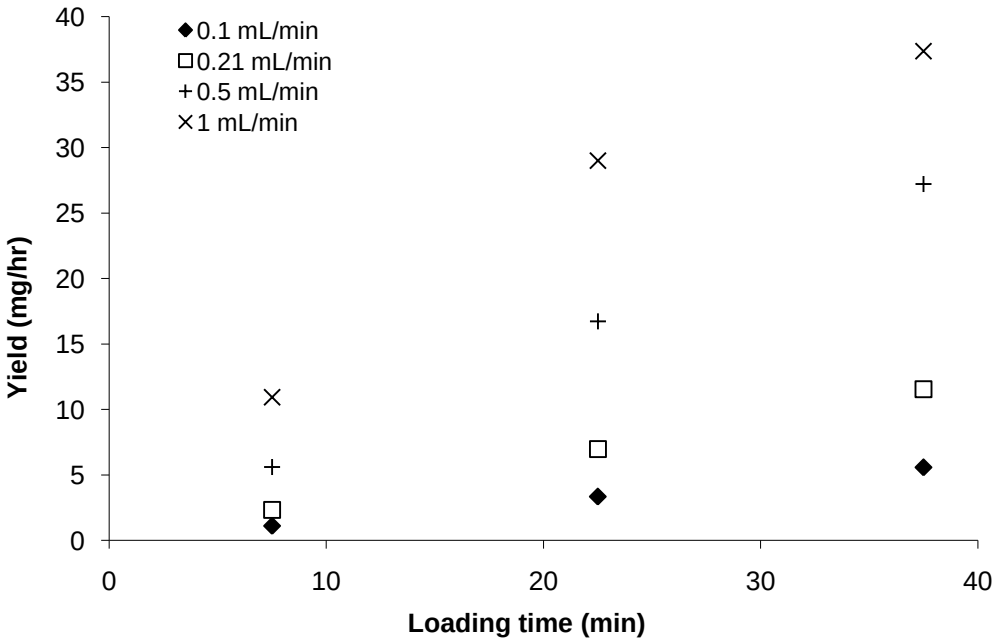

Figure 46. Yield with increasing loading sections under 1.5 mg/mL feed concentration, 1M elution buffer concentration and 360 deg/hr rotation speeds.

5.2.3.2 Elution sections

Results from trials with the same conditions were compared to observe effects of increasing elution sections on yield (Appendix G.2). Elution sections were in the range of 1-5 sections while loading section was maintained at one section. All comparisons showed no observable changes in yield with increasing elution sections similar to Figure 47. However, the observation is only restricted to one section of loading and does not predicted effect of increasing elution section with higher loading sections.

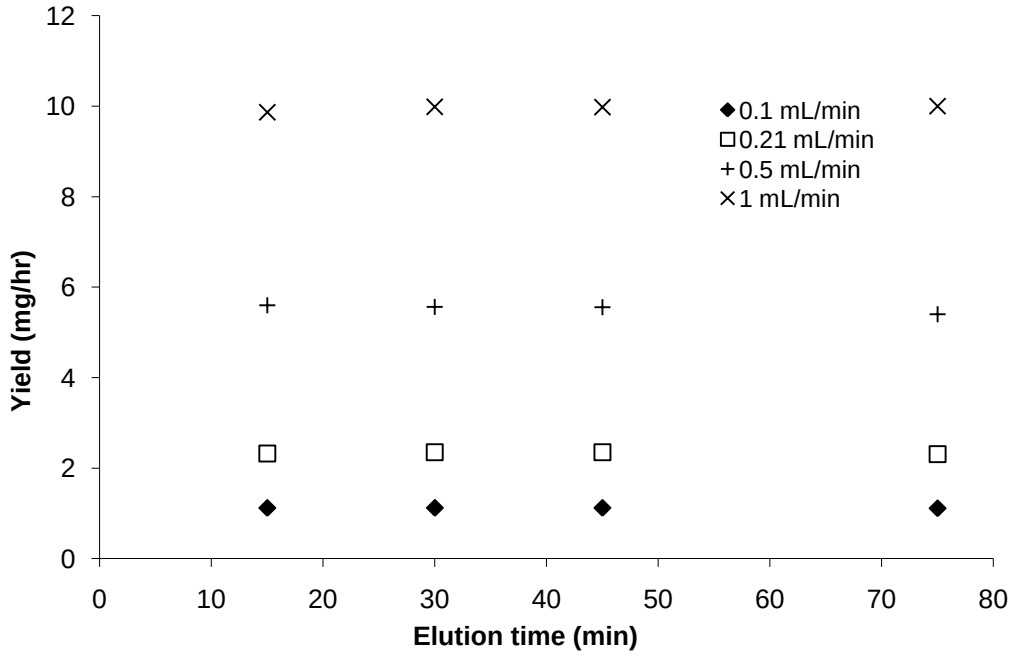

Figure 47. Yield with increasing elution sections under 1.5 mg/mL feed concentration, 1M elution buffer concentration and 180 deg/hr rotation speeds.

5.2.3.3 Rotation speed

Fast flow rates produced variable degree of yield increment with increasing rotation speed (Figure 48 and Appendix G.3). Among trials with increasing yield, most were trials with 1.0 mL/min flow rate followed by 0.5 mL/min flow rate. Yield increases were greater for higher loading sections and more concentrated feed solution. Trials with slow flow rates (0.1 and 0.21mL/min) did not show any change in yield with

increasing rotation speed for all conditions.

The slope of increase from 180 to 360 deg/hr is usually greater than from 360 to 720 deg/hr when trial have fewer loading sections and lower feed concentration. In trials with higher loading sections and feed concentration, yield increase from 360 to 720 deg/hr is similar to the increase in the lower rotation speed range. Assuming that yield is dependent on rotation speeds and increases with increasing speeds, then trials which show no change in yield with different rotation speeds may have one or more conditions as a limiting factor preventing further yield increase. The limiting factor is also likely to be more influential at higher rotation speeds.

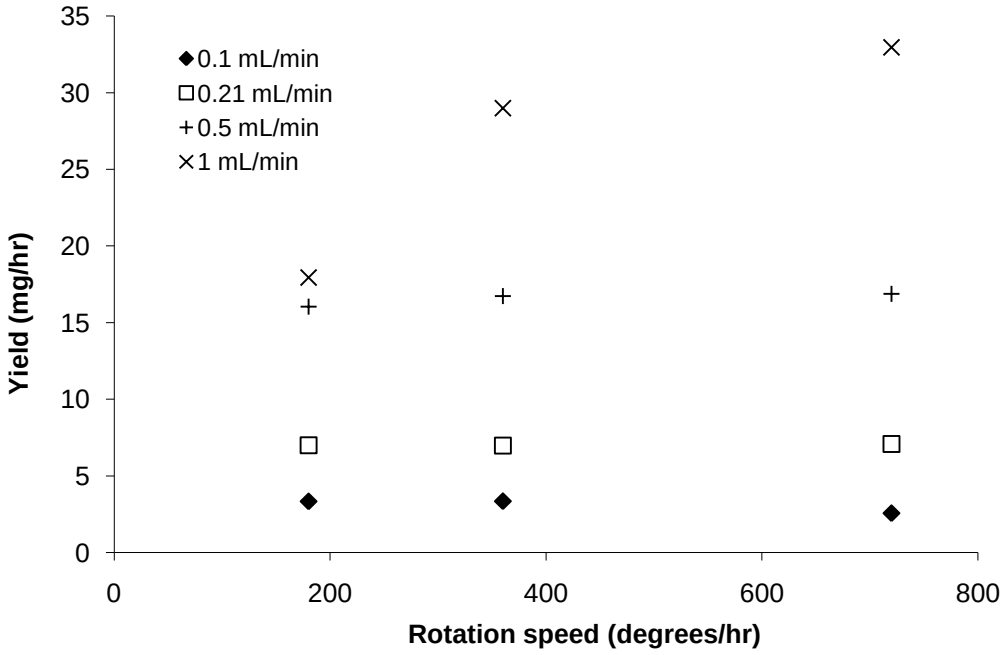

Figure 48. Yield with increasing rotation speed for Trial 2 under 1.5 mg/mL feed concentration and 1M elution buffer concentration.

5.2.3.4 Flow rate

Yield clearly increases with increasing flow rate when there are fewer loading sections and low feed concentration (Appendix G.4). Between 01mL/min to 0.5mL/min, yield at different rotation speed is equal and increase to a similar degree with increasing flow

rate (Figure 49). As flow rate becomes very high, the increase in yield is no longer equal for all rotation speeds. Higher rotation speeds would then give greater yield then lower rotation speeds.

Change in yield with increasing flow rate is affected by loading sections and feed concentration. The point of flow rate where yield with different rotation speeds start to differ may vary with different conditions. In some trials, increasing flow rate to 1mL/min causes a decrease in yield for trials with very low rotation speed (Figure 50).

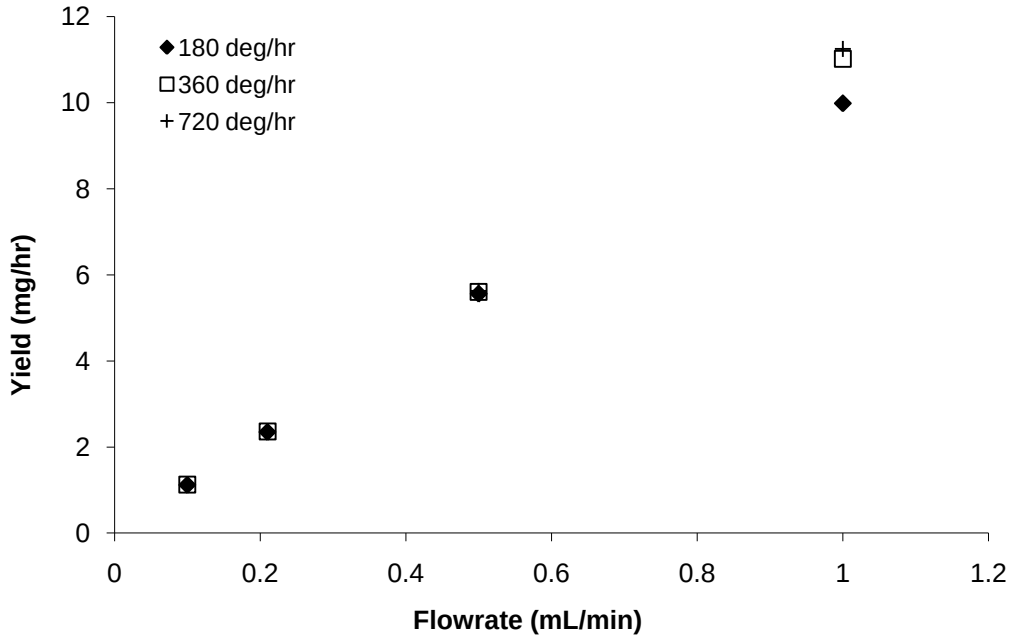

Figure 49 Yield with increasing flow rate for Trial 4 under 1.5 mg/mL feed concentration and 1M elution buffer concentration.

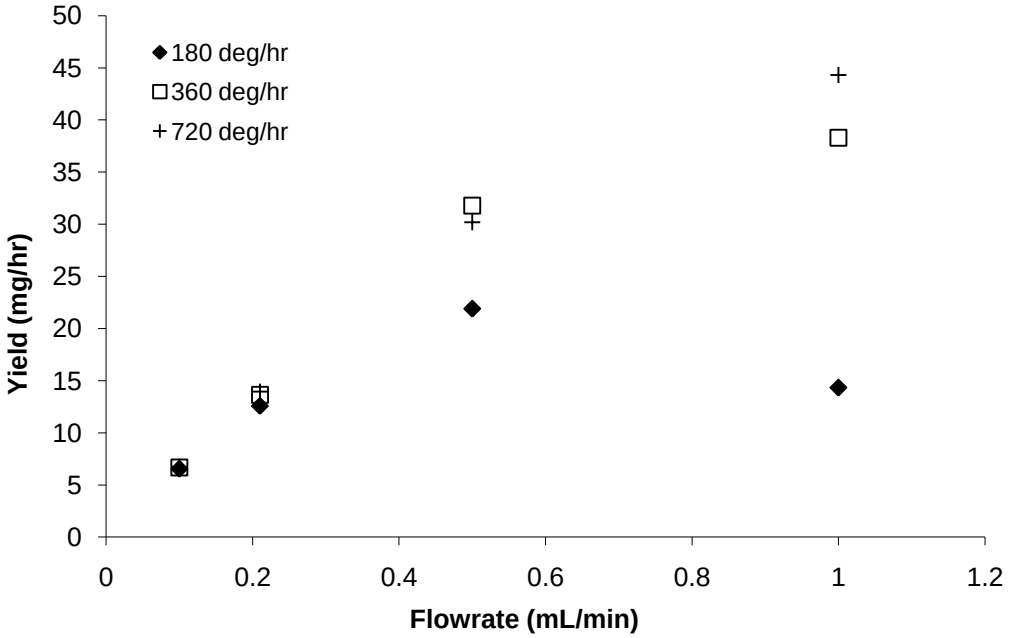

Figure 50 Yield with increasing flow rate for Trial 2 under 3 mg/mL feed concentration and 1M elution buffer concentration.

5.2.3.5 Feed concentration

Increase in feed concentration leads to greater yield for all trials at 720 deg/hr rotation speed (Figure 51 and Appendix G.5). A combination of high flow rate (0.5-1mL/min), large number of load sections (2-5 sections) and low rotation speeds (180-360 deg/hr) results in reduced yield at higher feed concentrations (Figure 52).

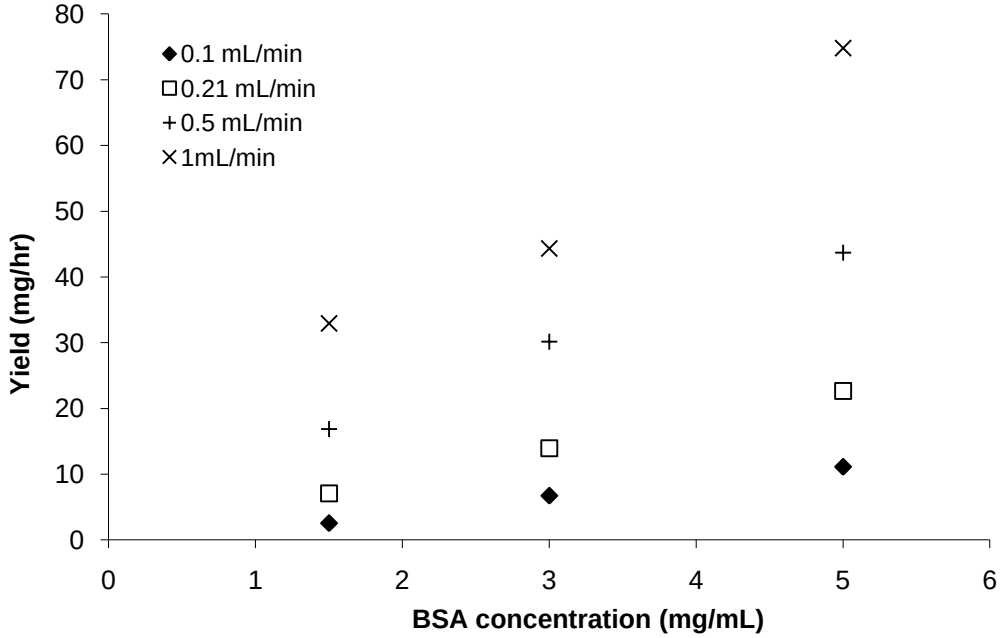

Figure 51. Yield with increasing feed concentration for Trial 2 under 720 deg/hr rotation speed and 1M elution buffer concentration.

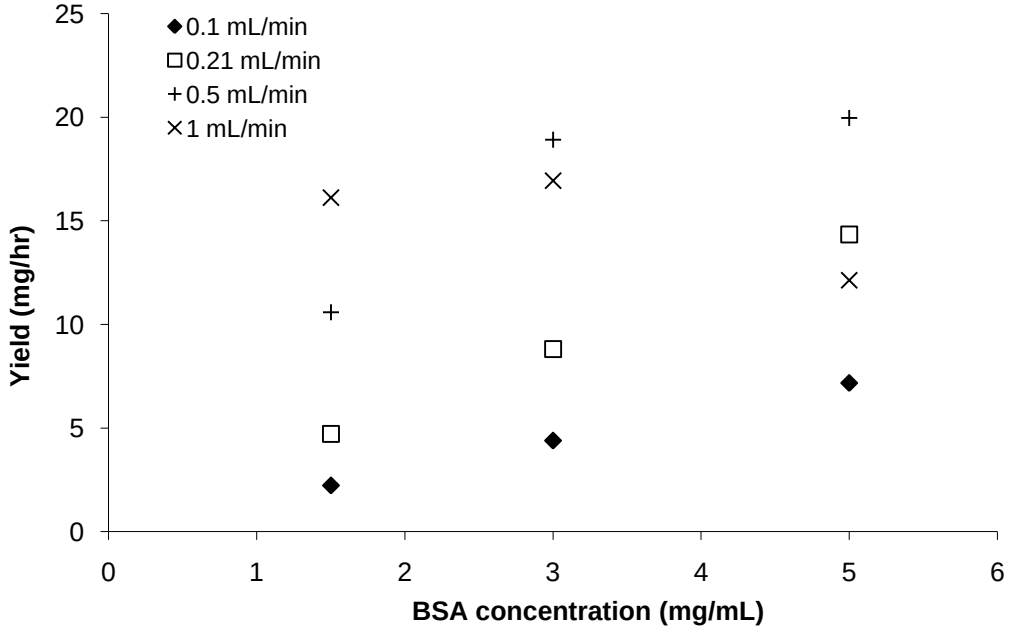

Figure 52. Yield with increasing feed concentration for Trial 7 under 180 deg/hr rotation speed and 1M elution buffer concentration.

5.2.3.6 Elution buffer concentration

Increasing elution buffer concentration did not cause any yield changes at lower flow rates. At higher flow rate of 1.0 mL/min and in some cases 0.5 mL/min, increasing elution buffer concentration to 2M NaCl resulted in a drop in yield (Figure 53 and Appendix G.6).

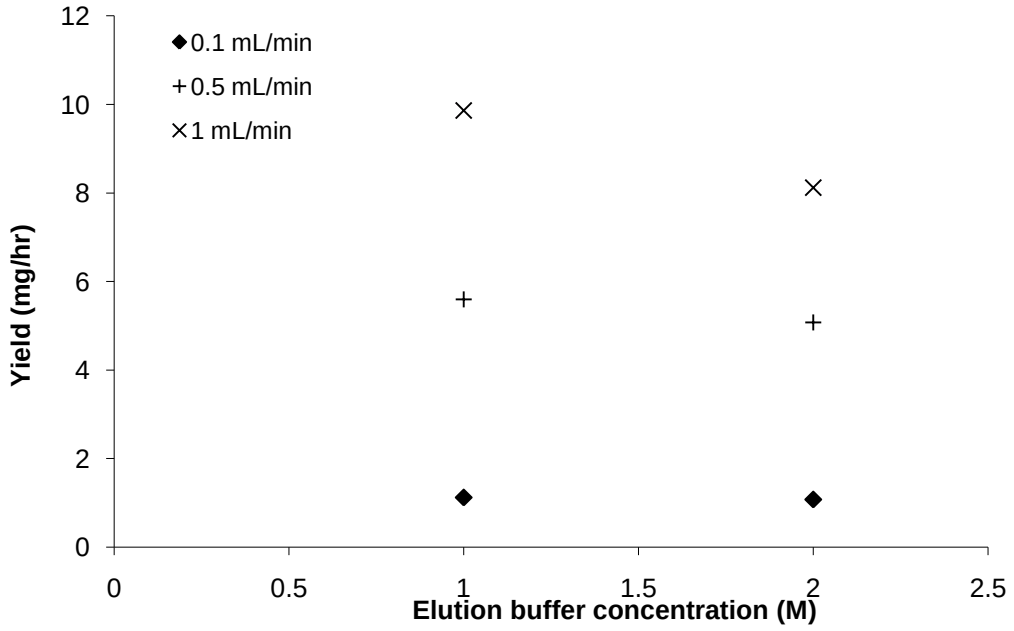

Figure 53. Yield with increasing elution buffer concentration for Trial 1 under 180 deg/hr rotation speed and 1.5 mg/mL feed concentration.

5.2.4 Trial ranking

Peak area analysis compares the amount of purified final product and protein loss separately for a single chromatography cycle. Yield analysis compares average productivity within a fixed timeframe of one hour. Peak area and yield of trials of similar conditions were compared in small numbers. Each set of data observed showed effects of varying one factor at a time and effects in combination with another variable. Changes in peak area and yield with respect to a single factor usually follow a trend but only within a particular range. Extremes of a certain parameter may cause unpredictable results or exhibit greater dependence on a second variable.

Both peak area and yield comparison gave a good indication of the best conditions to apply and the combinations to avoid. As the conclusions are based on observation of batches of data, an overall best trial and its corresponding conditions is inconclusive. In the search for the best conditions, each trial was ranked in terms of productivity, height to width ratio and overall ranking.

5.2.5 Productivity

Ranking based on productivity accounts for both product yield and loss. Yield and loss were calculated, giving amount of protein in mass per hour for each trial condition. The maximum yield and loss identified were 74.796 and 159.076 mg/hr respectively. Given that high yields are favourable while losses are unfavourable, these maximum values would correspond to the best ranked and worst ranked trials for yield and product loss respectively.

The ranking system is set in increasing order where the largest value represents the highest ranked trial. Ratio of yield for each trial to the maximum yield obtainable within the range of conditions tested would then produce the yield rank. For losses, ratio of product loss to maximum loss is subtracted from 1 to give rank in increasing order. Productivity rank is obtained from the sum of yield and loss ranks. The highest and lowest productivity rank was found to be 1.763 and 0.380 respectively.

From the list of productivity ranks calculated for each trial, the five highest and lowest ranked trials were identified (Table 7 and Table 8). All five highest ranked trials had

720 deg/hr rotation speed, 1 mL/min flow rate and 1 M elution buffer concentration. Most had feed concentration of 5 mg/mL. Loading were in the range of 2 to 5 sections while elution ranged from 1 to 3 sections.

Lowest productivity trials were found to have very low rotation speeds. Flow rate and elution buffer however, were the same with high ranking trials at 1mL/min and 1M. Loading and elution ranges were also similar to high ranking trials with loading from 3 to 5 sections and elution from 1 to 3 sections.

5.2.5.1 Rotation speed

Top five most productive trials were achieved at 720 deg/hr rotation speed. Looking further down at the next five trial ranks, 720 deg/hr rotation speeds remain most common. Lowest ranks were found in trials with 180 deg/hr rotation speed. Most productive and least productive trials had rotation speed on opposite ends of the range tested, suggesting that productivity is highly related to rotation speed. Previous results from peak area and yield analysis also indicated that as rotation speed increases, yield increase while the amount of product loss decreases.

For reconfirmation that productivity rank is higher with increasing rotation speed, five trials (A1-A5) were analyzed. The trials chosen were ones with conditions most similar to the top ranking trial conditions which also matched most of the lowest ranked trials. As the aim of understanding the effects of rotation speed on productivity is to determine the best possible conditions, it would be reasonable to analyse conditions similar to the highest ranked trials.

Trials A1-A5 showed that productivity rank is higher with faster rotation speeds (Appendix H.1.1). A more random pick of conditions (A6-A10) also showed that productivity is likely to increase with increasing rotation speeds. Therefore it is highly likely productivity increases with increasing rotation speeds within the range of 180 to 720 deg/hr.

Table 7. Highest productivity trial conditions.

Rank			Number of sections				Rotation speed (deg/hr)	Flow rate (mL/min)	Feed concentration (mg/mL)	Elution buffer concentration (M)
Productivity	Yield	Loss	Loading	Equilibration	Elution	Equilibration				
1.763	1	0.763	3	2	1	2	720	1	5	1
1.7144	0.9669	0.7474	3	1	3	1	720	1	5	1
1.7141	0.9667	0.7473	3	1	2	2	720	1	5	1
1.6946	0.7931	0.9015	2	2	2	2	720	1	5	1
1.6744	0.6992	0.9752	5	1	1	1	720	1	1.5	1

Table 8. Lowest productivity trial conditions.

Rank			Number of sections				Rotation speed (deg/hr)	Flow rate (mL/min)	Feed concentration (mg/mL)	Elution buffer concentration (M)
Productivity	Yield	Loss	Loading	Equilibration	Elution	Equilibration				
0.38	0.38	0	5	1	1	1	360	1	5	1
0.5734	0.1909	0.3825	3	2	1	2	180	1	5	1
0.5945	0.2052	0.3893	3	1	2	2	180	1	5	1
0.5962	0.2064	0.3898	3	1	3	1	180	1	5	1
0.7059	0.2008	0.5051	5	1	1	1	180	0.5	5	1

5.2.5.2 Flow rate

The highest ranking trials had 720 deg/hr rotation speeds while the lowest ranked had 180 deg/hr rotation speeds, suggesting productivity can be highly influenced by rotation speeds. In avoiding the effect of rotation speed overshadowing the effect of flow rate on productivity, trials with rotation speed of 360 deg/hr were chosen.

3 mg/mL feed concentration was used eventhough highest ranked trials were found to have feed concentrations of 5 mg/mL. Although it is possible to get a range of productivity with 5 mg/mL feed concentration, peak area and yield analysis indicated that very high feed concentration may adversely affect productivity especially when in combination with fast flow rates and high loading sections.

In trials B1-B5, productivity rank increased with increasing flow rate from 0.1 to 0.5 mL/min. From 0.5 to 1.0 mL/min, decrease in yield rank is observed for high loading sections (3-5) but not for 2 sections of loading. Trial B4 which has 5 sections of loading is affected most drastically (Appendix H.1.2).

Breakdown of the productivity into yield and product loss give a clearer view on how flow rate affects productivity ranking. Increasing flow rates increases supply of feed solution, giving the possibility of high yield. At slower flow rates, trials observed showed that protein loss is low and does not vary much with increasing flow rates. Productivity rank is therefore determined by the amount of protein captured which is reflected on flow rate. From increasing flow rate from 0.5 to 1.0mL/min, increase in protein loss is much greater than the increase in yield which results in the drop in productivity.

There is a general trend of increasing productivity with increasing flow rate but may be restricted to flow rates of 0.1 to 0.5 mL/min. Increasing productivity through increasing flow rate from 0.5 to 1.0 mL/min is only applicable when total protein load is not too high.

5.2.5.3 Feed concentration

High feed concentration can result in both high and low productivity as observed in the highest and lowest ranked trials with 5 mg/mL feed concentration. However, very high

productivity with 5 mg/mL feed concentration is found in trials with 720 deg/hr rotation speeds while 180 deg/hr rotation speeds results in very low productivity. Productivity is highly dependent on rotation speed. To observe changes in productivity with respect to feed concentration, productivity rank analysis with respect to decreasing feed concentration was carried for 180, 360 and 720 deg/hr rotation speeds (Appendix H.1.3).

Productivity was found to increase with decreasing feed concentration in all 180 rotation speed trials observed. The opposite effect was observed for trials at 720 deg/hr rotation speed. Productivity is lowered with reduced feed concentration. For 360 deg/hr rotation speed, productivity increased when feed concentration changes from 5 to 3 mg/ml. Further reducing feed concentration from 3 to 1.5 mg/mL at 360 deg/hr rotation speed resulted in 2 trials with lowered productivity and 3 trials with higher productivity.

The best combination for high productivity would be high feed concentration and high rotation speed. Other combinations giving good productivity include, 1.5 mg/mL feed concentration with 720 deg/hr rotation speed and 3 mg/mL feed concentration with 360 deg/hr rotation speed.

5.2.5.4 Loading sections

Productivity rank with respect to the number of loading sections is presented in Appendix H.1.4. At low flow rate of 0.21 mL/min, all trials observed showed an increase in productivity rank with increasing loading sections. Product loss is only reduced slightly with the increase in loading sections so increase in productivity with increasing loading section is mainly due to the increase in yield.

Productivity changes at 1.0 mL/min flow rate were more varied. When high flow rate is combined with 180 deg/hr rotation speed (Trial D6) or 5 mg/mL feed concentration (Trial D10), productivity decreases with more loading sections. Moderate feed concentration of 3 mg/mL at 360 and 720 deg/hr resulted in increases in productivity from 1 to 3 loading sections but productivity drops from 3 to 5 loading sections. When feed concentration is very low at 1.5 mg/mL, productivity increases with increasing loading section from 1 to 5 sections.

At high flow rates, product loss is more significant and increases with increasing

loading sections. Yield changes with increasing loading sections showed no common trend between the five trials observed as it is influenced differently depending on the range and combination of variables involved.

5.2.5.5 Elution sections

Trials with various combinations of rotation speed and feed concentration showed no significant changes in productivity with increasing elution sections, at both 0.21 and 1 mL/min flow rates. At 0.21 mL/min flow rate, both yield and product loss did not change with increasing elution sections. At 1 mL/min, there is slight increase in both yield and product loss. (Appendix H.1.5)

The number of elution sections has no effect on productivity, allowing flexibility in the ratio of loading to elution sections used to obtain high productivity. Any number of elution sections could produce high productivity given that the combination of conditions allows it. However, it is less cost effective to use high elution sections due to increased elution buffer volume requirements. Very high number of elution sections also results in very limited amount of possible load and reequilibration sections, which in turn limits the amount of protein load and yield.

5.2.5.6 Elution buffer concentration

Data available for observing the effect of changing elution buffer concentration on productivity is limited to feed concentration of 1.5 mg/mL. Increasing elution buffer concentration from 1M to 2M NaCl resulted in almost all trials to have decreased productivity (Appendix H.1.6).

The exceptions where productivity increased with increasing elution buffer concentration were two trials with 1.5 mg/mL feed concentration, 720 deg/hr rotation speed and mL/min flow rate. Theses two trial had load to elution section ratio of 1:1 and 3:1 respectively.

As the data collected is limited to conditions with 1.5 mg/mL feed concentration, more experimental work is required to accurately relate effect of elution buffer concentration to productivity. Within the range of conditions examined, elution buffer concentration is observed to adversely affect productivity.

5.2.5.7 Conclusion

High productivity is best achieved with rotation speed of 720 deg/hr. Using fast flow rates of 1 mL/min for high productivity is possible but not in combination with both high feed concentration and high number of loading sections. If both feed concentration and loading sections are very high, 0.5 mL/min flow rate may be more suitable.

5.2.6 Height to width

Height to width (HTW) ratio comparison of the elution zone protein peaks is an alternative way of searching for the best trial conditions. The greater the HTW ratio or sharper peaks, would represent a better chromatography run. In the HTW ranking system, the maximum value which was found to be 508.89 mAU/min represents the highest ranked trial. HTW ratio of a trial divided by the maximum HTW ratio would allocate a rank relative to other trials.

From the list of HTW ranks calculated, the five highest and lowest ranked trials were identified (Table 9 and Table 10). The highest ranked trials had 720 deg/hr rotation speed, 1 mL/min flow rate and 1 M elution buffer concentration. Feed concentration was observed to be between 1.5 and 5 mg/mLwhile loading and elution sections were varied from 1 to 5 sections.

Lowest ranked trials also had 720 deg/hr rotation speeds with one exception at 360 deg/hr. Feed concentration, flow rate and elution buffer were 1 mg/mL, 0.1 mL/min and 2M respectively, for all trials. Loading was restricted to one section while elution ranges from 1 to 5 sections.

5.2.6.1 Rotation speed

Rotation speed, on its own is unlikely a very important determinant of HTW ratio as indicated by both highest and lowest ranked trials having 720 deg/hr rotation speeds. Trials chosen in the investigation of changes in HTW ranking with increasing rotation speed include different combination of flow rate, feed concentration, loading sections, and elution sections (Appendix H.2.1).

HTW ratio was found to increase with increasing rotation speed for most trials examined. The cases (Trial A1, A6 and A7) where HTW ratio decreased with increasing rotation speeds showed common characteristic of 1 section loading. HTW ratio for some trials increase from 180 to 360 deg/hr and then decreases as rotation speeds increases from 360 to 720 deg/hr. This implies that drop in HTW ratio is more likely to occur at higher rotation speeds. HTW ratio is generally greater with faster rotation speeds.

HTW ratio evaluates protein peaks as output concentration over time. However it does

not show the angular distance at which eluted proteins exit the CRFC. Peak width measured as angular distance can be calculated by multiplying peak width in terms of time with the rotation speed of the annulus. Almost all trials compared showed an increase in total angle of elution with increasing rotation speeds (Appendix H.2.7).

5.2.6.2 Flow rate

Highest HTW ratio trials had 1 mL/min flow rate while the lowest ranked trials had 0.1 mL/min flow rate (Table 9 and Table 10). Although not shown, the next five highest and five lowest ranking trials also had 1 mL/min and 0.1 mL/min flow rates respectively.Flow rate is the only parameter with the ten highest ranking trials on one end of the range tested and the ten lowest ranks on the opposite end of the range. This implies that there is strong correlation between flow rate and HTW ratio.

Trials with various combinations of rotation speeds, feed concentration, loading sections and elution sections were analyzed for change in HTW ranking with increasing flow rate (H.2.2). All trials (B1-B10) analyzed showed an increase in HTW with increasing flow rate which concludes that HTW ratio increases with flow rate

5.2.6.3 Feed concentration

Most of the lowest ranked trials had 1.5 mg/mL feed concentration. However these low feed concentrations are in combination with 0.1 mL/min flow rate and flow rate was found to be highly influential on HTW ratio. In addition to that, very low ranks have conditions of 2M elution buffer concentration, which may be the main cause of low HTW ratio. Very high HTW ratio is achievable with 1.5 mg/mL feed concentration, which reinforces the fact that feed concentration alone may have very little or no effect on HTW ratio.

Table 9. Highest HTW ratio trial conditions.

Rank	Number of sections				Rotation speed (deg/hr)	Flow rate (mL/min)	Feed concentration (mg/mL)	Elution buffer concentration (M)
HTW	Loading	Equilibration	Elution	Equilibration				
1	3	2	1	2	720	1	1.5	1
0.9906	5	1	1	1	720	1	1.5	1
0.9492	1	1	5	1	720	1	5	1
0.9453	1	3	1	3	720	1	5	1
0.9341	2	2	2	2	720	1	1.5	1

Table 10. Lowest HTW ratio trial conditions.

Rank	Number of sections				Rotation speed (deg/hr)	Flow rate (mL/min)	Feed concentration (mg/mL)	Elution buffer concentration (M)
HTW	Loading	Equilibration	Elution	Equilibration				
0.0219	1	2	3	2	720	0.1	1.5	2
0.0302	1	1	5	1	720	0.1	1.5	2
0.0321	1	2	2	3	720	0.1	1.5	2
0.0352	1	2	3	2	360	0.1	1.5	2
0.0417	1	3	1	3	720	0.1	1.5	2

Further HTW rank analysis with 15 trials with a range of loading and elution sections, flow rate and rotation speeds showed that increasing feed concentration resulted in no obvious trend in HTW ratio changes with respect to feed concentration (Appendix H.2.3).

Various causes could have resulted in the different changes in HTW ratio with increasing feed concentration. Increasing feed concentration would be expected to increase the amount captured, thus giving higher concentration of eluted proteins. If loading zone protein peak is less distinctly separated from or overlaps the elution zone peak, then cut off point to obtain peak width would result in HTW ratio larger than trials with completely separated loading and elution peaks. The loading peaks may be due to overloading or insufficient reequilibration. When insufficient reequilibration results in elution peak shouldering or tailing, then the HTW is lowered.

5.2.6.4 Loading sections

Highest HTW ranks were found in trials with a wide range of loading sections while all ten lowest ranked trials had only one loading section. These trial conditions however, are not indicative of how HTW ratio changes with the number of loading sections. Further analysis was carried out with ten different trial conditions (Appendix H.2.4).

Most trials at 0.5 mL/min flow rate showed that HTW ratio increases with increasing loading sections. In increasing loading from 3 to 5 sections at this flow rate, both increasing and decreasing HTW ratio were observed. This inconsistent change in HTW ratio with increasing loading sections is not limited to a single rotation speed and feed concentration. At 1.0 mL/min flow rate, all trials increased in HTW ratio from 1 to 5 loading sections.

Although there were HTW ratio differences with different number of loading sections, the rank changes were very small. HTW ratios under the conditions examined were also of relatively good ranking, with the best trials within those analyzed being in the top 30 HTW ranking. When total protein input mass is not too high or too low, HTW is of good ranking and would remain or increase with increasing loading sections.

5.2.6.5 Elution sections

Both very high and very low HTW ratio can be obtained with any number of elution sections between 1 and 5. In search of the correlation between number of elution sections and HTW ratio, 15 trials were examined (Appendix H.2.5). Trials with one loading section were observed for HTW rank changes with increasing elution section from 1 to 5 sections. Trials with three loading section were observed from increasing elution sections from 1 to 3 sections.

No obvious trend of increasing or decreasing HTW ratio with increasing number of elution section was found with one section of loading. Among the ten trials with one loading section, six trials which consists mostly of trials with 3-5 mg/mL feed concentration, had highest HTW ranking with one elution section while four trials had highest HTW ratio at five elution sections. For trials with three sections of loading, HTW ratio was observed to decrease with increasing number of elution sections with no exceptions.

Results from comparing HTW ranking of trials with increasing elution sections may not be conclusive, but one section of elution would be compatible with a wider range of conditions in generating high HTW ratio.

5.2.6.6 Elution buffer concentration

All available trials with comparative conditions were observed for changes in HTW ratio with increasing elution buffer concentration (Appendix H.3.6). Most trials showed a decrease in HTW ratio from 1M to 2M elution buffer concentration. At 180 deg/hr rotation speed, less than half the trials observed had reduced HTW ratio. Among trials which showed greater HTW ratio, most were found to have 1 mL/min flow rates and five sections of loading.

As rotation speed increases, more trials had reduced HTW ratio with higher elution buffer concentration. At 720 deg/hr rotation speed, all trials were adversely affected by increasing elution buffer concentration. The combination of 720 deg/h rotation speed, 0.1 mL/min flow rate and 2M elution buffer concentration not only resulted in the worst HTW ratio within the range analyzed for the effect of elution buffer concentration but among all experimental trial conditions carried out.

5.2.6.7 Conclusion

In general, HTW ratio increases with increasing flow rate and rotation speed. However, very high rotation speeds may also cause HTW ratio decrease especially with very low protein load. Number of loading sections does not have much effect on HTW ratio, provided that total protein loaded is neither very high nor very low. One section of elution at 1M concentration would be sufficient and most compatible with a wide range of conditions. Higher elution buffer concentration may increase HTW ratio but only at 180 deg/hr rotation speeds. General correlation between feed concentration and HTW ratio could not be concluded from the results.

5.2.7 Overall ranking

Productivity measurements consider both the product output and product loss per unit input. HTW ratio measures the degree of product concentration per unit time. Both productivity and HTW ratio are important measurements of the quality of any protein purification processes. The range of productivity level and HTW ratio requirements could vary depending on the final product specifications or chromatographic objectives.

Overall rank is the sum of productivity rank and HTW ratio rank. Assuming that productivity and HTW ratio are equally favourable, overall rank would give a good representation of the best results. The highest and lowest overall ranked trials are presented in Table 11 and Table 12. Amoung the best overall ranks, the same conditions were found to have best productivity ranks too.

5.2.7.1 Rotation speed

Rotation speed for the lowest and highest ranking trials are at opposite extremities with 180 deg/hr and 720 deg/hr respectively. Therefore increasing rotation speed would be expected to increase ranking. By increasing rotation speed and maintaining all other conditions the same as the five lowest ranked trials, ranking was observed to increase significantly (Appendix H.3.1). At 720 deg/hr, the trials were in the top 20 ranks. As these trials had high flow rates and high feed concentrations, the assumption that overall rank increase with increasing rotation speeds may be biased.

Analysis of overall rank changes for other more trials were carried out to determine if effect of increasing rotation speeds on overall ranking is the same for all other conditions. Among the different combinations of flow rate, feed concentration loading sections and elution sections, overall rank was found to increase with increasing rotation speeds with the exception of 0.1 mL/min flow rate in combination with 1.5 mg/mL feed concentration.

Provided that the amount of protein loaded is not very small due to conditions such as low flow rate and low feed concentration, faster rotation speeds would result in higher overall ranking.

Table 11. Overall highest ranking trial conditions.

Rank	Number of sections				Rotation speed (deg/hr)	Flow rate (mL/min)	Feed concentration (mg/mL)	Elution buffer concentration (M)
Overall	Loading	Equilibration	Elution	Equilibration				
2.6884	3	2	1	2	720	1	5	1
2.6649	5	1	1	1	720	1	1.5	1
2.5191	3	1	2	2	720	1	5	1
2.4355	3	2	1	2	720	1	1.5	1
2.4222	1	1	5	1	720	1	5	1

Table 12. Overall lowest ranking trial conditions.

Rank	Number of sections				Rotation speed (deg/hr)	Flow rate (mL/min)	Feed concentration (mg/mL)	Elution buffer concentration (M)
Overall	Loading	Equilibration	Elution	Equilibration				
0.76215	3	1	3	1	180	1	5	1
0.7918	3	1	2	2	180	1	5	1
0.90665	3	2	1	2	180	1	5	1
0.93406	5	1	1	1	180	0.5	5	1
1.00768	2	2	2	2	180	1	5	1

5.2.7.2 Flow rate

Lowest and highest ranked trial have flow rates of 1 mL/min. Looking at the complete spreadsheet of data however shows that on average, low flow rates results in very low ranking and rank increases with increasing flow rate.

Based on ten selected trials, increasing flow rate from 0.1 to 0.5 mL/min was found to increase the overall trial ranks (Appendix). At higher flow rate range, there were seven trials with increased ranks. Another three trials which had conditions of 180-360 deg/hr rotation speed, 3-5 mg/mL feed concentration and 2-3 loading sections, showed a decrease in rank from increasing flow rate from 0.5 to 1 mL/min.

High flow rates, slow rotation speeds, high feed concentration and high number of loading sections increases protein load per chomatogrpahy cycle. Increasing protein load would normally result in greater product output. However, overloading above media capacity would only lead to increase in product loss. Therefore, high flow rates should only be applied when there is no protein overload with combined effects of rotation speed, feed concentration and loading sections.

5.2.7.3 Feed concentration

Highest ranked trials incorporated feed concentration of 1.5 and 5 mg/mL in combination with similar rotation speeds, flow rate, loading sections and elution buffer concentration, indicating variable effect of feed concentration on rank. Overall ranks with respect to feed concentration is shown in Appendix H.3.3.

Trial ranks compared at 180 deg/hr rotation speeds showed that decreasing feed concentration increases overall rank. At 360 deg/hr rotation speed, decreasing feed concentration resulted in four trials with increasing ranks and one trial best ranked with average (3 mg/mL) feed concentration. The exception would suggest that high loading sections would be best combined with 3 mg/mL feed concentration.

Most varied rank changes with feed concentration were observed with 720 deg/hr rotation speeds. At very high rotation speeds, the trial were mostly ranked lowest at 3 mg/mL feed concentration. Ranks were mostly highest at 5 mg/mL followed by 1.5 mg/mL feed concentration. Similar to the trials observed at 360 deg/hr, five loading

sections at 720 deg/hr rotation speed also gave highest ranking with 3 mg/mL feed concentration.

5.2.7.4 Loading sections

Very high overall rank can be achieved with any of the number of loading sections tested but depending on the number of loading sections, best results may be obtained with different combination of conditions. As high flow rates were found to produce better ranking trials, the trials conditions chosen for observing the effect of loading sections were restricted to 0.5 and 1 mL/min flow rates (Appendix H.3.4).

At 0.5 mL/min flow rate, most trial ranks increased with increasing loading sections. When conditions included either 180 deg/hr rotation speed or 5 mg/mL feed concentration ranks increased with increasing loading sections from 1 to 3 sections but is followed by a drop at five loading sections.

At 1 mL/min flow rate decrease in ranks from increasing loading section from 3 to 5 sections were observed in trials with higher rotation speeds of 360 and 720 deg/hr. For 180 deg/hr rotation speed and 5 mg/mL feed concentration trials, one section of loading gave the best ranks and continuously decreases with increasing loading sections. Results showed that higher flow rates caused the adverse effect of increasing loading section to be more severe and the onset of decrease in rank to start at lower number of loading sections. The only trial that increased in rank with increasing loading sections had 1.5 mg/mL feed concentration.

5.2.7.5 Elution sections

Both overall best and worst ranked trials consisted of conditions with the number of elution sections ranging from 1 to 5 sections, giving no indication of the preferred range to obtain higher overall rank. Therefore trials were analyzed under all rotation speeds, high flow rates and in combination with 1 and 3 loading sections (Appendix H.3.5).

The effect of increasing elution section from 1 to 5 sections resulted in varied changes in overall ranks when loading amounts to one section. For trials with loading of three sections, increasing elution sections from 1 to 3 sections caused an increase in overall trial ranking for all trials analyzed. However rank changes were very small, especially

between 2 to 3 elution sections.

Increasing elution sections produces very small increase in overall rank with higher loading sections and unpredictable changes with 1 section of loading. As the changes present, if any is very small, the least number of elution sections would be sufficient. Small elution sections would allow greater possible ranges for loading and equilibration steps.

5.2.7.6 Elution buffer concentration

The effect of increasing elution buffer concentration was investigated with 1M and 2M NaCl concentration. Out of the 80 trials observed, only ten cases increased in overall rank with increasing elution buffer concentration (Appendix H.3.6). These trials were mostly with conditions of 180 deg/hr rotation speeds and 1 mL/min flow rates.

Given that the majority of trials were adversely affected by higher elution buffer concentrations, 1M salt concentration would be appropriate for the elution of BSA under the range of conditions tested.

5.2.7.7 Conclusion

Faster rotation speeds produced higher overall ranking with the exception where the protein load is very small due to conditions such as low flow rate and low feed concentration. High flow rates can be applied for better overall ranking but not in combination with conditions which results in very high protein load. Feed concentration and number of loading sections for best results will be related to rotation speed and flow rate. Total amount of protein loaded should be high for efficient use of the media but must not exceed media capacity.

Increasing elution sections results in increase or variable changes in overall ranking but as effects are small one elution section would be sufficient. As increasing elution buffer concentration reduced overall ranking in most of the trials, 1M concentration should be used for the elution of BSA under range of conditions tested.

5.2.8 Recommended conditions

5.2.8.1 Protein load

Rotation speed sets the time spent by a section at an input port while the number of loading sections gives the total time allocated to the protein loading step. Flow rate determines the volume of solution supplied per unit time. The combination of rotation speed, loading sections and flow rate dictates the total volume of feed solution entering the column for each cycle. Feed concentration and the total volume of feed solution would then determine the mass input of protein per cycle.

Maximum binding capacity of the HiTrap DEAE Fast Flow column used for the experiments is ranged about 80-120 mg/mL. As the typical recommended range is 1-100 mg/mL, maximum capacity is taken as 100 mg/mL. Out of the total number of trials carried out, 17 trials had greater than 100 mg of protein load per cycle (Table 13). Among these trials, six trials had lowest overall ranked of the total 401 trials carried out. The other overloaded trials were also mostly ranked below average. Therefore, best conditions for BSA purification on the CRFC would exclude any of the combinations of feed concentration rotation speed, flow rate and load sections in Table 13.

Protein load near maximum media capacity is also not recommended. Although overall rank may not be very low in comparison with all trials that were carried out, results show that trials with protein load near 100 mg/mL is only ranked slightly above average. As the media approaches saturation point, protein adsorption slows down. The conditions which assist in producing good results from maximising productivity and HTW ratio would then be less efficient.

Table 13. Trials with protein load greater than 100 mg BSA per cycle.

Protein load mg	Overall rank	feed concentration mg/mL	Rotation speed deg/hr	Flow rate mL/min	Load sections
225	0.7621	5	180	1.0	3
225	0.7918	5	180	1.0	3
225	0.9067	5	180	1.0	3
187.5	0.9341	5	180	0.5	5
150	1.0077	5	180	1.0	2
187.5	1.0174	5	360	1.0	5
135	1.0595	3	180	1.0	3
135	1.0671	3	180	1.0	3
112.5	1.1341	5	180	0.5	3
112.5	1.1658	5	180	0.5	3
112.5	1.1807	5	180	0.5	3
135	1.2065	3	180	1.0	3
112.5	1.2454	3	180	0.5	5
112.5	1.3440	5	360	1.0	3
112.5	1.3484	5	360	1.0	3
112.5	1.3965	3	360	1.0	5
112.5	1.5504	5	360	1.0	3

Very low amounts of protein load can also lead to extremely low overall ranking. Small protein load is a result of low feed concentration, slow rotation speed, low flow rate and few load sections. Table 14 shows trials with protein load less than 1.2 mg and their conditions. When protein load is low, the amount of product would still be low even with maximum yield and no loss. Higher rotation speed may allow more purified protein to be obtained per unit time but it will not amount to much when protein load per cycle is extremely low.

Table 14. Trials with protein load less than 1.2 mg BSA per cycle.

Protein load mg	Overall rank	feed concentration mg/mL	Rotation speed deg/hr	Flow rate mL/min	Load sections
0.56	1.0325	1.5	720.0	0.1	1
0.56	1.0379	1.5	720.0	0.1	1
0.56	1.0440	1.5	720.0	0.1	1
1.13	1.0497	1.5	360.0	0.1	1
1.13	1.0549	1.5	360.0	0.1	1
0.56	1.0567	1.5	720.0	0.1	1
1.13	1.0570	1.5	360.0	0.1	1
0.56	1.0590	1.5	720.0	0.1	1
0.56	1.0633	1.5	720.0	0.1	1
1.13	1.0690	1.5	360.0	0.1	1
0.56	1.0710	1.5	720.0	0.1	1
0.56	1.0711	1.5	720.0	0.1	1
1.13	1.0846	3.0	720.0	0.1	1
1.13	1.0855	1.5	720.0	0.1	2
1.13	1.0895	3.0	720.0	0.1	1
1.13	1.0904	1.5	360.0	0.1	1
1.13	1.0990	3.0	720.0	0.1	1
1.13	1.0997	1.5	360.0	0.1	1
1.13	1.1092	1.5	360.0	0.1	1
1.13	1.1127	3.0	720.0	0.1	1
1.13	1.1263	1.5	360.0	0.1	1
1.13	1.1350	1.5	720.0	0.1	2
1.18	1.1478	1.5	720.0	0.21	1
1.18	1.1499	1.5	720.0	0.21	1
1.18	1.1539	1.5	720.0	0.21	1
1.18	1.1590	1.5	720.0	0.21	1

5.2.8.2 Flow rate

Flow rate is not only important in determining the mass protein load through manipulating the volume of feed solution entering the column. Flow rate also determines the supply of solutions for equilibration and elution. At flow rate of 0.1 mL/min and one section of loading, all corresponding trials ranked in the lowest 100 range except one trial (Table 15). These include trials with different rotation speeds, feed concentration and elution buffer concentration. Some of these trials had moderate

amount of protein loads.

Table 15. Trials with 0.1 mL/min flow rate and one loading section.

Solution input per section mL	Overall rank	Protein load mg	Solution input per section mL	Overall rank	Protein load mg
1.50	1.1187	2.25	1.50	1.1829	7.50
1.50	1.1172	2.25	1.50	1.1685	7.50
1.50	1.1287	2.25	1.50	1.1338	7.50
1.50	1.1224	2.25	1.50	1.1172	7.50
0.75	1.1092	1.13	0.75	1.1832	3.75
0.75	1.1263	1.13	0.75	1.1648	3.75
0.75	1.0997	1.13	0.75	1.1516	3.75
0.75	1.0904	1.13	0.75	1.1349	3.75
0.38	1.0711	0.56	0.38	1.1237	1.88
0.38	1.0710	0.56	0.38	1.1501	1.88
0.38	1.0633	0.56	0.38	1.1450	1.88
0.38	1.0590	0.56	0.38	1.1520	1.88
1.50	1.1447	4.50	1.50	1.1035	2.25
1.50	1.1205	4.50	1.50	1.0806	2.25
1.50	1.0982	4.50	1.50	1.0801	2.25
1.50	1.1139	4.50	1.50	1.0841	2.25
0.75	1.2280	2.25	0.75	1.0690	1.13
0.75	1.1325	2.25	0.75	1.0570	1.13
0.75	1.1119	2.25	0.75	1.0497	1.13
0.75	1.1151	2.25	0.75	1.0549	1.13
0.38	1.1127	1.13	0.38	1.0567	0.56
0.38	1.0990	1.13	0.38	1.0440	0.56
0.38	1.0895	1.13	0.38	1.0325	0.56
0.38	1.0846	1.13	0.38	1.0379	0.56

Trials with low flow rates have high risk of incomplete reequilibration as the small volume of equilibration buffer is incapable of washing out all the salt introduced in the elution step. Remaining salts from one cycle would result in high protein loss in the next separation cycle. Low flow rates also result in peak broadening which would lower the HTW ratio ranking. Dispersion occurs as proteins slowly travel through the chromatography system.

5.2.8.3 Throughput

Protein load per cycle must neither be too high (above resin capacity) nor too low to allow average to high amounts of protein to be adsorbed onto the resin without high losses. Next important factor to consider is the amount of protein that can be processed within a fixed amount of time. Throughput is obtained as protein mass per unit time, allows comparative efficiency of trials with different rotation speeds.

Trials with rotation speeds of 720, 360 and 180 deg/hr would require 30, 60 and 120 minutes respectively, for a complete chromatography cycle. Given that the protein load is equal in all trials compared, different rotation speeds would result in different amounts of throughput within an hour with 720 deg/hr rotation speed producing the most throughput. Therefore, overall best results can be obtained with 720 deg/hr rotation speeds.

5.2.8.4 Best CRFC operation conditions

A good chromatography separation in any column would involve efficient utilisation of the media to produce high productivity and high HTW ratio peaks. In the continuous purification of BSA in the CRFC, best overall results is produced when protein load per cycle is within a good range, flow rate is sufficiently high and rotation speeds gives the highest throughput.The corresponding conditions would include high flow rate, high rotation speed, high feed concentration, high loading sections, low elution section where possible and1M elution buffer concentration. These conditions however exclude combinations which result in protein overload (Table 13) and protein load close to maximum binding capacity of the media (80-100 mg)

High rotation speeds produce greater throughput while fast flow rates prevent salt effects and increases HTW ratio. Therefore these two parameters should be kept within

the upper range. When protein load is sufficiently high, either the number of loading sections or feed concentration can be at a lower range. Following the criteria and restrictions discussed, the recommended conditions would then match the five highest overall ranked trials (Table 11).

Table 16. Recommended conditions for best results

Rotation speed	Flow rate	BSA	NaCl	Loading	Equilibration	Elution	Equilibration
deg/hr	mL/min	mg/mL	M	sections			
720	1	5	1	3	2	1	2
720	1	5	1	3	1	2	2
720	1	5	1	1	1	5	1
720	1	5	1	1	3	1	3
720	1	5	1	3	1	3	1
720	1	5	1	2	2	2	2
720	1	5	1	1	2	2	3
720	1	1.5	1	5	1	1	1
720	1	1.5	1	3	2	1	2
720	1	1.5	1	3	1	3	1

5.2.9 Problems

Various problems were encountered during the course of collected experimental data. Any affected results were rejected and the trial repeated.

5.2.9.1 Overpressure

Axial flow column experiments were carried out in trials of three with each trial having three continuous cycles. The total run time which includes additional equilibration time between trials with different conditions and after the final cycle, ranges between 8 and 21.5 hours. As these experiments were run daily, over time high pressures from clogging of the solution filter would occur and was solved by replacing the filter. BSA accumulation in the column also resulted in overpressure in the system during earlier trial runs with 1 mL/min flow rate and 120 min cycle time (slow rotation speed). This is however rare, as the column was regenerated periodically and usually prior to trials with high protein loads.

5.2.9.2 Air bubbles

Air introduced into the system resulted in poor elution peak profiles. This problem was eliminated with the flushing of the pumps and spectrophotometer, and degassing of the solutions prior to each run.

5.2.9.3 Data export

Results from the AKTA system exported into Excel spreadsheets may not accurately represent the actual peaks. The number of data points exported remains the same regardless of the duration of the run or the number of peaks present. Therefore when many trials were fitted into a single run, some data points were lost during data export. The resulting peaks plotted in excel were inconsistent. Three trials with three replicates each in one run gave good peak resolution from the exported data.

5.3 Comparison between simulated and experimental results

BSA elution in the CRFC was modelled under the recommended conditions (Table 16) and compared to the experimental results.Simulations were programmed in Matlab as given in (Appendix J.1). Although experiments were carried out to represent the continuous operation of the CRFC, model simulations were based on an axial column of the same dimensions used for the experimental work for a more accurate comparison.

Initial model parameters used were obtained from earlier works on the CRFC (Lay 2005). This set of parameters was not suitable for many of the experimental conditions, including the recommended best conditions used for model comparison. Unsuccessful simulation was due to insufficient computer memory and unstable simulations resulting in negative solute concentration. A range of values for individual parameters and in combination with each other was tested to produce a successful elution profile. The parameters were then adjusted to achieve a better fit experimental data.

The set of parameter which gave good comparative protein profiles are shown in Table 17. Simulated data and the corresponding experimental data are presented in Figure 54-Figure 56 and Appendix I.

Table 17. BSA and NaCl parameters for simulation data and experimental data comparison.

Parameters	BSA	NaCl
k_f (cm/s)	0.003	0.0001
K (mL/ mg	47	1500
k_1 (mL/ mg.s)	0.001	0.001
k_2 (1/s)	0.00002	0.0000007
C_{Rmax} (mg/mL)	100	1.5

Column bed was modelled in N number of stages. Simulations with larger number of stages produce better resolution. However, large number of stages may not be applicable when the Matlab simulations require larger memory than which is available in the operating system. The maximum number of stages that can be applied with the

model as programmed, decreases with increasing flow rate. At 1 mL/min, the number of stages is set at 10. The J factor sets the number of simulation time steps by fixing the change in time from one step to the next. Higher number of steps produces greater prediction accuracy but requires longer processing time. Simulations were carried out at J=5.

5.3.1 Loading zone peak

Breakthrough or loading zone peaks from the experimental results which was thought to be an unusual occurance as protein load was below maximum resin capacity, was also produced in the simulation. As the modelled column is salt free at the loading step, the breakthrough peak is not due to residual salts. Simulated breakthrough may be a result of the protein rate parameters or maximum resin capacity set.

Simulation and experimental loading zone peaks match well for both retention time and peak width. However sharper peaks and tailing were observed in the experimental results. For conditions with three loading sections and 5 mg/mL feed concentration (Figure 54), column experiments produced more proteins in the loading zone.

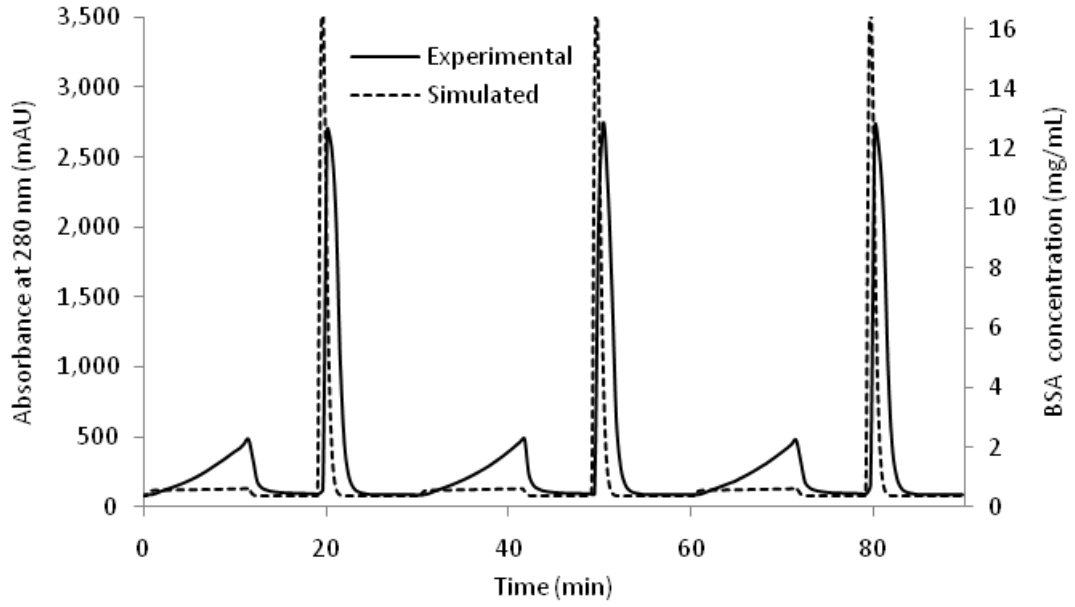

Figure 54. Simulated and experimental BSA elution profiles with 5 mg/mL BSA concentration, 720 rotation speed, 1 mL/min flow rate, 1M NaCl concentration, 11.25 min loading, 7.5 min equilibration, 3.75 min elution and 7.5 min reequilibration.

Condition of one loading section and 5 mg/mL (Figure 55) on the other hand produced less protein loss in the loading zone than simulated. At 1.5 mg/mL feed concentration and three loading sections, experimental data showed no obvious protein peaks while simulated loading zone peaks were observed (Figure 56). Protein parameters may need to be adjusted to different loading time and feed concentration to match experimental loading zone peaks.

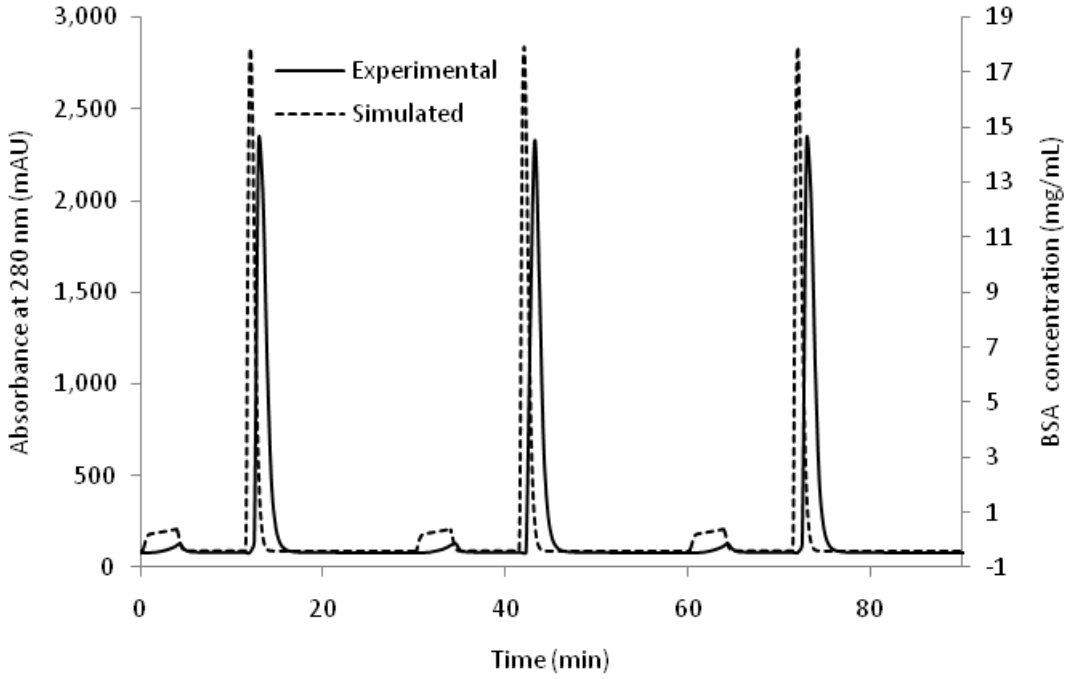

Figure 55. (a) Simulated and (b) experimental BSA elution with 5 mg/mL BSA concentration, 720 rotation speed, 1 mL/min flow rate, 1M NaCl concentration, 3.75 min loading, 7.5 min equilibration, 7.5 min elution and 11.25 min reequilibration.

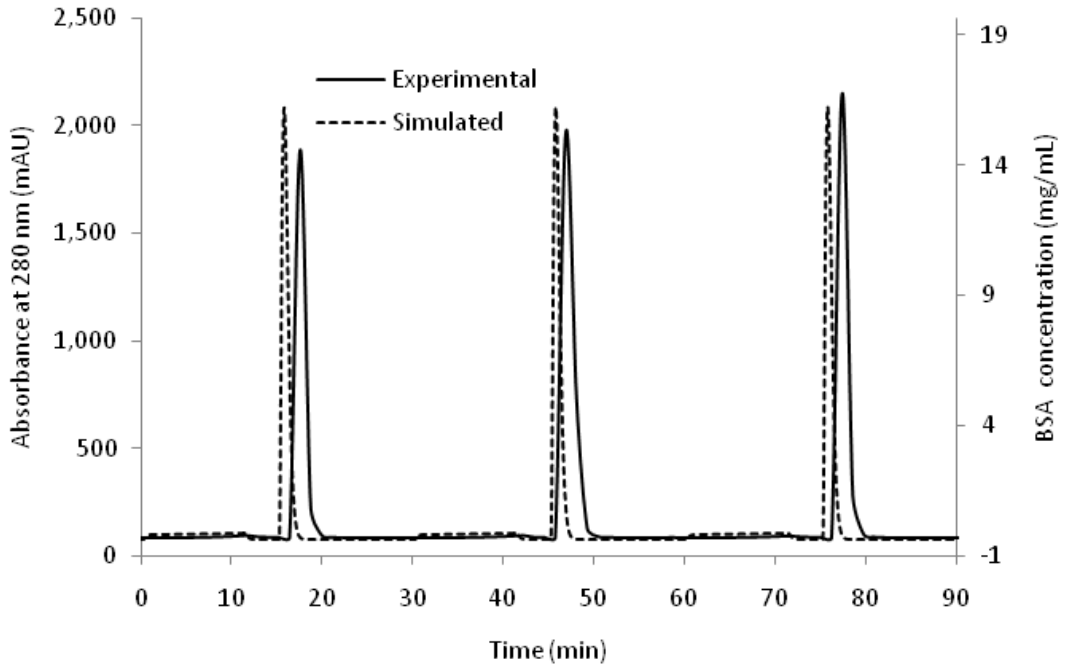

Figure 56. Simulated and experimental BSA elution profile with 1.5 mg/mL BSA concentration, 720 rotation speed, 1 mL/min flow rate, 1M NaCl concentration, 11.25 min loading, 3.75 min equilibration, 11.25 min elution and 3.75 min reequilibration.

5.3.2 Elution zone peak

Simulated data agreed well with the experimental data in the elution zone but the experiments produced broader and higher elution peaks. Figure 54-56 show simulated elution peaks with maximum protein concentration at about 50, 18 and 16 mg/mL. The experimental elution peaks under the same conditions had higher protein concentrations at 70, 22 and 27 mg/mL.

The retention time was also slightly different with simulated peaks occurring earlier. This may be an indication that there Cl^- ion competes with BSA for the resin matrix to a greater degree causing faster protein desorption in the model. Peak tailing were found in both simulated and experimental peaks.

Varying the model parameters changes the loading zone and elution zone peaks. Decreasing protein kf and k1 resulted in more unadsorbed proteins which is observed by the increase in loading zone peaks area. Increasing CRmax increases protein elution peaks. Manipulating k1 and k2 for NaCl also result in changes to protein peaks while varying CRBmax had no effect.

Chapter 6: Conclusion

5.4 Conclusions

Continuous radial flow chromatography (CRFC) combines two separate systems; the radial flow chromatography and rotating annular bed chromatography. Thus the CRFC has added advantages of multicomponent separations at higher throughput and lowered pressure drop compared to conventional axial flow chromatography systems. The overall cost of operation is reduced giving it the potential for industrial application.

An efficient chromatography separation maximises the usage of the media, has high productivity and high HTW ratio (or peak resolution for multicomponent separations). As observed in axial flow column experiments which represents the continuous operation of the CRFC, the best conditions for efficient BSA purification under the current CRFC prototype are:

- 720 deg/hr rotation speed
- 1 mL/min flow rate,
- 5 or 1.5 mg/mL BSA
- 1M NaCl
- Loading sections which gives good total protein load (e.g. 3 sections at 720 deg/hr, 1 mL/min and 5 mg/mL BSA, or 5 sections at 720 deg/hr, 1 mL/min and 1.5 mg/mL BSA)
- Any number of elution sections

A major part of understanding any chromatography systems can be obtained using mathematical models which predicts the separation process. The models can also be used to predict effects of alternative CRFC configuration such as overall column volume, feed chamber volume and bed depth, for further improvements on the system.

Model simulations agreed well with experimental results for both loading and elution zone peaks. Loading peak width is similar while experimental elution peak was wider than that simulated. Elution peak height for all simulations was greater while loading peak height were more variable than in the experiments. Elution peak tailing was observed in both experimental and model data.

5.5 Recommendations

The following are recommendations for CRFC model improvement and future work.

- Experimental work could be carried out on the CRFC for the recovery of bovine serum albumin using the recommended conditions.
- CRFC experimental results could be used to evaluate the mathematical model.
- Alternative feed solutions such whey protein solution could be carried out using the CRFC to evaluate multicomponent separation models.
- Performance differences between the current CRFC and new CRFC could be compared both experimentally and using the models.
- A more accurate salt model could be derived.

References

Barker, P. E. and G. Ganetsos (1988). "Chemical and Biochemical Separations Using Preparative and Large Scale Batch and Continuous Chromatography." Separation & Purification Reviews **17**(1): 1 - 65.

Bart, H. J., R. C. Messenböcl, et al. (1996). "Continuous Chromatographic Separation of Fructose, Mannitol and Sorbitol." Chemical Engineering and Processing **35**(6): 459-471.

Begovich, J. M., C. H. Byers, et al. (1983). "A High-Capacity Pressurized Continuous Chromatograph." Separation Science and Technology **18**(12): 1167 - 1191.

Begovich, J. M. and W. G. Sisson (1981). Rotating Annular Chromatograph for Continuous Metal Separations and Recovery. **30:** 705 - 710.

Begovich, J. M. and W. G. Sisson (1984). "Rotating Annular Chromatograph for Continuous Separations." A.I.Ch.E. J. **30**(5): 705-710.

Bloomingburg, G. F., J. S. Bauer, et al. (1991). "Continuous Separation of Proteins by Annular Chromatography." Industrial & Engineering Chemistry Research **30**(5): 1061-1067.

Bloomingburg, G. F. and G. Carta (1994). "Separation of Protein Mixtures by Continuous Annular Chromatography with Step Elution." The Chemical Engineering Journal(55): B19-B27.

Buchacher, A., G. Iberer, et al. (2001). "Continuous Removal of Protein Aggregates by Annular Chromatography." Biotechnology Progress **17**(1): 140-149.

Byers, C., W. Sisson, et al. (1989). "Pilot-Scale Studies of Sugar Separations by Continuous Chromatography." Applied Biochemistry and Biotechnology **20-21**(1): 635-654.

Cabanne, C., M. Raedts, et al. (2007). "Evaluation of Radial Chromatography Versus Axial Chromatography, Practical Approach." Journal of Chromatography B **845**(2): 191-199.

Canon, R. M., J. M. Begovich, et al. (1980). "Pressurized Continuous Chromatography." Separation Science and Technology **15**(3): 655 - 678.

Canon, R. M. and W. G. Sisson (1978). "Operation of an Improved, Continuous Annular Chromatograph." Journal of Liquid Chromatography **1**(4): 427-441.

Carta, G., J. P. DeCarli, et al. (1989). "Separation of Metals by Continuous Annular Chromatography with Step Elution." Chemical Engineering Communications **79**(1): 207 - 227.

Chen, H.-L. and K. C. Hou (1985). "Bioseparation by Cartridge Chromatography." Annual Reports on Fermentation Processes. Annual Reports on Fermentation Processes **8**: 59-71.

Ching, C. B., B. G. Lim, et al. (1993). "Preparative Resolution of Praziquantel Enantiomers by Simulated Counter-Current Chromatography." Journal of Chromatography A **634**(2): 215-219.

De Carli, J. P., G. Carta, et al. (1990). "Displacement Separations by Sontinuous Annular Chromatography." AIChE Journal **36**(8): 1220-1228.

Dinelli, D., S. Polezzo, et al. (1962). "Rotating Unit for Preparative-Scale Gas Chromatography." Journal of Chromatography(7): 477-484.

Fox, J. B., R. C. Calhoun, et al. (1969). "Continuous Chromatography Apparatus : I. Construction." Journal of Chromatography A **43**: 48-54.

Giddings, J. C. (1962). "Theoretical Basis for a Continuous, Large-Capacity Gas Chromatographic Apparatus." Analytical Chemistry **34**(1): 37-39.

Giovannini, R. and R. Freitag (2001). "Isolation of a Recombinant Antibody from Cell Culture Supernatant: Continuous Annular Versus Batch and Expanded-Bed Chromatography." Biotechnology and Bioengineering **73**(6): 522-529.

Giovannini, R. and R. Freitag (2002). "Continuous Isolation of Plasmid DNA by Annular Chromatography." Biotechnology and Bioengineering **77**(4): 445-454.

Gu, T. (1999a). Radial Flow Chromatography. Encyclopedia of Bioprocess Technology: Fermentation, Biocatalysis and Bioseparation. M. C. Flickinger and S. W. Drew, John Wiley & Sons, Inc.**:** 627-638.

Gu, T., G. J. Tsai, et al. (1991). "Theoretical Study of Multi Component Radial Flow Chromatography." Chemical Engineering Science **46**(5-6): 1279-1288.

Gu, T. and Y. Zheng (1999b). "A Study of the Scale-up of Reversed-Phase Lliquid Chromatography." Separation and Purification Technology **15**(1): 41-58.

Hall, L. G. and L. G. Cole (1959). Chromatography. **US Patent 2,891,630**.

Hashimoto, K., M. Yamada, et al. (1989). "A Simulated Moving-Bed Adsorber with Three Zones for Continuous Separation of Image -Phenylalanine and Nacl." Journal of Chemical Engineering of Japan(22): 432.

Heaton, W. B. (1963). Chromatographic Method and Apparatus. **US Patent 3,077,103**.

Heftmann, E., J. M., D. F. F. Krochta, et al. (1972). "The Chromatofuge, an Apparatus for Preparative Rapid Radial Column Chromatography." Journal of Chromatography **66**: 365-369.

Hopf, P. P. (1947). "Radial Chromatography in Industry." Industrial & Engineering Chemistry **39**(8): 938-940.

Hou, K. C. and R. Zaniewski (1990). "Purification of Urokinase by Combined Cation Exchanger and Affinity Chromatographic Cartridges." Journal of Chromatography B: Biomedical Sciences and Applications **525**: 297-306.

Howard, A. J., G. Carta, et al. (1988). "Separation of Sugars by Sontinuous Annular Shromatography." Industrial & Engineering Chemistry Research **27**(10): 1873-1882.

Huang, S. H., W.-C. Lee, et al. (1988). "Mathematical Models of Radial Chromatography." Chemical Engineering Journal and the Biochemical Engineering Journal **38**(3): 179-186.

Huang, S. H., S. Roy, et al. (1988). "Scaling-up of Affinity Chromatography by Radial-Flow Cartridges." Biotechnology Progress **4**(3): 159-165.

Humphrey, J. L. (1995). "Separation Processes: Playing a Critical Role." Chemical Engineering Progress **91**(10): 31–41.

Hunter, A. K. and G. Carta (2001). "Effects of Bovine Serum Albumin Heterogeneity on Frontal Analysis with Anion-Exchange Media." Journal of Chromatography A **937**(1-2): 13-19.

Iberer, G., H. Schwinn, et al. (2001). "Improved Performance of Protein Separation by Continuous Annular Chromatography in the Size-Exclusion Mode." Journal of Chromatography A **921**(1): 15-24.

Jungbauer, A., F. Unterluggauer, et al. (1988). "Scaleup of Monoclonal Antibody Purification Using Radial Streaming Ion Exchange Chromatography." Biotechnology and Bioengineering **32**(3): 326-333.

Kaczmarski, K., D. Antos, et al. (2001). "Comparative Modeling of Breakthrough Curves of Bovine Serum Albumin in Anion-Exchange Chromatography." Journal of Chromatography A(925): 1-17.

Kishihara, S., H. Horikawa, et al. (1989). "Continuous Chromatographic Separation of Palatinose and Trehalulose Using a Simulated Moving-Bed Adsorber." Journal of Chemical Engineering of Japan **22**(4): 434-436.

Kitakawa, A., Y. Yamanishi, et al. (1997). "Complete Separation of Amino Acids Using Continuous Rotating Annular Ion Exchange Chromatography with Partial Recycle of Effluent." Industrial & Engineering Chemistry Research **36**(9): 3809-3814.

Kitakawa, A., Y. Yamanishi, et al. (1995). "Modeling and Simulation of Continuous Rotating Annular Ion-Exchange Chromatography for Separation of Amino Acids." Separation Science and Technology **30**(16): 3089-3110.

Lanckriet, H. and A. P. J. Middelberg (2004). "Continuous Chromatographic Protein Refolding." Journal of Chromatography A **1022**(1-2): 103-113.

Lapidus, L. and N. R. Amundson (1952). "The Rate-Determining Steps in Radial Adsorption Analysis." Journal of Physical Chemistry(56): 373-383.

Lay, M. C. (1998). Continuous Radial Flow Chromatography. MSc Thesis, Hamilton,

New Zealand, University of Waikato.

Lay, M. C. (2005). Continuous Radial Flow Chromatography. PhD Thesis, Hamilton, New Zealand, University of Waikato.

Lay, M. C., C. J. Fee, et al. (2006). "Continuous Radial Flow Chromatography of Proteins." Food and Bioproducts Processing **84**(1 C): 78-83.

LeVan, A. D., M. Carta, et al. (1997). Adsorption and Ion Exchange. Perry's Chemical Engineers' Handbook, 7th Edition. R. H. Perry, D. W. Green and J. O. Maloney. New York, McGraw-Hill**:** 16.1-16.66.

Levison, P. R. (2003). "Large-Scale Ion-Exchange Column Chromatography of Proteins: Comparison of Different Formats." Journal of Chromatography B **790**(1-2): 17-33.

Liapis, A. I. (1989). "Theoretical Aspects of Affinity Chromatography." Journal of Biotechnology **11**(2-3): 143-160.

Luft, L. (1962). Apparatus for Continuous Separation of Volatile Components of a Gaseous Mixture. **US Patent 3,016,106**.

Martin, A. J. P. (1949). "Summarizing Paper." Discussions of the Faraday Society(7): 332 - 336.

Mosier, L. C. (1963). Continuous Gas Chromatography. **US Patent 3,078,647**.

Navarro, A., H. Caruel, et al. (1997). "Continuous Chromatographic Separation Process: Simulated Moving Bed Allowing Simultaneous Withdrawal of Three Fractions." Journal of Chromatography A(770): 39-50.

Nicholas, R. A. and J. B. Fox (1969). "Continuous Chromatography Apparatus : Iii. Application." Journal of Chromatography A **43**: 61-65.

Pais, L. S., J. M. Loureiro, et al. (1997). "Modeling, Simulation and Operation of a Simulated Moving Bed for Continuous Chromatographic Separation of 1,1'-Bi-2-Naphthol Enantiomers." Journal of Chromatography A **769**(1): 25-35.

Plaigin, M., J. F. Lacoste-Bourgeacq, et al. (1989). "Purification of Plasma Fractions by Radial Flow Chromatography Cartridges." Colloque INSERM(175): 169-176.

Reissner, K., A. Prior, et al. (1996). Preparative Desalting of Bovine Serum Albumin by Continuous Annular Chromatography. 20th International Symposium on High Performance Liquid Phase Separations and Related Techniques, San Francisco, Ca, Elsevier Science Bv.

Roger-Marc, N., F. Géraldine, et al. (1993). "Preparative Scale Enantioseparation of a Chiral Epoxide: Comparison of Liquid Chromatography and Simulated Moving Bed Adsorption Technology." Chirality **5**(4): 267-271.

Saxena, V. and M. Dunn (1989). "Solving Scale-Up: Radial Flow Chromatography." Bio/Technology **7**(3): 250.

Schlegl, R., G. Iberer, et al. (2003). "Continuous Matrix-Assisted Refolding of Proteins." Journal of Chromatography A **1009**(1-2): 119-132.

Scott, C. D., R. D. Spence, et al. (1976). "Pressurized, Annular Chromatograph for Continuous Separations." Journal of Chromatography(126): 381-400.

Scott, R. P. W. (2000). "Moving Bed Chromatography." Journal of Liquid Chromatography & Related Technologies **23**(20): 3069 - 3082.

Sisson, W. G., J. M. Begovich, et al. (1987). Application of Continuous Annular Chromatography to Size-Exclusion Separations, United States.

Solms, J. J. (1955). Process for the Continuous Chromatographic Separation of Mixtures. **US Patent 786,896**.

Strancar, A., M. Barut, et al. (1997). "Application of Compact Porous Tubes for Preparative Isolation of Clotting Factor Viii from Human Plasma." Journal of Chromatography A **760**(1): 117-123.

Sun, T., C. Ge, et al. (2000). "Chromatography of Human Prothrombin from Nitschmann Fraction Iii on Q Sepharose Fast Flow Using Axial and Radial Flow Column." Bioprocess and Biosystems Engineering **23**(2): 121-125.

Sussman, M. and R. Rathore (1975). "Continuous Modes of Chromatography." Chromatographia **8**(2): 55-59.

Sussman, M. V. (1970). Apparatus for Effecting Interactions of Fluids at Extended Solid Surfaces. **US Patent 3,503,712**.

Sussman, M. V. (1976). "Continuous Chromatography." ChemTech **6**: 260.

Svensson, H., C.-E. Agrell, et al. (1955). "An Apparatus for Continuous Chromatographic Separation." Science Tools(2): 17-21.

Takahashi, Y. and S. Goto (1991). "Continuous Separations of Amino Acids by Using an Annular Chromatograph with Rotating Inlet and Outlet." Separation Science and Technology **26**(1): 1 - 13.

Takahashi, Y. and S. Goto (1992). "Continuous Separation and Concentration of Proteins Using an Annular Chromatograph." Journal of Chemical Engineering of Japan(25): 403-407.

Taramasso, M. and D. Dinelli (1964). ""Preparative Scale Gas Chromatography by a Laboratory Rotating Unit." Journal of Gas Chromatography: 150-153.

Thiele, A., T. Falk, et al. (2001). "Prediction of Elution Profiles in Annular Chromatography." Computers & Chemical Engineering **25**(7-8): 1089-1101.

Tsaur, Y. and D. C. Shallcross (1997). "Modeling of Ion Exchange Performance in a Fixed Radial Flow Annular Bed." Industrial & Engineering Chemistry Research **36**(6): 2359-2367.

Tuthill, E. J. (1970). Apparatus for Continuous Chromatography. **US Patent 3,527,350**.

Vogel, J. H., H. Nguyen, et al. (2002). "Continuous Annular Chromatography: General Characterization and Application for the Isolation of Recombinant Protein Drugs." Biotechnology and Bioengineering **80**(5): 559-568.

Wankat, P. C. (1977). "Therelationship between One-Dimensional and Two-Dimensional Separation Processes." AIChE Journal **23**(6): 859-867.

Wolfgang, J., A. Prior, et al. (1995). Continuous Separation of Carbohydrates by Ion-Exchange Chromatography. 9th Symposium on Separation Science and Technology for Energy Applications, Gatlinburg, Tn, Marcel Dekker Inc.

Yonemoto, T., A. Kitakawa, et al. (1993). "A Novel Continuous Rotating Annular Liquid Chromatograph with a Multichannel Peristaltic Pump for Variable Eluent Withdrawal." Separation Science and Technology **28**(17): 2587 - 2605.

Appendices

Appendix A Column Properties and Dimensions

Table 18. HiTrap DEAE Fast Flow column properties

Height	2.50 cm
Diameter	0.70 cm
Column volume	0.96 ml
Technique	Anion_Exchange
Vt	0.86 ml
Vo	0.00 ml
Max pressure	0.3 MPa
Default flow rate	1.0 ml/min
Max flow rate	4.0 ml/min
Typ. peak width at base	3.0 ml
pH High value, longterm	12
pH Low value, longterm	2
pH High value, shortterm	14
pH Low value, shortterm	1
Average particle diam.	90 µm
Code no	17-5055-01
Typical loading range	1-100 mg

Table 19. CRFC dimensions

	O.D. (cm)	I.D. (cm)	Height (cm)	Volume (mL)	Void fraction, ε
Outer sintered wall	15.2	14.6	3	42.13	0.25
Resin bed	14.6	8.6	3	327.98	0.33
Inner sintered wall	8.6	8	3	23.47	0.25

Appendix B Calibration Data

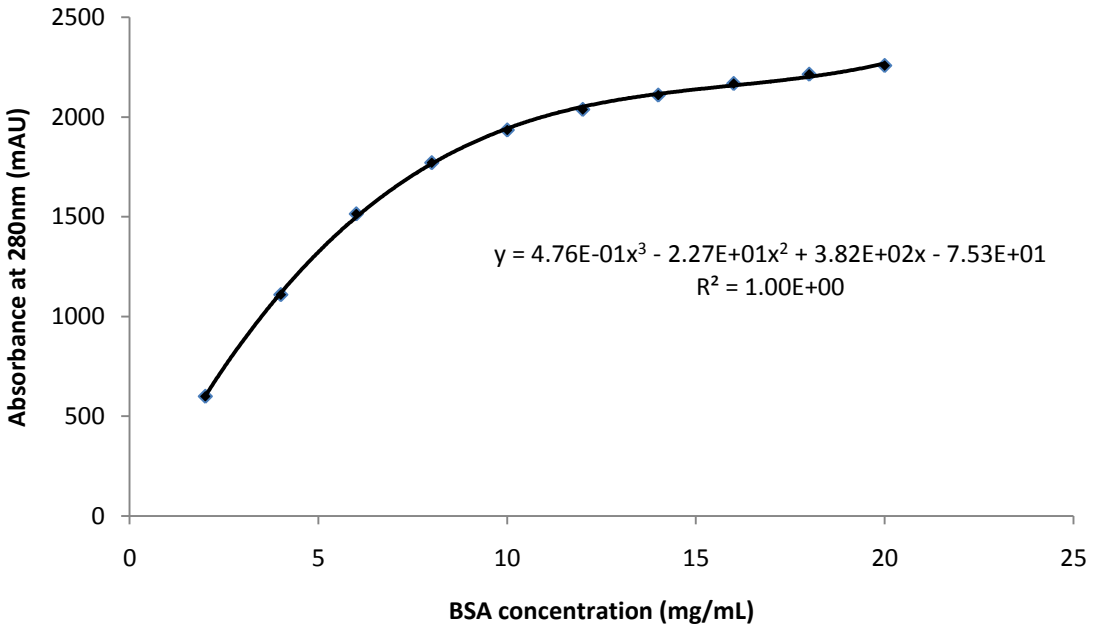

Figure 57. BSA concentration calibration curve using the AKTA FPLC inline UV spectrophotometer at 280 nm

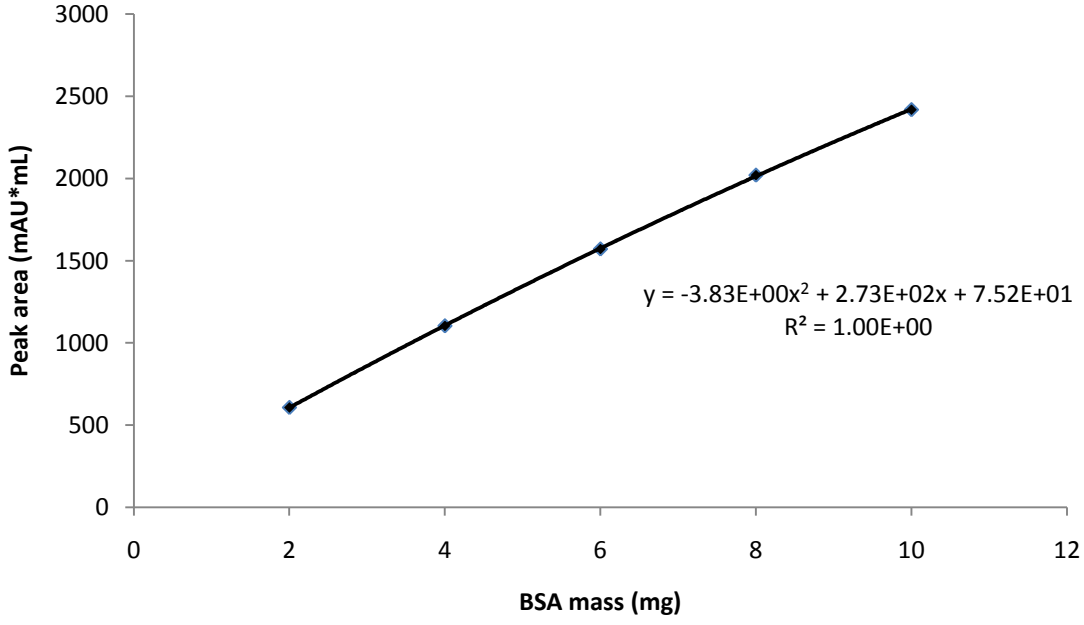

Figure 58. BSA mass calibration curve using the AKTA FPLC inline UV spectrophotometer at 280 nm

Appendix C AKTA FPLC Methods

C.1 Axial column experiments

C.1.1 Flow rate 0.1 mL/min, Rotation speed 180 degrees/hr, Trial 1-3

Main method:

¤ (Main)
0.00 Base Time 0.962 {ml} HiTrap_DEAE_FF_1_ml
0.00 Flow 0.1 {ml/min}
0.00 InjectionValve Load
0.00 ColumnPosition Position2
0.00 Alarm_Pressure Enabled 1 {MPa} 0.000 {MPa}
0.00 OutletValve F1
0.00 BufferValveA A1
0.00 BufferValveB B1
¤ 0.00 Block Equilibration
(Equilibration)
0.00 Base SameAsMain
30.00 End_Block
0.00 Loop 3
¤ 0.00 Block Inject
(Inject)
0.00 Base SameAsMain
0.00 InjectionValve Inject
15.00 InjectionValve Load
15.00 End_Block
¤ 0.00 Block Wash
(Wash)
0.00 Base SameAsMain
45.00 End_Block
¤ 0.00 Block Elution
(Elution)
0.00 Base SameAsMain
0.00 Gradient 100 {%B} 0.00 {base}
15.00 End_Block
¤ 0.00 Block Reequilibration
(Reequilibration)
0.00 Base SameAsMain
0.00 Gradient 0.0 {%B} 0.00 {base}
45.00 End_Block
0.00 Loop_End
¤ 0.00 Block Equilibration2
(Equilibration2)
0.00 Base SameAsMain
60.00 End_Block
0.00 Loop 3

¤ 0.00 Block Inject2
(Inject2)
0.00 Base SameAsMain
0.00 InjectionValve Inject
45.00 InjectionValve Load
45.00 End_Block
¤ 0.00 Block Wash2
(Wash2)
0.00 Base SameAsMain
30.00 End_Block
¤ 0.00 Block Elution2
(Elution2)
0.00 Base SameAsMain
0.00 Gradient 100 {%B} 0.00 {base}
15.00 End_Block
¤ 0.00 Block Reequilibration2
(Reequilibration2)
0.00 Base SameAsMain
0.00 Gradient 0.0 {%B} 0.00 {base}
30.00 End_Block
0.00 Loop_End
¤ 0.00 Block Equilibration3
(Equilibration3)
0.00 Base SameAsMain
60.00 End_Block
0.00 Loop 3
¤ 0.00 Block Inject3
(Inject3)
0.00 Base SameAsMain
0.00 InjectionValve Inject
75.00 InjectionValve Load
75.00 End_Block
¤ 0.00 Block Wash3
(Wash3)
0.00 Base SameAsMain
15.00 End_Block
¤ 0.00 Block Elution3
(Elution3)
0.00 Base SameAsMain
0.00 Gradient 100 {%B} 0.00 {base}
15.00 End_Block
¤ 0.00 Block Reequilibration3
(Reequilibration3)
0.00 Base SameAsMain
0.00 Gradient 0.0 {%B} 0.00 {base}
15.00 End_Block
0.00 Loop_End
¤ 0.00 Block Final
(Final)
0.00 Base SameAsMain
60.00 End_Block

C.1.2 Flow rate 0.1 mL/min, Rotation speed 180 degrees/hr, Trial 4-6

Main method:

¤ (Main)
0.00 Base Time 0.962 {ml} HiTrap_DEAE_FF_1_ml
0.00 Flow 0.1 {ml/min}
0.00 InjectionValve Load
0.00 ColumnPosition Position2
0.00 Alarm_Pressure Enabled 1 {MPa} 0.000 {MPa}
0.00 OutletValve F1
0.00 BufferValveA A1
0.00 BufferValveB B1
¤ 0.00 Block Equilibration
(Equilibration)
0.00 Base SameAsMain
30.00 End_Block
0.00 Loop 3
¤ 0.00 Block Inject4
(Inject4)
0.00 Base SameAsMain
0.00 InjectionValve Inject
15.00 InjectionValve Load
15.00 End_Block
¤ 0.00 Block Wash4
(Wash4)
0.00 Base SameAsMain
30.00 End_Block
¤ 0.00 Block Elution4
(Elution4)
0.00 Base SameAsMain
0.00 Gradient 100 {%B} 0.00 {base}
30.00 End_Block
¤ 0.00 Block Reequilibration4
(Reequilibration4)
0.00 Base SameAsMain
0.00 Gradient 0.0 {%B} 0.00 {base}
45.00 End_Block
0.00 Loop_End
¤ 0.00 Block Equilibration5
(Equilibration5)
0.00 Base SameAsMain
60.00 End_Block
0.00 Loop 3
¤ 0.00 Block Inject5
(Inject5)
0.00 Base SameAsMain
0.00 InjectionValve Inject
15.00 InjectionValve Load
15.00 End_Block
¤ 0.00 Block Wash5

(Wash5)
0.00 Base SameAsMain
30.00 End_Block
¤ 0.00 Block Elution5
(Elution5)
0.00 Base SameAsMain
0.00 Gradient 100 {%B} 0.00 {base}
45.00 End_Block
¤ 0.00 Block Reequilibration5
(Reequilibration5)
0.00 Base SameAsMain
0.00 Gradient 0.0 {%B} 0.00 {base}
30.00 End_Block
0.00 Loop_End
¤ 0.00 Block Equilibration6
(Equilibration6)
0.00 Base SameAsMain
60.00 End_Block
0.00 Loop 3
¤ 0.00 Block Inject6
(Inject6)
0.00 Base SameAsMain
0.00 InjectionValve Inject
15.00 InjectionValve Load
15.00 End_Block
¤ 0.00 Block Wash6
(Wash6)
0.00 Base SameAsMain
15.00 End_Block
¤ 0.00 Block Elution6
(Elution6)
0.00 Base SameAsMain
0.00 Gradient 100 {%B} 0.00 {base}
75.00 End_Block
¤ 0.00 Block Reequilibration6
(Reequilibration6)
0.00 Base SameAsMain
0.00 Gradient 0.0 {%B} 0.00 {base}
15.00 End_Block
0.00 Loop_End
¤ 0.00 Block Final
(Final)
0.00 Base SameAsMain
60.00 End_Block

C.1.3 Flow rate 0.1 mL/min, Rotation speed 180 degrees/hr, Trial 7-9

Main method:
¤ (Main)
0.00 Base Time 0.962 {ml} HiTrap_DEAE_FF_1_ml
0.00 Flow 0.1 {ml/min}

0.00 InjectionValve Load
0.00 ColumnPosition Position2
0.00 Alarm_Pressure Enabled 1 {MPa} 0.000 {MPa}
0.00 OutletValve F1
0.00 BufferValveA A1
0.00 BufferValveB B1
¤ 0.00 Block Equilibration
(Equilibration)
0.00 Base SameAsMain
30.00 End_Block
0.00 Loop 3
¤ 0.00 Block Inject7
(Inject7)
0.00 Base SameAsMain
0.00 InjectionValve Inject
30.00 InjectionValve Load
30.00 End_Block
¤ 0.00 Block Wash7
(Wash7)
0.00 Base SameAsMain
30.00 End_Block
¤ 0.00 Block Elution7
(Elution7)
0.00 Base SameAsMain
0.00 Gradient 100 {%B} 0.00 {base}
30.00 End_Block
¤ 0.00 Block Reequilibration7
(Reequilibration7)
0.00 Base SameAsMain
0.00 Gradient 0.0 {%B} 0.00 {base}
30.00 End_Block
0.00 Loop_End
¤ 0.00 Block Equilibration8
(Equilibration8)
0.00 Base SameAsMain
60.00 End_Block
0.00 Loop 3
¤ 0.00 Block Inject8
(Inject8)
0.00 Base SameAsMain
0.00 InjectionValve Inject
45.00 InjectionValve Load
45.00 End_Block
¤ 0.00 Block Wash8
(Wash8)
0.00 Base SameAsMain
15.00 End_Block
¤ 0.00 Block Elution8
(Elution8)
0.00 Base SameAsMain
0.00 Gradient 100 {%B} 0.00 {base}

30.00 End_Block
¤ 0.00 Block Reequilibration8
(Reequilibration8)
0.00 Base SameAsMain
0.00 Gradient 0.0 {%B} 0.00 {base}
30.00 End_Block
0.00 Loop_End
¤ 0.00 Block Equilibration9
(Equilibration9)
0.00 Base SameAsMain
60.00 End_Block
0.00 Loop 3
¤ 0.00 Block Inject9
(Inject9)
0.00 Base SameAsMain
0.00 InjectionValve Inject
45.00 InjectionValve Load
45.00 End_Block
¤ 0.00 Block Wash9
(Wash9)
0.00 Base SameAsMain
15.00 End_Block
¤ 0.00 Block Elution9
(Elution9)
0.00 Base SameAsMain
0.00 Gradient 100 {%B} 0.00 {base}
45.00 End_Block
¤ 0.00 Block Reequilibration9
(Reequilibration9)
0.00 Base SameAsMain
0.00 Gradient 0.0 {%B} 0.00 {base}
15.00 End_Block
0.00 Loop_End
¤ 0.00 Block Final
(Final)
0.00 Base SameAsMain
60.00 End_Block

C.1.4 Flow rate 0.1 mL/min, rotation speed 360 degrees/hr, Trial 1-3

Main method:
¤ (Main)
0.00 Base Time 0.962 {ml} HiTrap_DEAE_FF_1_ml
0.00 Flow 0.1 {ml/min}
0.00 InjectionValve Load
0.00 ColumnPosition Position2
0.00 Alarm_Pressure Enabled 1 {MPa} 0.000 {MPa}
0.00 OutletValve F1
0.00 BufferValveA A1
0.00 BufferValveB B1
¤ 0.00 Block Equilibration

(Equilibration)
0.00 Base SameAsMain
30.00 End_Block
0.00 Loop 3
¤ 0.00 Block Inject
(Inject)
0.00 Base SameAsMain
0.00 InjectionValve Inject
7.50 InjectionValve Load
7.50 End_Block
¤ 0.00 Block Wash
(Wash)
0.00 Base SameAsMain
22.50 End_Block
¤ 0.00 Block Elution
(Elution)
0.00 Base SameAsMain
0.00 Gradient 100 {%B} 0.00 {base}
7.50 End_Block
¤ 0.00 Block Reequilibration
(Reequilibration)
0.00 Base SameAsMain
0.00 Gradient 0.0 {%B} 0.00 {base}
22.50 End_Block
0.00 Loop_End
¤ 0.00 Block Equilibration2
(Equilibration2)
0.00 Base SameAsMain
60.00 End_Block
0.00 Loop 3
¤ 0.00 Block Inject2
(Inject2)
0.00 Base SameAsMain
0.00 InjectionValve Inject
22.50 InjectionValve Load
22.50 End_Block
¤ 0.00 Block Wash2
(Wash2)
0.00 Base SameAsMain
15.00 End_Block
¤ 0.00 Block Elution2
(Elution2)
0.00 Base SameAsMain
0.00 Gradient 100 {%B} 0.00 {base}
7.50 End_Block
¤ 0.00 Block Reequilibration2
(Reequilibration2)
0.00 Base SameAsMain
0.00 Gradient 0.0 {%B} 0.00 {base}
15.00 End_Block
0.00 Loop_End

¤ 0.00 Block Equilibration3
(Equilibration3)
0.00 Base SameAsMain
60.00 End_Block
0.00 Loop 3
¤ 0.00 Block Inject3
(Inject3)
0.00 Base SameAsMain
0.00 InjectionValve Inject
37.50 InjectionValve Load
37.50 End_Block
¤ 0.00 Block Wash3
(Wash3)
0.00 Base SameAsMain
7.50 End_Block
¤ 0.00 Block Elution3
(Elution3)
0.00 Base SameAsMain
0.00 Gradient 100 {%B} 0.00 {base}
7.50 End_Block
¤ 0.00 Block Reequilibration3
(Reequilibration3)
0.00 Base SameAsMain
0.00 Gradient 0.0 {%B} 0.00 {base}
7.50 End_Block
0.00 Loop_End
¤ 0.00 Block Final
(Final)
0.00 Base SameAsMain
60.00 End_Block

C.1.5 Flow rate 0.1 mL/min, rotation speed 360 degrees/hr, Trial 4-6

Main method:
¤ (Main)
0.00 Base Time 0.962 {ml} HiTrap_DEAE_FF_1_ml
0.00 Flow 0.1 {ml/min}
0.00 InjectionValve Load
0.00 ColumnPosition Position2
0.00 Alarm_Pressure Enabled 1 {MPa} 0.000 {MPa}
0.00 OutletValve F1
0.00 BufferValveA A1
0.00 BufferValveB B1
¤ 0.00 Block Equilibration
(Equilibration)
0.00 Base SameAsMain
30.00 End_Block
0.00 Loop 3
¤ 0.00 Block Inject4
(Inject4)
0.00 Base SameAsMain

0.00 InjectionValve Inject
7.50 InjectionValve Load
7.50 End_Block
¤ 0.00 Block Wash4
(Wash4)
0.00 Base SameAsMain
15.00 End_Block
¤ 0.00 Block Elution4
(Elution4)
0.00 Base SameAsMain
0.00 Gradient 100 {%B} 0.00 {base}
15.00 End_Block
¤ 0.00 Block Reequilibration4
(Reequilibration4)
0.00 Base SameAsMain
0.00 Gradient 0.0 {%B} 0.00 {base}
22.50 End_Block
0.00 Loop_End
¤ 0.00 Block Equilibration5
(Equilibration5)
0.00 Base SameAsMain
60.00 End_Block
0.00 Loop 3
¤ 0.00 Block Inject5
(Inject5)
0.00 Base SameAsMain
0.00 InjectionValve Inject
7.50 InjectionValve Load
7.50 End_Block
¤ 0.00 Block Wash5
(Wash5)
0.00 Base SameAsMain
15.00 End_Block
¤ 0.00 Block Elution5
(Elution5)
0.00 Base SameAsMain
0.00 Gradient 100 {%B} 0.00 {base}
22.50 End_Block
¤ 0.00 Block Reequilibration5
(Reequilibration5)
0.00 Base SameAsMain
0.00 Gradient 0.0 {%B} 0.00 {base}
15.00 End_Block
0.00 Loop_End
¤ 0.00 Block Equilibration6
(Equilibration6)
0.00 Base SameAsMain
60.00 End_Block
0.00 Loop 3
¤ 0.00 Block Inject6
(Inject6)

0.00 Base SameAsMain
0.00 InjectionValve Inject
7.50 InjectionValve Load
7.50 End_Block
¤ 0.00 Block Wash6
(Wash6)
0.00 Base SameAsMain
7.50 End_Block
¤ 0.00 Block Elution6
(Elution6)
0.00 Base SameAsMain
0.00 Gradient 100 {%B} 0.00 {base}
37.50 End_Block
¤ 0.00 Block Reequilibration6
(Reequilibration6)
0.00 Base SameAsMain
0.00 Gradient 0.0 {%B} 0.00 {base}
7.50 End_Block
0.00 Loop_End
¤ 0.00 Block Final
(Final)
0.00 Base SameAsMain
60.00 End_Block

C.1.6 Flow rate 0.1 mL/min, Rotation speed 360 degrees/hr, Trial 7-9

Main method:
¤ (Main)
0.00 Base Time 0.962 {ml} HiTrap_DEAE_FF_1_ml
0.00 Flow 0.1 {ml/min}
0.00 InjectionValve Load
0.00 ColumnPosition Position2
0.00 Alarm_Pressure Enabled 1 {MPa} 0.000 {MPa}
0.00 OutletValve F1
0.00 BufferValveA A1
0.00 BufferValveB B1
¤ 0.00 Block Equilibration
(Equilibration)
0.00 Base SameAsMain
30.00 End_Block
0.00 Loop 3
¤ 0.00 Block Inject7
(Inject7)
0.00 Base SameAsMain
0.00 InjectionValve Inject
15.00 InjectionValve Load
15.00 End_Block
¤ 0.00 Block Wash7
(Wash7)
0.00 Base SameAsMain
15.00 End_Block

¤ 0.00 Block Elution7
(Elution7)
0.00 Base SameAsMain
0.00 Gradient 100 {%B} 0.00 {base}
15.00 End_Block
¤ 0.00 Block Reequilibration7
(Reequilibration7)
0.00 Base SameAsMain
0.00 Gradient 0.0 {%B} 0.00 {base}
15.00 End_Block
0.00 Loop_End
¤ 0.00 Block Equilibration8
(Equilibration8)
0.00 Base SameAsMain
60.00 End_Block
0.00 Loop 3
¤ 0.00 Block Inject8
(Inject8)
0.00 Base SameAsMain
0.00 InjectionValve Inject
22.50 InjectionValve Load
22.50 End_Block
¤ 0.00 Block Wash8
(Wash8)
0.00 Base SameAsMain
7.50 End_Block
¤ 0.00 Block Elution8
(Elution8)
0.00 Base SameAsMain
0.00 Gradient 100 {%B} 0.00 {base}
15.00 End_Block
¤ 0.00 Block Reequilibration8
(Reequilibration8)
0.00 Base SameAsMain
0.00 Gradient 0.0 {%B} 0.00 {base}
15.00 End_Block
0.00 Loop_End
¤ 0.00 Block Equilibration9
(Equilibration9)
0.00 Base SameAsMain
60.00 End_Block
0.00 Loop 3
¤ 0.00 Block Inject9
(Inject9)
0.00 Base SameAsMain
0.00 InjectionValve Inject
22.50 InjectionValve Load
22.50 End_Block
¤ 0.00 Block Wash9
(Wash9)
0.00 Base SameAsMain

7.50 End_Block
¤ 0.00 Block Elution9
(Elution9)
0.00 Base SameAsMain
0.00 Gradient 100 {%B} 0.00 {base}
22.50 End_Block
¤ 0.00 Block Reequilibration9
(Reequilibration9)
0.00 Base SameAsMain
0.00 Gradient 0.0 {%B} 0.00 {base}
7.50 End_Block
0.00 Loop_End
¤ 0.00 Block Final
(Final)
0.00 Base SameAsMain
60.00 End_Block

C.1.7 Flow rate 0.1 mL/min, Rotation speed 720 degrees/hr, Trial 1-3

Main method:
¤ (Main)
0.00 Base Time 0.962 {ml} HiTrap_DEAE_FF_1_ml
0.00 Flow 0.1 {ml/min}
0.00 InjectionValve Load
0.00 ColumnPosition Position2
0.00 Alarm_Pressure Enabled 1 {MPa} 0.000 {MPa}
0.00 OutletValve F1
0.00 BufferValveA A1
0.00 BufferValveB B1
¤ 0.00 Block Equilibration
(Equilibration)
0.00 Base SameAsMain
30.00 End_Block
0.00 Loop 3
¤ 0.00 Block Inject
(Inject)
0.00 Base SameAsMain
0.00 InjectionValve Inject
3.75 InjectionValve Load
3.75 End_Block
¤ 0.00 Block Wash
(Wash)
0.00 Base SameAsMain
11.25 End_Block
¤ 0.00 Block Elution
(Elution)
0.00 Base SameAsMain
0.00 Gradient 100 {%B} 0.00 {base}
3.75 End_Block
¤ 0.00 Block Reequilibration
(Reequilibration)

0.00 Base SameAsMain
0.00 Gradient 0.0 {%B} 0.00 {base}
11.25 End_Block
0.00 Loop_End
¤ 0.00 Block Equilibration2
(Equilibration2)
0.00 Base SameAsMain
60.00 End_Block
0.00 Loop 3
¤ 0.00 Block Inject2
(Inject2)
0.00 Base SameAsMain
0.00 InjectionValve Inject
11.25 InjectionValve Load
11.25 End_Block
¤ 0.00 Block Wash2
(Wash2)
0.00 Base SameAsMain
7.50 End_Block
¤ 0.00 Block Elution2
(Elution2)
0.00 Base SameAsMain
0.00 Gradient 100 {%B} 0.00 {base}
3.75 End_Block
¤ 0.00 Block Reequilibration2
(Reequilibration2)
0.00 Base SameAsMain
0.00 Gradient 0.0 {%B} 0.00 {base}
7.50 End_Block
0.00 Loop_End
¤ 0.00 Block Equilibration3
(Equilibration3)
0.00 Base SameAsMain
60.00 End_Block
0.00 Loop 3
¤ 0.00 Block Inject3
(Inject3)
0.00 Base SameAsMain
0.00 InjectionValve Inject
18.75 InjectionValve Load
18.75 End_Block
¤ 0.00 Block Wash3
(Wash3)
0.00 Base SameAsMain
3.75 End_Block
¤ 0.00 Block Elution3
(Elution3)
0.00 Base SameAsMain
0.00 Gradient 100 {%B} 0.00 {base}
3.75 End_Block
¤ 0.00 Block Reequilibration3

(Reequilibration3)
0.00 Base SameAsMain
0.00 Gradient 0.0 {%B} 0.00 {base}
3.75 End_Block
0.00 Loop_End
¤ 0.00 Block Final
(Final)
0.00 Base SameAsMain
60.00 End_Block

C.1.8 Flow rate 0.1 mL/min, Rotation speed 720 degrees/hr, Trial 4-6

Main method:
¤ (Main)
0.00 Base Time 0.962 {ml} HiTrap_DEAE_FF_1_ml
0.00 Flow 0.1 {ml/min}
0.00 InjectionValve Load
0.00 ColumnPosition Position2
0.00 Alarm_Pressure Enabled 1 {MPa} 0.000 {MPa}
0.00 OutletValve F1
0.00 BufferValveA A1
0.00 BufferValveB B1
¤ 0.00 Block Equilibration
(Equilibration)
0.00 Base SameAsMain
30.00 End_Block
0.00 Loop 3
¤ 0.00 Block Inject4
(Inject4)
0.00 Base SameAsMain
0.00 InjectionValve Inject
3.75 InjectionValve Load
3.75 End_Block
¤ 0.00 Block Wash4
(Wash4)
0.00 Base SameAsMain
7.50 End_Block
¤ 0.00 Block Elution4
(Elution4)
0.00 Base SameAsMain
0.00 Gradient 100 {%B} 0.00 {base}
7.50 End_Block
¤ 0.00 Block Reequilibration4
(Reequilibration4)
0.00 Base SameAsMain
0.00 Gradient 0.0 {%B} 0.00 {base}
11.25 End_Block
0.00 Loop_End
¤ 0.00 Block Equilibration5
(Equilibration5)
0.00 Base SameAsMain

60.00 End_Block
0.00 Loop 3
¤ 0.00 Block Inject5
(Inject5)
0.00 Base SameAsMain
0.00 InjectionValve Inject
3.75 InjectionValve Load
3.75 End_Block
¤ 0.00 Block Wash5
(Wash5)
0.00 Base SameAsMain
7.50 End_Block
¤ 0.00 Block Elution5
(Elution5)
0.00 Base SameAsMain
0.00 Gradient 100 {%B} 0.00 {base}
11.25 End_Block
¤ 0.00 Block Reequilibration5
(Reequilibration5)
0.00 Base SameAsMain
0.00 Gradient 0.0 {%B} 0.00 {base}
7.50 End_Block
0.00 Loop_End
¤ 0.00 Block Equilibration6
(Equilibration6)
0.00 Base SameAsMain
60.00 End_Block
0.00 Loop 3
¤ 0.00 Block Inject6
(Inject6)
0.00 Base SameAsMain
0.00 InjectionValve Inject
3.75 InjectionValve Load
3.75 End_Block
¤ 0.00 Block Wash6
(Wash6)
0.00 Base SameAsMain
3.75 End_Block
¤ 0.00 Block Elution6
(Elution6)
0.00 Base SameAsMain
0.00 Gradient 100 {%B} 0.00 {base}
18.75 End_Block
¤ 0.00 Block Reequilibration6
(Reequilibration6)
0.00 Base SameAsMain
0.00 Gradient 0.0 {%B} 0.00 {base}
3.75 End_Block
0.00 Loop_End
¤ 0.00 Block Final
(Final)

0.00 Base SameAsMain
60.00 End_Block

C.1.9 Flow rate 0.1 mL/min, Rotation speed 720 degrees/hr, Trial 7-9

Main method:
¤ (Main)
0.00 Base Time 0.962 {ml} HiTrap_DEAE_FF_1_ml
0.00 Flow 0.1 {ml/min}
0.00 InjectionValve Load
0.00 ColumnPosition Position2
0.00 Alarm_Pressure Enabled 1 {MPa} 0.000 {MPa}
0.00 OutletValve F1
0.00 BufferValveA A1
0.00 BufferValveB B1
¤ 0.00 Block Equilibration
(Equilibration)
0.00 Base SameAsMain
30.00 End_Block
0.00 Loop 3
¤ 0.00 Block Inject7
(Inject7)
0.00 Base SameAsMain
0.00 InjectionValve Inject
7.50 InjectionValve Load
7.50 End_Block
¤ 0.00 Block Wash7
(Wash7)
0.00 Base SameAsMain
7.50 End_Block
¤ 0.00 Block Elution7
(Elution7)
0.00 Base SameAsMain
0.00 Gradient 100 {%B} 0.00 {base}
7.50 End_Block
¤ 0.00 Block Reequilibration7
(Reequilibration7)
0.00 Base SameAsMain
0.00 Gradient 0.0 {%B} 0.00 {base}
7.50 End_Block
0.00 Loop_End
¤ 0.00 Block Equilibration8
(Equilibration8)
0.00 Base SameAsMain
60.00 End_Block
0.00 Loop 3
¤ 0.00 Block Inject8
(Inject8)
0.00 Base SameAsMain
0.00 InjectionValve Inject
11.25 InjectionValve Load

11.25 End_Block
¤ 0.00 Block Wash8
(Wash8)
0.00 Base SameAsMain
3.75 End_Block
¤ 0.00 Block Elution8
(Elution8)
0.00 Base SameAsMain
0.00 Gradient 100 {%B} 0.00 {base}
7.50 End_Block
¤ 0.00 Block Reequilibration8
(Reequilibration8)
0.00 Base SameAsMain
0.00 Gradient 0.0 {%B} 0.00 {base}
7.50 End_Block
0.00 Loop_End
¤ 0.00 Block Equilibration9
(Equilibration9)
0.00 Base SameAsMain
60.00 End_Block
0.00 Loop 3
¤ 0.00 Block Inject9
(Inject9)
0.00 Base SameAsMain
0.00 InjectionValve Inject
11.25 InjectionValve Load
11.25 End_Block
¤ 0.00 Block Wash9
(Wash9)
0.00 Base SameAsMain
3.75 End_Block
¤ 0.00 Block Elution9
(Elution9)
0.00 Base SameAsMain
0.00 Gradient 100 {%B} 0.00 {base}
11.25 End_Block
¤ 0.00 Block Reequilibration9
(Reequilibration9)
0.00 Base SameAsMain
0.00 Gradient 0.0 {%B} 0.00 {base}
3.75 End_Block
0.00 Loop_End
¤ 0.00 Block Final
(Final)
0.00 Base SameAsMain
60.00 End_Block

Appendix D Axial Column Experimental Results

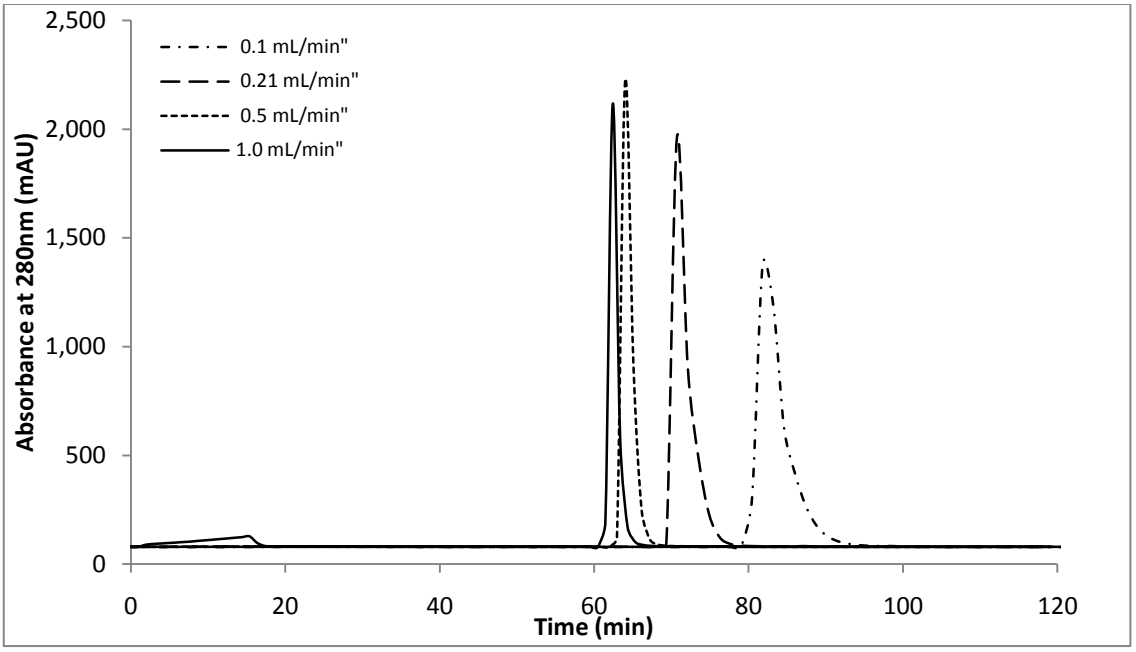

Figure 59. 1.5 mg/mL BSA concentration, 1M NaCl concentration, 180 degrees/hr rotation speed, flow rates 0.1-1.0 mL/min, Trial 1: 15 min loading, 45 min equilibration, 15 min elution, 45 min equilibration

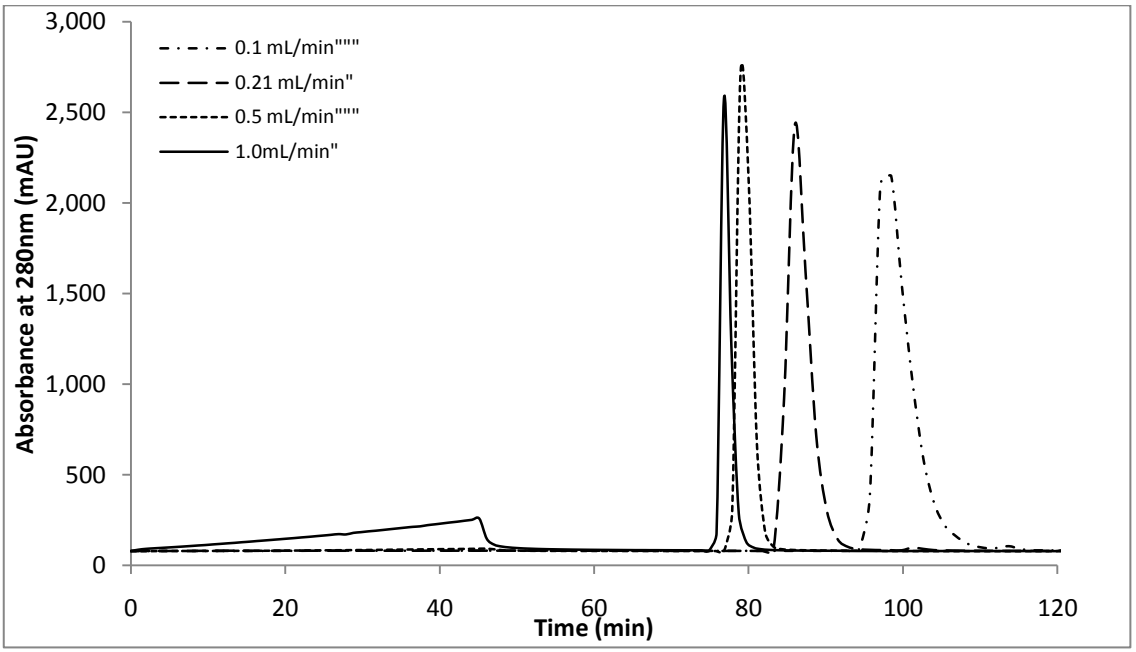

Figure 60. 1.5 mg/mL BSA concentration, 1M NaCl concentration, 180 degrees/hr rotation speed, Flow rates 0.1-1.0 mL/min, Trial 2: 45 min loading, 30 min equilibration, 15 min elution, 30 min equilibration.

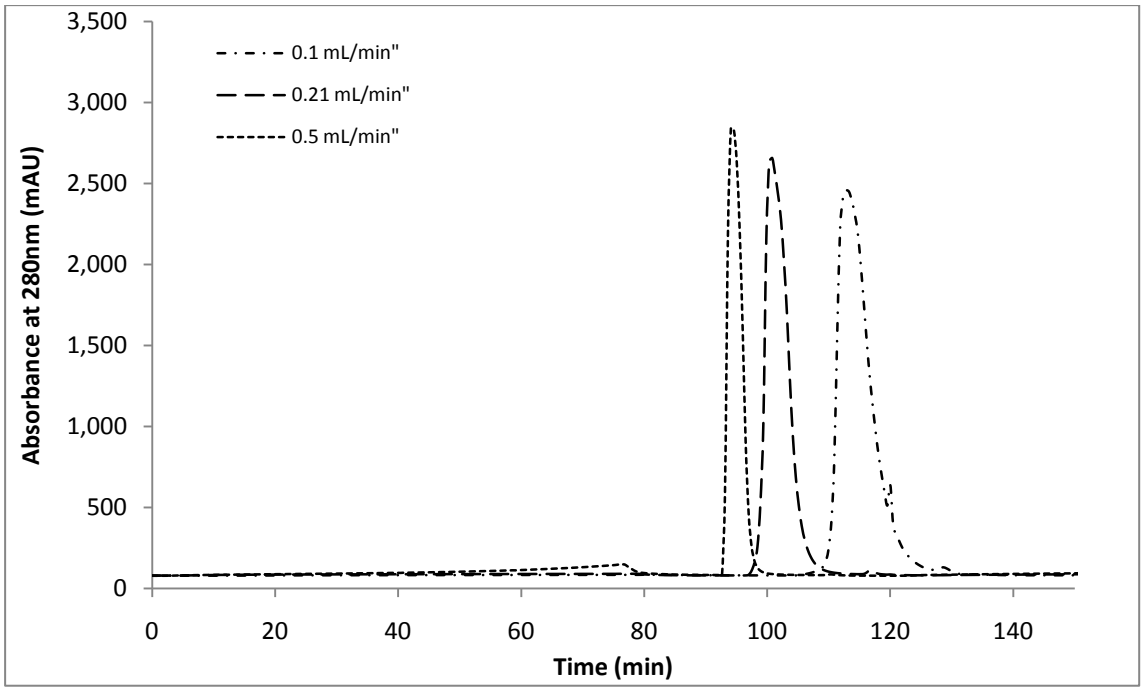

Figure 61. 1.5 mg/mL BSA concentration, 1M NaCl concentration, 180 degrees/hr rotation speed, flow rates 0.1-0.5 mL/min, Trial 3: 75 min loading, 15 min equilibration, 15 min elution, 15 min equilibration.

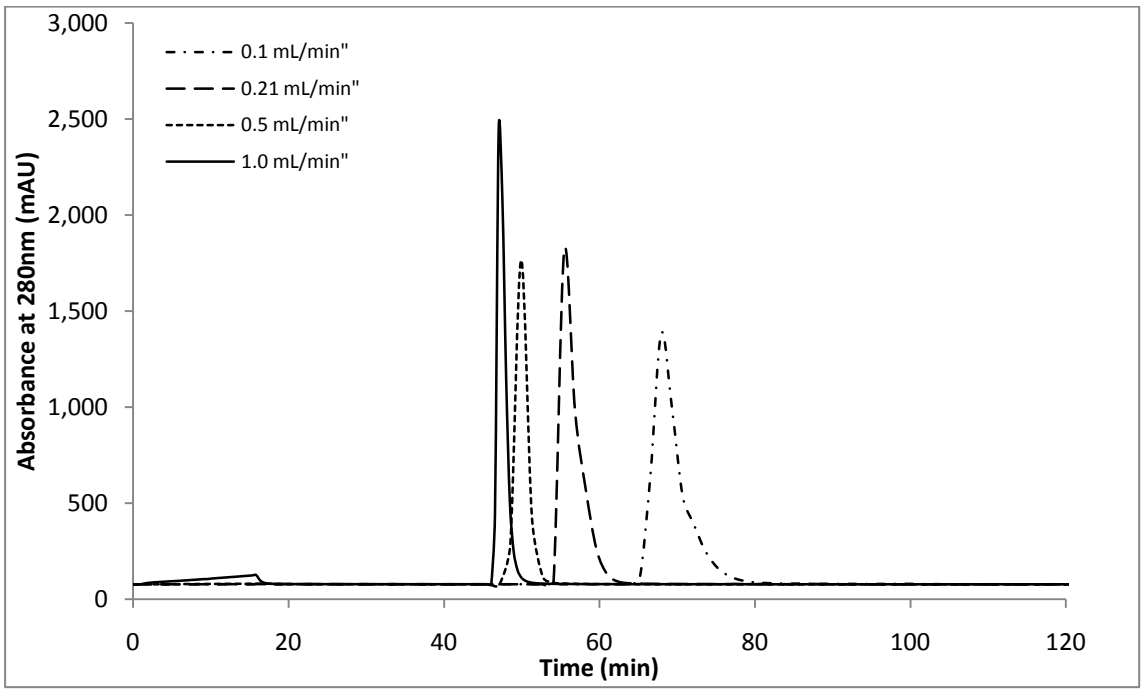

Figure 62. 1.5 mg/mL BSA concentration, 1M NaCl concentration, 180 degrees/hr rotation speed, flow rates 0.1-1.0 mL/min, Trial 4: 15 min loading, 30 min equilibration, 30 min elution, 45 min equilibration.

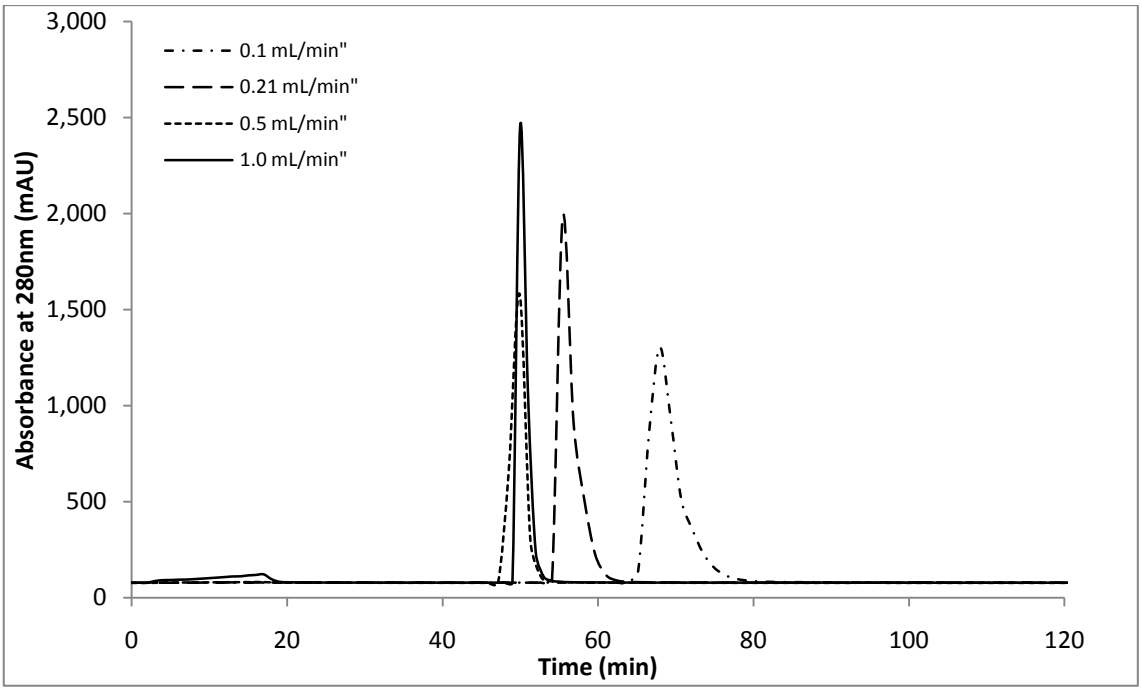

Figure 63. 1.5 mg/mL BSA concentration, 1M NaCl concentration, 180 degrees/hr rotation speed, flow rates 0.1-1.0 mL/min, Trial 5: 15 min loading, 30 min equilibration, 45 min elution, 30 min equilibration.

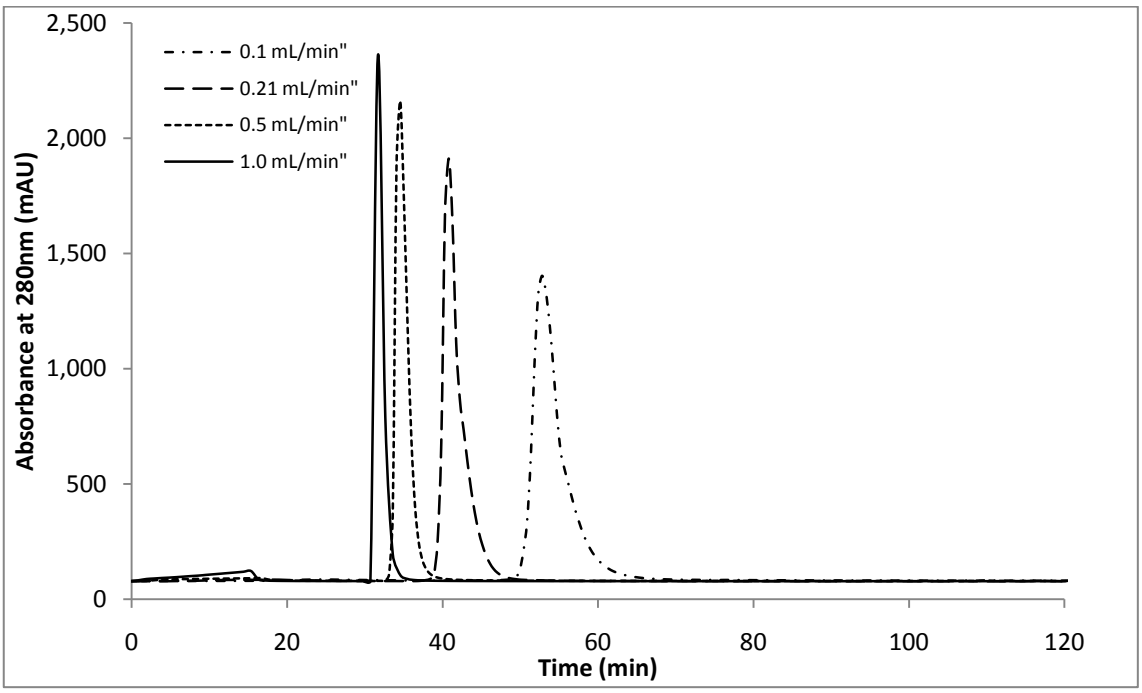

Figure 64. 1.5 mg/mL BSA concentration, 1M NaCl concentration, 180 degrees/hr rotation speed, flow rates 0.1-1.0 mL/min, Trial 6: 15 min loading, 15 min equilibration, 75 min elution, 15 min equilibration.

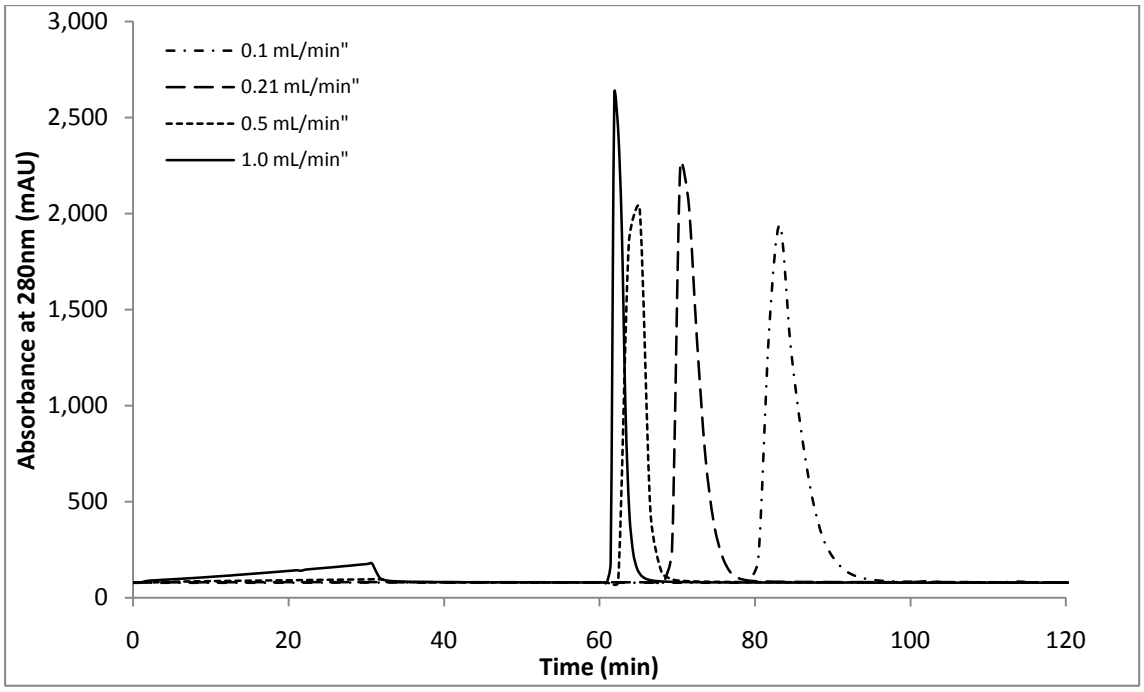

Figure 65. 1.5 mg/mL BSA concentration, 1M NaCl concentration, 180 degrees/hr rotation speed, flow rates 0.1-1.0 mL/min, Trial 7: 30 min loading, 30 min equilibration, 30 min elution, 30 min equilibration.

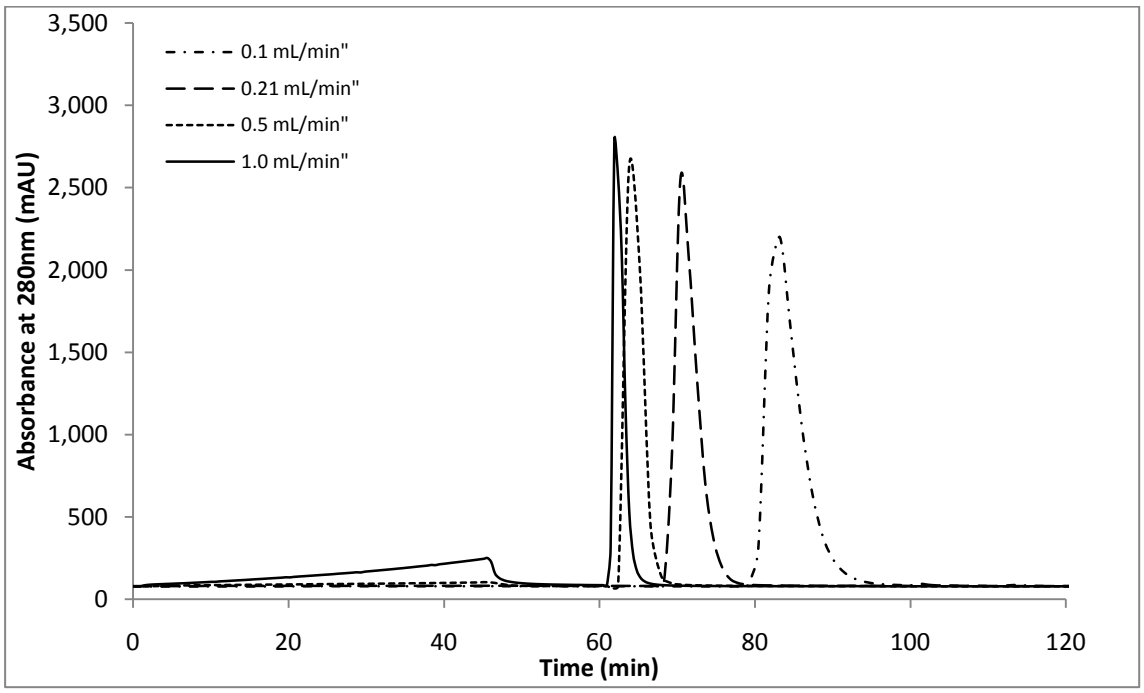

Figure 66. 1.5 mg/mL BSA concentration, 1M NaCl concentration, 180 degrees/hr rotation speed, flow rates 0.1-1.0 mL/min, Trial 8: 45 min loading, 15 min equilibration, 30 min elution, 30 min equilibration.

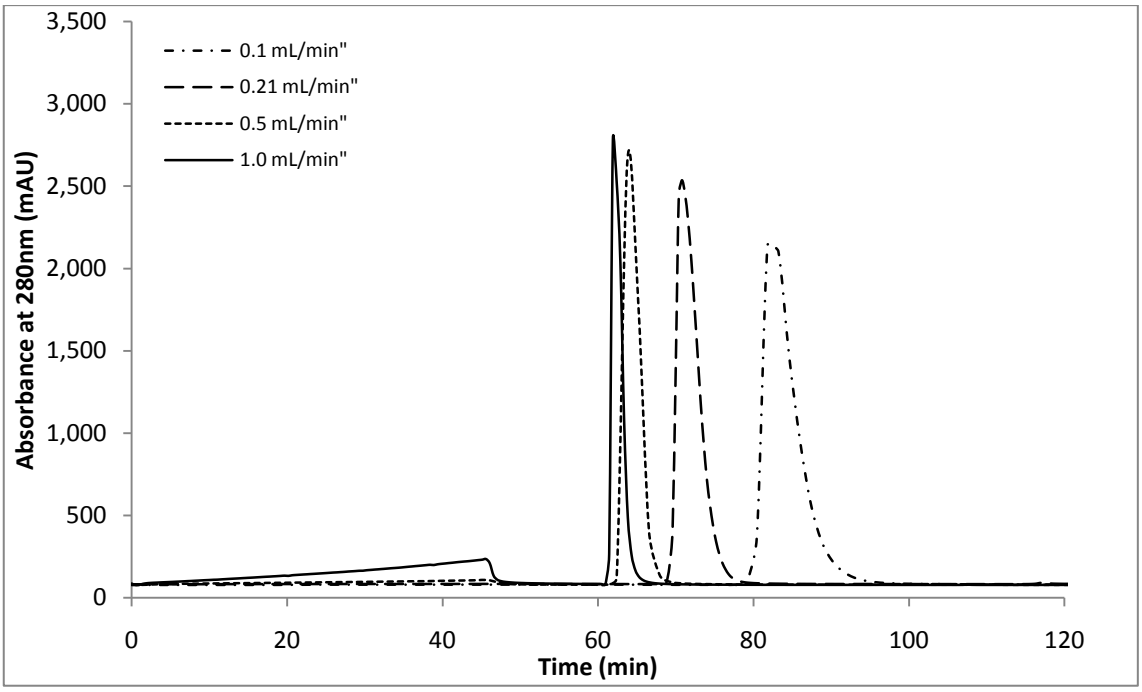

Figure 67. 1.5 mg/mL BSA concentration, 1M NaCl concentration, 180 degrees/hr rotation speed, flow rates 0.1-1.0 mL/min, Trial 9: 45 min loading, 15 min equilibration, 45 min elution, 15 min equilibration.

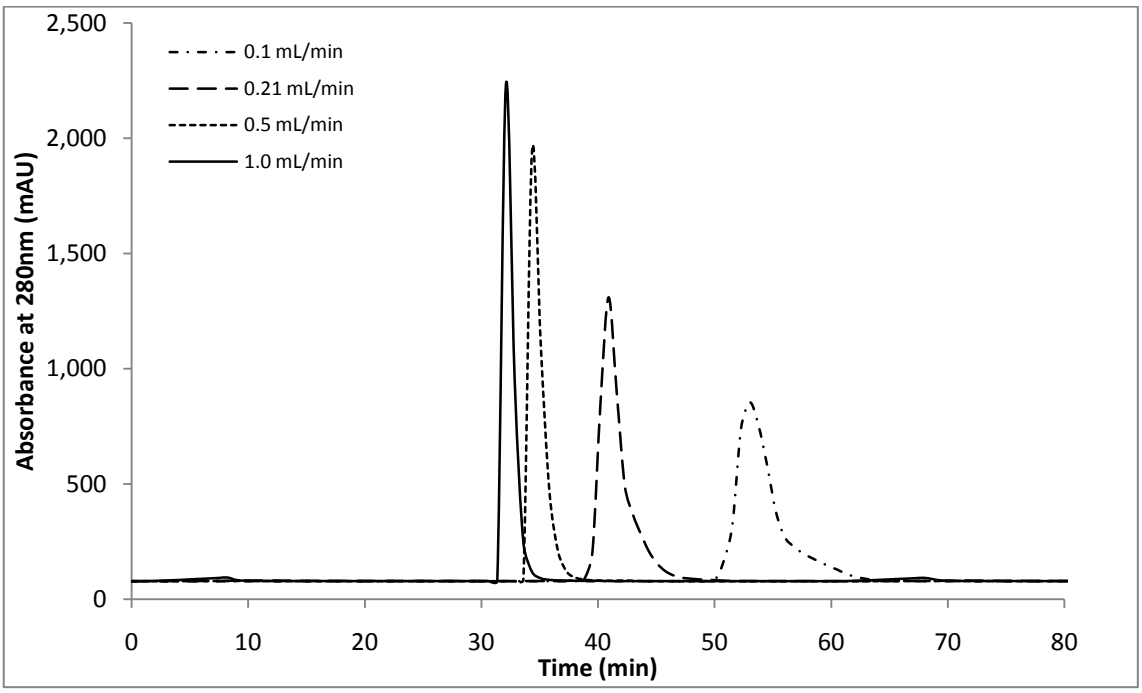

Figure 68. 1.5 mg/mL BSA concentration, 1M NaCl concentration, 360 degrees/hr rotation speed, flow rates 0.1-1.0 mL/min, Trial 1: 7.5 min loading, 22.5 min equilibration, 7.5 min elution, 22.5 min equilibration.

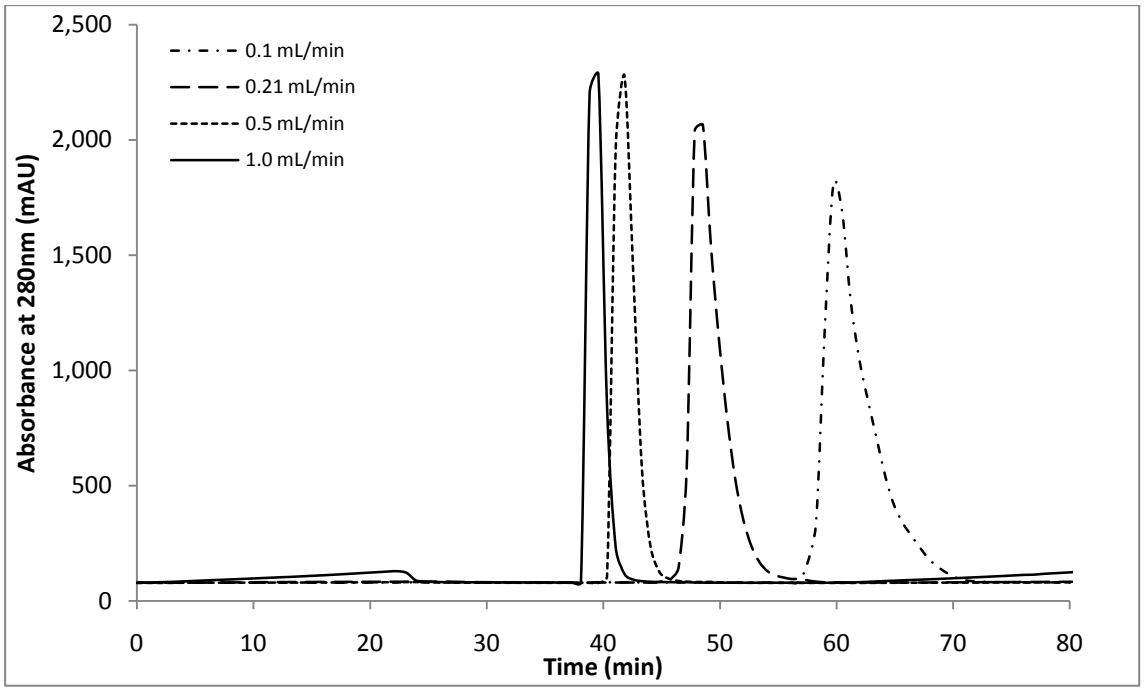

Figure 69. 1.5 mg/mL BSA concentration, 1M NaCl concentration, 360 degrees/hr rotation speed, flow rates 0.1-1.0 mL/min, Trial 2: 22.5 min loading, 15 min equilibration, 7.5 min elution, 15 min equilibration.

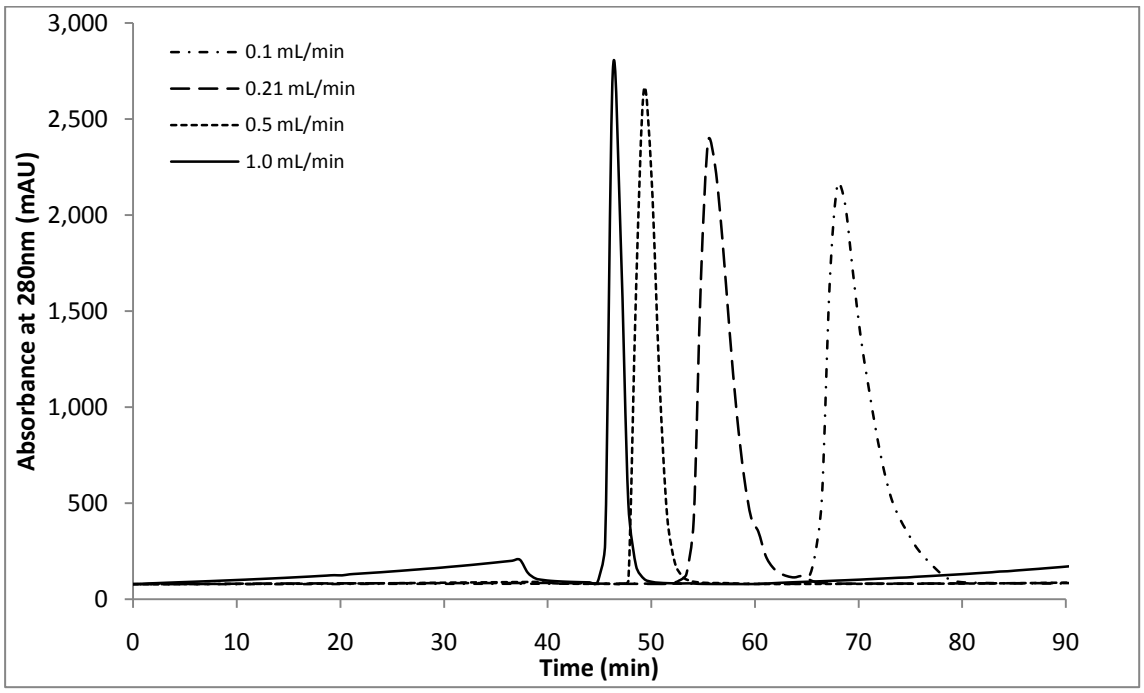

Figure 70. 1.5 mg/mL BSA concentration, 1M NaCl concentration, 360 degrees/hr rotation speed, flow rates 0.1-1.0 mL/min, Trial 3: 37.5 min loading, 7.5 min equilibration, 7.5 min elution, 7.5 min equilibration.

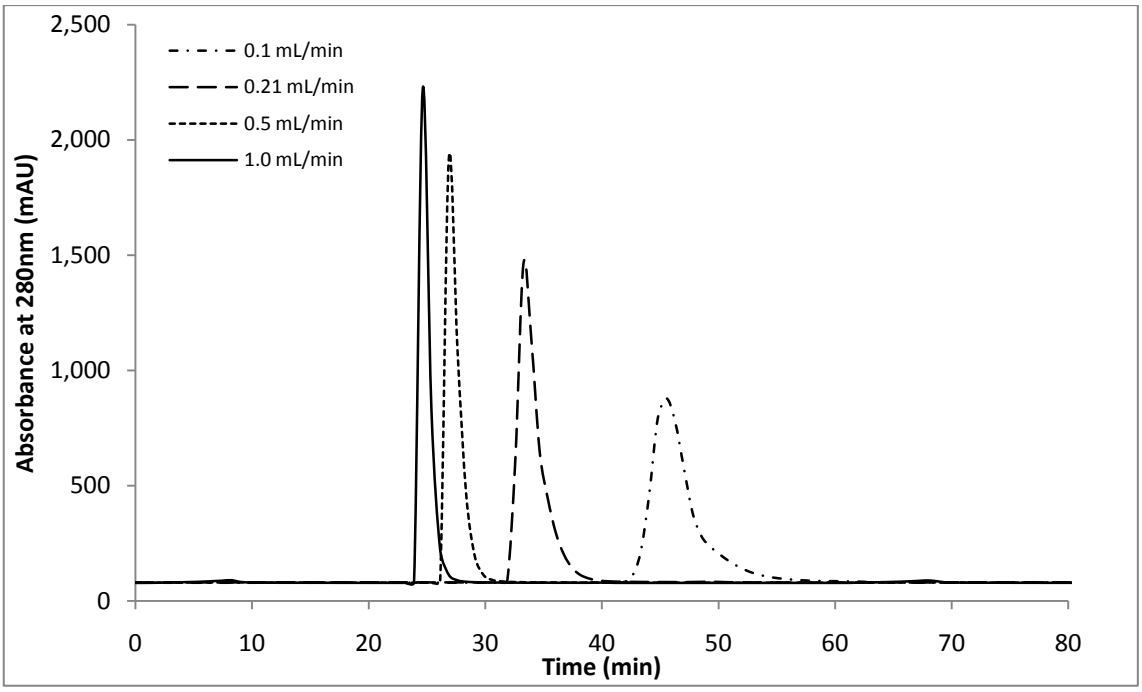

Figure 71. 1.5 mg/mL BSA concentration, 1M NaCl concentration, 360 degrees/hr rotation speed, flow rates 0.1-1.0 mL/min, Trial 4: 7.5 min loading, 15 min equilibration, 15 min elution, 22.5 min equilibration.

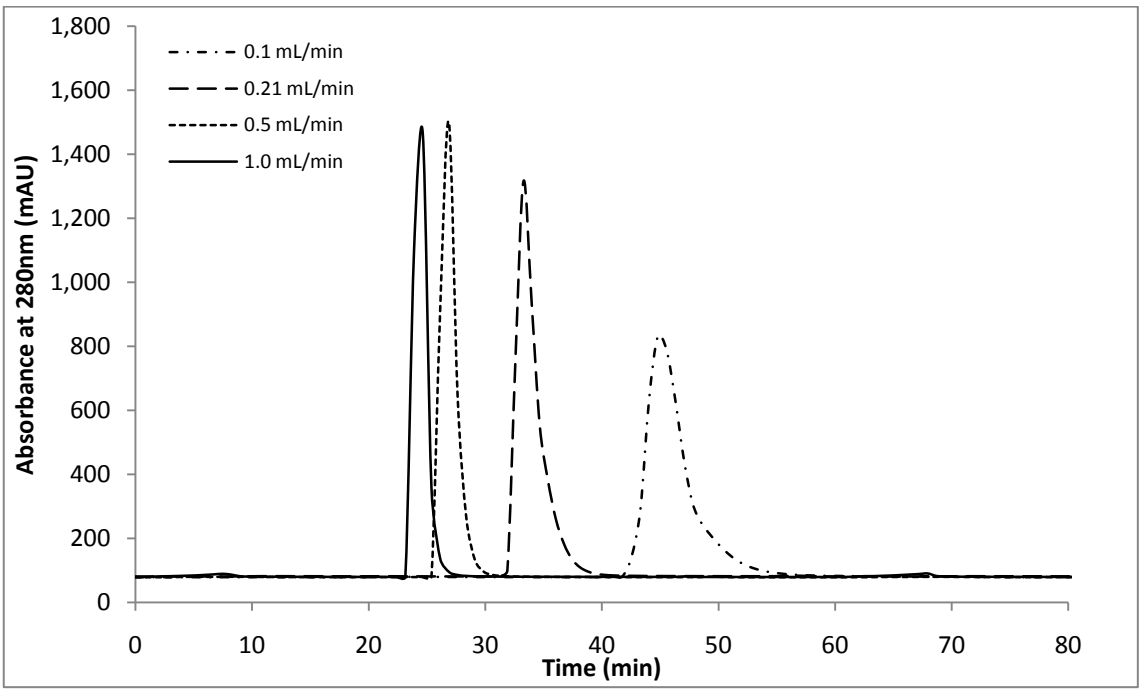

Figure 72. 1.5 mg/mL BSA concentration, 1M NaCl concentration, 360 degrees/hr rotation speed, flow rates 0.1-1.0 mL/min, Trial 5: 7.5 min loading, 15 min equilibration, 22.5 min elution, 15 min equilibration.

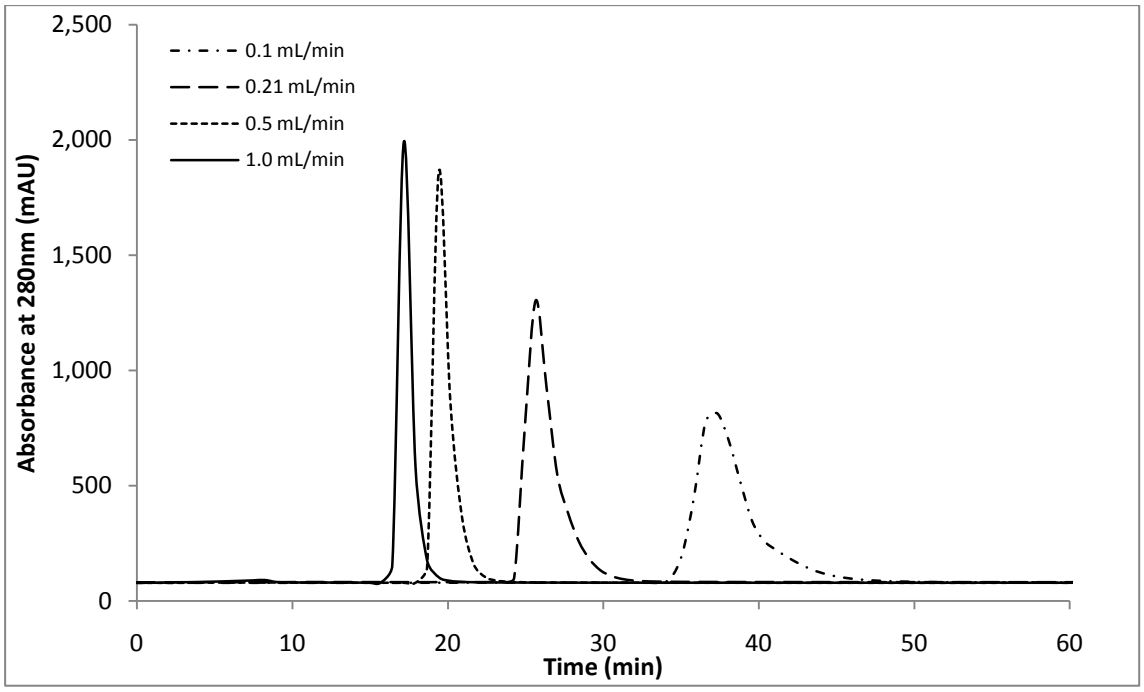

Figure 73. 1.5 mg/mL BSA concentration, 1M NaCl concentration, 360 degrees/hr rotation speed, flow rates 0.1-1.0 mL/min, Trial 6: 7.5 min loading, 7.5 min equilibration, 37.5 min elution, 7.5 min equilibration.

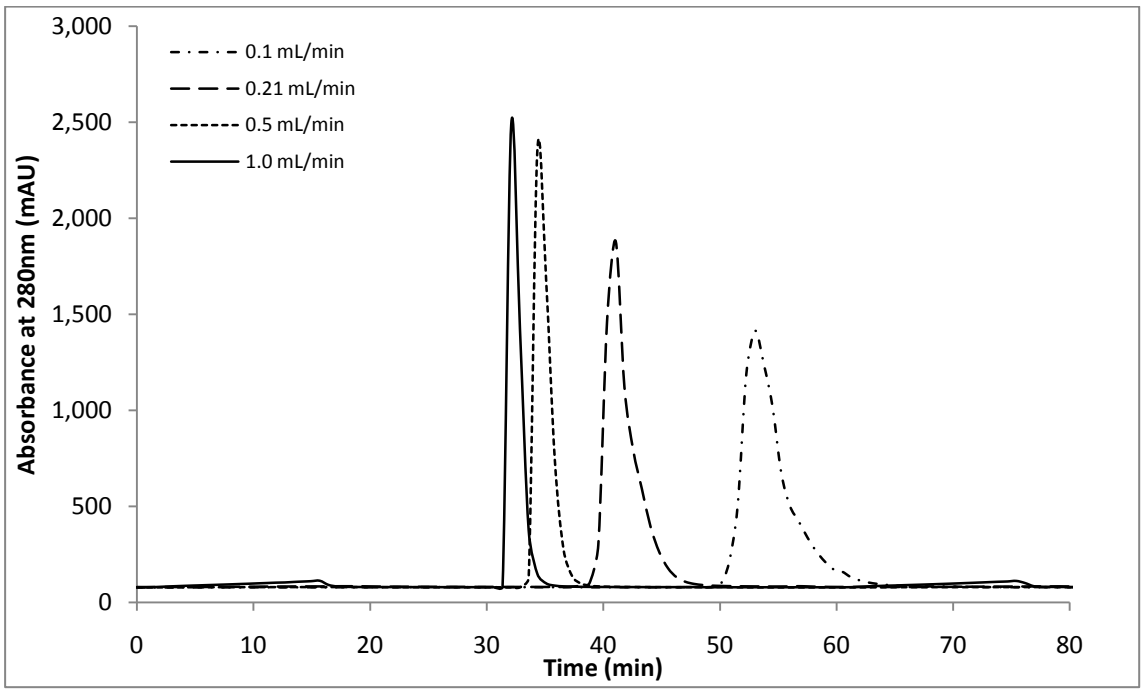

Figure 74. 1.5 mg/mL BSA concentration, 1M NaCl concentration, 360 degrees/hr rotation speed, flow rates 0.1-1.0 mL/min, Trial 7: 15 min loading, 15 min equilibration, 15 min elution, 15 min equilibration.

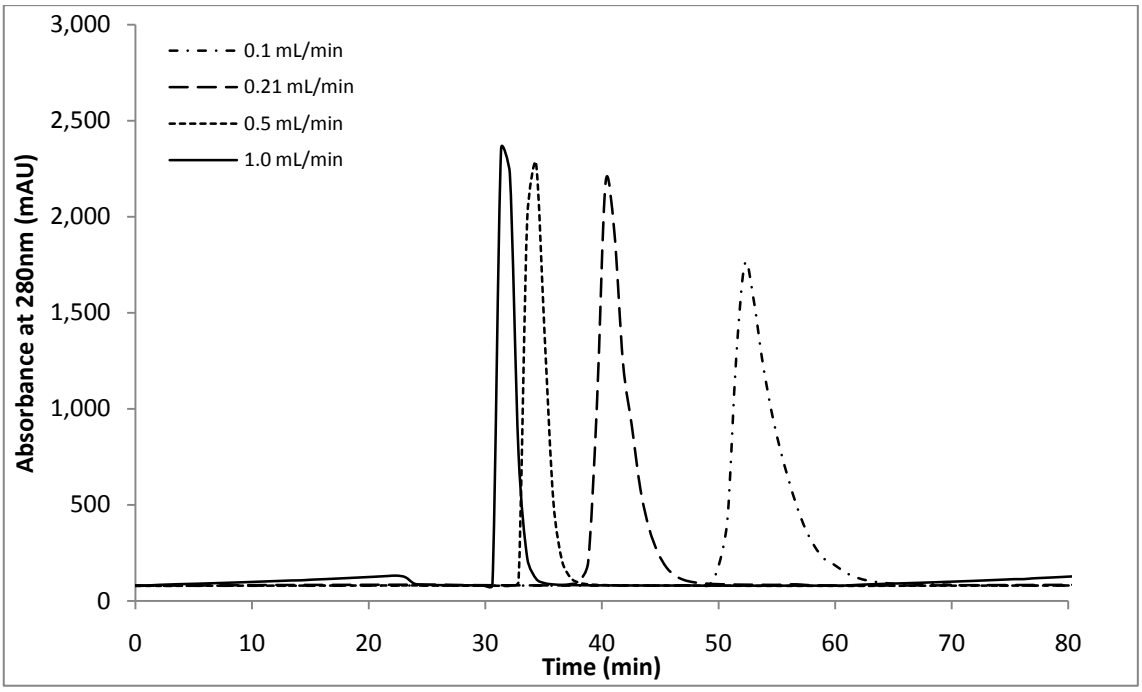

Figure 75. 1.5 mg/mL BSA concentration, 1M NaCl concentration, 360 degrees/hr rotation speed, flow rates 0.1-1.0 mL/min, Trial 8: 22.5 min loading, 7.5 min equilibration, 15 min elution, 15 min equilibration.

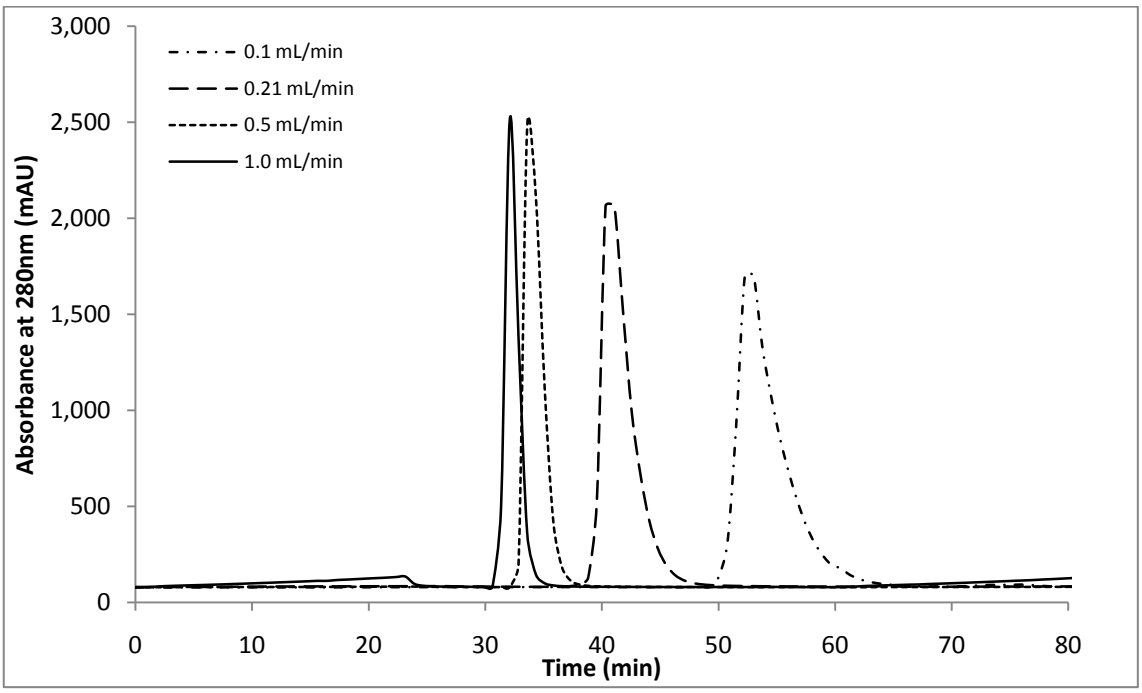

Figure 76. 1.5 mg/mL BSA concentration, 1M NaCl concentration, 360 degrees/hr rotation speed, flow rates 0.1-1.0 mL/min, Trial 9: 22.5 min loading, 7.5 min equilibration, 22.5 min elution, 7.5 min equilibration.

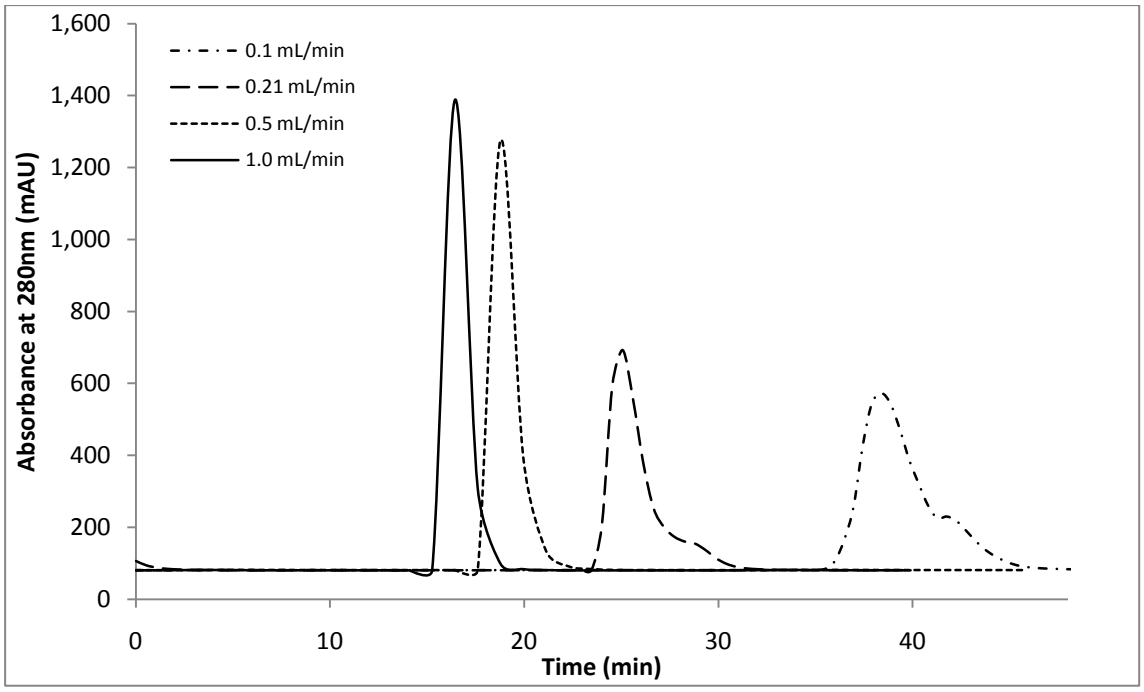

Figure 77. 1.5 mg/mL BSA concentration, 1M NaCl concentration, 720 degrees/hr rotation speed, flow rates 0.1-1.0 mL/min, Trial 1: 3.75 min loading, 11.25 min equilibration, 3.75 min elution, 11.25 min equilibration.

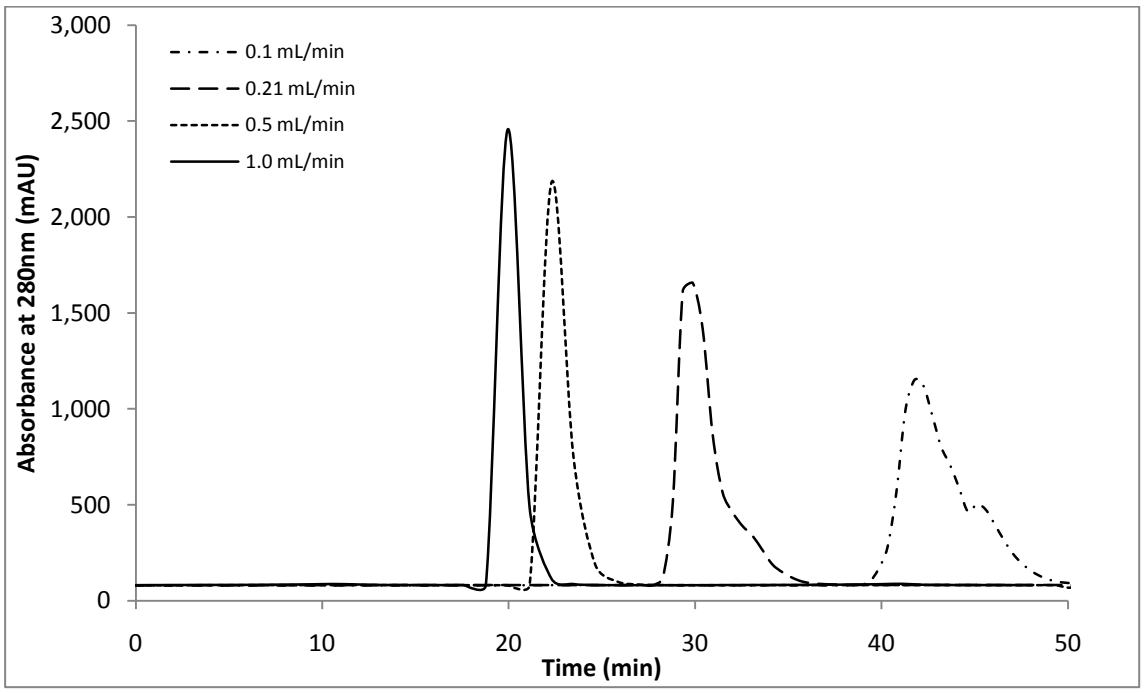

Figure 78. 1.5 mg/mL BSA concentration, 1M NaCl concentration, 720 degrees/hr rotation speed, flow rates 0.1-1.0 mL/min, Trial 2: 11.25 min loading, 7.5 min equilibration, 3.75 min elution, 7.5 min equilibration.

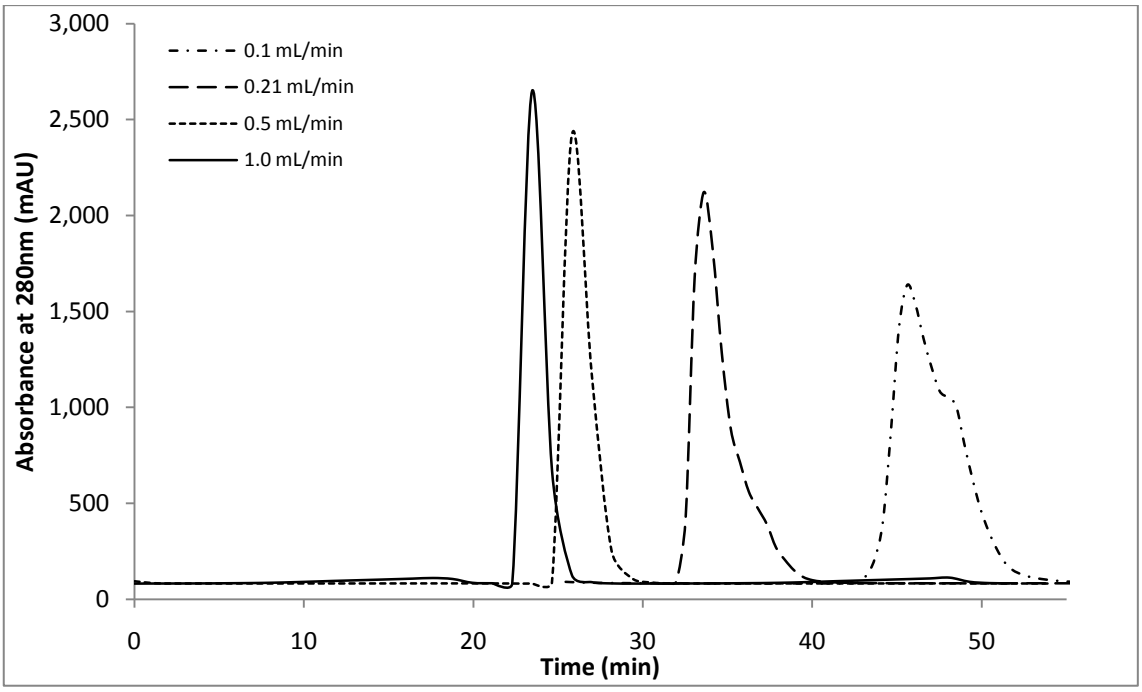

Figure 79. 1.5 mg/mL BSA concentration, 1M NaCl concentration, 720 degrees/hr rotation speed, flow rates 0.1-1.0 mL/min, Trial 3: 18.75 min loading, 3.75 min equilibration, 3.75 min elution, 3.75 min equilibration.

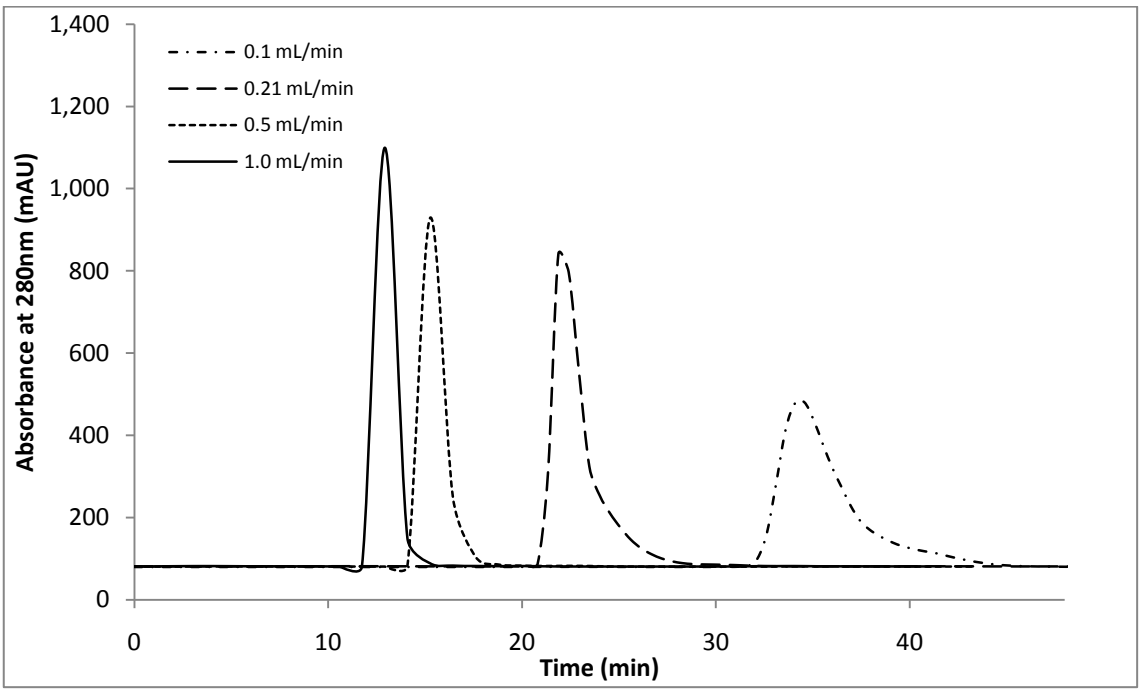

Figure 80. 1.5 mg/mL BSA concentration, 1M NaCl concentration, 720 degrees/hr rotation speed, flow rates 0.1-1.0 mL/min, Trial 4: 3.75 min loading, 7.5 min equilibration, 7.5 min elution, 11.25 min equilibration.

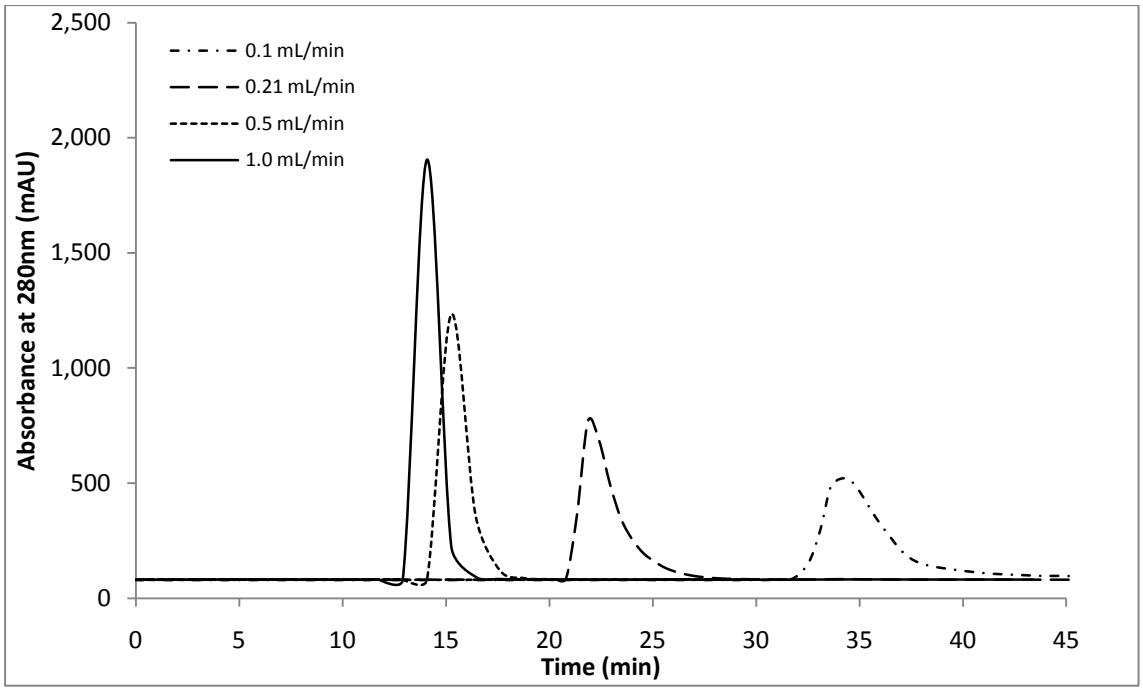

Figure 81. 1.5 mg/mL BSA concentration, 1M NaCl concentration, 720 degrees/hr rotation speed, flow rates 0.1-1.0 mL/min, Trial 5: 3.75 min loading, 7.5 min equilibration, 11.25 min elution, 7.5 min equilibration.

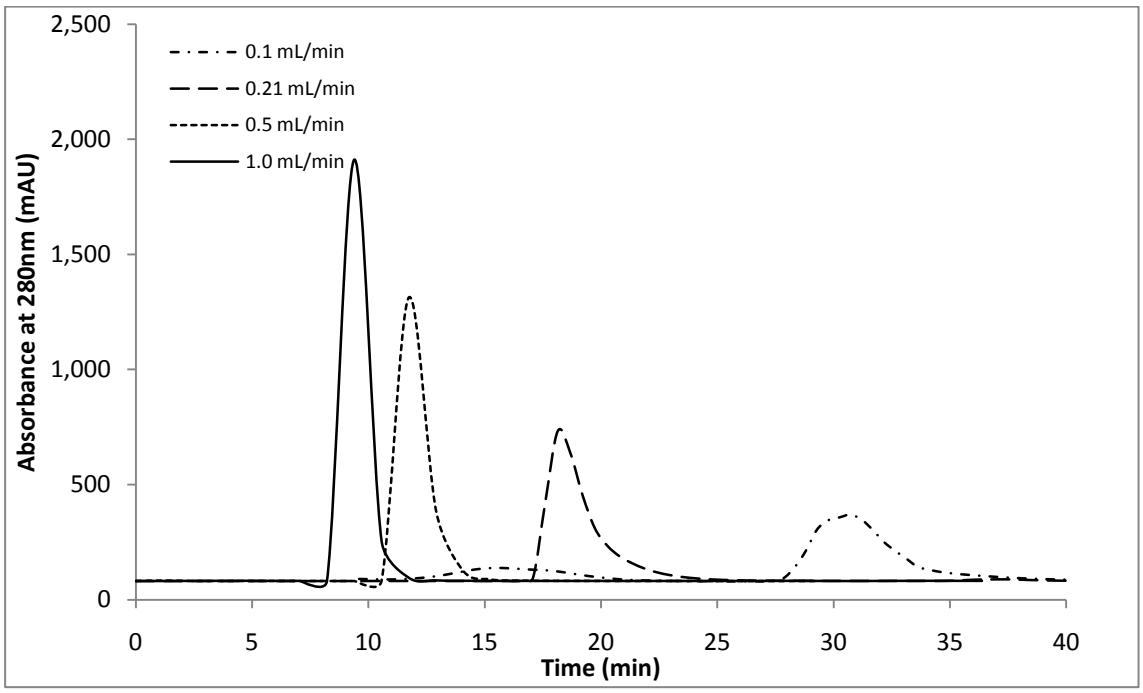

Figure 82. 1.5 mg/mL BSA concentration, 1M NaCl concentration, 720 degrees/hr rotation speed, flow rates 0.1-1.0 mL/min, Trial 6: 3.75 min loading, 3.75 min equilibration, 18.75 min elution, 3.75 min equilibration.

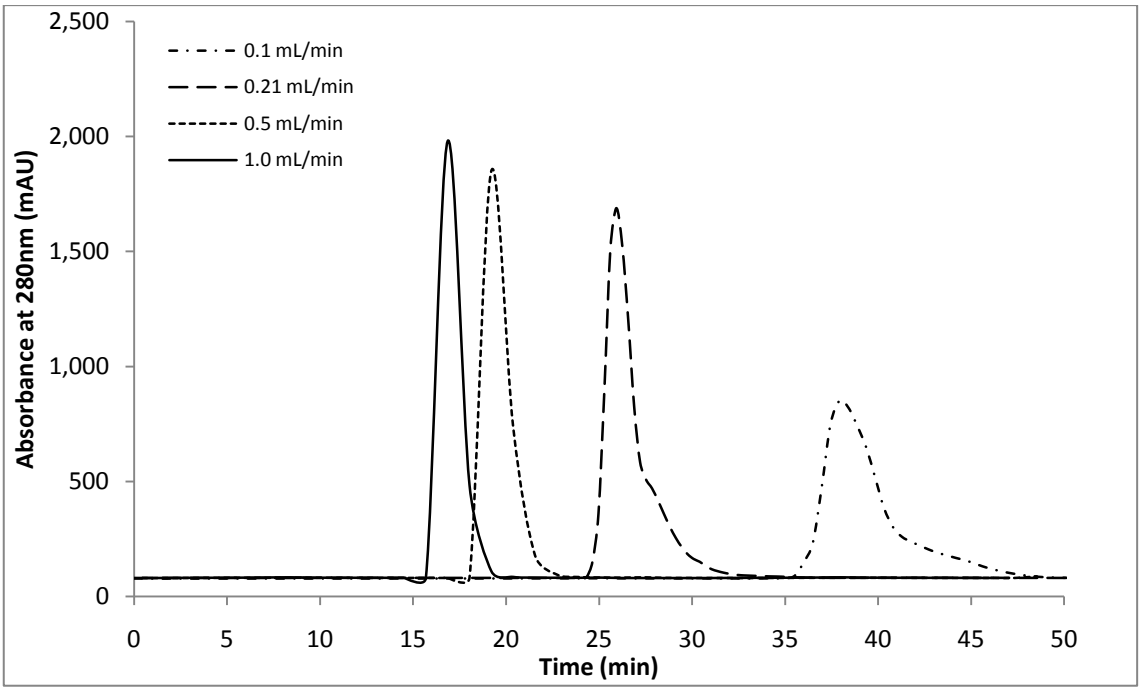

Figure 83. 1.5 mg/mL BSA concentration, 1M NaCl concentration, 720 degrees/hr rotation speed, flow rates 0.1-1.0 mL/min, Trial 7: 7.5 min loading, 7.5 min equilibration, 7.5 min elution, 7.5 min equilibration.

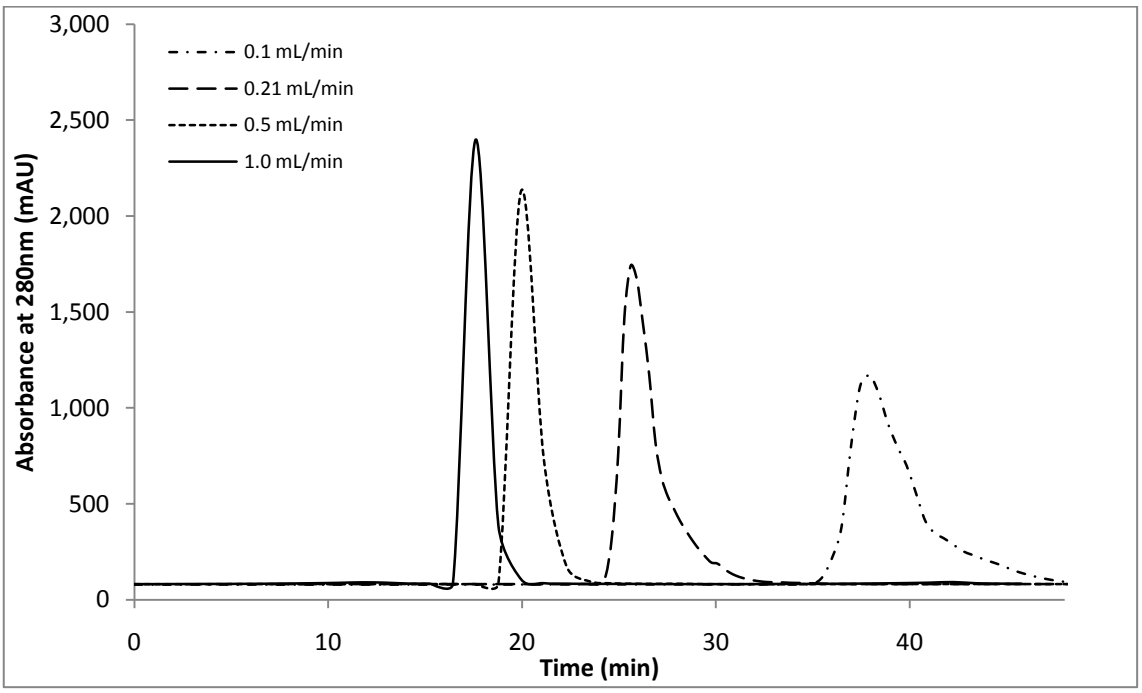

Figure 84. 1.5 mg/mL BSA concentration, 1M NaCl concentration, 720 degrees/hr rotation speed, flow rates 0.1-1.0 mL/min, Trial 8: 11.25 min loading, 3.75 min equilibration, 7.5 min elution, 7.5 min equilibration.

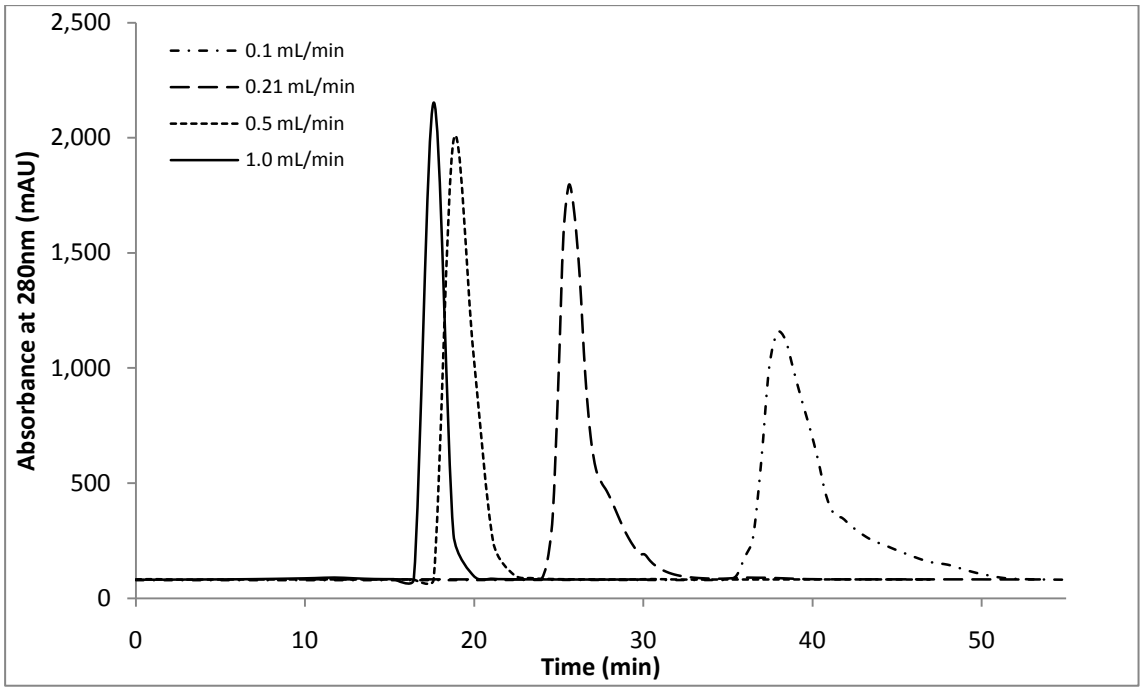

Figure 85. 1.5 mg/mL BSA concentration, 1M NaCl concentration, 720 degrees/hr rotation speed, flow rates 0.1-1.0 mL/min, Trial 9: 11.25 min loading, 3.75 min equilibration, 11.25 min elution, 3.75 min equilibration.

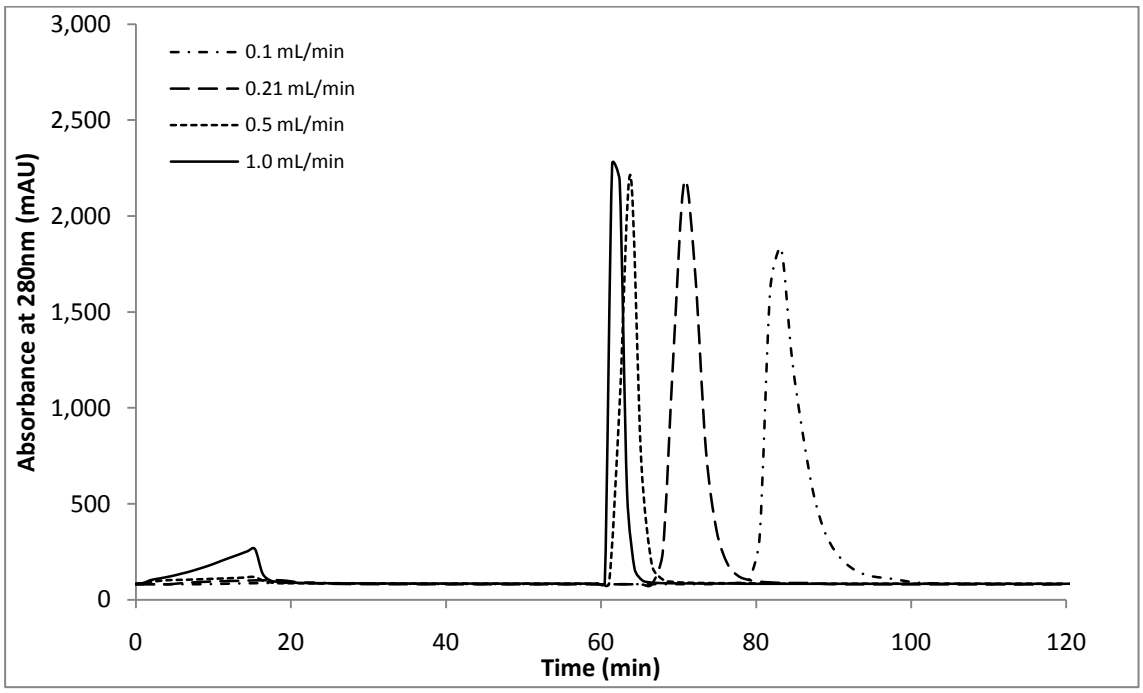

Figure 86. 3 mg/mL BSA concentration, 1M NaCl concentration, 180 degrees/hr rotation speed, flow rates 0.1-1.0 mL/min, Trial 1: 15 min loading, 45 min equilibration, 15 min elution, 45 min equilibration.

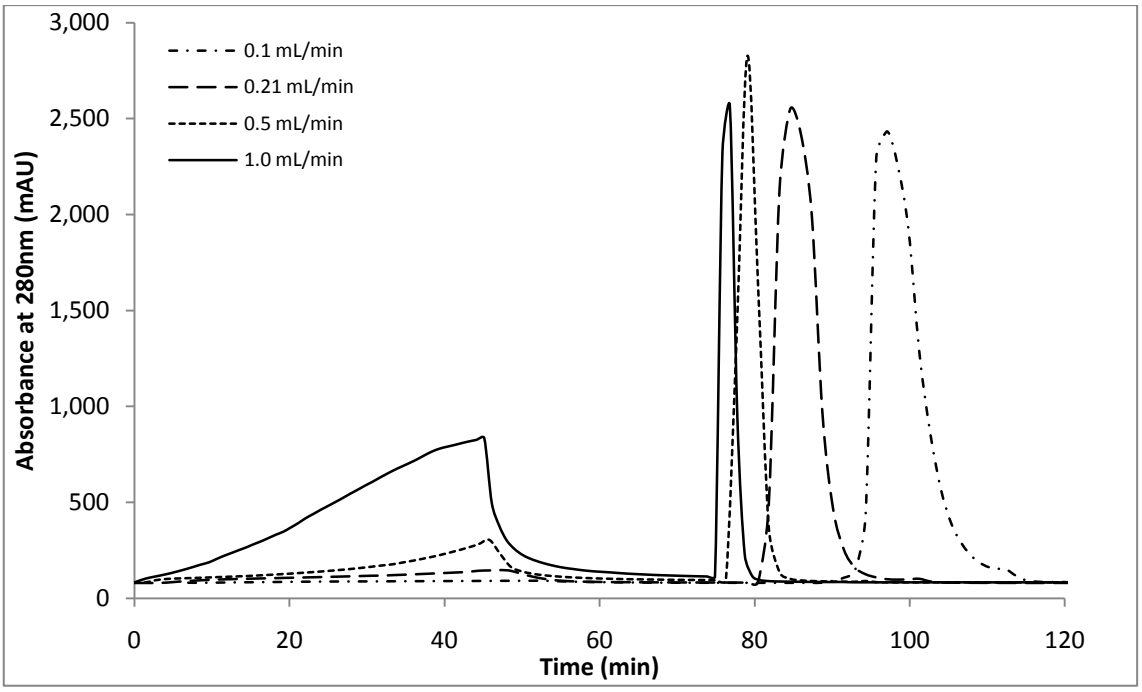

Figure 87. 3 mg/mL BSA concentration, 1M NaCl concentration, 180 degrees/hr rotation speed, flow rates 0.1-1.0 mL/min, Trial 2: 45 min loading, 40 min equilibration, 15 min elution, 30 min equilibration.

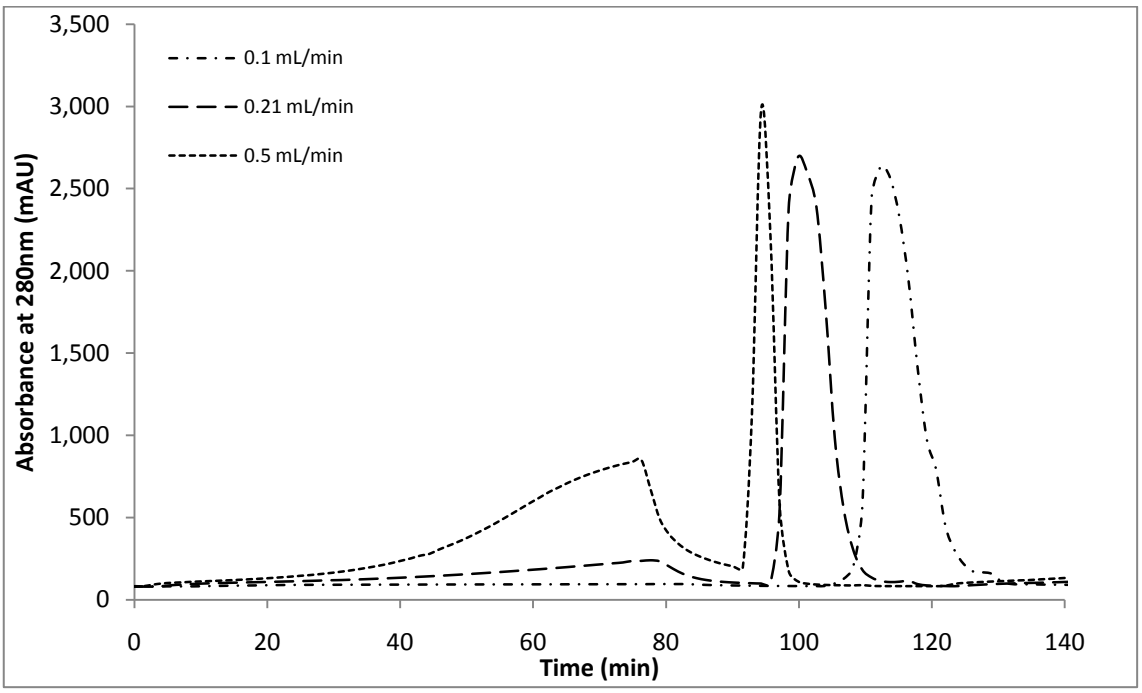

Figure 88. 3 mg/mL BSA concentration, 1M NaCl concentration, 180 degrees/hr rotation speed, flow rates 0.1-0.5 mL/min, Trial 3: 75 min loading, 15 min equilibration, 15 min elution, 15 min equilibration.

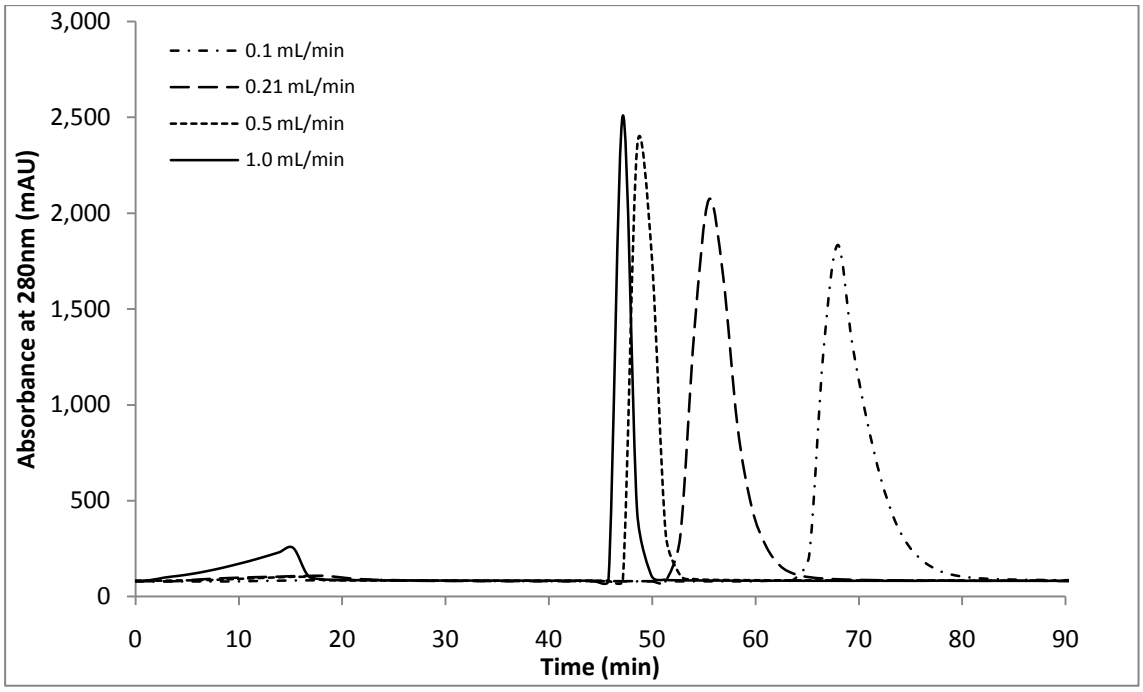

Figure 89. 3 mg/mL BSA concentration, 1M NaCl concentration, 180 degrees/hr rotation speed, flow rates 0.1-1.0 mL/min, Trial 4: 15 min loading, 30 min equilibration, 30 min elution, 45 min equilibration.

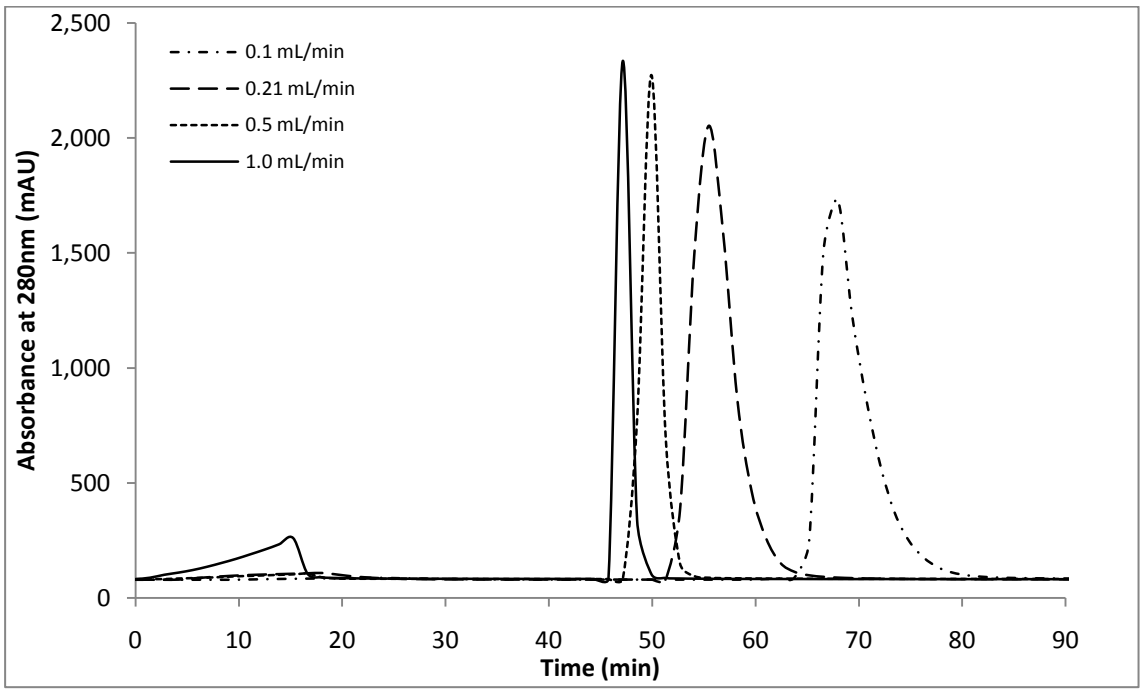

Figure 90. 3 mg/mL BSA concentration, 1M NaCl concentration, 180 degrees/hr rotation speed, flow rates 0.1-1.0 mL/min, Trial 5: 15 min loading, 30 min equilibration, 45 min elution, 30 min equilibration.

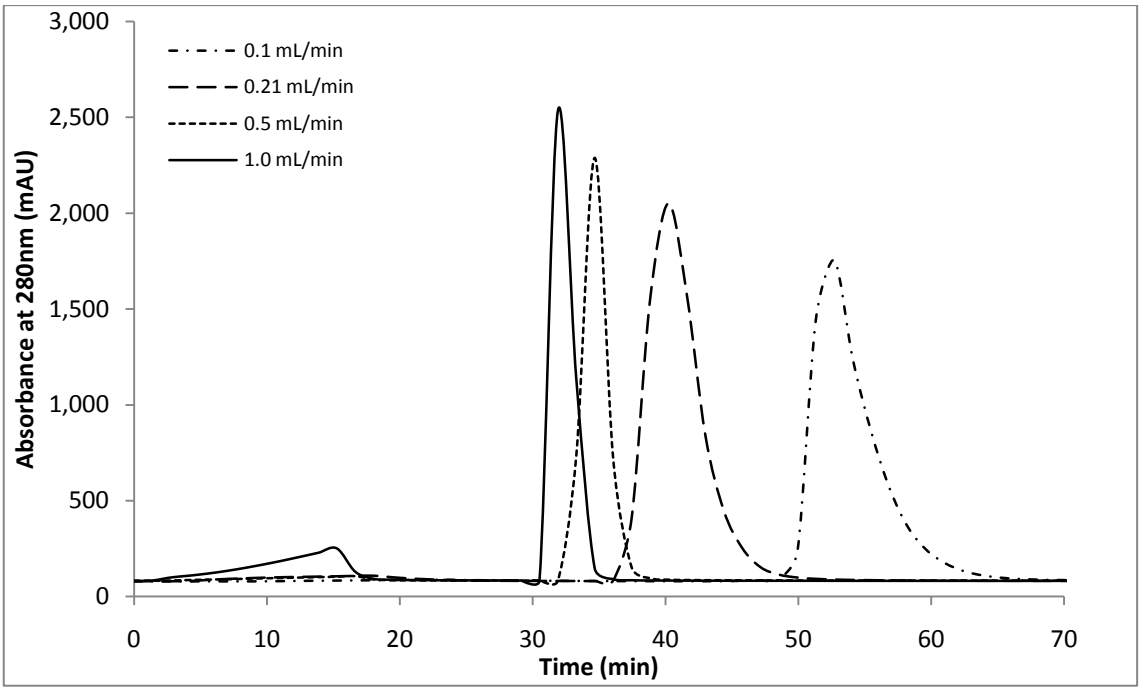

Figure 91. 3 mg/mL BSA concentration, 1M NaCl concentration, 180 degrees/hr rotation speed, flow rates 0.1-1.0 mL/min, Trial 6: 15 min loading, 15 min equilibration, 75 min elution, 15equilibration.

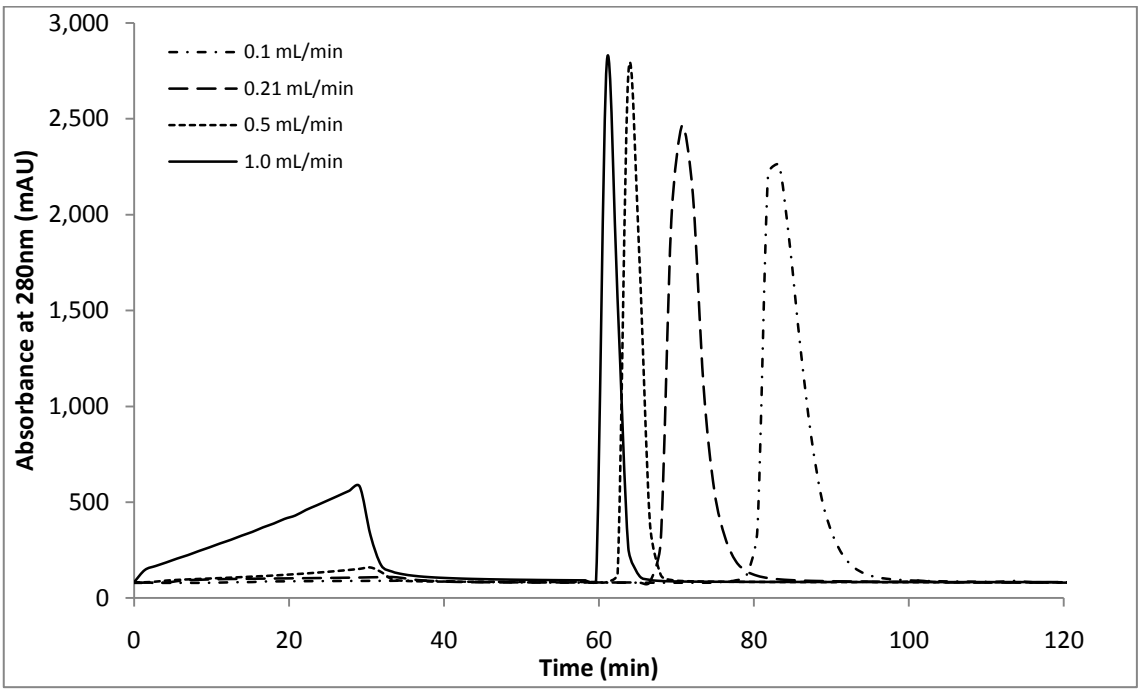

Figure 92. 3 mg/mL BSA concentration, 1M NaCl concentration, 180 degrees/hr rotation speed, flow rates 0.1-1.0 mL/min, Trial 7: 30 min loading, 30 min equilibration, 30 min elution, 30 min equilibration.

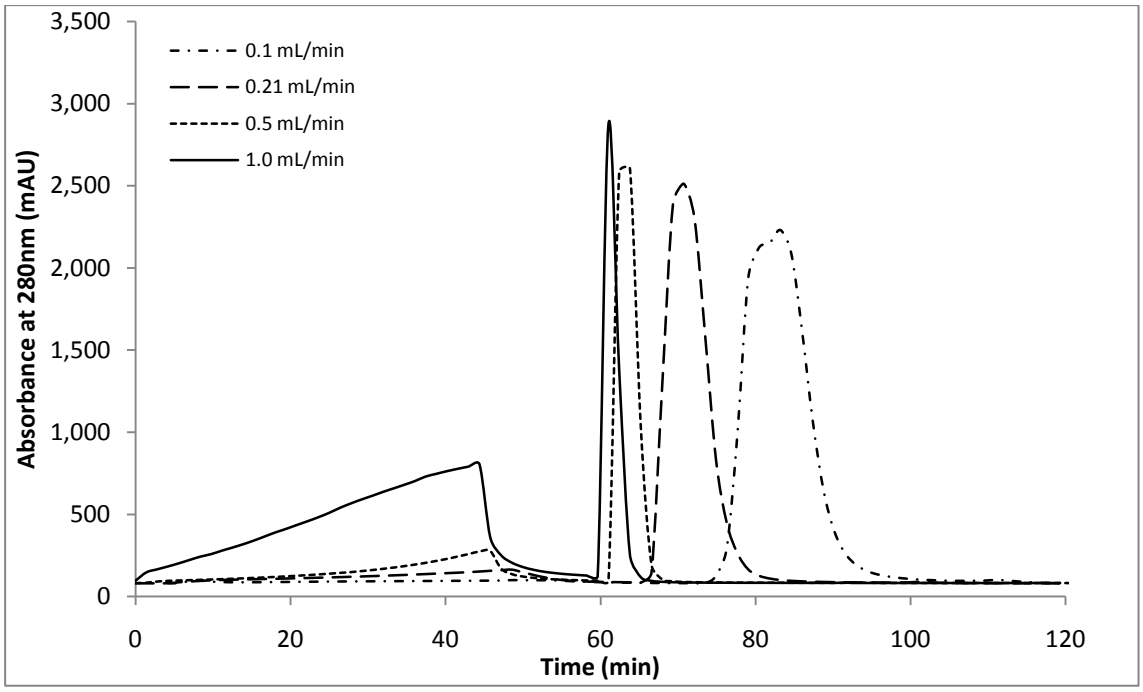

Figure 93. 3 mg/mL BSA concentration, 1M NaCl concentration, 180 degrees/hr rotation speed, flow rates 0.1-1.0 mL/min, Trial 8: 45 min loading, 15 min equilibration, 30 min elution, 30 min equilibration.

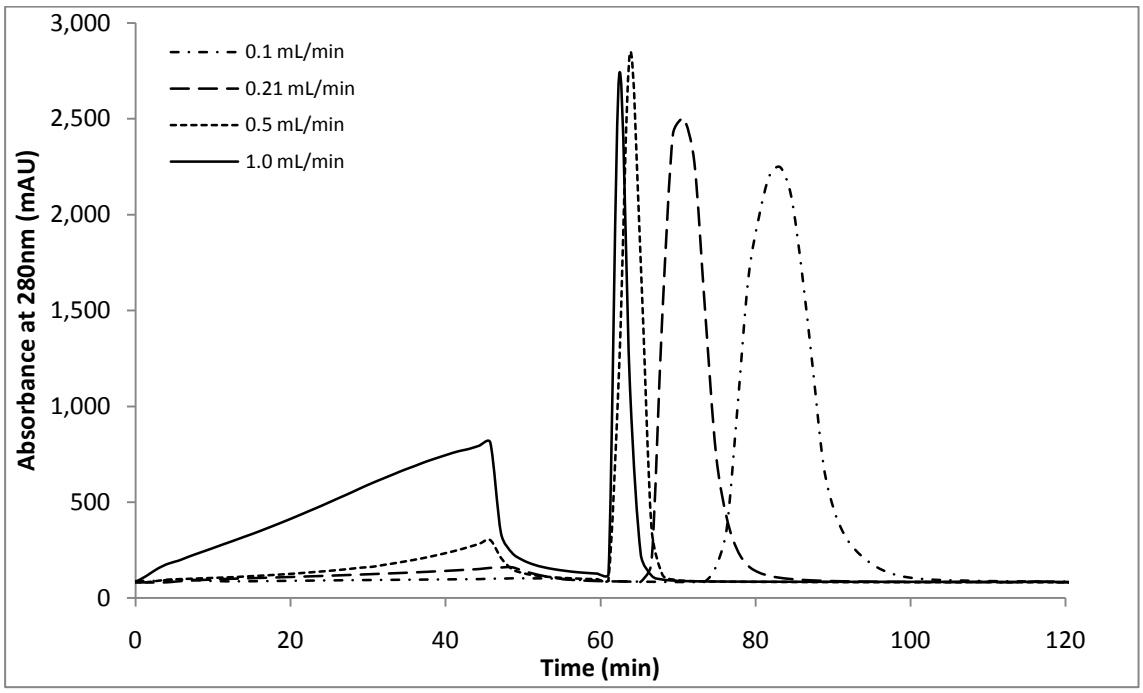

Figure 94. 3 mg/mL BSA concentration, 1M NaCl concentration, 180 degrees/hr rotation speed, flow rates 0.1-1.0 mL/min, Trial 9: 45 min loading, 15 min equilibration, 45 min elution, 15 min equilibration.

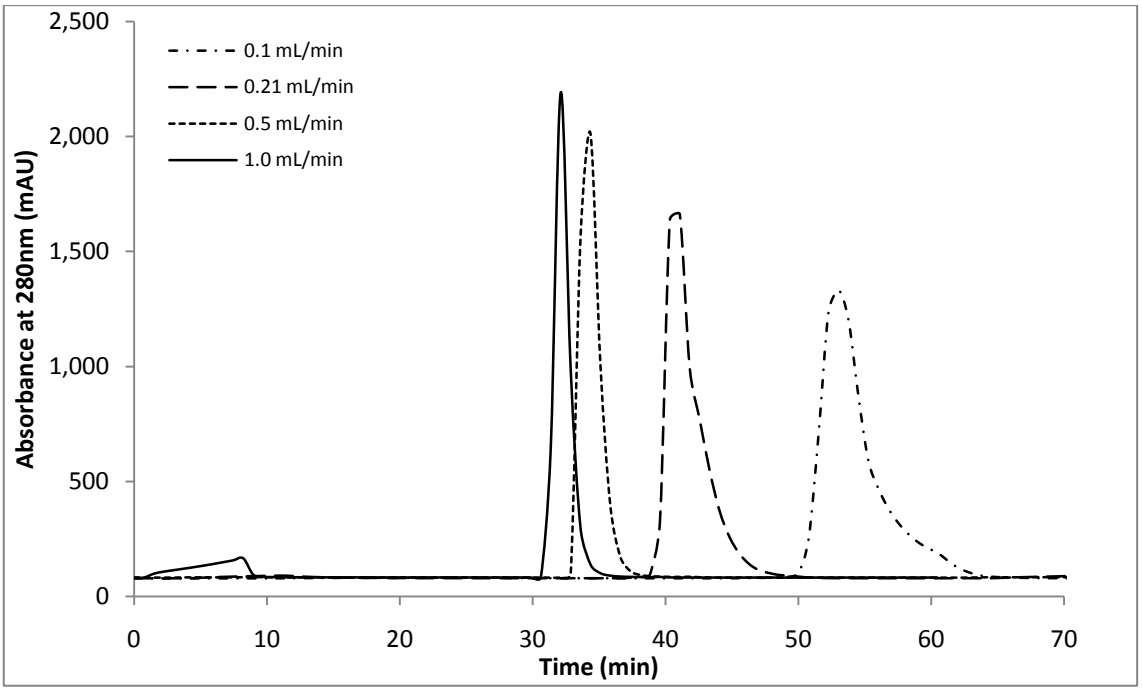

Figure 95. 3 mg/mL BSA concentration, 1M NaCl concentration, 360 degrees/hr rotation speed, flow rates 0.1-1.0 mL/min, Trial 1: 7.5 min loading, 22.5 min equilibration, 7.5 min elution, 22.5 min equilibration.

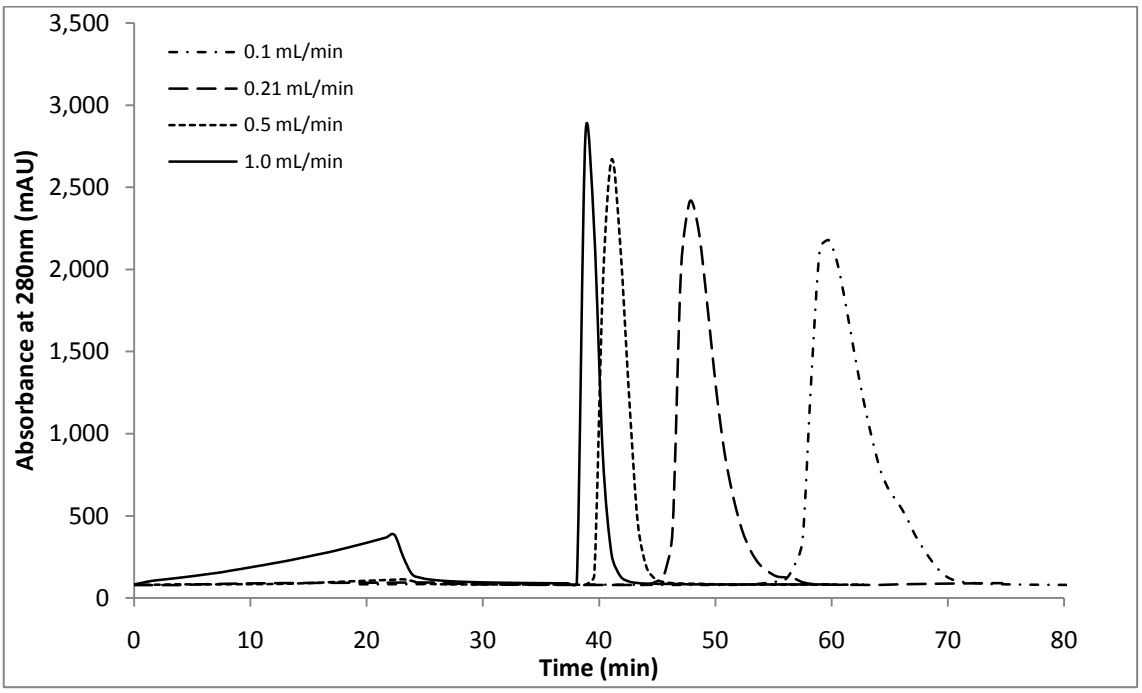

Figure 96. 3 mg/mL BSA concentration, 1M NaCl concentration, 360 degrees/hr rotation speed, flow rates 0.1-1.0 mL/min, Trial 2: 22.5 min loading, 15 min equilibration, 7.5 min elution, 15 min equilibration.

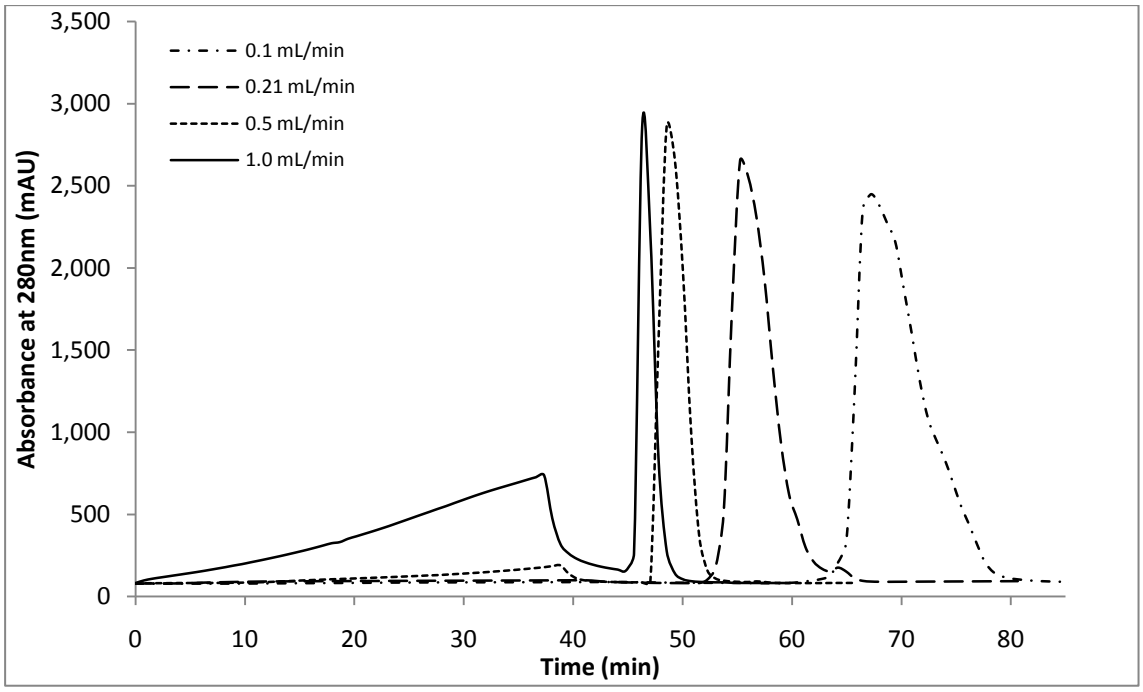

Figure 97. 3 mg/mL BSA concentration, 1M NaCl concentration, 360 degrees/hr rotation speed, flow rates 0.1-1.0 mL/min, Trial 3: 37.5 min loading, 7.5 min equilibration, 7.5 min elution, 7.5 min equilibration.

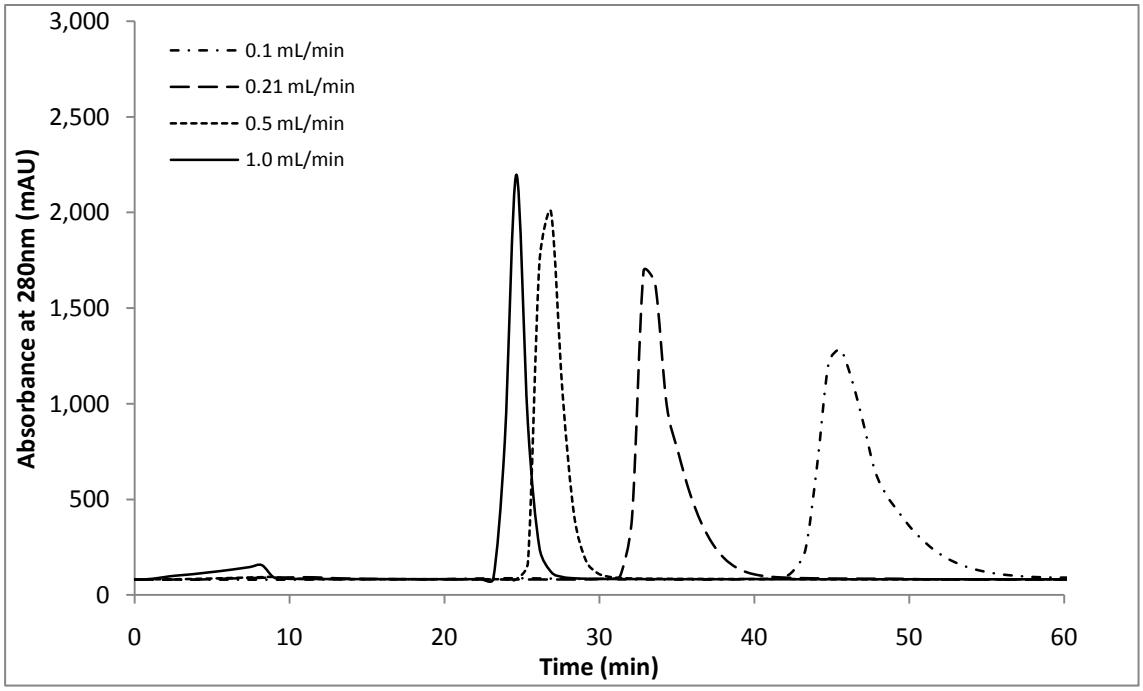

Figure 98. 3 mg/mL BSA concentration, 1M NaCl concentration, 360 degrees/hr rotation speed, flow rates 0.1-1.0 mL/min, Trial 4: 7.5 min loading, 15 min equilibration, 15 min elution, 22.5 min equilibration.

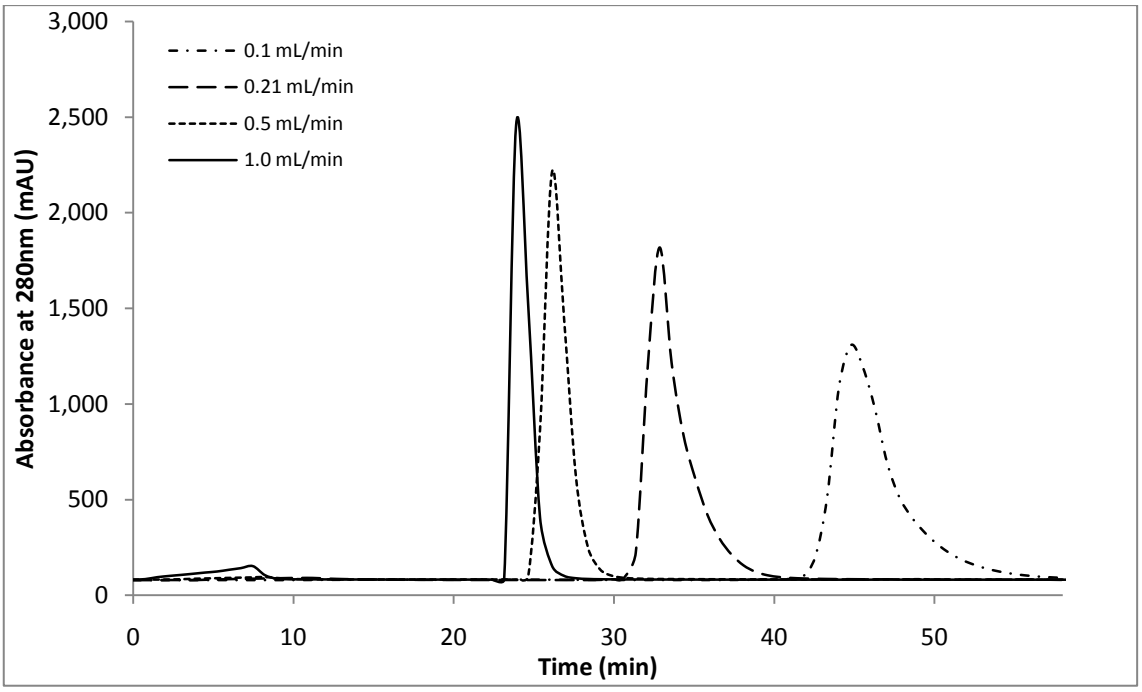

Figure 99. 3 mg/mL BSA concentration, 1M NaCl concentration, 360 degrees/hr rotation speed, flow rates 0.1-1.0 mL/min, Trial 5: 7.5 min loading, 15 min equilibration, 22.5 min elution, 15 min equilibration.

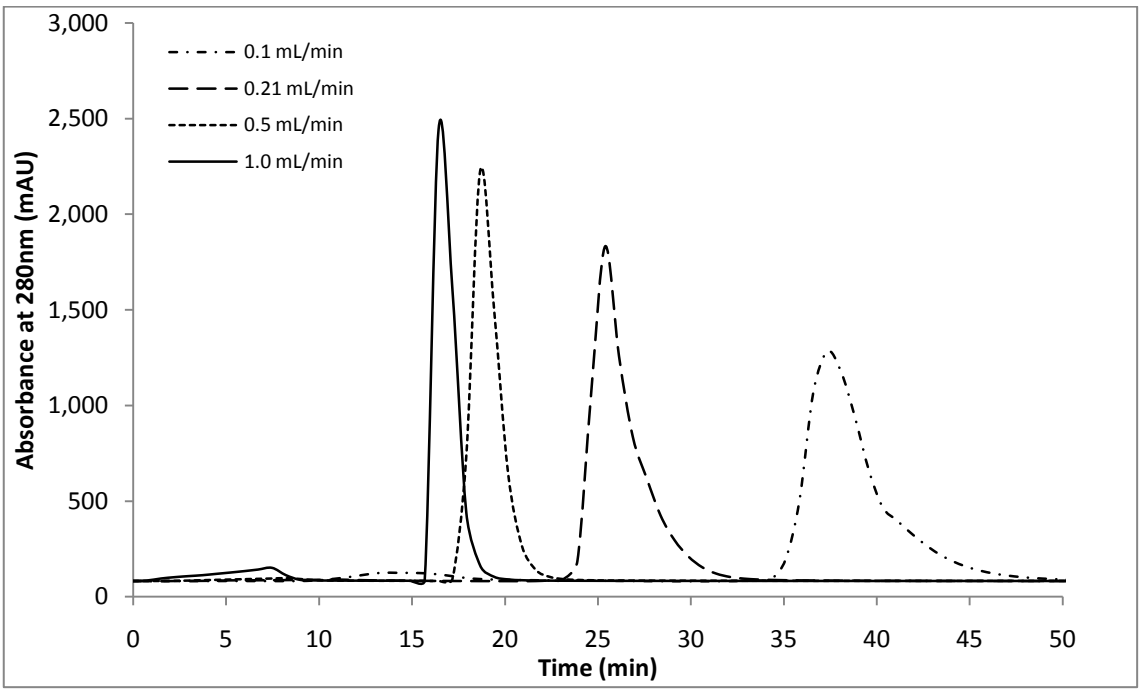

Figure 100. 3 mg/mL BSA concentration, 1M NaCl concentration, 360 degrees/hr rotation speed, flow rates 0.1-1.0 mL/min, Trial 6: 7.5 min loading, 7.5 min equilibration, 37.5 min elution, 7.5 min equilibration.

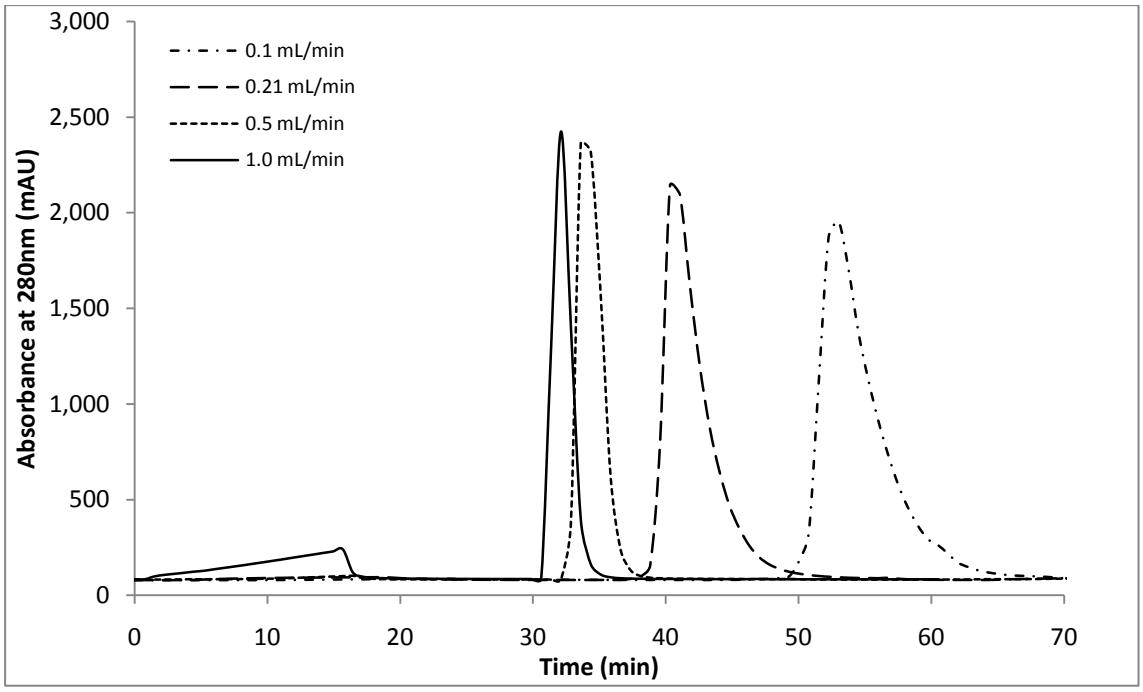

Figure 101. 3 mg/mL BSA concentration, 1M NaCl concentration, 360 degrees/hr rotation speed, flow rates 0.1-1.0 mL/min, Trial 7: 15 min loading, 15 min equilibration, 15 min elution, 15 min equilibration.

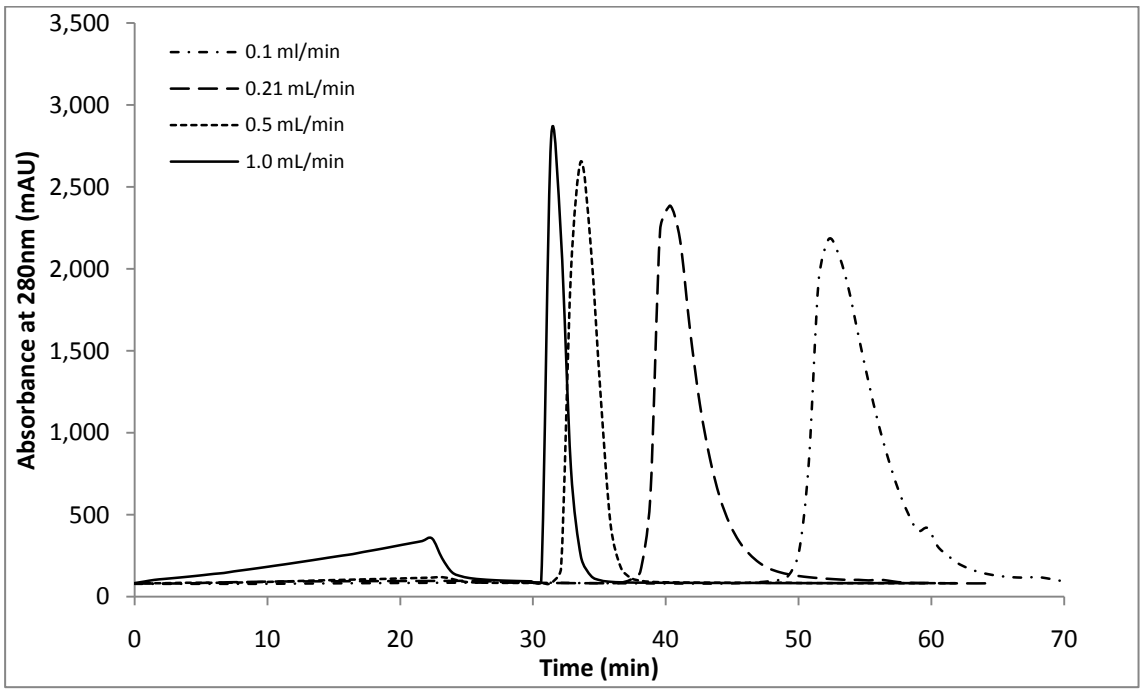

Figure 102. 3 mg/mL BSA concentration, 1M NaCl concentration, 360 degrees/hr rotation speed, flow rates 0.1-1.0 mL/min, Trial 8: 22.5 min loading, 7.5 min equilibration, 15 min elution, 15 min equilibration.

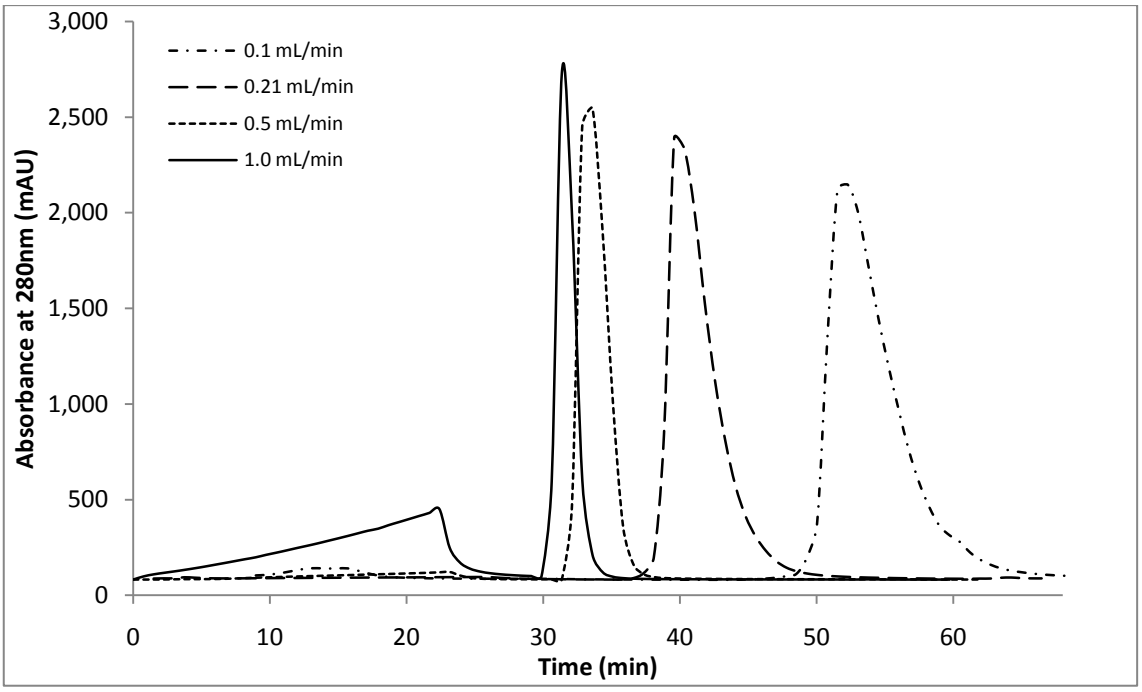

Figure 103. 3 mg/mL BSA concentration, 1M NaCl concentration, 360 degrees/hr rotation speed, flow rates 0.1-1.0 mL/min, Trial 9: 22.5 min loading, 7.5 min equilibration, 22.5 min elution, 7.5 min equilibration.

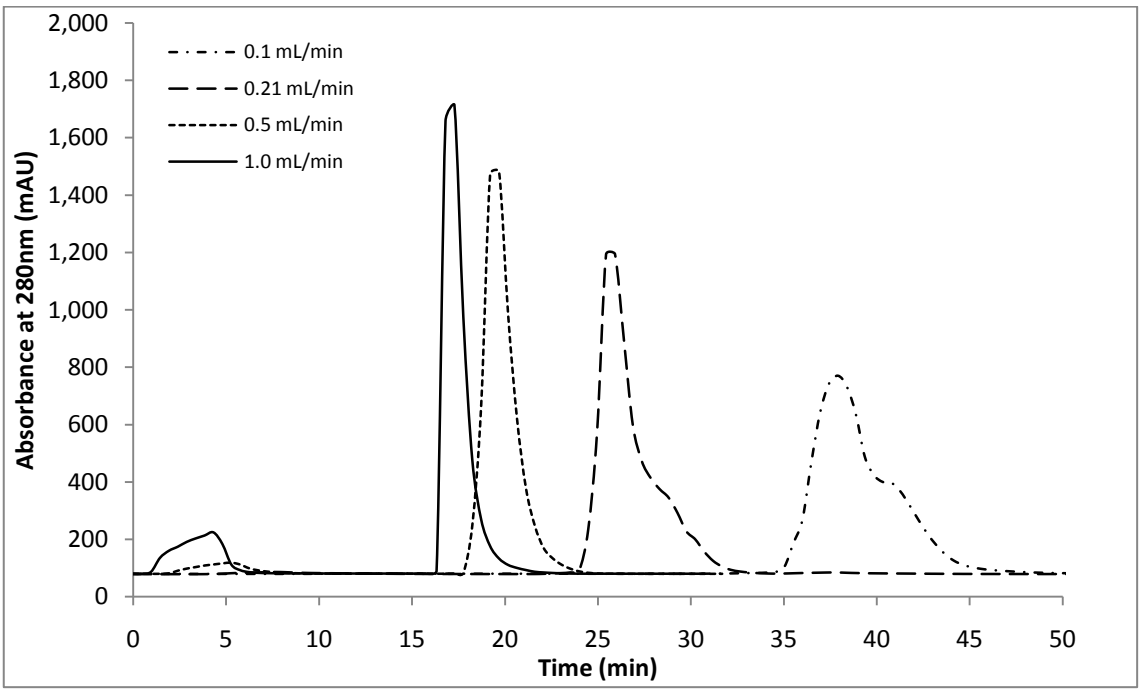

Figure 104. 3 mg/mL BSA concentration, 1M NaCl concentration, 720 degrees/hr rotation speed, flow rates 0.1-1.0 mL/min, Trial 1: 3.75 min loading, 11.25 min equilibration, 3.75 min elution, 11.25 min equilibration.

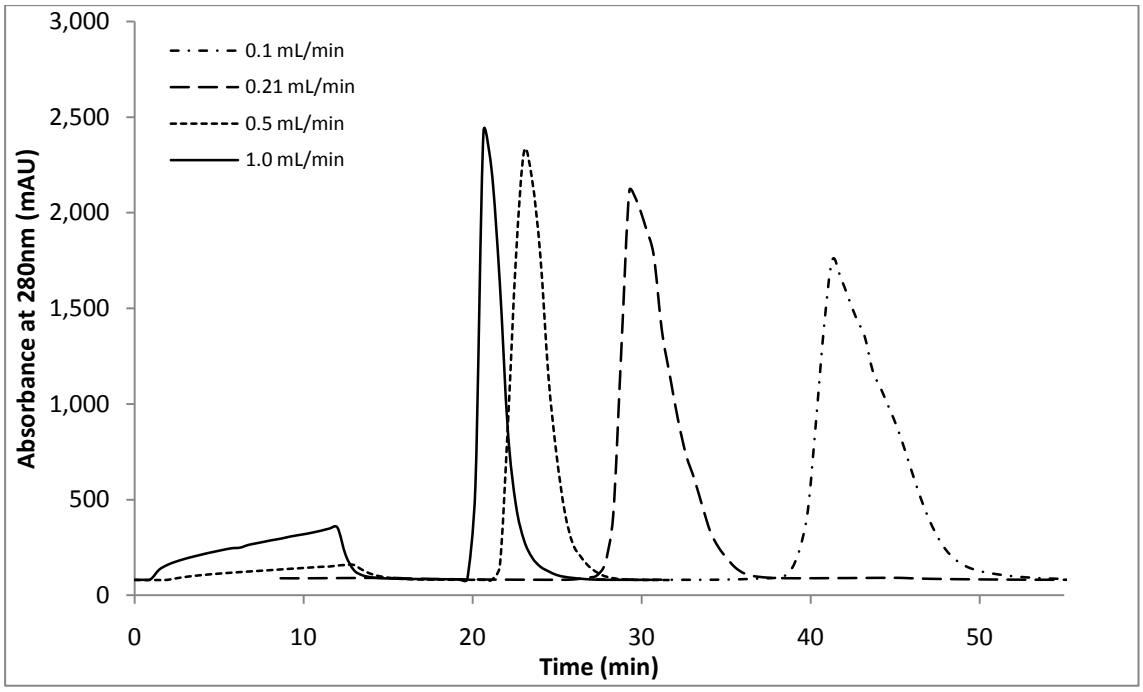

Figure 105. 3 mg/mL BSA concentration, 1M NaCl concentration, 720 degrees/hr rotation speed, flow rates 0.1-1.0 mL/min, Trial 2: 11.25 min loading, 7.5 min equilibration, 3.75 min elution, 7.5 min equilibration.

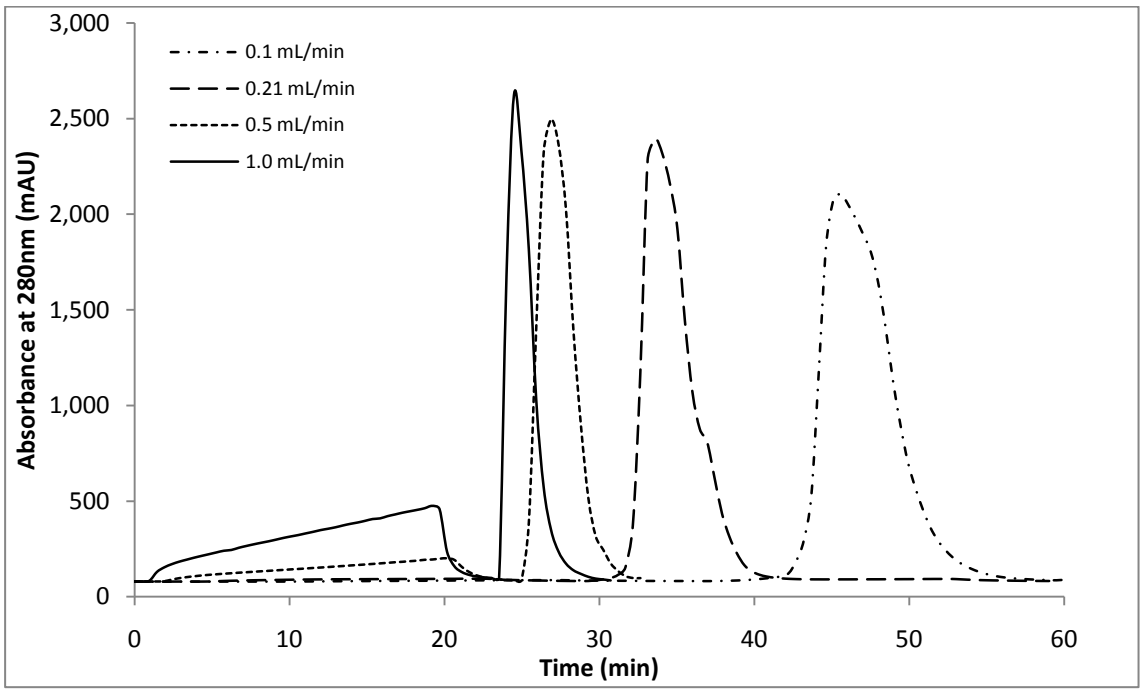

Figure 106. 3 mg/mL BSA concentration, 1M NaCl concentration, 720 degrees/hr rotation speed, flow rates 0.1-1.0 mL/min, Trial 3: 18.75 min loading, 3.75 min equilibration, 3.75 min elution, 3.75 min equilibration.

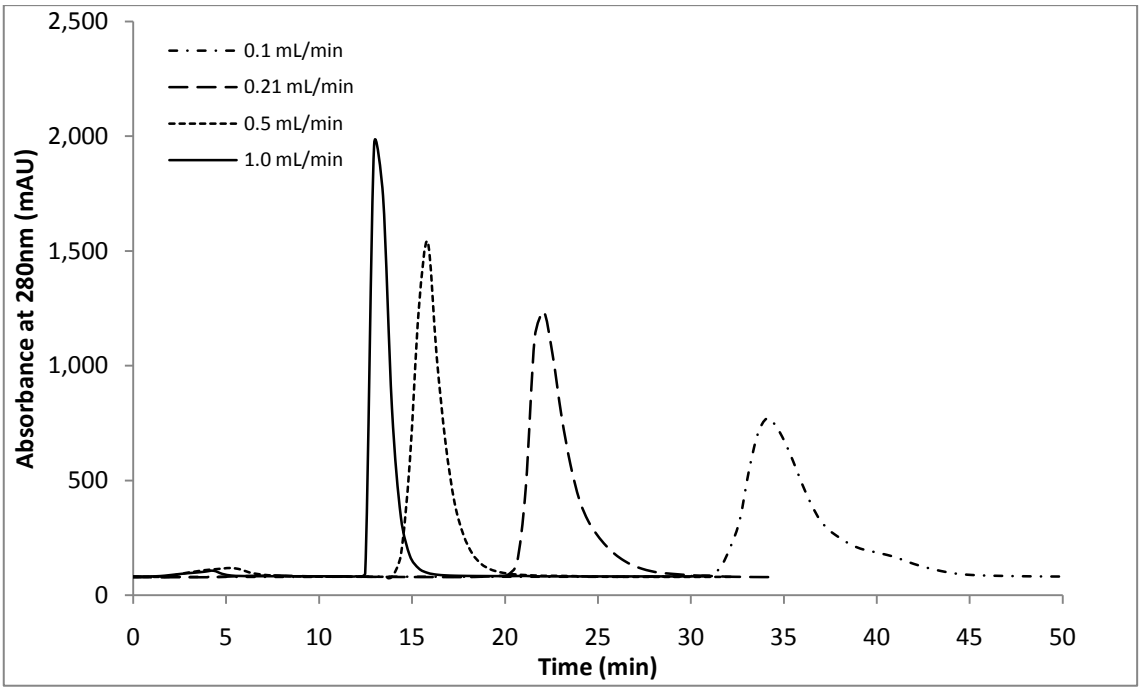

Figure 107. 3 mg/mL BSA concentration, 1M NaCl concentration, 720 degrees/hr rotation speed, flow rates 0.1-1.0 mL/min, Trial 4: 3.75 min loading, 7.5 min equilibration, 7.5 min elution, 11.25 min equilibration.

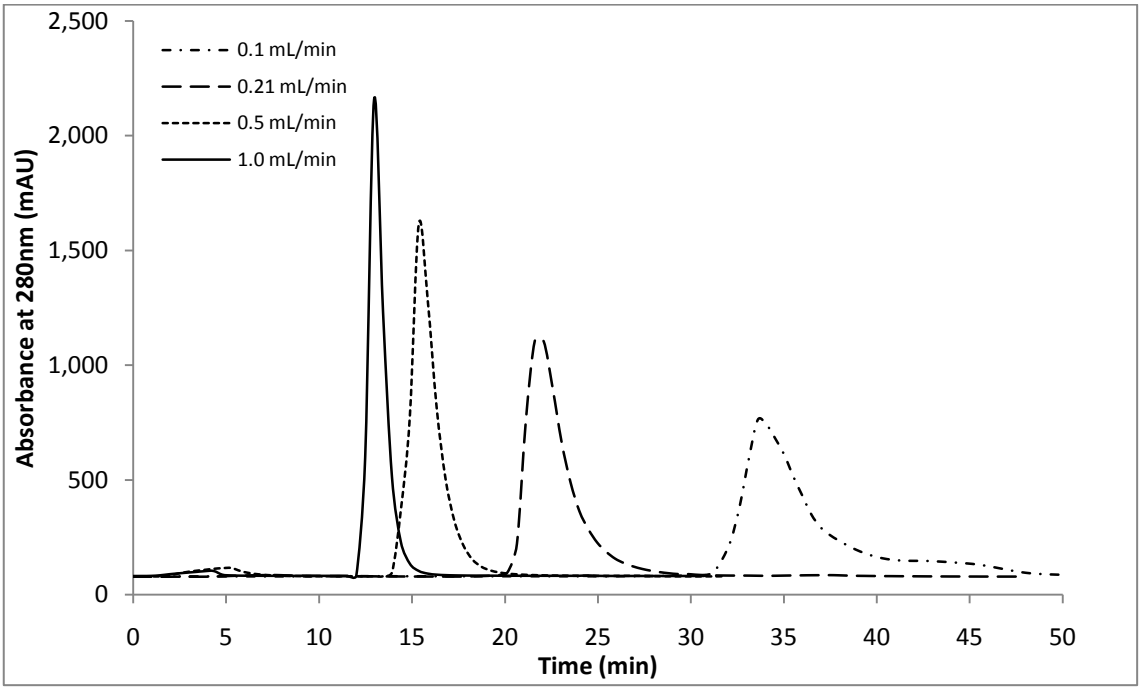

Figure 108. 3 mg/mL BSA concentration, 1M NaCl concentration, 720 degrees/hr rotation speed, flow rates 0.1-1.0 mL/min, Trial 5: 3.75 min loading, 7.5 min equilibration, 11.25 min elution, 7.5 min equilibration.

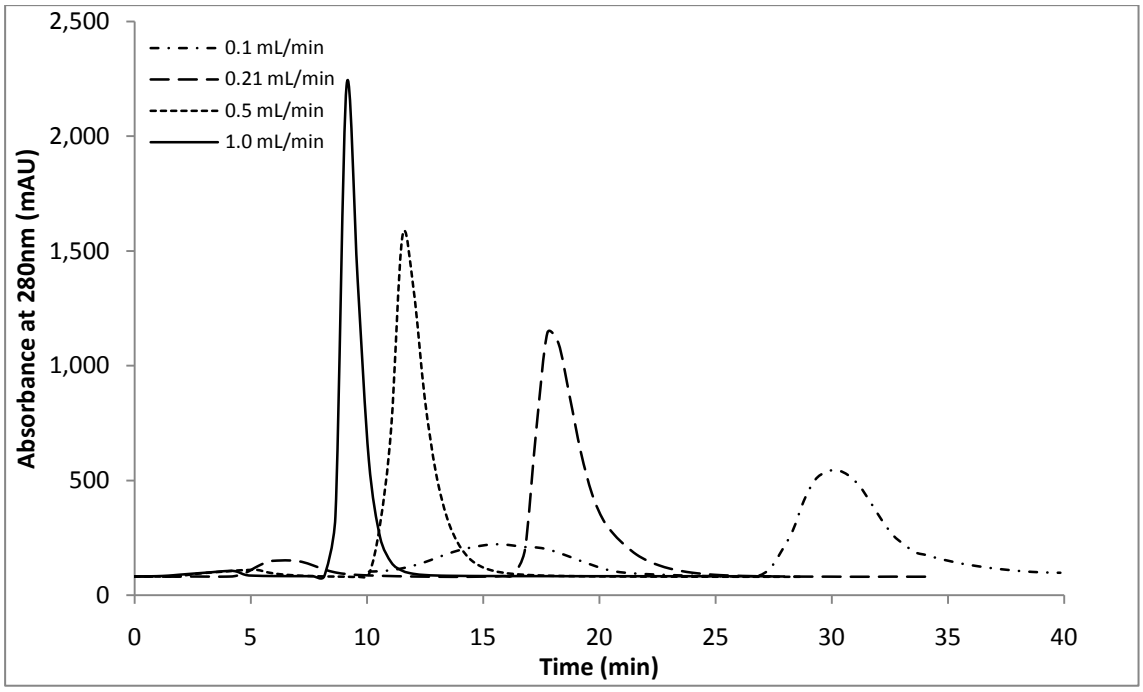

Figure 109. 3 mg/mL BSA concentration, 1M NaCl concentration, 720 degrees/hr rotation speed, flow rates 0.1-1.0 mL/min, Trial 6: 3.75 min loading, 3.75 min equilibration, 18.75 min elution, 3.75 min equilibration.

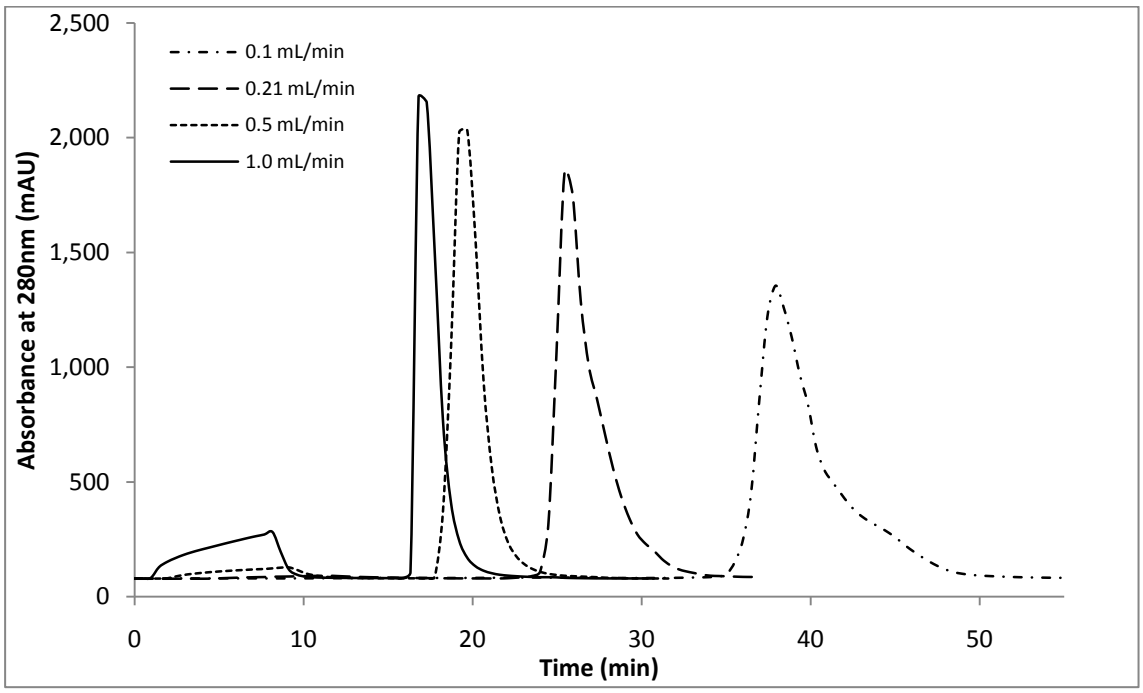

Figure 110. 3 mg/mL BSA concentration, 1M NaCl concentration, 720 degrees/hr rotation speed, flow rates 0.1-1.0 mL/min, Trial 7: 7.5 min loading, 7.5 min equilibration, 7.5 min elution, 7.5 min equilibration.

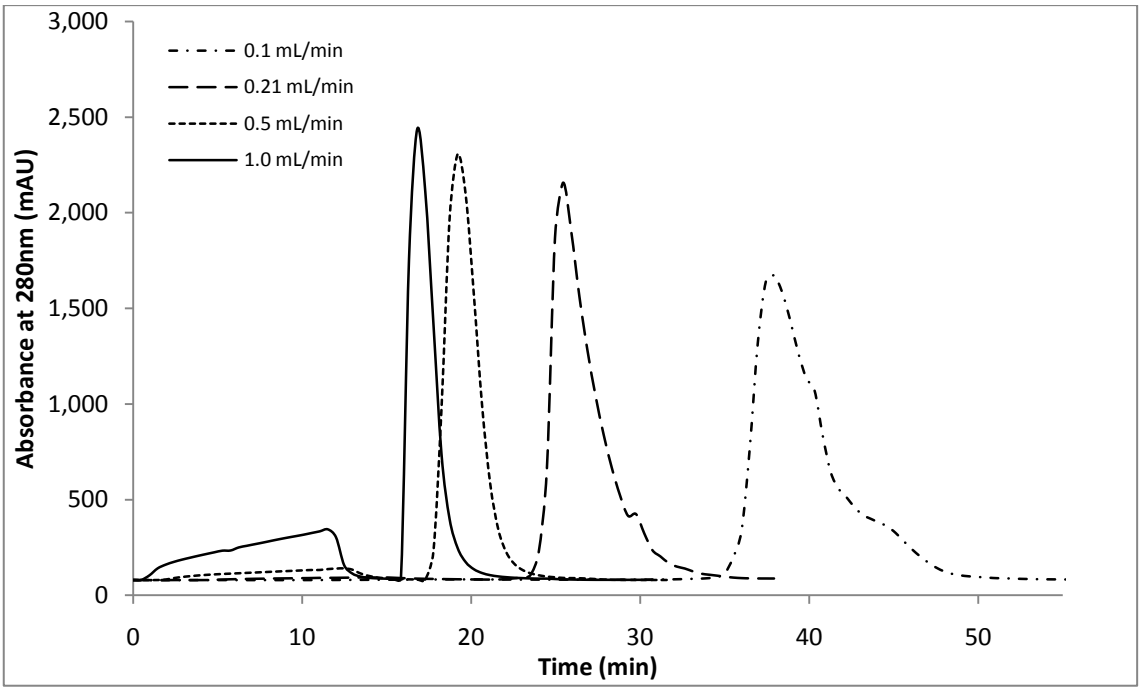

Figure 111. 3 mg/mL BSA concentration, 1M NaCl concentration, 720 degrees/hr rotation speed, flow rates 0.1-1.0 mL/min, Trial 8: 11.25 min loading, 3.75 min equilibration, 7.5 min elution, 7.5 min equilibration.

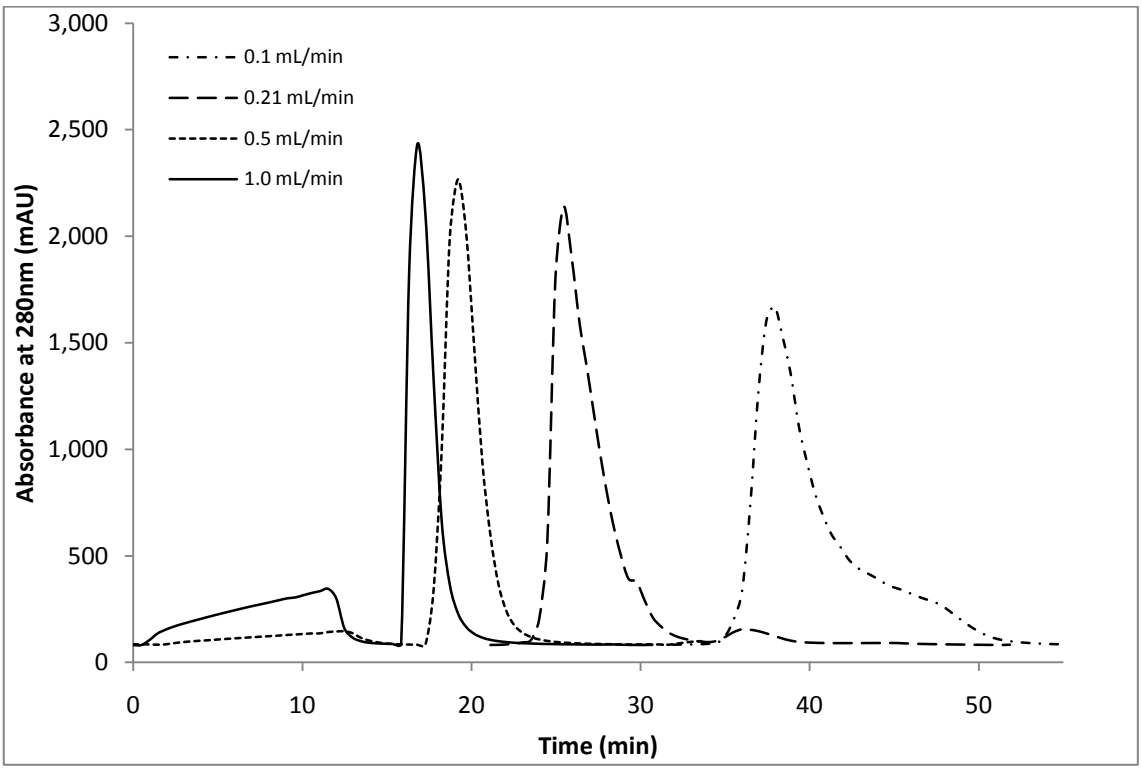

Figure 112. 3 mg/mL BSA concentration, 1M NaCl concentration, 720 degrees/hr rotation speed, flow rates 0.1-1.0 mL/min, Trial 9: 11.25 min loading, 3.75 min equilibration, 11.25 min elution, 3.75 min equilibration.

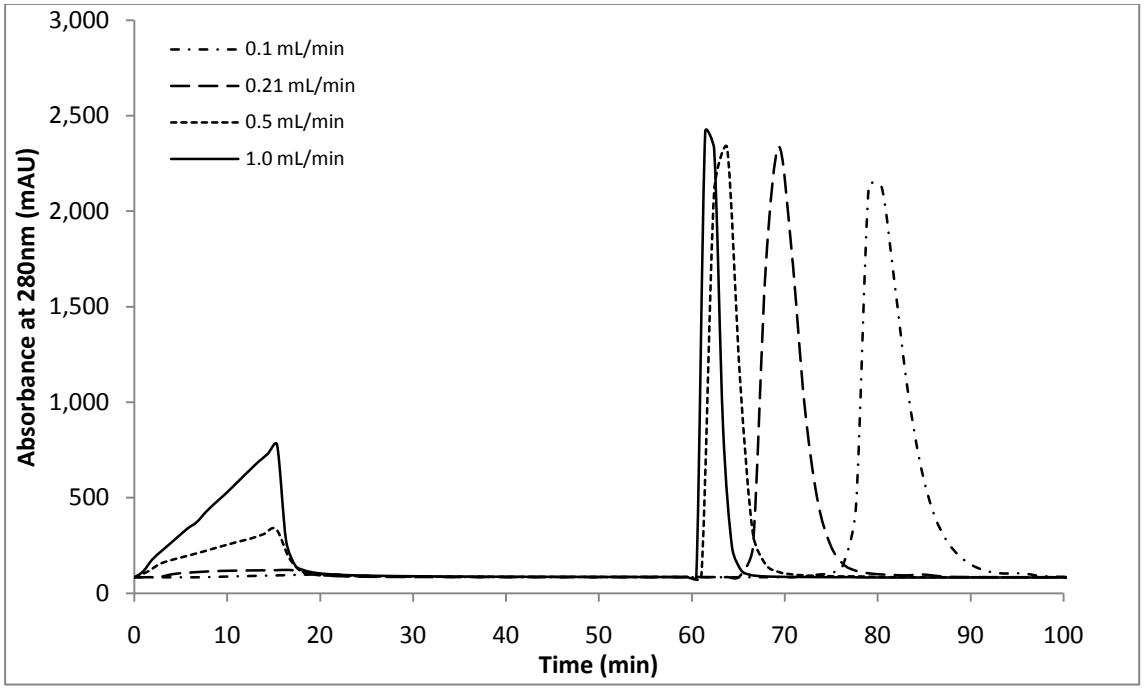

Figure 113. 5 mg/mL BSA concentration, 1M NaCl concentration, 180 degrees/hr rotation speed, flow rates 0.1-1.0 mL/min, Trial 1: 15 min loading, 45 min equilibration, 15 min elution, 45 min equilibration.

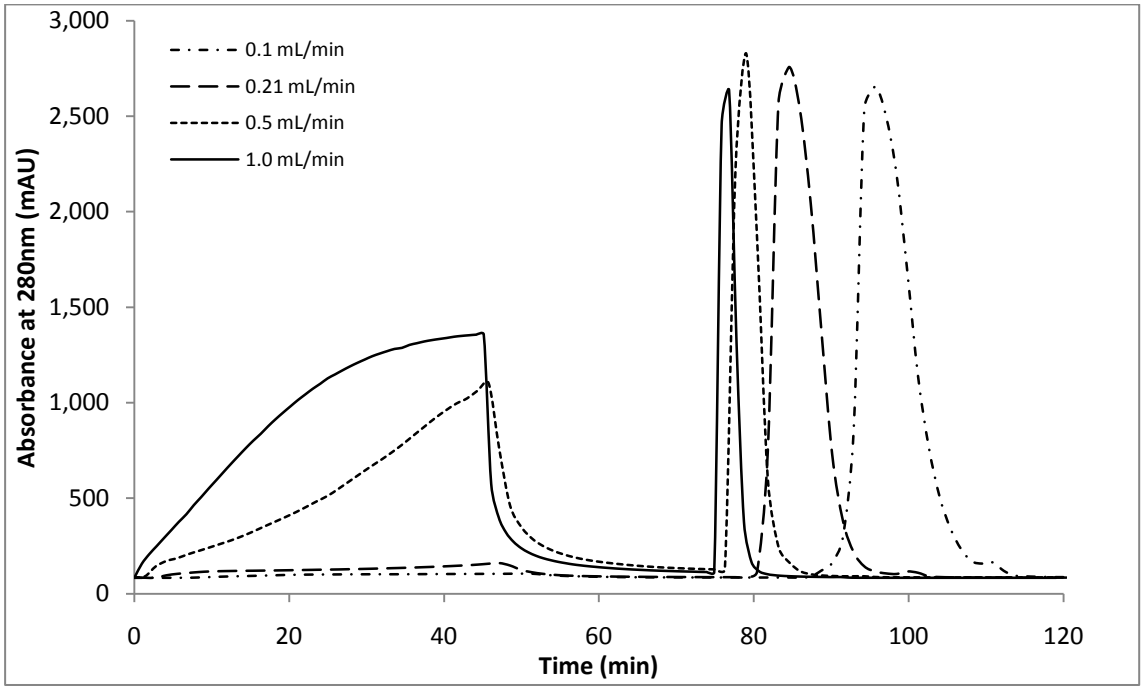

Figure 114. 5 mg /mL BSA concentration, 1M NaCl concentration, 180 degrees/hr rotation speed, flow rates 0.1-1.0 mL/min Trial 2: 45 min loading, 30 min equilibration, 15 min elution, 30 min equilibration.

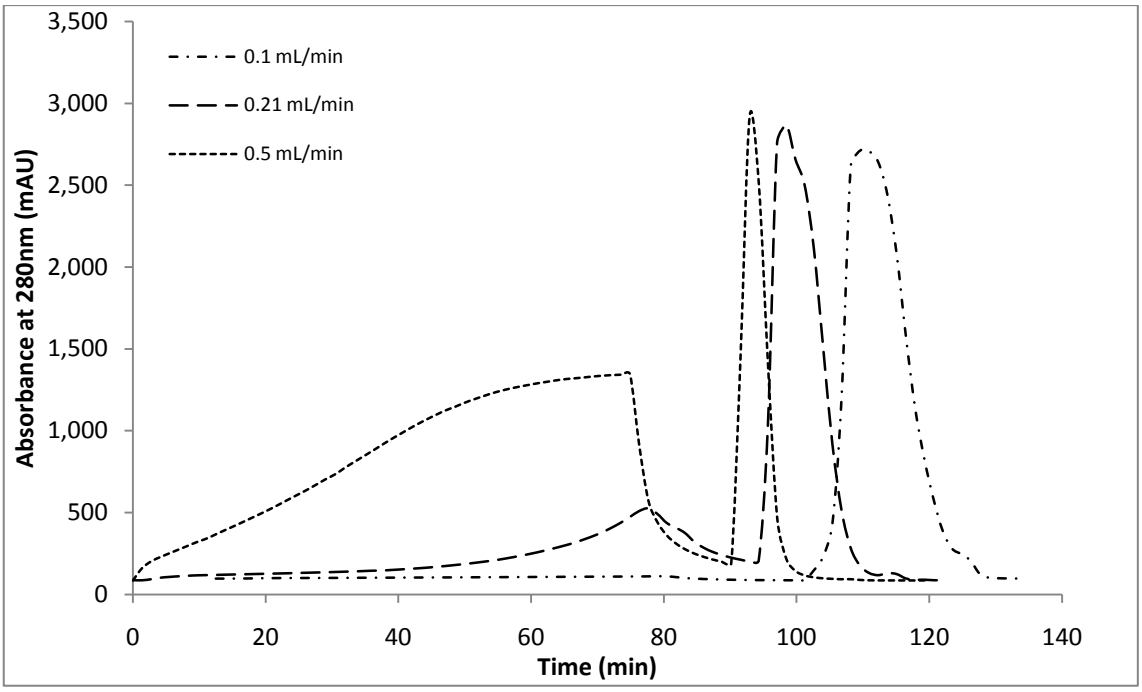

Figure 115. 5 mg /mL BSA concentration, 1M NaCl concentration, 180 degrees/hr rotation speed, flow rates 0.1-0.5 mL/min Trial 3: 75 min loading, 15 min equilibration, 15 min elution, 15 min equilibration.

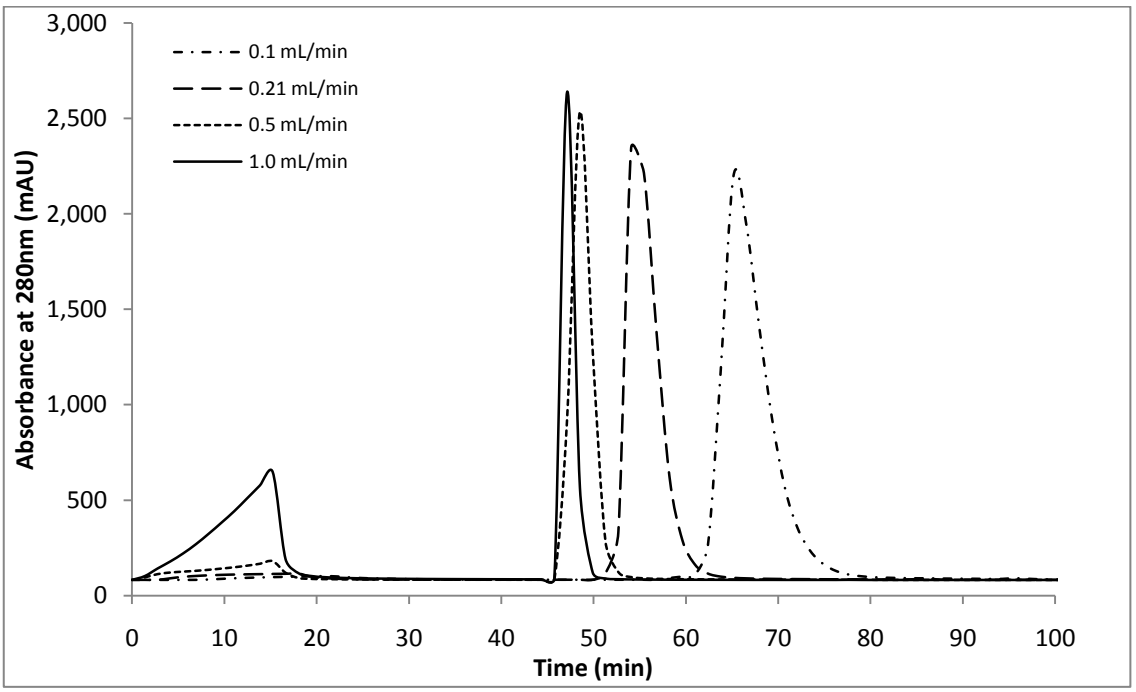

Figure 116. 5 mg /mL BSA concentration, 1M NaCl concentration, 180 degrees/hr rotation speed, , flow rates 0.1-1.0 mL/min, Trial 4: 15 min loading, 30 min equilibration, 30 min elution, 45 min equilibration.

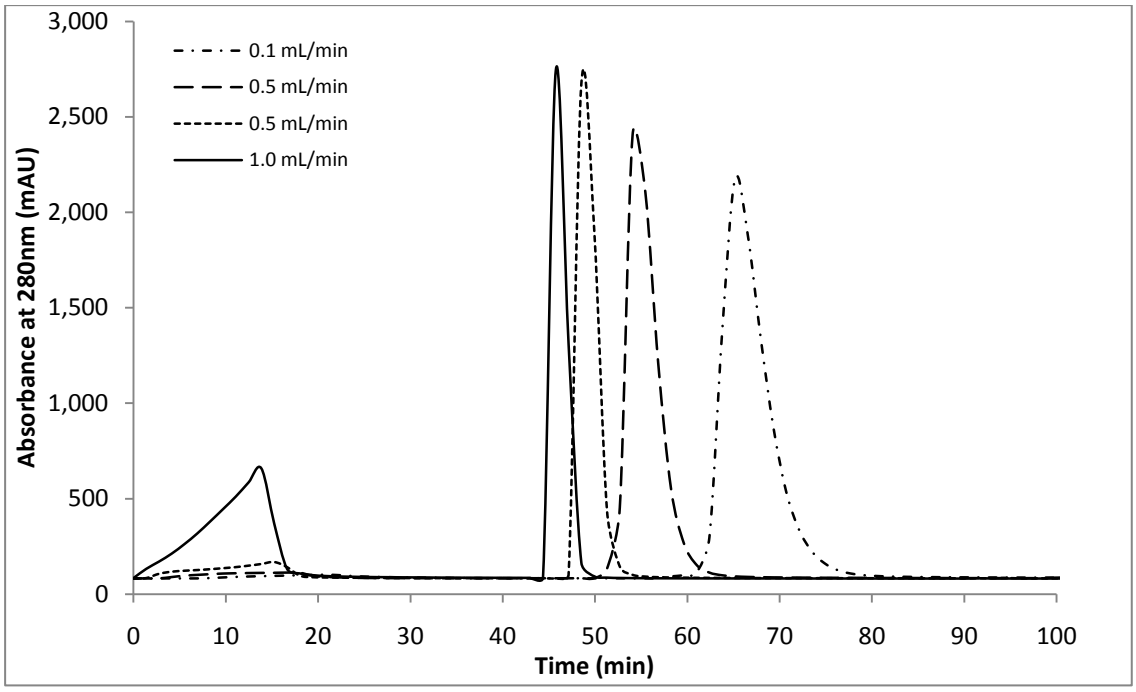

Figure 117. 5 mg /mL BSA concentration, 1M NaCl concentration, 180 degrees/hr rotation speed, flow rates 0.1-1.0 mL/min, Trial 5: 15 min loading, 30 min equilibration, 45 min elution, 30 min equilibration.

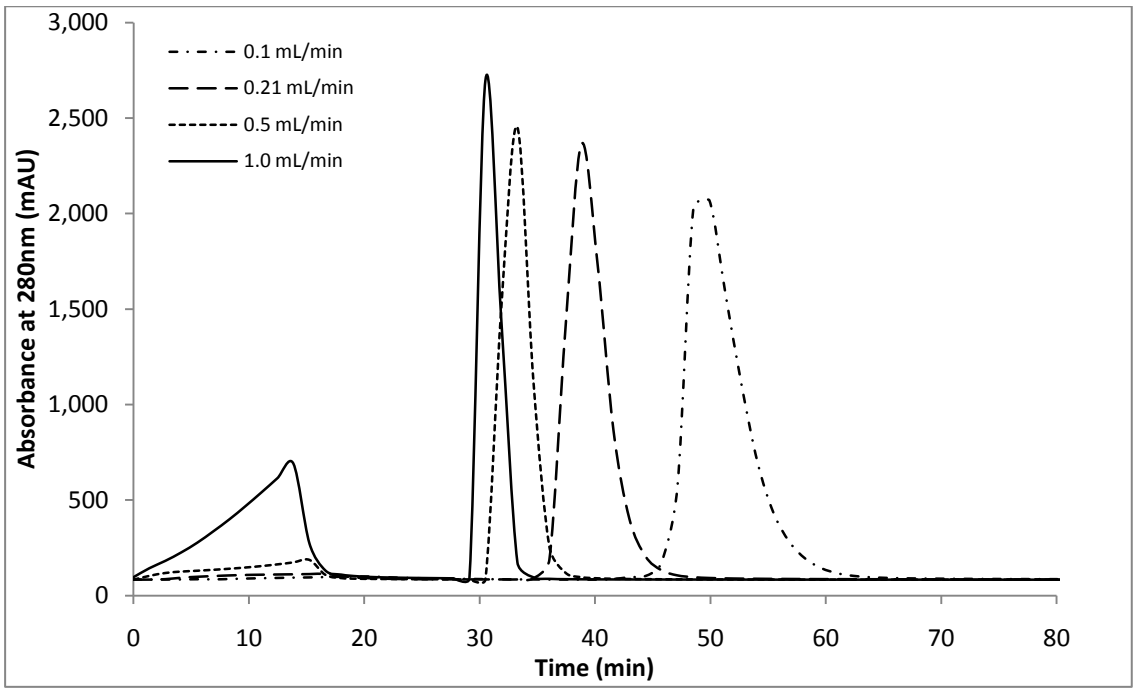

Figure 118. 5 mg /mL BSA concentration, 1M NaCl concentration, 180 degrees/hr rotation speed, flow rates 0.1-1.0 mL/min, Trial 6: 15 min loading, 15 min equilibration, 75 min elution, 15 min equilibration.

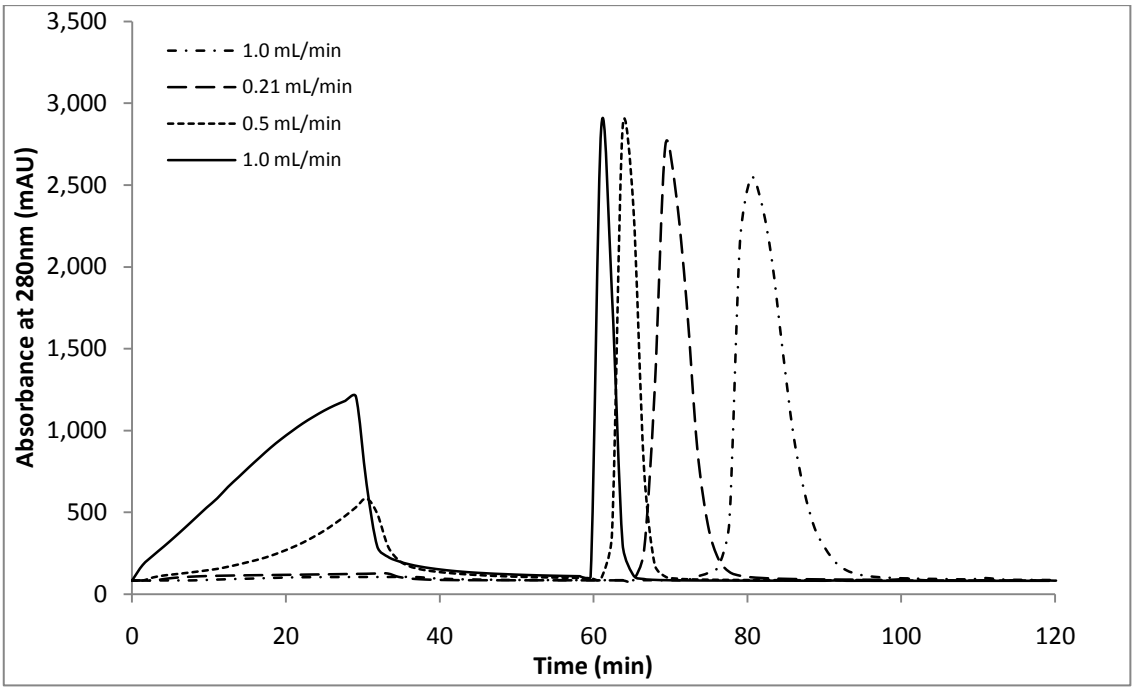

Figure 119. 5 mg /mL BSA concentration, 1M NaCl concentration, 180 degrees/hr rotation speed, flow rates 0.1-1.0 mL/min, Trial 7: 30 min loading, 30 min equilibration, 30 min elution, 30 min equilibration.

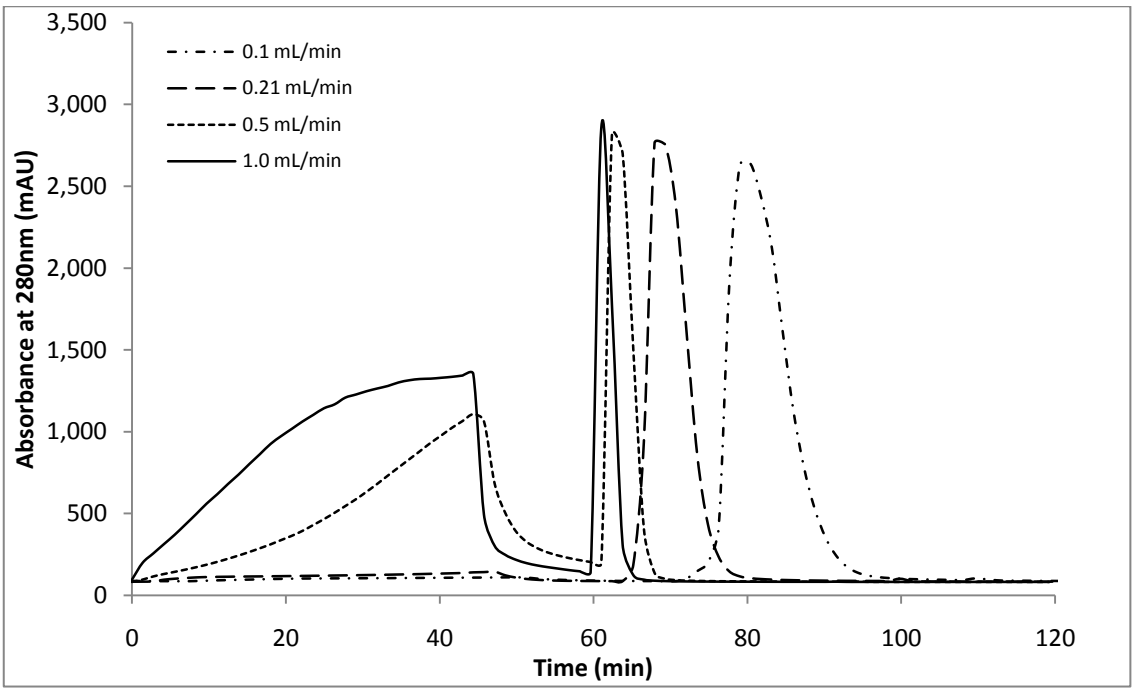

Figure 120. 5 mg /mL BSA concentration, 1M NaCl concentration, 180 degrees/hr rotation speed, flow rates 0.1-1.0 mL/min, Trial 8: 45 min loading, 15 min equilibration, 30 min elution, 30 min equilibration.

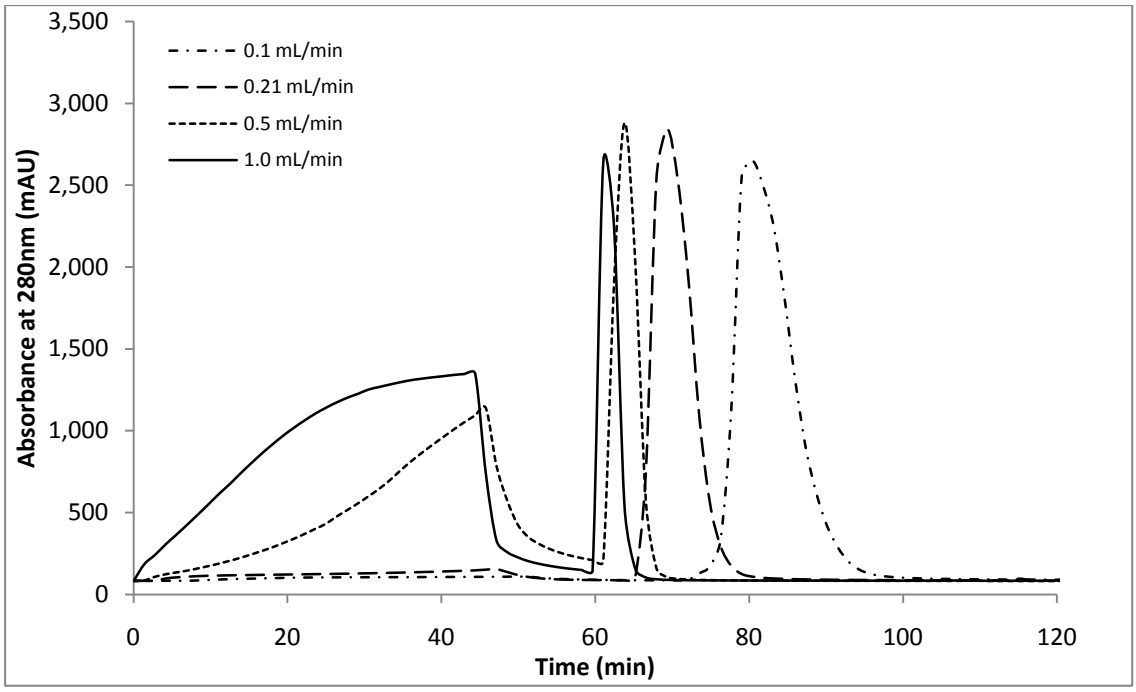

Figure 121. 5 mg /mL BSA concentration, 1M NaCl concentration, 180 degrees/hr rotation speed, flow rates 0.1-1.0 mL/min, Trial 9: 45 min loading, 15 min equilibration, 45 min elution, 15 min equilibration.

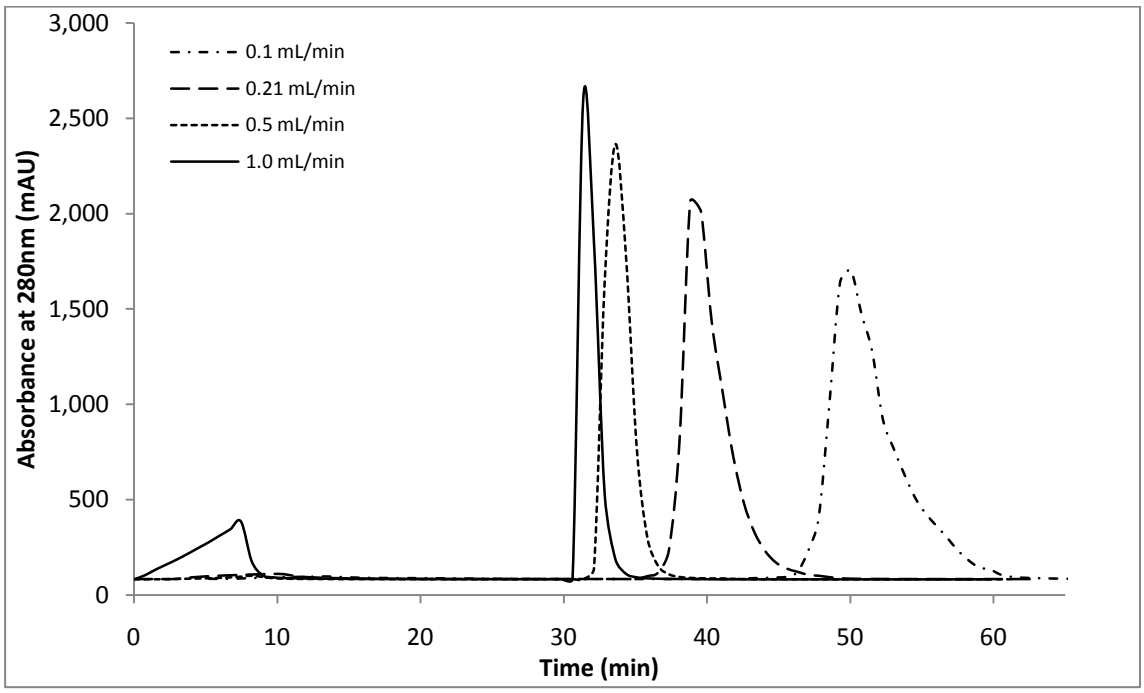

Figure 122. 5 mg/mL BSA concentration, 1M NaCl concentration, 360 degrees/hr rotation speed, flow rates 0.1-1.0 mL/min, Trial 1: 7.5 min loading, 22.5 min equilibration, 7.5 min elution, 22.5 min equilibration.

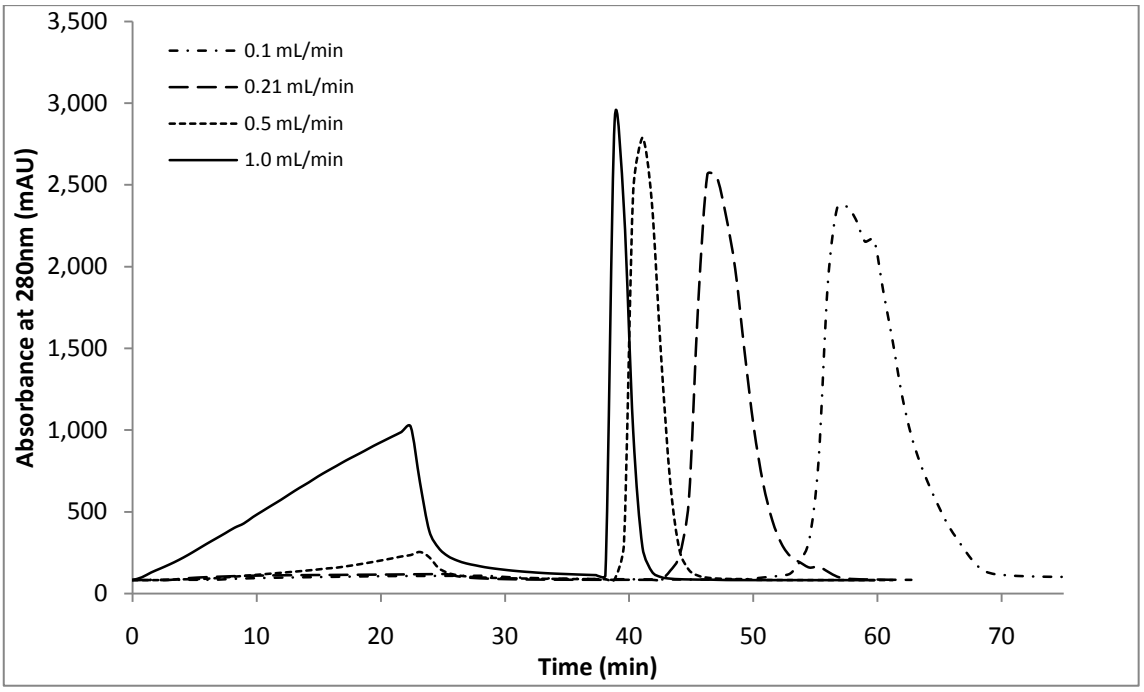

Figure 123. 5 mg /mL BSA concentration, 1M NaCl concentration, 360 degrees/hr rotation speed, flow rates 0.1-1.0 mL/min, Trial 2: 22.5 min loading, 15 min equilibration, 7.5 min elution, 15 min equilibration.

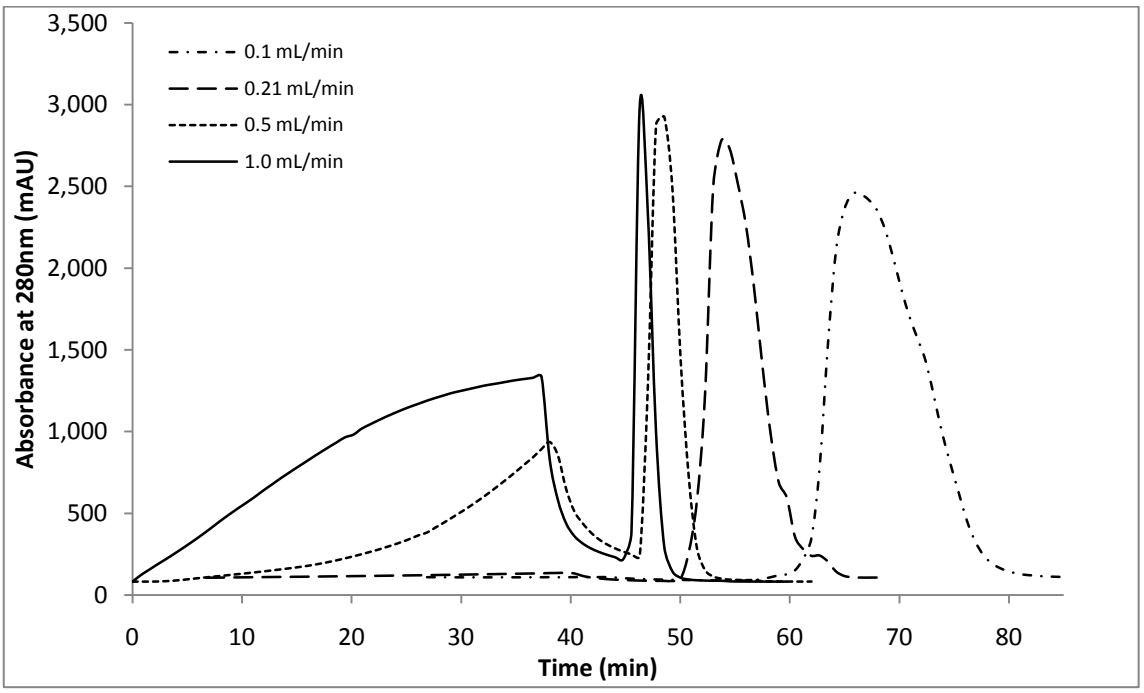

Figure 124. 5 mg /mL BSA concentration, 1M NaCl concentration, 360 degrees/hr rotation speed, flow rates 0.1-1.0 mL/min, Trial 3: 37.5 min loading, 7.5 min equilibration, 7.5 min elution, 7.5 min equilibration.

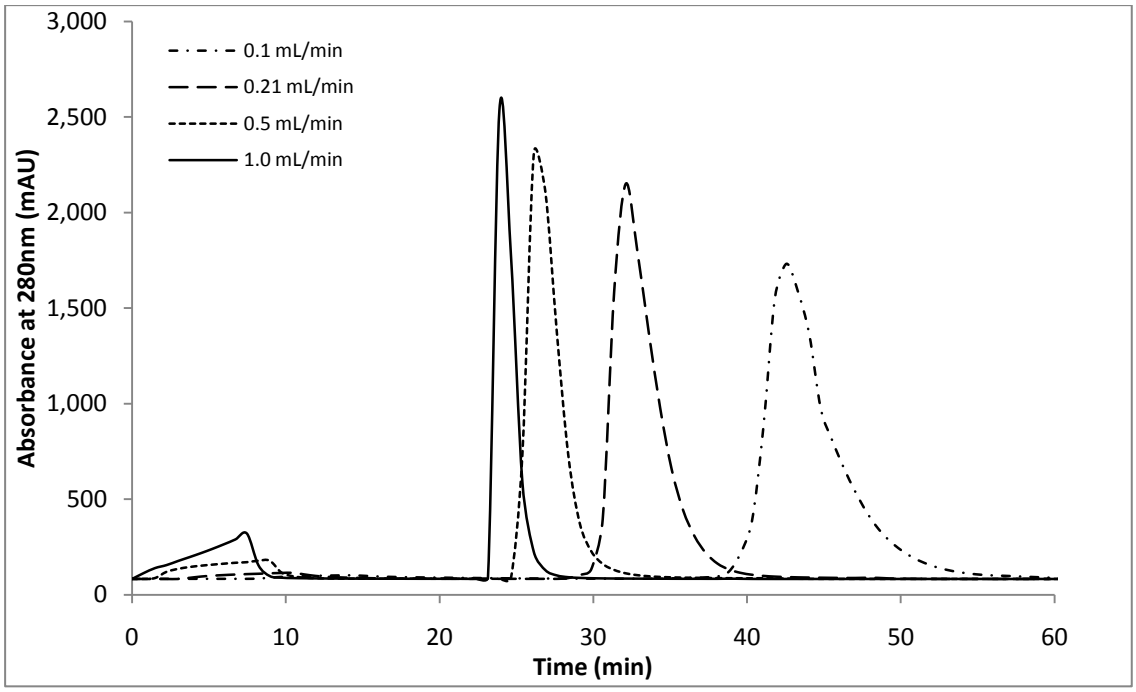

Figure 125. 5 mg /mL BSA concentration, 1M NaCl concentration, 360 degrees/hr rotation speed, flow rates 0.1-1.0 mL/min, Trial 4: 7.5 min loading, 15 min equilibration, 15 min elution, 22.5 min equilibration.

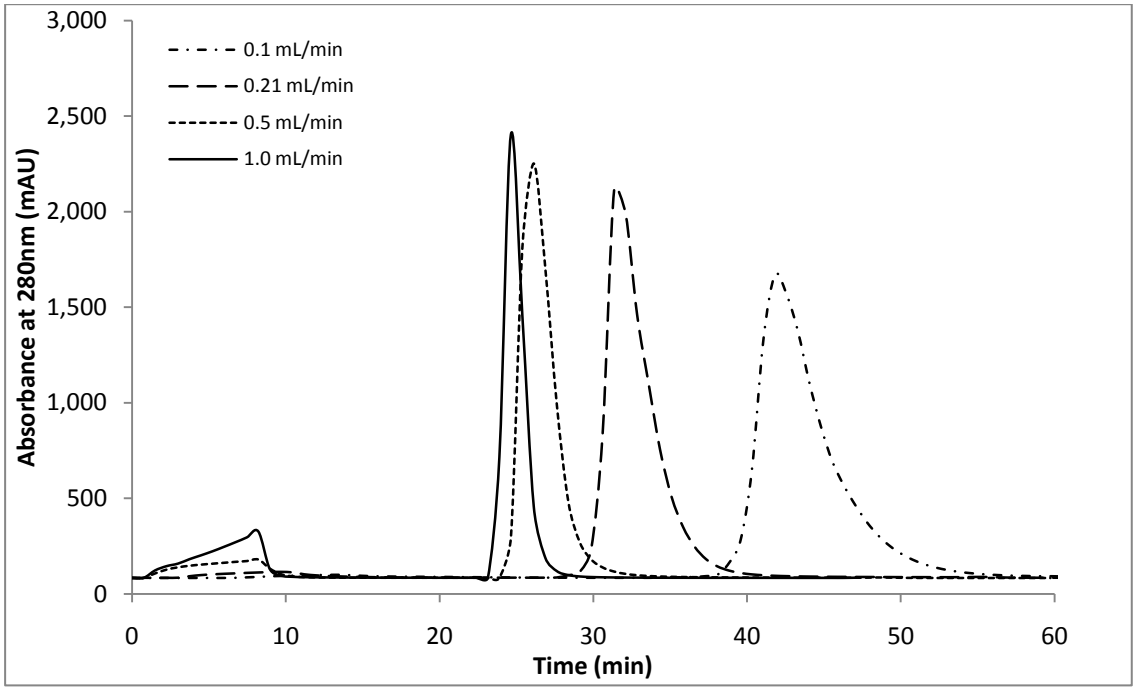

Figure 126. 5 mg /mL BSA concentration, 1M NaCl concentration, 360 degrees/hr rotation speed, flow rates 0.1-1.0 mL/min, Trial 5: 7.5 min loading, 15 min equilibration, 22.5 min elution, 15 min equilibration.

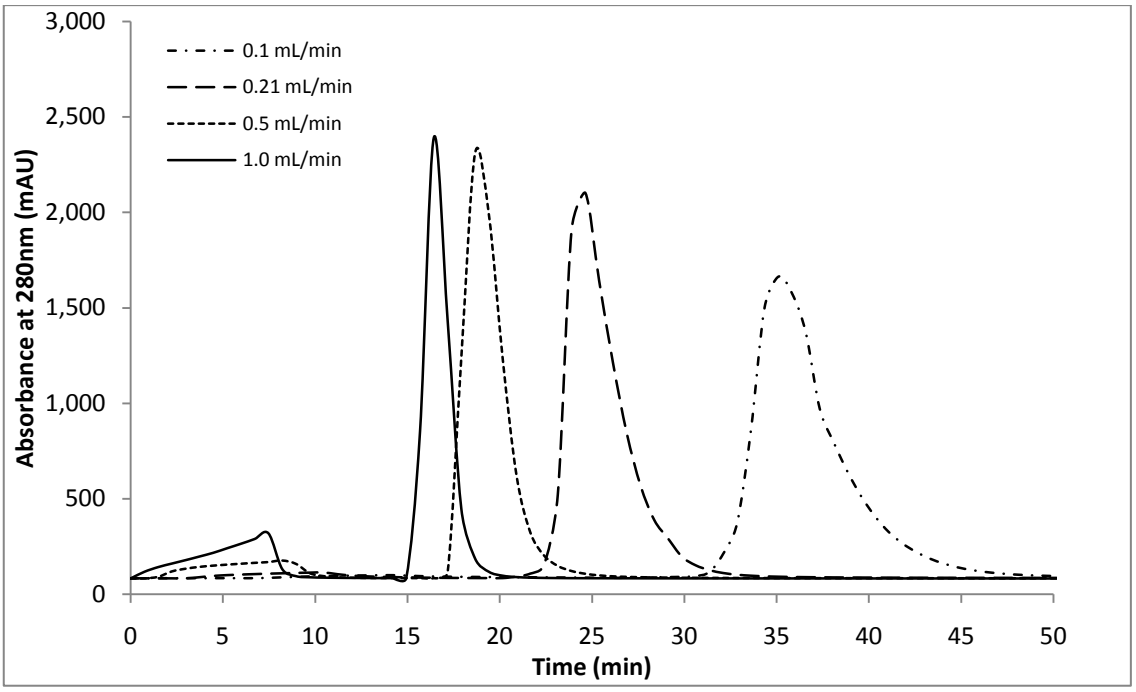

Figure 127. 5 mg /mL BSA concentration, 1M NaCl concentration, 360 degrees/hr rotation speed, flow rates 0.1-1.0 mL/min, Trial 6: 7.5 min loading, 7.5 min equilibration, 37.5 min elution, 7.5 min equilibration.

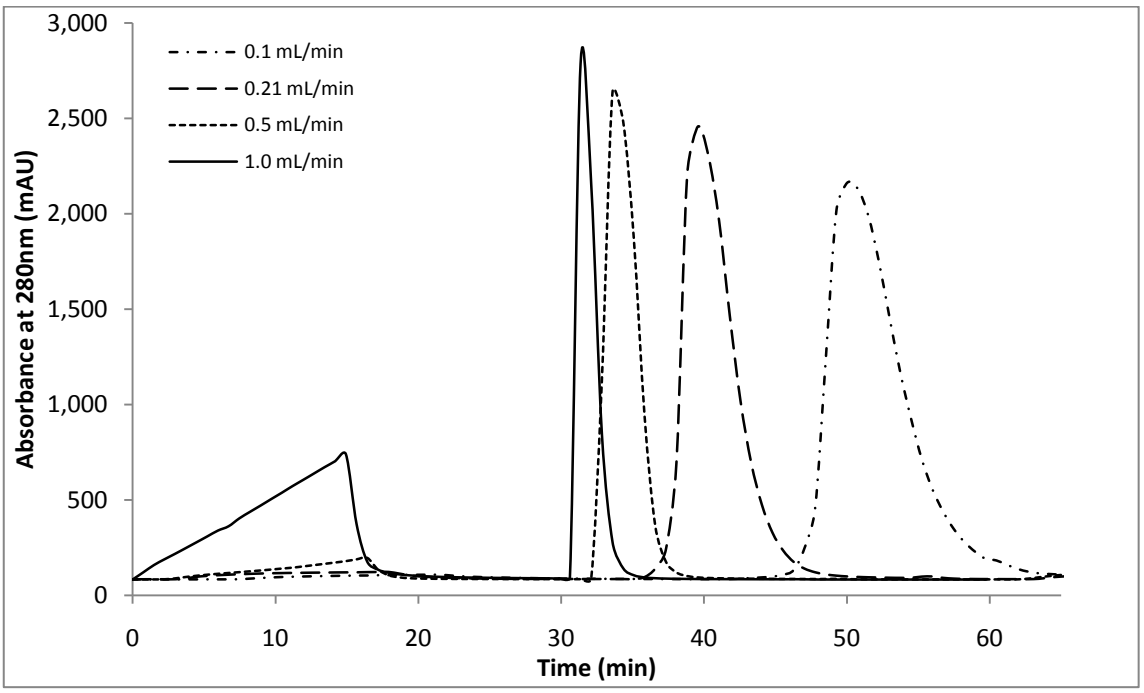

Figure 128. 5 mg /mL BSA concentration, 1M NaCl concentration, 360 degrees/hr rotation speed, flow rates 0.1-1.0 mL/min, Trial 7: 15 min loading, 15 min equilibration, 15 min elution, 15 min equilibration.

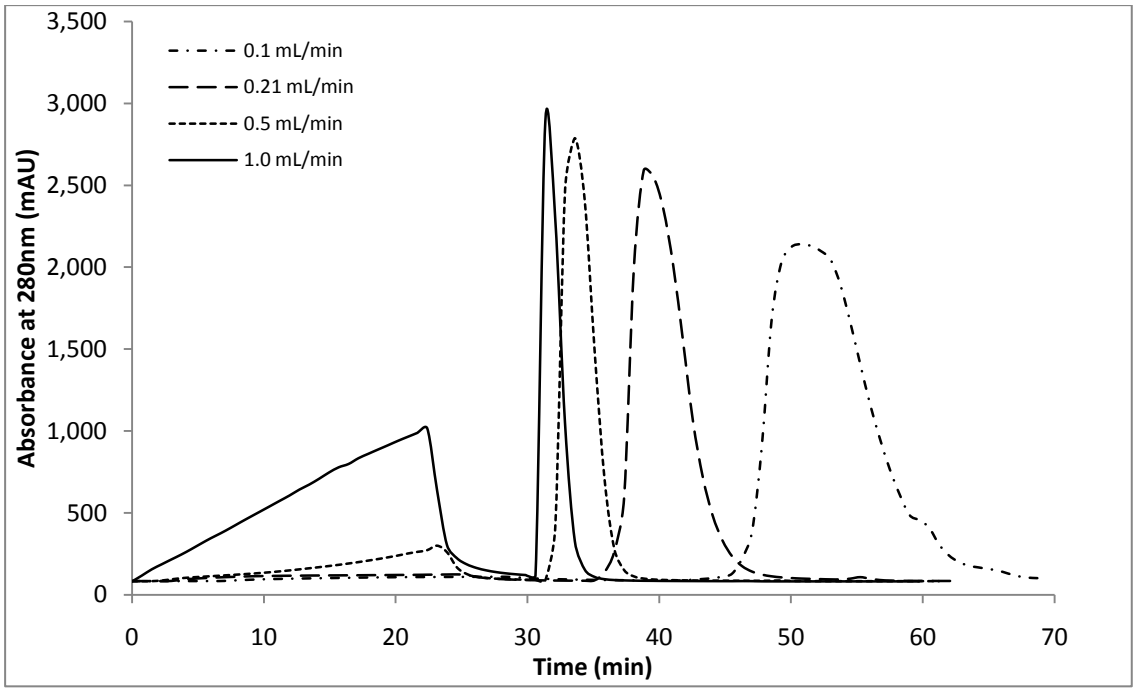

Figure 129. 5 mg /mL BSA concentration, 1M NaCl concentration, 360 degrees/hr rotation speed, flow rates 0.1-1.0 mL/min, Trial 8: 22.5 min loading, 7.5 min equilibration, 15 min elution, 15 min equilibration.

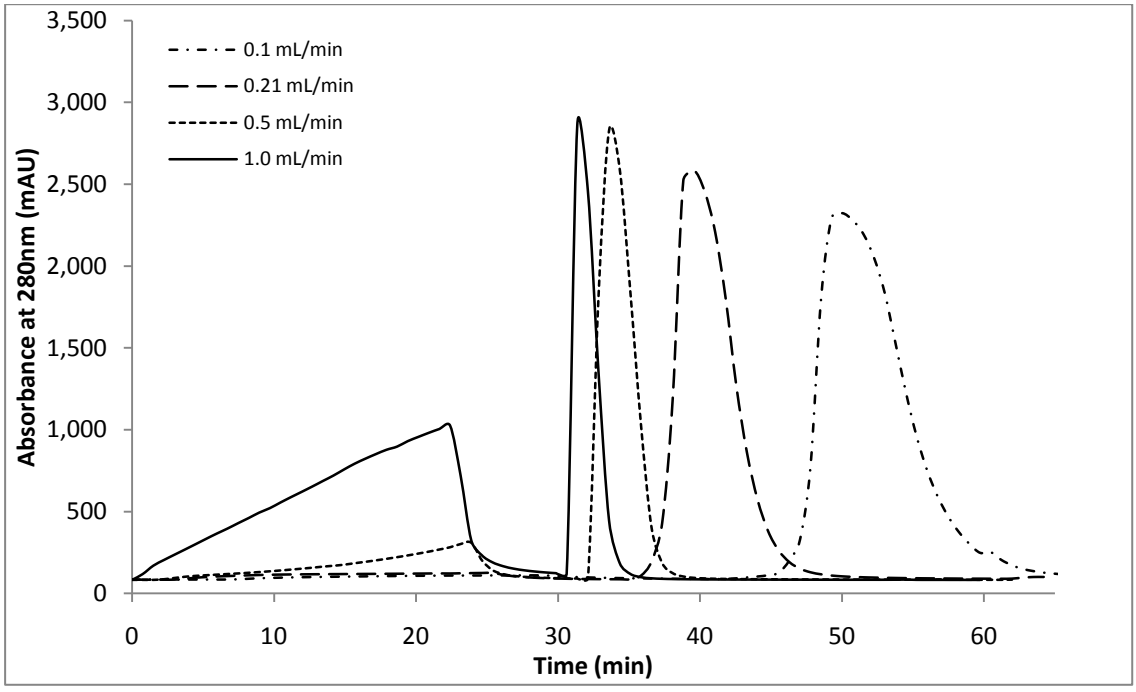

Figure 130. 5 mg /mL BSA concentration, 1M NaCl concentration, 360 degrees/hr rotation speed, flow rates 0.1-1.0 mL/min, Trial 9: 22.5 min loading, 7.5 min equilibration, 22.5 min elution, 7.5 min equilibration.

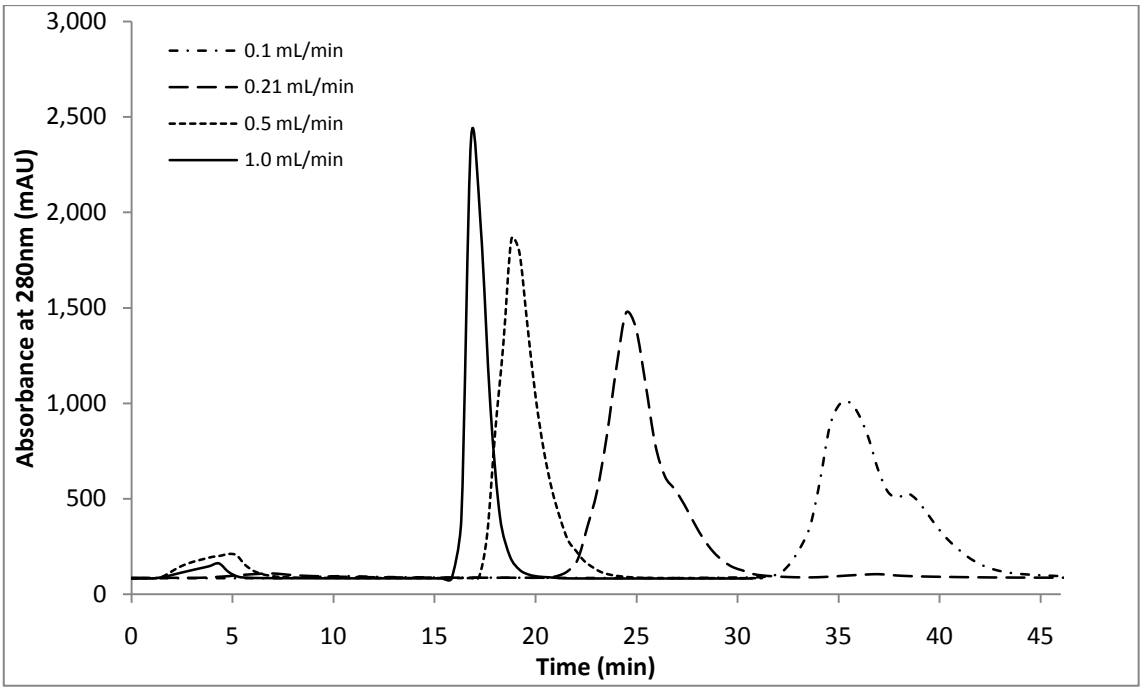

Figure 131. 5 mg /mL BSA concentration, 1M NaCl concentration, 720 degrees/hr rotation speed, flow rates 0.1-1.0 mL/min, Trial 1: 3.75 min loading, 11.25 min equilibration, 3.75 min elution, 11.25 min equilibration.

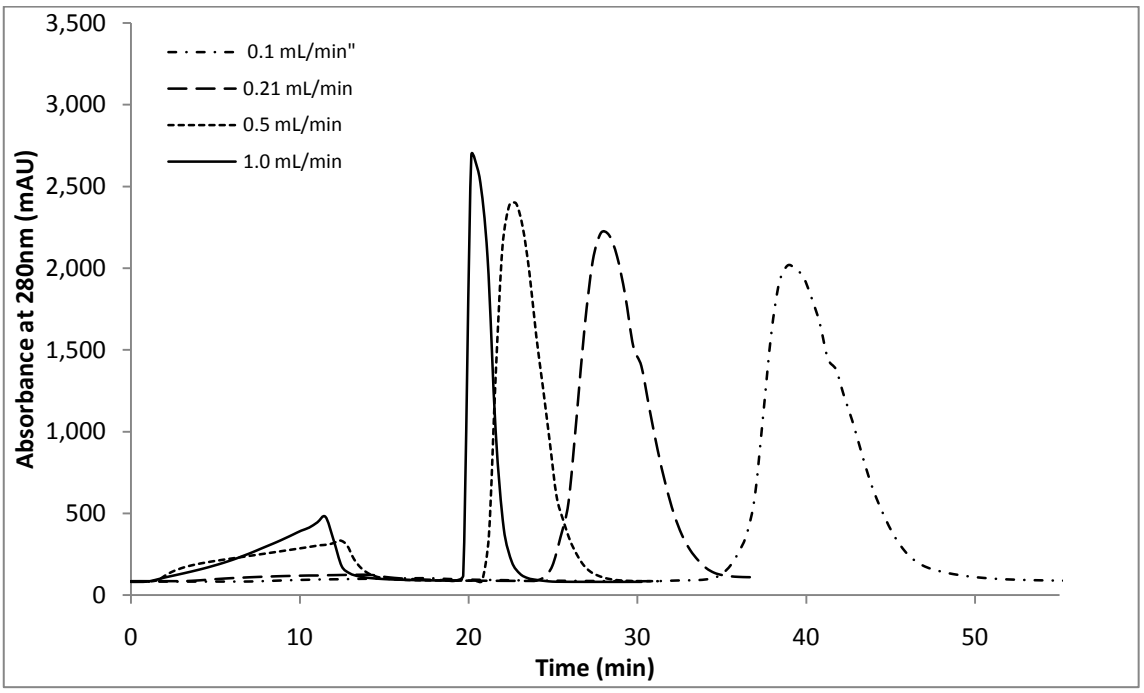

Figure 132. 5 mg /mL BSA concentration, 1M NaCl concentration, 720 degrees/hr rotation speed, flow rates 0.1-1.0 mL/min, Trial 2: 11.25 min loading, 7.5 min equilibration, 3.75 min elution, 7.5 min equilibration.

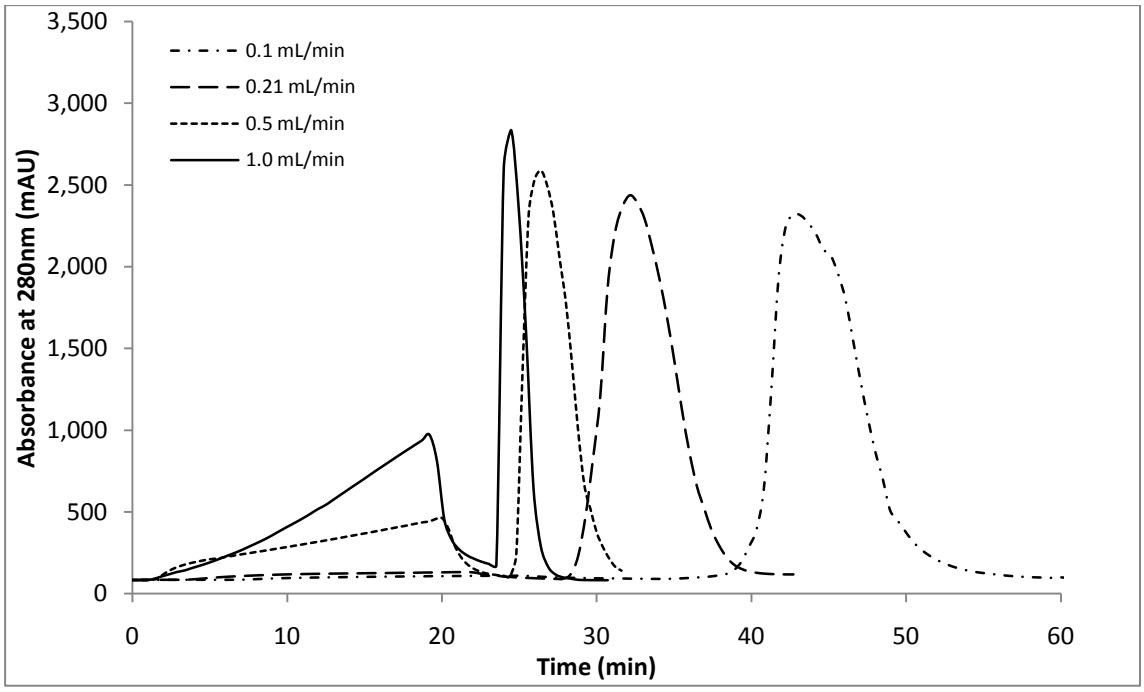

Figure 133. 5 mg /mL BSA concentration, 1M NaCl concentration, 720 degrees/hr rotation speed, flow rates 0.1-1.0 mL/min, Trial 3: 18.75 min loading, 3.75 min equilibration, 3.75 min elution, 3.75 min equilibration.

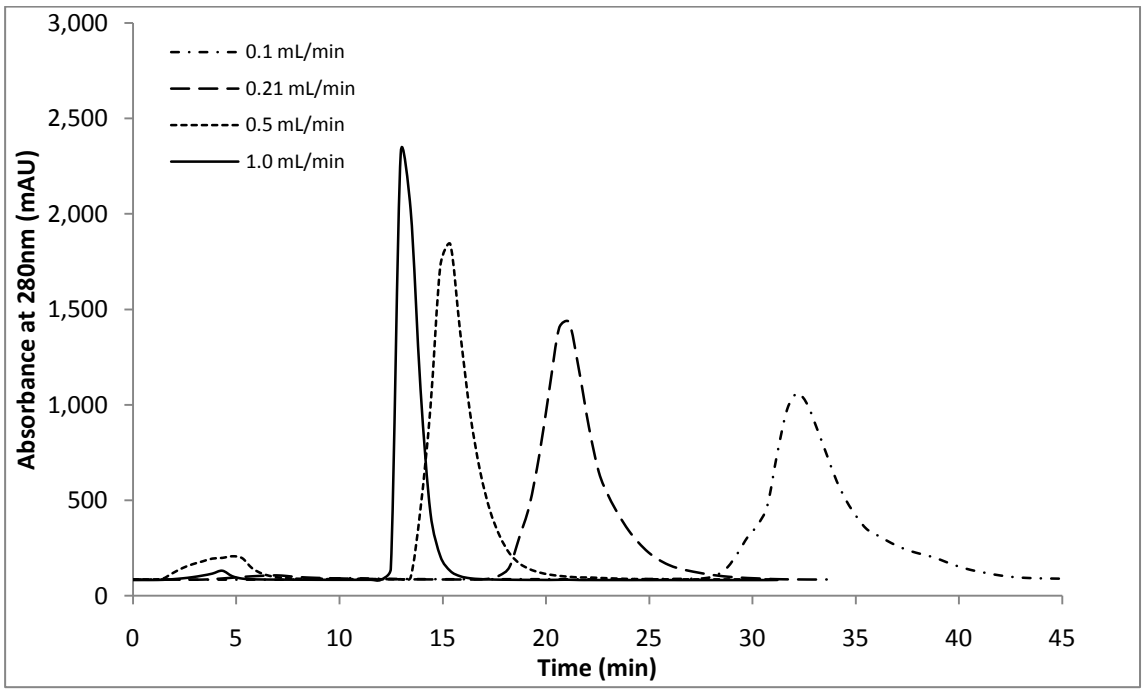

Figure 134. 5 mg /mL BSA concentration, 1M NaCl concentration, 720 degrees/hr rotation speed, flow rates 0.1-1.0 mL/min, Trial 4: 3.75 min loading, 7.5 min equilibration, 7.5 min elution, 11.25 min equilibration.

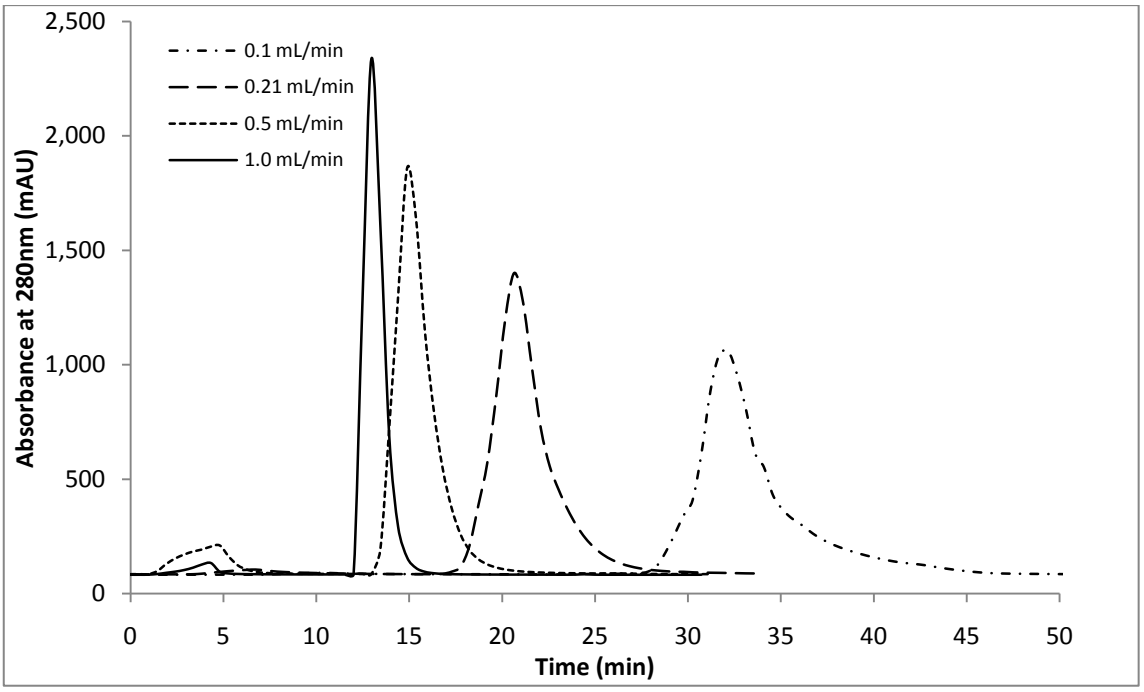

Figure 135. 5 mg /mL BSA concentration, 1M NaCl concentration, 720 degrees/hr rotation speed, flow rates 0.1-1.0 mL/min, Trial 5: 3.75 min loading, 7.5 min equilibration, 11.25 min elution, 7.5 min equilibration.

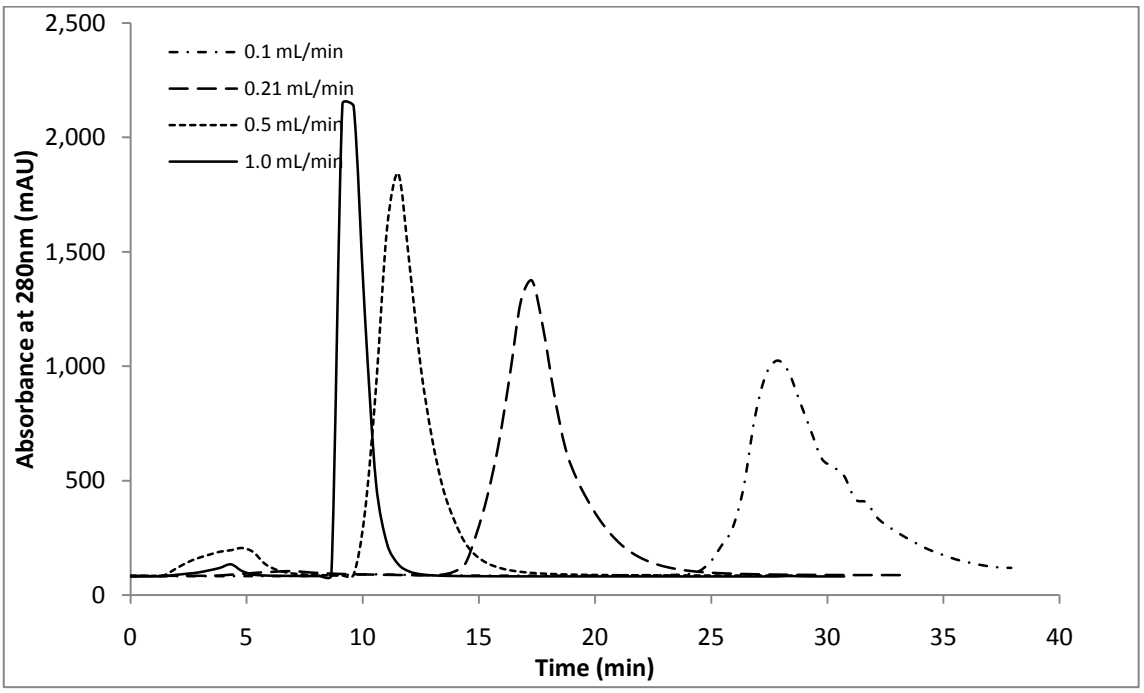

Figure 136. 5 mg /mL BSA concentration, 1M NaCl concentration, 720 degrees/hr rotation speed, flow rates 0.1-1.0 mL/min, Trial 6: 3.75 min loading, 3.75 min equilibration, 18.75 min elution, 3.75 min equilibration.

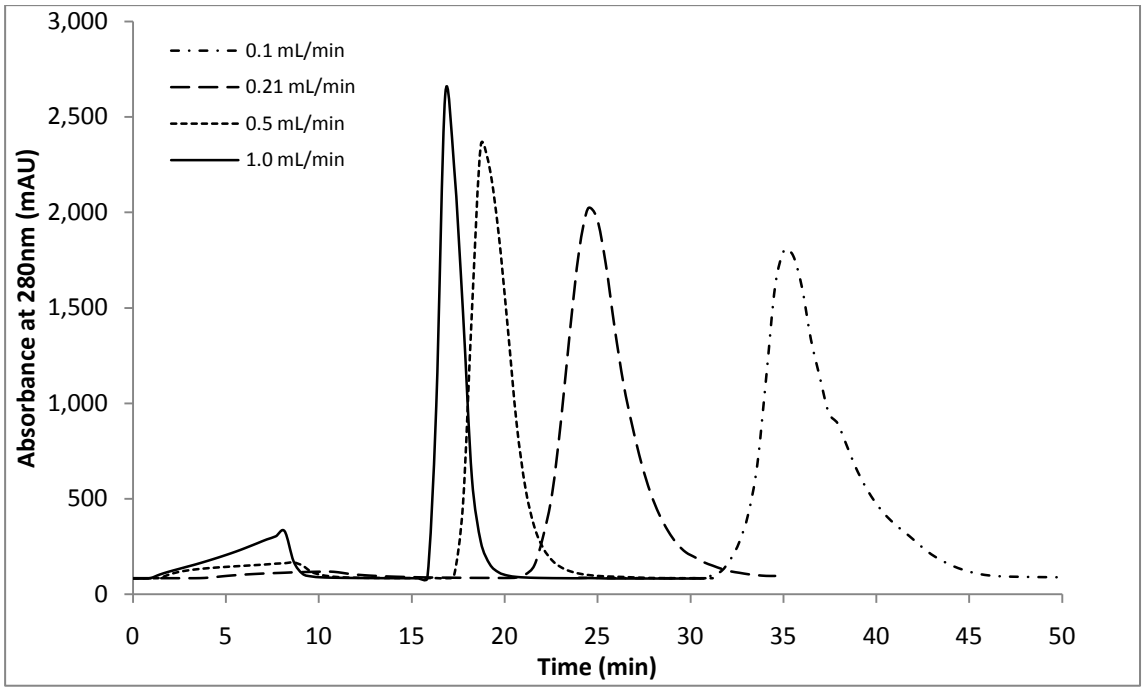

Figure 137. 5 mg /mL BSA concentration, 1M NaCl concentration, 720 degrees/hr rotation speed, flow rates 0.1-1.0 mL/min, Trial 7: 7.5 min loading, 7.5 min equilibration, 7.5 min elution, 7.5 min equilibration.

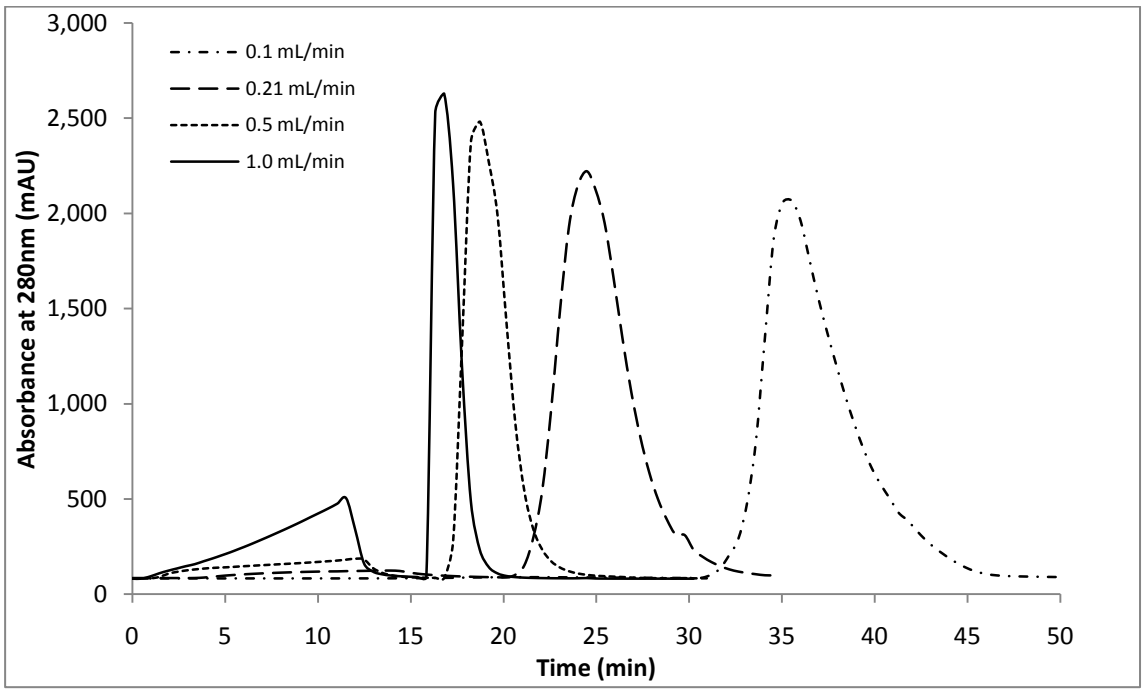

Figure 138. 5 mg /mL BSA concentration, 1M NaCl concentration, 720 degrees/hr rotation speed, flow rates 0.1-1.0 mL/min, Trial 8: 11.25 min loading, 3.75 min equilibration, 7.5 min elution, 7.5 min equilibration.

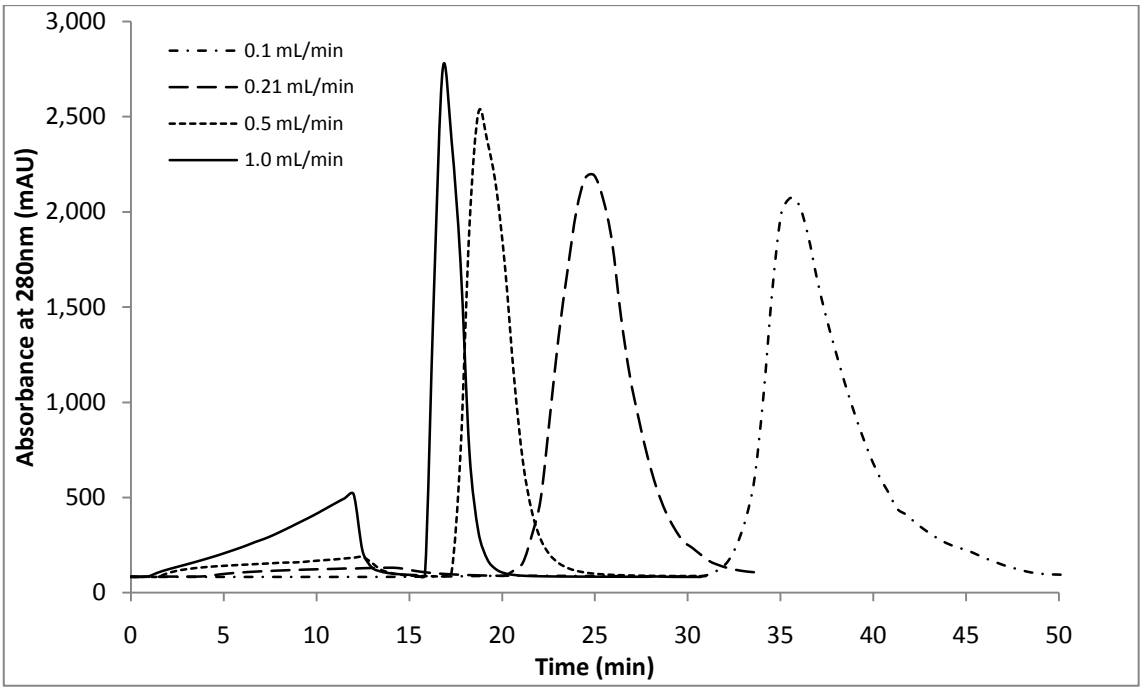

Figure 139. 5 mg /mL BSA concentration, 1M NaCl concentration, 720 degrees/hr rotation speed, flow rates 0.1-1.0 mL/min, Trial 9: 11.25 min loading, 3.75 min equilibration, 11.25 min elution, 3.75 min equilibration.

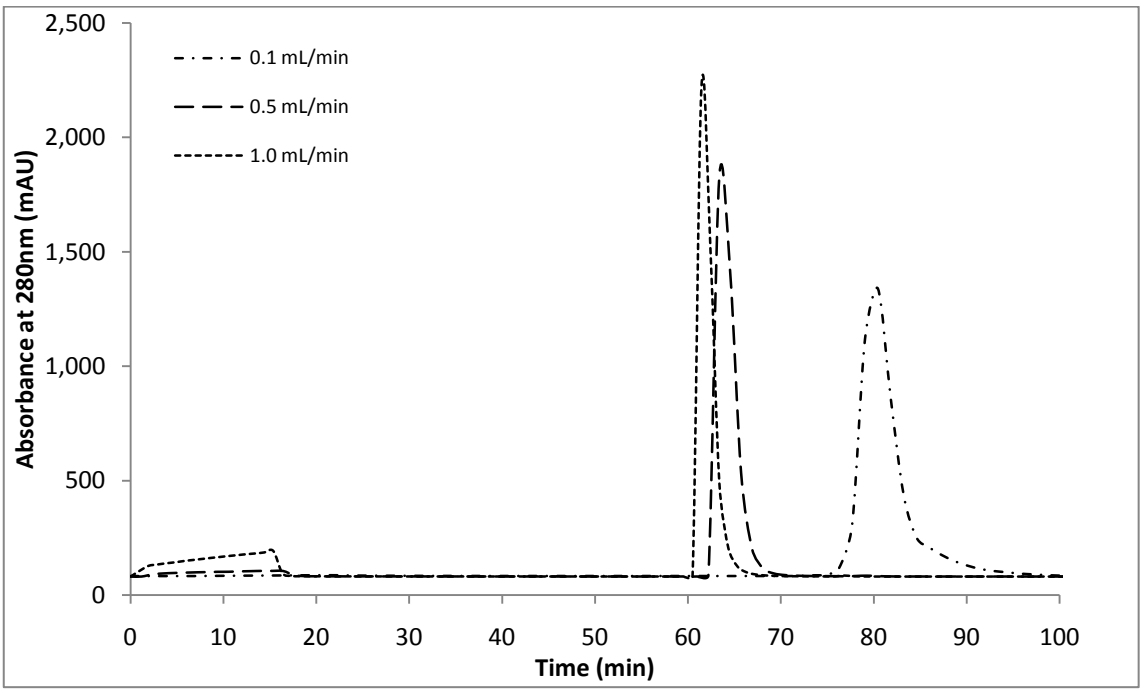

Figure 140. 1.5 mg/mL BSA concentration, 2M NaCl concentration, 180 degrees/hr rotation speed, flow rates 0.1-1.0 mL/min, Trial 1: 15 min loading, 45 min equilibration, 15 min elution, 45 min equilibration.

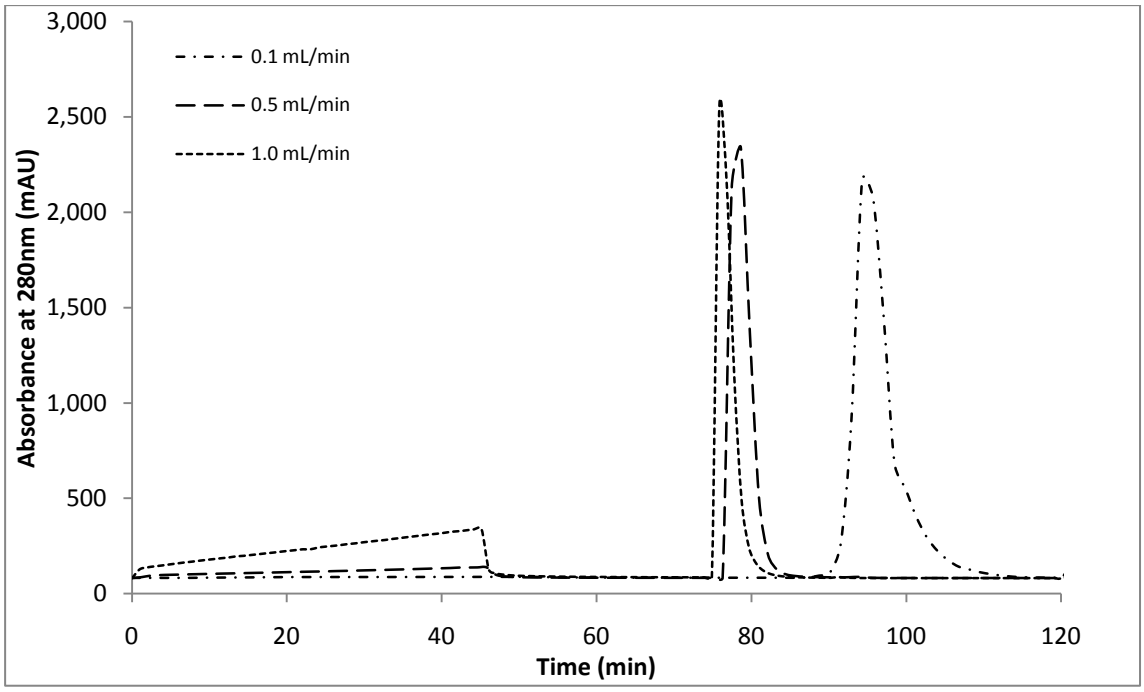

Figure 141. 1.5 mg/mL BSA concentration, 2M NaCl concentration, 180 degrees/hr rotation speed, flow rates 0.1-1.0 mL/min, Trial 2: 45 min loading, 30 min equilibration, 15 min elution, 30 min equilibration.

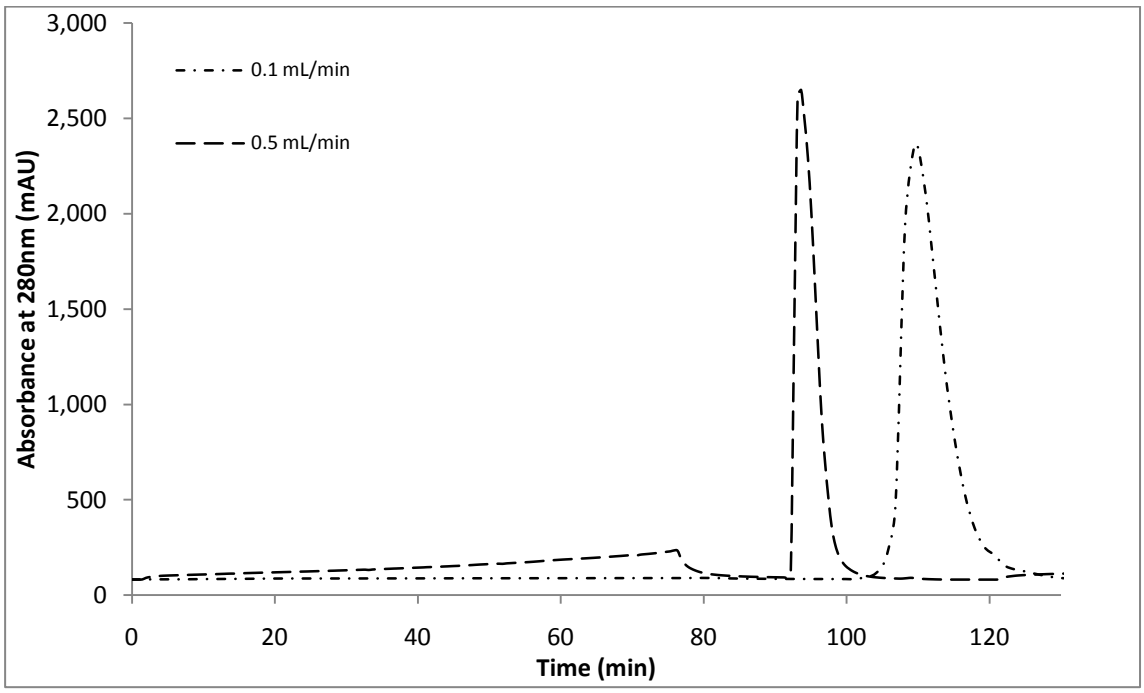

Figure 142. 1.5 mg/mL BSA concentration, 2M NaCl concentration, 180 degrees/hr rotation speed, flow rates 0.1-0.5 mL/min, Trial 3: 75 min loading, 15 min equilibration, 15 min elution, 15 min equilibration.

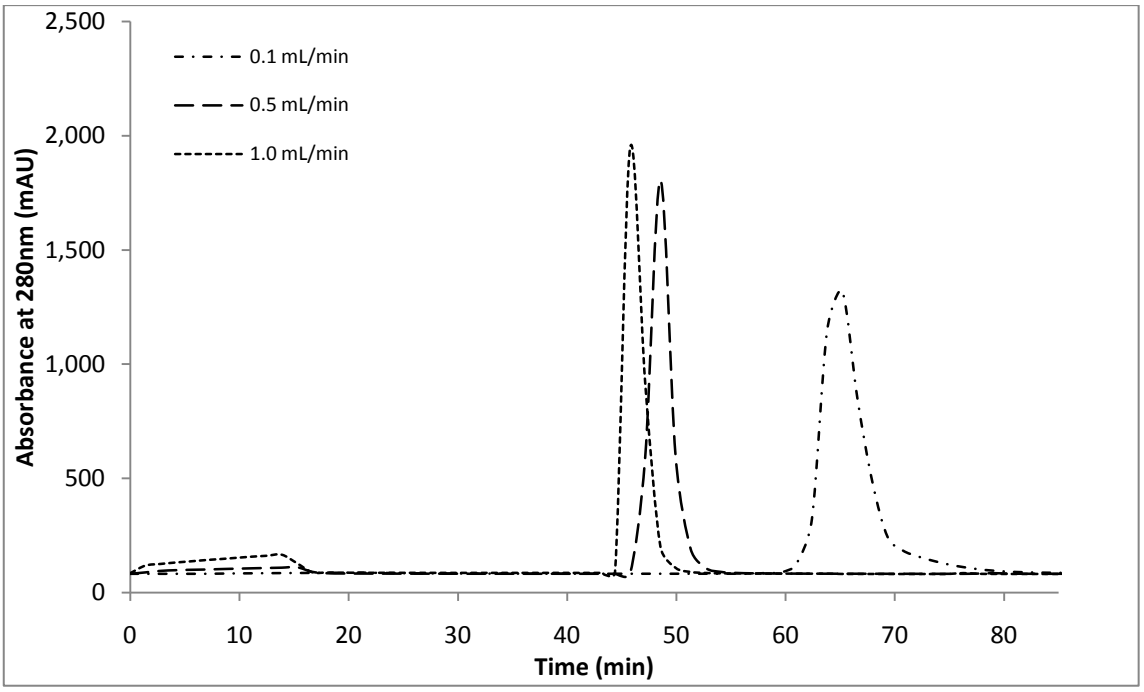

Figure 143. 1.5 mg/mL BSA concentration, 2M NaCl concentration, 180 degrees/hr rotation speed, flow rates 0.1-1.0 mL/min, Trial 4: 15 min loading, 30 min equilibration, 30 min elution, 45 min equilibration.

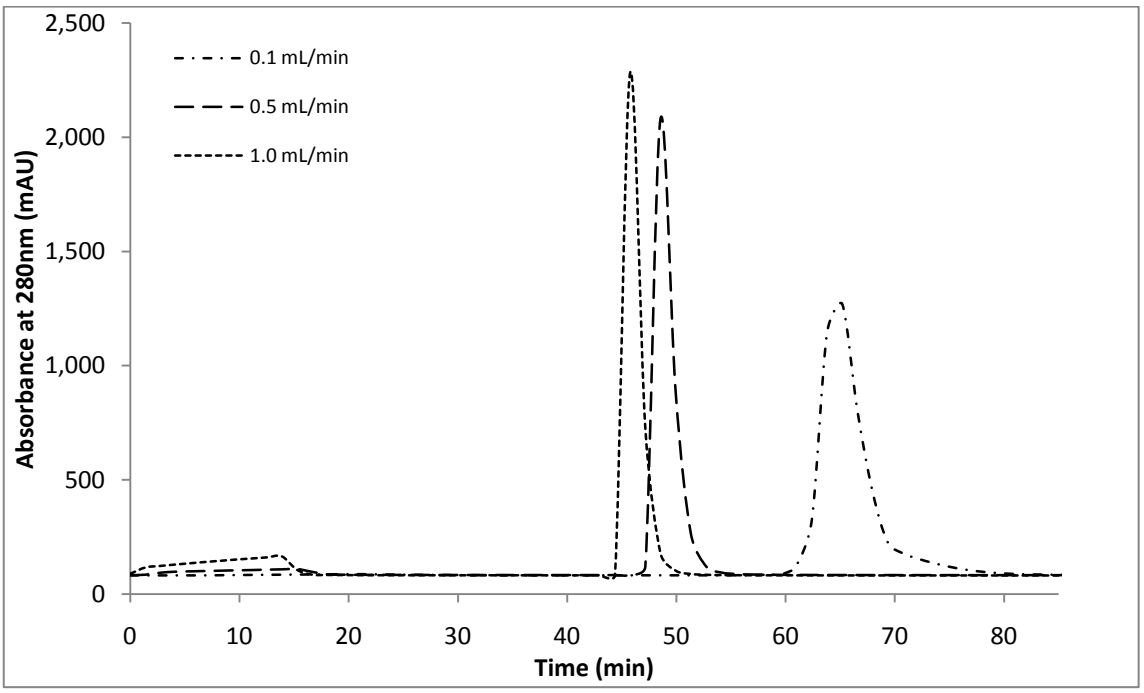

Figure 144. 1.5 mg/mL BSA concentration, 2M NaCl concentration, 180 degrees/hr rotation speed, flow rates 0.1-1.0 mL/min, Trial 5: 15 min loading, 30 min equilibration, 45 min elution, 30 min equilibration.

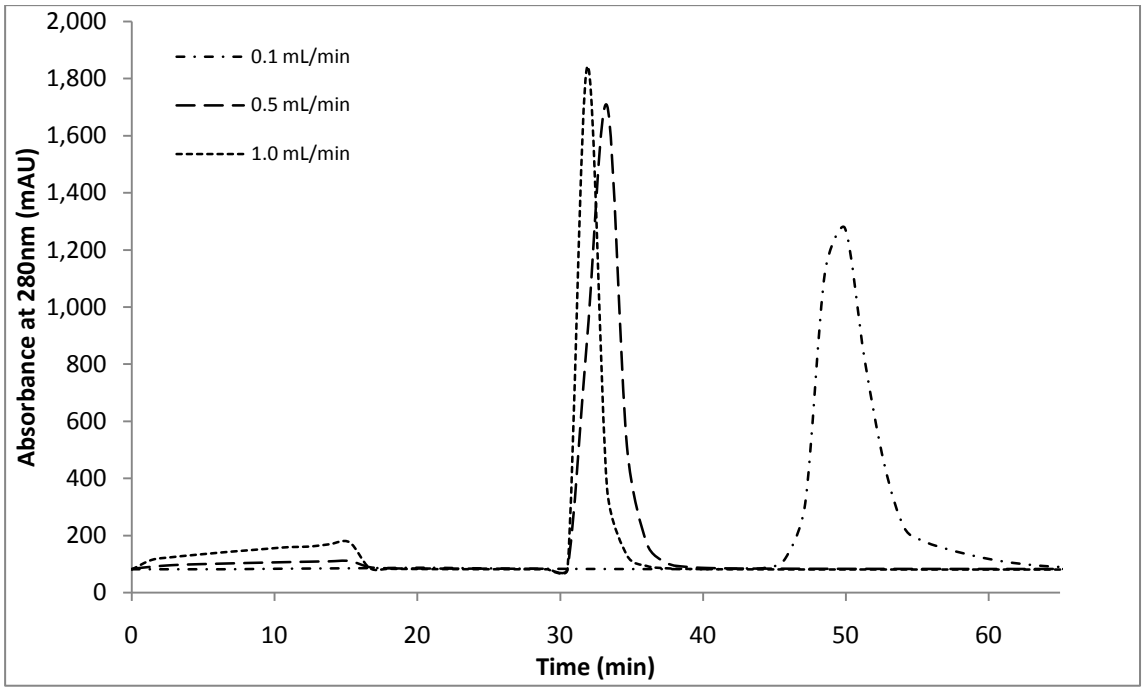

Figure 145. 1.5 mg/mL BSA concentration, 2M NaCl concentration, 180 degrees/hr rotation speed, flow rates 0.1-1.0 mL/min, Trial 6: 15 min loading, 15 min equilibration, 75 min elution, 15 min equilibration.

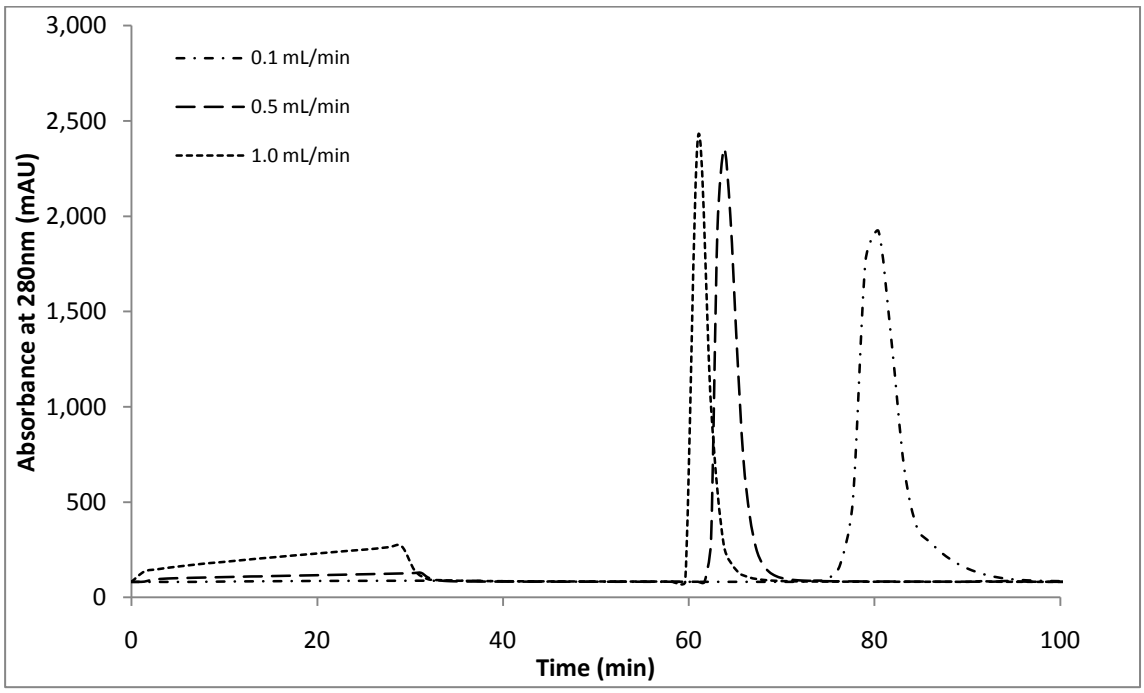

Figure 146. 1.5 mg/mL BSA concentration, 2M NaCl concentration, 180 degrees/hr rotation speed, flow rates 0.1-1.0 mL/min, Trial 7: 30 min loading, 30 min equilibration, 30 min elution, 30 min equilibration.

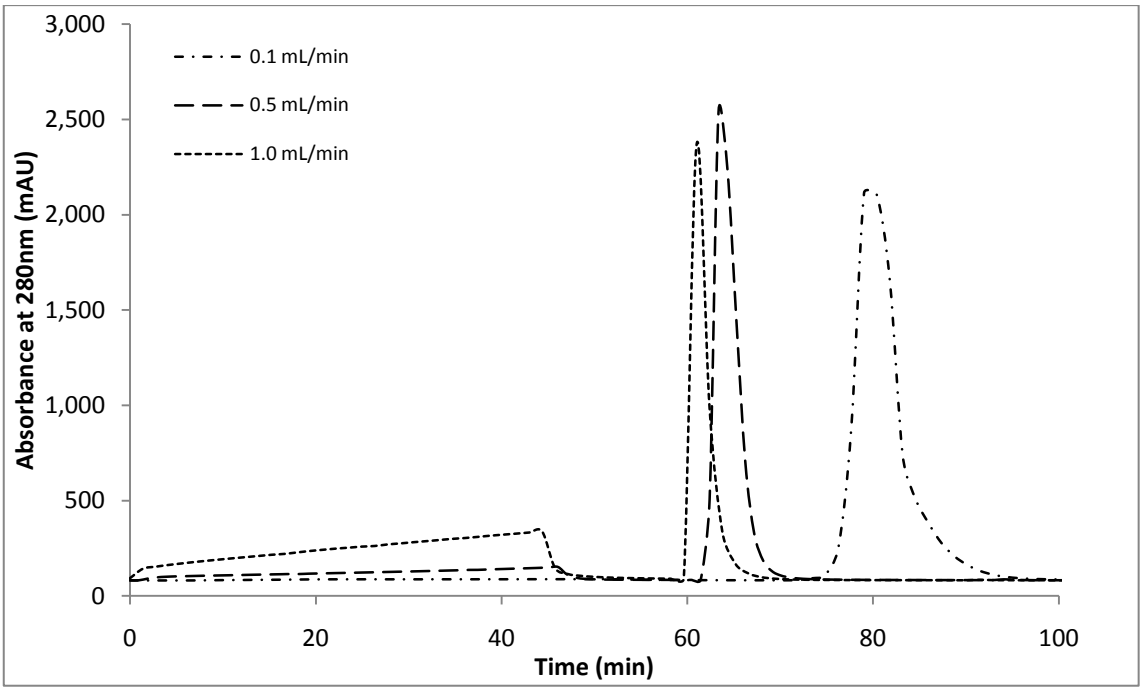

Figure 147. 1.5 mg/mL BSA concentration, 2M NaCl concentration, 180 degrees/hr rotation speed, flow rates 0.1-1.0 mL/min, Trial 8: 45 min loading, 15 min equilibration, 30 min elution, 30 min equilibration.

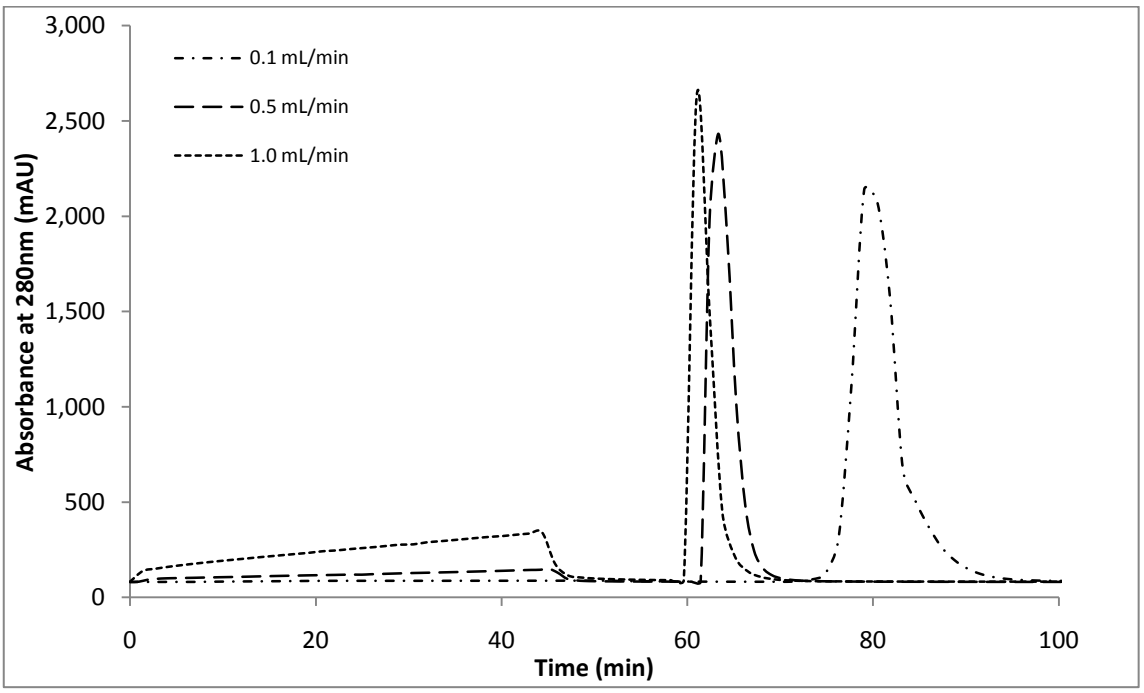

Figure 148. 1.5 mg/mL BSA concentration, 2M NaCl concentration, 180 degrees/hr rotation speed, flow rates 0.1-1.0 mL/min, Trial 9: 45 min loading, 15 min equilibration, 45 min elution, 15 min equilibration.

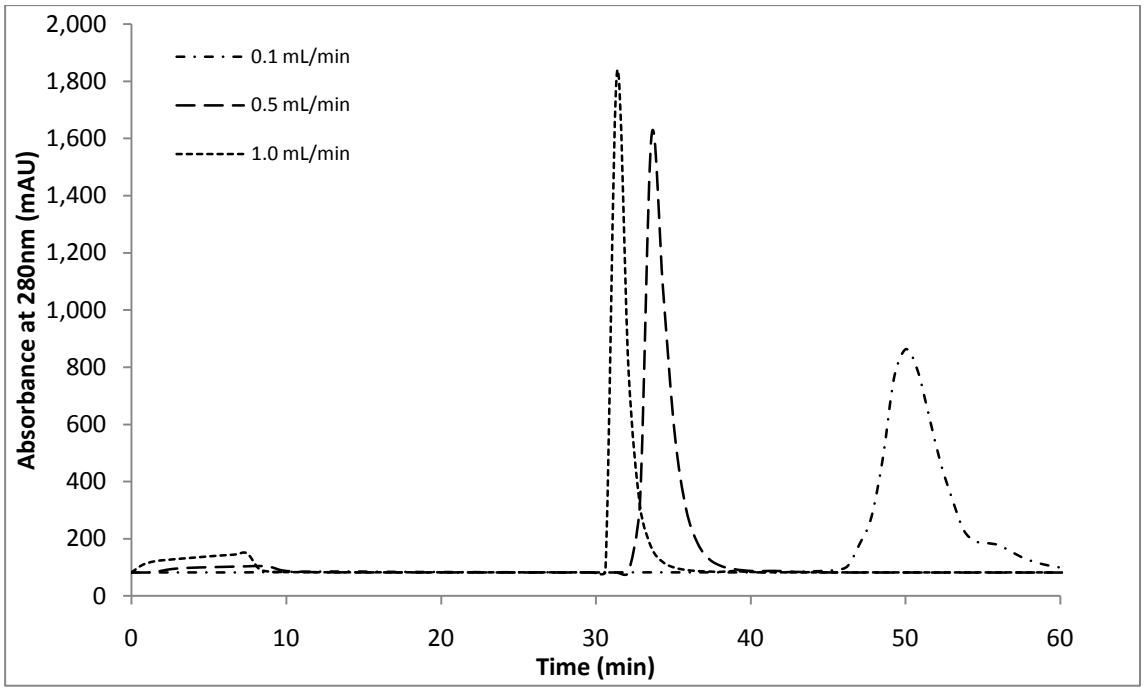

Figure 149. 1.5 mg/mL BSA concentration, 2M NaCl concentration, 360 degrees/hr rotation speed, flow rates 0.1-1.0 mL/min, Trial 1: 7.5 min loading, 22.5 min equilibration, 7.5 min elution, 22.5 min equilibration.

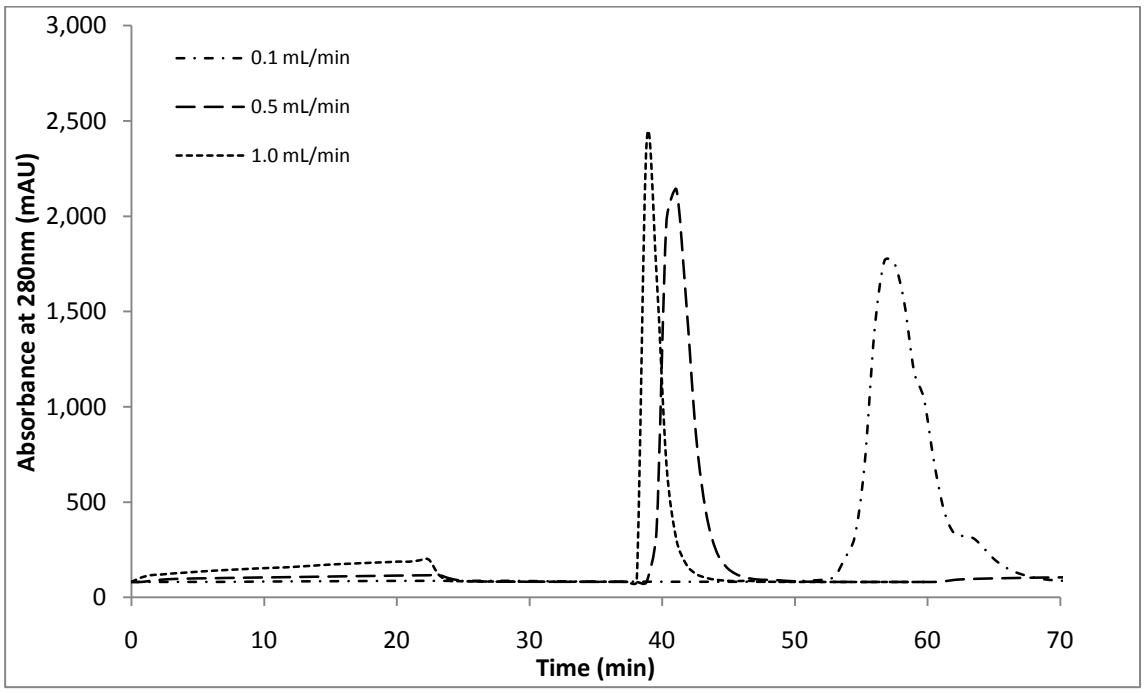

Figure 150. 1.5 mg/mL BSA concentration, 2M NaCl concentration, 360 degrees/hr rotation speed, flow rates 0.1-1.0 mL/min, Trial 2: 22.5 min loading, 15 min equilibration, 7.5 min elution, 15 min equilibration.

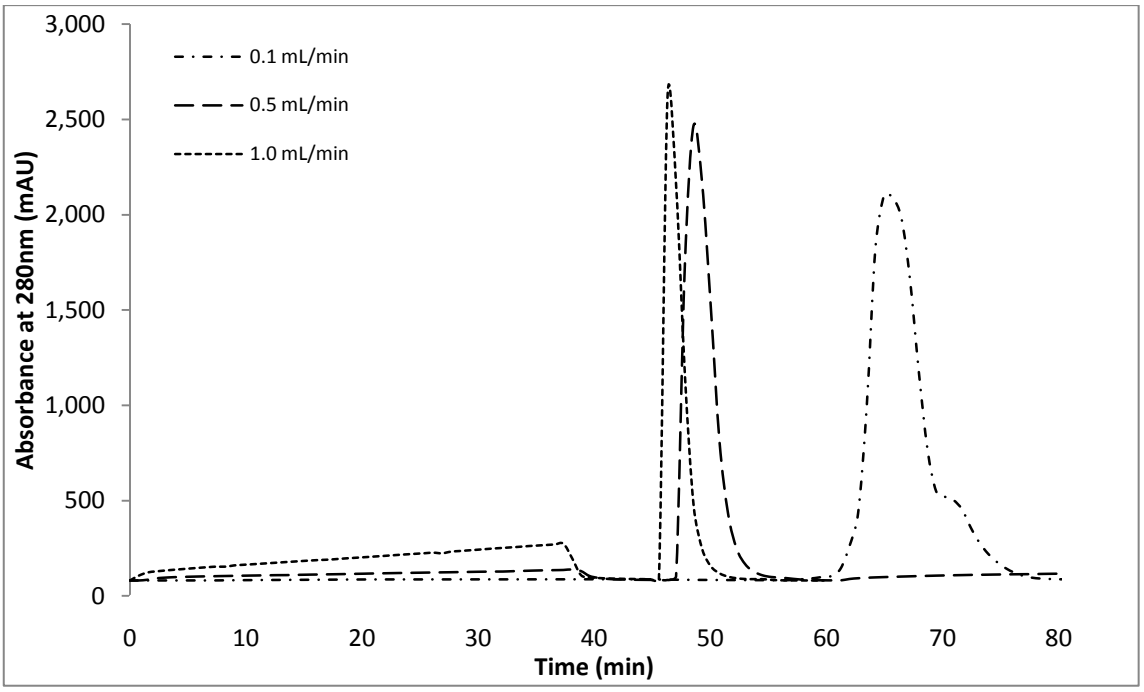

Figure 151. 1.5 mg/mL BSA concentration, 2M NaCl concentration, 360 degrees/hr rotation speed, flow rates 0.1-1.0 mL/min, Trial 3: 37.5 min loading, 7.5 min equilibration, 7.5 min elution, 7.5 min equilibration.

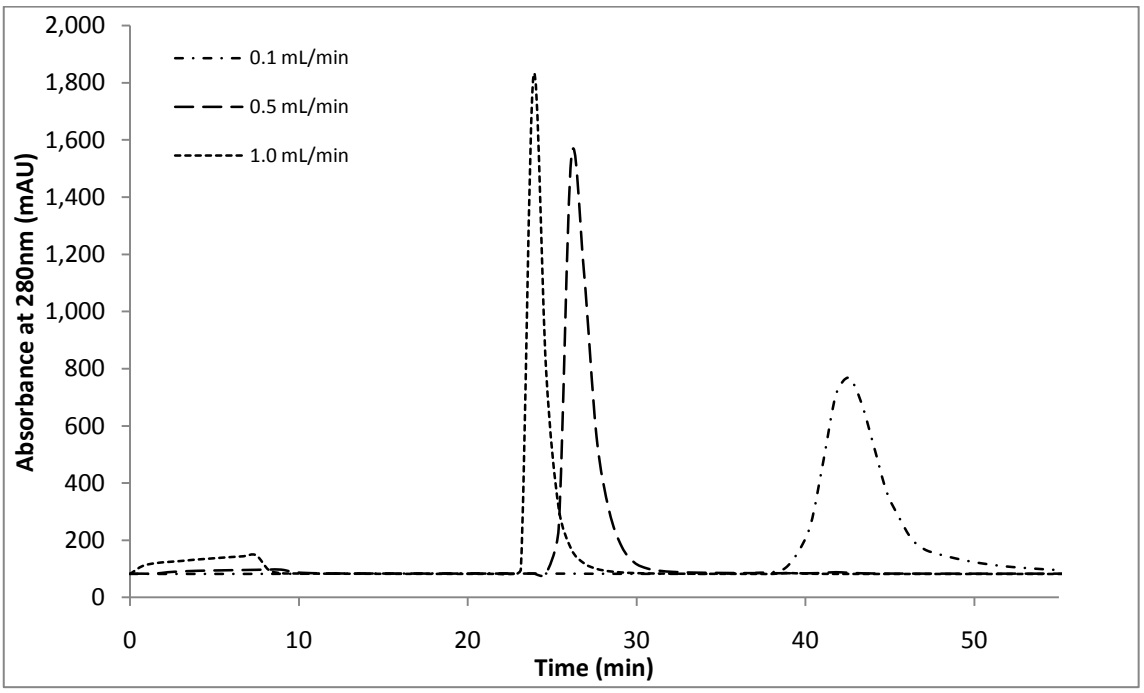

Figure 152. 1.5 mg/mL BSA concentration, 2M NaCl concentration, 360 degrees/hr rotation speed, flow rates 0.1-1.0 mL/min, Trial 4: 7.5 min loading, 15 min equilibration, 15 min elution, 22.5 min equilibration.

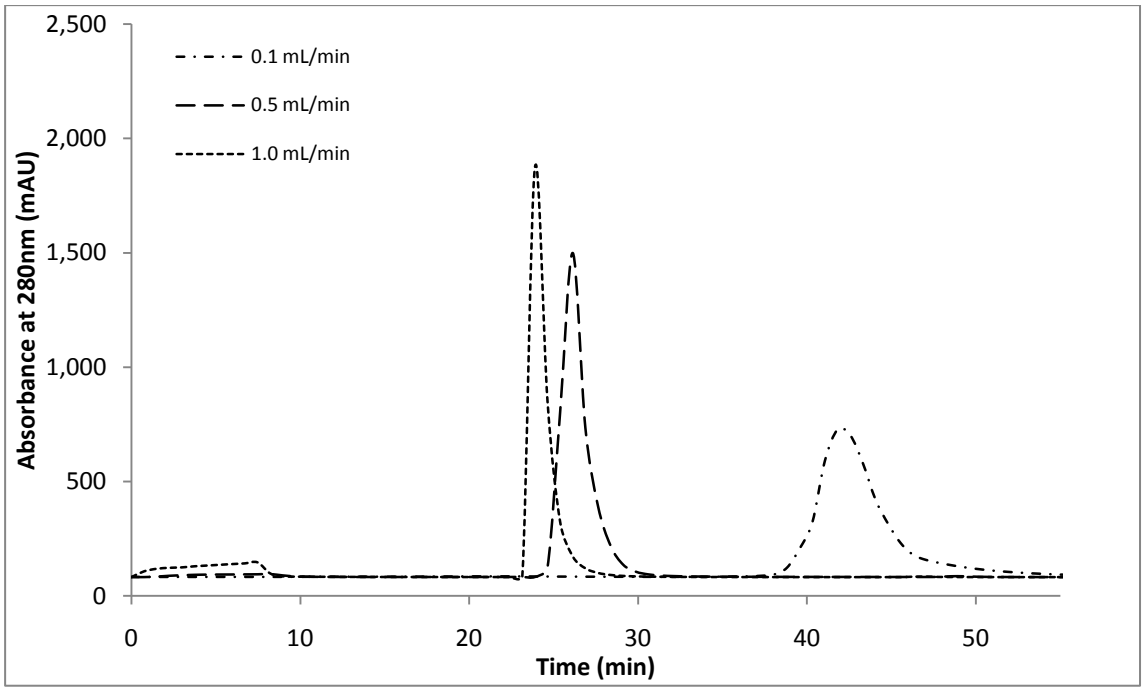

Figure 153. 1.5 mg/mL BSA concentration, 2M NaCl concentration, 360 degrees/hr rotation speed, flow rates 0.1-1.0 mL/min, Trial 5: 7.5 min loading, 15 min equilibration, 22.5 min elution, 15 min equilibration.

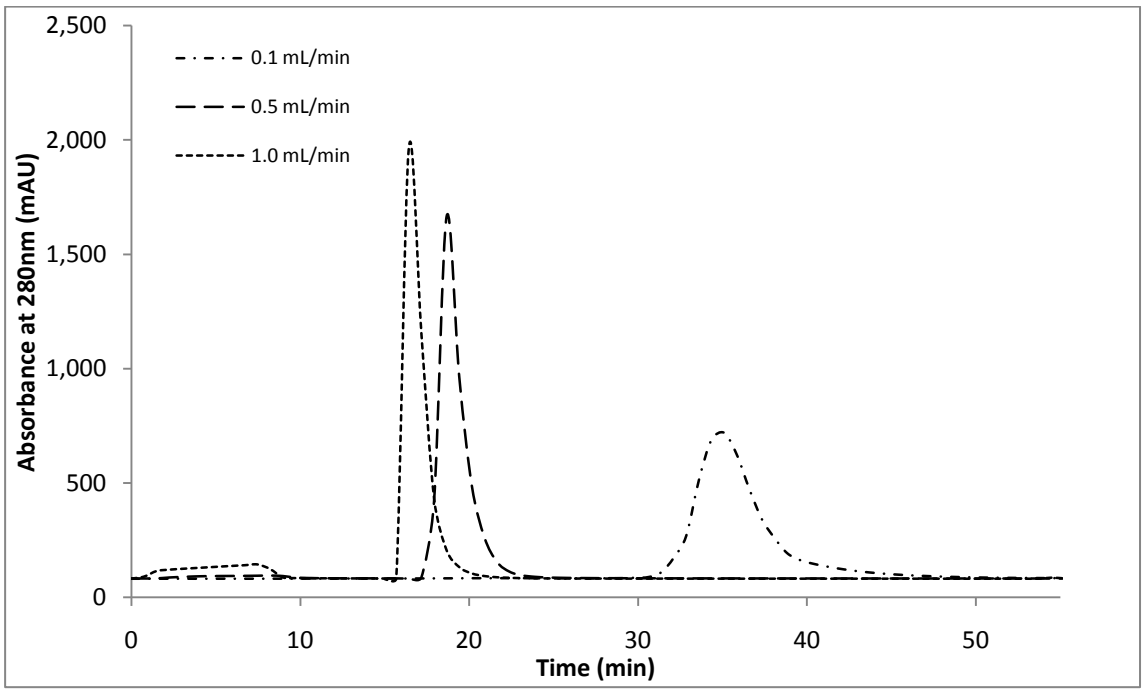

Figure 154. 1.5 mg/mL BSA concentration, 2M NaCl concentration, 360 degrees/hr rotation speed, flow rates 0.1-1.0 mL/min, Trial 6: 7.5 min loading, 7.5 min equilibration, 37.5 min elution, 7.5 min equilibration.

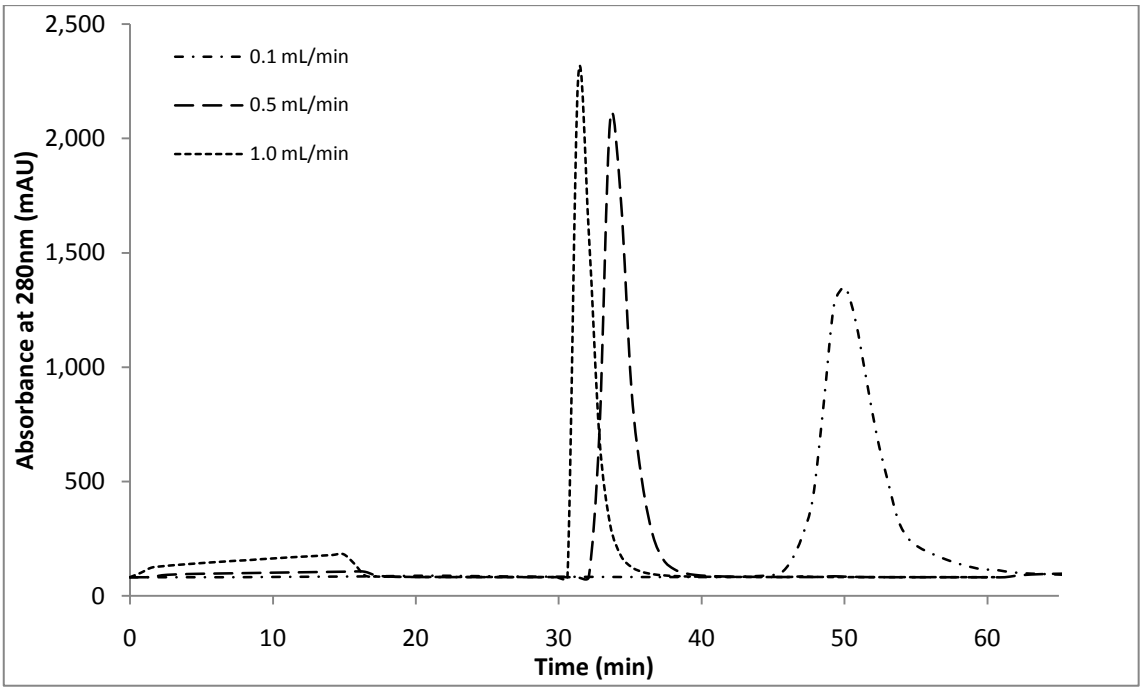

Figure 155. 1.5 mg/mL BSA concentration, 2M NaCl concentration, 360 degrees/hr rotation speed, flow rates 0.1-1.0 mL/min, Trial 7: 15 min loading, 15 min equilibration, 15 min elution, 15 min equilibration.

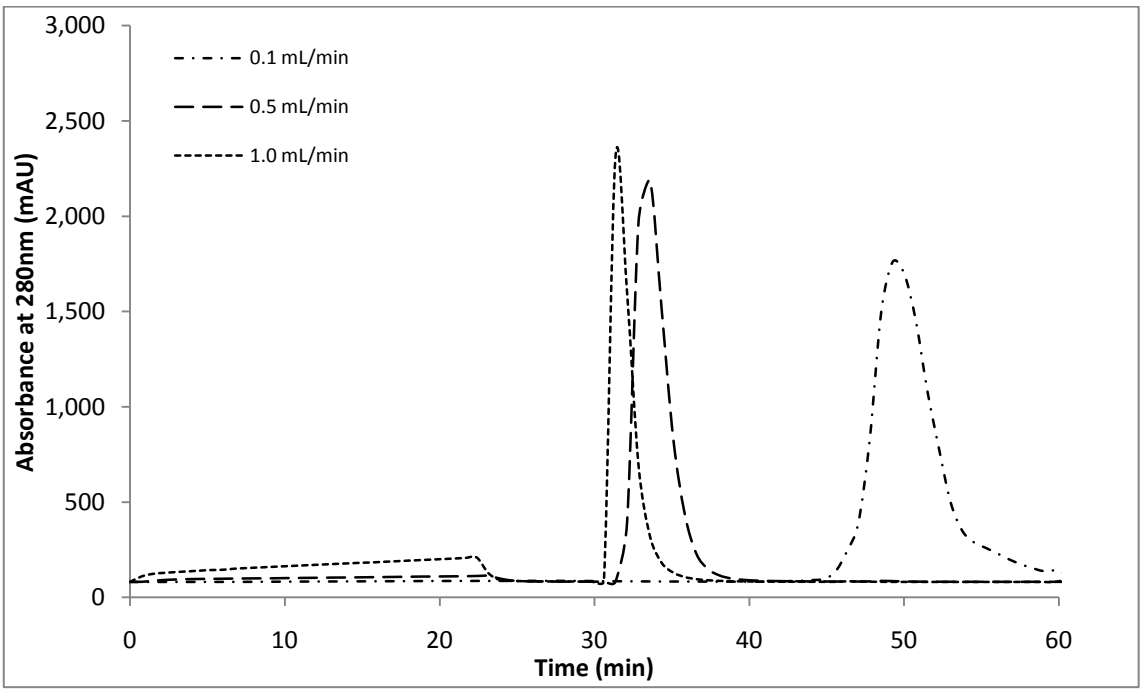

Figure 156. 1.5 mg/mL BSA concentration, 2M NaCl concentration, 360 degrees/hr rotation speed, flow rates 0.1-1.0 mL/min, Trial 8: 22.5 min loading, 7.5 min equilibration, 15 min elution, 15 min equilibration.

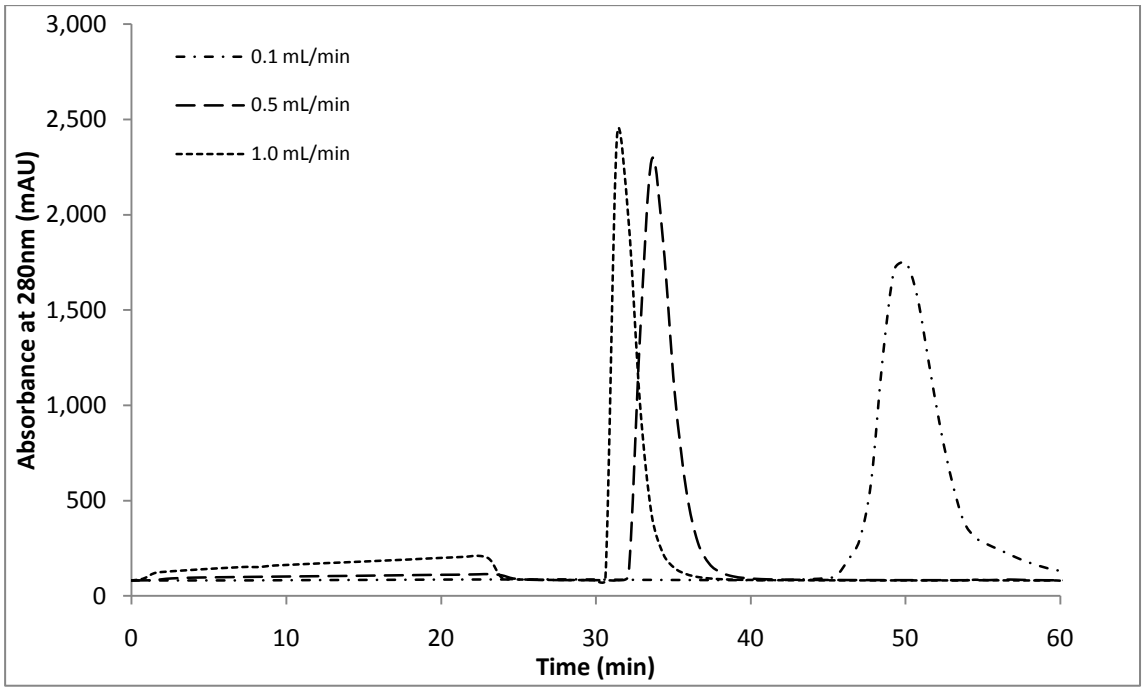

Figure 157. 1.5 mg/mL BSA concentration, 2M NaCl concentration, 360 degrees/hr rotation speed, flow rates 0.1-1.0 mL/min, Trial 9: 22.5 min loading, 7.5 min equilibration, 22.5 min elution, 7.5 min equilibration.

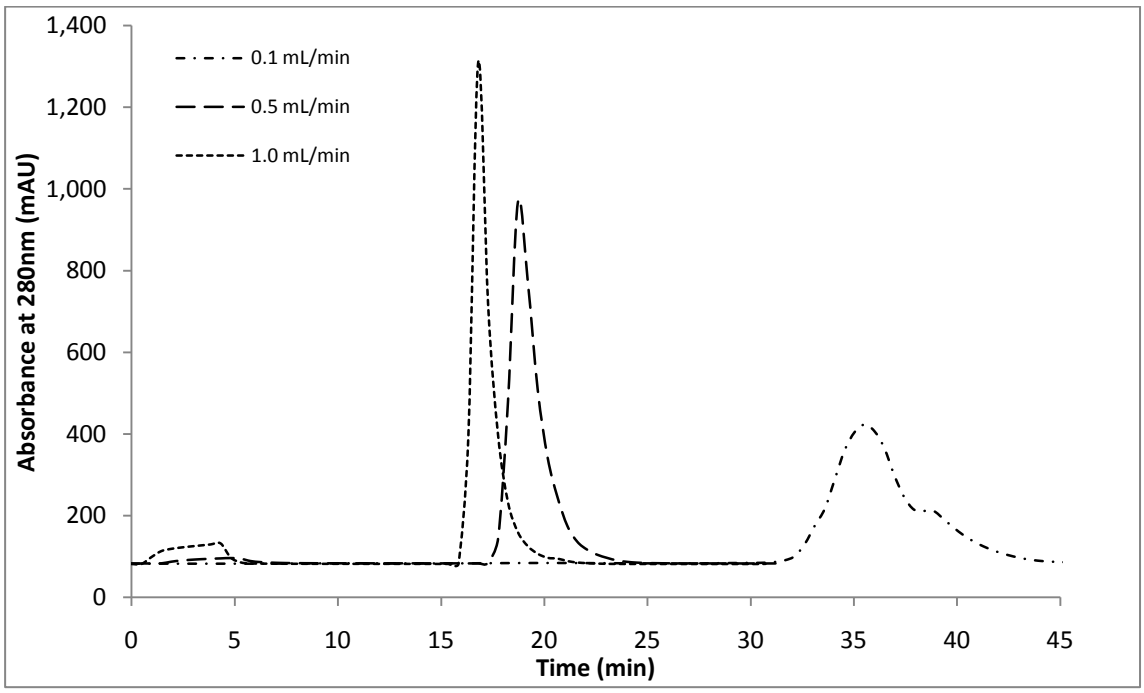

Figure 158. 1.5 mg/mL BSA concentration, 2M NaCl concentration, 720 degrees/hr rotation speed, flow rates 0.1-1.0 mL/min, Trial 1: 3.75 min loading, 11.25 min equilibration, 3.75 min elution, 11.25 min equilibration.

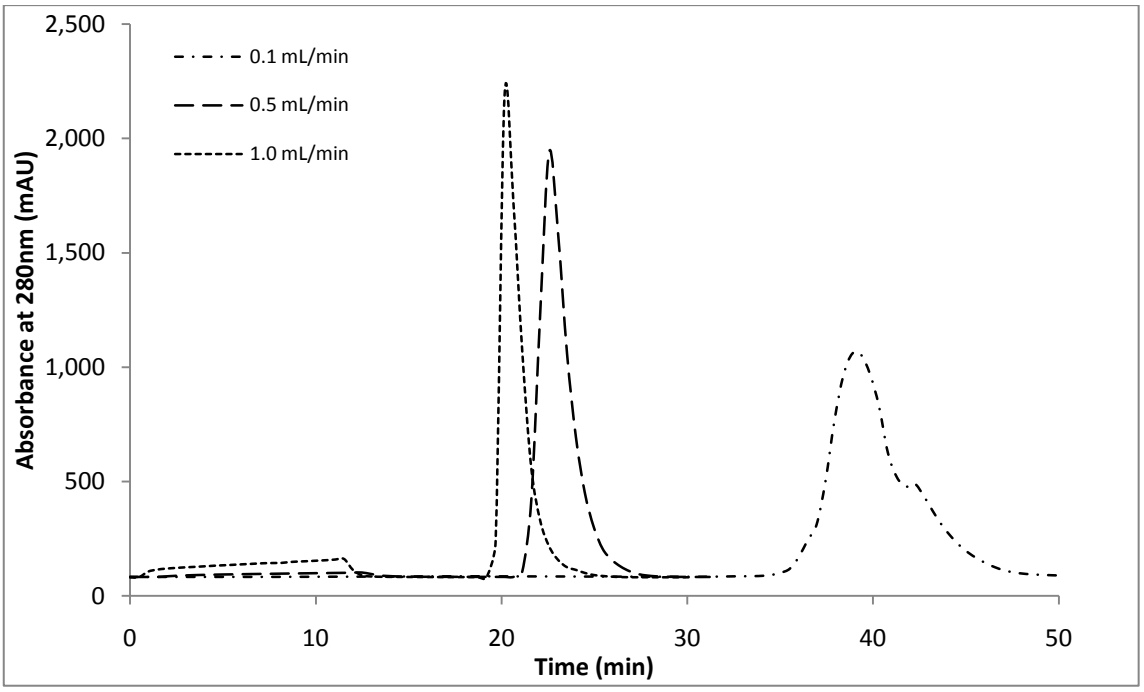

Figure 159. 1.5 mg/mL BSA concentration, 2M NaCl concentration, 720 degrees/hr rotation speed, flow rates 0.1-1.0 mL/min, Trial 2: 11.25 min loading, 7.5 min equilibration, 3.75 min elution, 7.5 min equilibration.

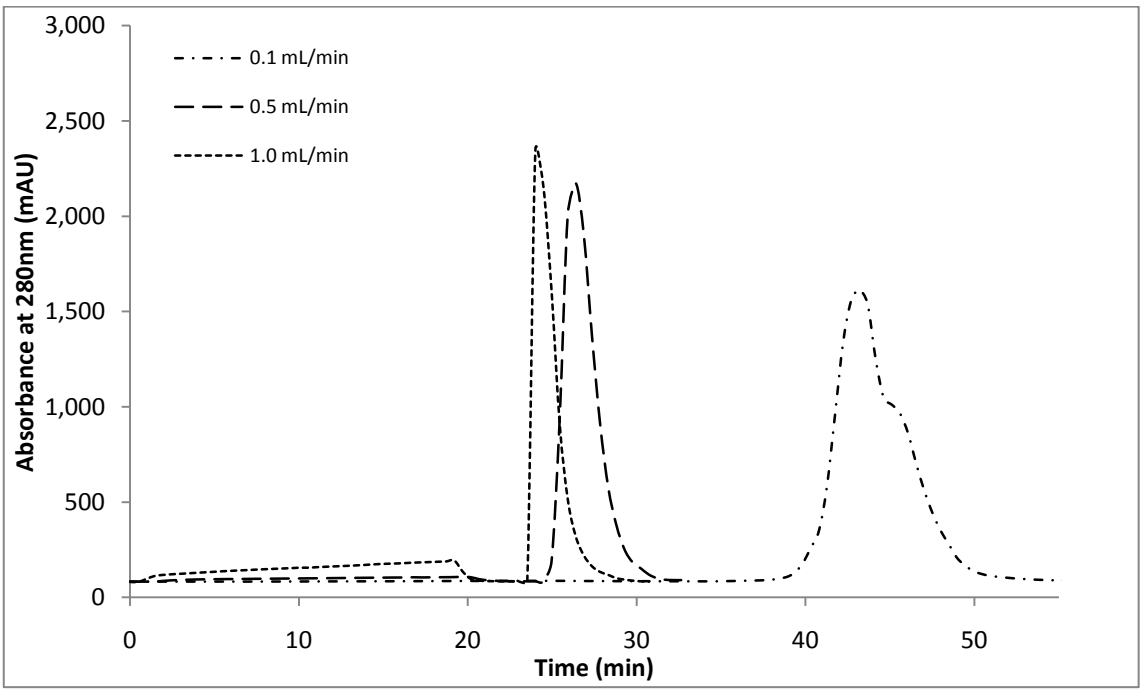

Figure 160. 1.5 mg/mL BSA concentration, 2M NaCl concentration, 720 degrees/hr rotation speed, flow rates 0.1-1.0 mL/min, Trial 3: 18.75 min loading, 3.75 min equilibration, 3.75 min elution, 3.75 min equilibration.

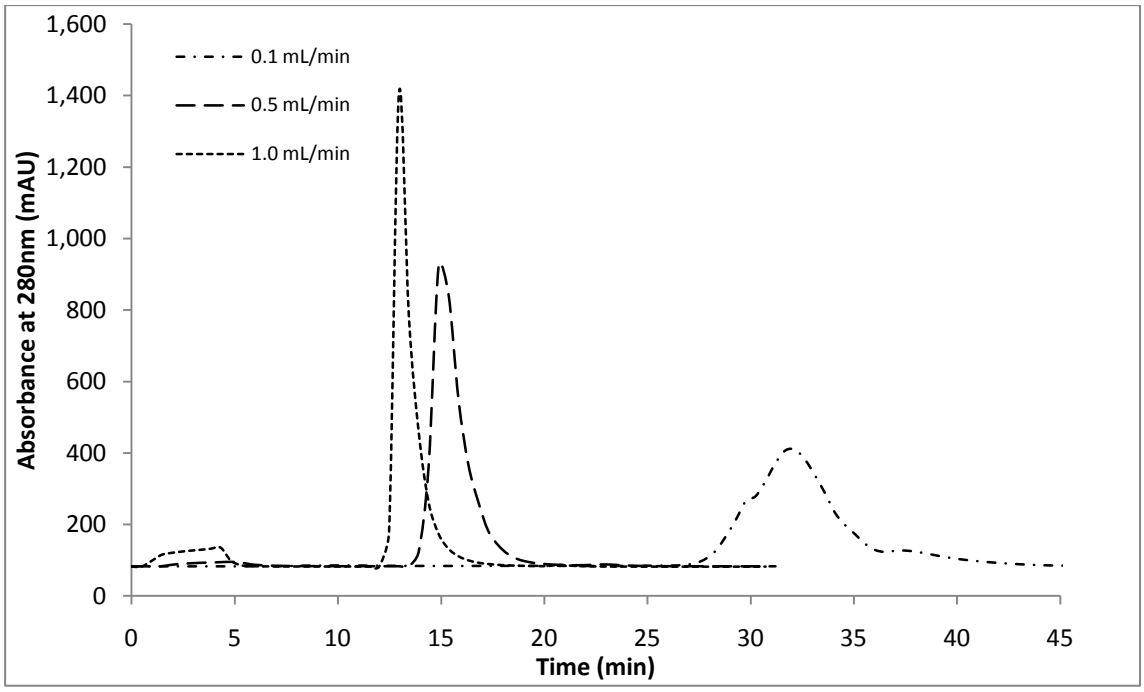

Figure 161. 1.5 mg/mL BSA concentration, 2M NaCl concentration, 720 degrees/hr rotation speed, flow rates 0.1-1.0 mL/min, Trial 4: 3.75 min loading, 7.5 min equilibration, 7.5 min elution, 11.25 min equilibration.

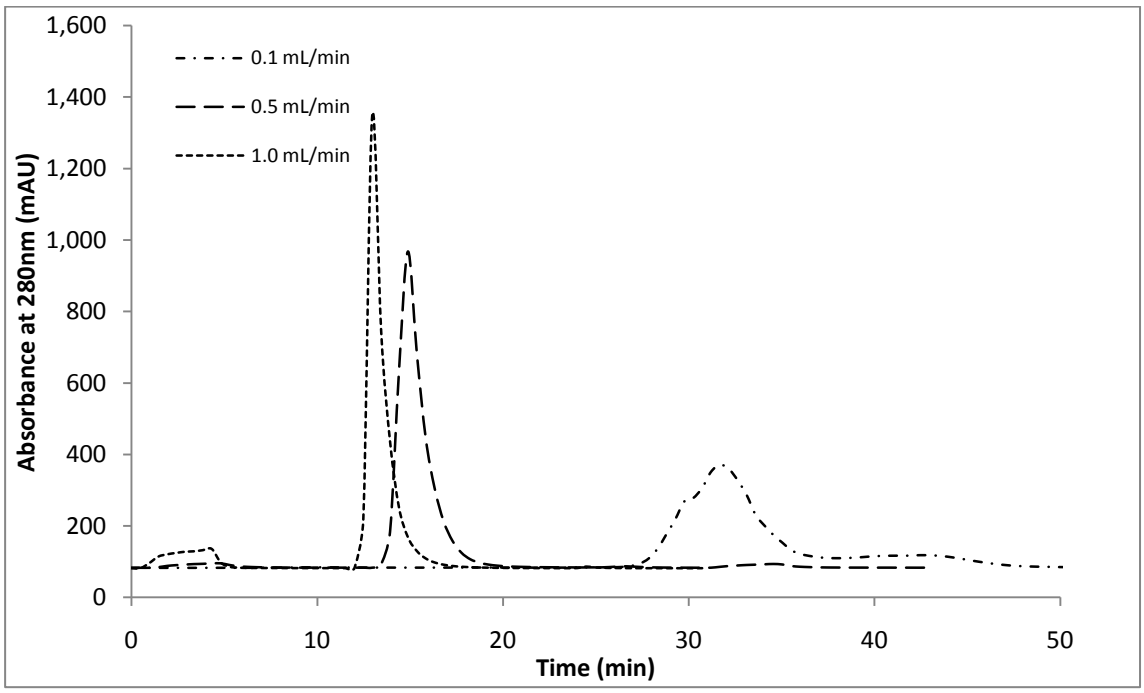

Figure 162. 1.5 mg/mL BSA concentration, 2M NaCl concentration, 720 degrees/hr rotation speed, flow rates 0.1-1.0 mL/min, Trial 5: 3.75 min loading, 7.5 min equilibration, 11.25 min elution, 7.5 min equilibration.

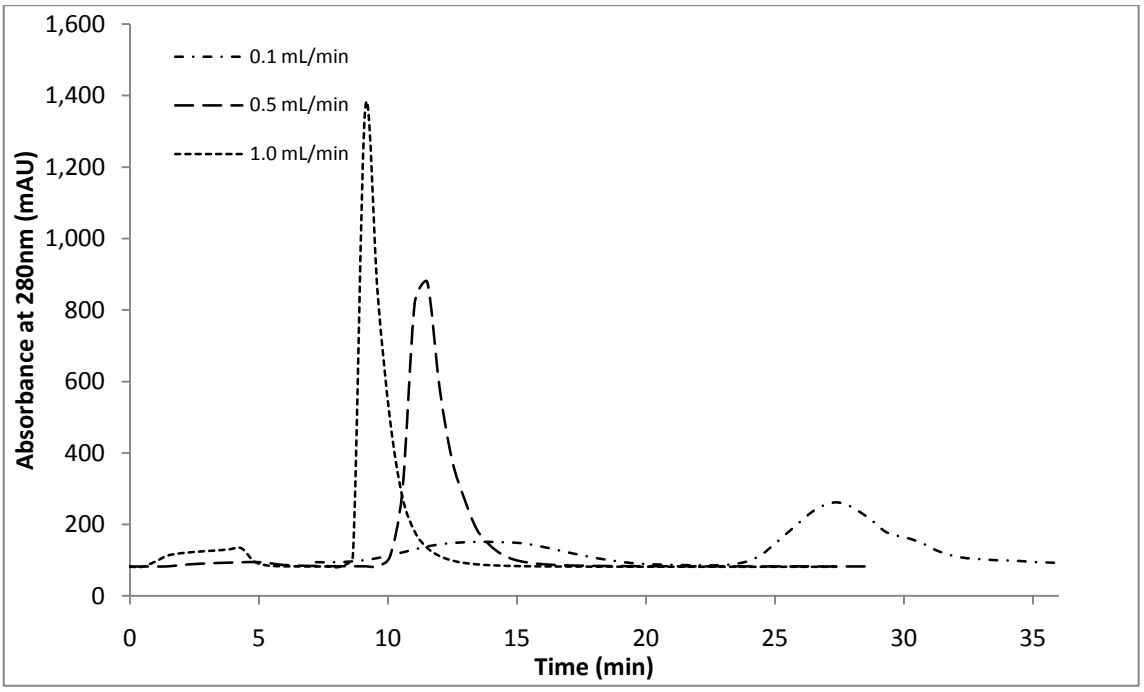

Figure 163. 1.5 mg/mL BSA concentration, 2M NaCl concentration, 720 degrees/hr rotation speed, flow rates 0.1-1.0 mL/min, Trial 6: 3.75 min loading, 3.75 min equilibration, 18.75 min elution, 3.75 min equilibration.

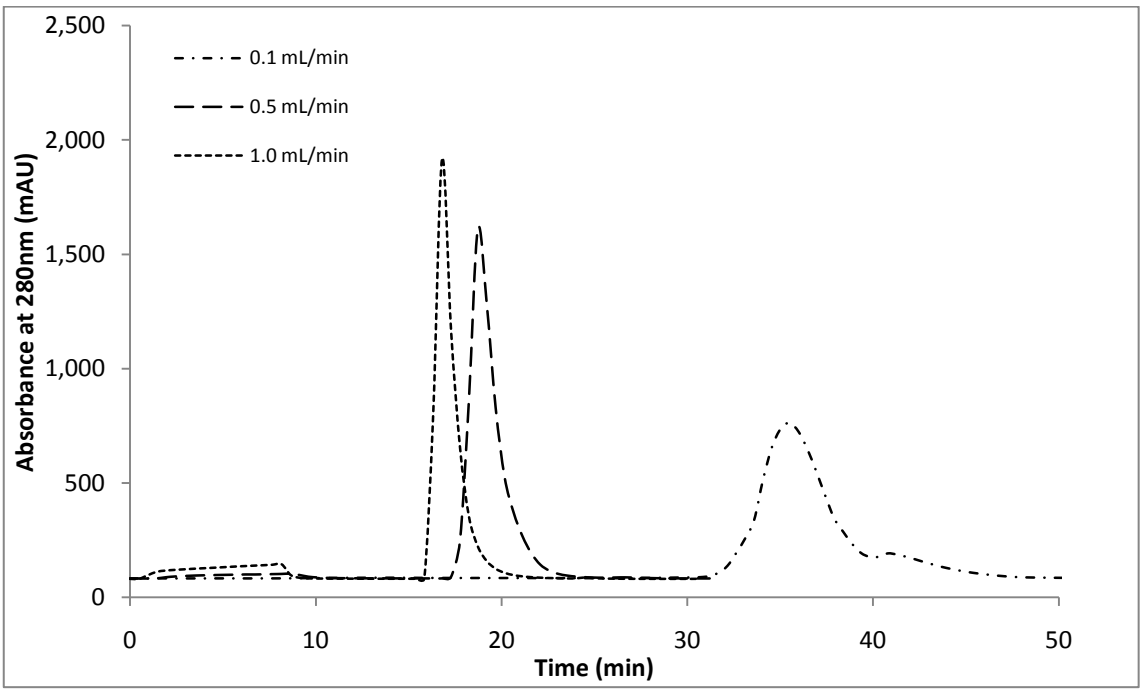

Figure 164. 5 mg/mL BSA concentration, 2M NaCl concentration, 720 degrees/hr rotation speed, flow rates 0.1-1.0 mL/min, Trial 7: 7.5 min loading, 7.5 min equilibration, 7.5 min elution, 7.5 min equilibration.

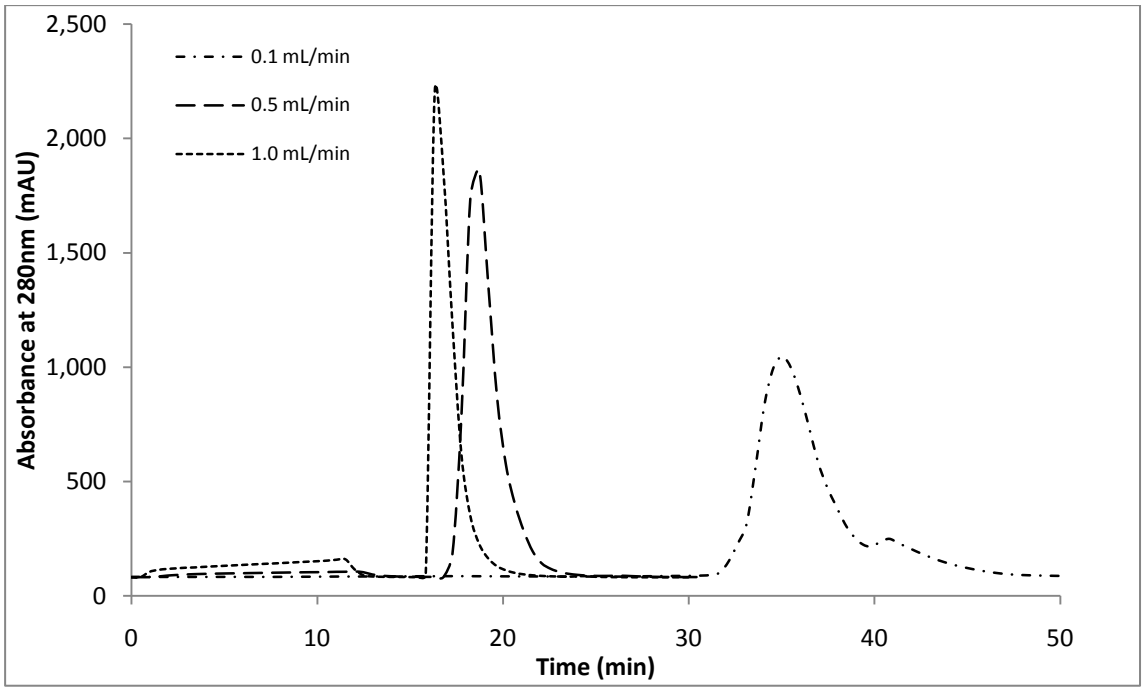

Figure 165. 1.5 mg/mL BSA concentration, 2M NaCl concentration, 720 degrees/hr rotation speed, flow rates 0.1-1.0 mL/min, Trial 8: 11.25 min loading, 3.75 min equilibration, 7.5 min elution, 7.5 min equilibration

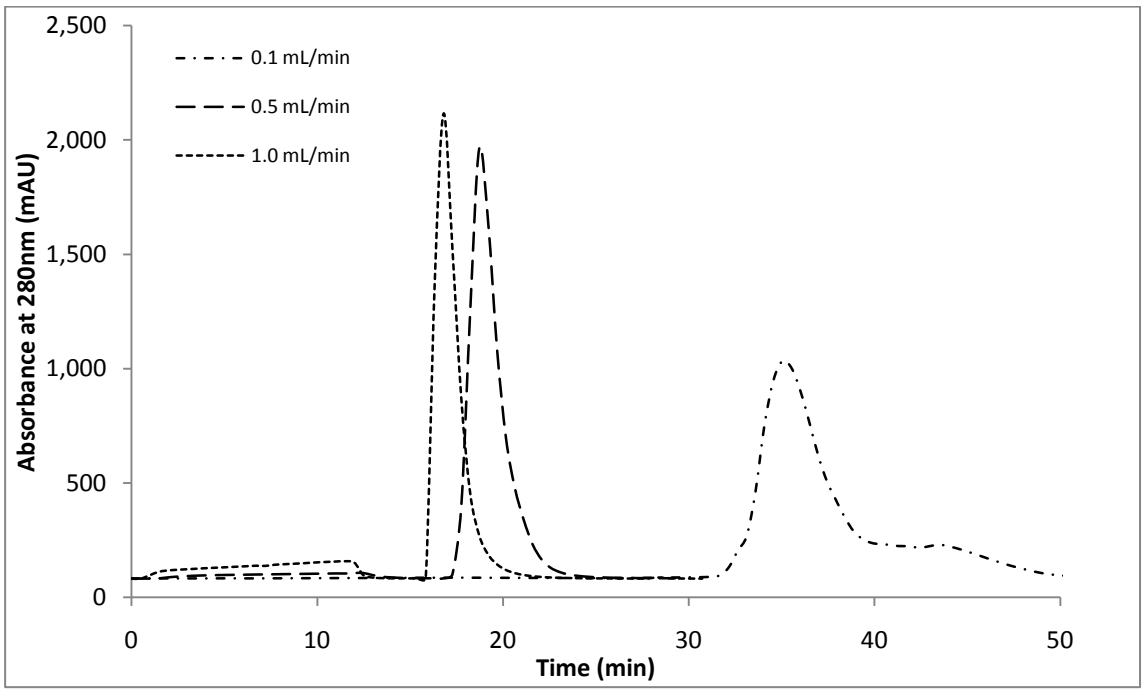

Figure 166. 1.5 mg/mL BSA concentration, 2M NaCl concentration, 720 degrees/hr rotation speed, flow rates 0.1-1.0 mL/min, Trial 9: 11.25 min loading, 3.75 min equilibration, 11.25 min elution, 3.75 min equilibration.

Appendix E Elution Zone Peak Area

E.1 Loading sections

E.1.1 1.5 mg/mL BSA concentration, 1M NaCl concentration, 180 deg/hr rotation speed, 0.1-1.0mL/min flow rate

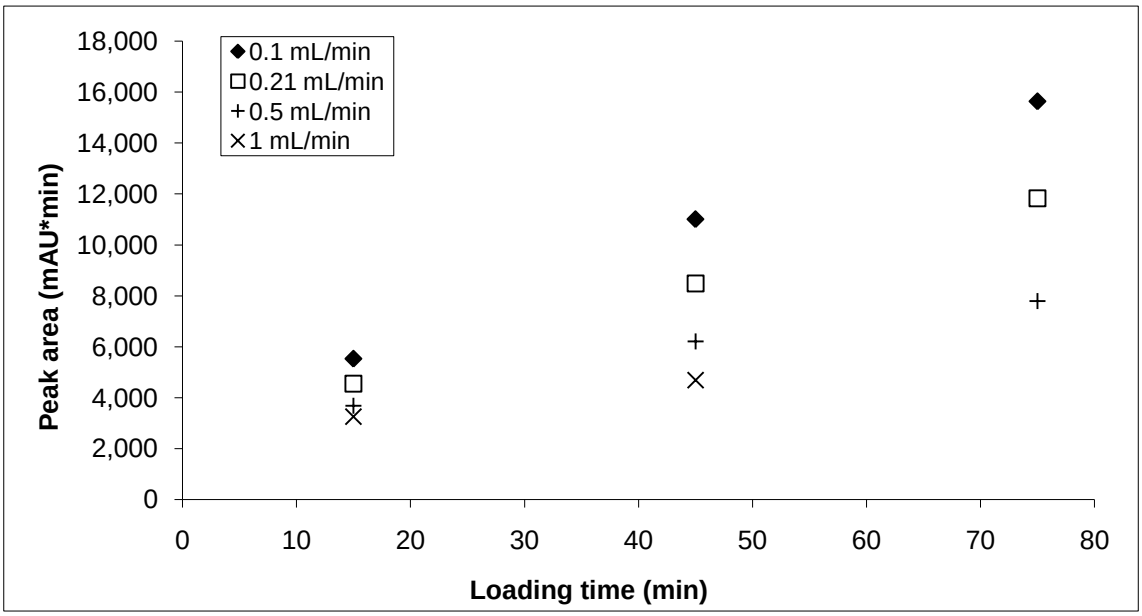

E.1.2 1.5 mg/mL BSA concentration, 1M NaCl concentration, 360 deg/hr rotation speed, 0.1-1.0 mL/min flow rate

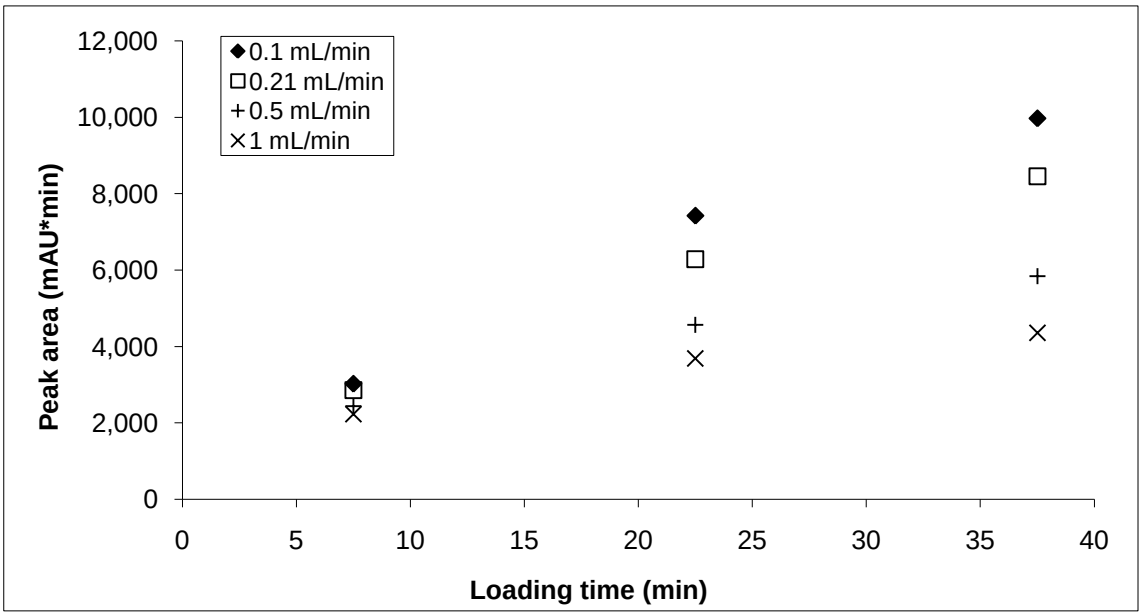

E.1.3 1.5 mg/mL BSA concentration, 1M NaCl concentration, 720 deg/hr rotation speed, 0.1-1.0 mL/min flow rate

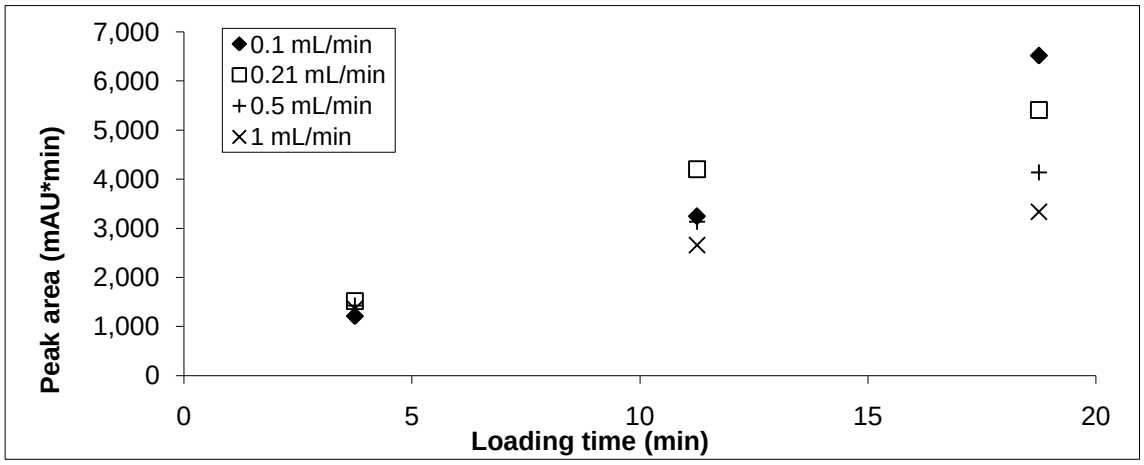

E.1.4 3 mg/mL BSA concentration, 1M NaCl concentration, 180 deg/hr rotation speed, 0.1-1.0 mL/min flow rate

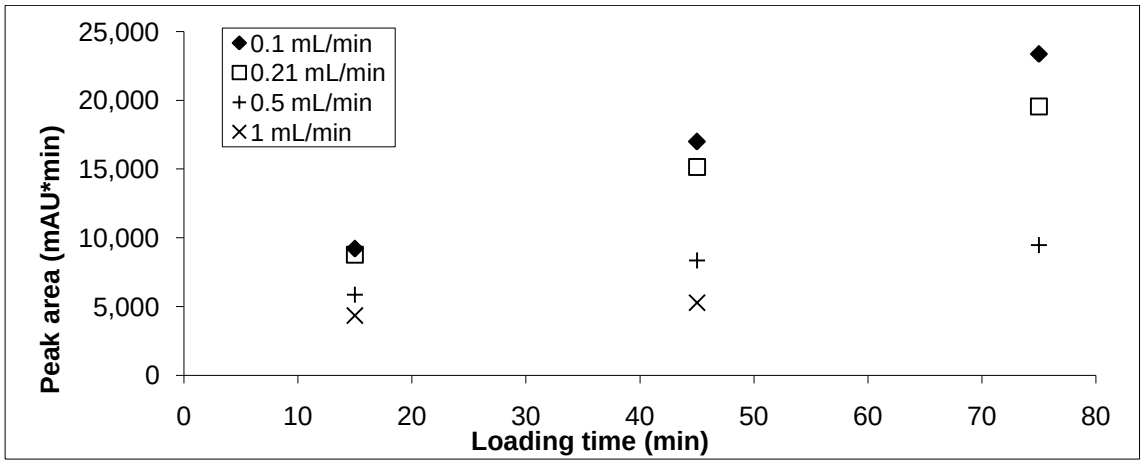

E.1.5 3 mg/mL BSA concentration, 1M NaCl concentration, 360 deg/hr rotation speed, 0.1-1.0 mL/min flow rate

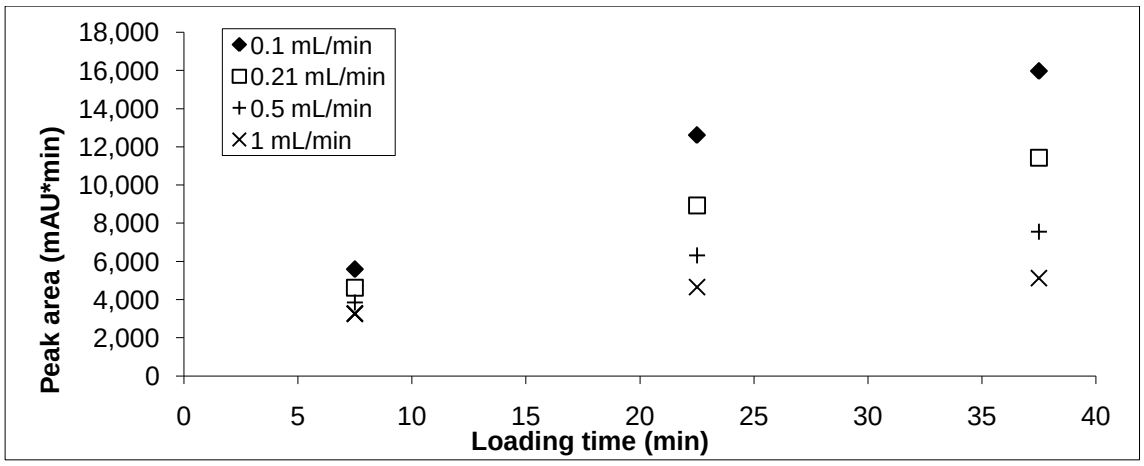

E.1.6 3 mg/mL BSA concentration, 1M NaCl concentration, 720 deg/hr rotation speed, 0.1-1.0 mL/min flow rate

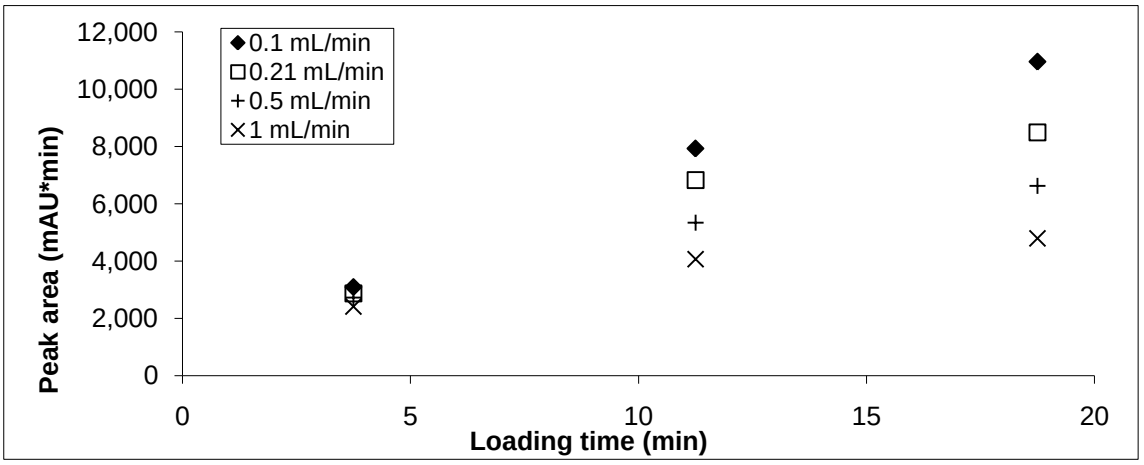

E.1.7 5 mg/mL BSA concentration, 1M NaCl concentration, 180 deg/hr rotation speed, 0.1-1.0 mL/min flow rate

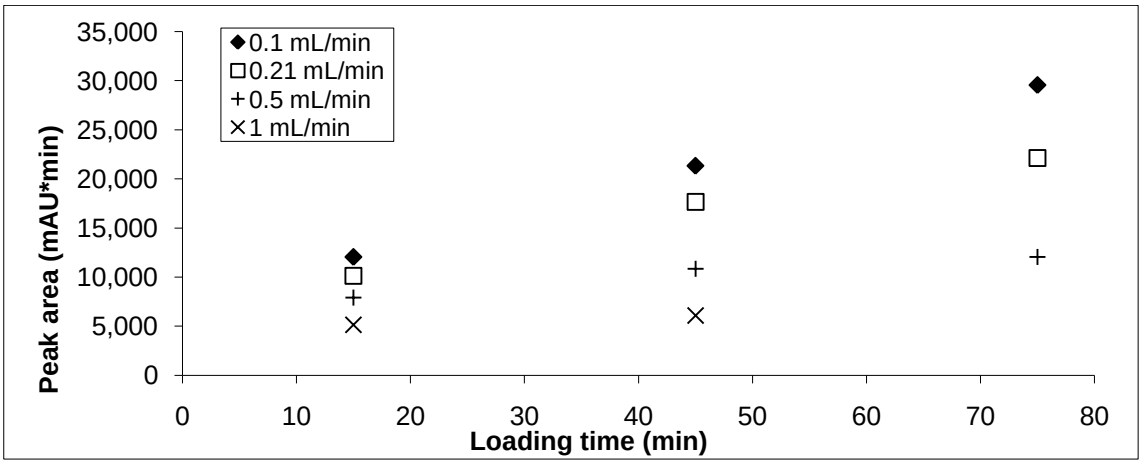

E.1.8 5 mg/mL BSA concentration, 1M NaCl concentration, 360 deg/hr rotation speed, 0.1-1.0 mL/min flow rate

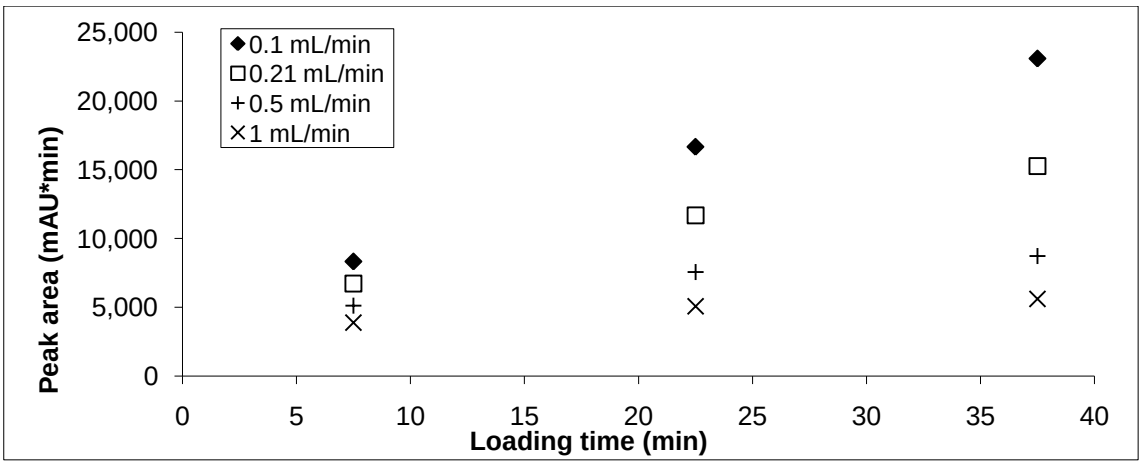

E.1.9 5 mg/mL BSA concentration, 1M NaCl concentration, 720 deg/hr rotation speed, 0.1-1.0 mL/min flow rate

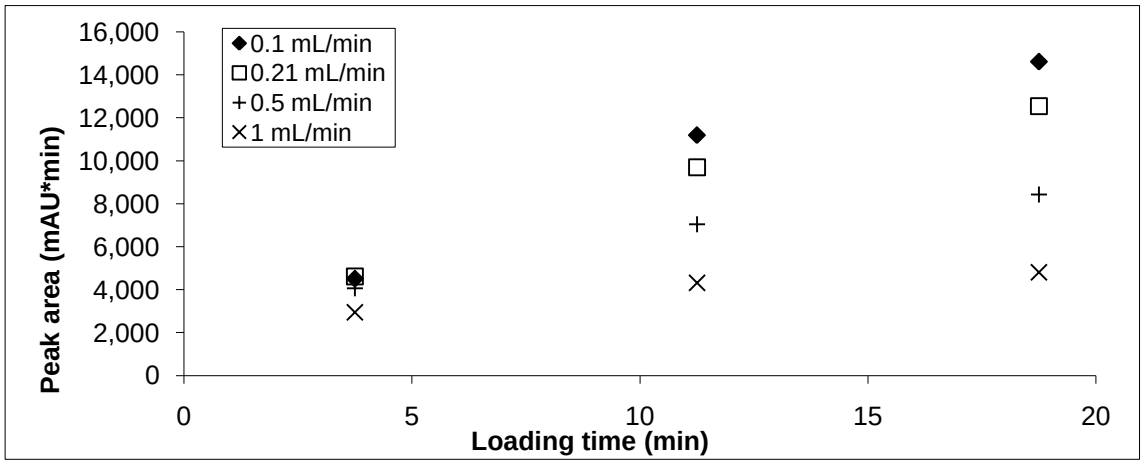

E.1.10 1.5 mg/mL BSA concentration, 2M NaCl concentration, 180 deg/hr rotation speed, 0.1-1.0 mL/min flow rate

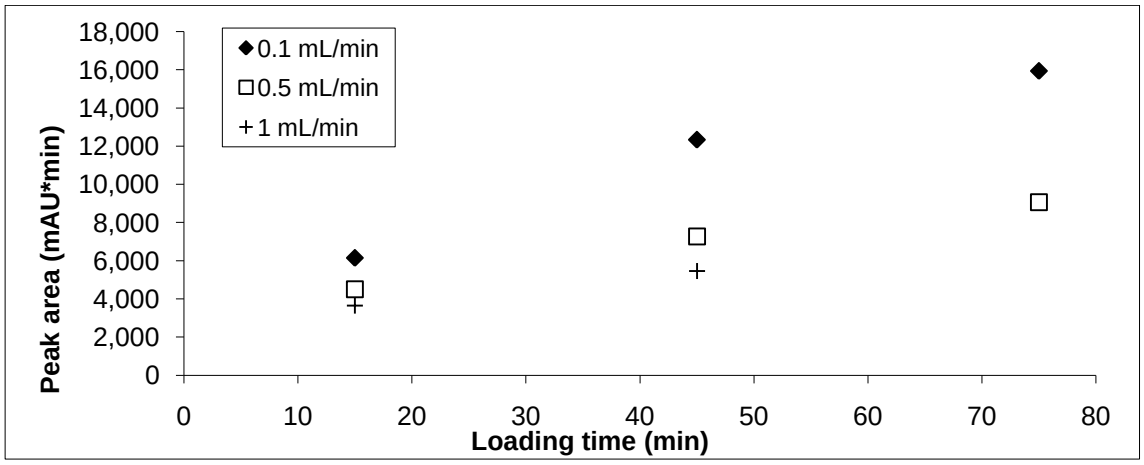

E.1.11 1.5 mg/mL BSA concentration, 2M NaCl concentration, 360 deg/hr rotation speed, 0.1-1.0 mL/min flow rate

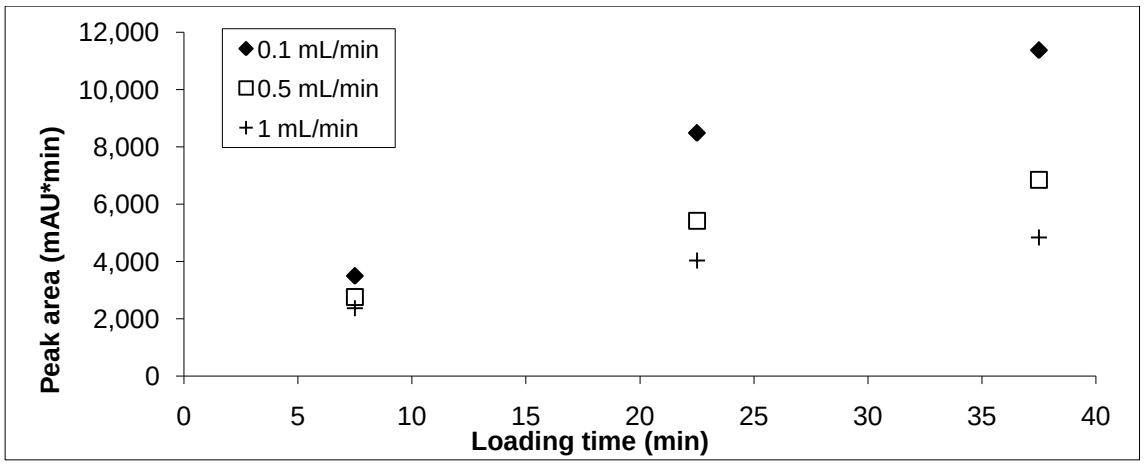

E.1.12 1.5 mg/mL BSA concentration, 2M NaCl concentration, 720 deg/hr rotation speed, 0.1-1.0 mL/min flow rate

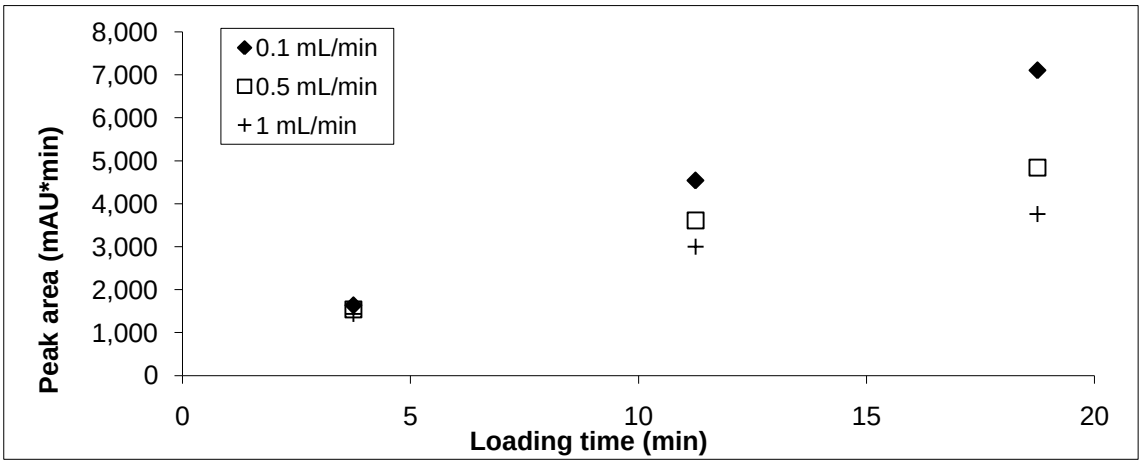

E.2 Elution sections

E.2.1 1.5 mg/mL BSA concentration, 1M NaCl concentration, 180 deg/hr rotation speed, 0.1-1.0 mL/min flow rate

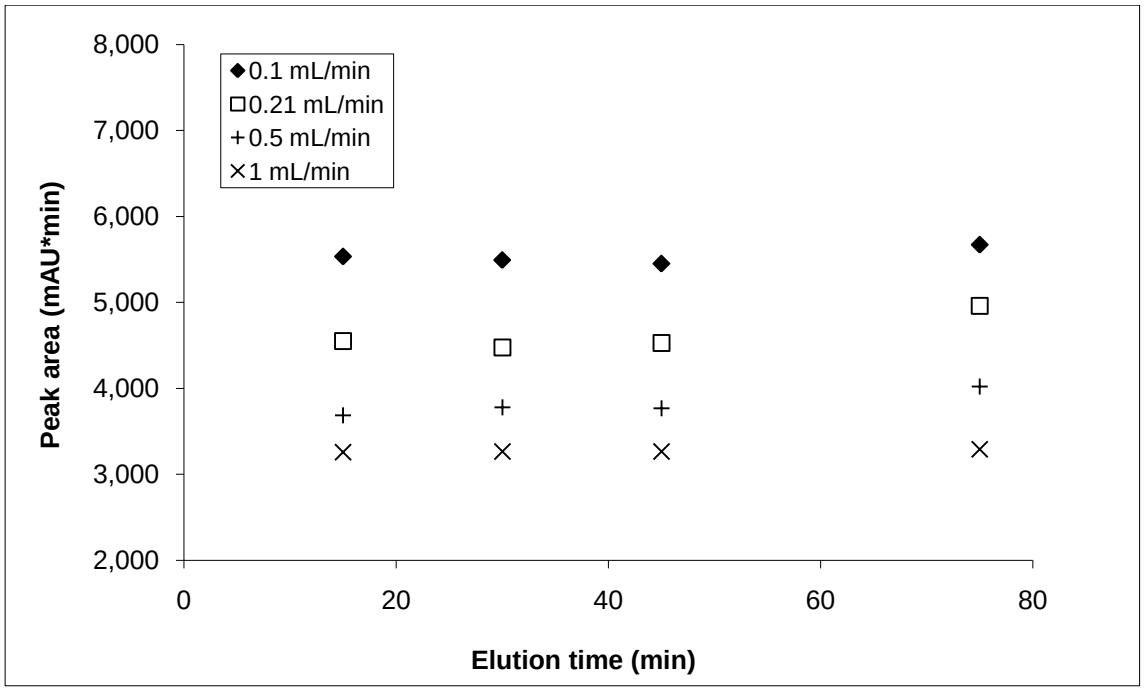

E.2.2 1.5 mg/mL BSA concentration, 1M NaCl concentration, 360 deg/hr rotation speed, 0.1-1.0 mL/min flow rate

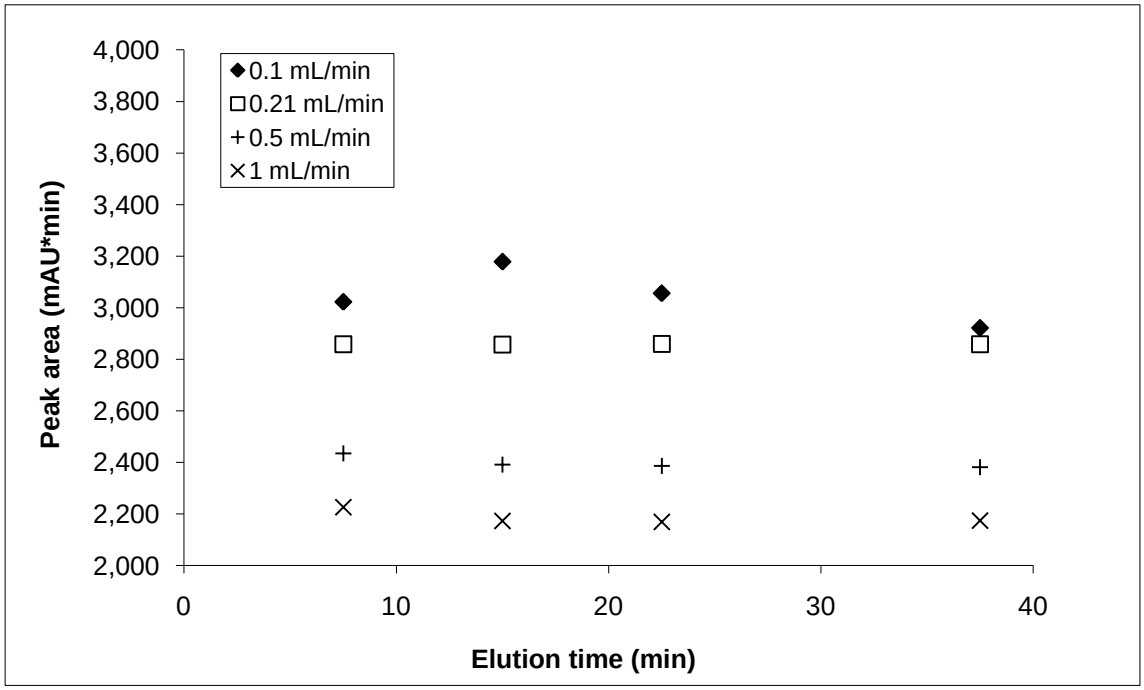

E.2.3 1.5 mg/mL BSA concentration, 1M NaCl concentration, 720 deg/hr rotation speed, 0.1-1.0 mL/min flow rate

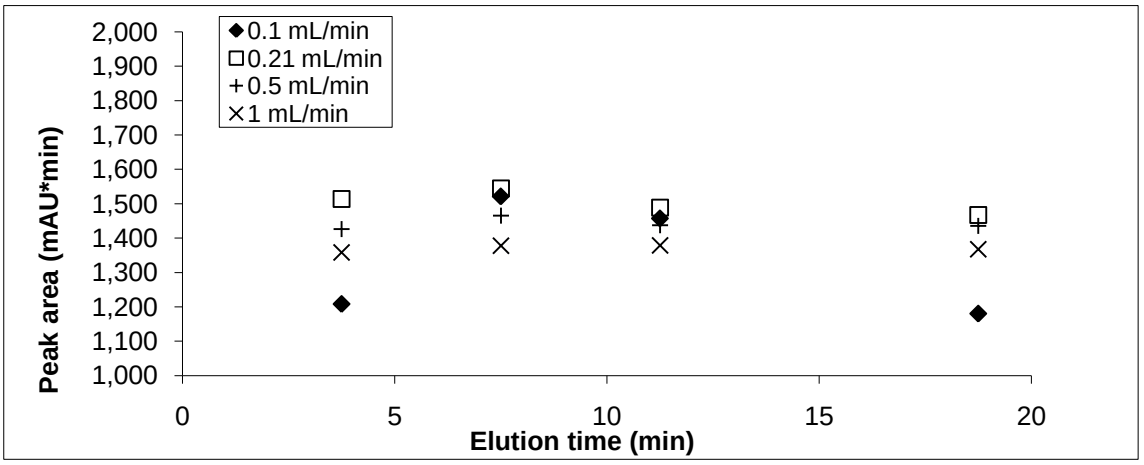

E.2.4 3 mg/mL BSA concentration, 1M NaCl concentration, 180 deg/hr rotation speed, 0.1-1.0 mL/min flow rate

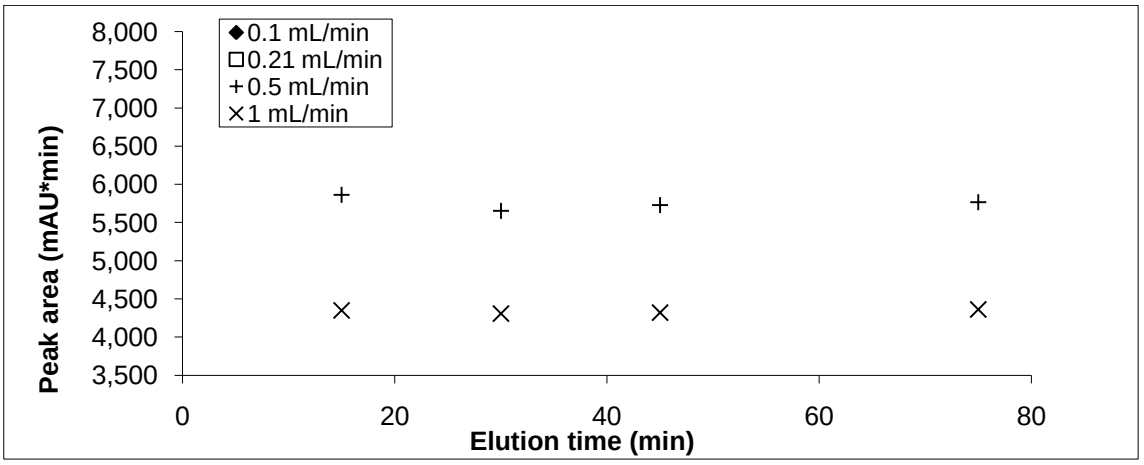

E.2.5 3 mg/mL BSA concentration, 1M NaCl concentration, 360 deg/hr rotation speed, 0.1-1.0 mL/min flow rate

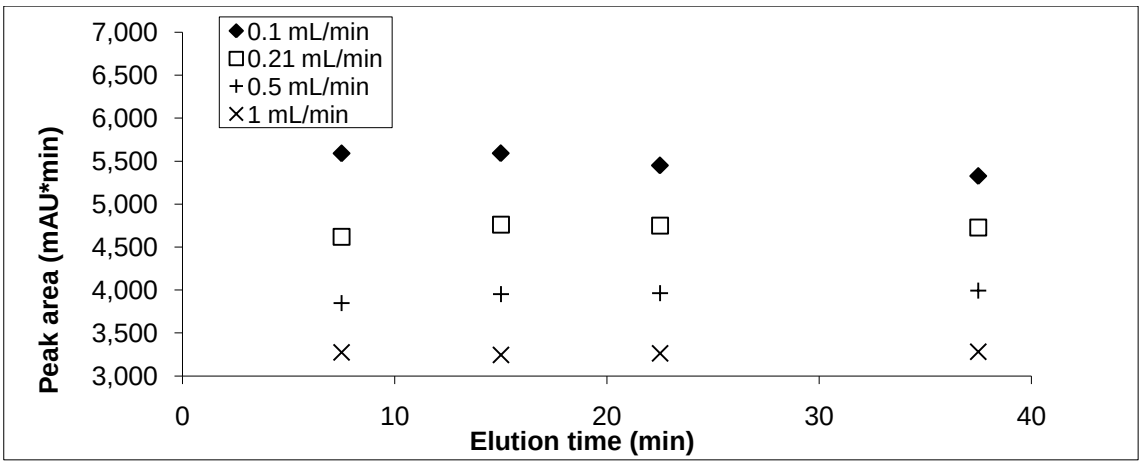

E.2.6 3 mg/mL BSA concentration, 1M NaCl concentration, 720 deg/hr rotation speed, 0.1-1.0 mL/min flow rate

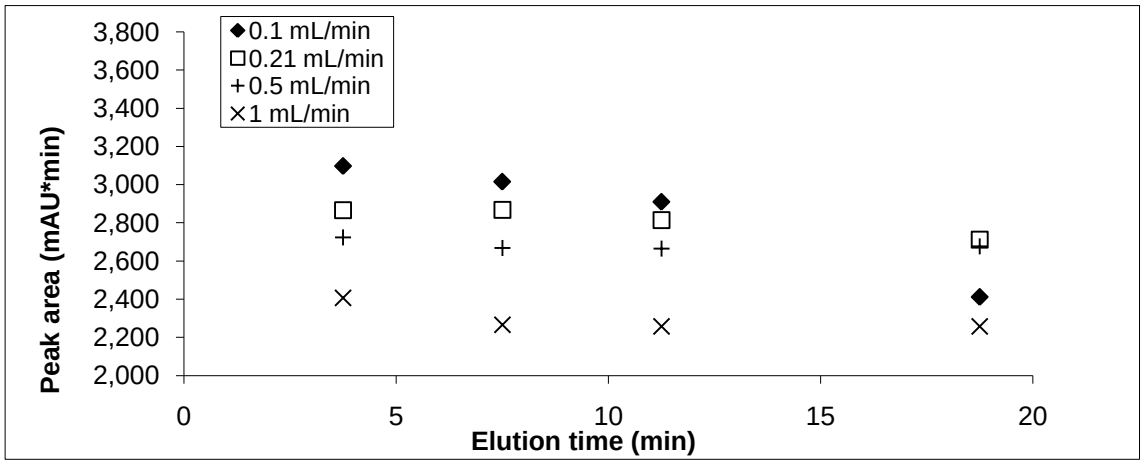

E.2.7 5 mg/mL BSA concentration, 1M NaCl concentration, 180 deg/hr rotation speed, 0.1-1.0 mL/min flow rate

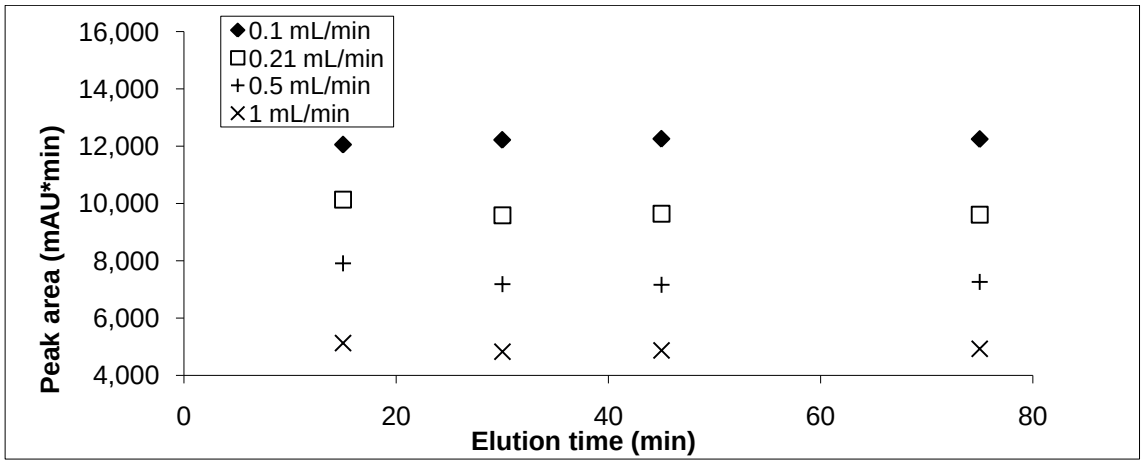

E.2.8 5 mg/mL BSA concentration, 1M NaCl concentration, 360 deg/hr rotation speed, 0.1-1.0 mL/min flow rate

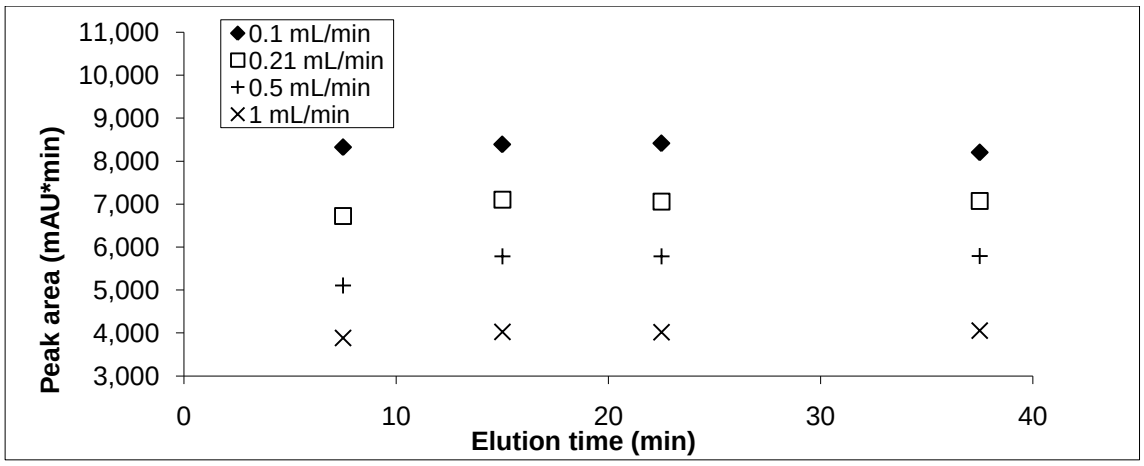

E.2.9 5 mg/mL BSA concentration, 1M NaCl concentration, 720 deg/hr rotation speed, 0.1-1.0 mL/min flow rate

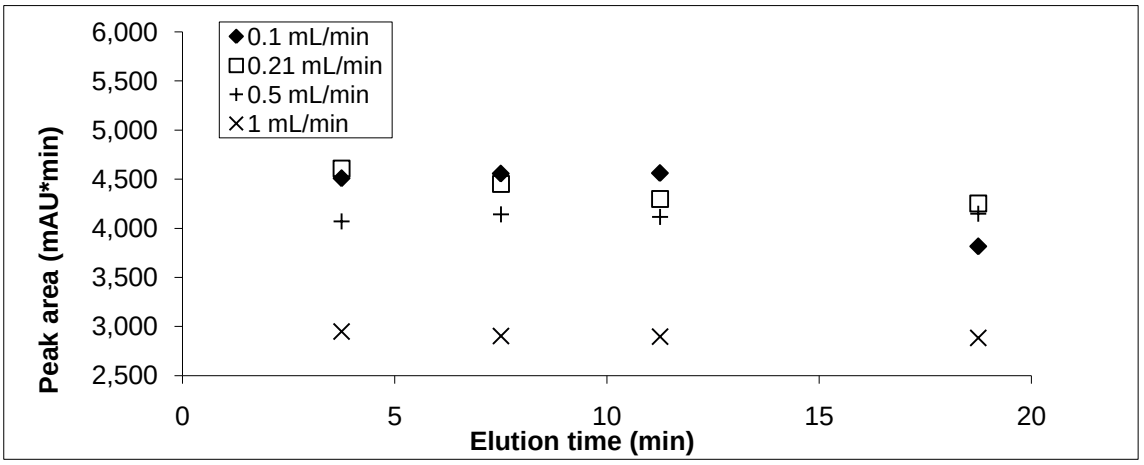

E.2.10 1.5 mg/mL BSA concentration, 2M NaCl concentration, 180 deg/hr rotation speed, 0.1-1.0 mL/min flow rate

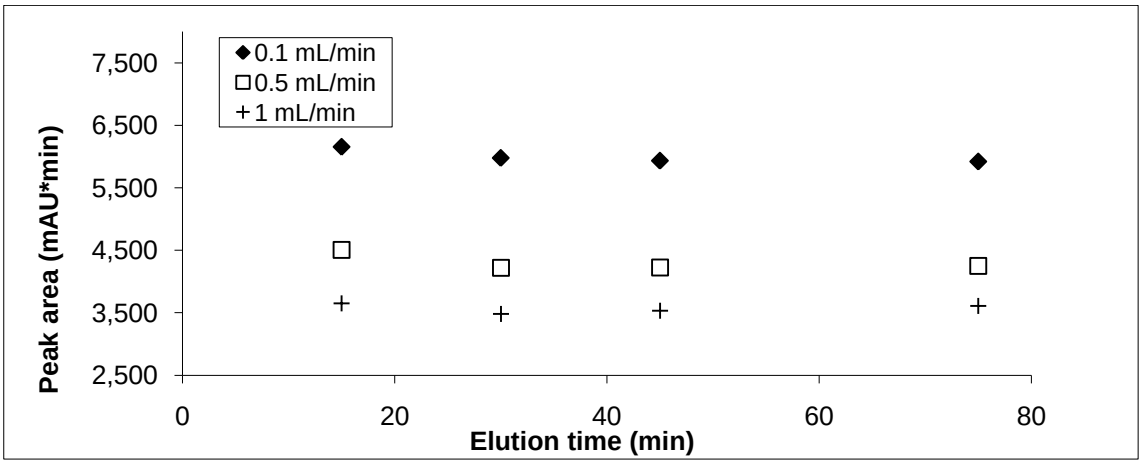

E.2.11 1.5 mg/mL BSA concentration, 2M NaCl concentration, 360 deg/hr rotation speed, 0.1-1.0 mL/min flow rate

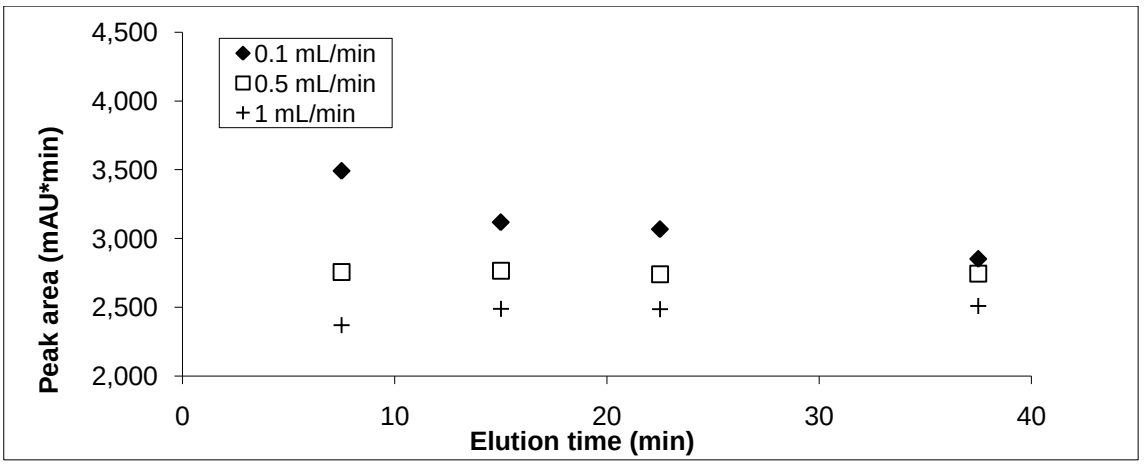

E.2.12 1.5 mg/mL BSA concentration, 2M NaCl concentration, 720 deg/hr rotation speed, 0.1-1.0 mL/min flow rate

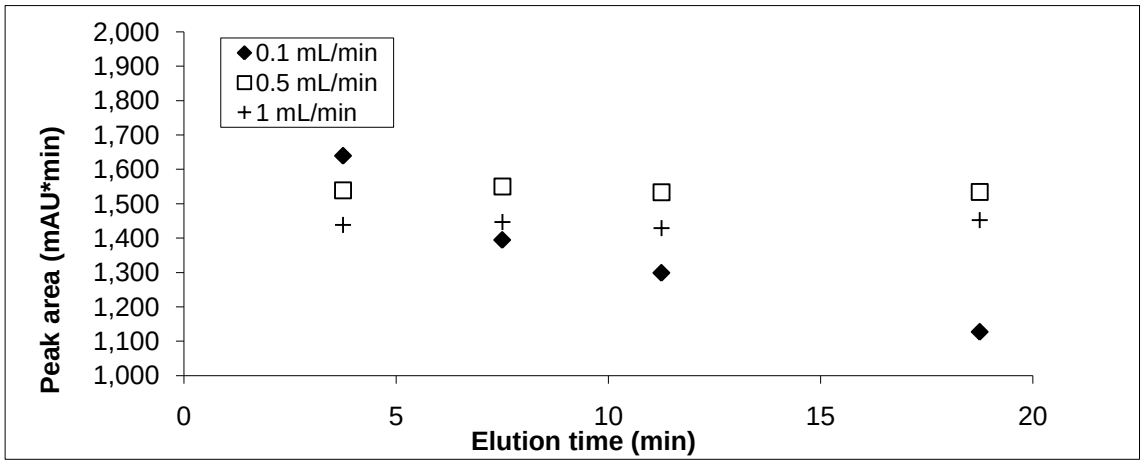

E.3 Rotation speed

E.3.1 1.5 mg/mL BSA concentration, 1M NaCl concentration, Trial 1, 0.1-1.0 mL/min flow rate

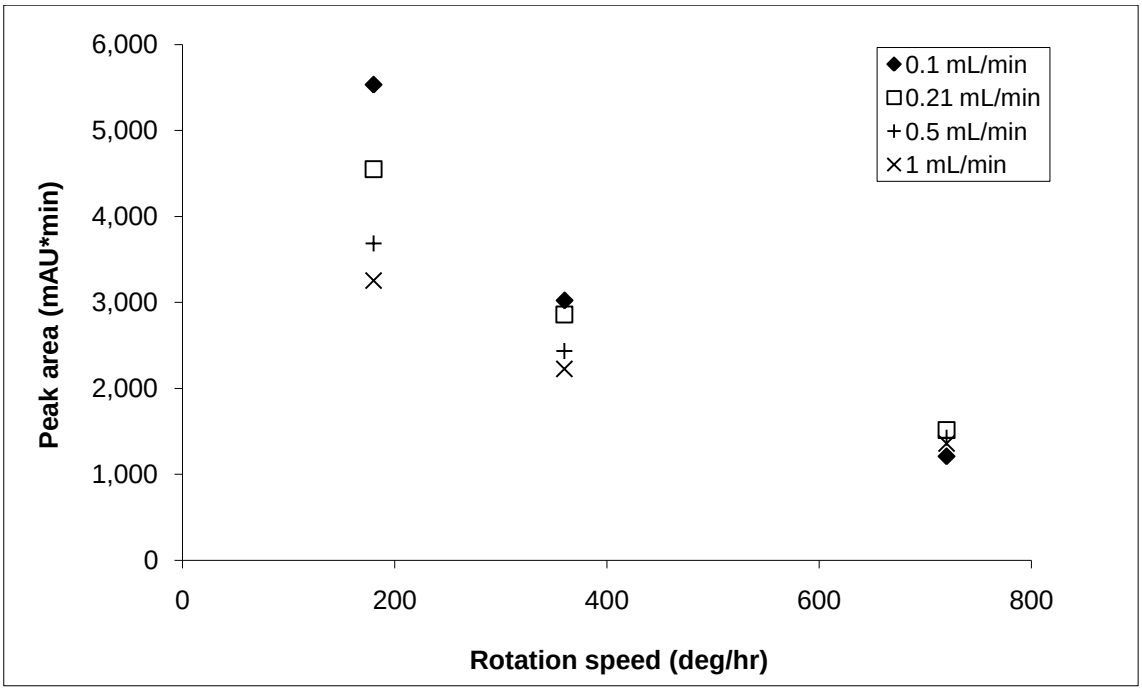

E.3.2 1.5 mg/mL BSA concentration, 1M NaCl concentration, Trial 2, 0.1-1.0 mL/min flow rate

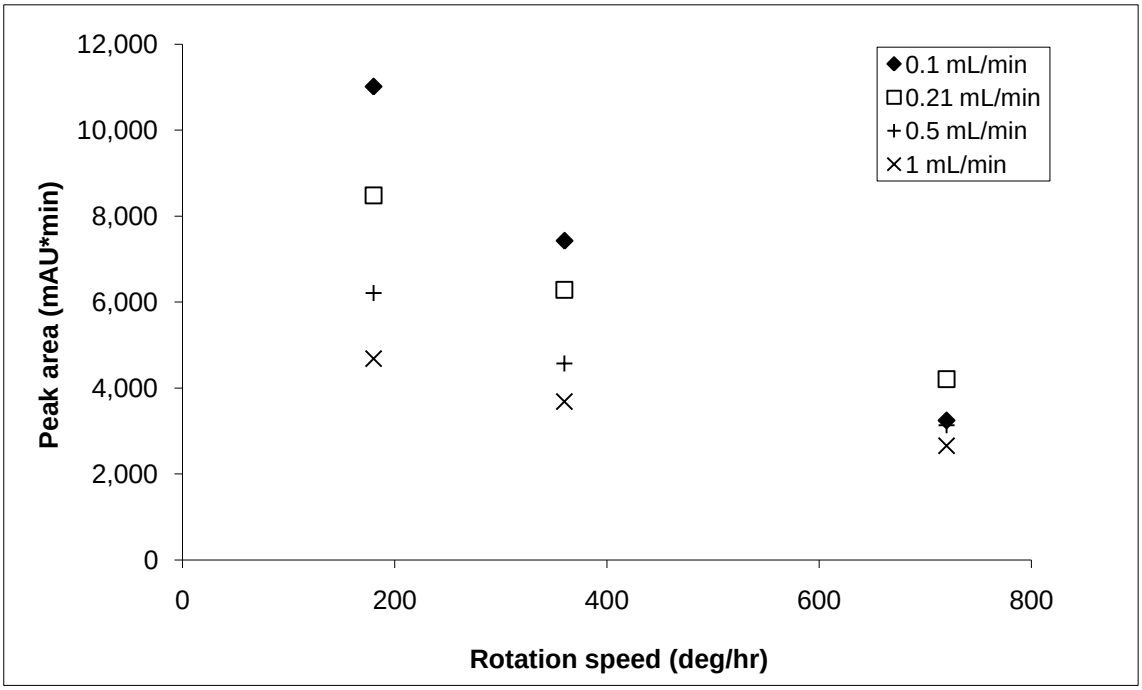

E.3.3 1.5 mg/mL BSA concentration, 1M NaCl concentration, Trial 3, 0.1-1.0 mL/min flow rate

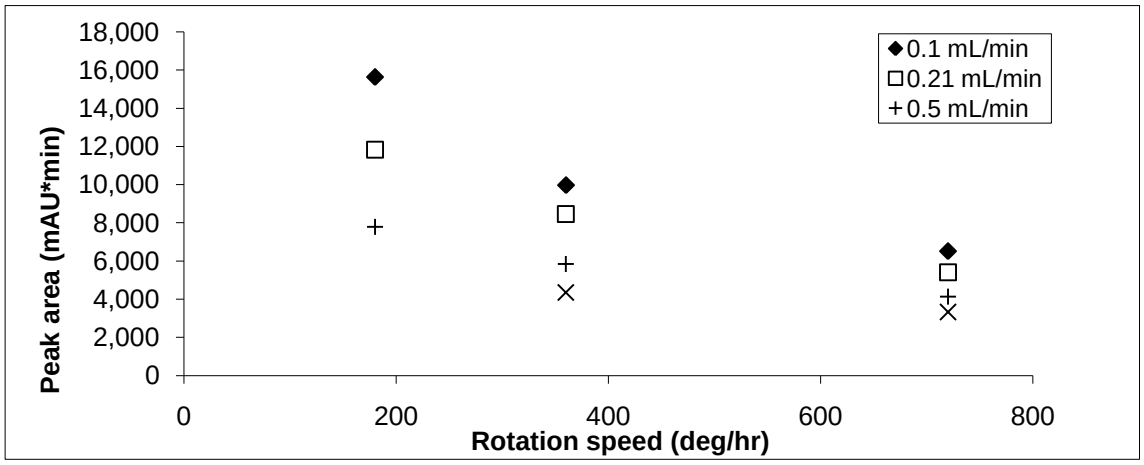

E.3.4 1.5 mg/mL BSA concentration, 1M NaCl concentration, Trial 4, 0.1-1.0 mL/min flow rate

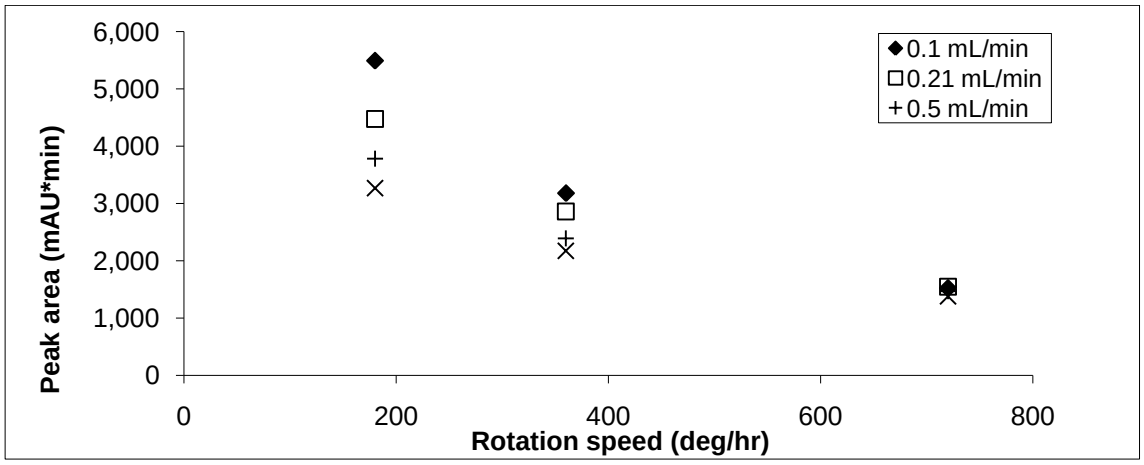

E.3.5 1.5 mg/mL BSA concentration, 1M NaCl concentration, Trial 5, 0.1-1.0 mL/min flow rate

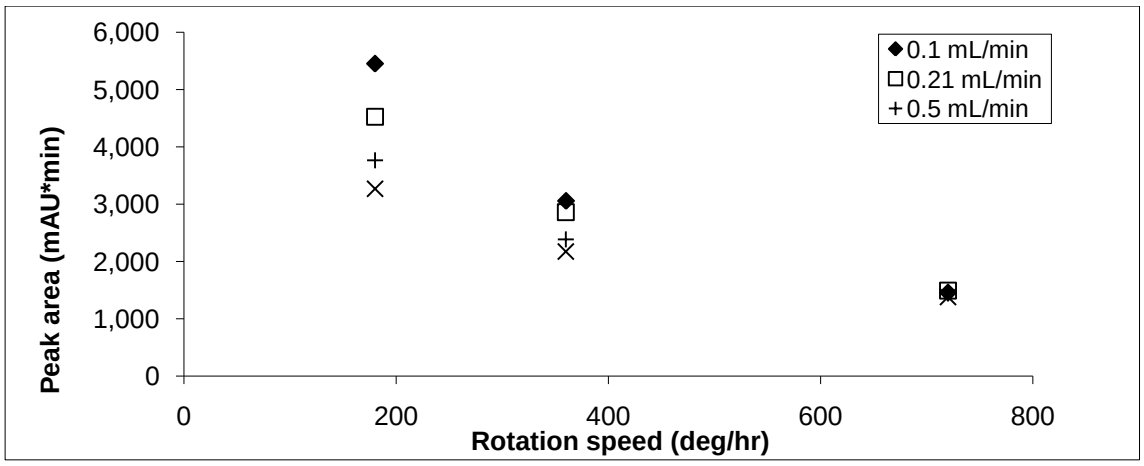

E.3.6 1.5 mg/mL BSA concentration, 1M NaCl concentration, Trial 6, 0.1-1.0 mL/min flow rate

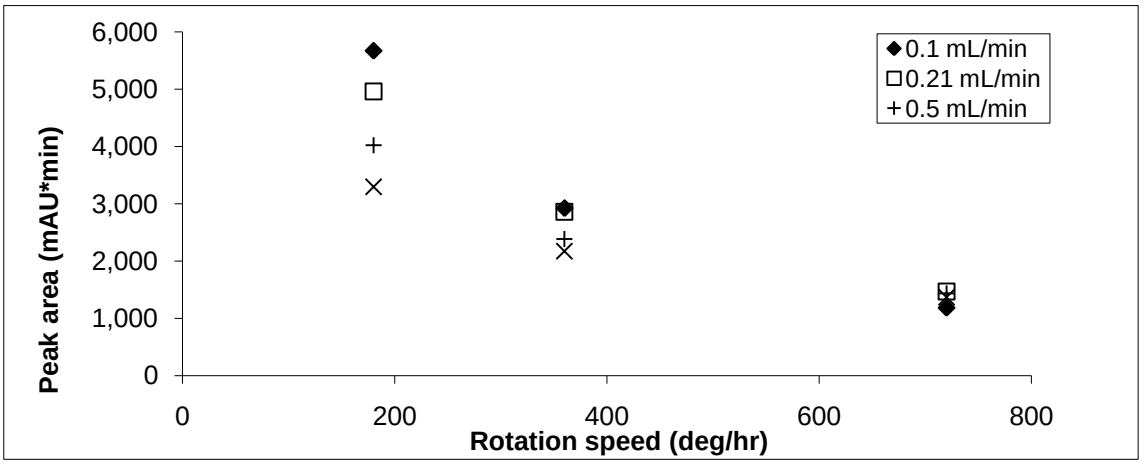

E.3.7 1.5 mg/mL BSA concentration, 1M NaCl concentration, Trial 7, 0.1-1.0 mL/min flow rate

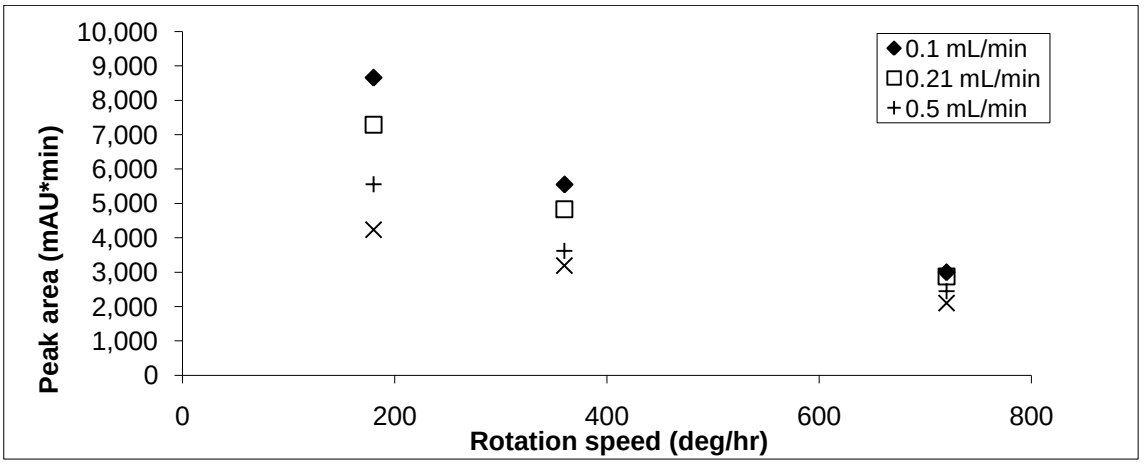

E.3.8 1.5 mg/mL BSA concentration, 1M NaCl concentration, Trial 8, 0.1-1.0 mL/min flow rate

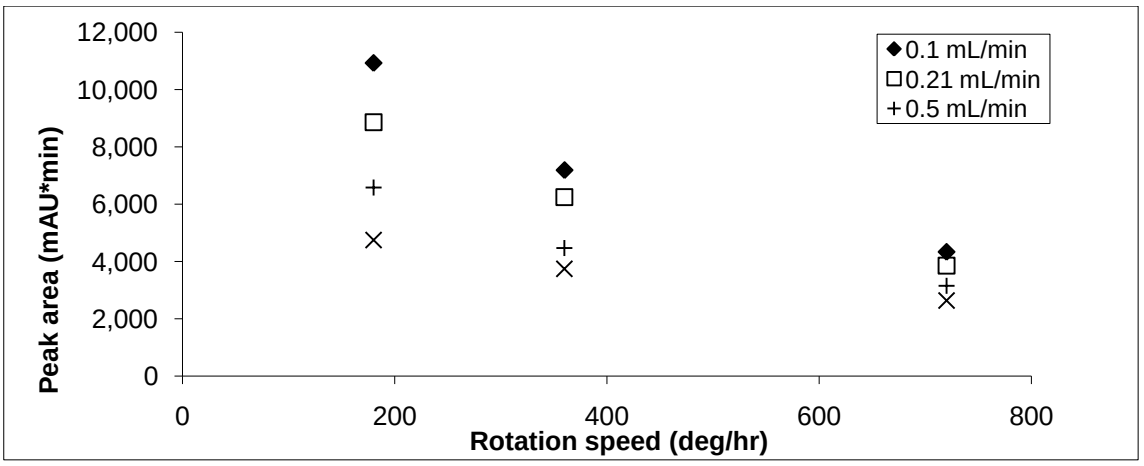

E.3.9 1.5 mg/mL BSA concentration, 1M NaCl concentration, Trial 9, 0.1-1.0 mL/min flow rate

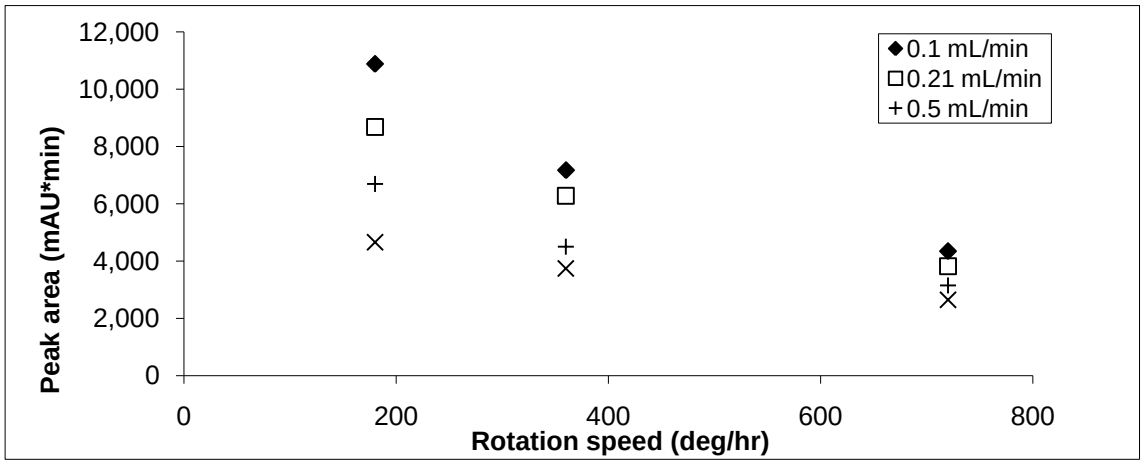

E.3.10 3 mg/mL BSA concentration, 1M NaCl concentration, Trial 1, 0.1-1.0 mL/min flow rate

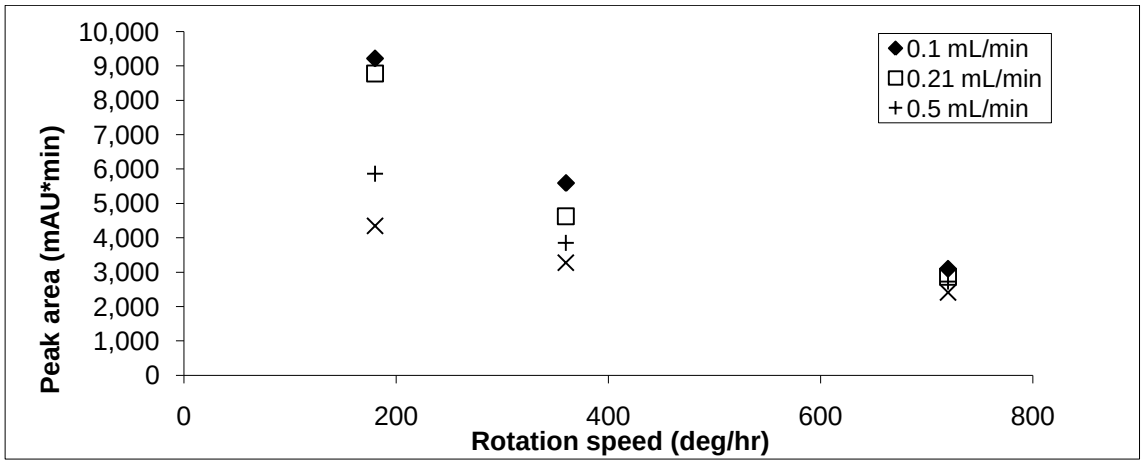

E.3.11 3 mg/mL BSA concentration, 1M NaCl concentration, Trial 2, 0.1-1.0 mL/min flow rate

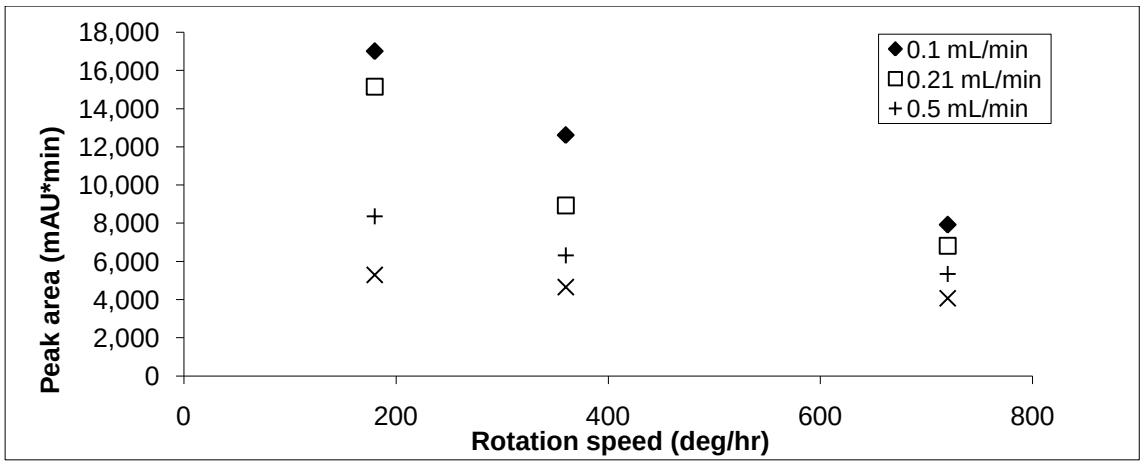

E.3.12 3 mg/mL BSA concentration, 1M NaCl concentration, Trial 3, 0.1-1.0 mL/min flow rate

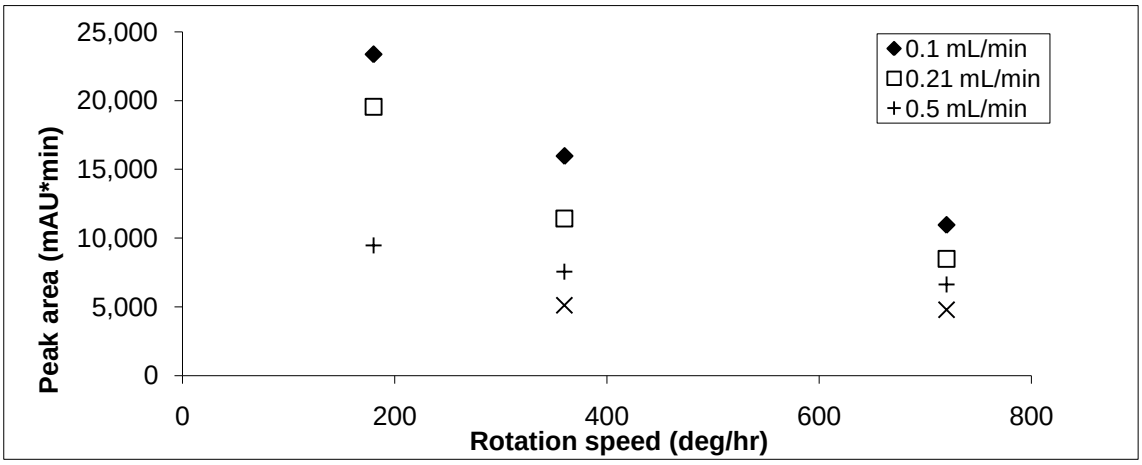

E.3.13 3 mg/mL BSA concentration, 1M NaCl concentration, Trial 4, 0.1-1.0 mL/min flow rate

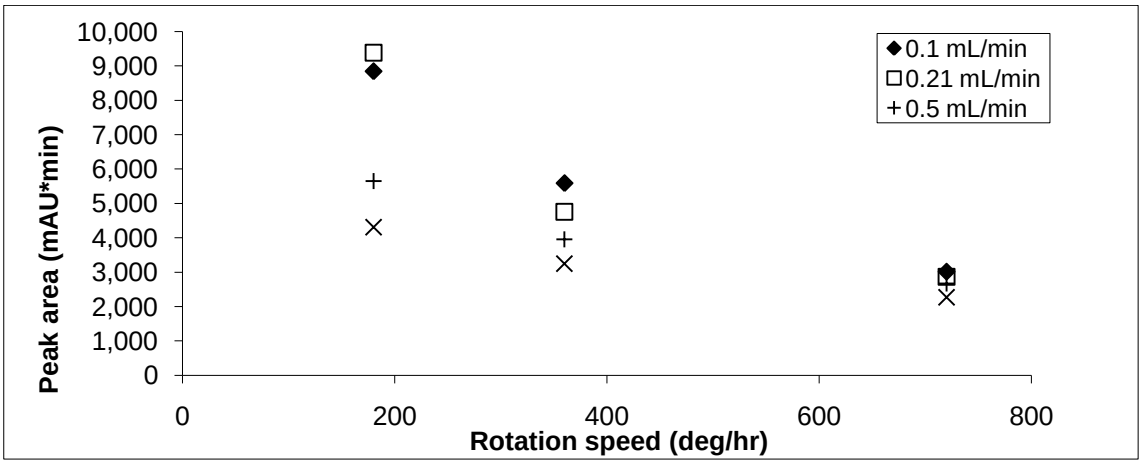

E.3.14 3 mg/mL BSA concentration, 1M NaCl concentration, Trial 5, 0.1-1.0 mL/min flow rate

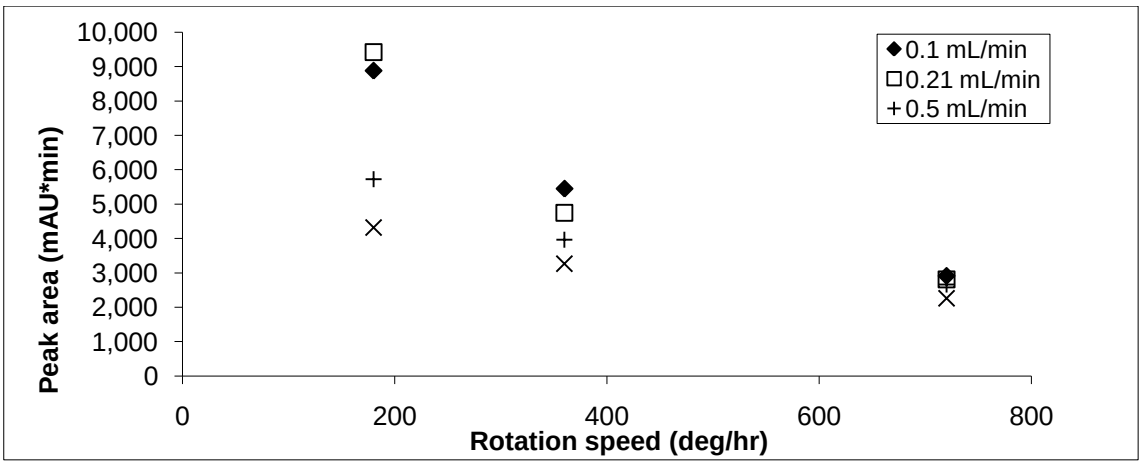

E.3.15 3 mg/mL BSA concentration, 1M NaCl concentration, Trial 6, 0.1-1.0 mL/min flow rate

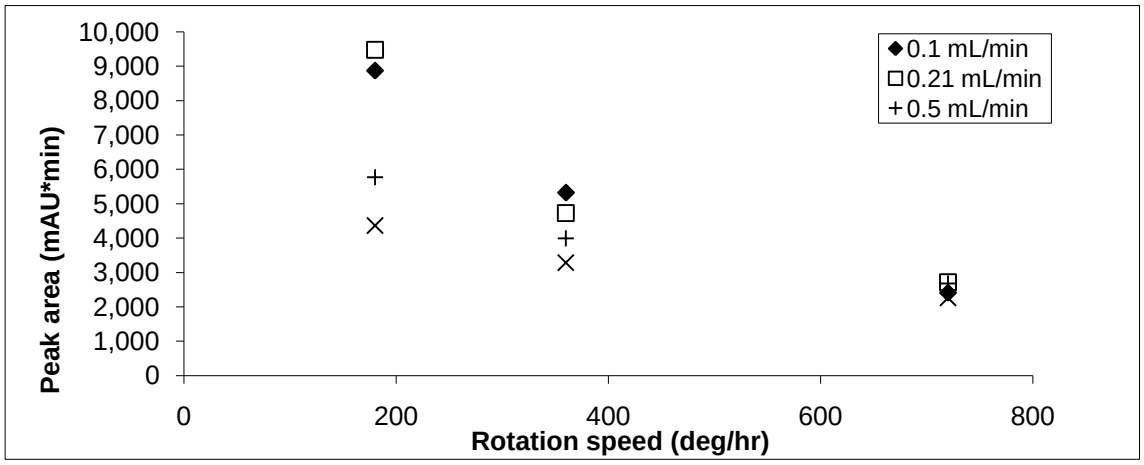

E.3.16 3 mg/mL BSA concentration, 1M NaCl concentration, Trial 7, 0.1-1.0 mL/min flow rate

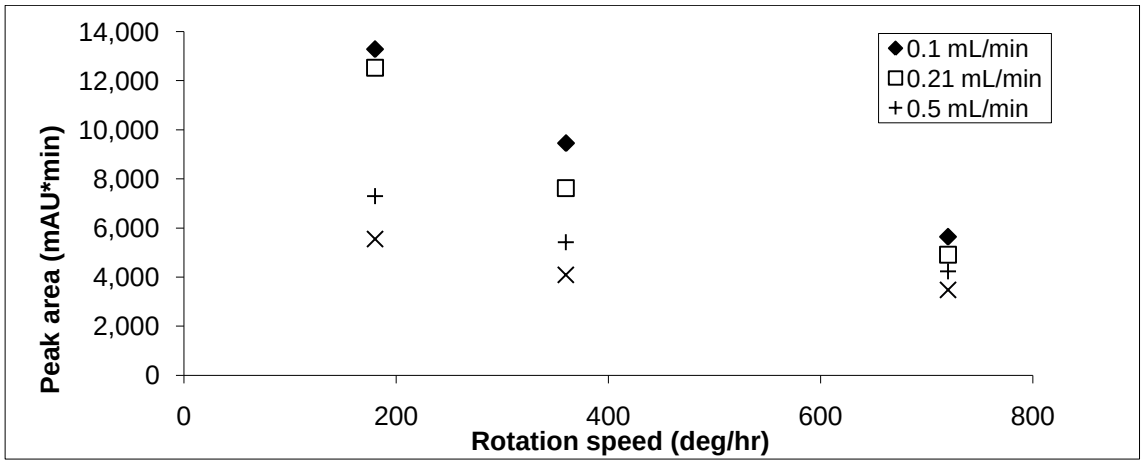

E.3.17 3 mg/mL BSA concentration, 1M NaCl concentration, Trial 8, 0.1-1.0 mL/min flow rate

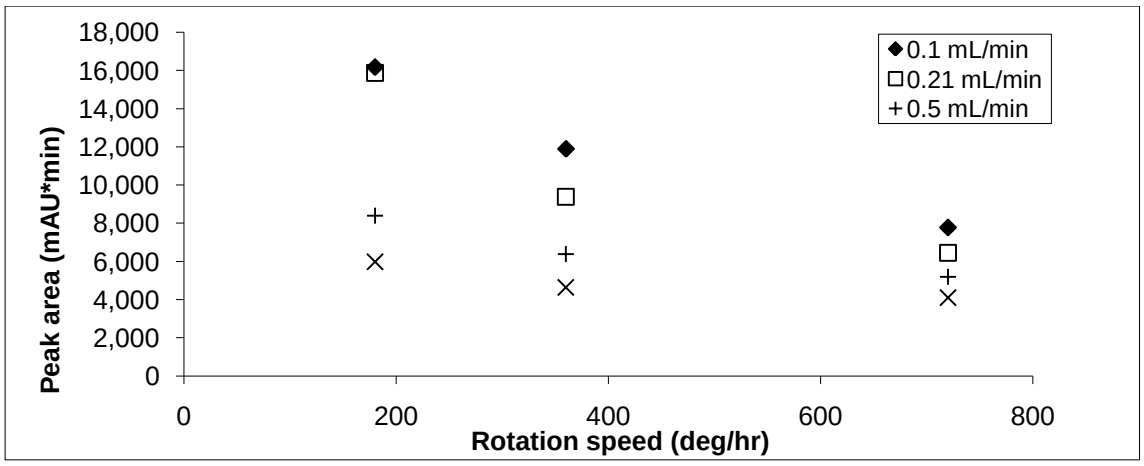

E.3.18 3 mg/mL BSA concentration, 1M NaCl concentration, Trial 9, 0.1-1.0 mL/min flow rate

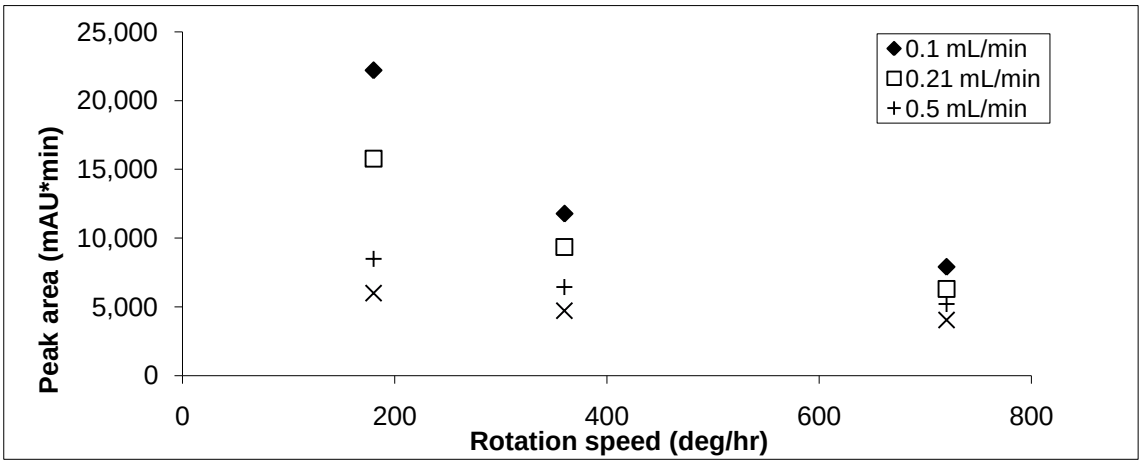

E.3.19 5 mg/mL BSA concentration, 1M NaCl concentration, Trial 1, 0.1-1.0 mL/min flow rate

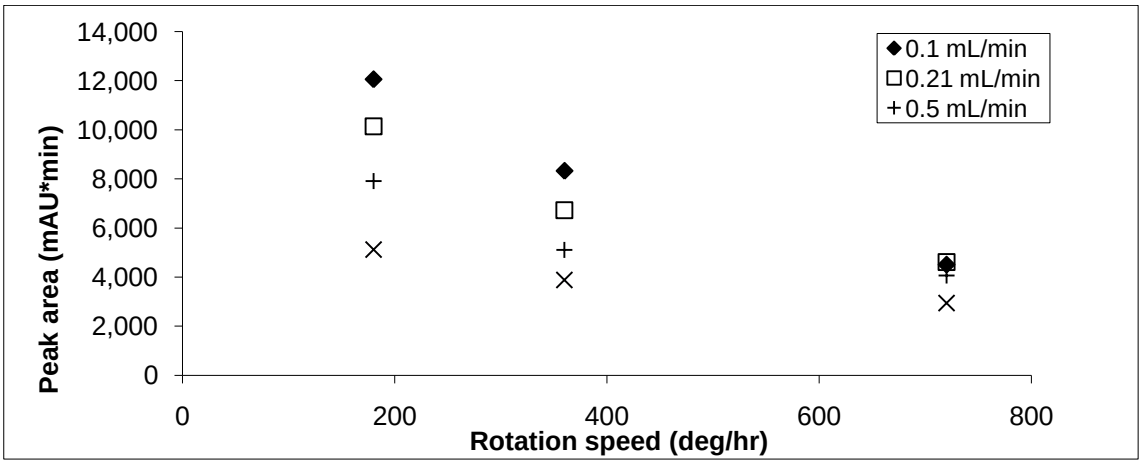

E.3.20 5 mg/mL BSA concentration, 1M NaCl concentration, Trial 2, 0.1-1.0 mL/min flow rate

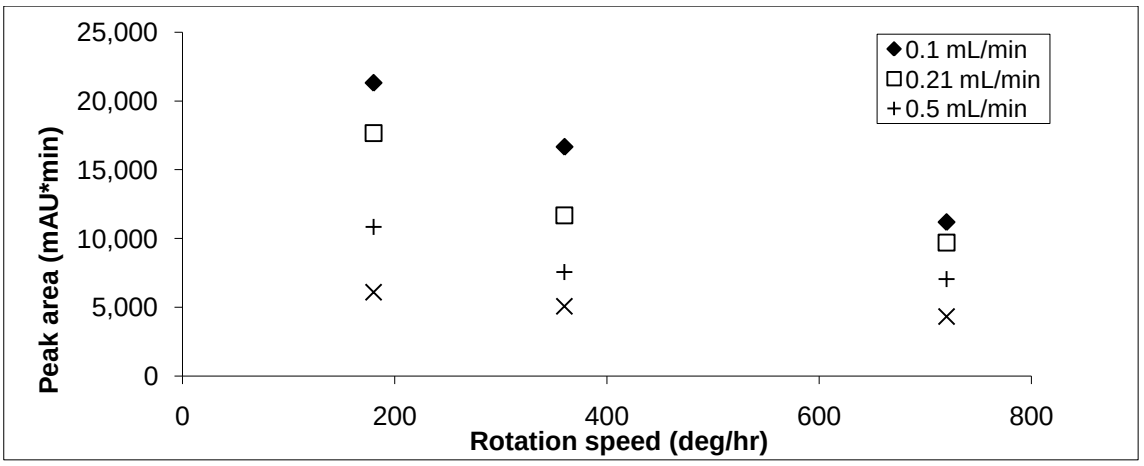

E.3.21 5 mg/mL BSA concentration, 1M NaCl concentration, Trial 3, 0.1-1.0 mL/min flow rate

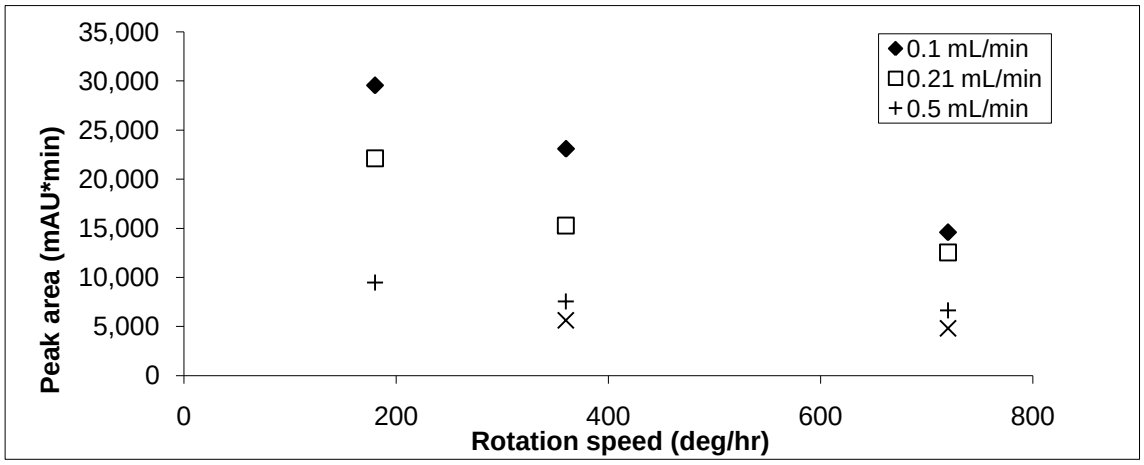

E.3.22 5 mg/mL BSA concentration, 1M NaCl concentration, Trial 4, 0.1-1.0 mL/min flow rate

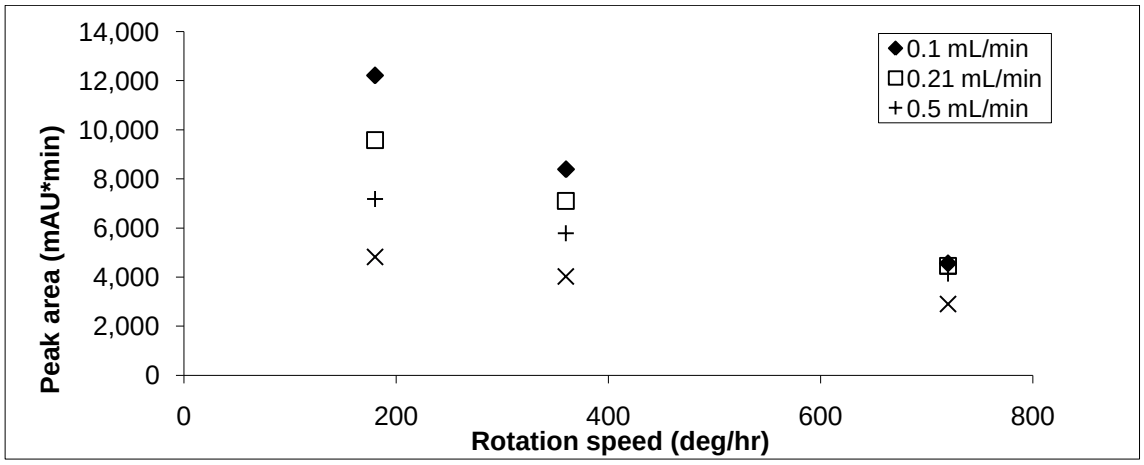

E.3.23 5 mg/mL BSA concentration, 1M NaCl concentration, Trial 5, 0.1-1.0 mL/min flow rate

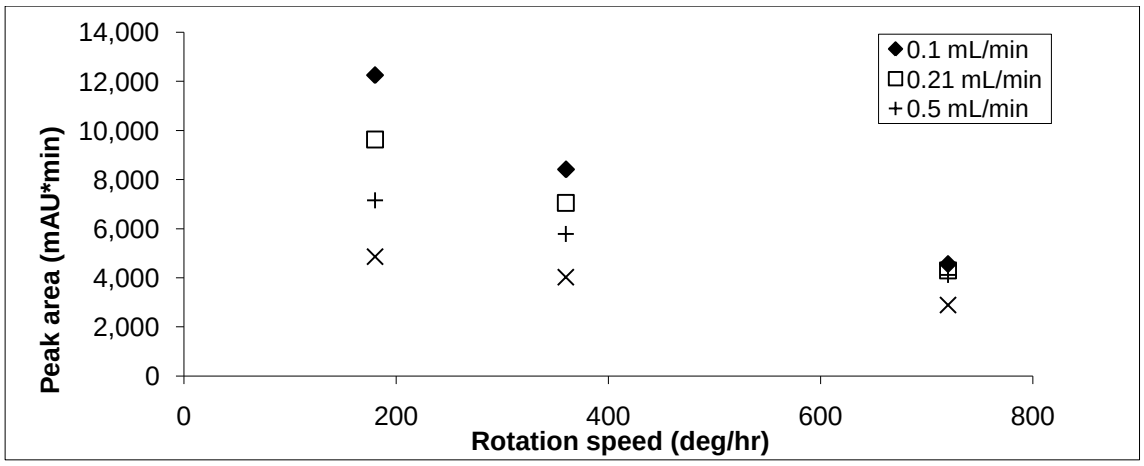

E.3.24 5 mg/mL BSA concentration, 1M NaCl concentration, Trial 6 0.1-1.0 mL/min flow rate

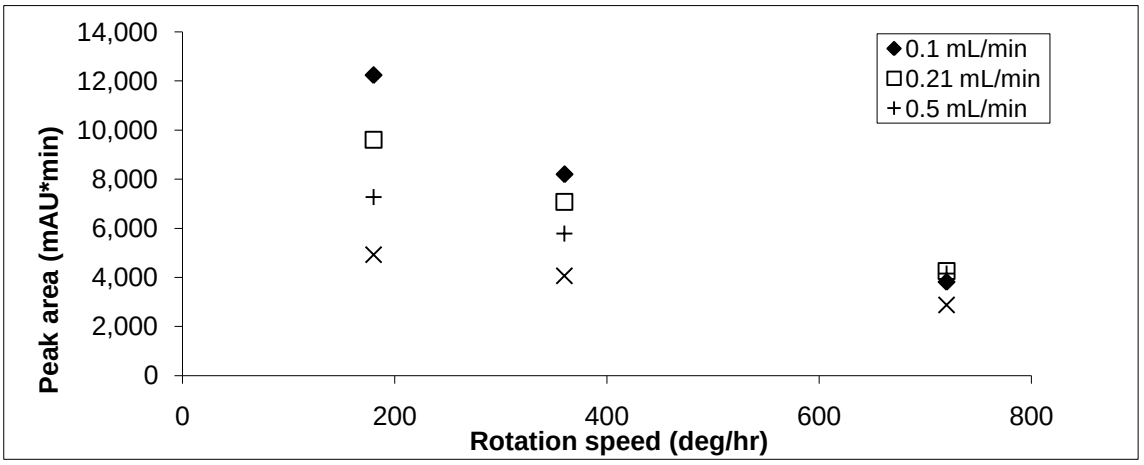

E.3.25 5 mg/mL BSA concentration, 1M NaCl concentration, Trial 7, 0.1-1.0 mL/min flow rate

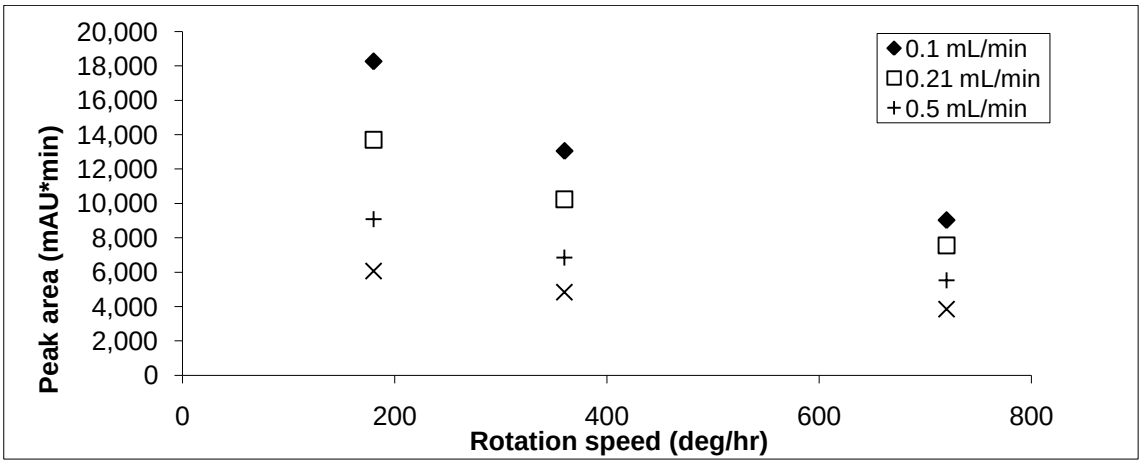

E.3.26 5 mg/mL BSA concentration, 1M NaCl concentration, Trial 8, 0.1-1.0 mL/min flow rate

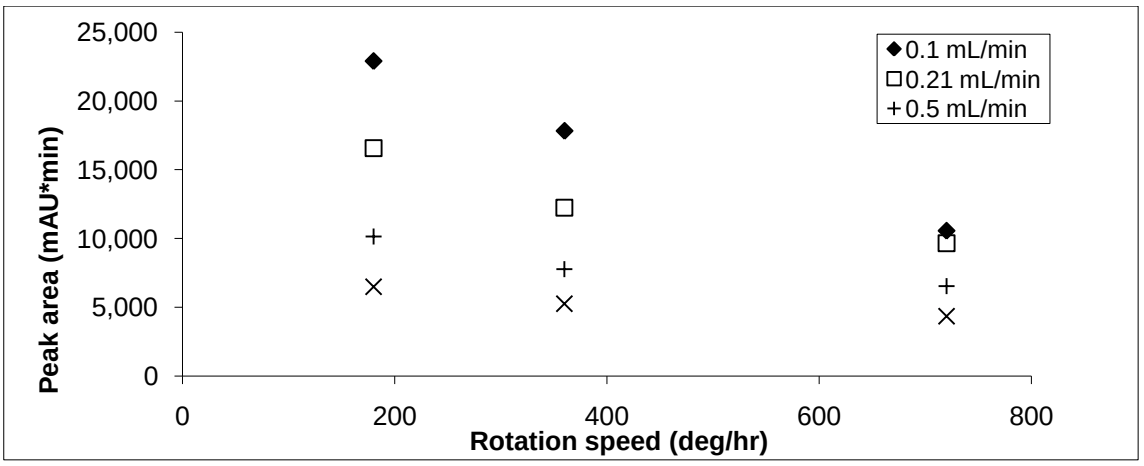

E.3.27 5 mg/mL BSA concentration, 1M NaCl concentration, Trial 9, 0.1-1.0 mL/min flow rate

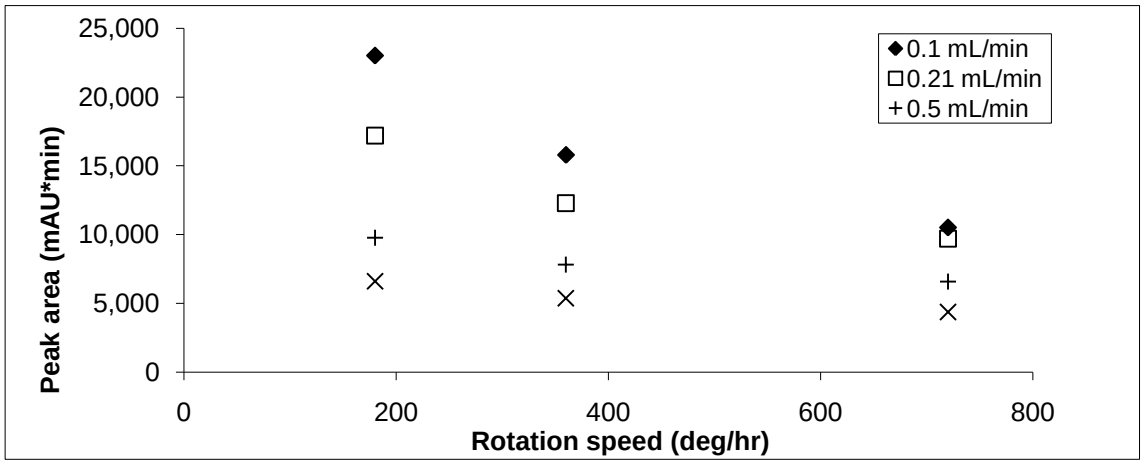

E.3.28 1.5 mg/mL BSA concentration, 2M NaCl concentration, Trial 1, 0.1-1.0 mL/min flow rate

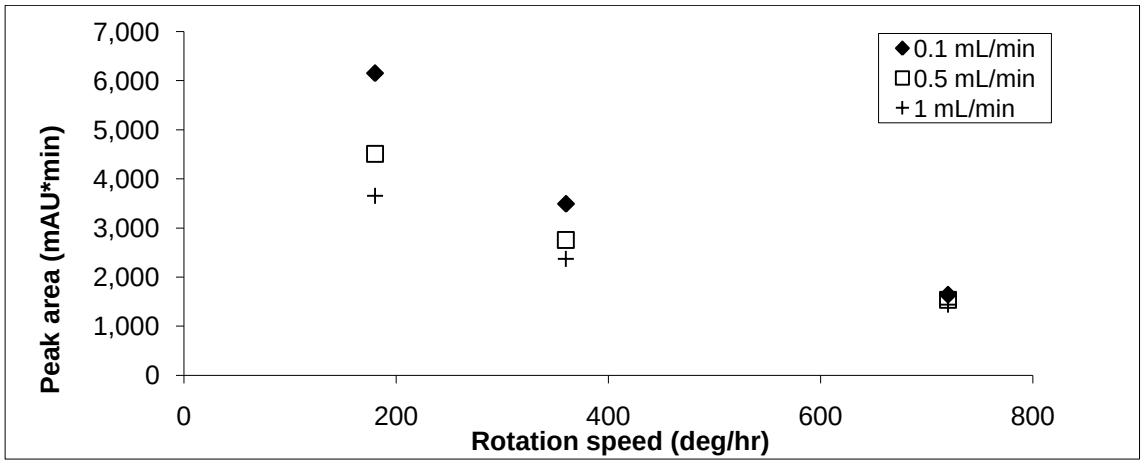

E.3.29 1.5 mg/mL BSA concentration, 2M NaCl concentration, Trial 2, 0.1-1.0 mL/min flow rate

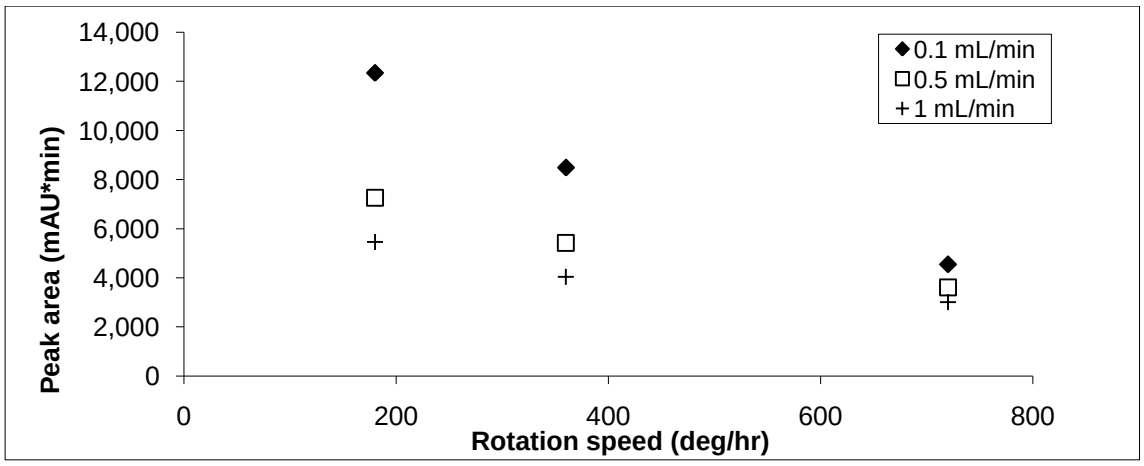

E.3.30 1.5 mg/mL BSA concentration, 2M NaCl concentration, Trial 3, 0.1-1.0 mL/min flow rate

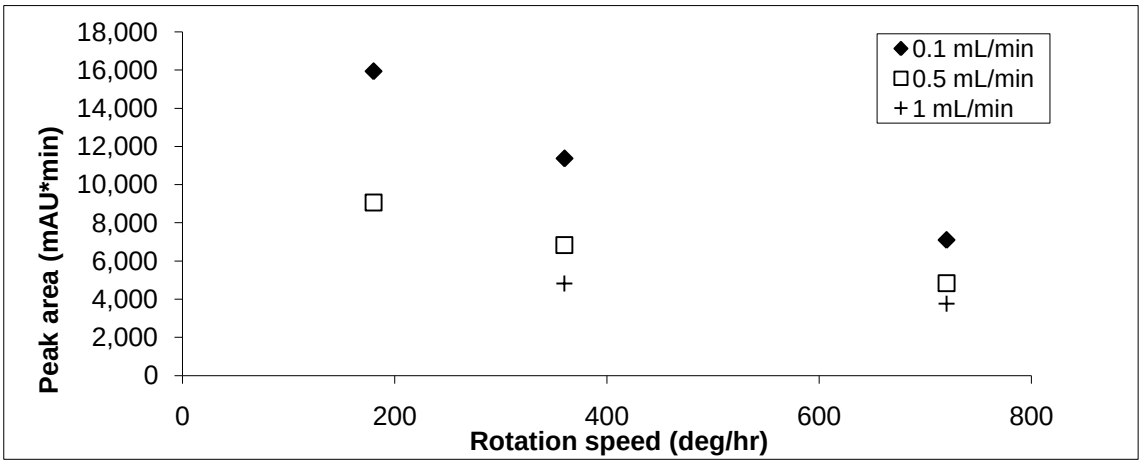

E.3.31 1.5 mg/mL BSA concentration, 2M NaCl concentration, Trial 4, 0.1-1.0 mL/min flow rate

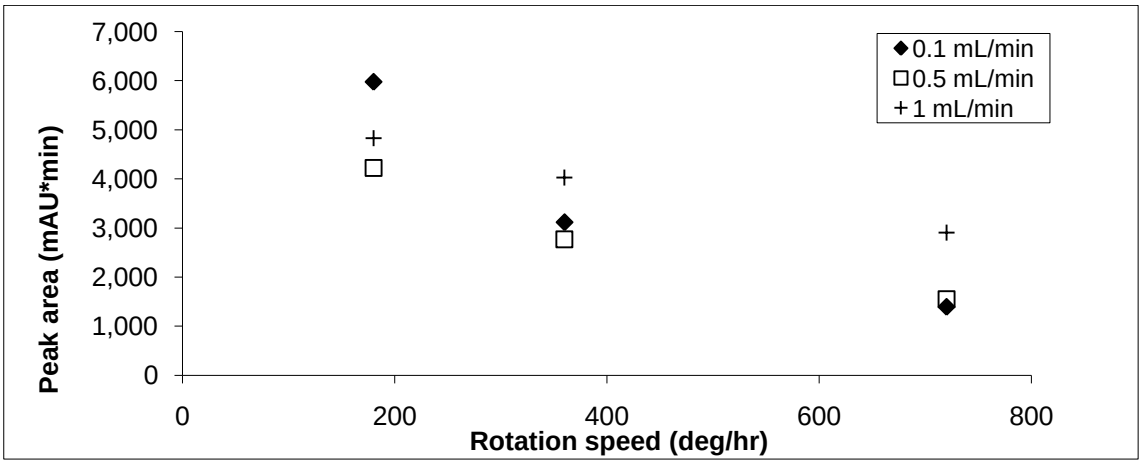

E.3.32 1.5 mg/mL BSA concentration, 2M NaCl concentration, Trial 5, 0.1-1.0 mL/min flow rate

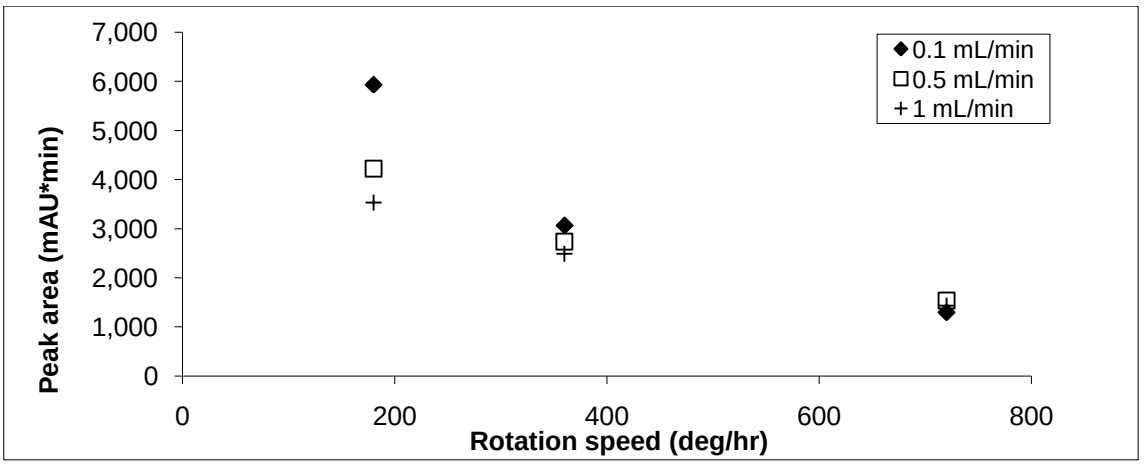

E.3.33 1.5 mg/mL BSA concentration, 2M NaCl concentration, Trial 6, 0.1-1.0 mL/min flow rate

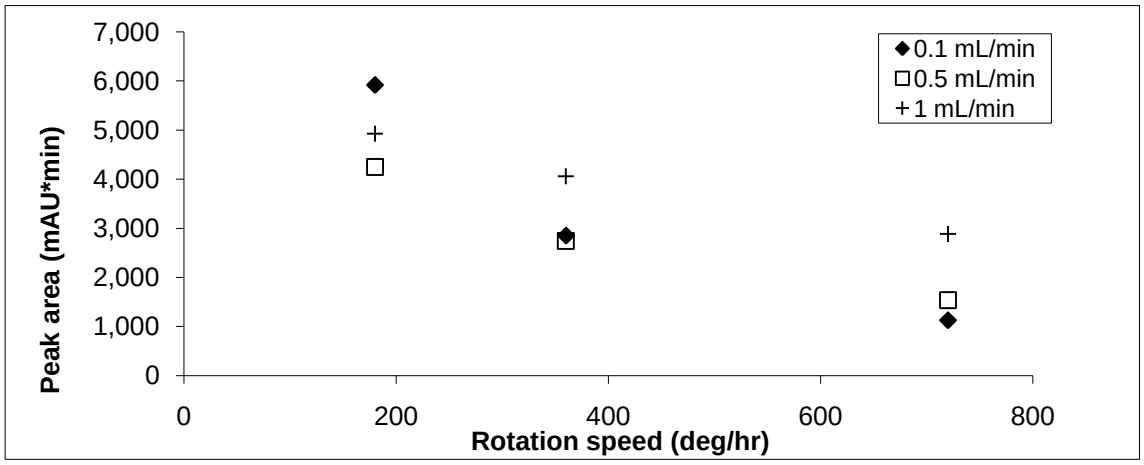

E.3.34 1.5 mg/mL BSA concentration, 2M NaCl concentration, Trial 7, 0.1-1.0 mL/min flow rate

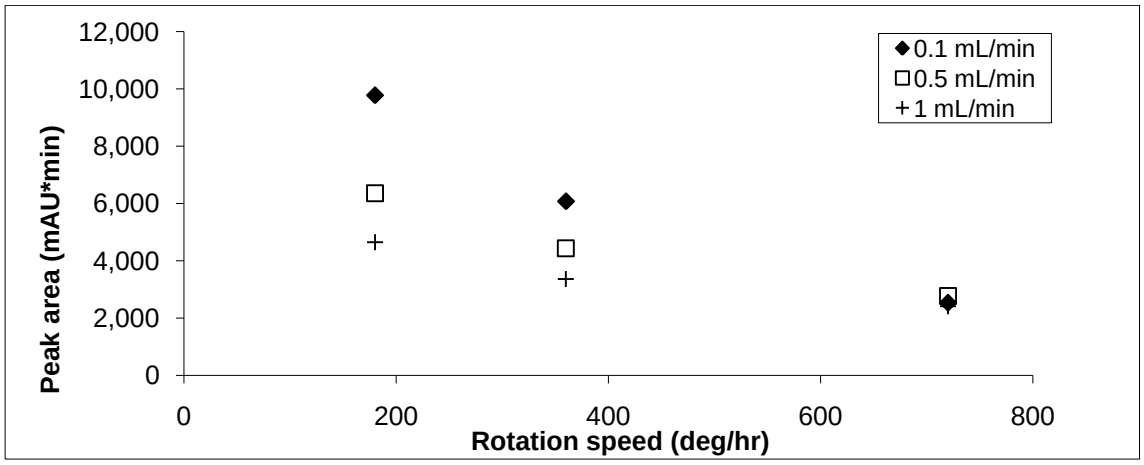

E.3.35 1.5 mg/mL BSA concentration, 2M NaCl concentration, Trial 8, 0.1-1.0 mL/min flow rate

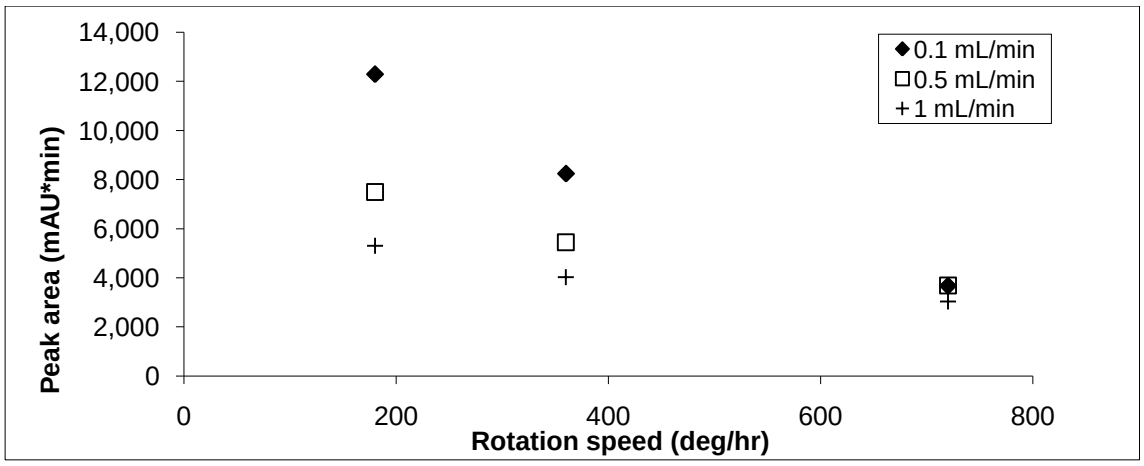

E.3.36 1.5 mg/mL BSA concentration, 2M NaCl concentration, Trial 9, 0.1-1.0 mL/min flow rate

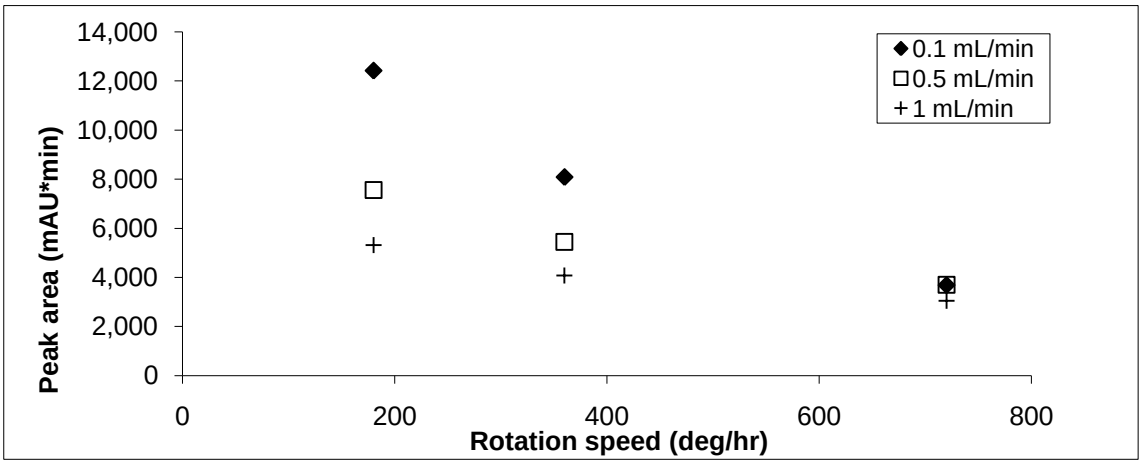

E.4 Flow rate

E.4.1 1.5 mg/mL BSA concentration, 1M NaCl concentration, Trial 1, 180-720 deg/hr rotation speed

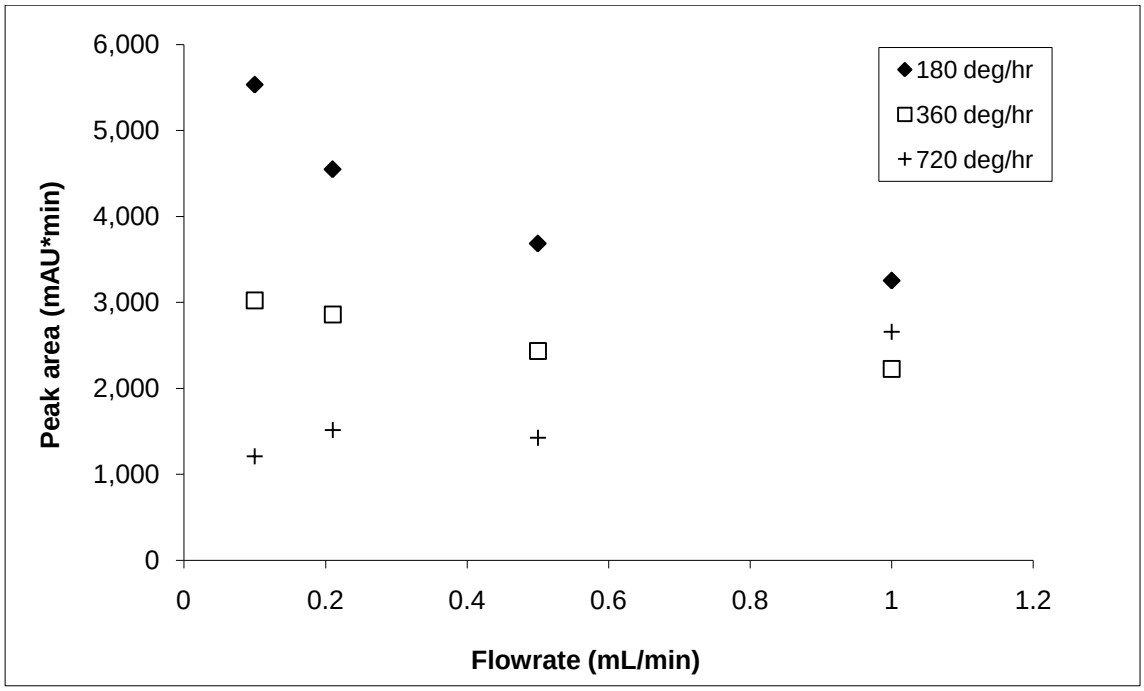

E.4.2 1.5 mg/mL BSA concentration, 1M NaCl concentration, Trial 2, 180-720 deg/hr rotation speed

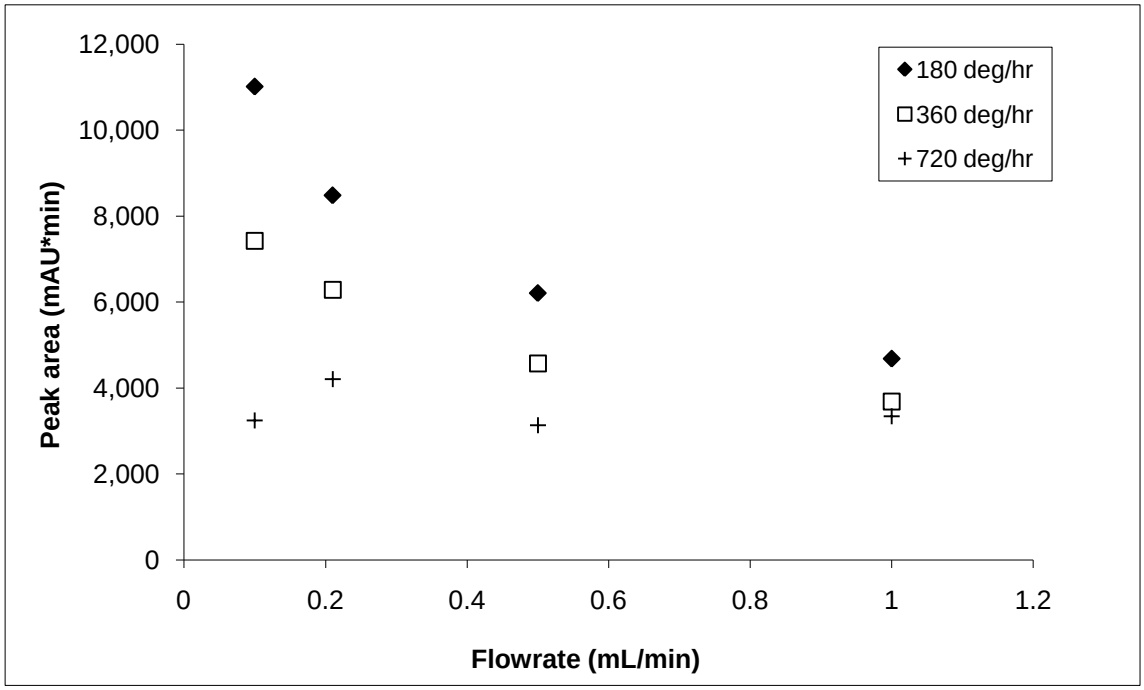

E.4.3 1.5 mg/mL BSA concentration, 1M NaCl concentration, Trial 3, 180-720 deg/hr rotation speed

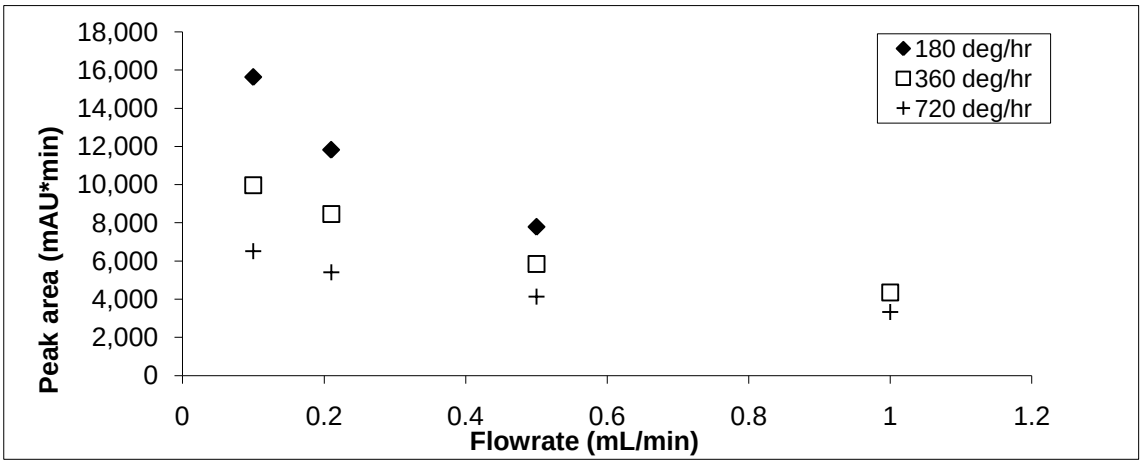

E.4.4 1.5 mg/mL BSA concentration, 1M NaCl concentration, Trial 4, 180-720 deg/hr rotation speed

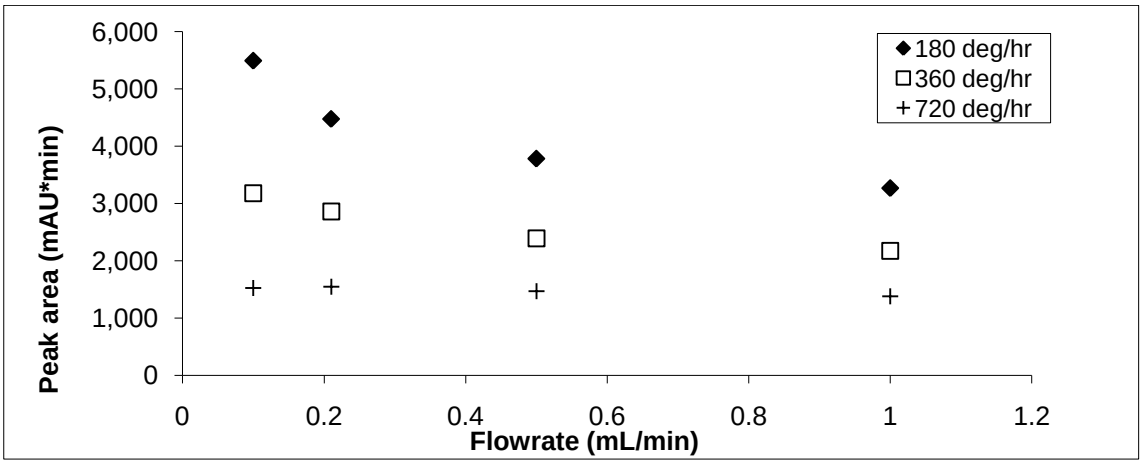

E.4.5 1.5 mg/mL BSA concentration, 1M NaCl concentration, Trial 5, 180-720 deg/hr rotation speed

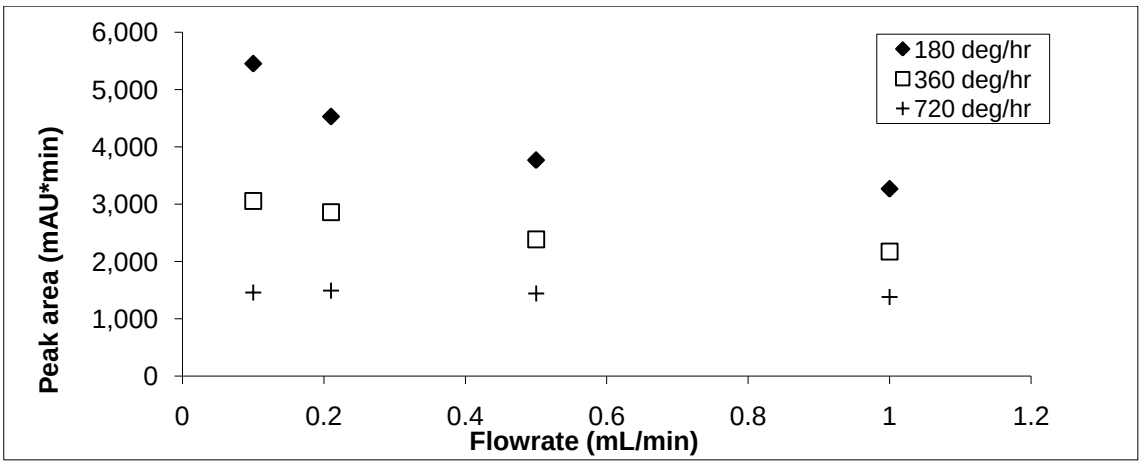

E.4.6 1.5 mg/mL BSA concentration, 1M NaCl concentration, Trial 6, 180-720 deg/hr rotation speed

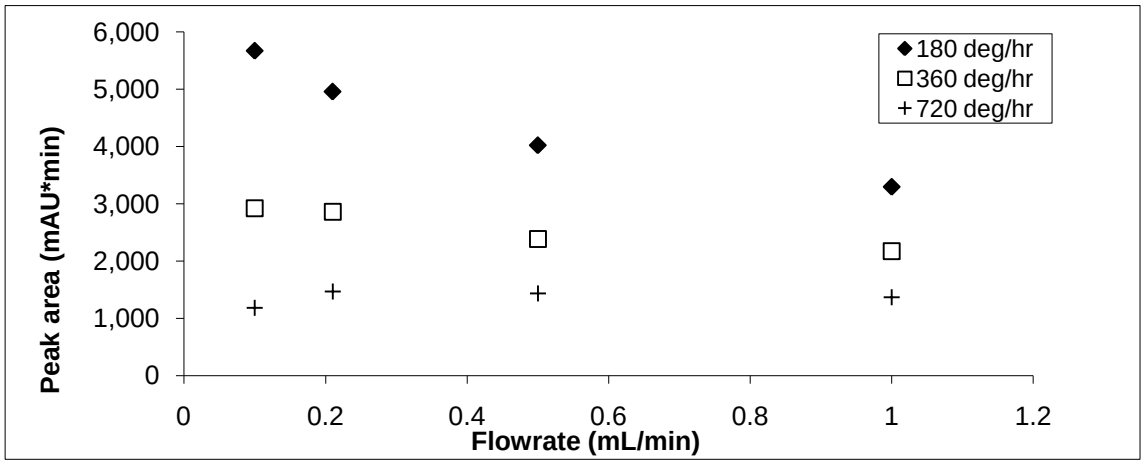

E.4.7 1.5 mg/mL BSA concentration, 1M NaCl concentration, Trial 7, 180-720 deg/hr rotation speed

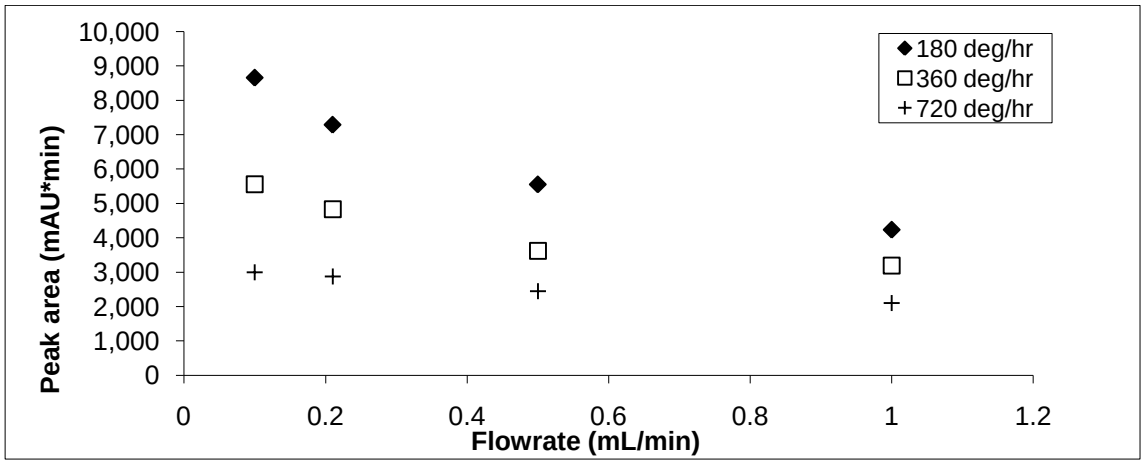

E.4.8 1.5 mg/mL BSA concentration, 1M NaCl concentration, Trial 8, 180-720 deg/hr rotation speed

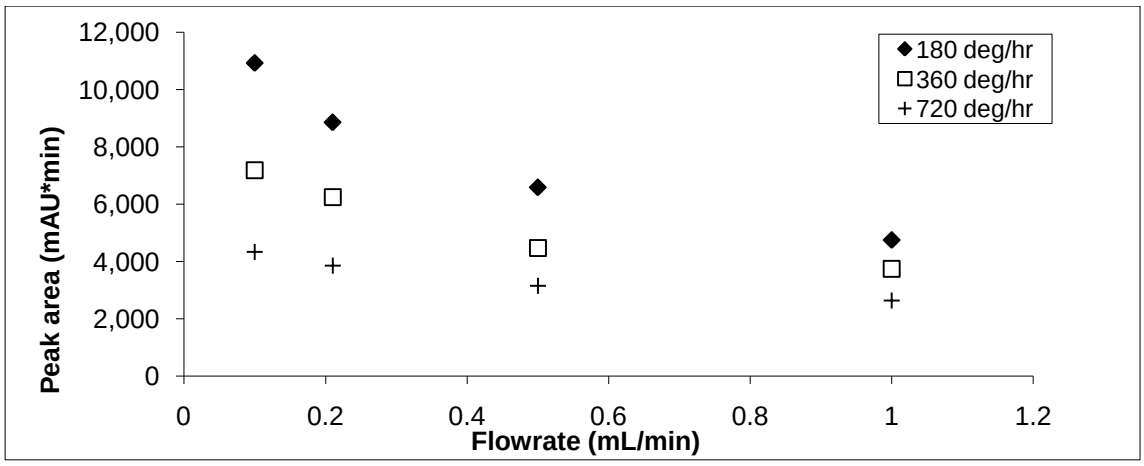

E.4.9 1.5 mg/mL BSA concentration, 1M NaCl concentration, Trial 9, 180-720 deg/hr rotation speed

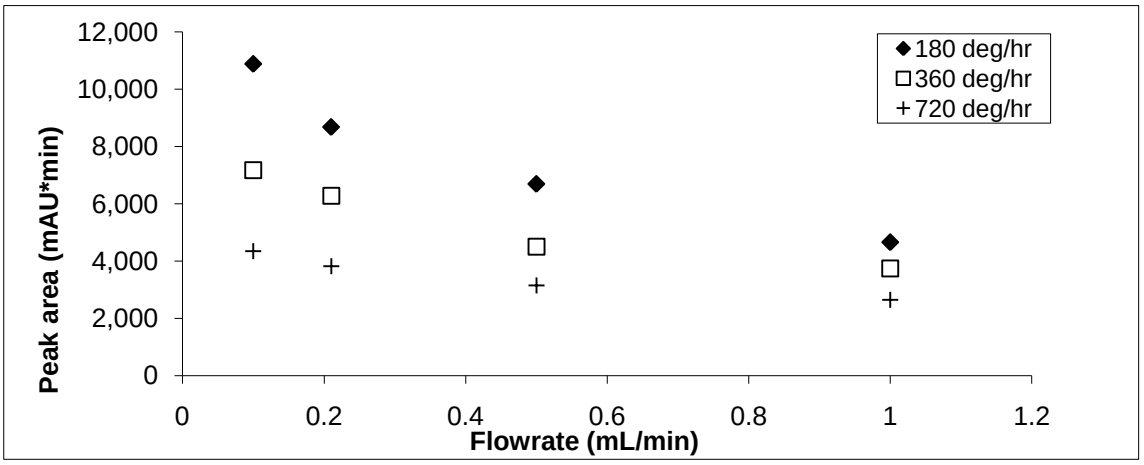

E.4.10 3 mg/mL BSA concentration, 1M NaCl concentration, Trial 1, 180-720 deg/hr rotation speed

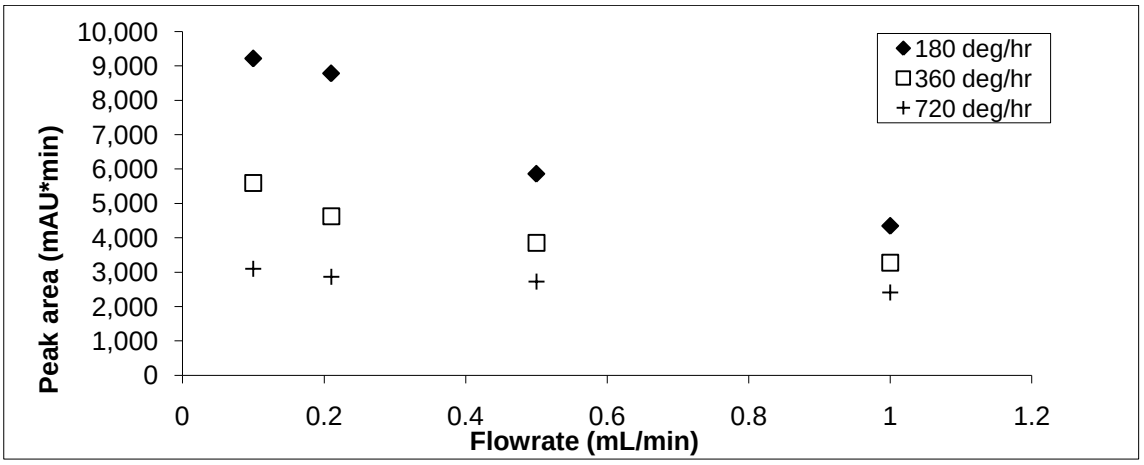

E.4.11 3 mg/mL BSA concentration, 1M NaCl concentration, Trial 2, 180-720 deg/hr rotation speed

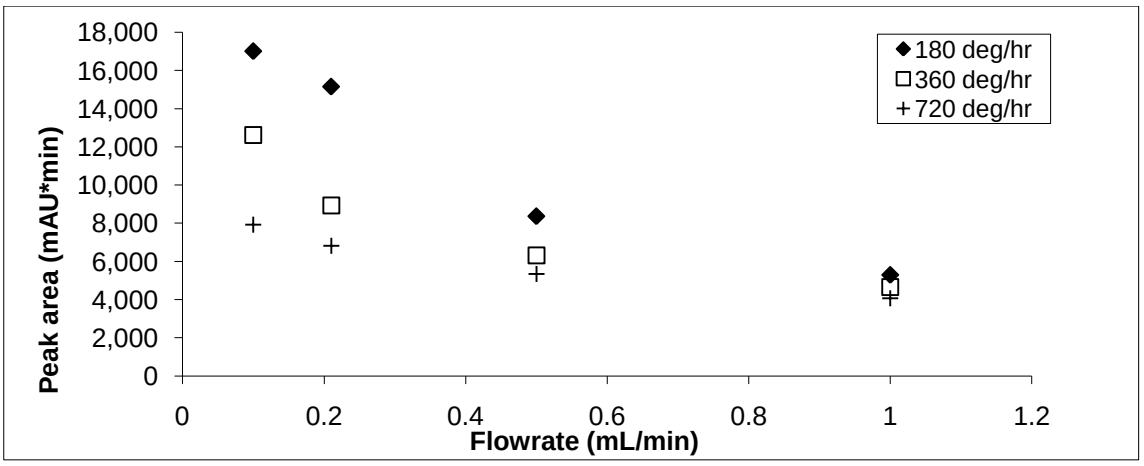

E.4.12 3 mg/mL BSA concentration, 1M NaCl concentration, Trial 3, 180-720 deg/hr rotation speed

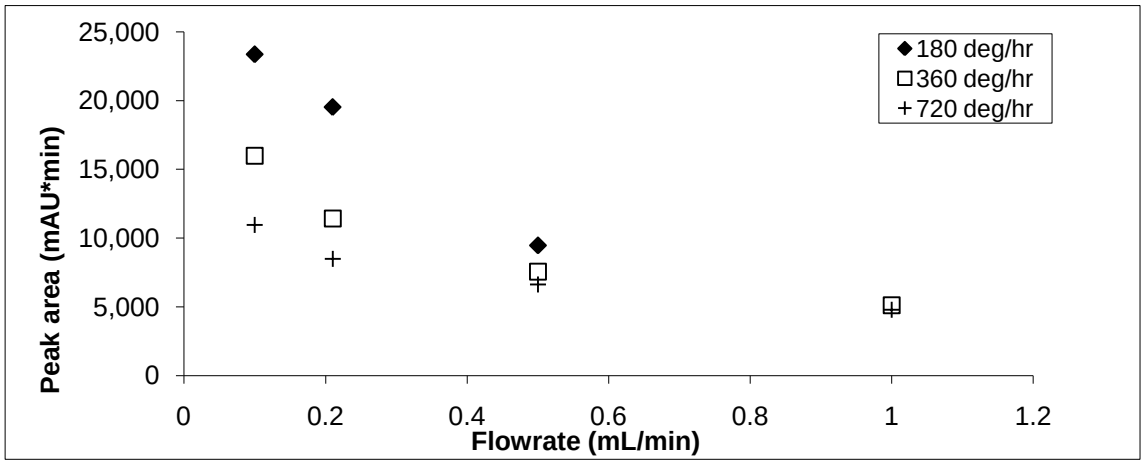

E.4.13 3 mg/mL BSA concentration, 1M NaCl concentration, Trial 4, 180-720 deg/hr rotation speed

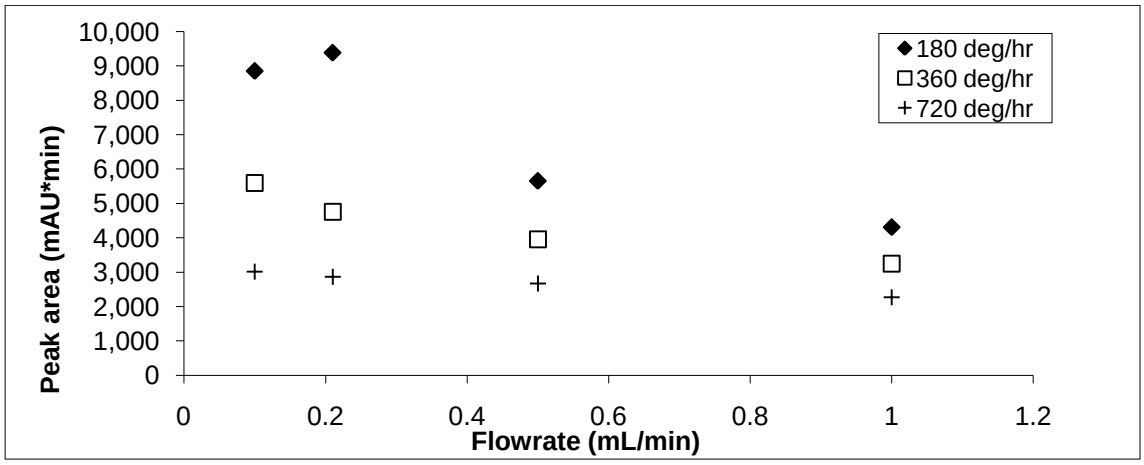

E.4.14 3 mg/mL BSA concentration, 1M NaCl concentration, Trial 5, 180-720 deg/hr rotation speed

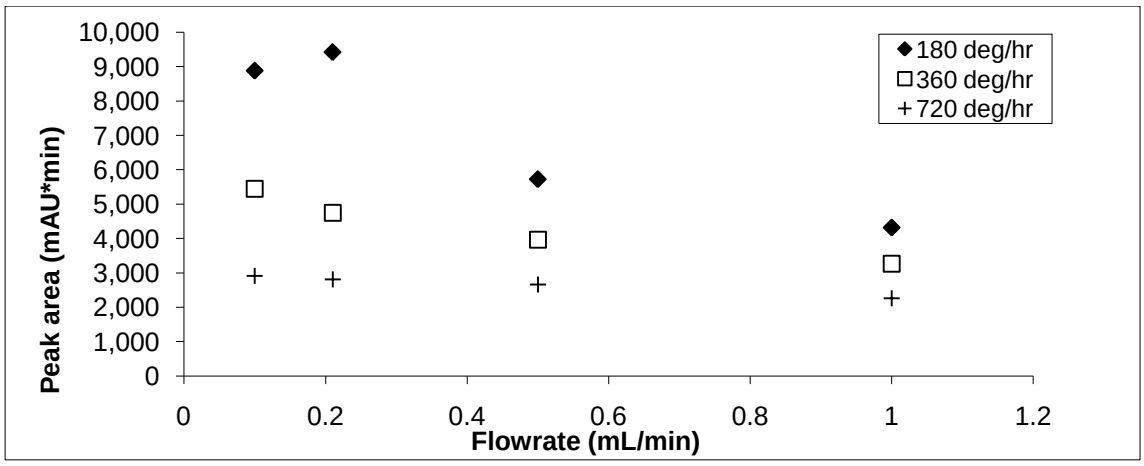

E.4.15 3 mg/mL BSA concentration, 1M NaCl concentration, Trial 6, 180-720 deg/hr rotation speed

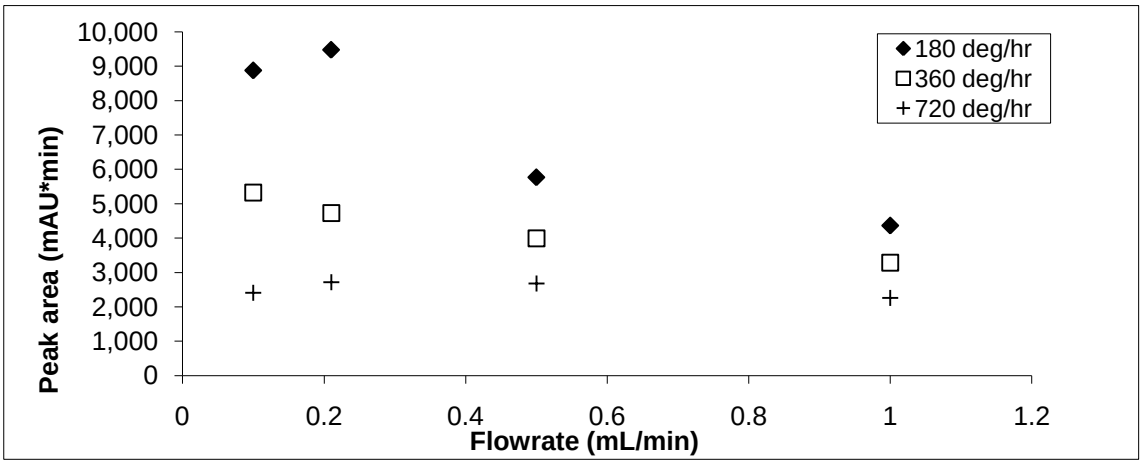

E.4.16 3 mg/mL BSA concentration, 1M NaCl concentration, Trial 7, 180-720 deg/hr rotation speed

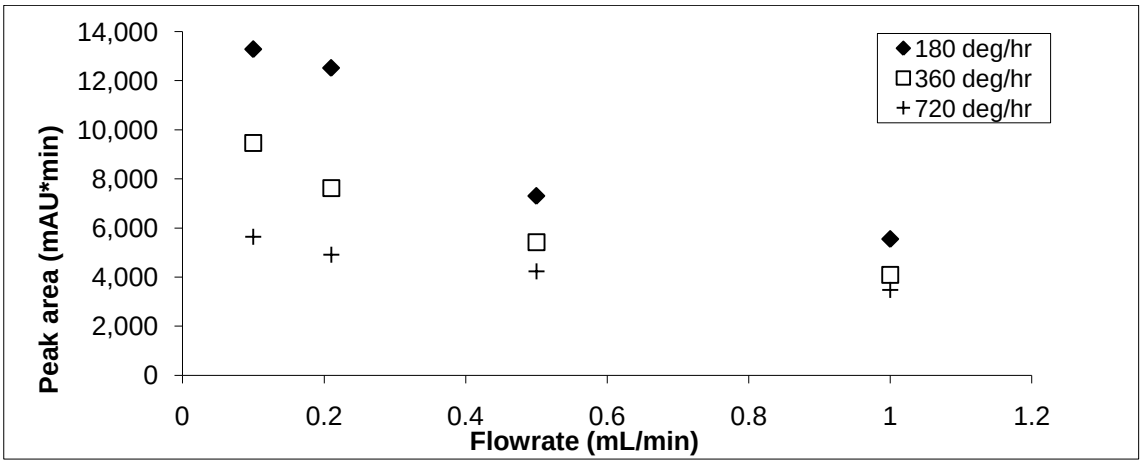

E.4.17 3 mg/mL BSA concentration, 1M NaCl concentration, Trial 8, 180-720 deg/hr rotation speed

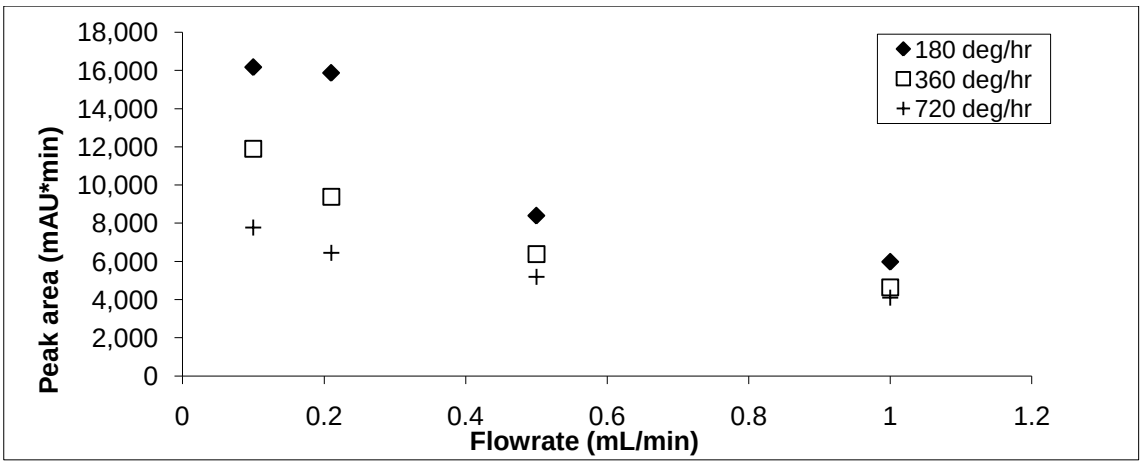

E.4.18 3 mg/mL BSA concentration, 1M NaCl concentration, Trial 9, 180-720 deg/hr rotation speed

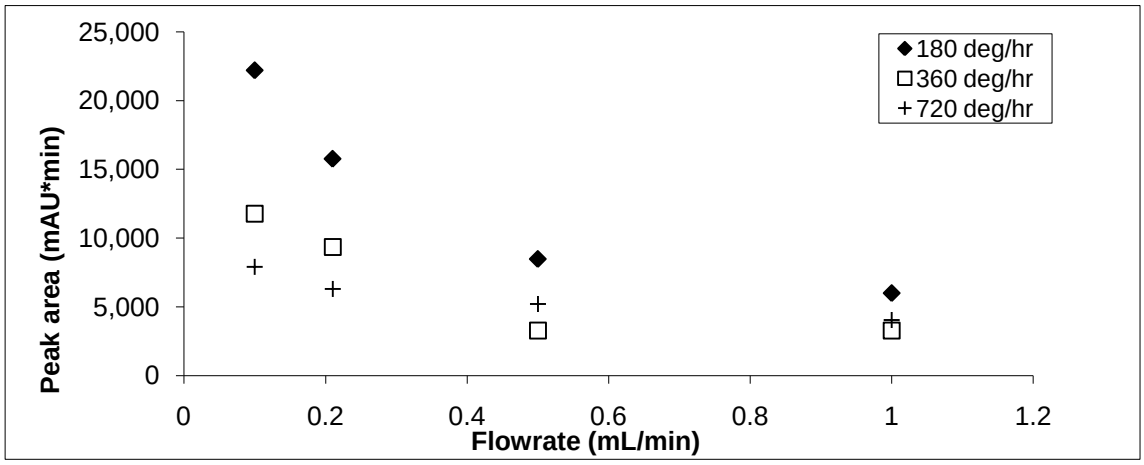

E.4.19 5 mg/mL BSA concentration, 1M NaCl concentration, Trial 1, 180-720 deg/hr rotation speed

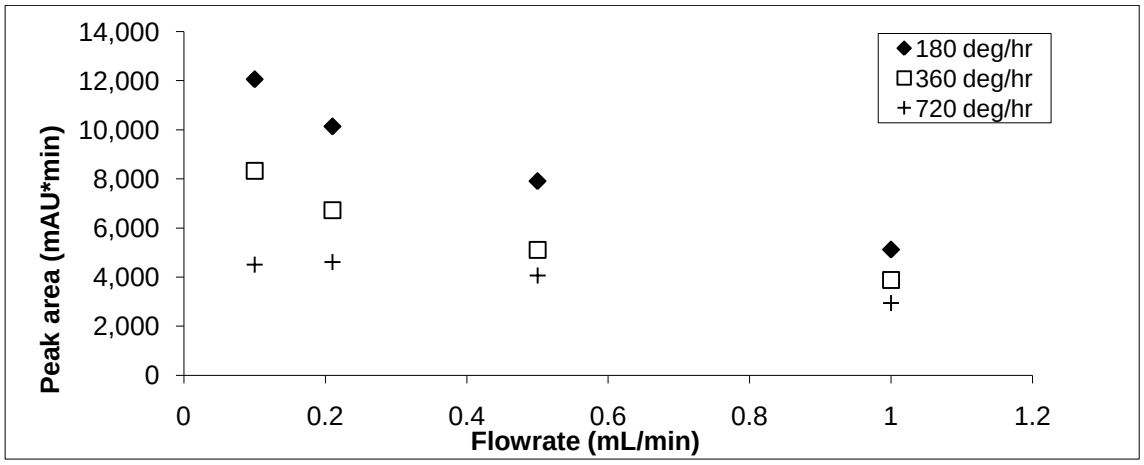

E.4.20 5 mg/mL BSA concentration, 1M NaCl concentration, Trial 2, 180-720 deg/hr rotation speed

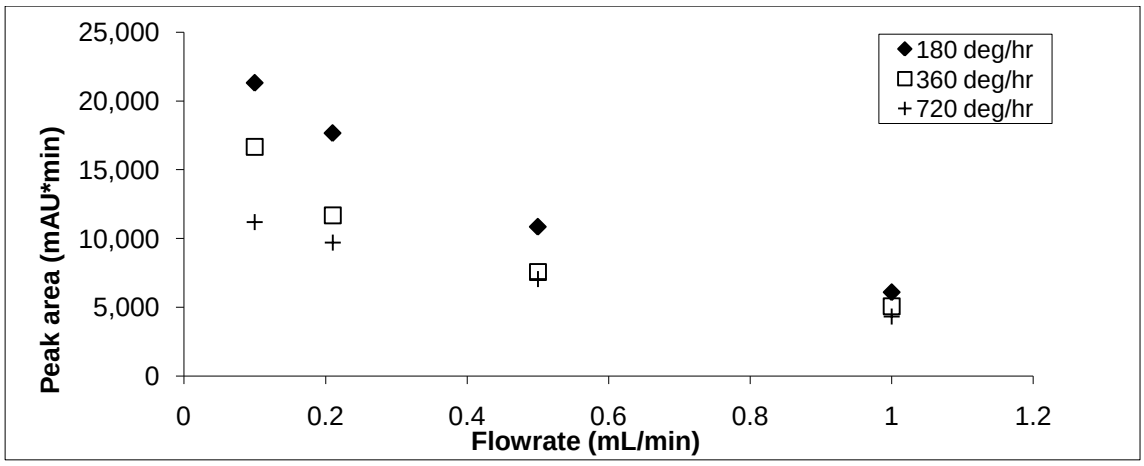

E.4.21 5 mg/mL BSA concentration, 1M NaCl concentration, Trial 3, 180-720 deg/hr rotation speed

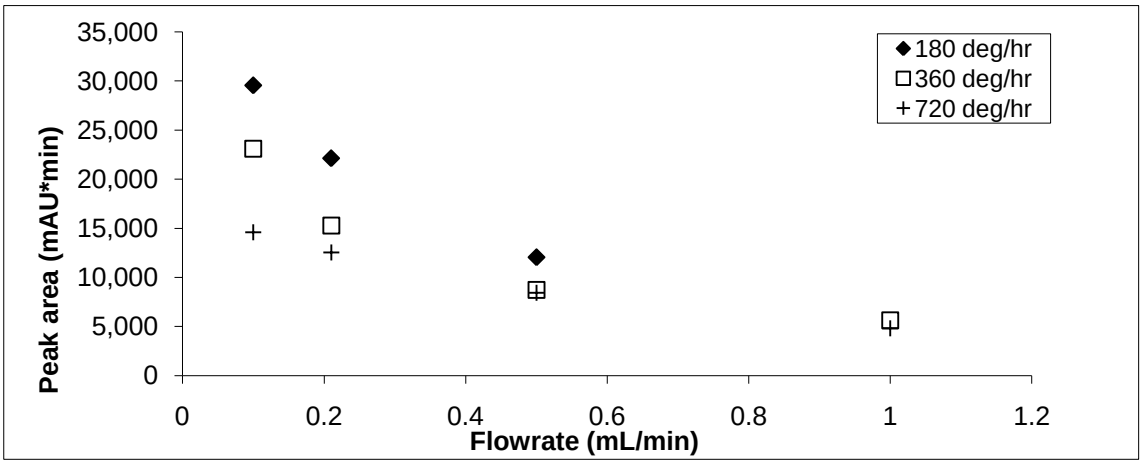

E.4.22 5 mg/mL BSA concentration, 1M NaCl concentration, Trial 4, 180-720 deg/hr rotation speed

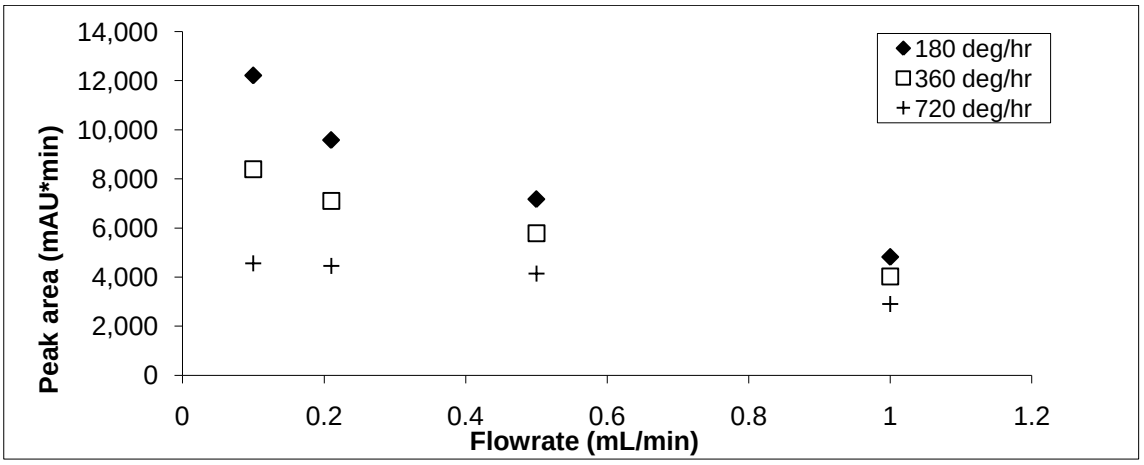

E.4.23 5 mg/mL BSA concentration, 1M NaCl concentration, Trial 5, 180-720 deg/hr rotation speed

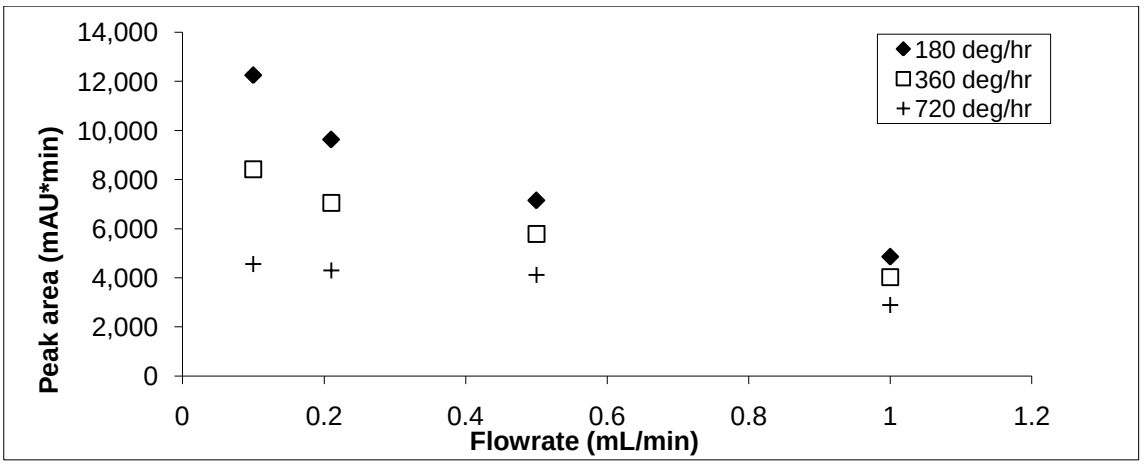

E.4.24 5 mg/mL BSA concentration, 1M NaCl concentration, Trial 6, 180-720 deg/hr rotation speed

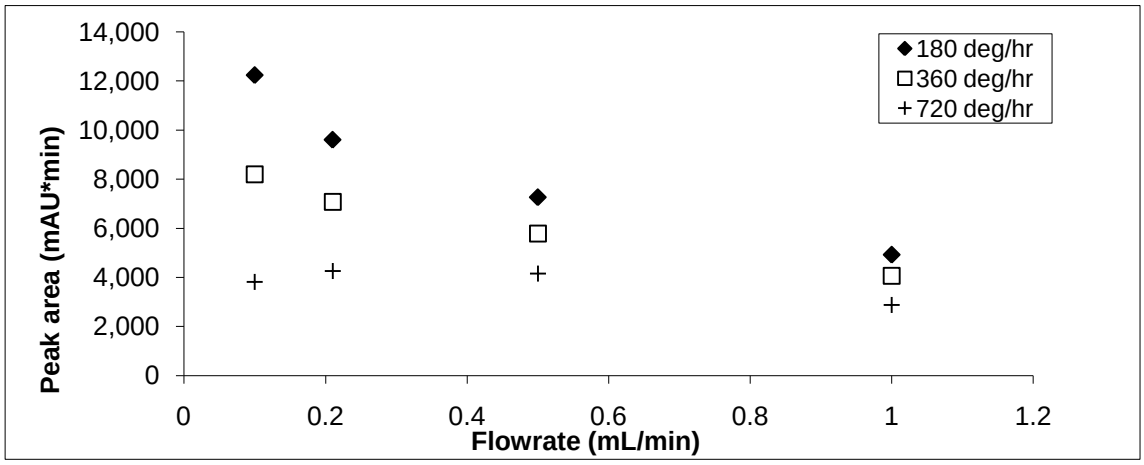

E.4.25 5 mg/mL BSA concentration, 1M NaCl concentration, Trial 7, 180-720 deg/hr rotation speed

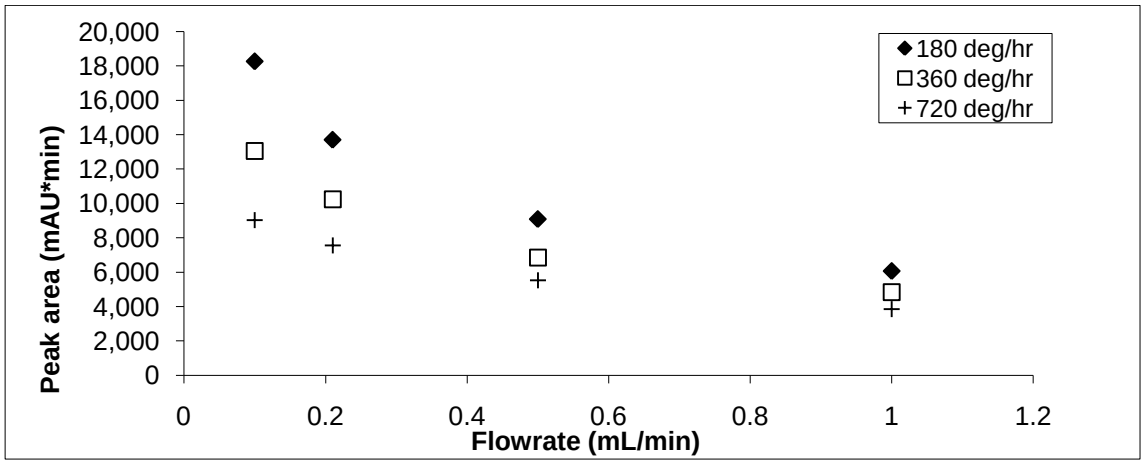

E.4.26 5 mg/mL BSA concentration, 1M NaCl concentration, Trial 8, 180-720 deg/hr rotation speed

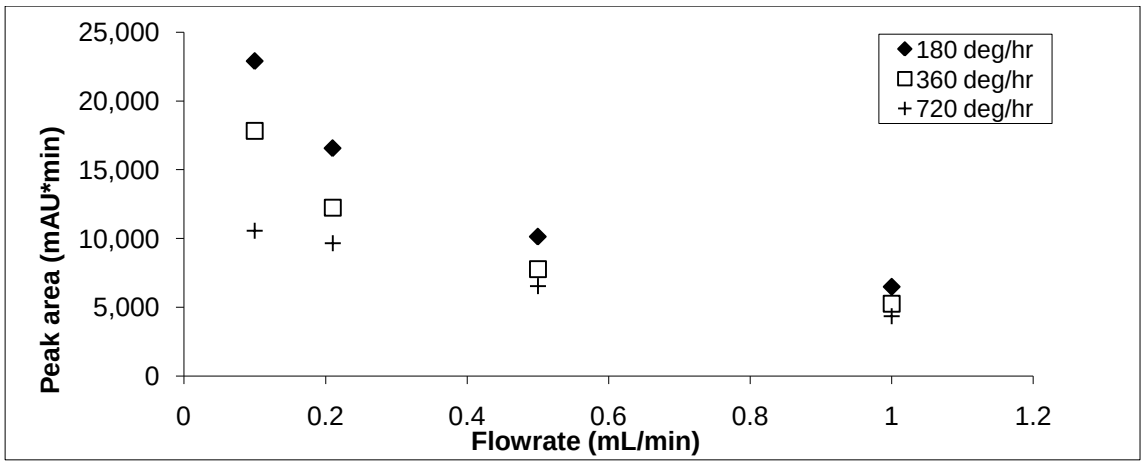

E.4.27 5 mg/mL BSA concentration, 1M NaCl concentration, Trial 9, 180-720 deg/hr rotation speed

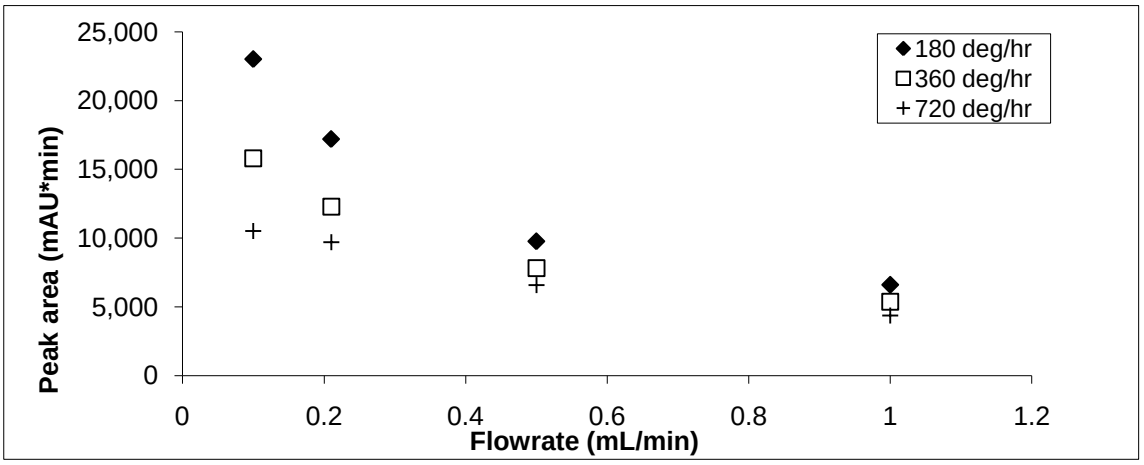

E.4.28 1.5 mg/mL BSA concentration, 2M NaCl concentration, Trial 1, 180-720 deg/hr rotation speed

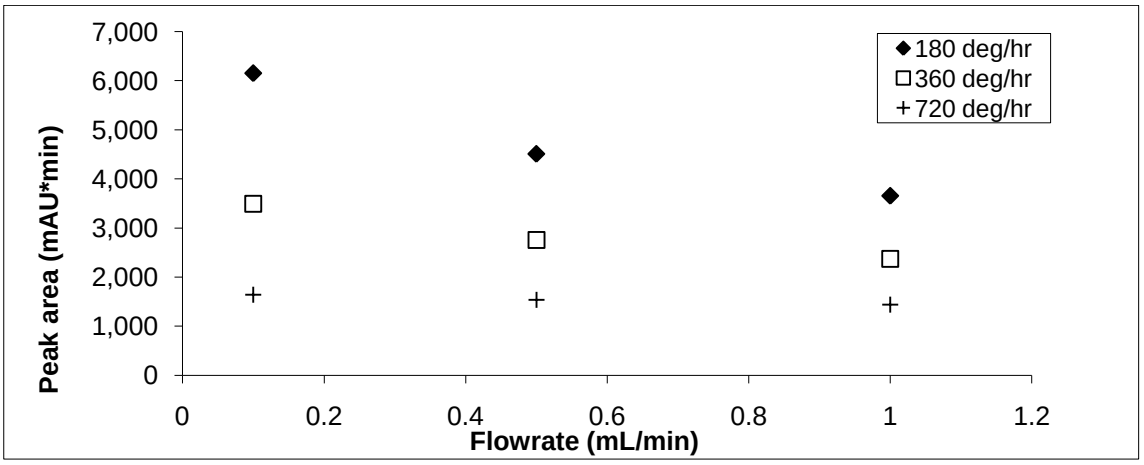

E.4.29 1.5 mg/mL BSA concentration, 2M NaCl concentration, Trial 2, 180-720 deg/hr rotation speed

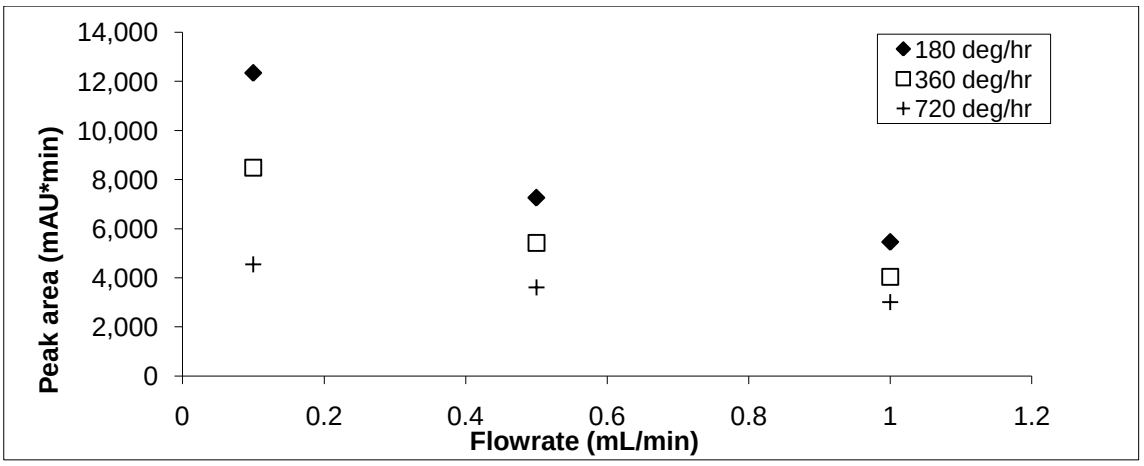

E.4.30 1.5 mg/mL BSA concentration, 2M NaCl concentration, Trial 3, 180-720 deg/hr rotation speed

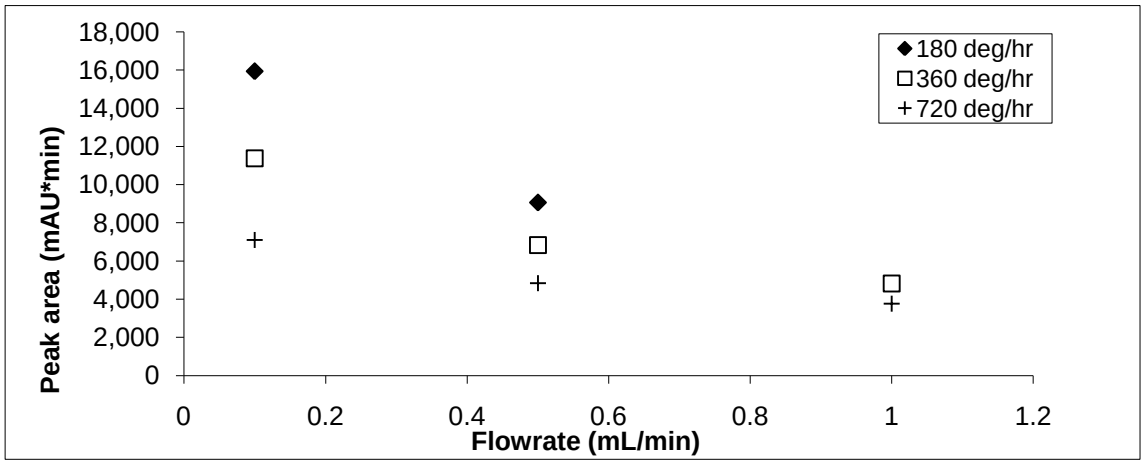

E.4.31 1.5 mg/mL BSA concentration, 2M NaCl concentration, Trial 4, 180-720 deg/hr rotation speed

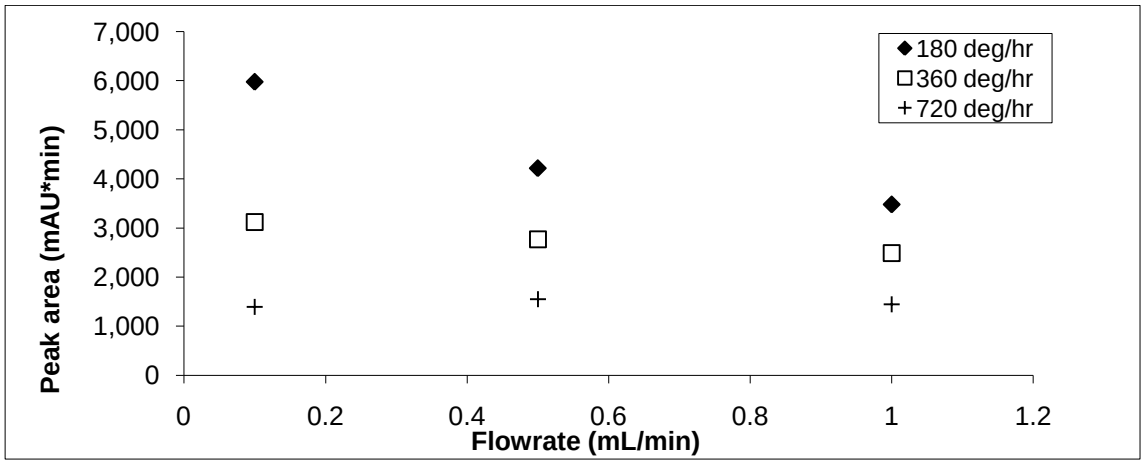

E.4.32 1.5 mg/mL BSA concentration, 2M NaCl concentration, Trial 5, 180-720 deg/hr rotation speed

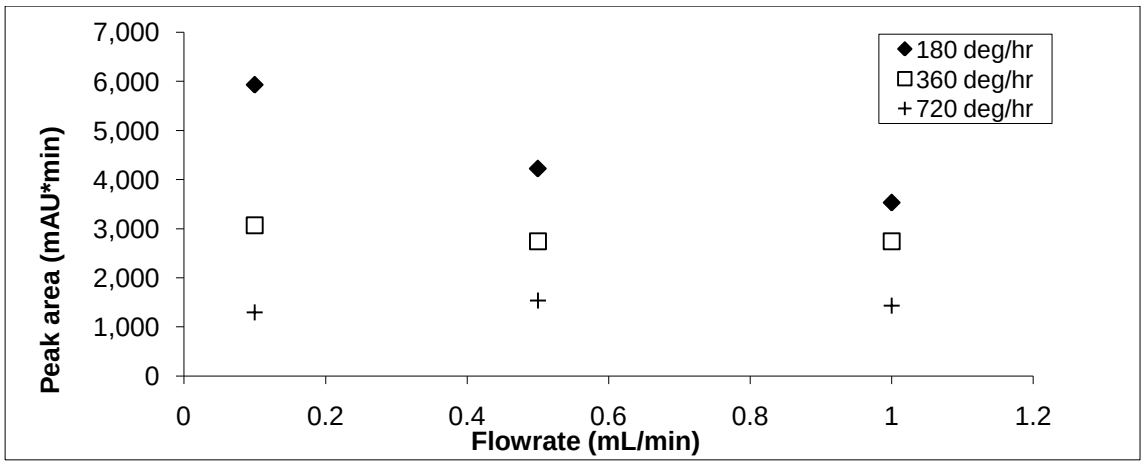

E.4.33 1.5 mg/mL BSA concentration, 2M NaCl concentration, Trial 6, 180-720 deg/hr rotation speed

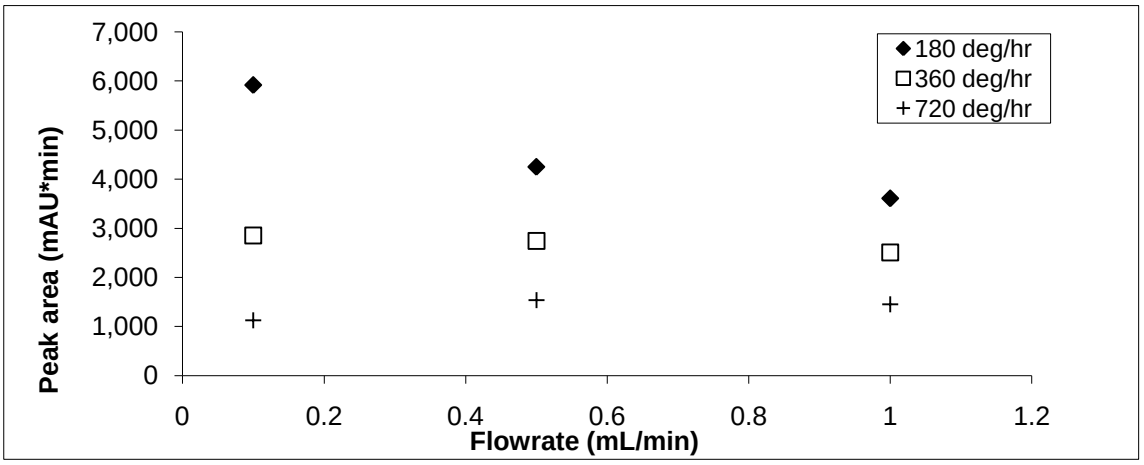

E.4.34 1.5 mg/mL BSA concentration, 2M NaCl concentration, Trial 7, 180-720 deg/hr rotation speed

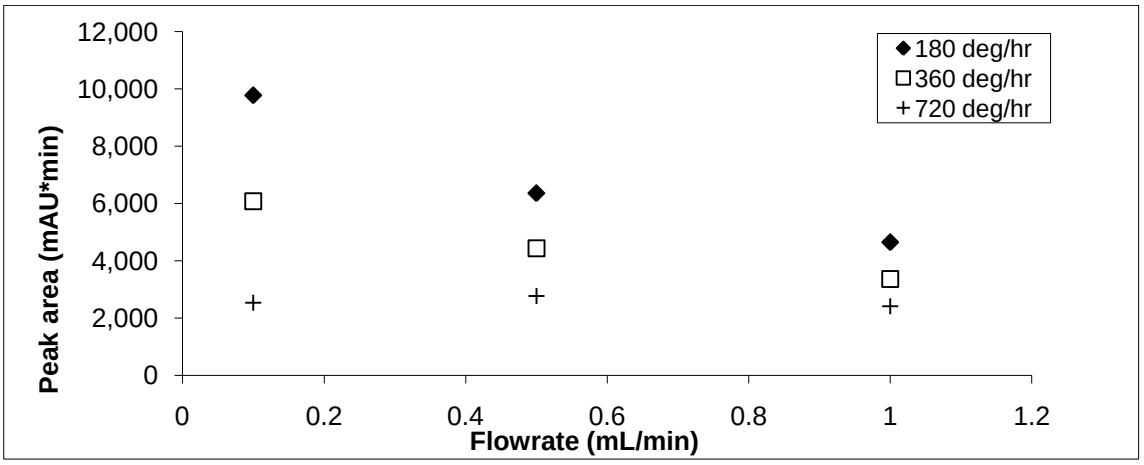

E.4.35 1.5 mg/mL BSA concentration, 2M NaCl concentration, Trial 8, 180-720 deg/hr rotation speed

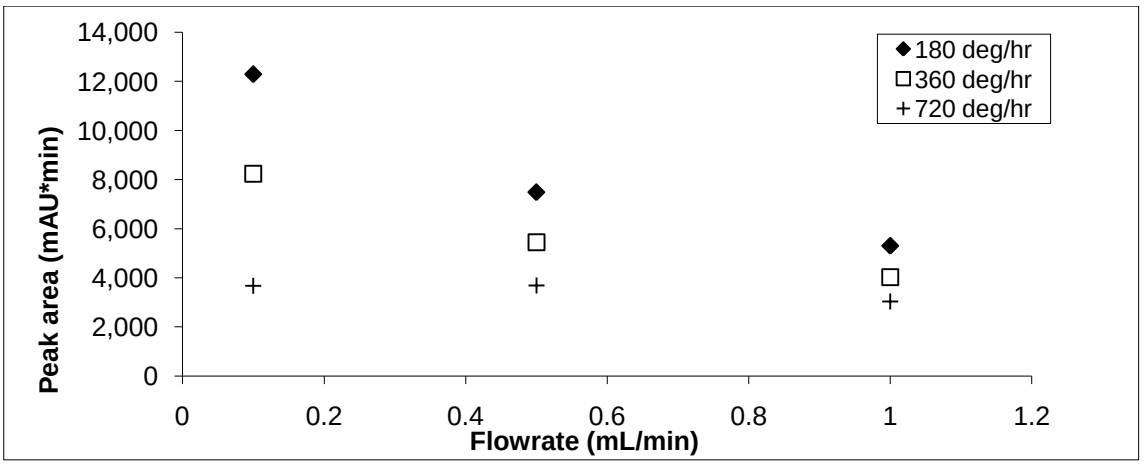

E.4.36 1.5 mg/mL BSA concentration, 2M NaCl concentration, Trial 9, 180-720 deg/hr rotation speed

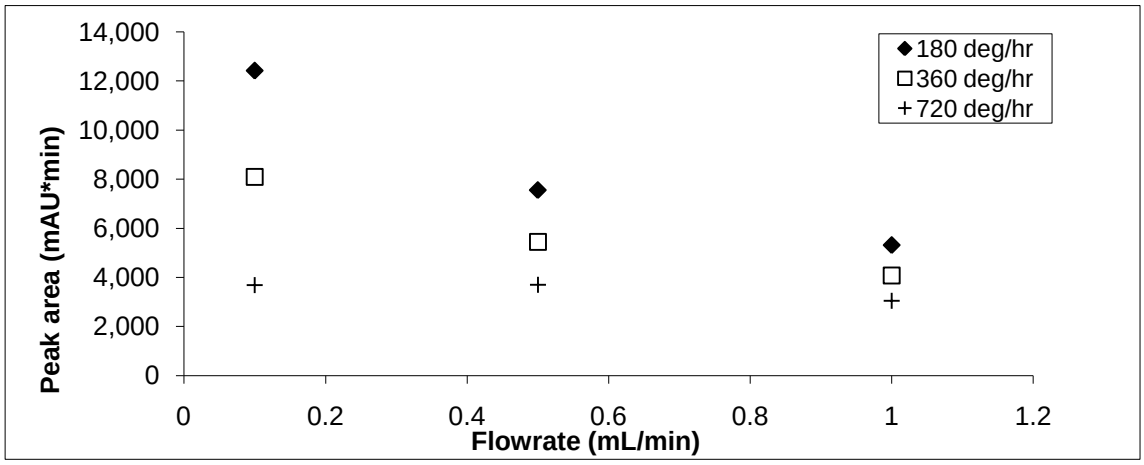

E.5 Feed concentration

E.5.1 180 deg/hr rotation speed, 1M NaCl concentration, Trial 1, 0.1-1.0 mL/min flow rate

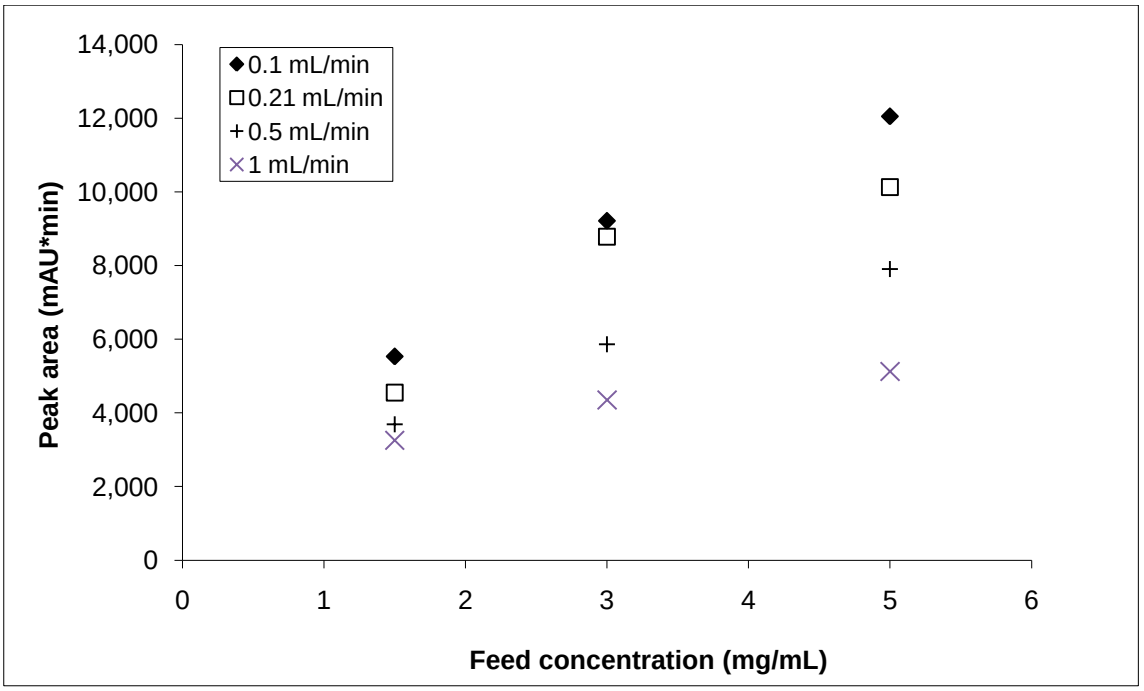

E.5.2 180 deg/hr rotation speed, 1M NaCl concentration, Trial 2, 0.1-1.0 mL/min flow rate

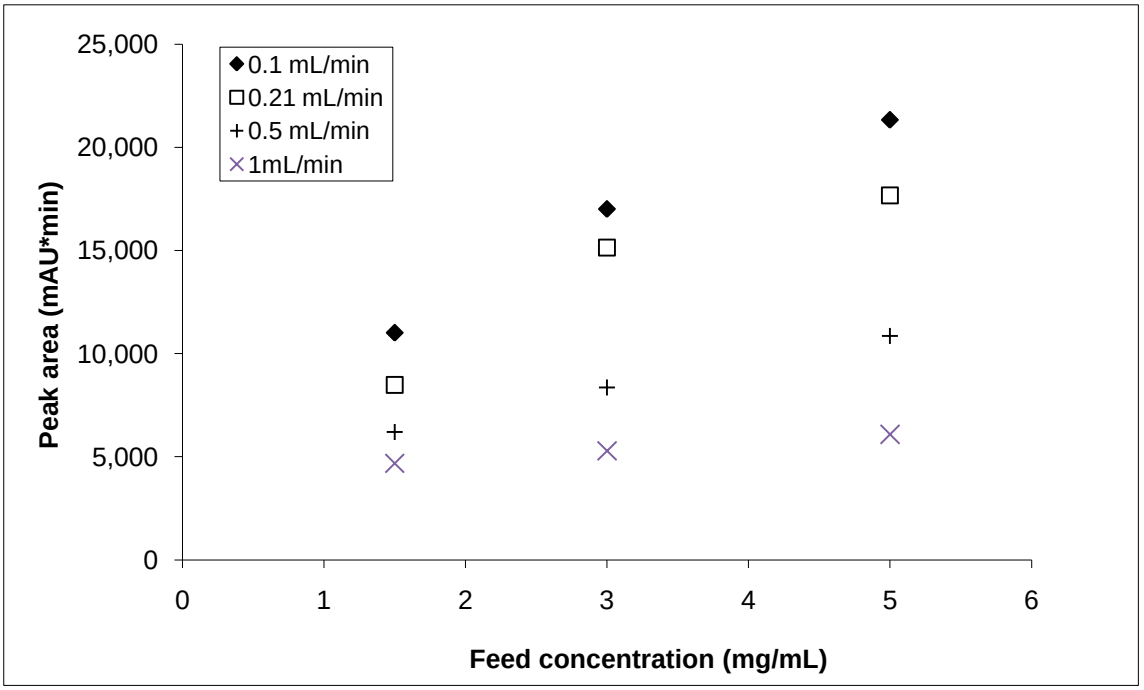

E.5.3 180 deg/hr rotation speed, 1M NaCl concentration, Trial 3, 0.1-0.5 mL/min flow rate

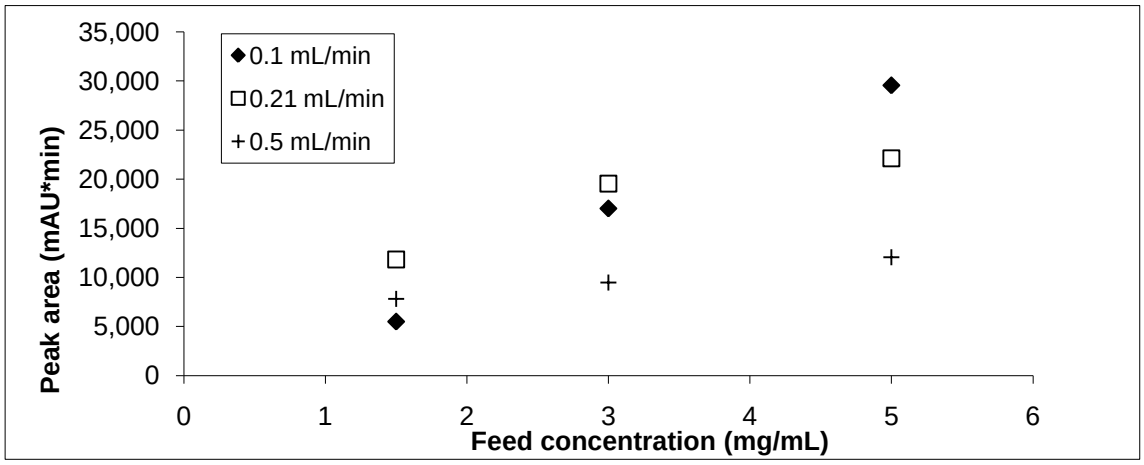

E.5.4 180 deg/hr rotation speed, 1M NaCl concentration, Trial 4, 0.1-1.0 mL/min flow rate

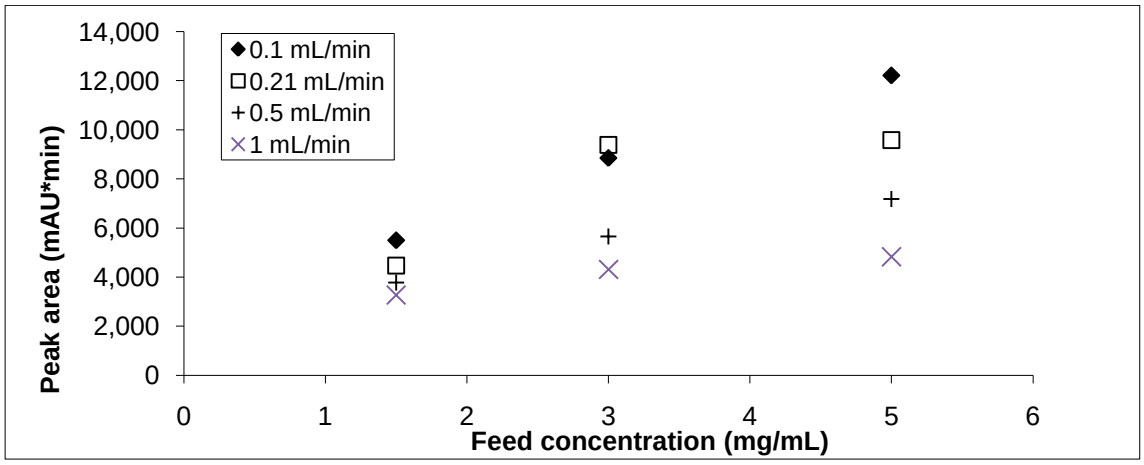

E.5.5 180 deg/hr rotation speed, 1M NaCl concentration, Trial 5, 0.1-1.0 mL/min flow rate

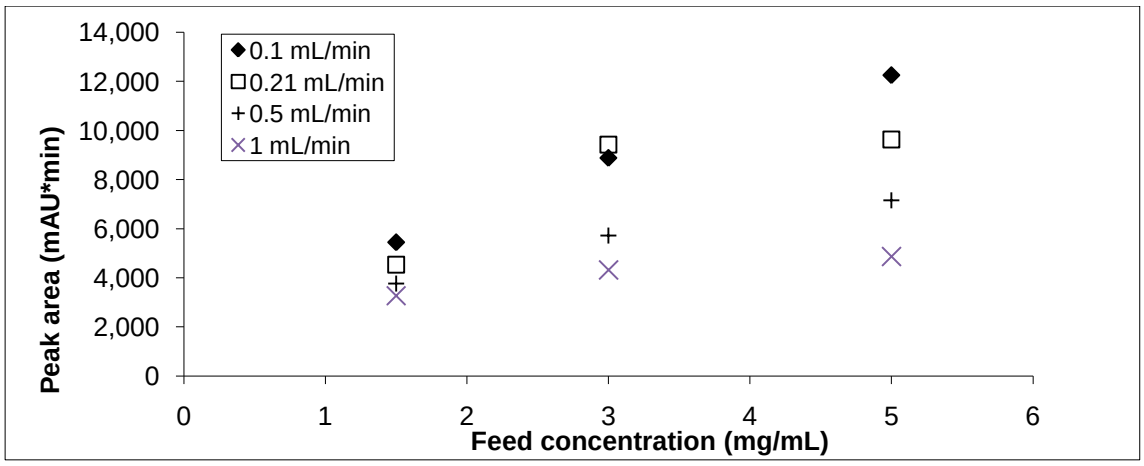

E.5.6 180 deg/hr rotation speed, 1M NaCl concentration, Trial 6, 0.1-1.0 mL/min flow rate

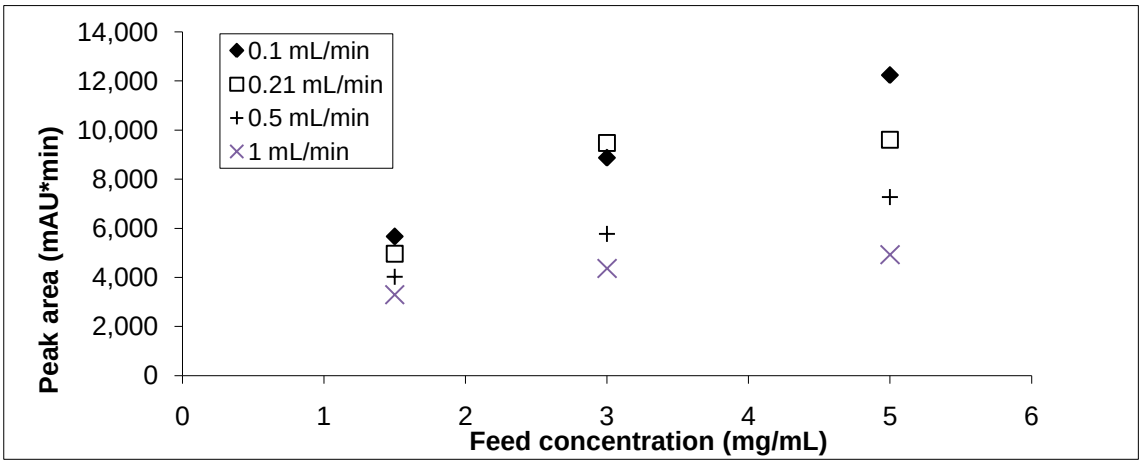

E.5.7 180 deg/hr rotation speed, 1M NaCl concentration, Trial 7, 0.1-1.0 mL/min flow rate

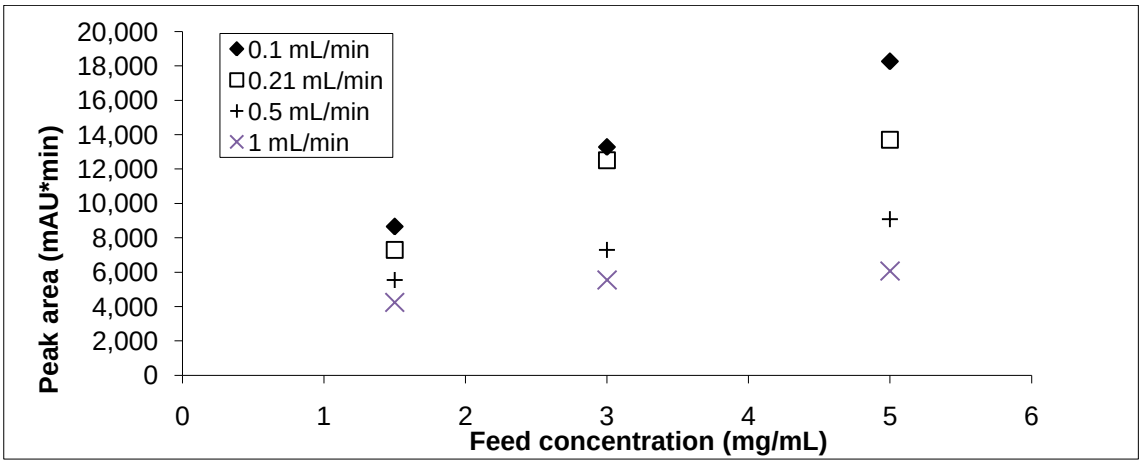

E.5.8 180 deg/hr rotation speed, 1M NaCl concentration, Trial 8, 0.1-1.0 mL/min flow rate

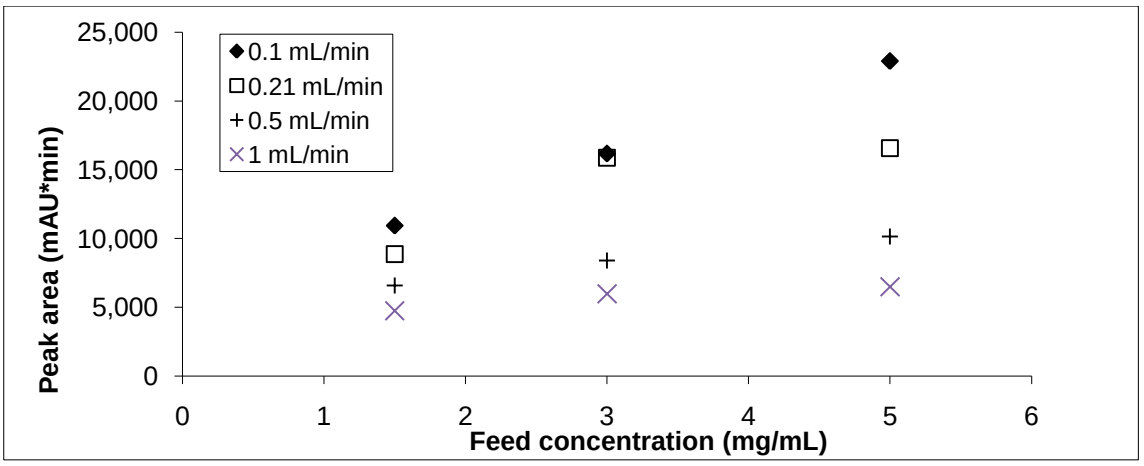

E.5.9 180 deg/hr rotation speed, 1M NaCl concentration, Trial 9, 0.1-1.0 mL/min flow rate

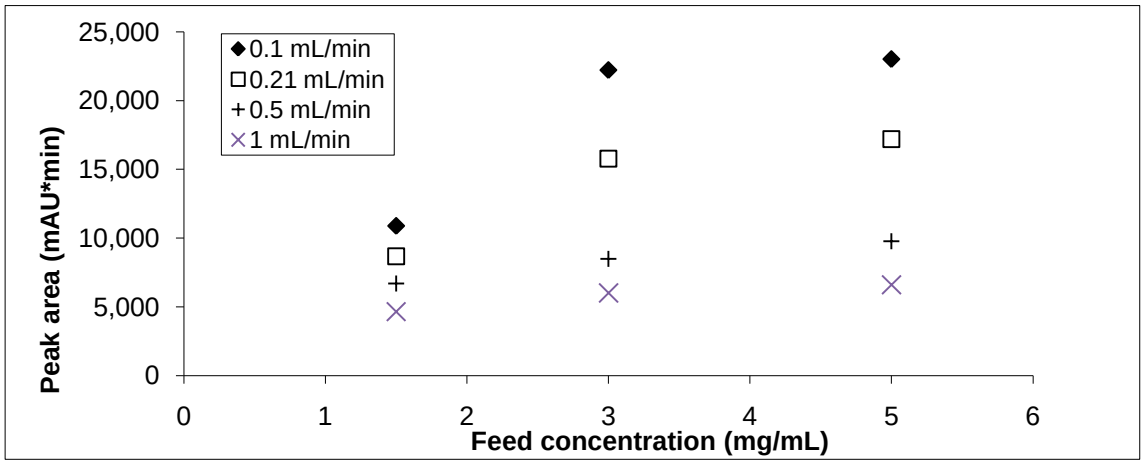

E.5.10 360 deg/hr rotation speed, 1M NaCl concentration, Trial 1, 0.1-1.0 mL/min flow rate

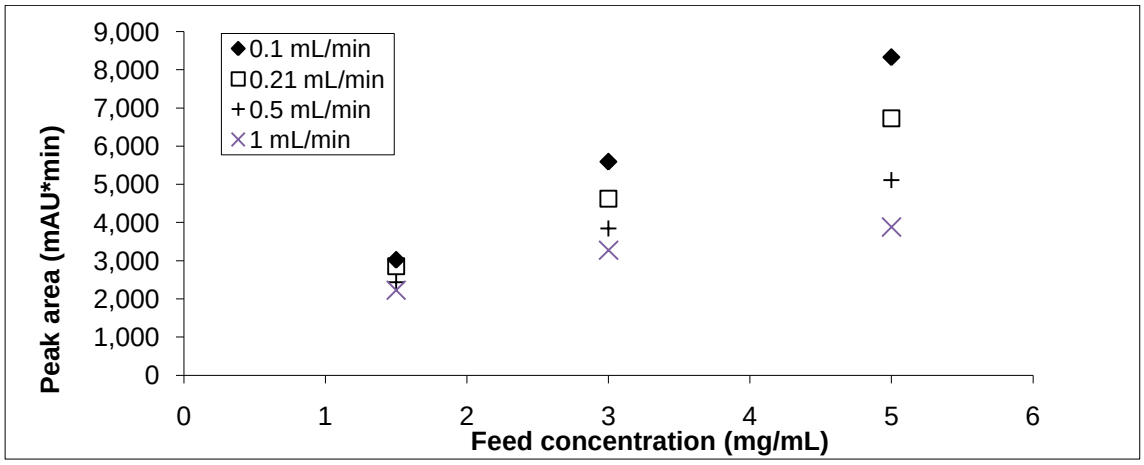

E.5.11 360 deg/hr rotation speed, 1M NaCl concentration, Trial 2, 0.1-1.0 mL/min flow rate

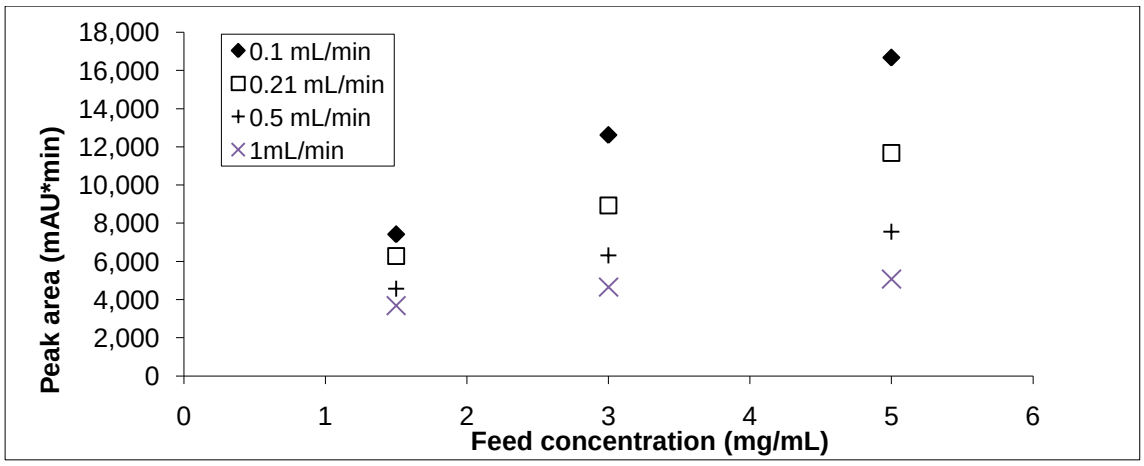

E.5.12 360 deg/hr rotation speed, 1M NaCl concentration, Trial 3, 0.1-1.0 mL/min flow rate

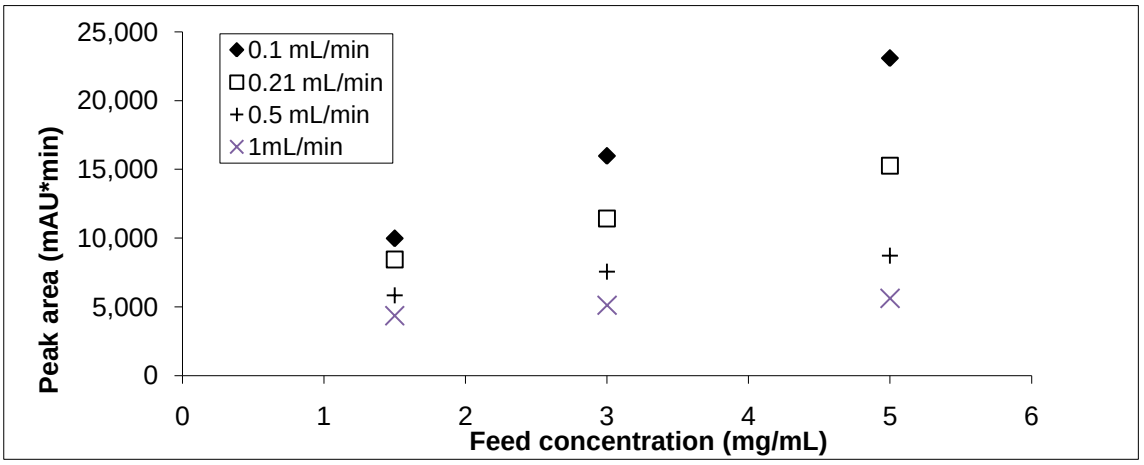

E.5.13 360 deg/hr rotation speed, 1M NaCl concentration, Trial 4, 0.1-1.0 mL/min flow rate

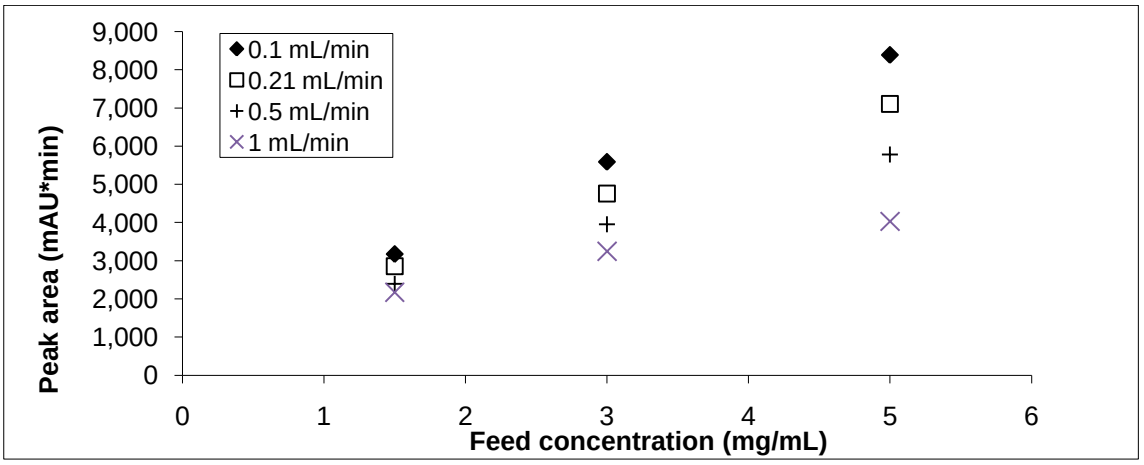

E.5.14 360 deg/hr rotation speed, 1M NaCl concentration, Trial 5, 0.1-1.0 mL/min flow rate

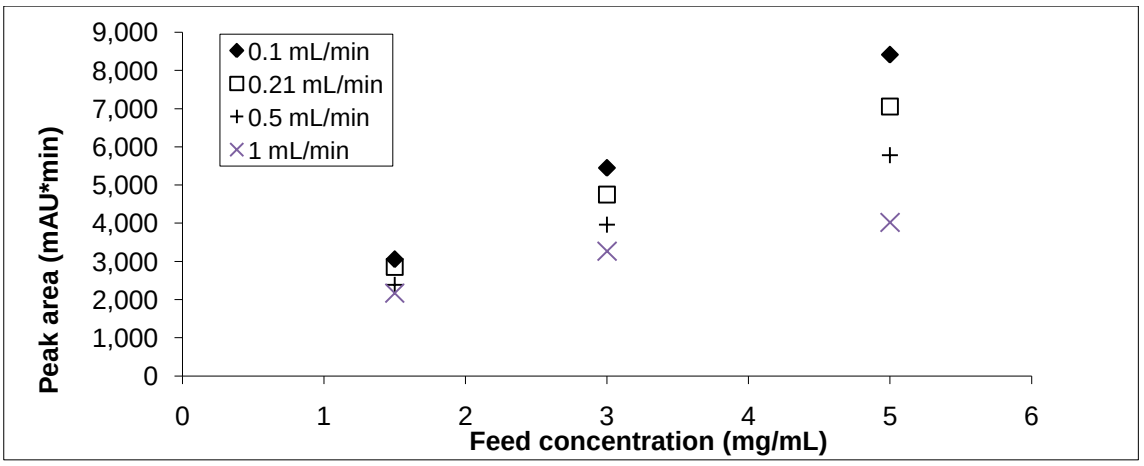

E.5.15 360 deg/hr rotation speed, 1M NaCl concentration, Trial 6, 0.1-1.0 mL/min flow rate

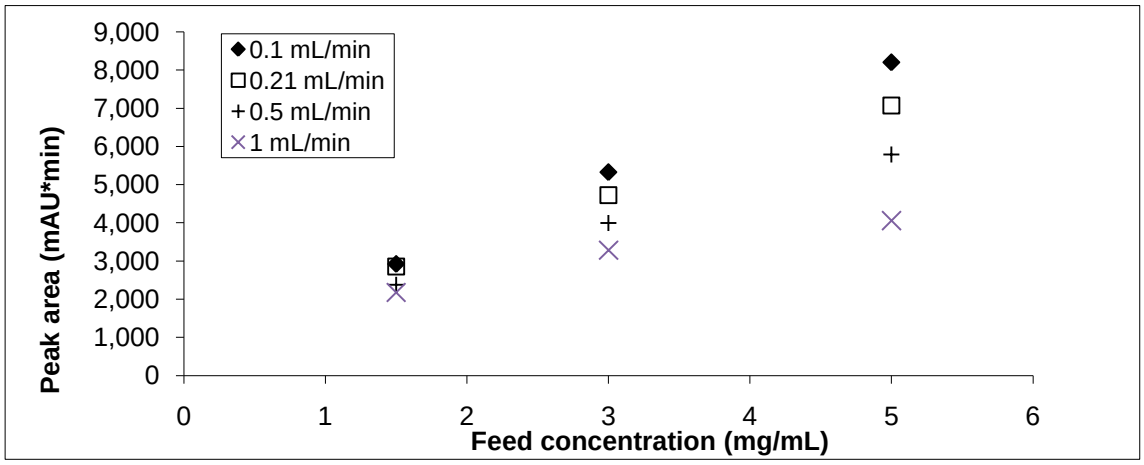

E.5.16 360 deg/hr rotation speed, 1M NaCl concentration, Trial 7, 0.1-1.0 mL/min flow rate

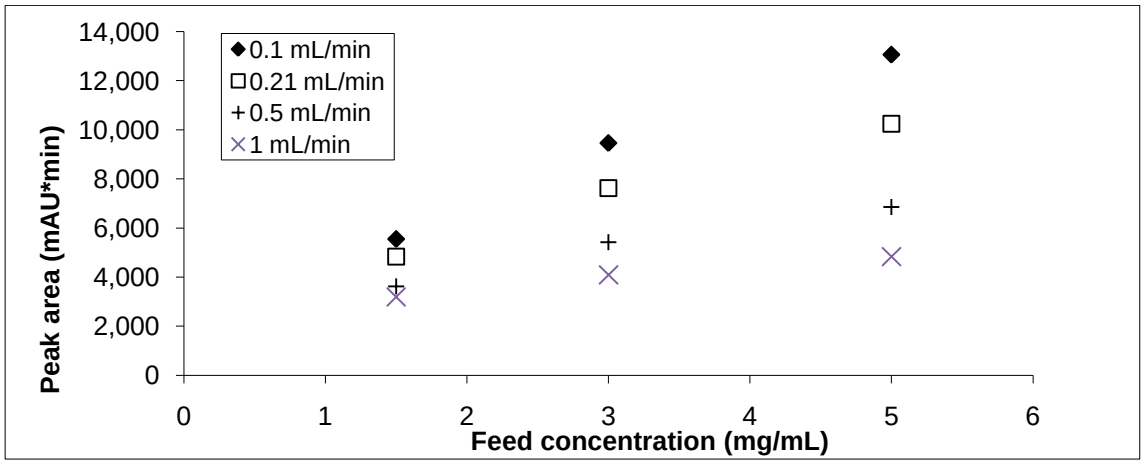

E.5.17 360 deg/hr rotation speed, 1M NaCl concentration, Trial 8, 0.1-1.0 mL/min flow rate

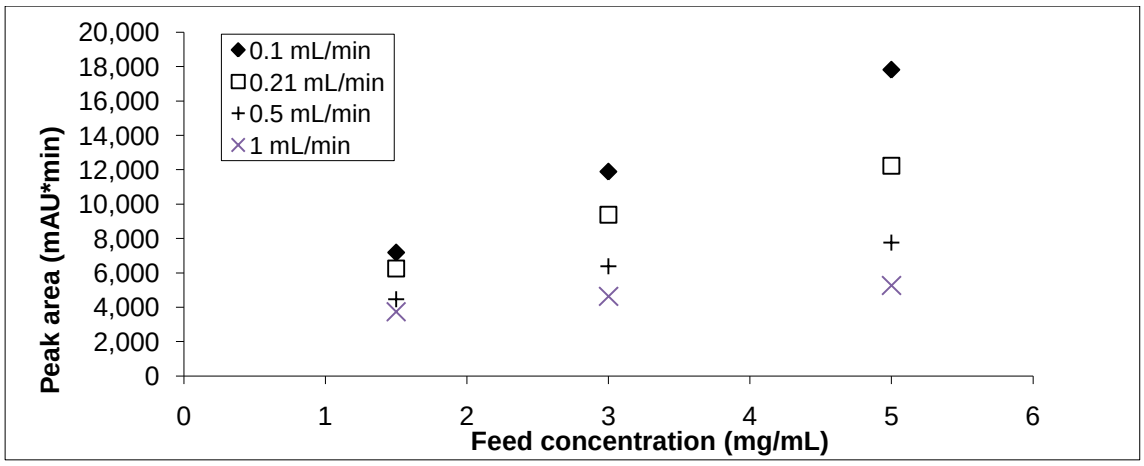

E.5.18 360 deg/hr rotation speed, 1M NaCl concentration, Trial 9, 0.1-1.0 mL/min flow rate

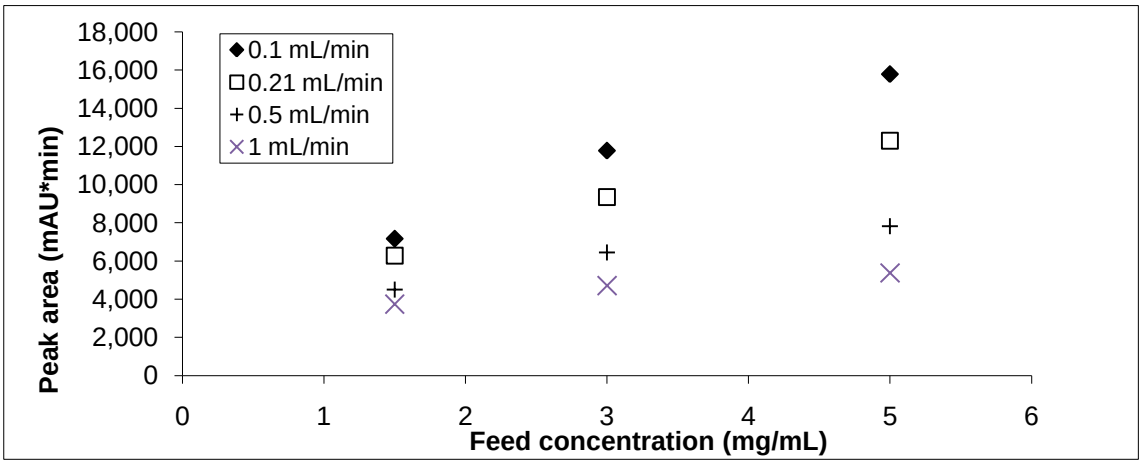

E.5.19 720 deg/hr rotation speed, 1M NaCl concentration, Trial 1, 0.1-1.0 mL/min flow rate

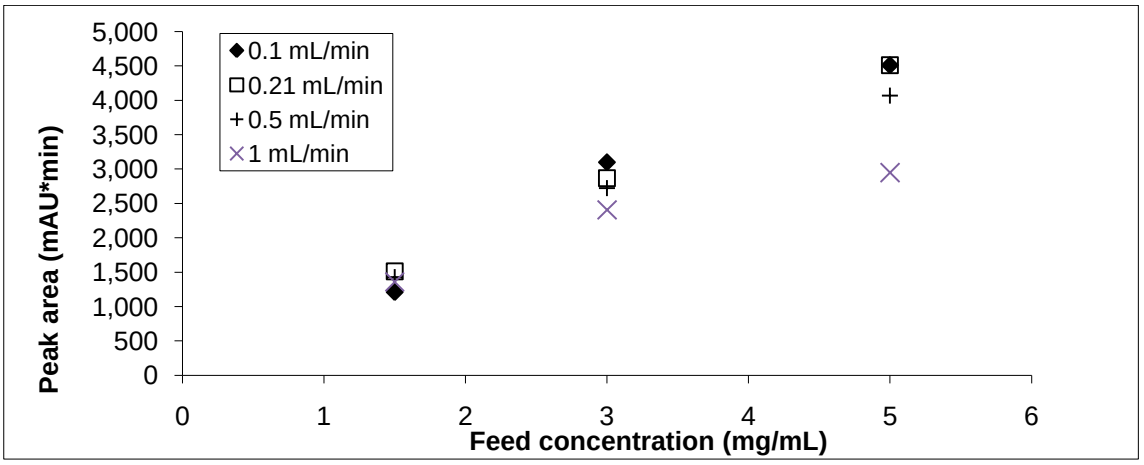

E.5.20 720 deg/hr rotation speed, 1M NaCl concentration, Trial 2, 0.1-1.0 mL/min flow rate

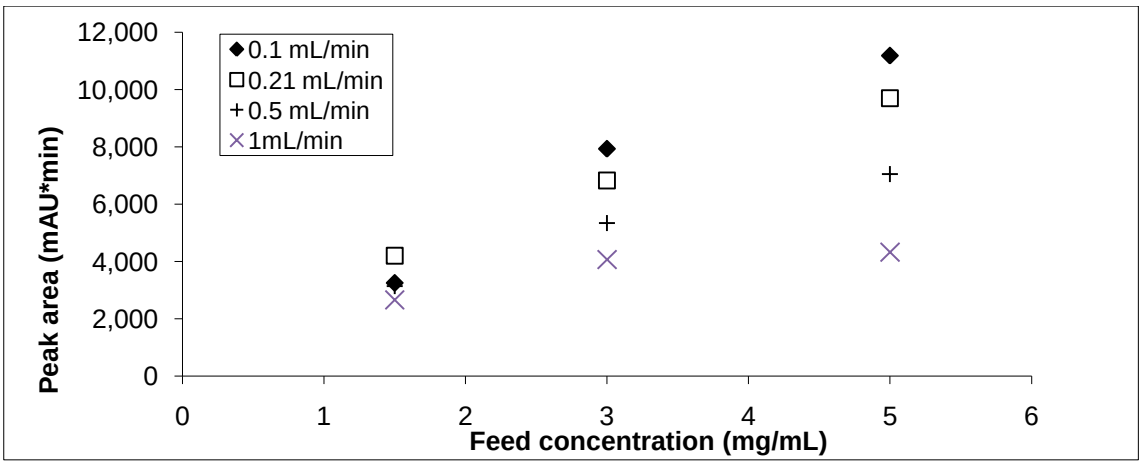

E.5.21 720 deg/hr rotation speed, 1M NaCl concentration, Trial 3, 0.1-1.0 mL/min flow rate

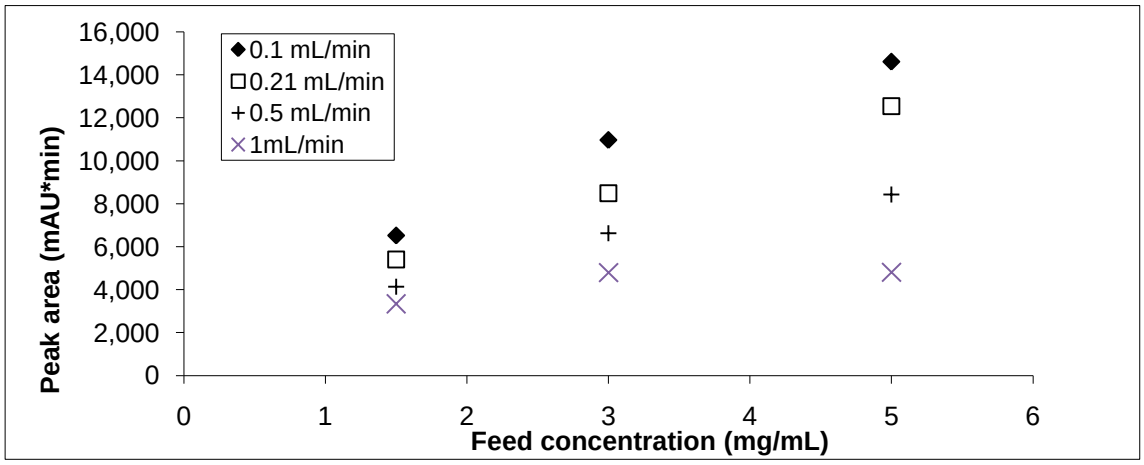

E.5.22 720 deg/hr rotation speed, 1M NaCl concentration, Trial 4, 0.1-1.0 mL/min flow rate

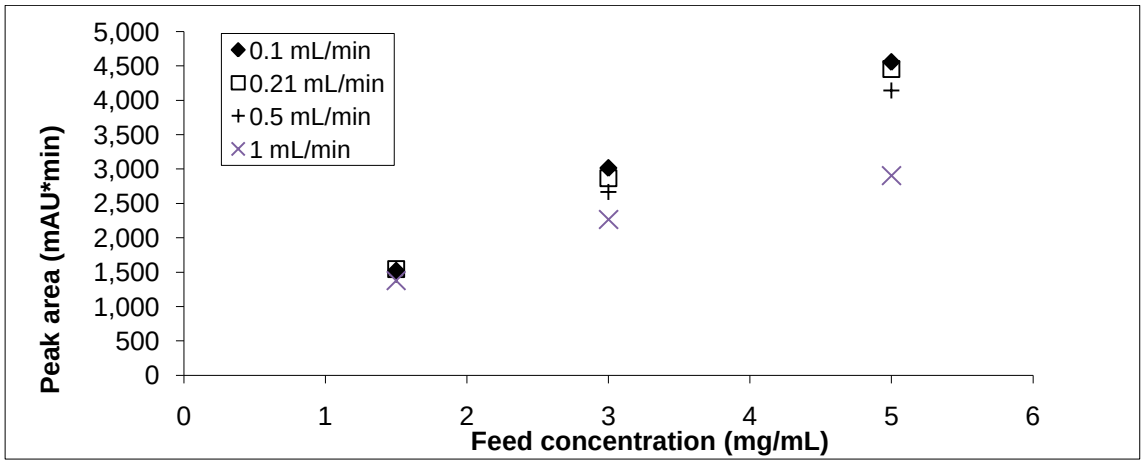

E.5.23 720 deg/hr rotation speed, 1M NaCl concentration, Trial 5, 0.1-1.0 mL/min flow rate

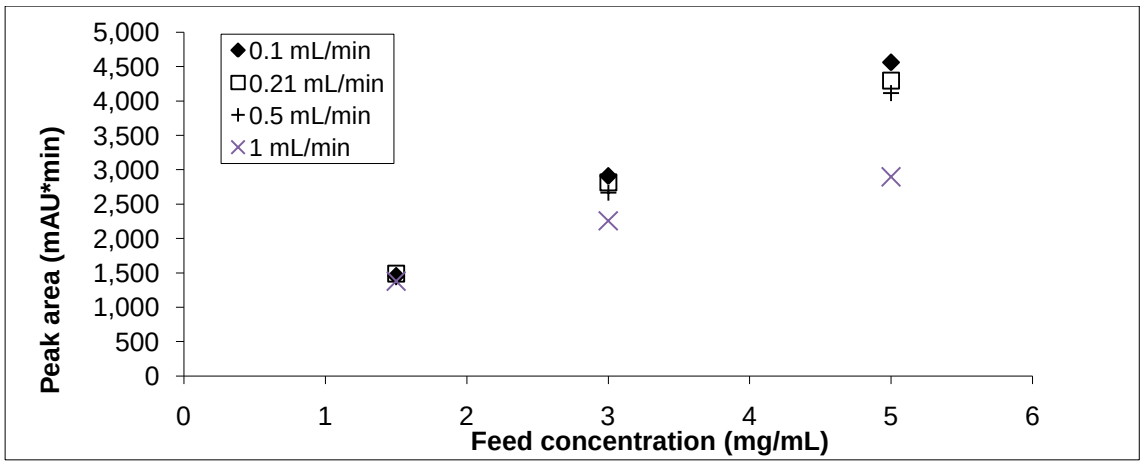

E.5.24 720 deg/hr rotation speed, 1M NaCl concentration, Trial 6, 0.1-1.0 mL/min flow rate

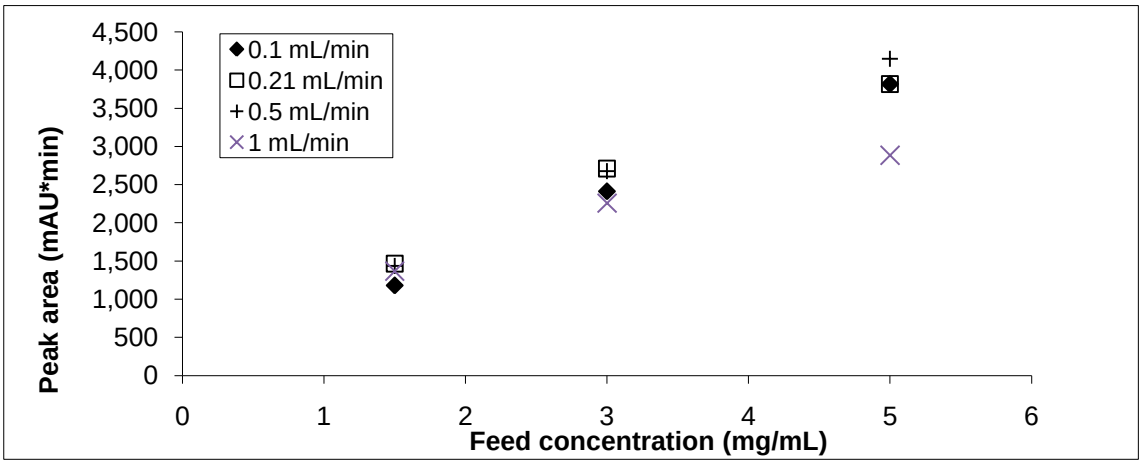

E.5.25 720 deg/hr rotation speed, 1M NaCl concentration, Trial 7, 0.1-1.0 mL/min flow rate

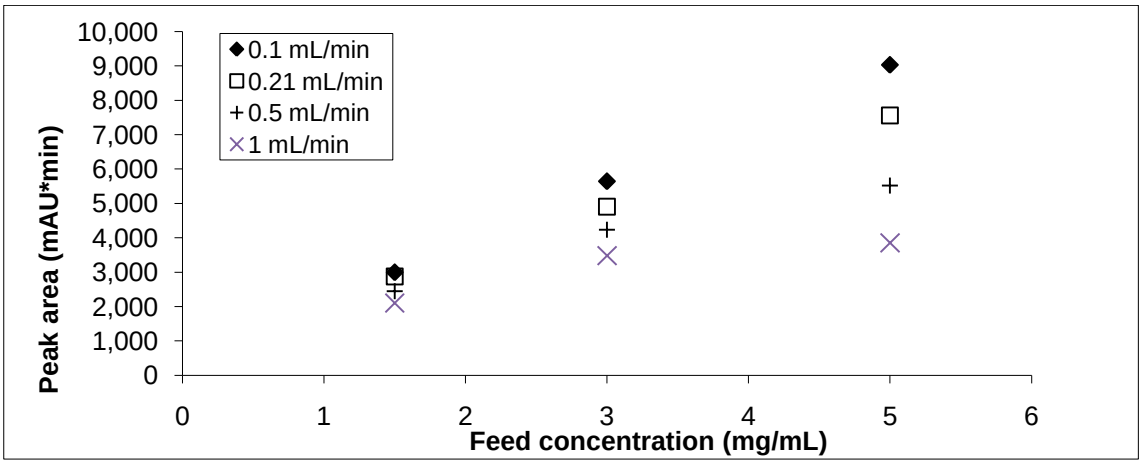

E.5.26 720 deg/hr rotation speed, 1M NaCl concentration, Trial 8, 0.1-1.0 mL/min flow rate

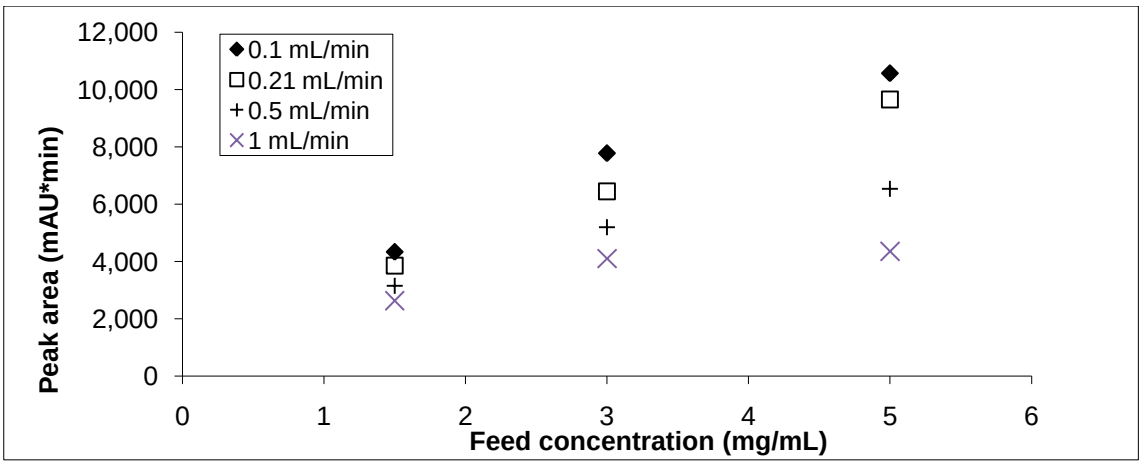

E.5.27 720 deg/hr rotation speed, 1M NaCl concentration, Trial 9, 0.1-1.0 mL/min flow rate

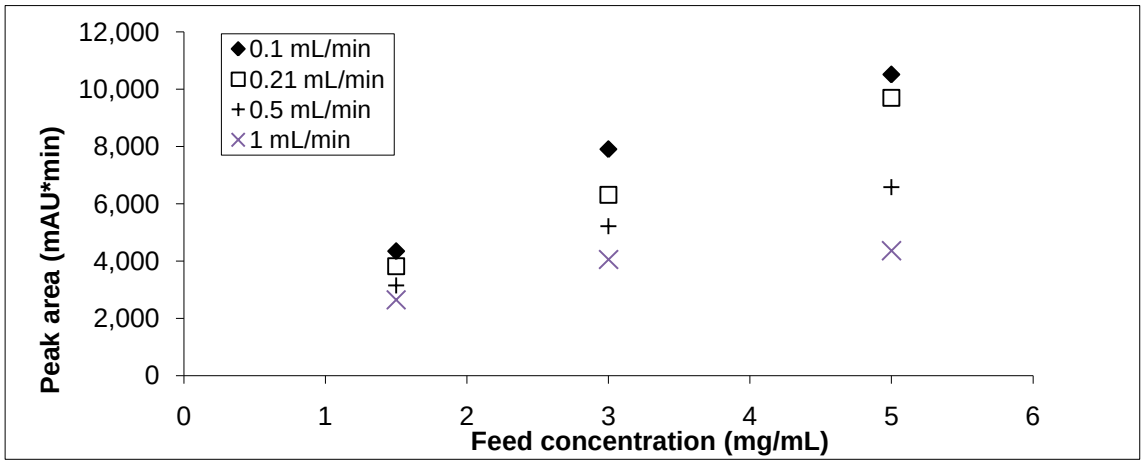

E.6 Elution buffer concentration

E.6.1 180 deg/hr rotation speed, 1.5 mg/mL BSA concentration, Trial 1, 0.1-1.0 mL/min flow rate

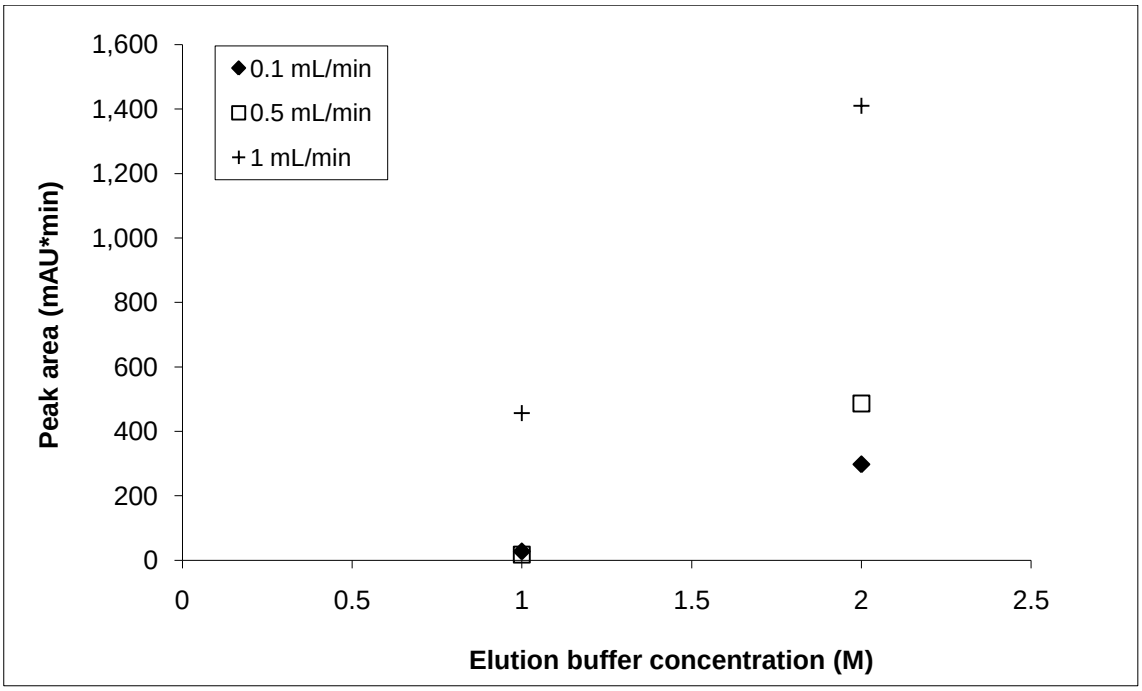

E.6.2 180 deg/hr rotation speed, 1.5 mg/mL BSA concentration, Trial 2, 0.1-1.0 mL/min flow rate

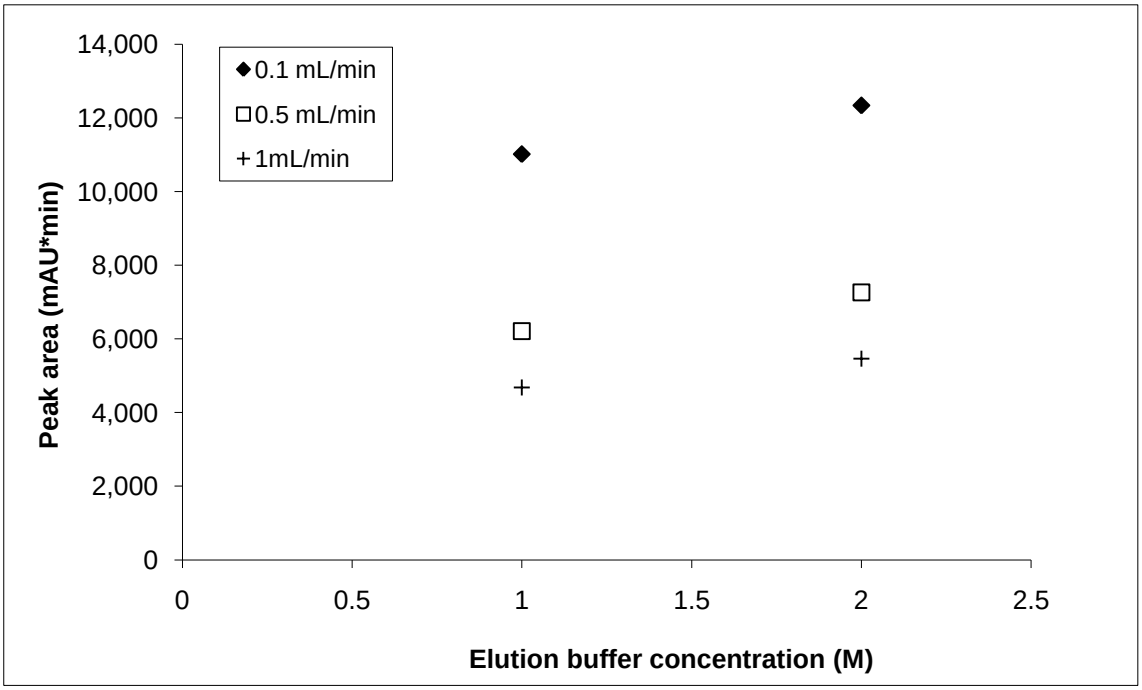

E.6.3 180 deg/hr rotation speed, 1.5 mg/mL BSA concentration, Trial 3, 0.1-0.5 mL/min flow rate

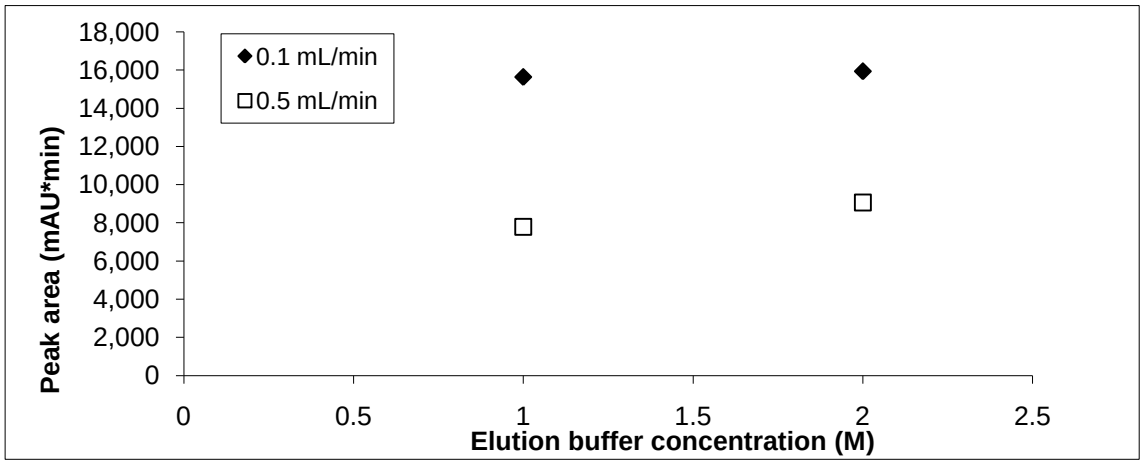

E.6.4 180 deg/hr rotation speed, 1.5 mg/mL BSA concentration, Trial 4, 0.1-1.0 mL/min flow rate

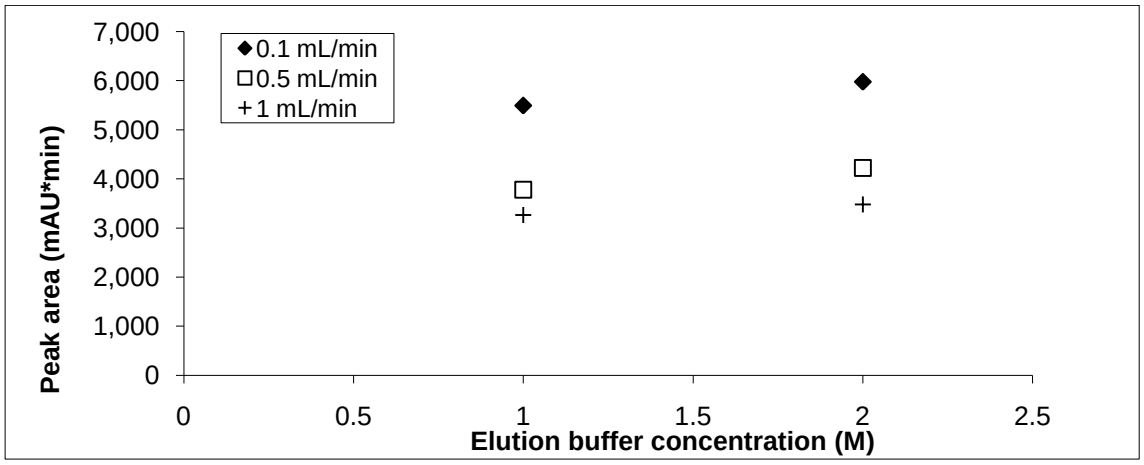

E.6.5 180 deg/hr rotation speed, 1.5 mg/mL BSA concentration, Trial 5, 0.1-1.0 mL/min flow rate

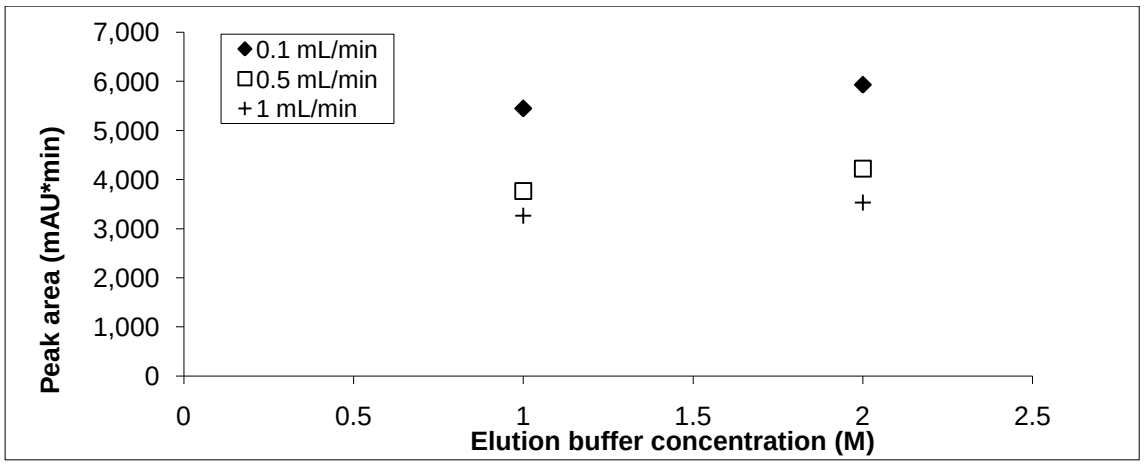

E.6.6 180 deg/hr rotation speed, 1.5 mg/mL BSA concentration, Trial 6, 0.1-1.0 mL/min flow rate

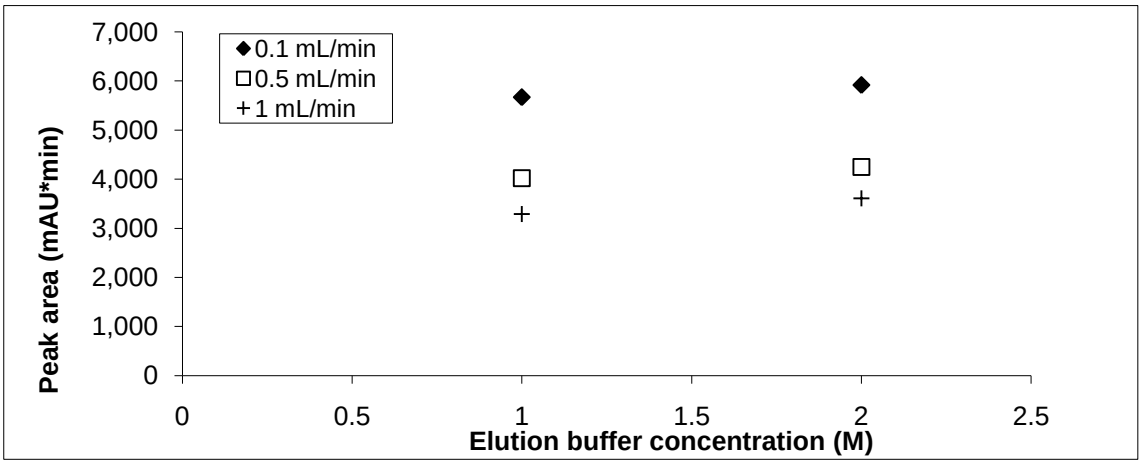

E.6.7 180 deg/hr rotation speed, 1.5 mg/mL BSA concentration, Trial 7, 0.1-1.0 mL/min flow rate

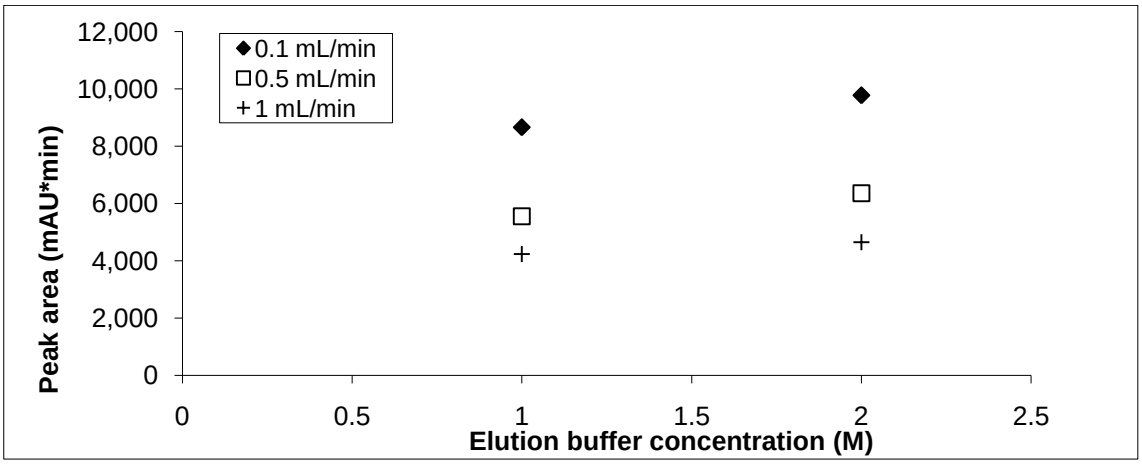

E.6.8 180 deg/hr rotation speed, 1.5 mg/mL BSA concentration, Trial 8, 0.1-1.0 mL/min flow rate

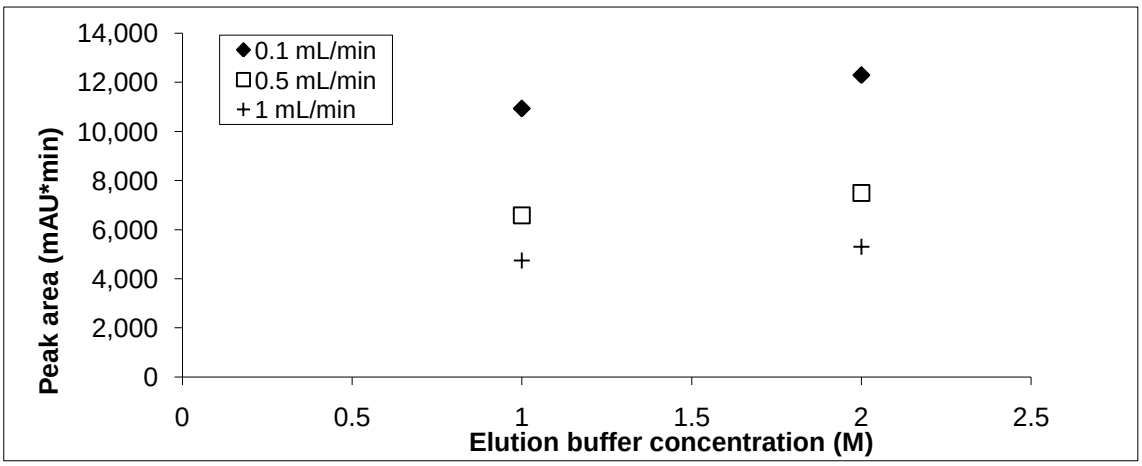

E.6.9 180 deg/hr rotation speed, 1.5 mg/mL BSA concentration, Trial 9, 0.1-1.0 mL/min flow rate

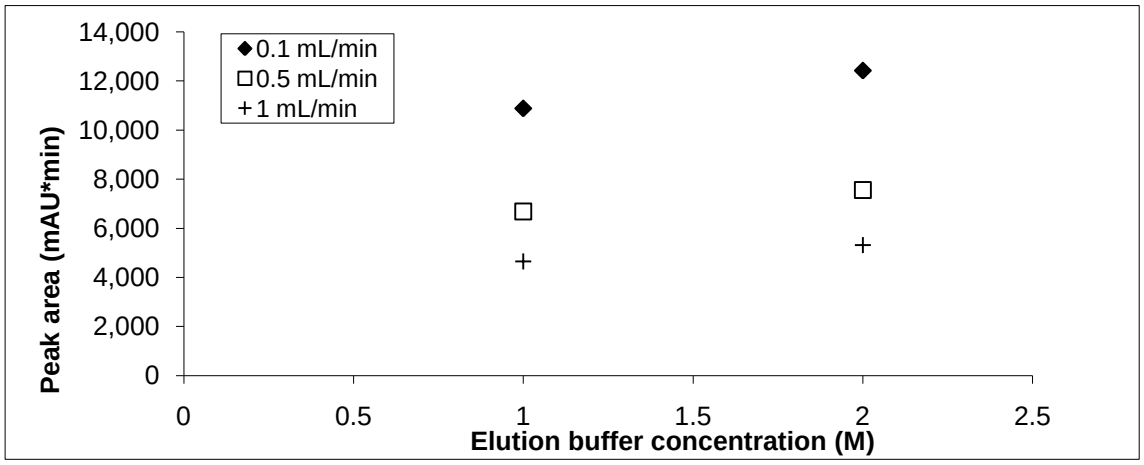

E.6.10 360 deg/hr rotation speed, 1.5 mg/mL BSA concentration, Trial 1, 0.1-1.0 mL/min flow rate

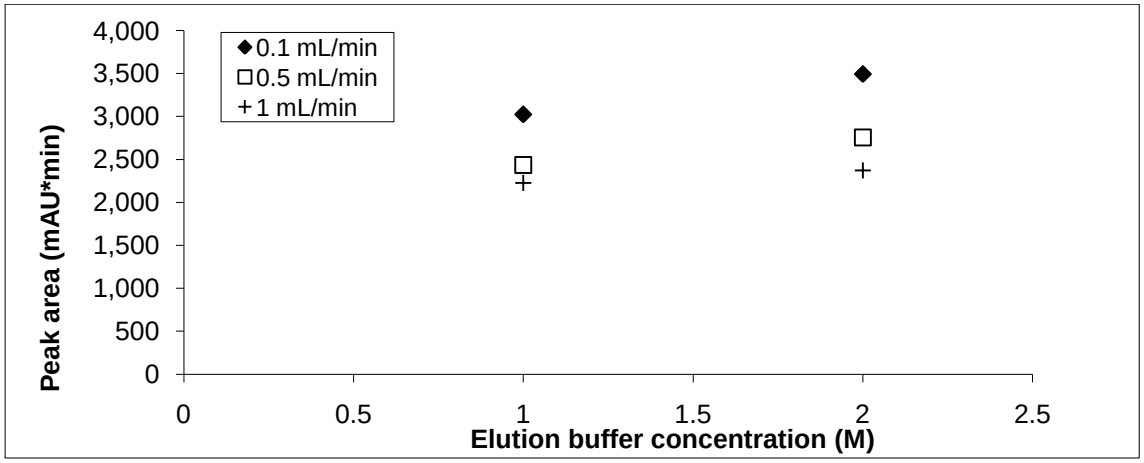

E.6.11 360 deg/hr rotation speed, 1.5 mg/mL BSA concentration, Trial 2, 0.1-1.0 mL/min flow rate

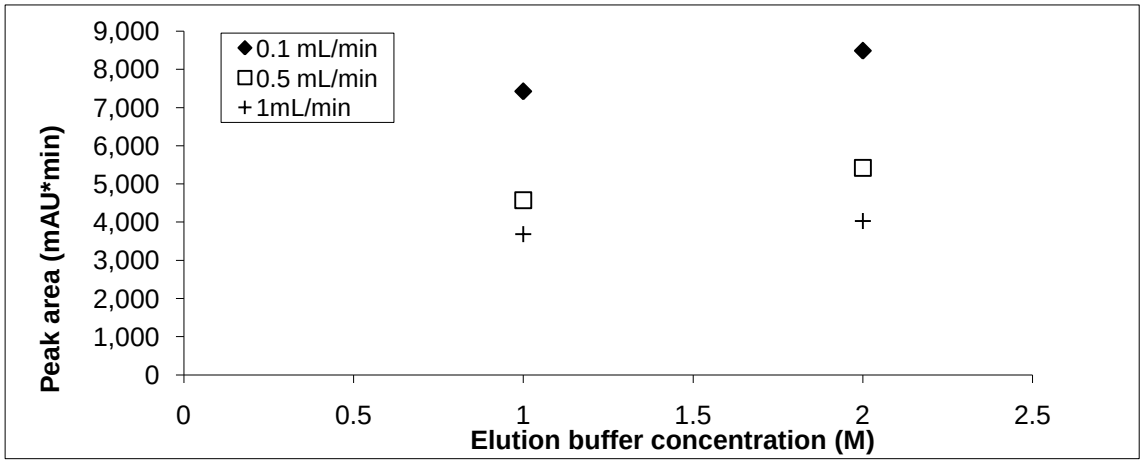

E.6.12 360 deg/hr rotation speed, 1.5 mg/mL BSA concentration, Trial 3, 0.1-1.0 mL/min flow rate

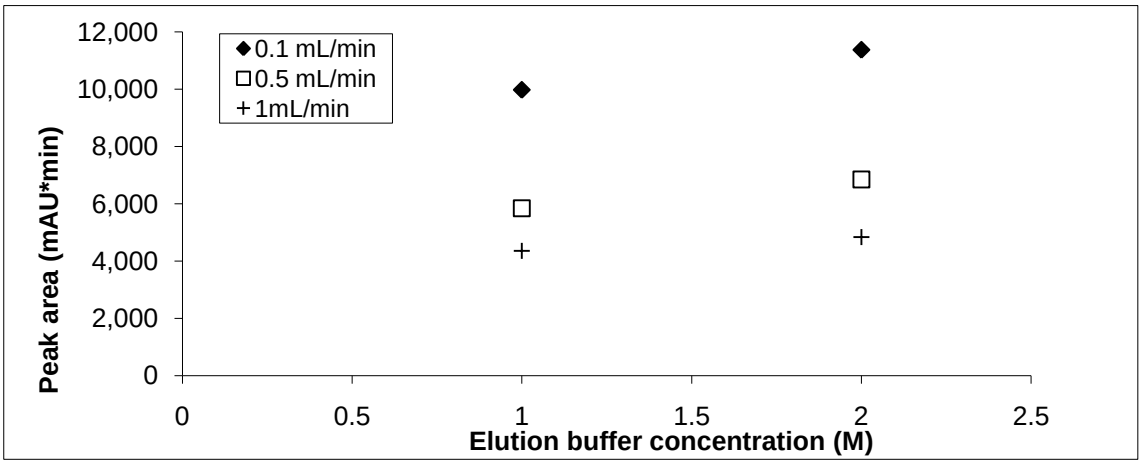

E.6.13 360 deg/hr rotation speed, 1.5 mg/mL BSA concentration, Trial 4, 0.1-1.0 mL/min flow rate

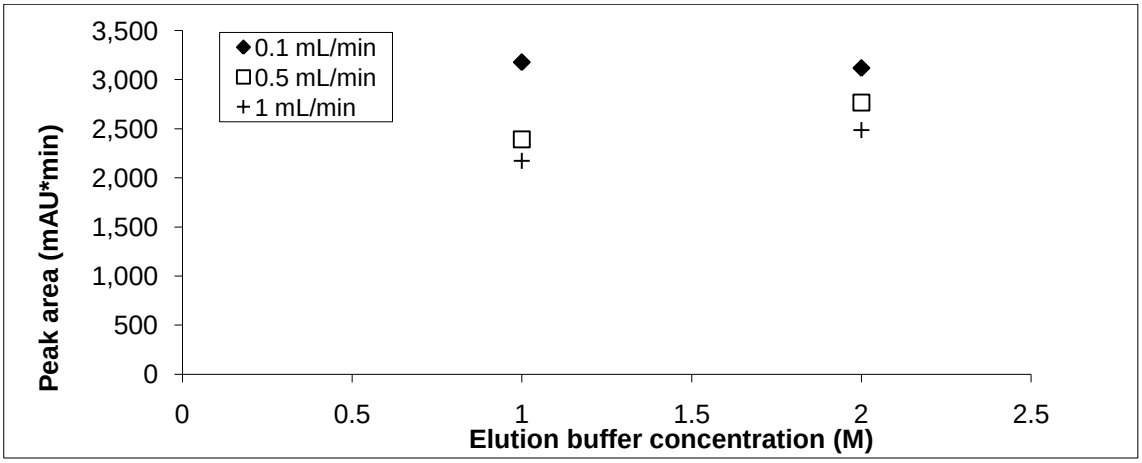

E.6.14 360 deg/hr rotation speed, 1.5 mg/mL BSA concentration, Trial 5, 0.1-1.0 mL/min flow rate

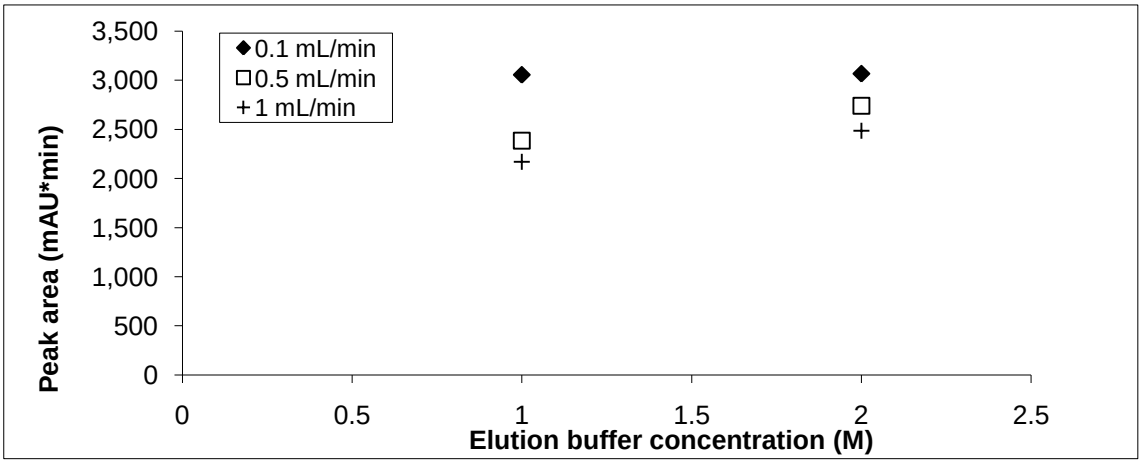

E.6.15 360 deg/hr rotation speed, 1.5 mg/mL BSA concentration, Trial 6, 0.1-1.0 mL/min flow rate

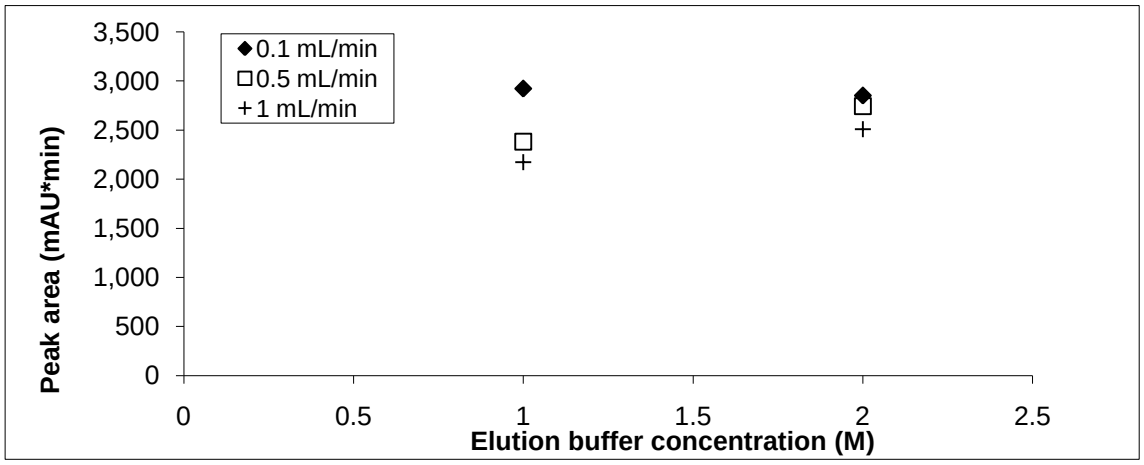

E.6.16 360 deg/hr rotation speed, 1.5 mg/mL BSA concentration, Trial 7, 0.1-1.0 mL/min flow rate

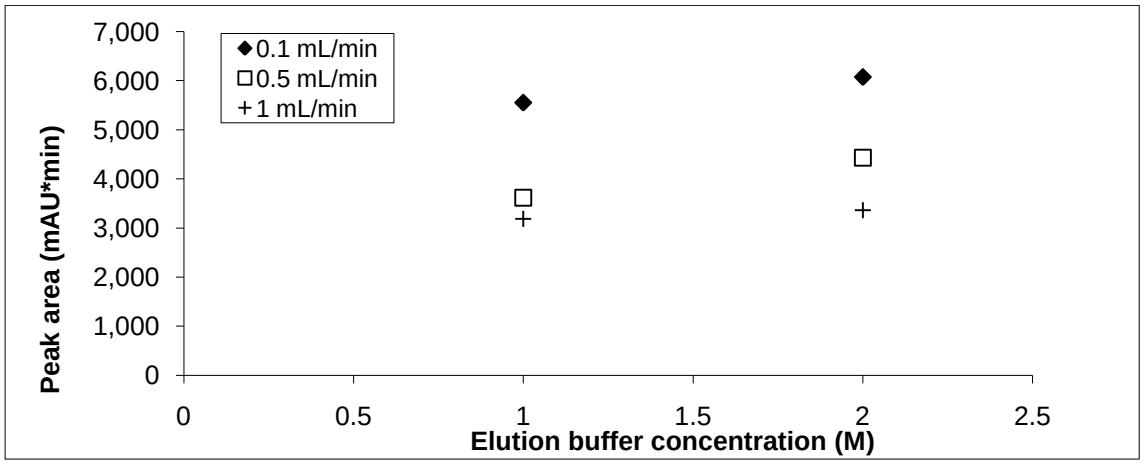

E.6.17 360 deg/hr rotation speed, 1.5 mg/mL BSA concentration, Trial 8, 0.1-1.0 mL/min flow rate

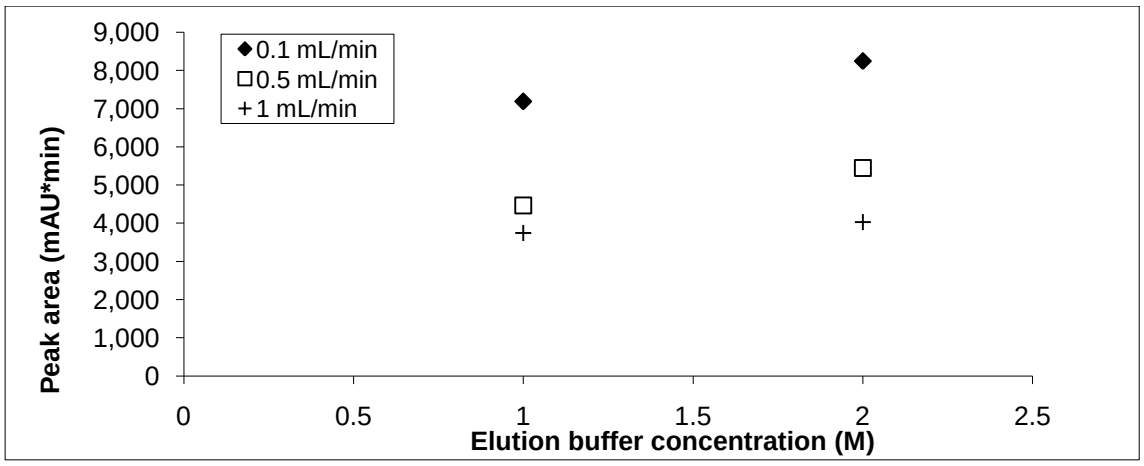

E.6.18 360 deg/hr rotation speed, 1.5 mg/mL BSA concentration, Trial 9, 0.1-1.0 mL/min flow rate

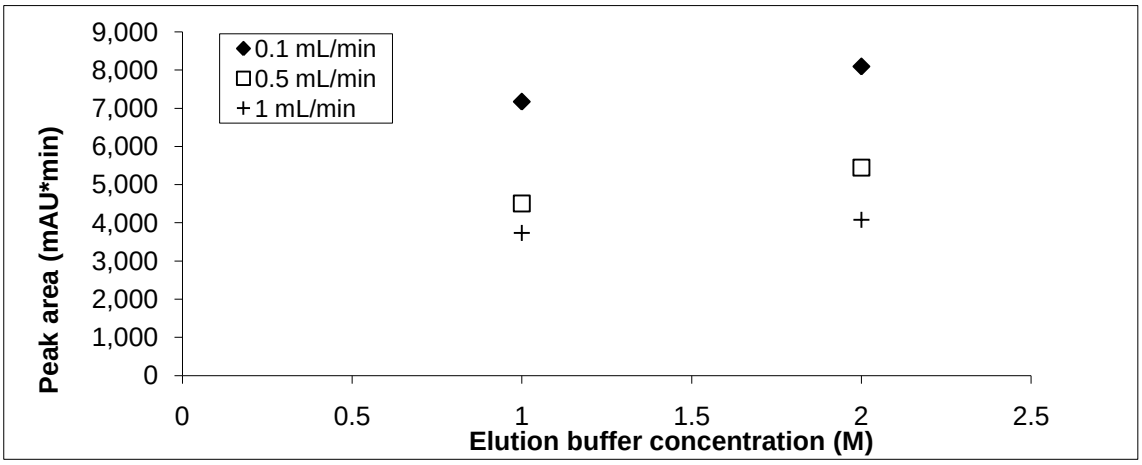

E.6.19 720 deg/hr rotation speed, 1.5 mg/mL BSA concentration, Trial 1, 0.1-1.0 mL/min flow rate

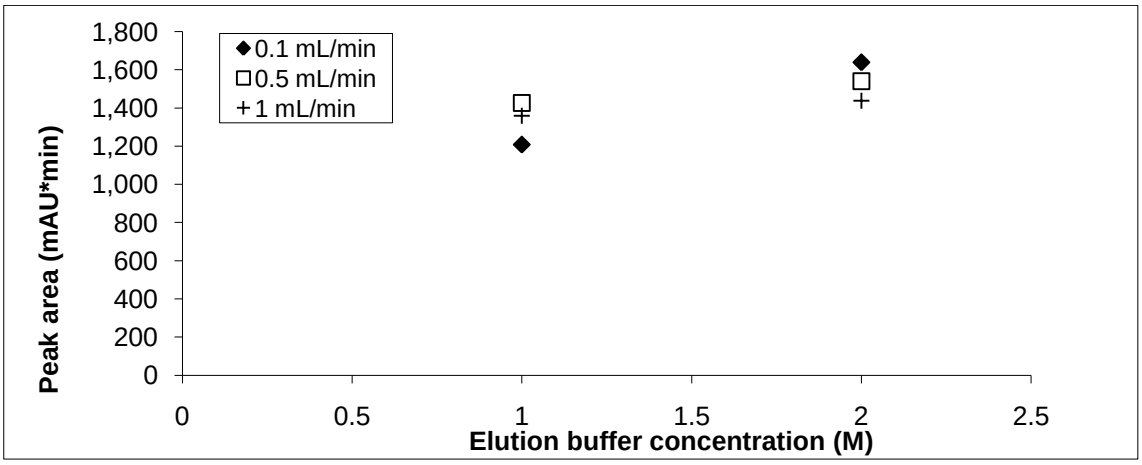

E.6.20 720 deg/hr rotation speed, 1.5 mg/mL BSA concentration, Trial 2, 0.1-1.0 mL/min flow rate

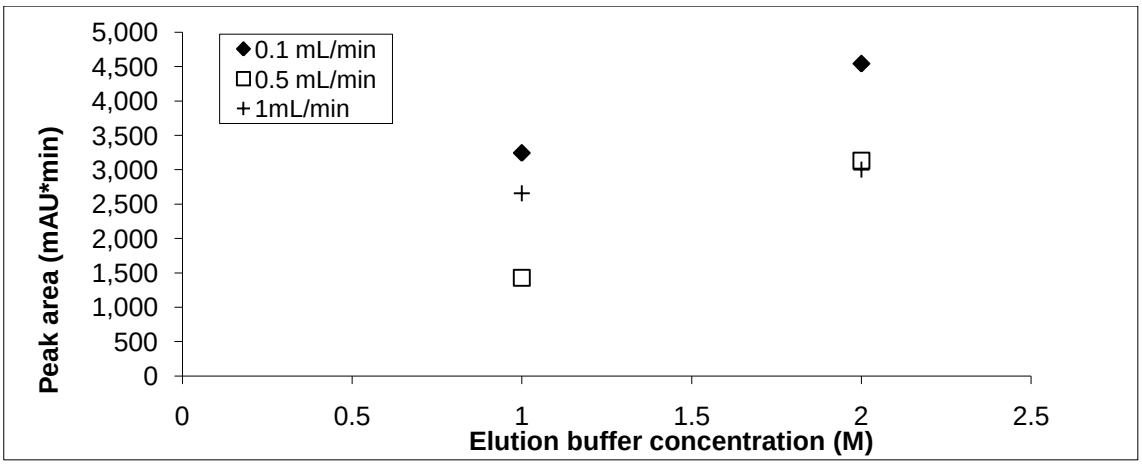

E.6.21 720 deg/hr rotation speed, 1.5 mg/mL BSA concentration, Trial 3, 0.1-1.0 mL/min flow rate

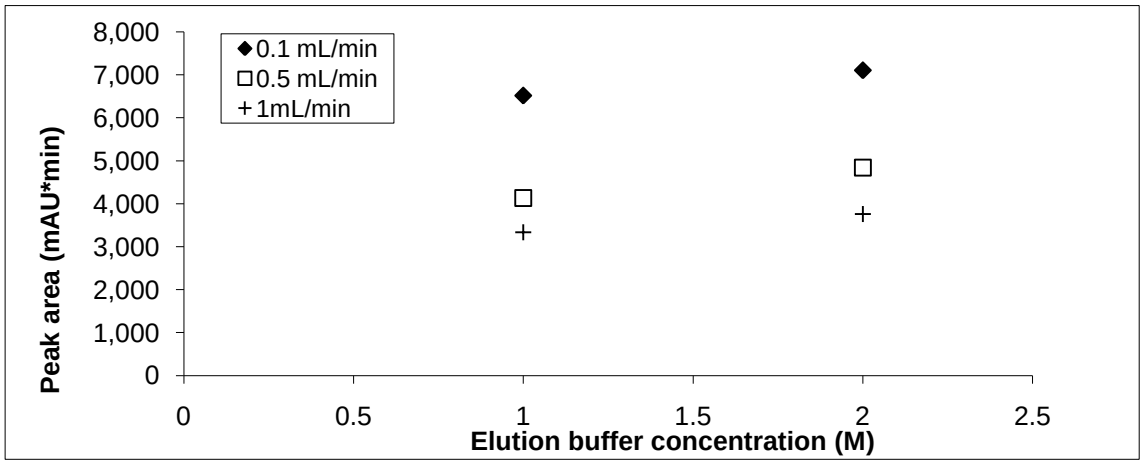

E.6.22 720 deg/hr rotation speed, 1.5 mg/mL BSA concentration, Trial 4, 0.1-1.0 mL/min flow rate

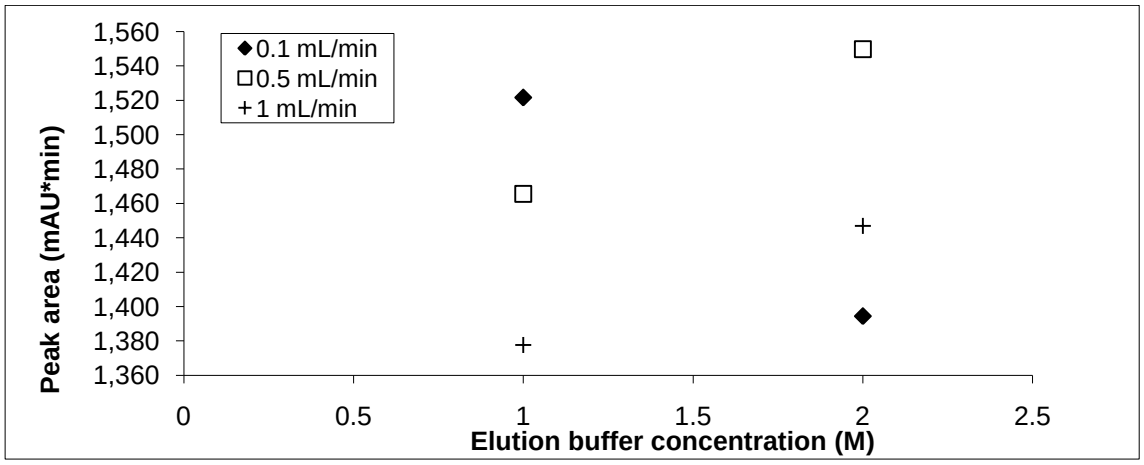

E.6.23 720 deg/hr rotation speed, 1.5 mg/mL BSA concentration, Trial 5, 0.1-1.0 mL/min flow rate

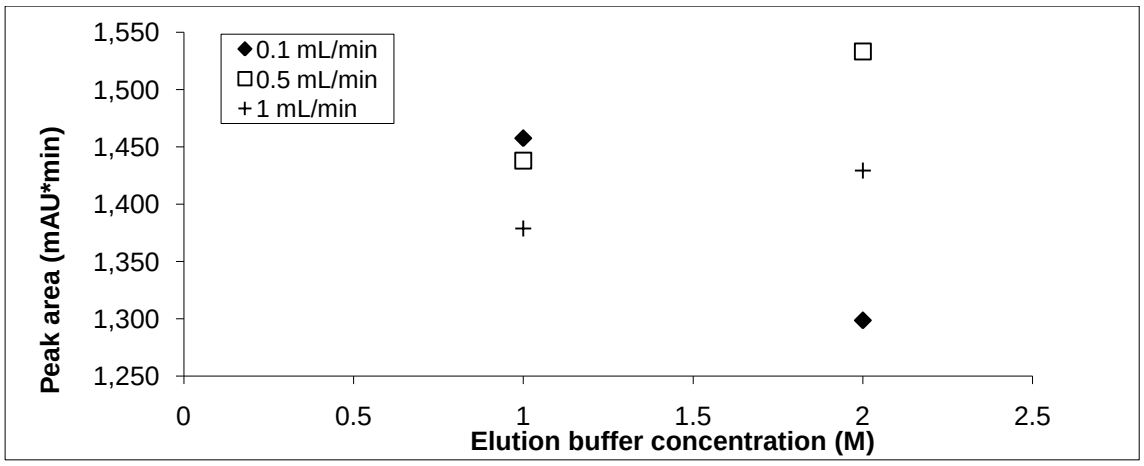

E.6.24 720 deg/hr rotation speed, 1.5 mg/mL BSA concentration, Trial 6, 0.1-1.0 mL/min flow rate

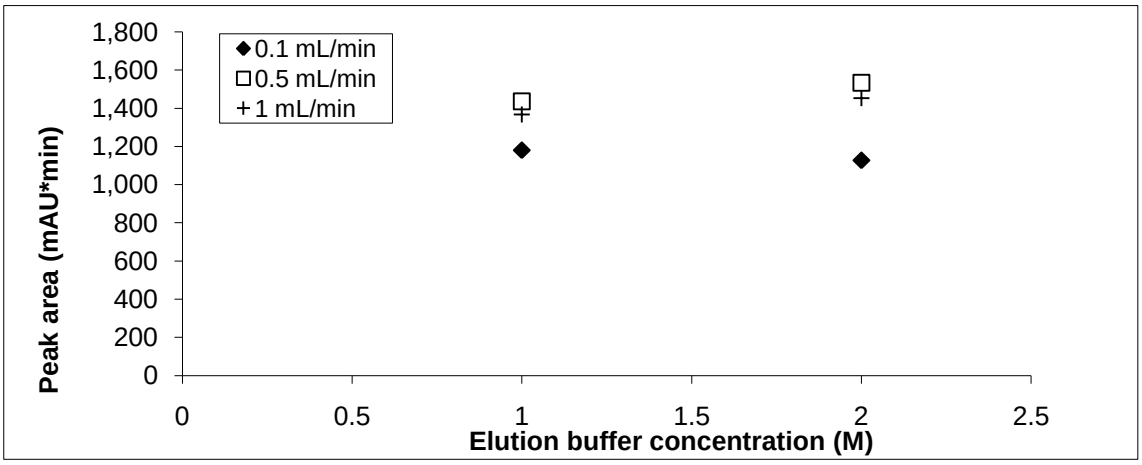

E.6.25 720 deg/hr rotation speed, 1.5 mg/mL BSA concentration, Trial 7, 0.1-1.0 mL/min flow rate

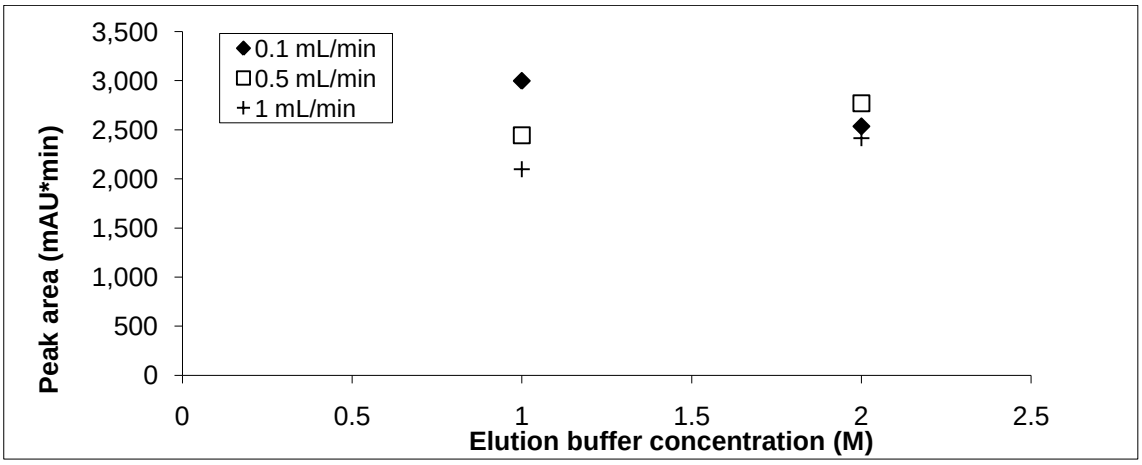

E.6.26 720 deg/hr rotation speed, 1.5 mg/mL BSA concentration, Trial 8, 0.1-1.0 mL/min flow rate

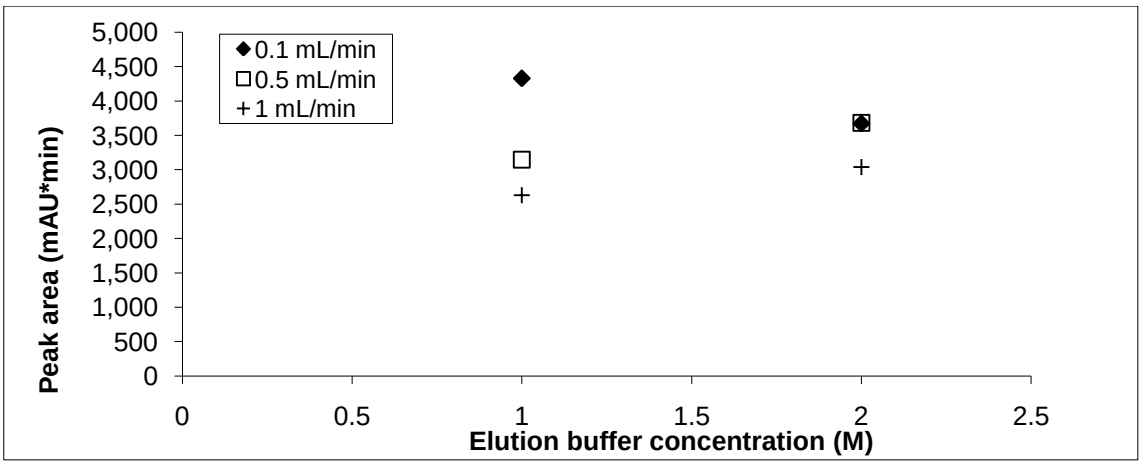

E.6.27 720 deg/hr rotation speed, 1.5 mg/mL BSA concentration, Trial 9, 0.1-1.0 mL/min flow rate

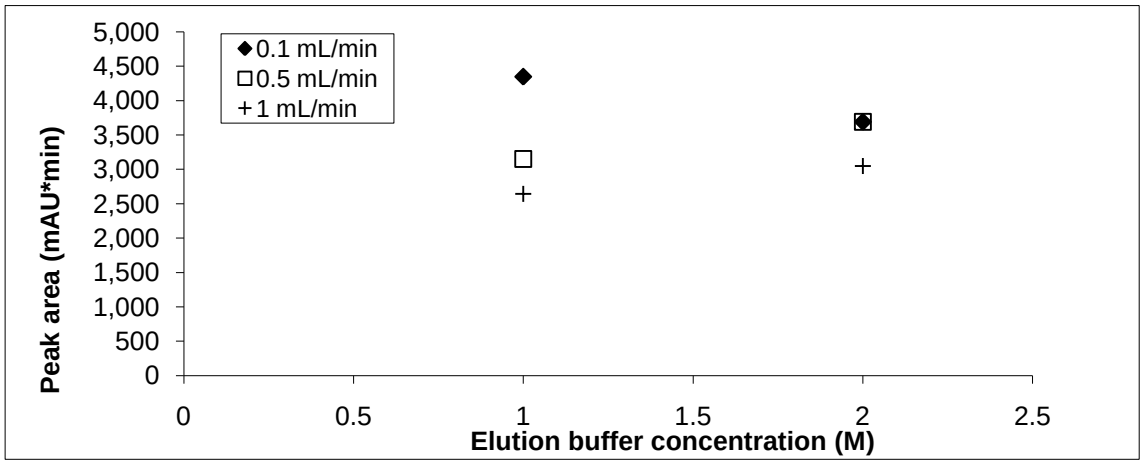

Appendix F Loading Zone Peak Area

F.1 Loading sections

F.1.1 180 deg/hr rotation speed, 1.5 mg/mL BSA concentration, 1M NaCl concentration, 0.1-1.0 mL/min flow rate

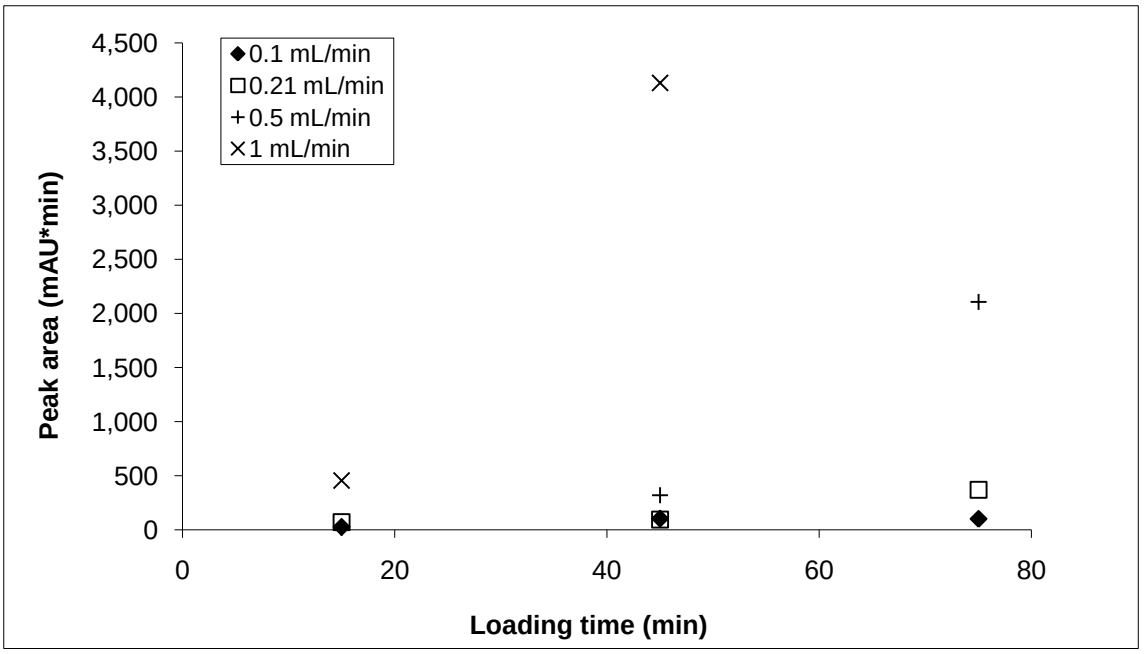

F.1.2 360 deg/hr rotation speed, 1.5 mg/mL BSA concentration, 1M NaCl concentration, 0.1-1.0 mL/min flow rate

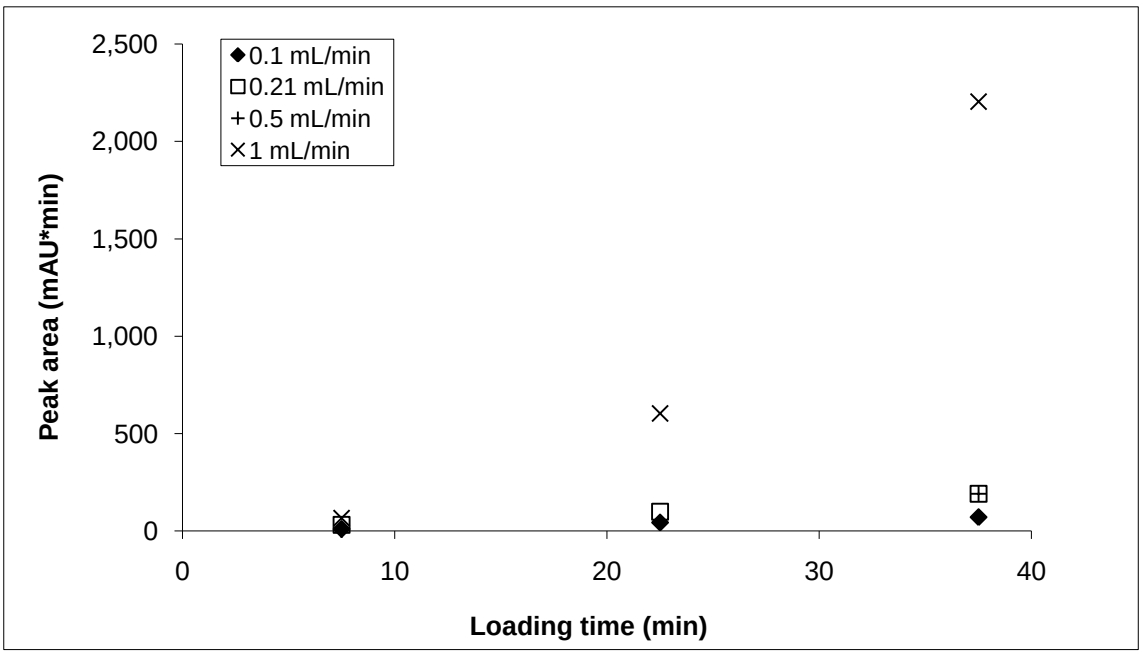

F.1.3 720 deg/hr rotation speed, 1.5 mg/mL BSA concentration, 1M NaCl concentration, 0.1-1.0 mL/min flow rate

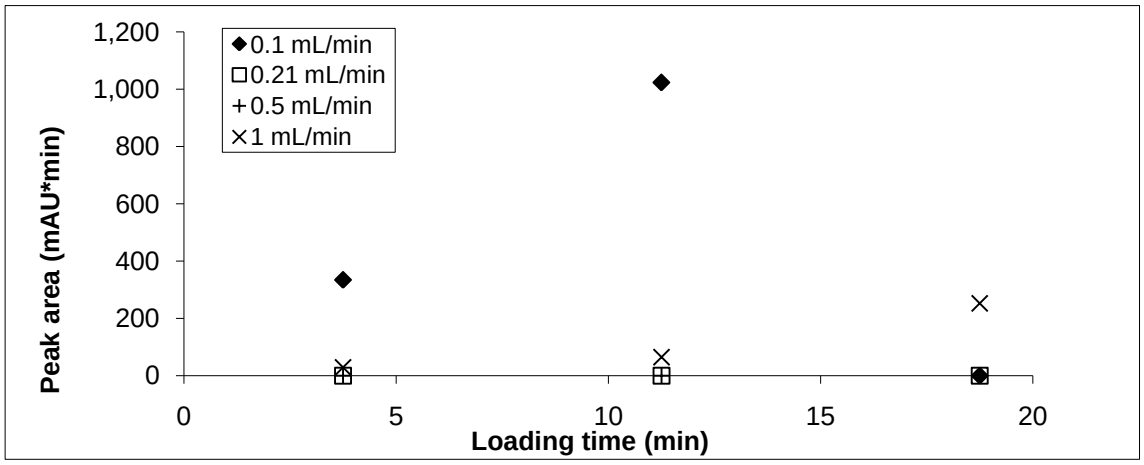

F.1.4 180 deg/hr rotation speed, 3 mg/mL BSA concentration, 1M NaCl concentration, 0.1-1.0 mL/min flow rate

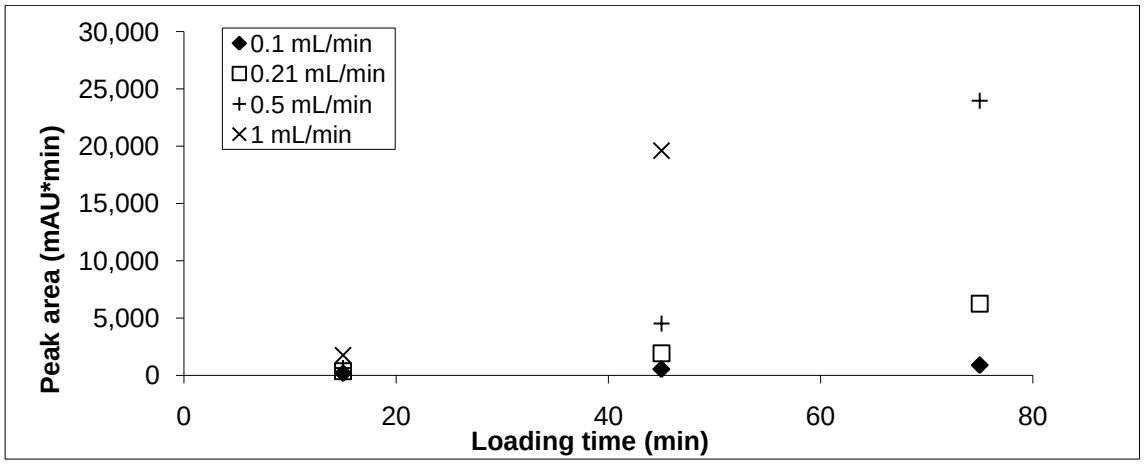

F.1.5 360 deg/hr rotation speed, 3 mg/mL BSA concentration, 1M NaCl concentration, 0.1-1.0 mL/min flow rate

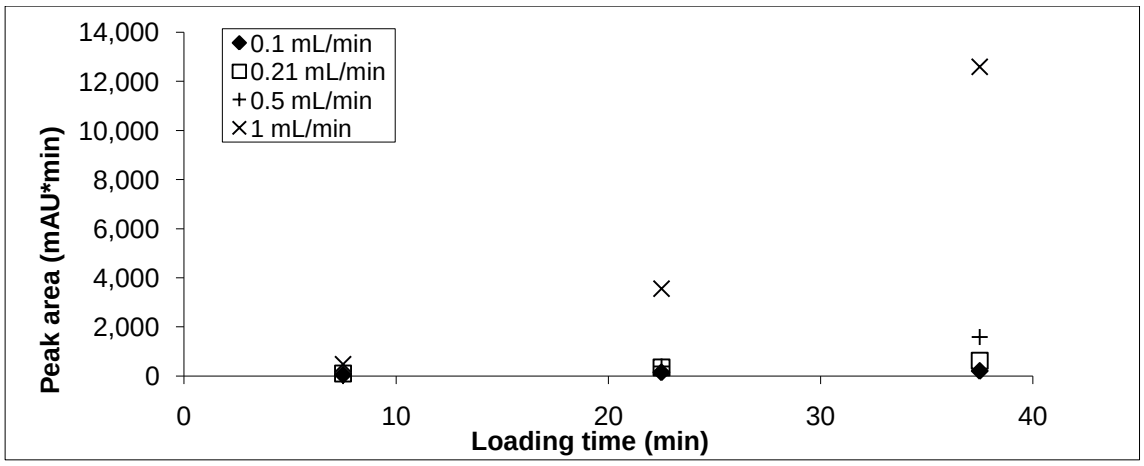

F.1.6 720 deg/hr rotation speed, 3 mg/mL BSA concentration, 1M NaCl concentration, 0.1-1.0 mL/min flow rate

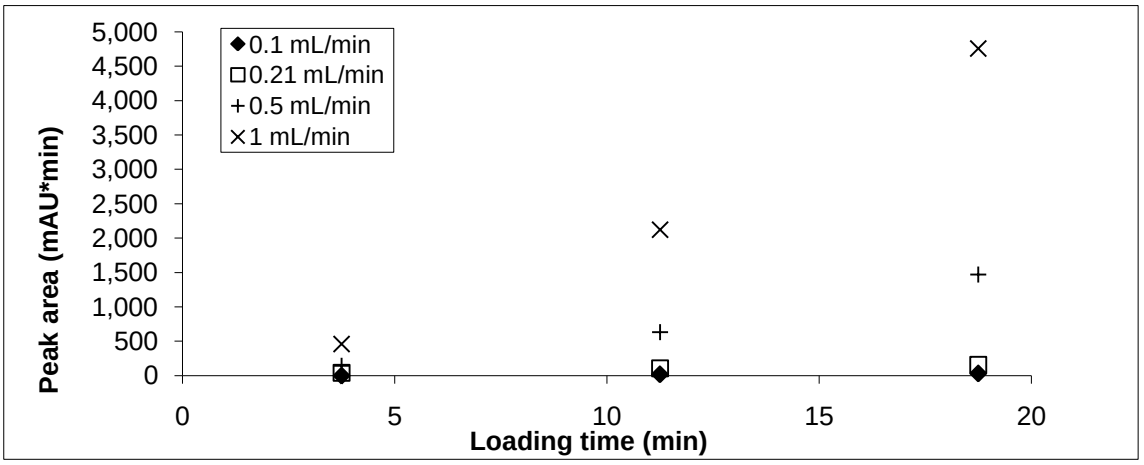

F.1.7 180 deg/hr rotation speed, 5 mg/mL BSA concentration, 1M NaCl concentration, 0.1-1.0 mL/min flow rate

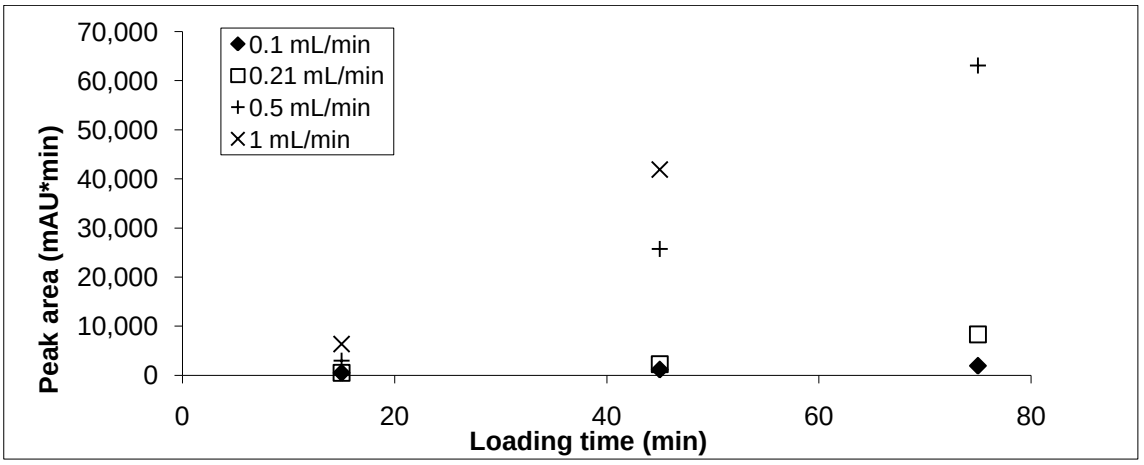

F.1.8 360 deg/hr rotation speed, 5 mg/mL BSA concentration, 1M NaCl concentration, 0.1-1.0 mL/min flow rate

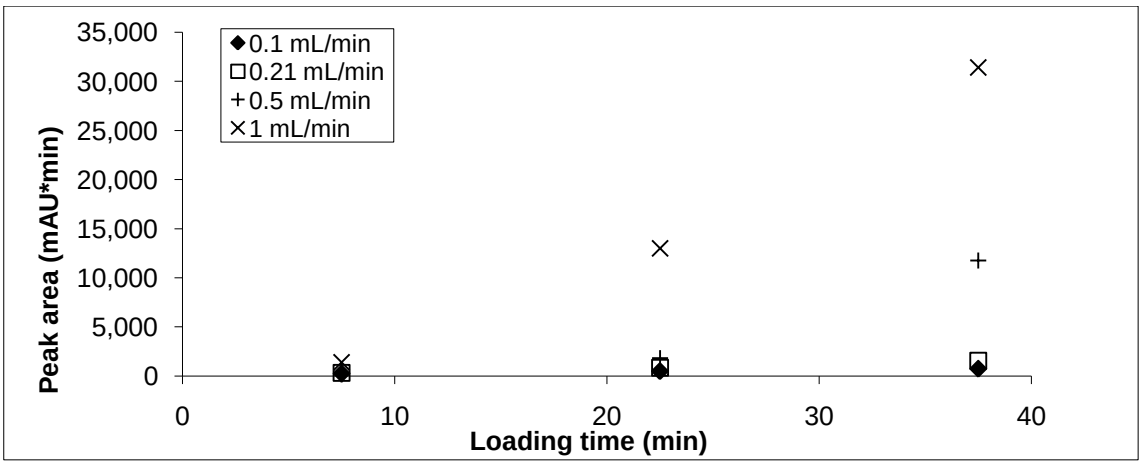

F.1.9 720 deg/hr rotation speed, 5 mg/mL BSA concentration, 1M NaCl concentration, 0.1-1.0 mL/min flow rate

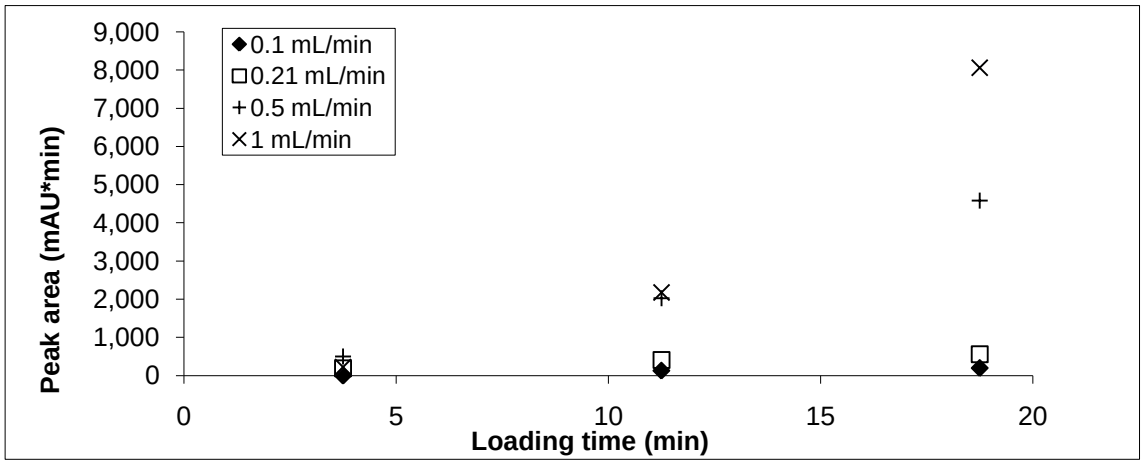

F.1.10 180 deg/hr rotation speed, 1.5 mg/mL BSA concentration, 2M NaCl concentration, 0.1-1.0 mL/min flow rate

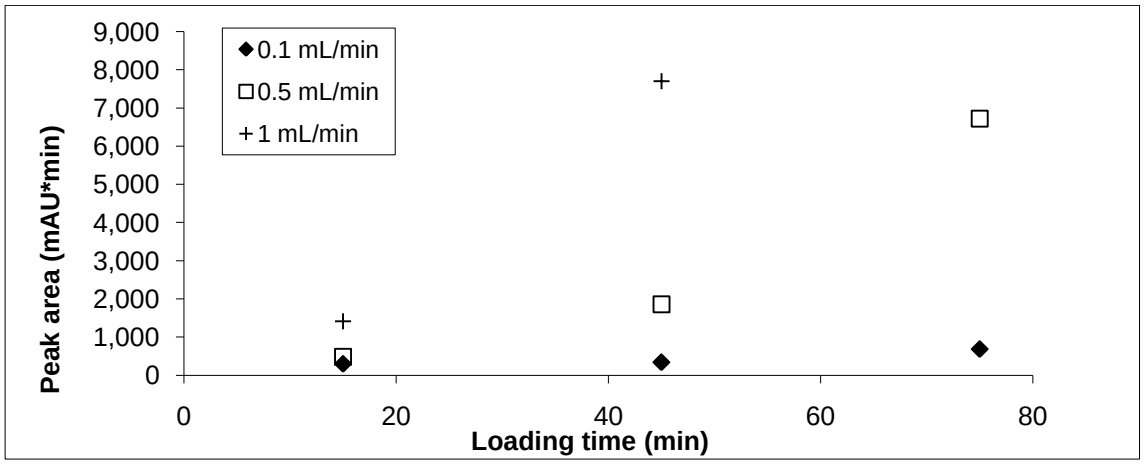

F.1.11 360 deg/hr rotation speed, 1.5 mg/mL BSA concentration, 2M NaCl concentration, 0.1-1.0 mL/min flow rate

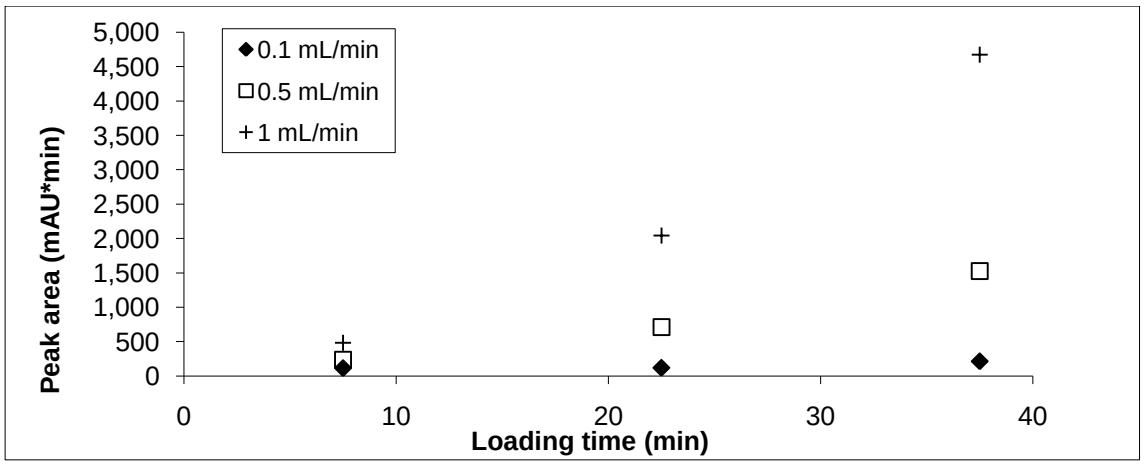

F.1.12 720 deg/hr rotation speed, 1.5 mg/mL BSA concentration, 2M NaCl concentration, 0.1-1.0 mL/min flow rate

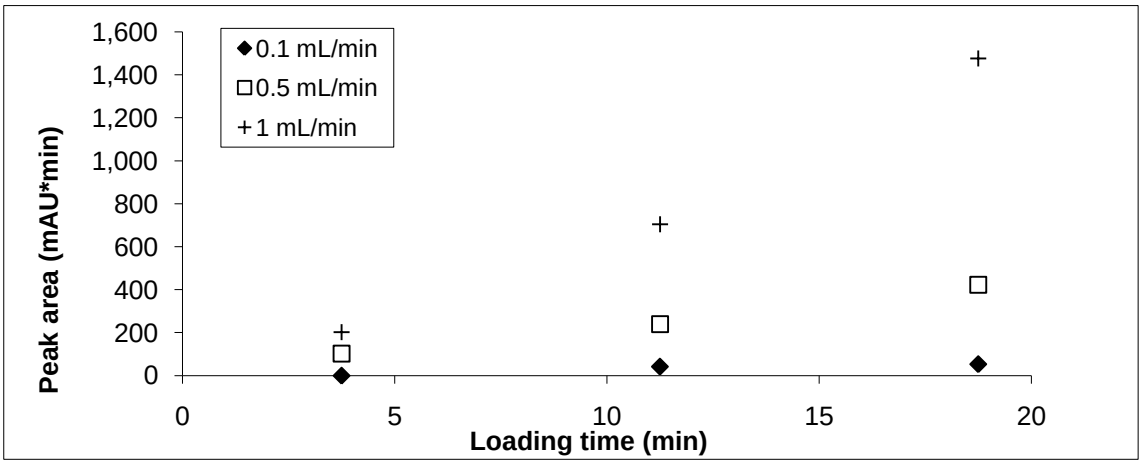

F.2 Elution sections

F.2.1 180 deg/hr rotation speed, 1.5 mg/mL BSA concentration, 1M NaCl concentration, 0.1-1.0 mL/min flow rate

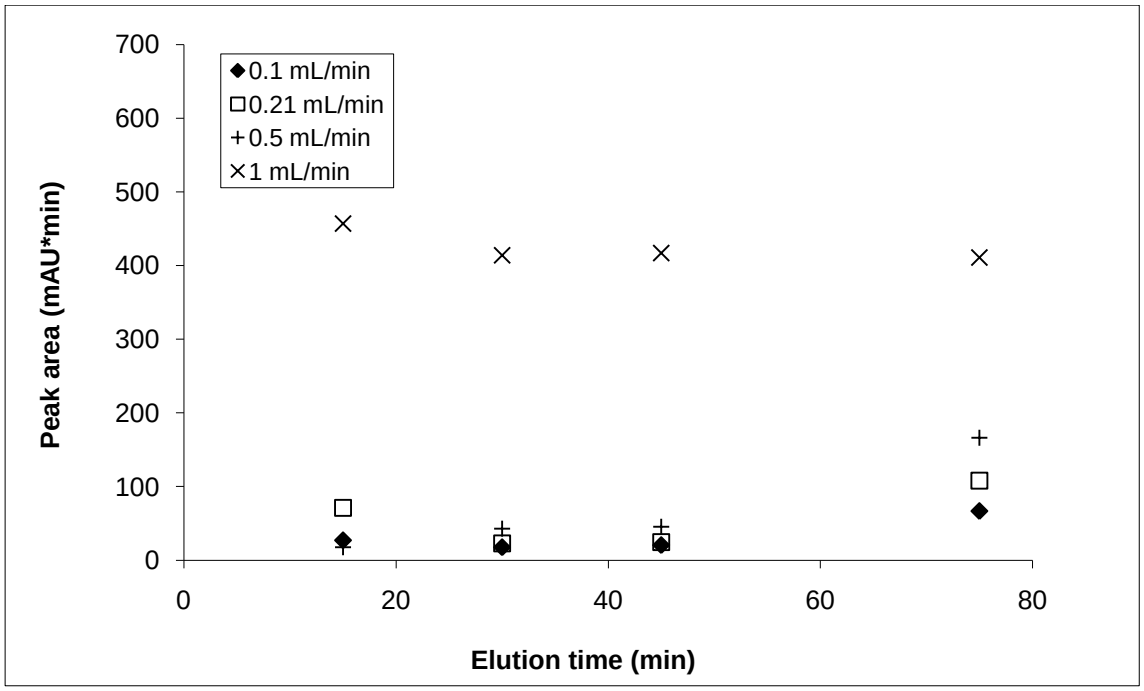

F.2.2 360 deg/hr rotation speed, 1.5 mg/mL BSA concentration, 1M NaCl concentration, 0.1-1.0 mL/min flow rate

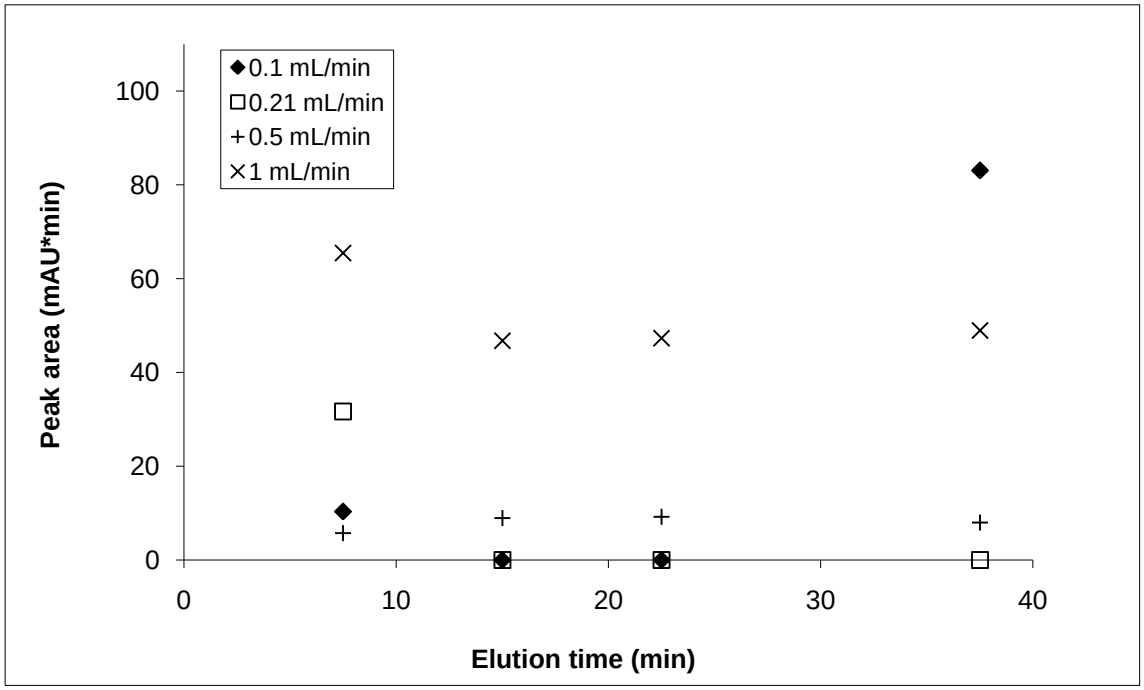

F.2.3 720 deg/hr rotation speed, 1.5 mg/mL BSA concentration, 1M NaCl concentration, 0.1-1.0 mL/min flow rate

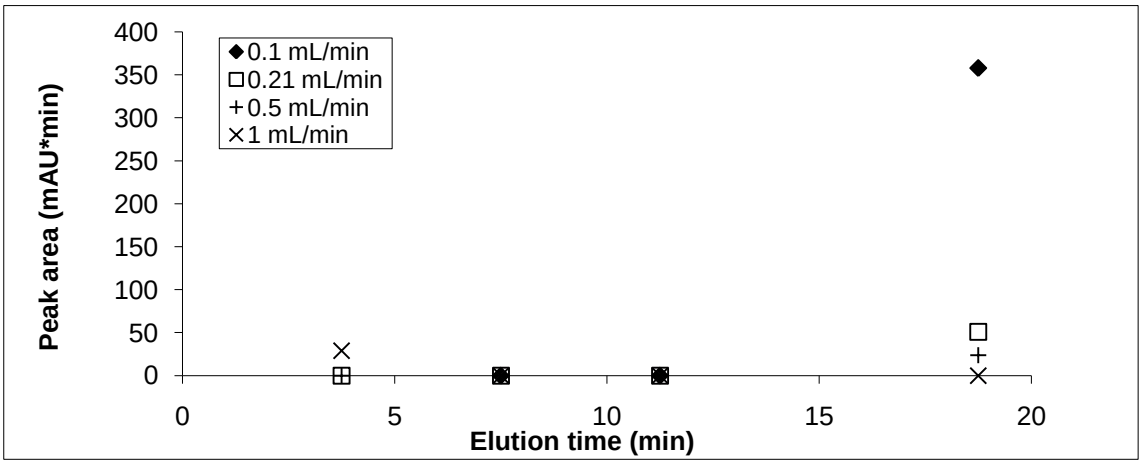

F.2.4 180 deg/hr rotation speed, 3 mg/mL BSA concentration, 1M NaCl concentration, 0.1-1.0 mL/min flow rate

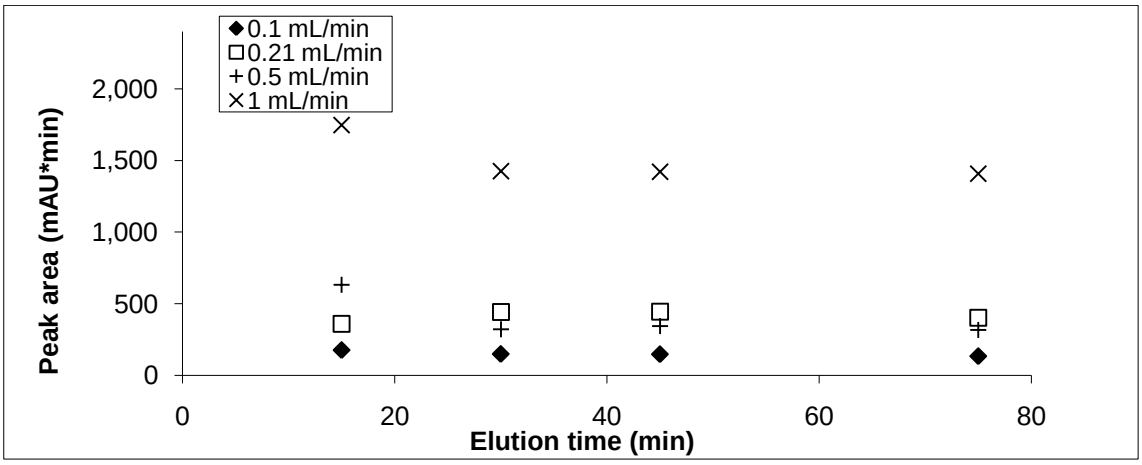

F.2.5 360 deg/hr rotation speed, 3 mg/mL BSA concentration, 1M NaCl concentration, 0.1-1.0 mL/min flow rate

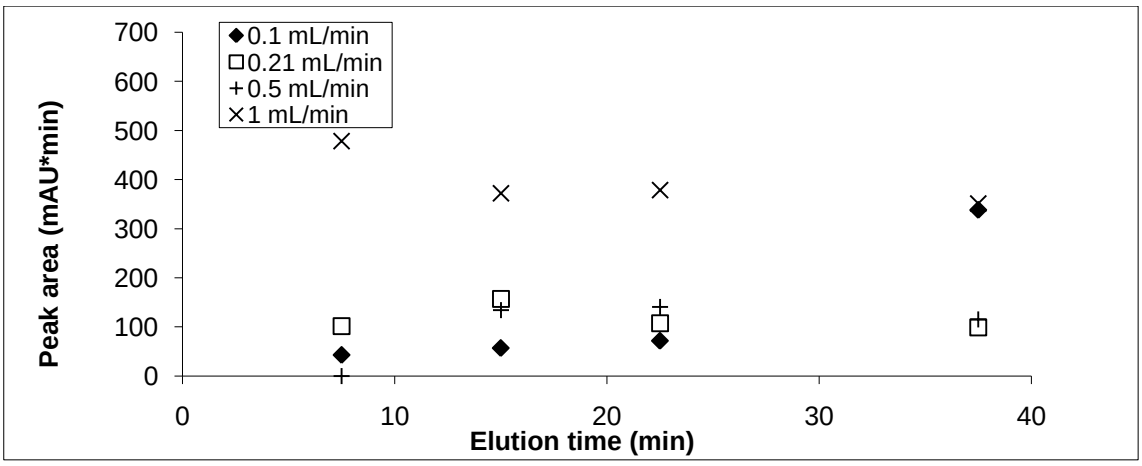

F.2.6 720 deg/hr rotation speed, 3 mg/mL BSA concentration, 1M NaCl concentration, 0.1-1.0 mL/min flow rate

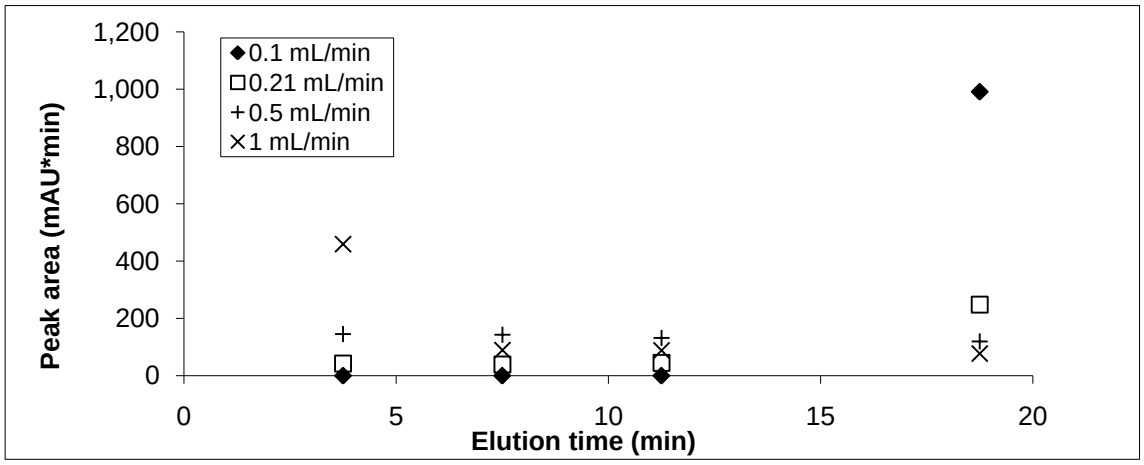

F.2.7 180 deg/hr rotation speed, 5 mg/mL BSA concentration, 1M NaCl concentration, 0.1-1.0 mL/min flow rate

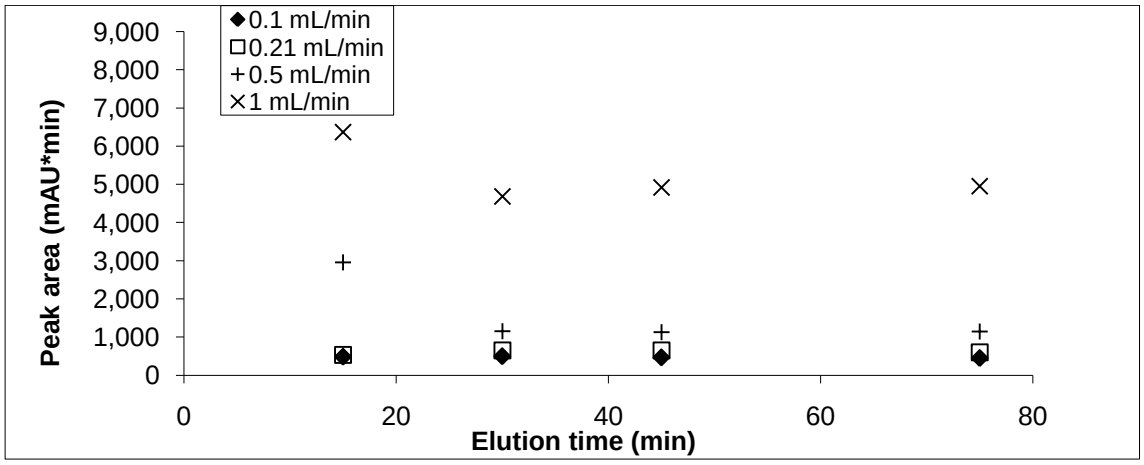

F.2.8 360 deg/hr rotation speed, 5 mg/mL BSA concentration, 1M NaCl concentration, 0.1-1.0 mL/min flow rate

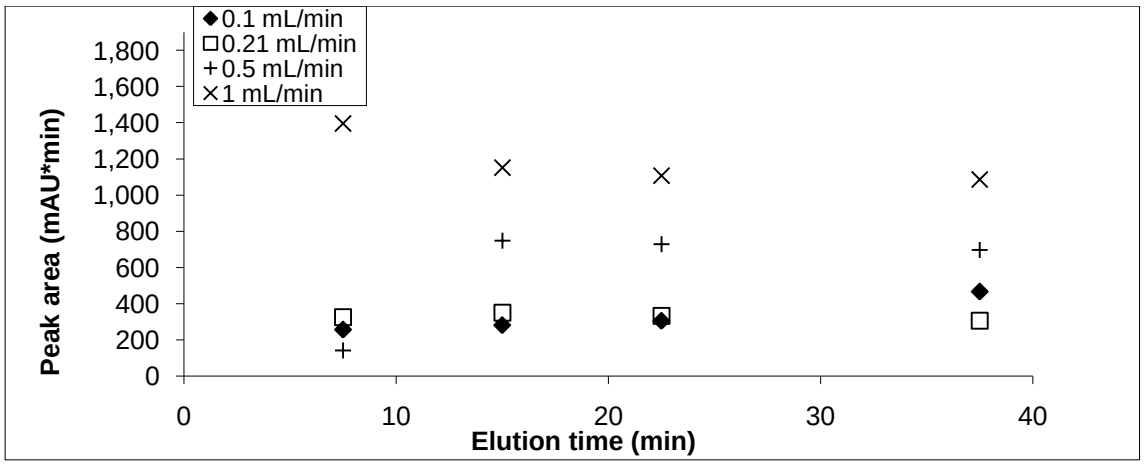

F.2.9 720 deg/hr rotation speed, 5 mg/mL BSA concentration, 1M NaCl concentration, 0.1-1.0 mL/min flow rate

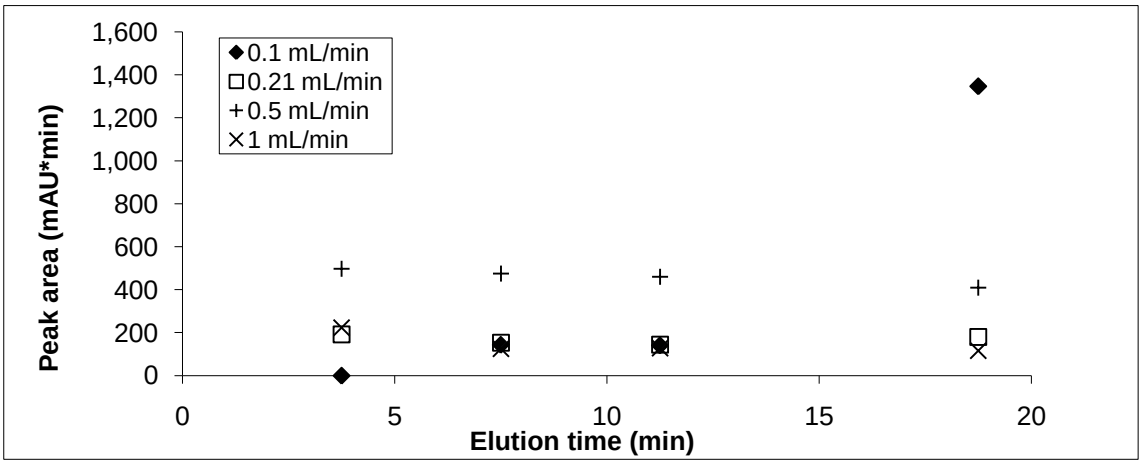

F.2.10 180 deg/hr rotation speed, 1.5 mg/mL BSA concentration, 2M NaCl concentration, 0.1-1.0 mL/min flow rate

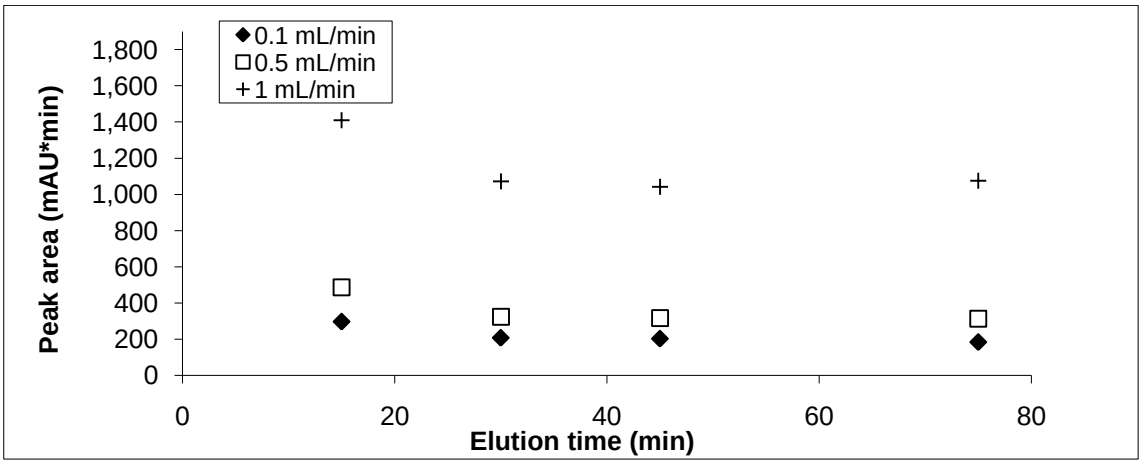

F.2.11 360 deg/hr rotation speed, 1.5 mg/mL BSA concentration, 2M NaCl concentration, 0.1-1.0 mL/min flow rate

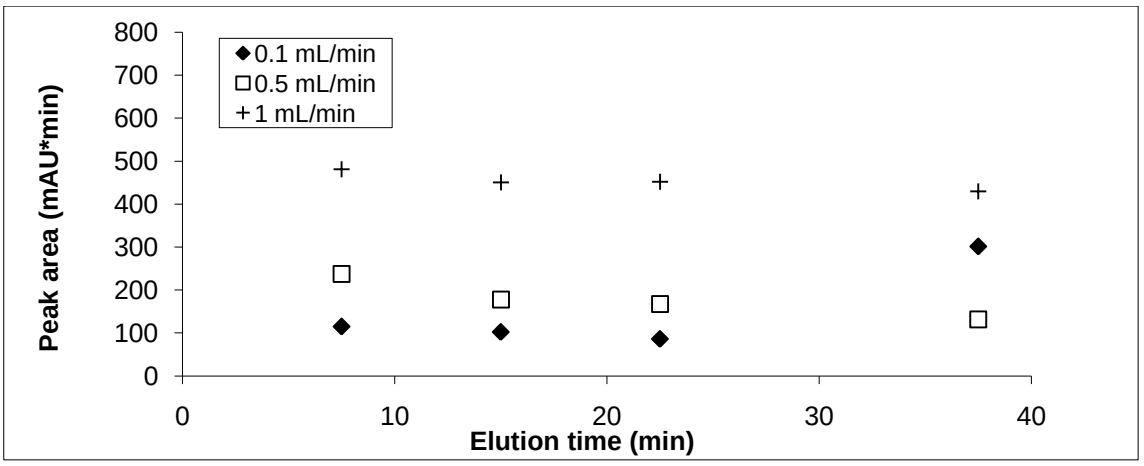

F.2.12 720 deg/hr rotation speed, 1.5 mg/mL BSA concentration, 2M NaCl concentration, 0.1-1.0 mL/min flow rate

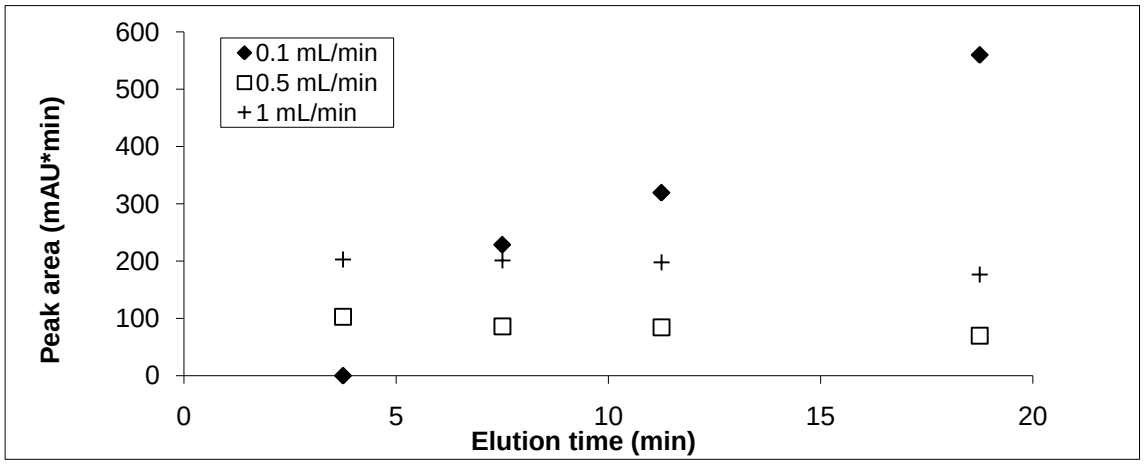

F.3 Rotation speed

F.3.1 1.5 mg/mL BSA concentration, 1M NaCl concentration, Trial 1, 0.1-1.0mL/min flow rate

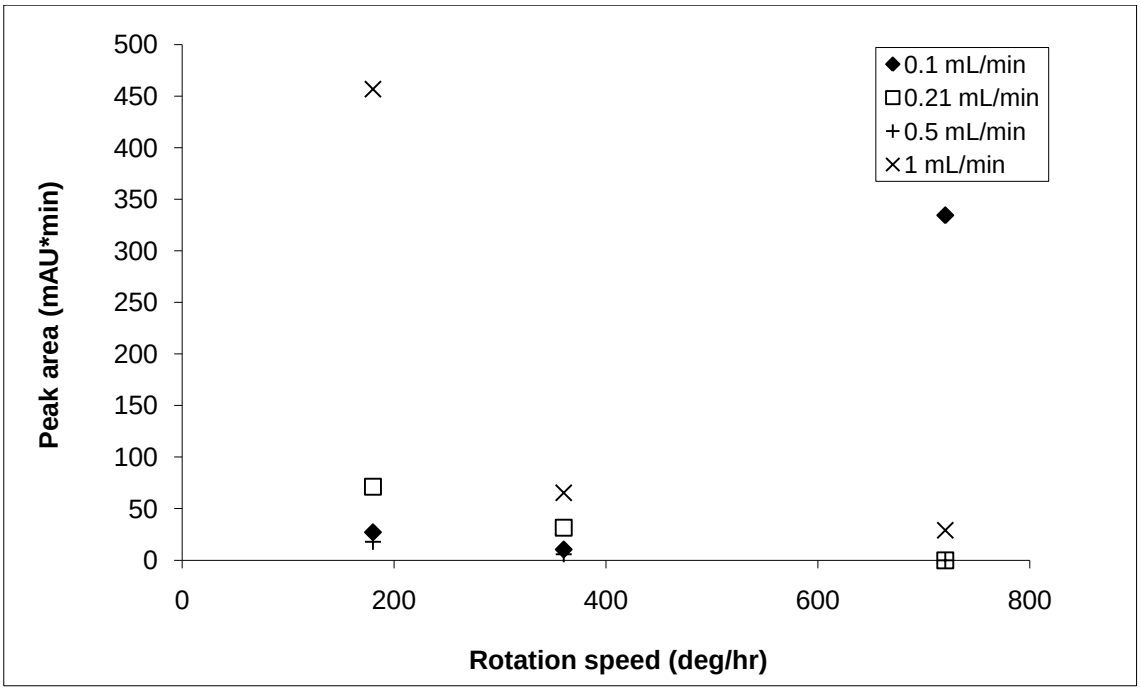

F.3.2 1.5 mg/mL BSA concentration, 1M NaCl concentration, Trial 2, 0.1-1.0mL/min flow rate

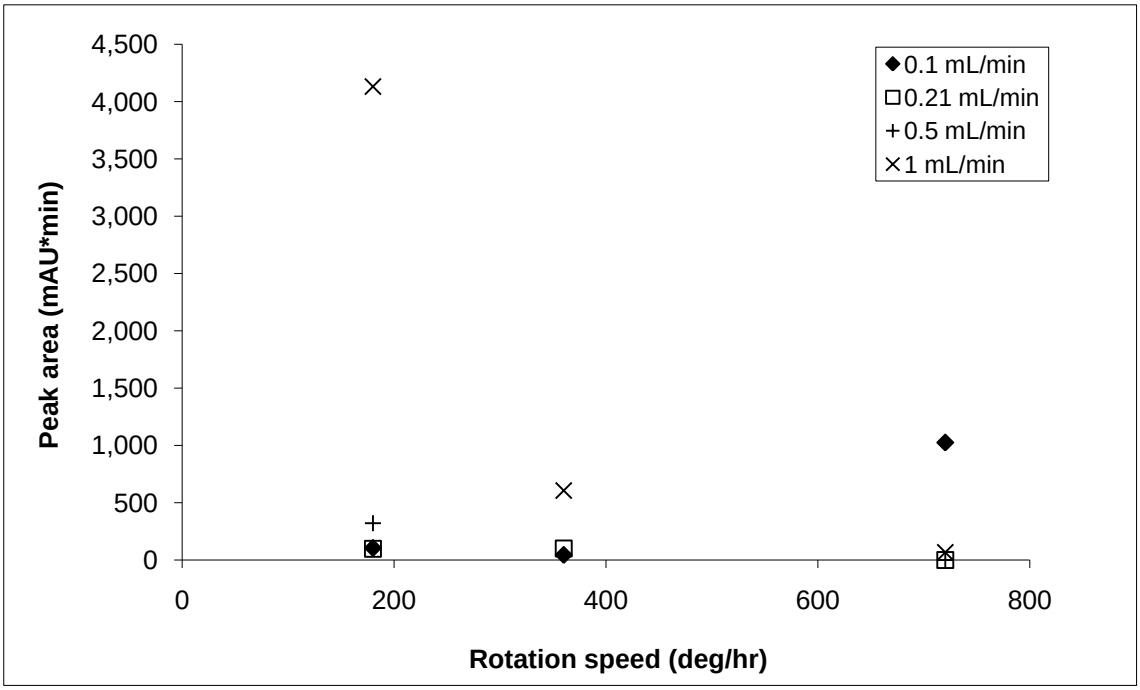

F.3.3 1.5 mg/mL BSA concentration, 1M NaCl concentration, Trial 3 0.1-1.0mL/min flow rate

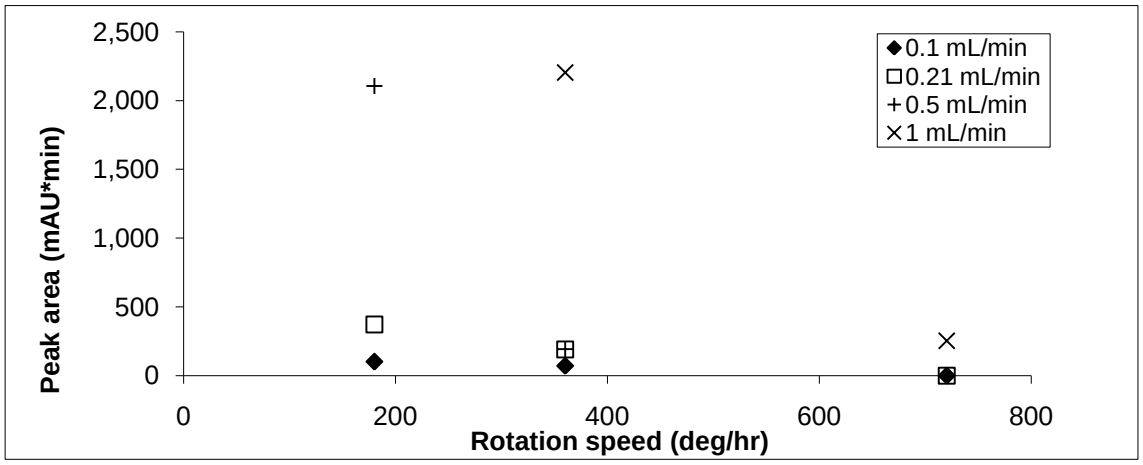

F.3.4 1.5 mg/mL BSA concentration, 1M NaCl concentration, Trial 4, 0.1-1.0mL/min flow rate

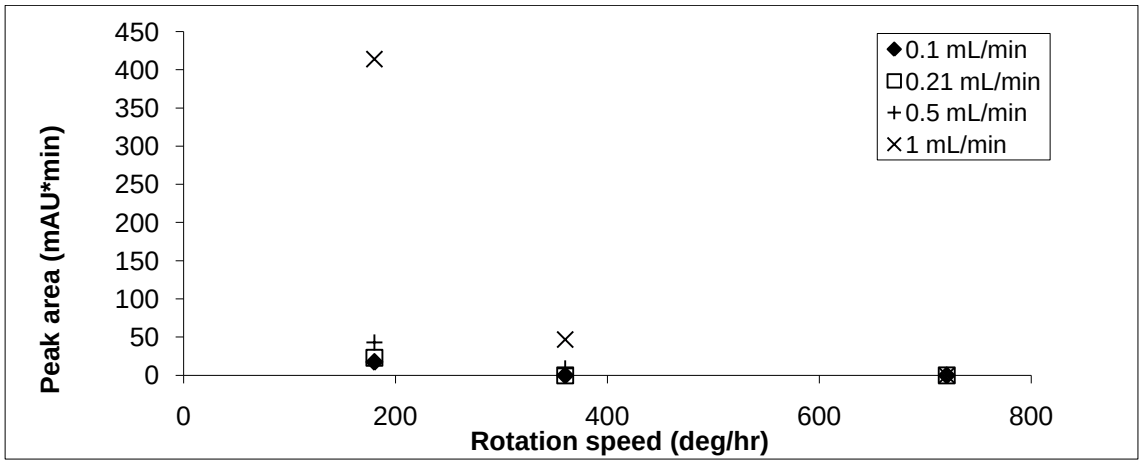

F.3.5 1.5 mg/mL BSA concentration, 1M NaCl concentration, Trial 5, 0.1-1.0mL/min flow rate

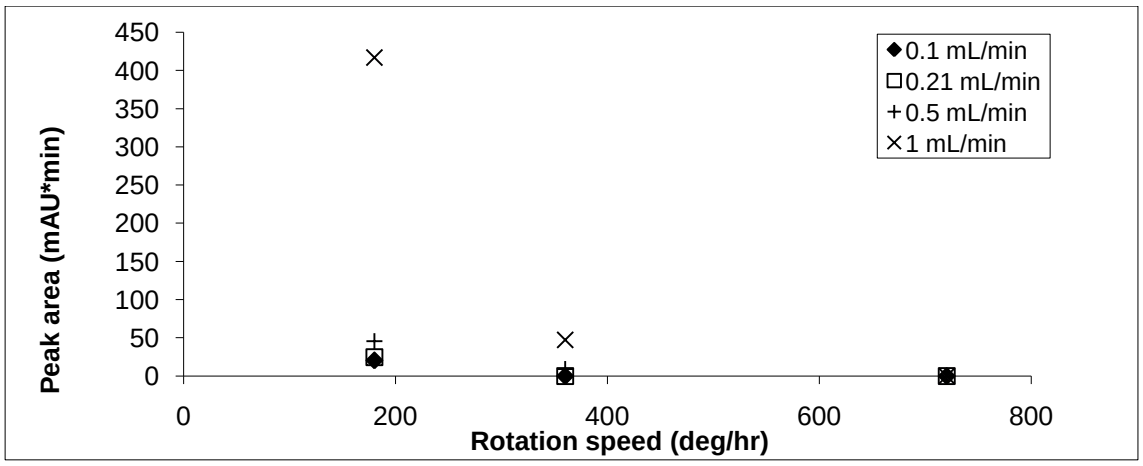

F.3.6 1.5 mg/mL BSA concentration, 1M NaCl concentration, Trial 6, 0.1-1.0mL/min flow rate

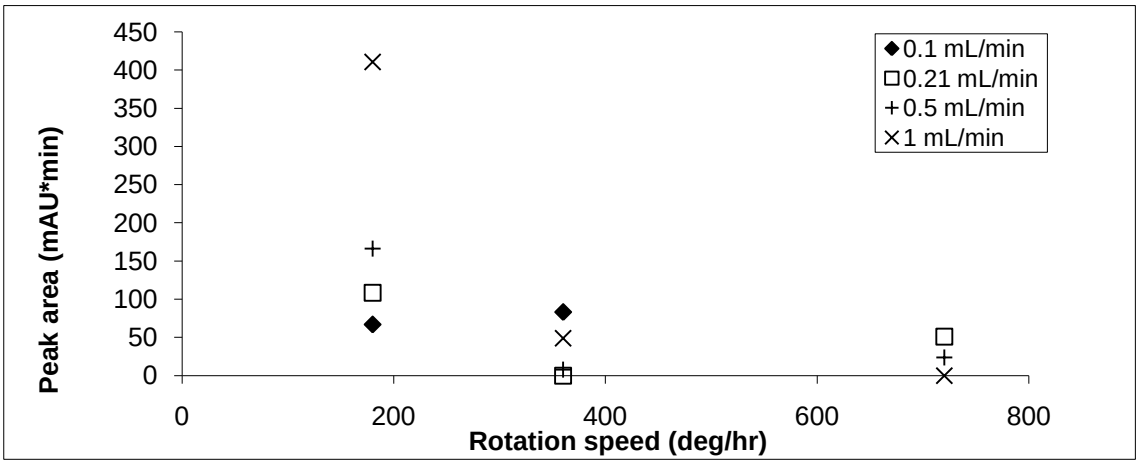

F.3.7 1.5 mg/mL BSA concentration, 1M NaCl concentration, Trial 7, 0.1-1.0mL/min flow rate

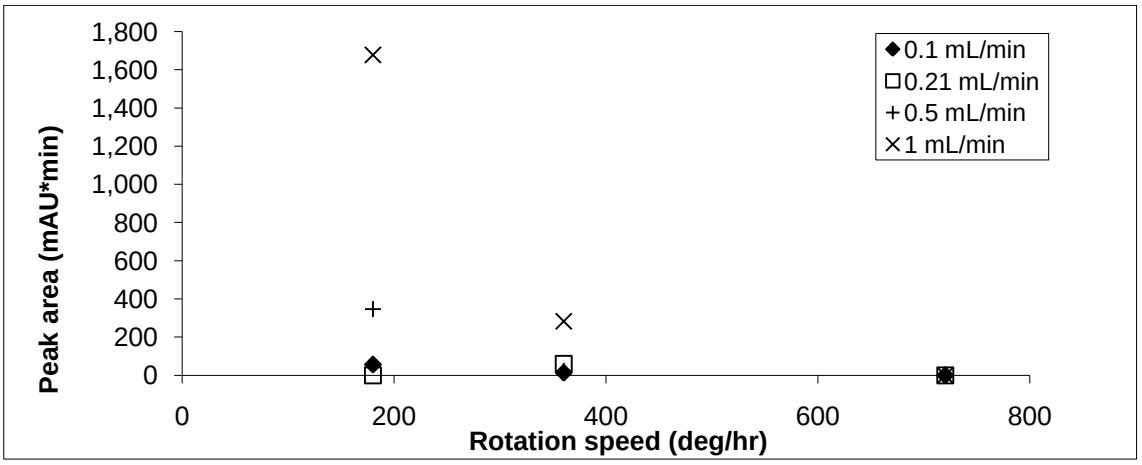

F.3.8 1.5 mg/mL BSA concentration, 1M NaCl concentration, Trial 8, 0.1-1.0mL/min flow rate

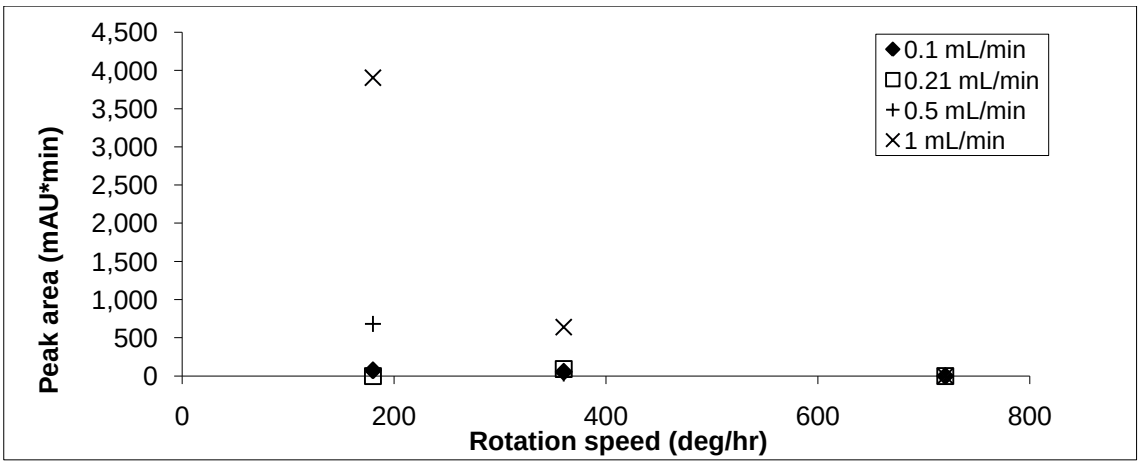

F.3.9 1.5 mg/mL BSA concentration, 1M NaCl concentration, Trial 9, 0.1-1.0mL/min flow rate

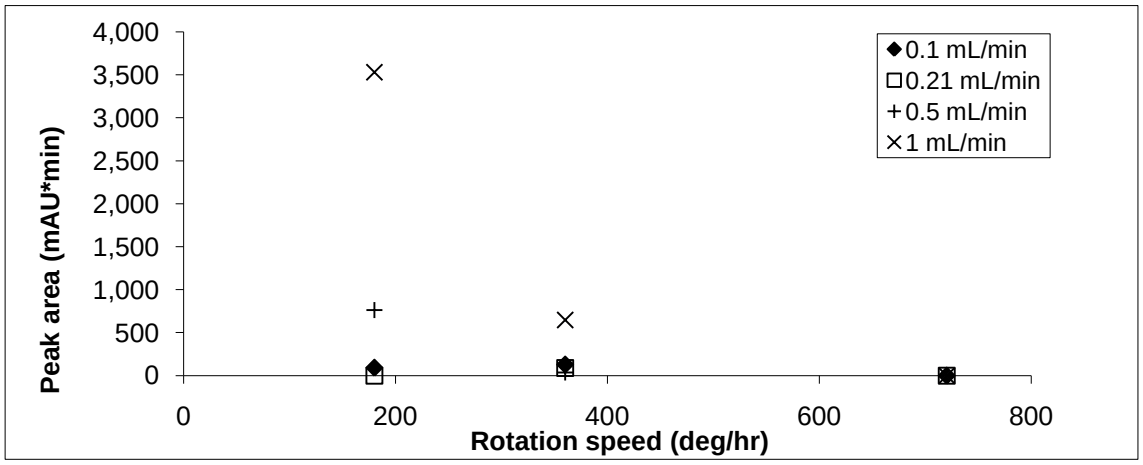

F.3.10 3 mg/mL BSA concentration, 1M NaCl concentration, Trial 1, 0.1-1.0mL/min flow rate

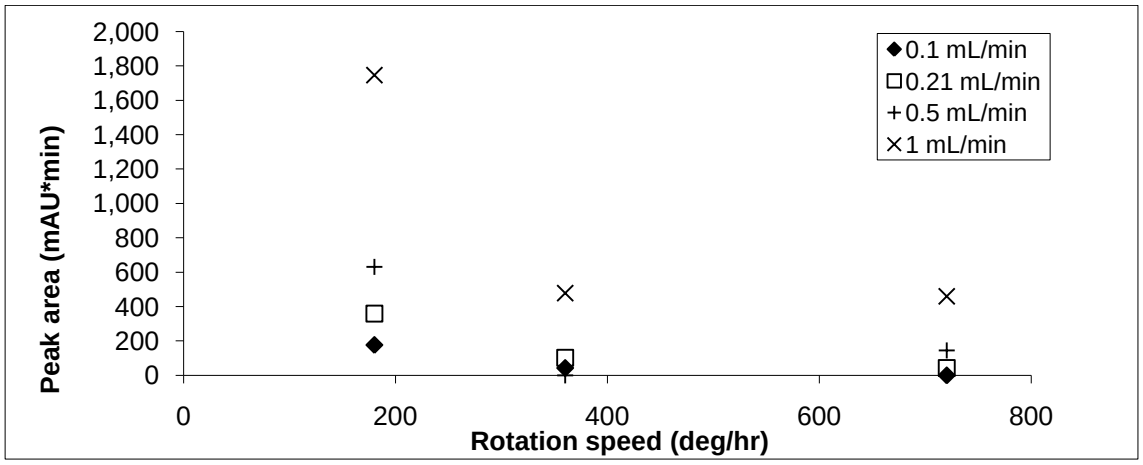

F.3.11 3 mg/mL BSA concentration, 1M NaCl concentration, Trial 2, 0.1-1.0mL/min flow rate

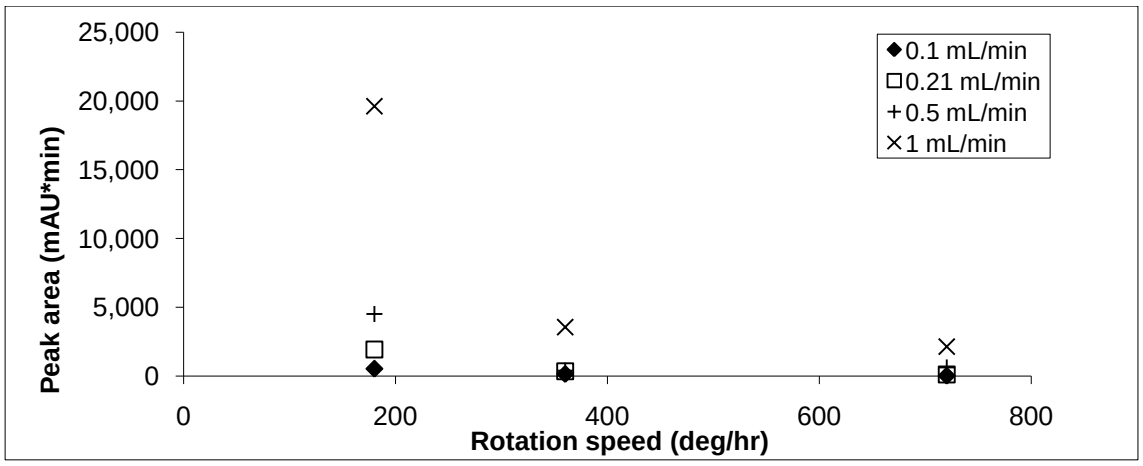

F.3.12 3 mg/mL BSA concentration, 1M NaCl concentration, Trial 3, 0.1-1.0mL/min flow rate

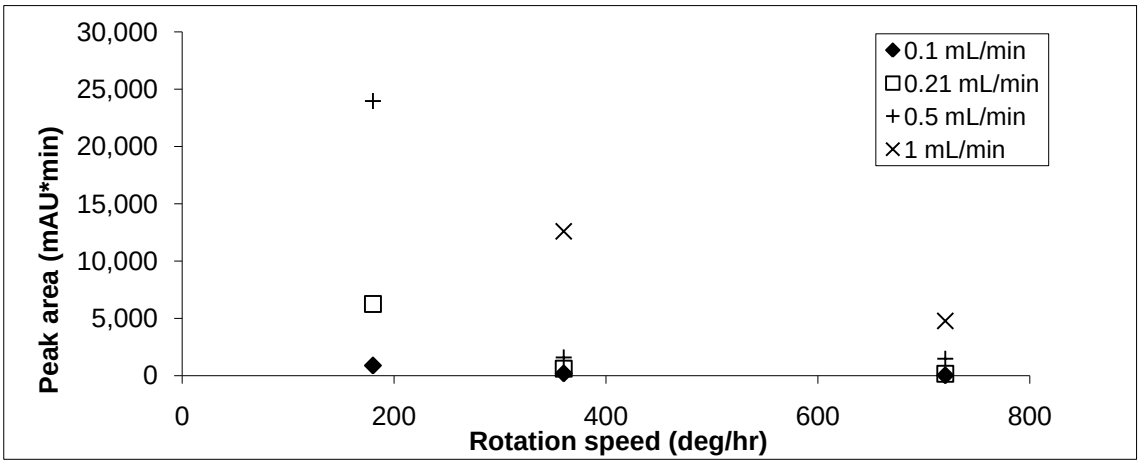

F.3.13 3 mg/mL BSA concentration, 1M NaCl concentration, Trial 4, 0.1-1.0mL/min flow rate

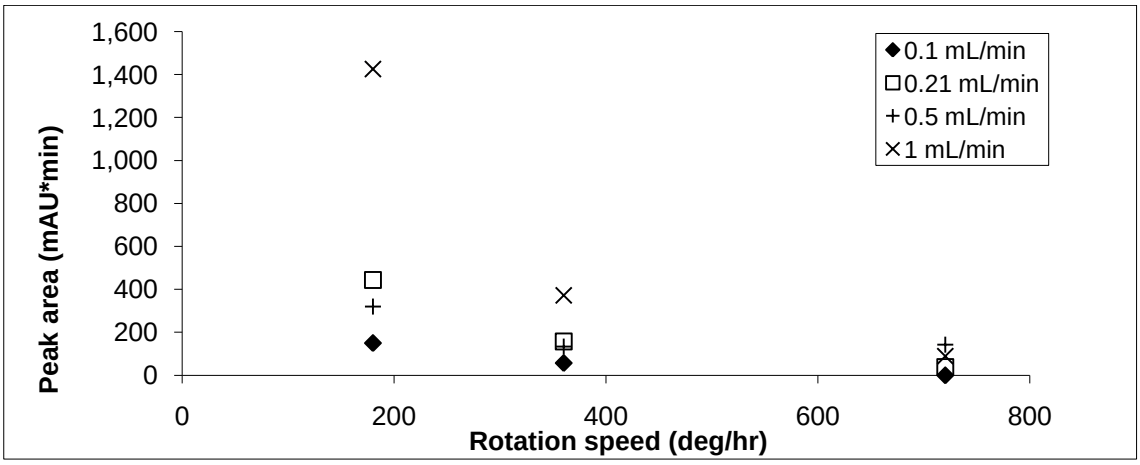

F.3.14 3 mg/mL BSA concentration, 1M NaCl concentration, Trial 5, 0.1-1.0mL/min flow rate

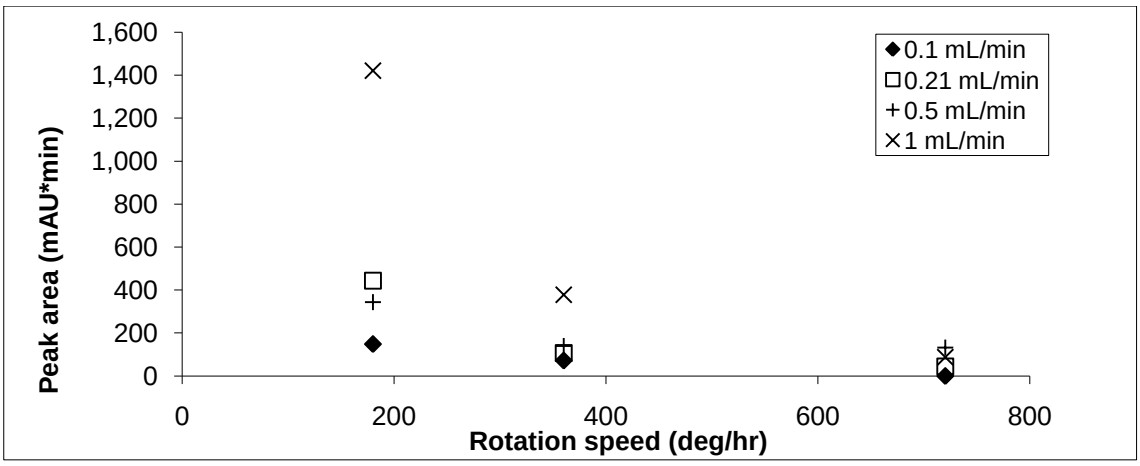

F.3.15 3 mg/mL BSA concentration, 1M NaCl concentration, Trial 6, 0.1-1.0mL/min flow rate

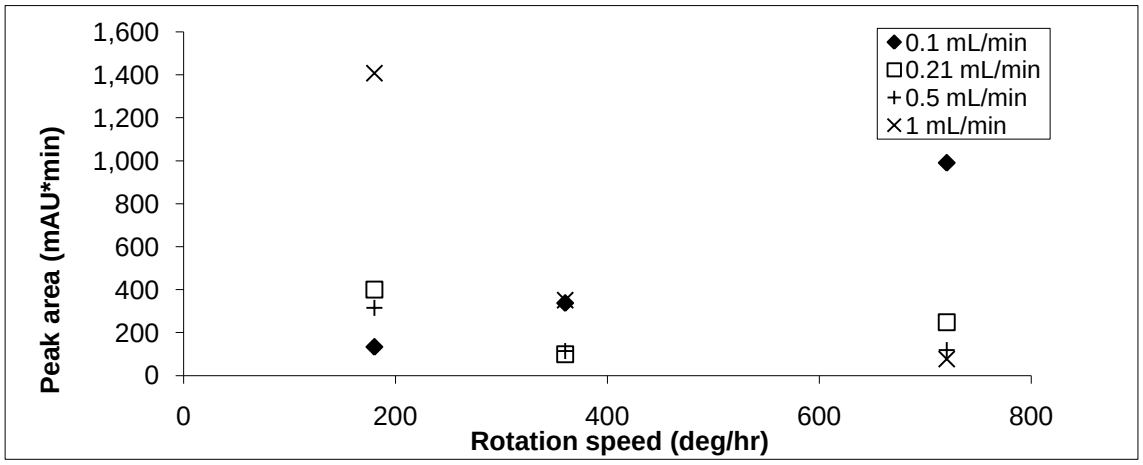

F.3.16 3 mg/mL BSA concentration, 1M NaCl concentration, Trial 7, 0.1-1.0mL/min flow rate

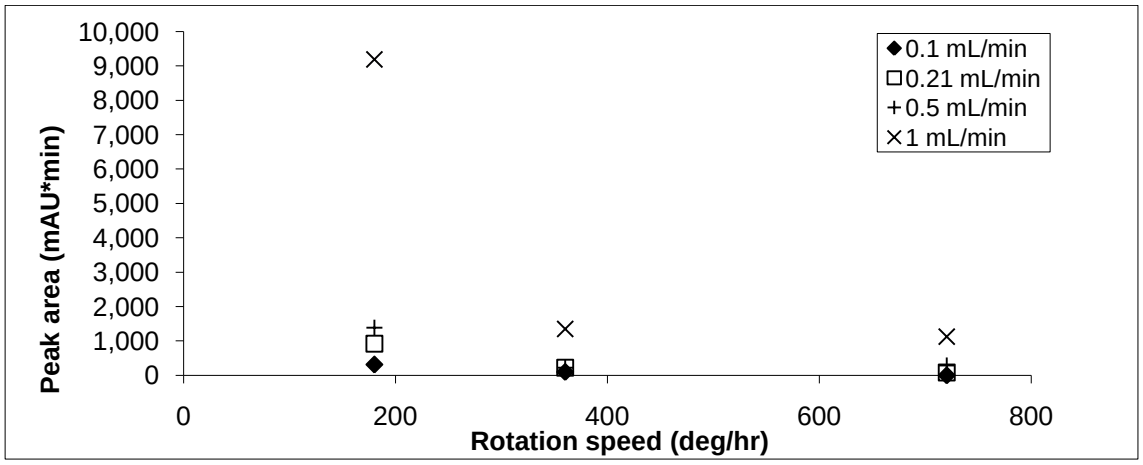

F.3.17 3 mg/mL BSA concentration, 1M NaCl concentration, Trial 8, 0.1-1.0mL/min flow rate

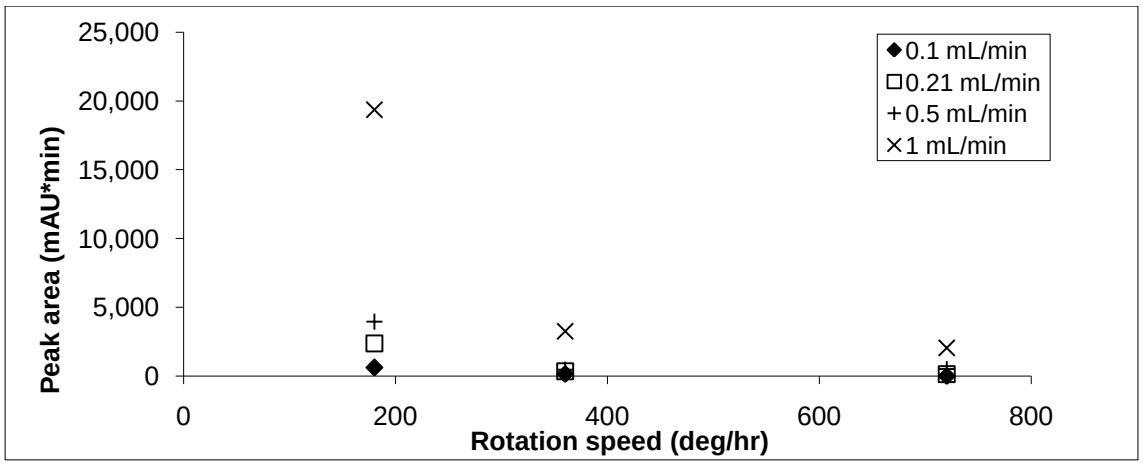

F.3.18 3 mg/mL BSA concentration, 1M NaCl concentration, Trial 9, 0.1-1.0mL/min flow rate

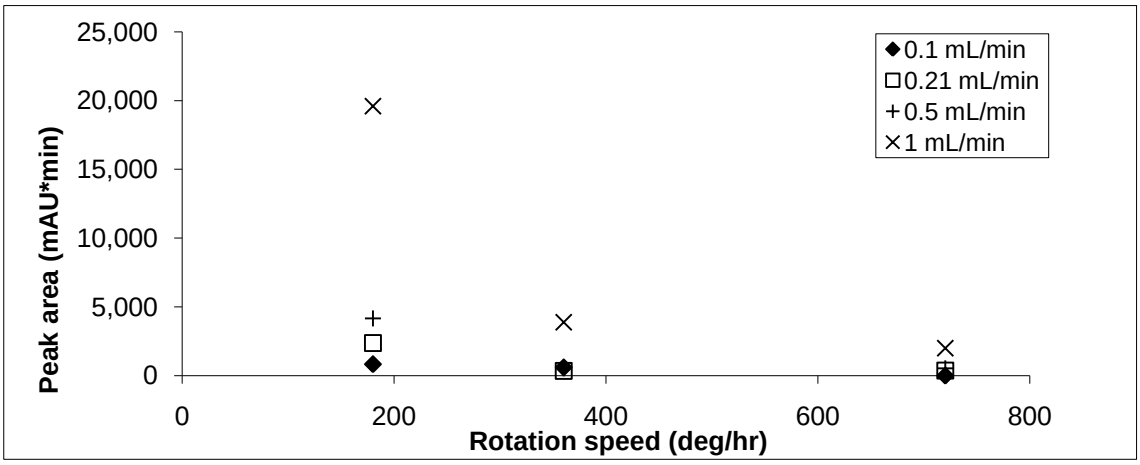

F.3.19 5 mg/mL BSA concentration, 1M NaCl concentration, Trial 1, 0.1-1.0mL/min flow rate

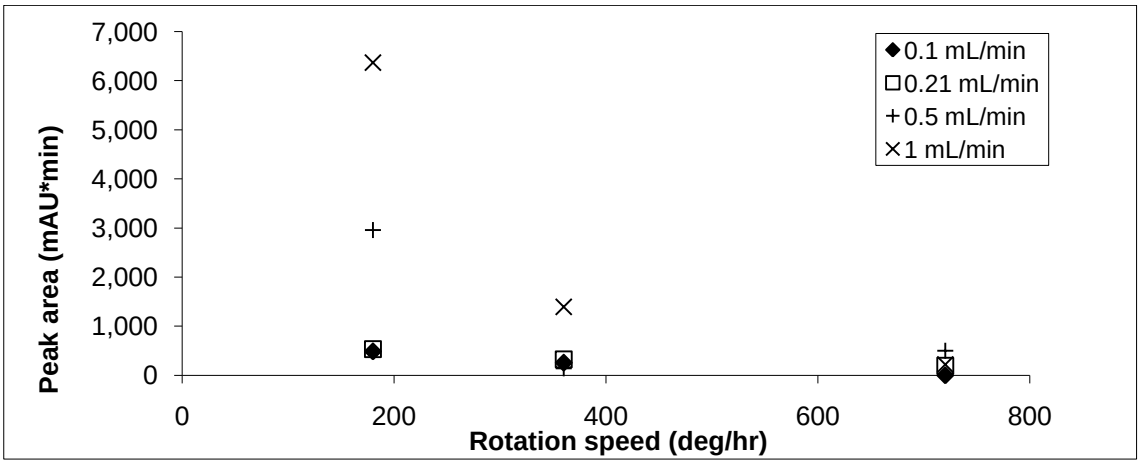

F.3.20 5 mg/mL BSA concentration, 1M NaCl concentration, Trial 2, 0.1-1.0mL/min flow rate

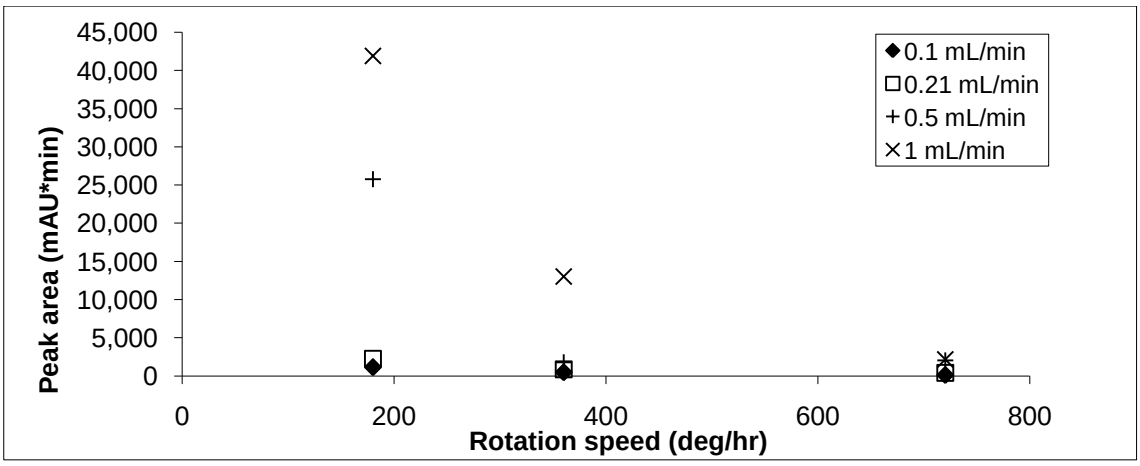

F.3.21 5 mg/mL BSA concentration, 1M NaCl concentration, Trial 3, 0.1-1.0mL/min flow rate

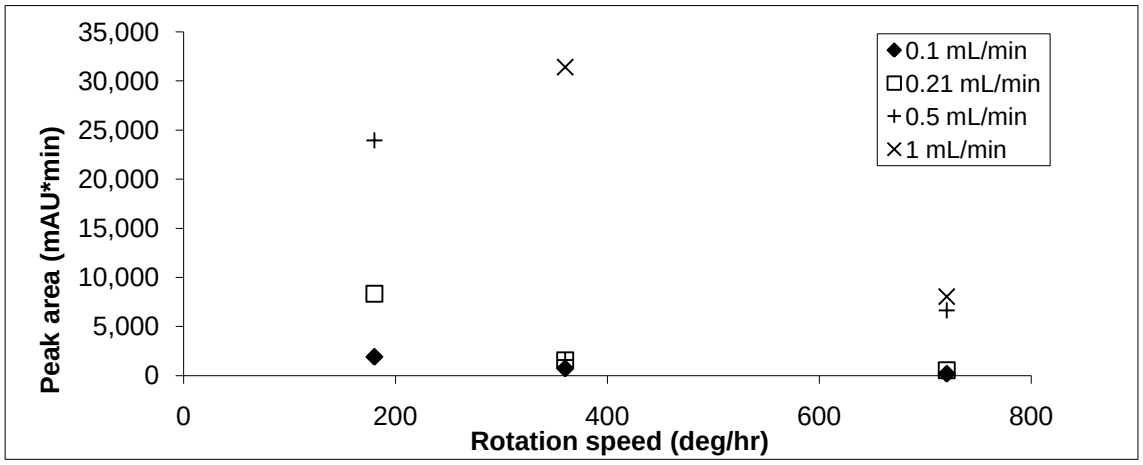

F.3.22 5 mg/mL BSA concentration, 1M NaCl concentration, Trial 4, 0.1-1.0mL/min flow rate

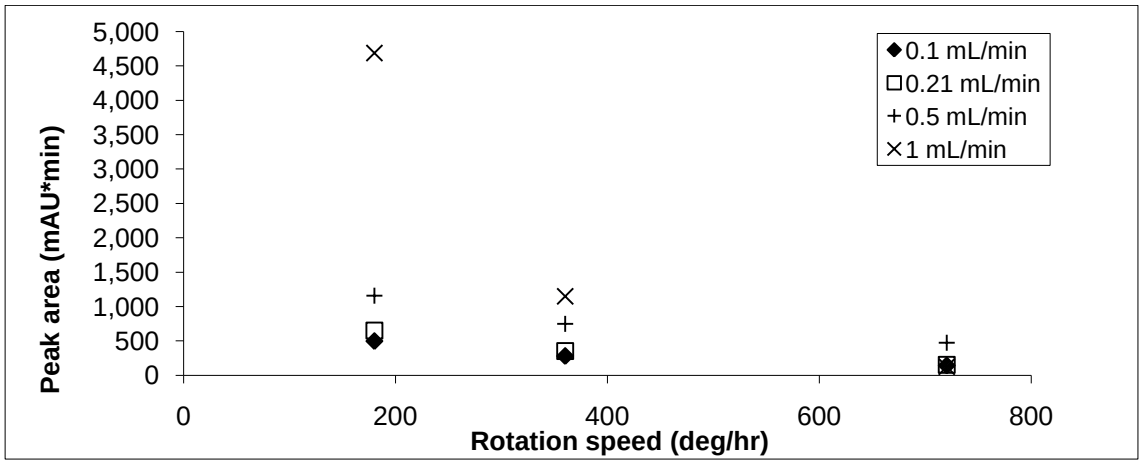

F.3.23 5 mg/mL BSA concentration, 1M NaCl concentration, Trial 5, 0.1-1.0mL/min flow rate

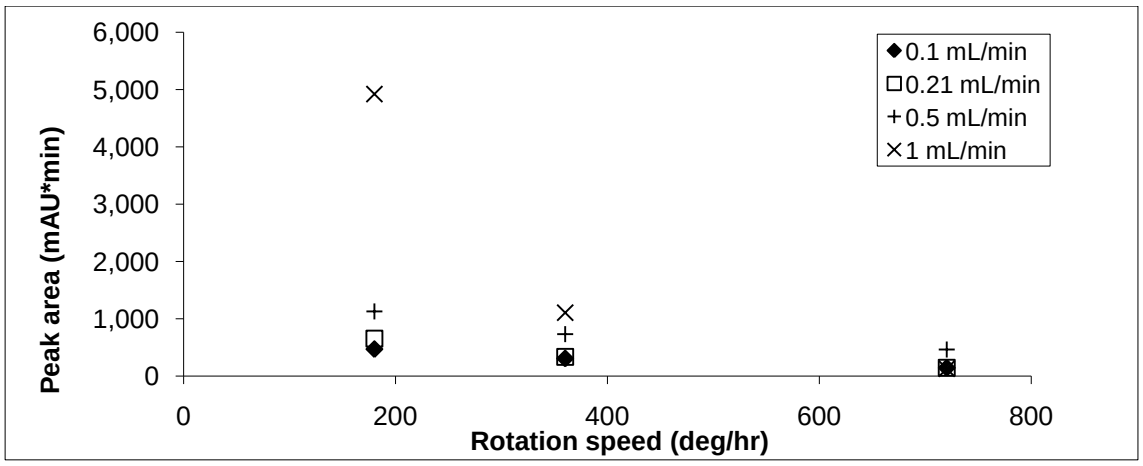

F.3.24 5 mg/mL BSA concentration, 1M NaCl concentration, Trial 6, 0.1-1.0mL/min flow rate

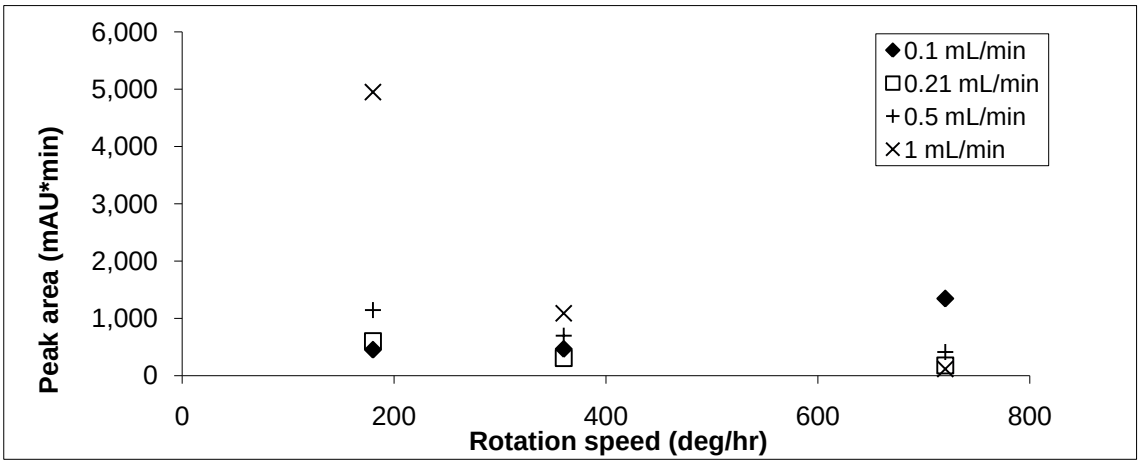

F.3.25 5 mg/mL BSA concentration, 1M NaCl concentration, Trial 7, 0.1-1.0mL/min flow rate

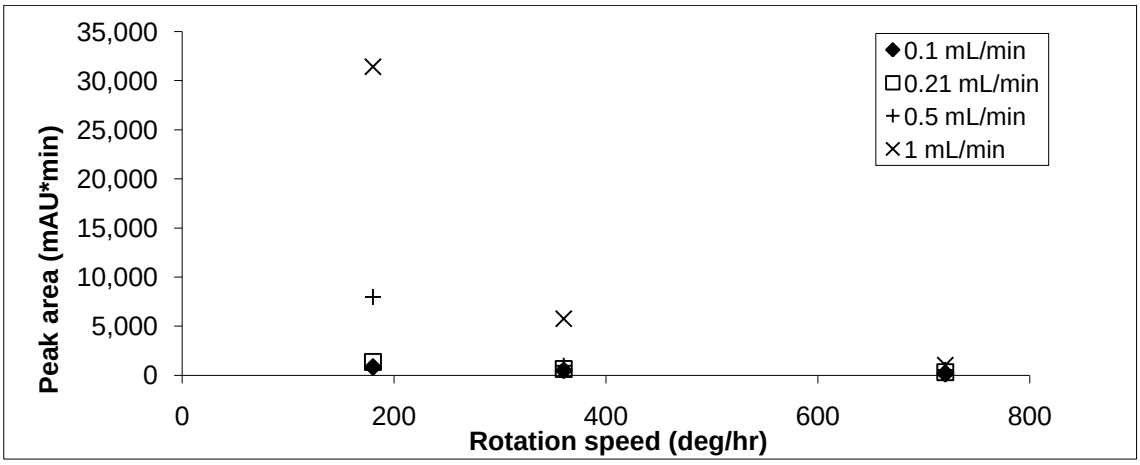

F.3.26 5 mg/mL BSA concentration, 1M NaCl concentration, Trial 8, 0.1-1.0mL/min flow rate

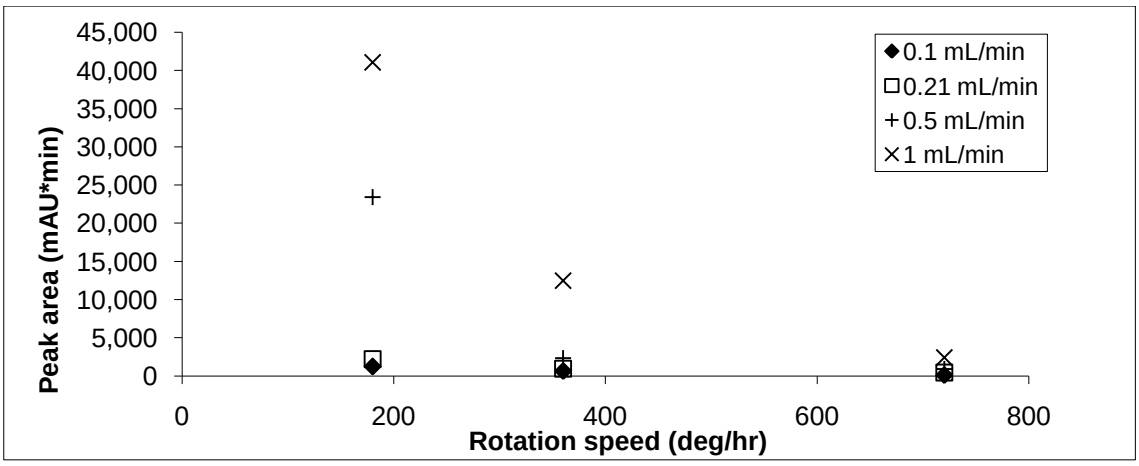

F.3.27 5 mg/mL BSA concentration, 1M NaCl concentration, Trial 9, 0.1-1.0mL/min flow rate

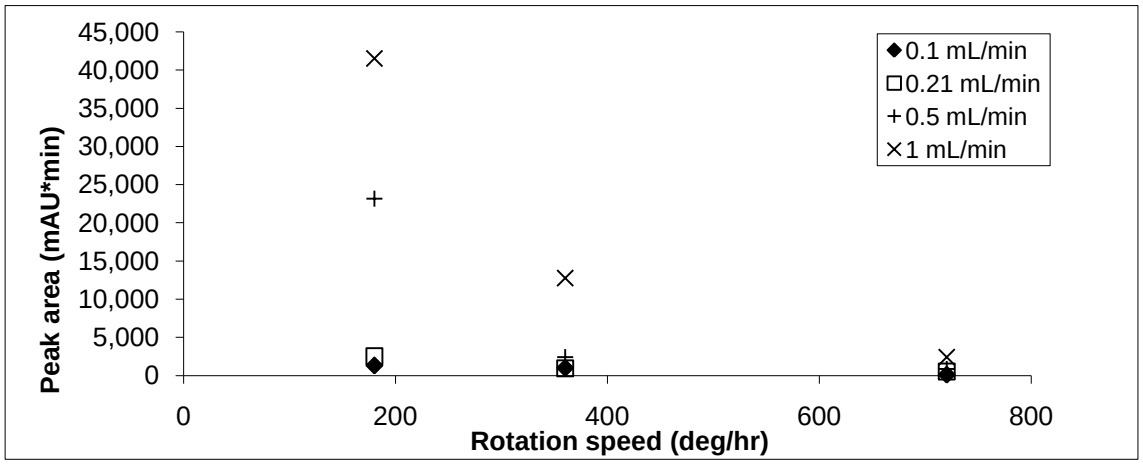

F.3.28 1.5 mg/mL BSA concentration, 2M NaCl concentration, Trial 1, 0.1-1.0mL/min flow rate

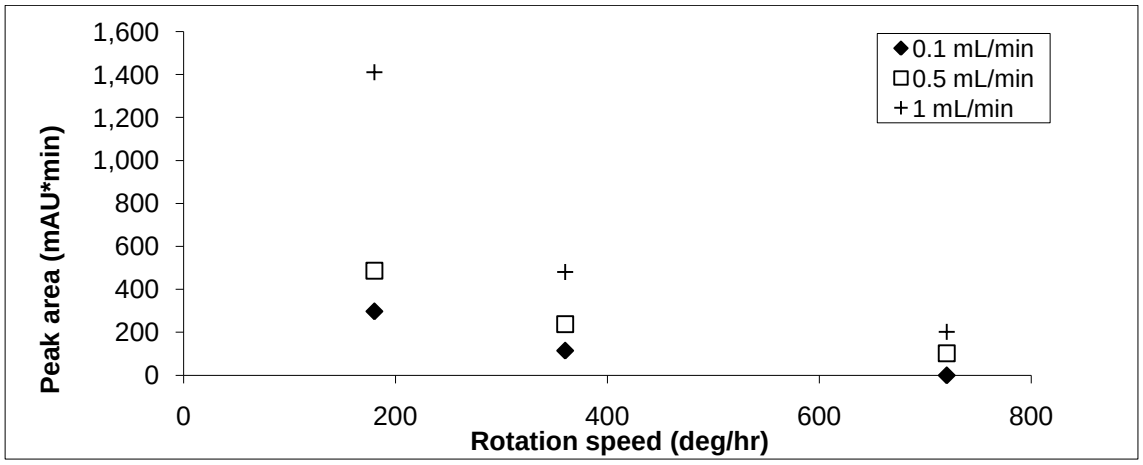

F.3.29 1.5 mg/mL BSA concentration, 2M NaCl concentration, Trial 2, 0.1-1.0mL/min flow rate

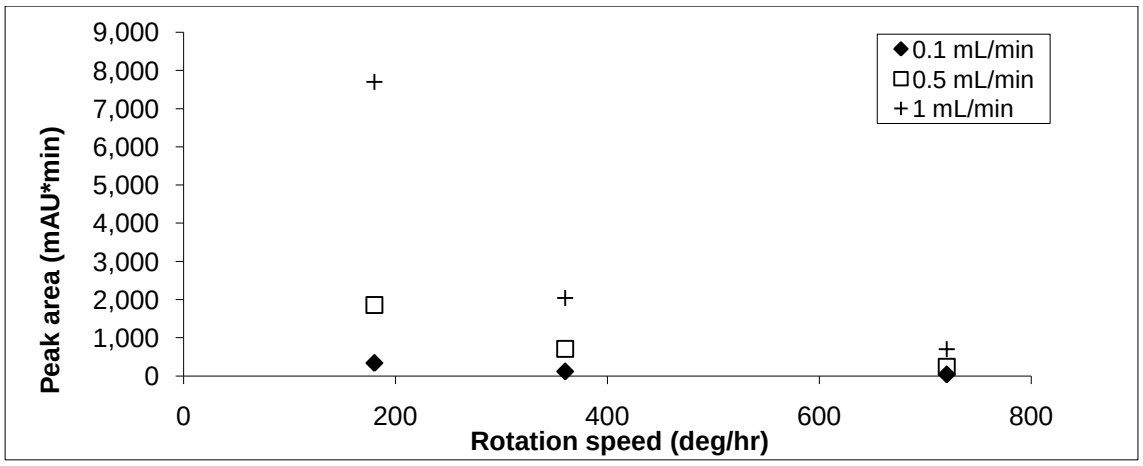

F.3.30 1.5 mg/mL BSA concentration, 2M NaCl concentration, Trial 3, 0.1-1.0mL/min flow rate

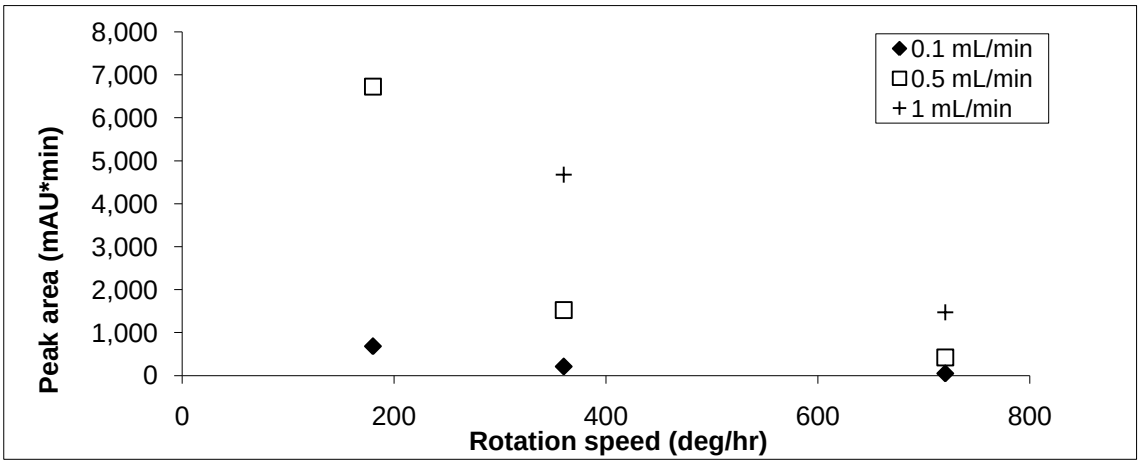

F.3.31 1.5 mg/mL BSA concentration, 2M NaCl concentration, Trial 4, 0.1-1.0mL/min flow rate

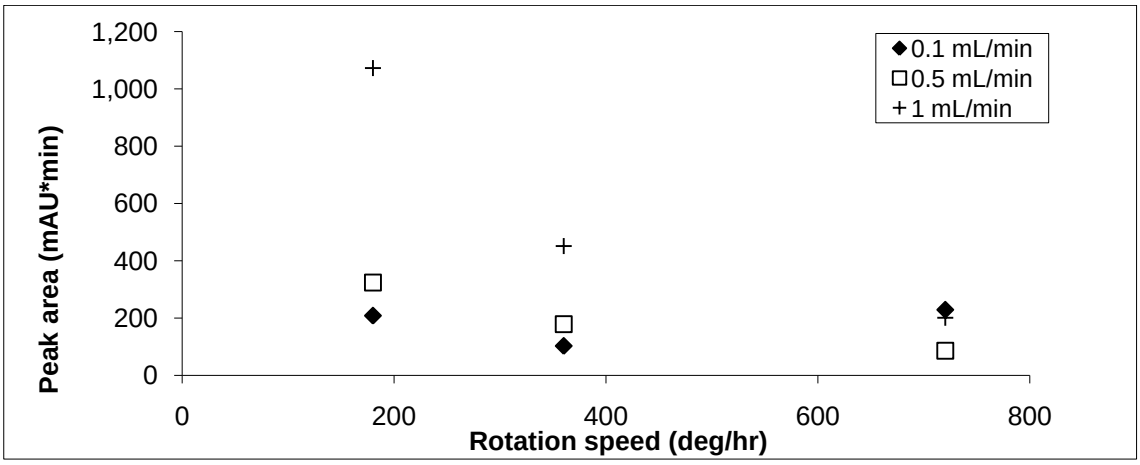

F.3.32 1.5 mg/mL BSA concentration, 2M NaCl concentration, Trial 5, 0.1-1.0mL/min flow rate

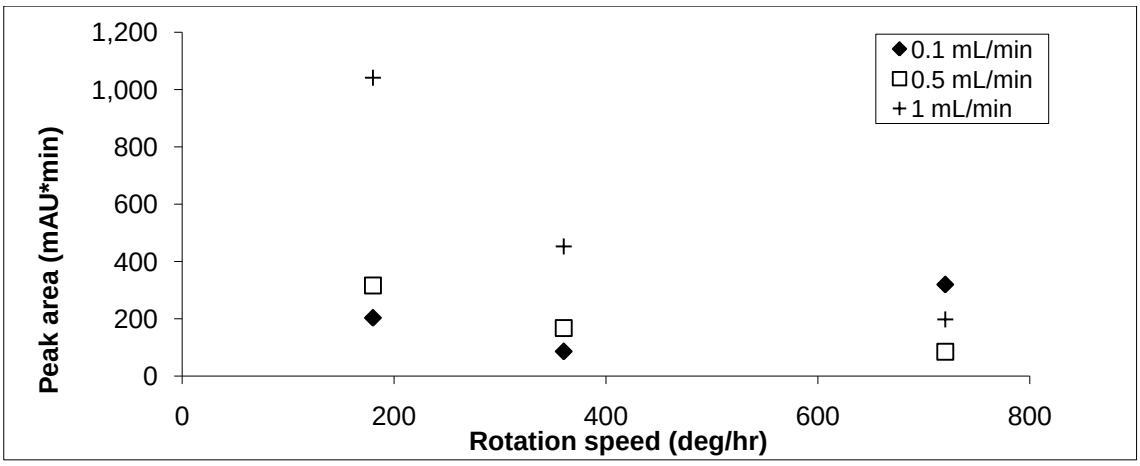

F.3.33 1.5 mg/mL BSA concentration, 2M NaCl concentration, Trial 6, 0.1-1.0mL/min flow rate

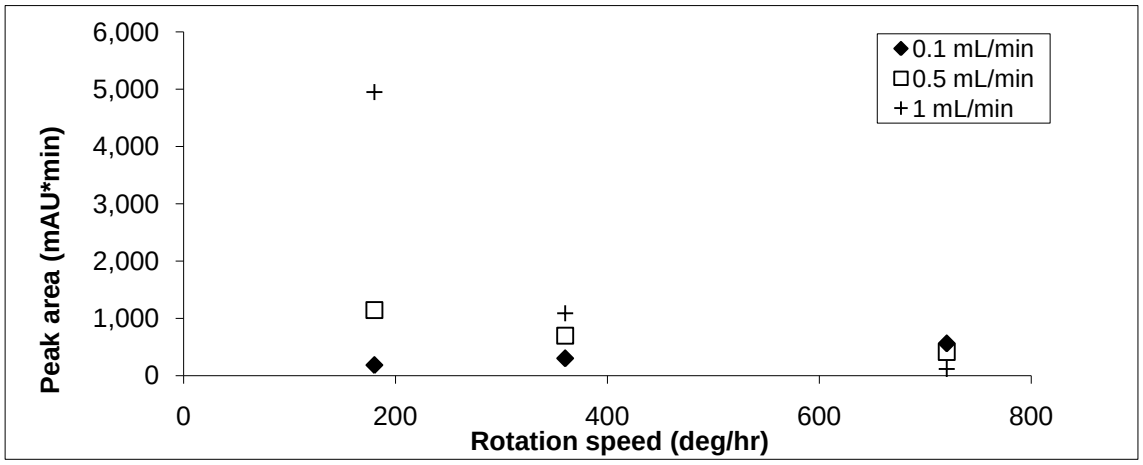

F.3.34 1.5 mg/mL BSA concentration, 2M NaCl concentration, Trial 7, 0.1-1.0mL/min flow rate

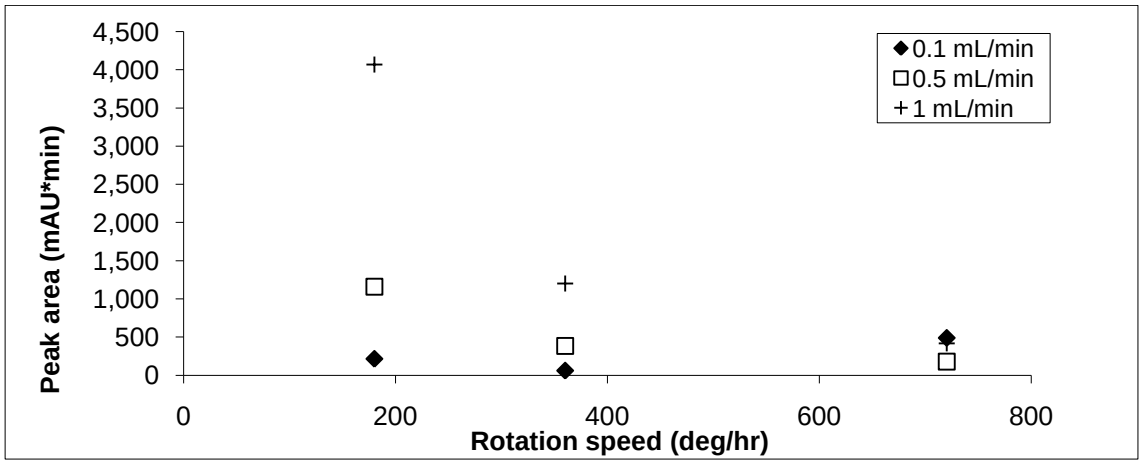

F.3.35 1.5 mg/mL BSA concentration, 2M NaCl concentration, Trial 8, 0.1-1.0mL/min flow rate

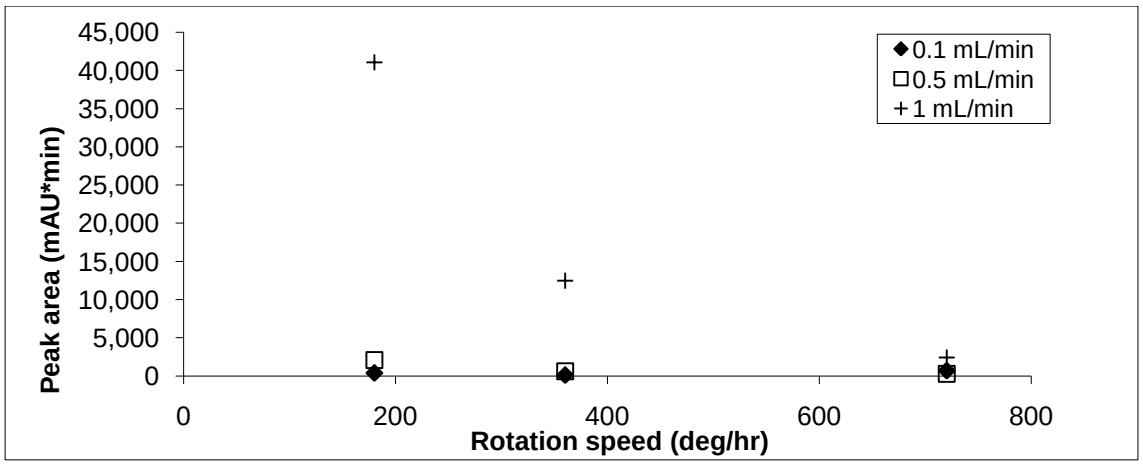

F.3.36 1.5 mg/mL BSA concentration, 2M NaCl concentration, Trial 9, 0.1-1.0mL/min flow rate

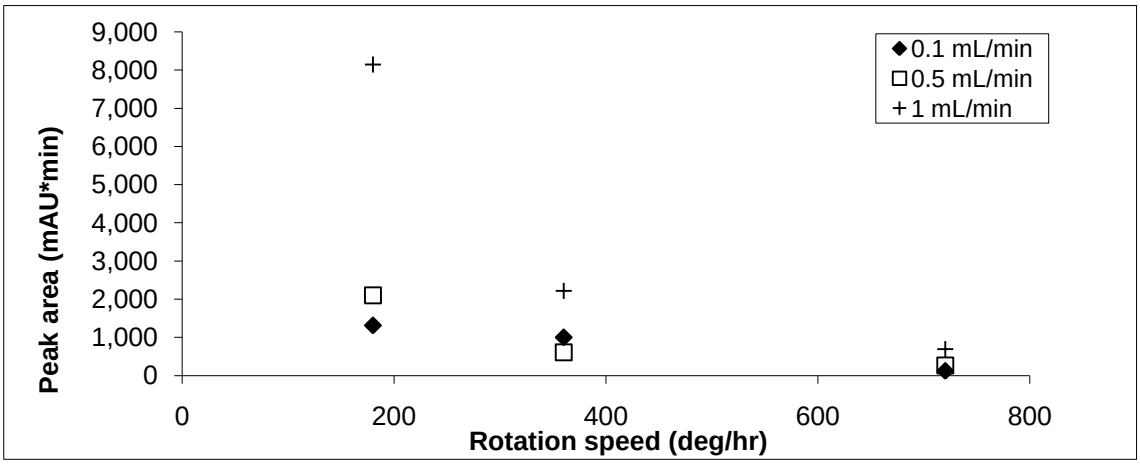

F.4 Flow rate

F.4.1 1.5 mg/mL BSA concentration, 1M NaCl concentration, Trial 1, 180-720 deg/hr rotation speed

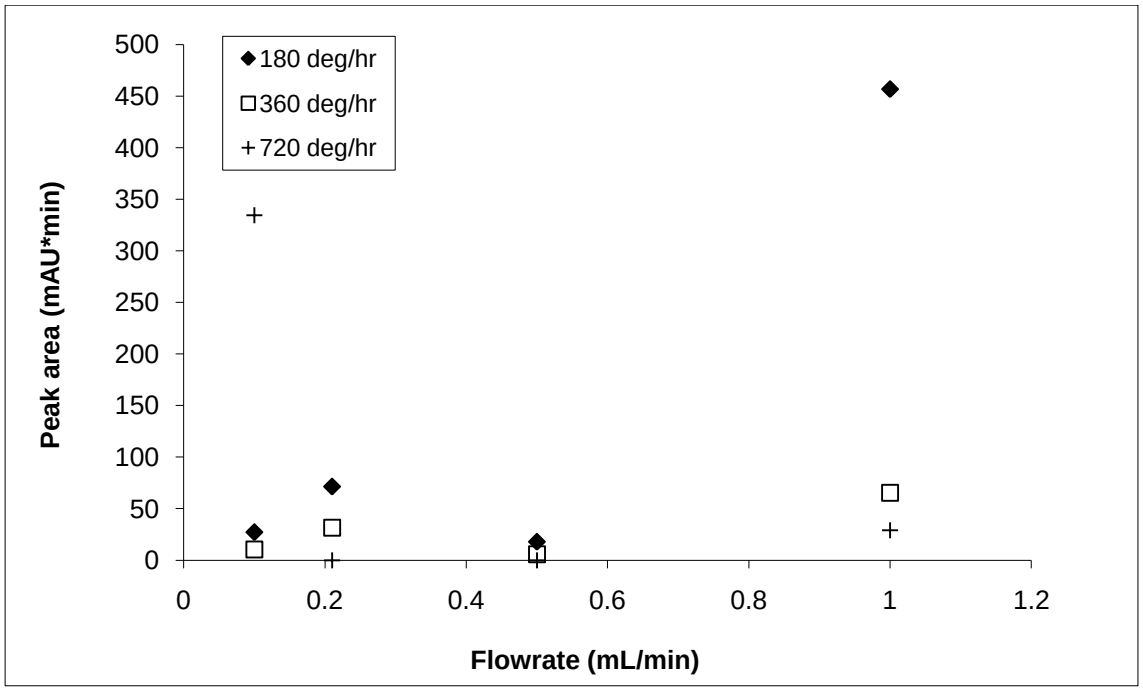

F.4.2 1.5 mg/mL BSA concentration, 1M NaCl concentration, Trial 2, 180-720 deg/hr rotation speed

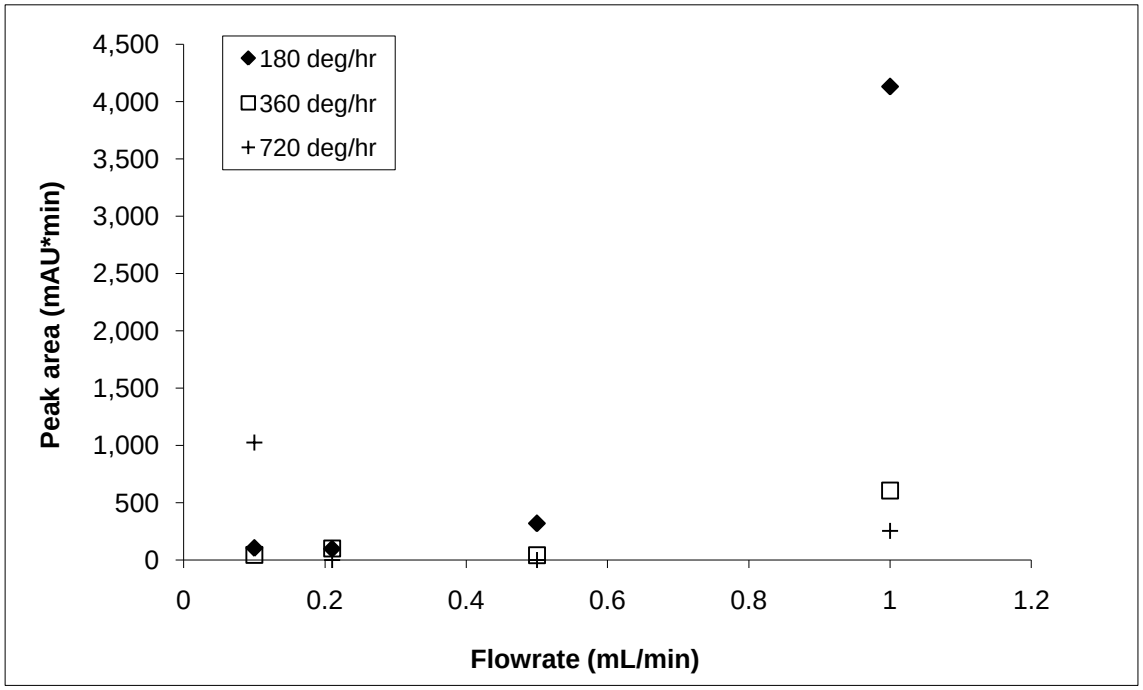

F.4.3 1.5 mg/mL BSA concentration, 1M NaCl concentration, Trial 3, 180-720 deg/hr rotation speed

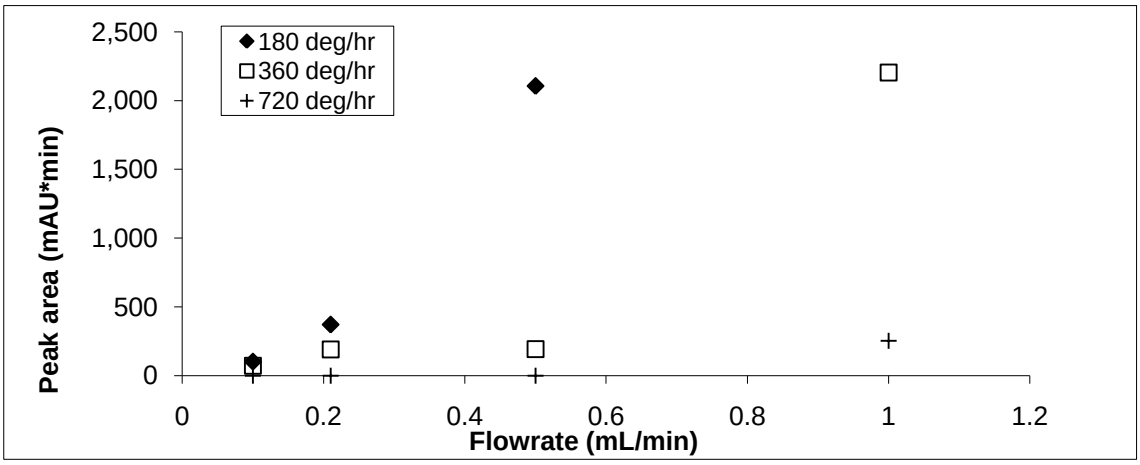

F.4.4 1.5 mg/mL BSA concentration, 1M NaCl concentration, Trial 4, 180-720 deg/hr rotation speed

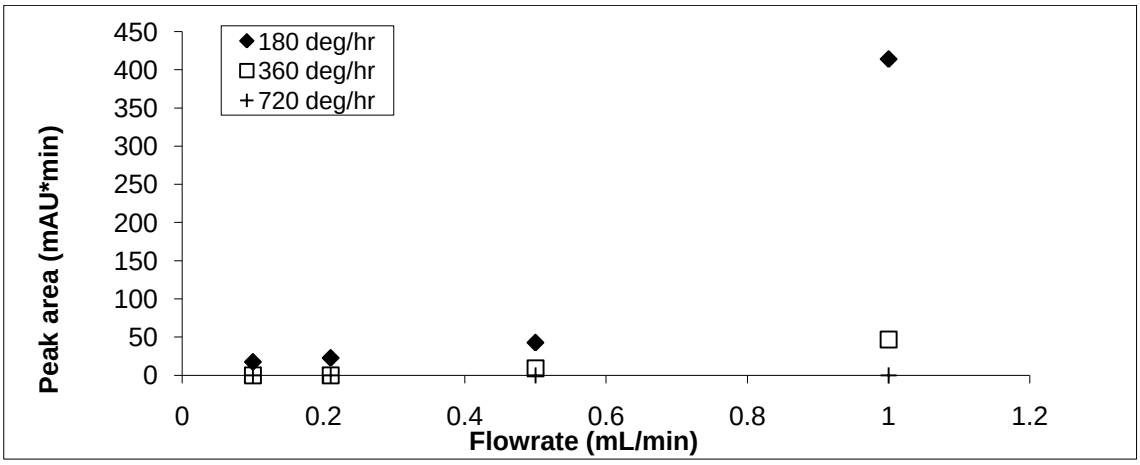

F.4.5 1.5 mg/mL BSA concentration, 1M NaCl concentration, Trial 5, 180-720 deg/hr rotation speed

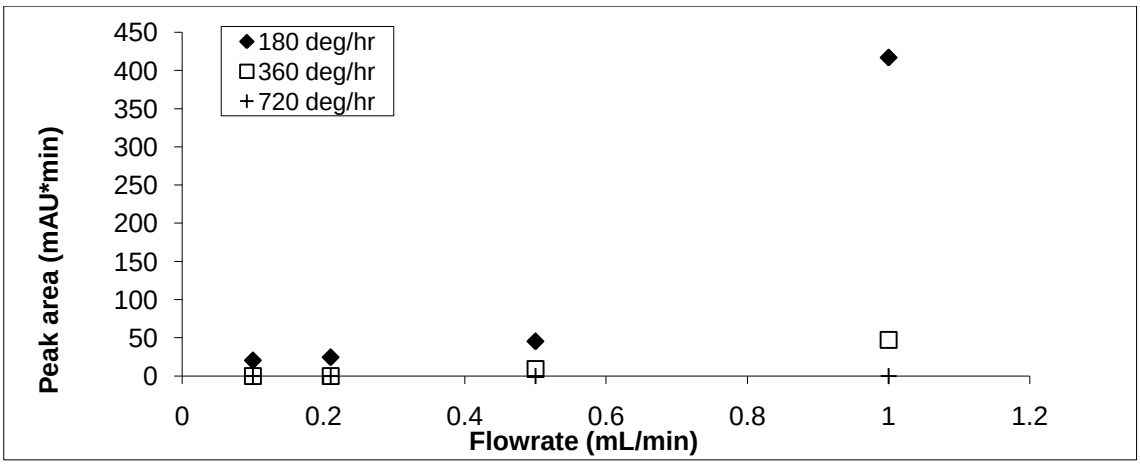

F.4.6 1.5 mg/mL BSA concentration, 1M NaCl concentration, Trial 6, 180-720 deg/hr rotation speed

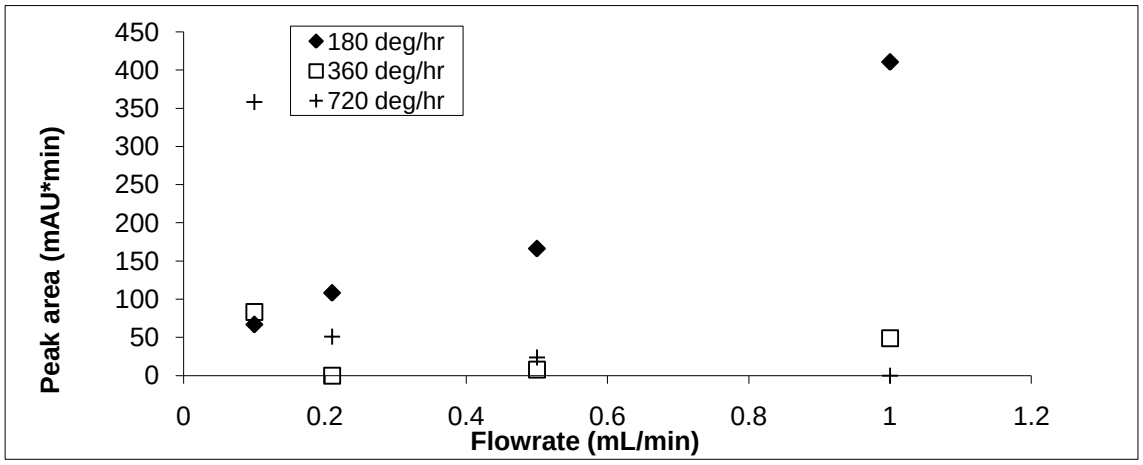

F.4.7 1.5 mg/mL BSA concentration, 1M NaCl concentration, Trial 7, 180-720 deg/hr rotation speed

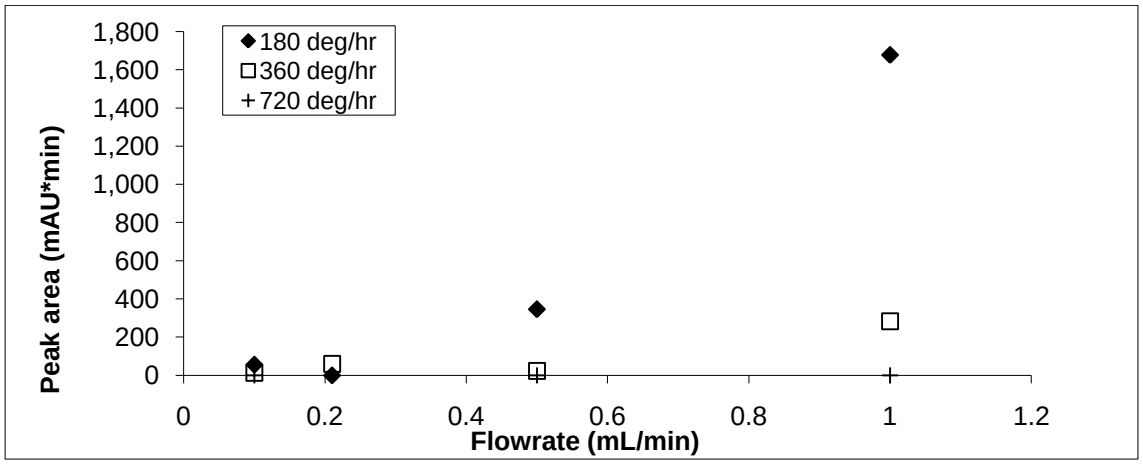

F.4.8 1.5 mg/mL BSA concentration, 1M NaCl concentration, Trial 8, 180-720 deg/hr rotation speed

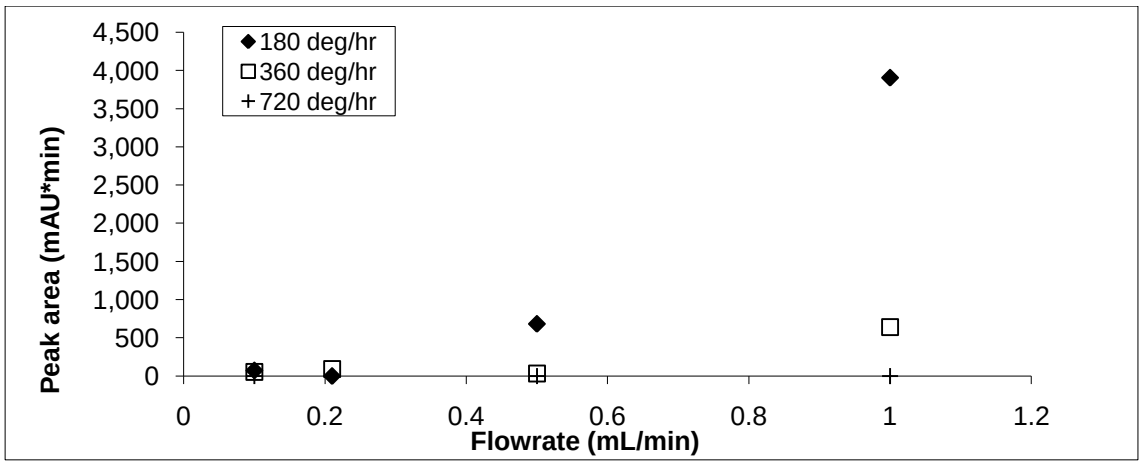

F.4.9 1.5 mg/mL BSA concentration, 1M NaCl concentration, Trial 9, 180-720 deg/hr rotation speed

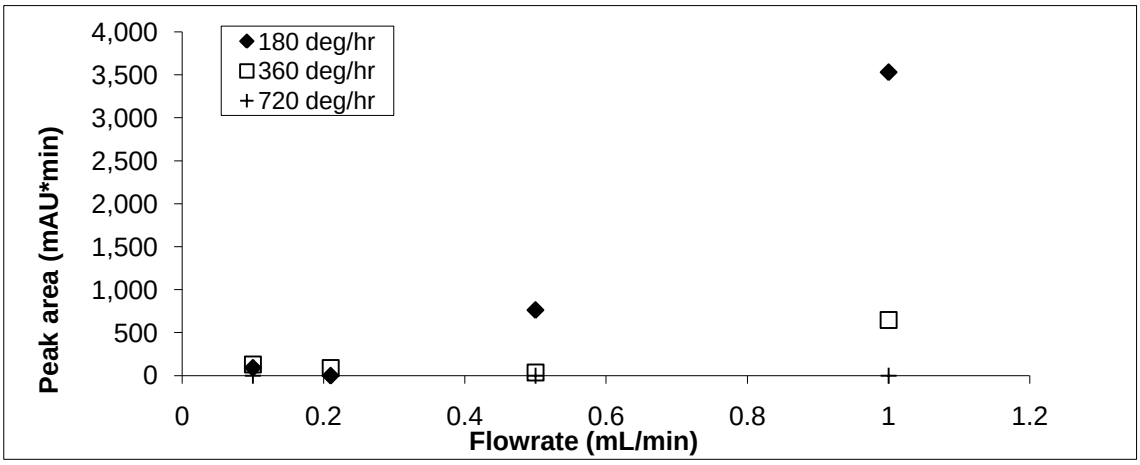

F.4.10 3 mg/mL BSA concentration, 1M NaCl concentration, Trial 1, 180-720 deg/hr rotation speed

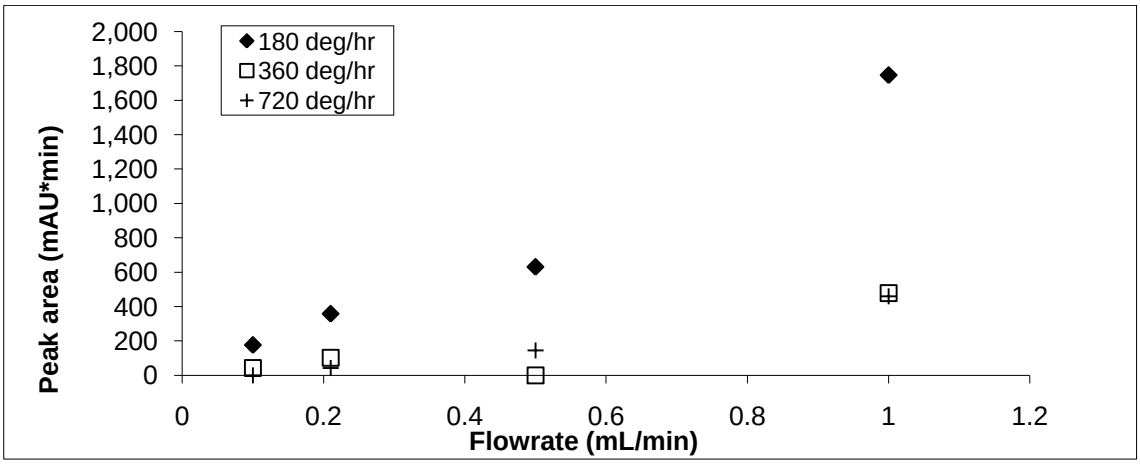

F.4.11 3 mg/mL BSA concentration, 1M NaCl concentration, Trial 2, 180-720 deg/hr rotation speed

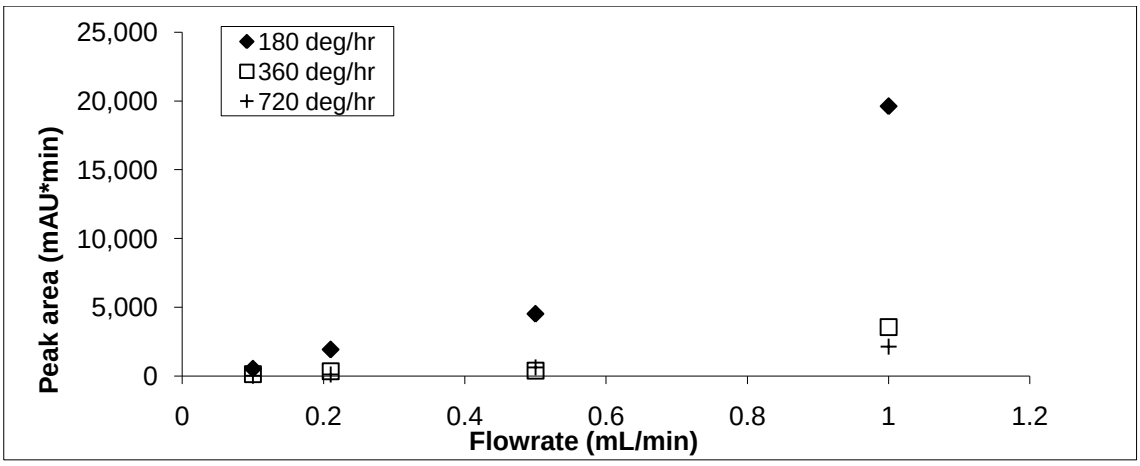

F.4.12 3 mg/mL BSA concentration, 1M NaCl concentration, Trial 3, 180-720 deg/hr rotation speed

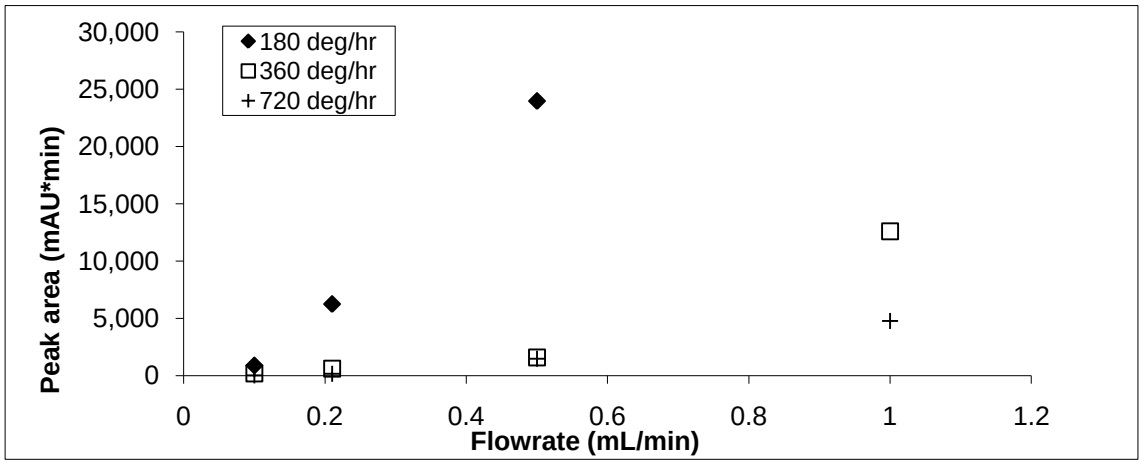

F.4.13 3 mg/mL BSA concentration, 1M NaCl concentration, Trial 4, 180-720 deg/hr rotation speed

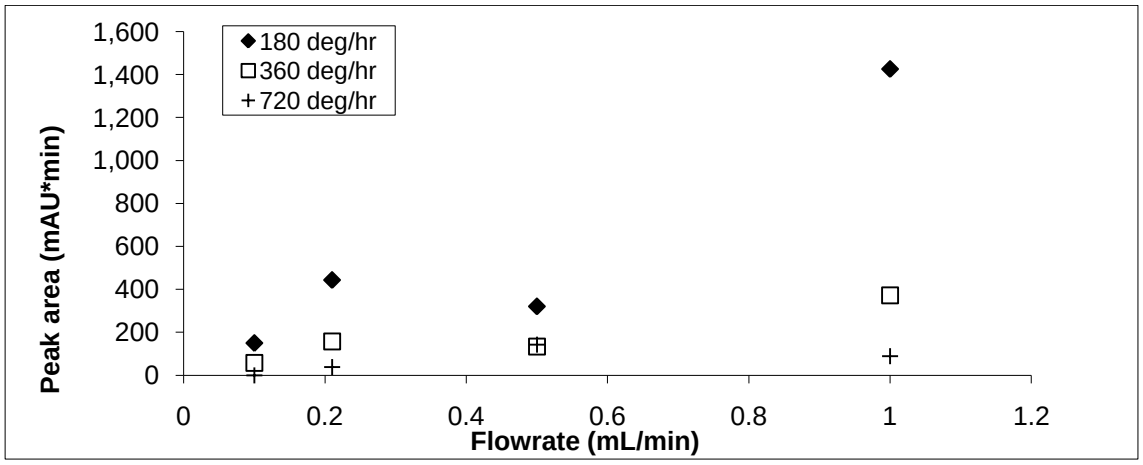

F.4.14 3 mg/mL BSA concentration, 1M NaCl concentration, Trial 5, 180-720 deg/hr rotation speed

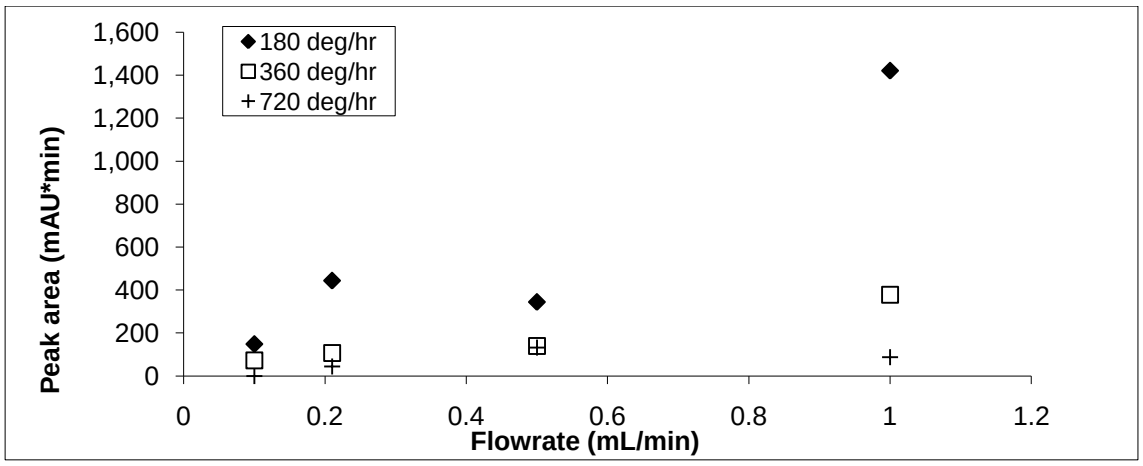

F.4.15 3 mg/mL BSA concentration, 1M NaCl concentration, Trial 6, 180-720 deg/hr rotation speed

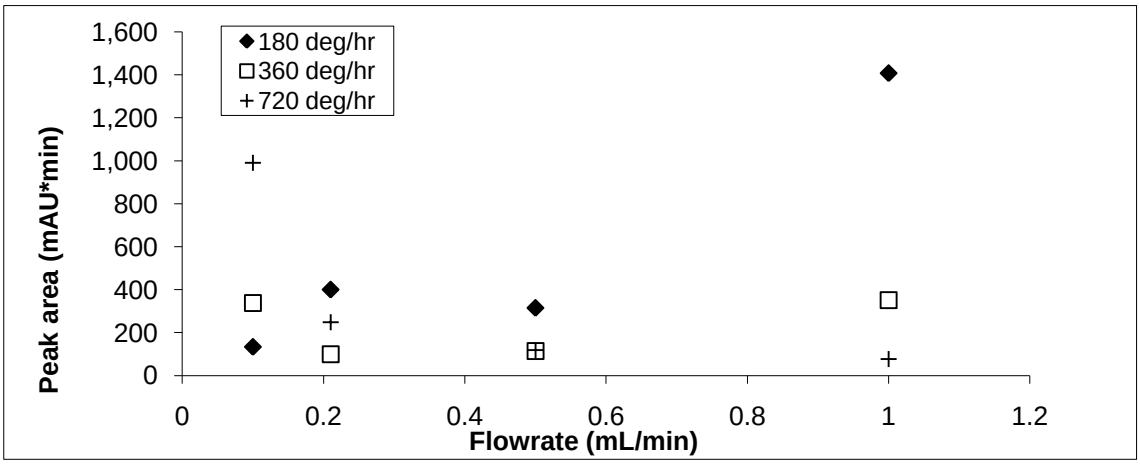

F.4.16 3 mg/mL BSA concentration, 1M NaCl concentration, Trial 7, 180-720 deg/hr rotation speed

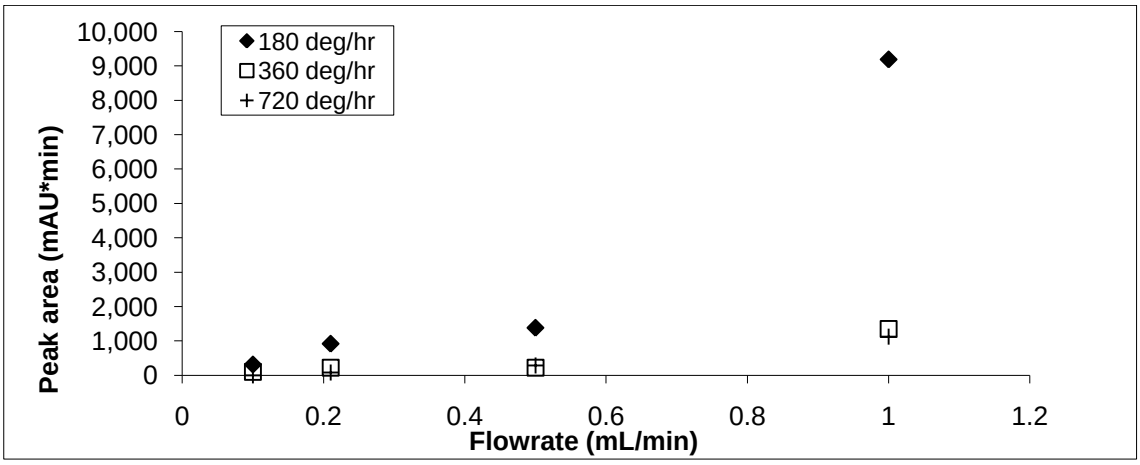

F.4.17 3 mg/mL BSA concentration, 1M NaCl concentration, Trial 8, 180-720 deg/hr rotation speed

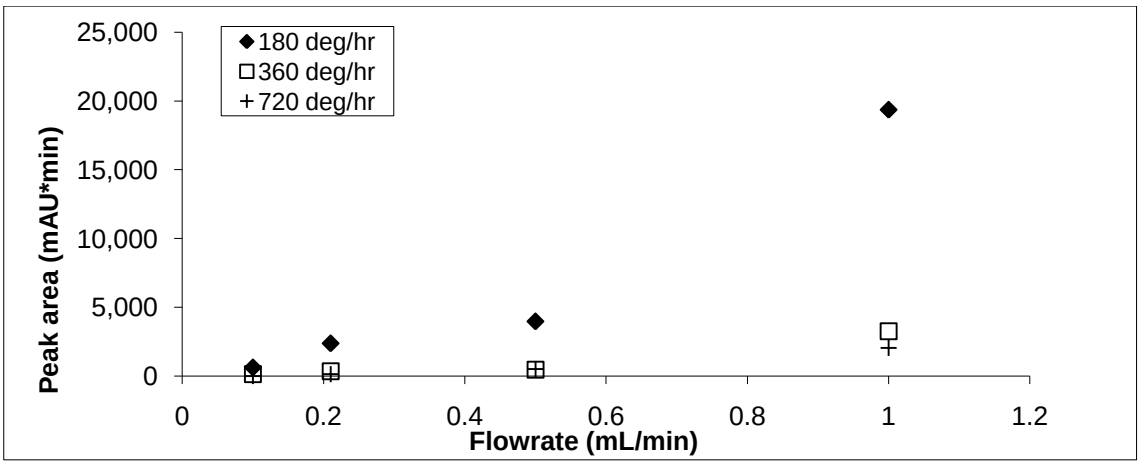

F.4.18 3 mg/mL BSA concentration, 1M NaCl concentration, Trial 9, 180-720 deg/hr rotation speed

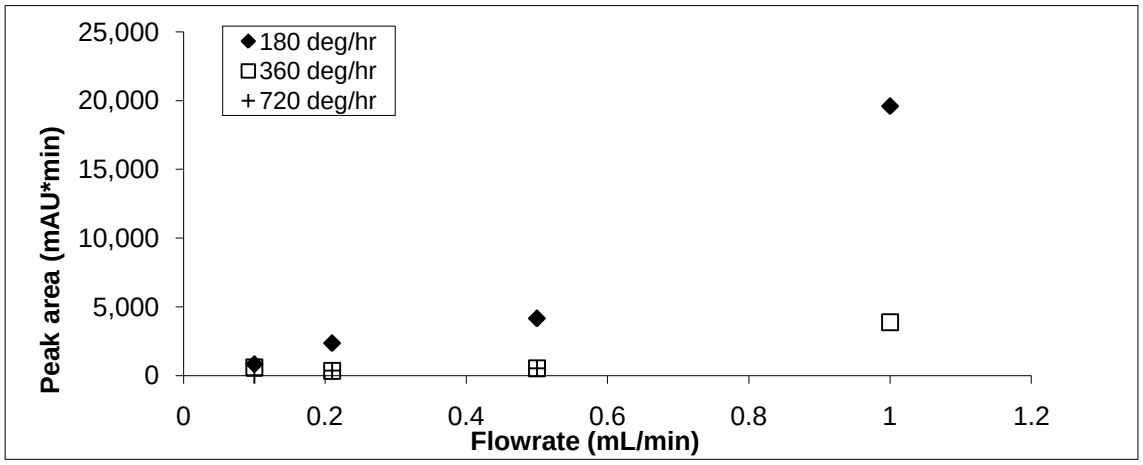

F.4.19 5 mg/mL BSA concentration, 1M NaCl concentration, Trial 1, 180-720 deg/hr rotation speed

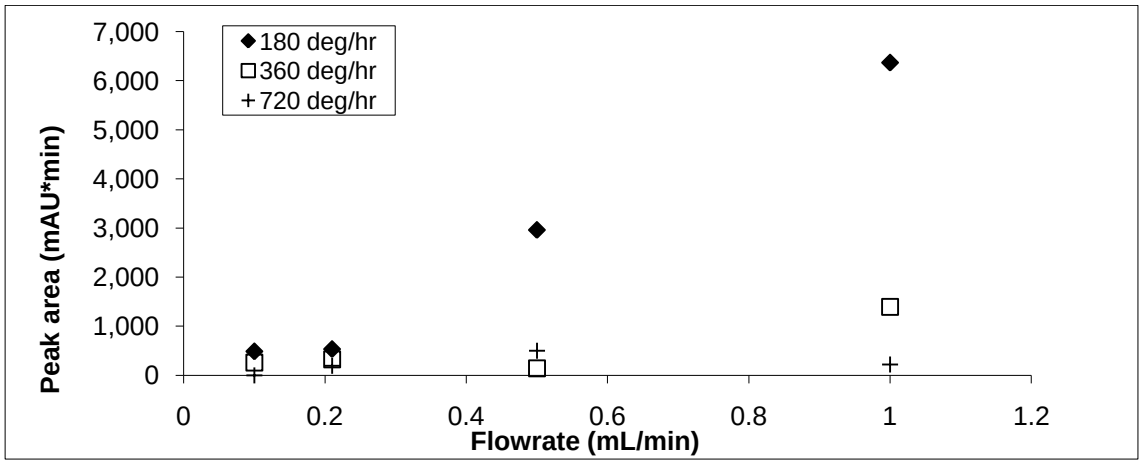

F.4.20 5 mg/mL BSA concentration, 1M NaCl concentration, Trial 2, 180-720 deg/hr rotation speed

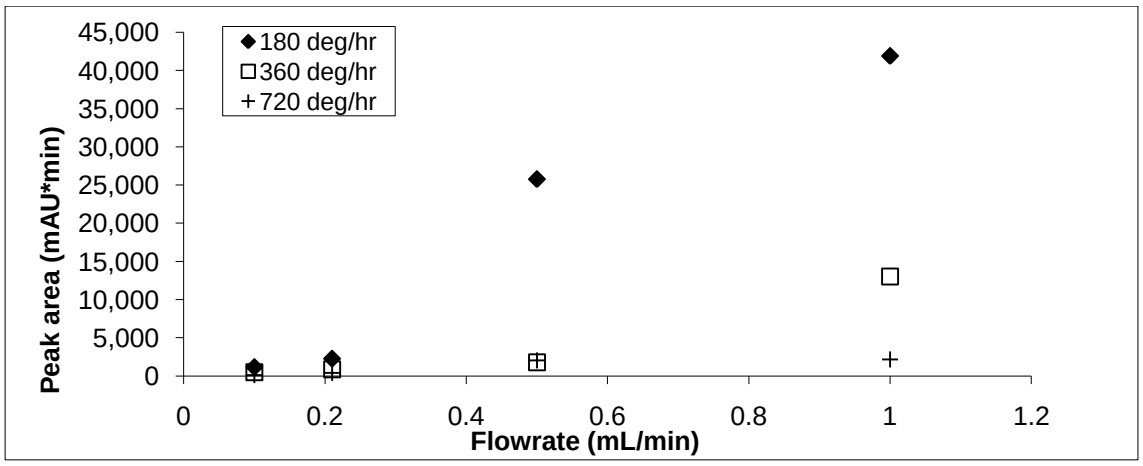

F.4.21 5 mg/mL BSA concentration, 1M NaCl concentration, Trial 3, 180-720 deg/hr rotation speed

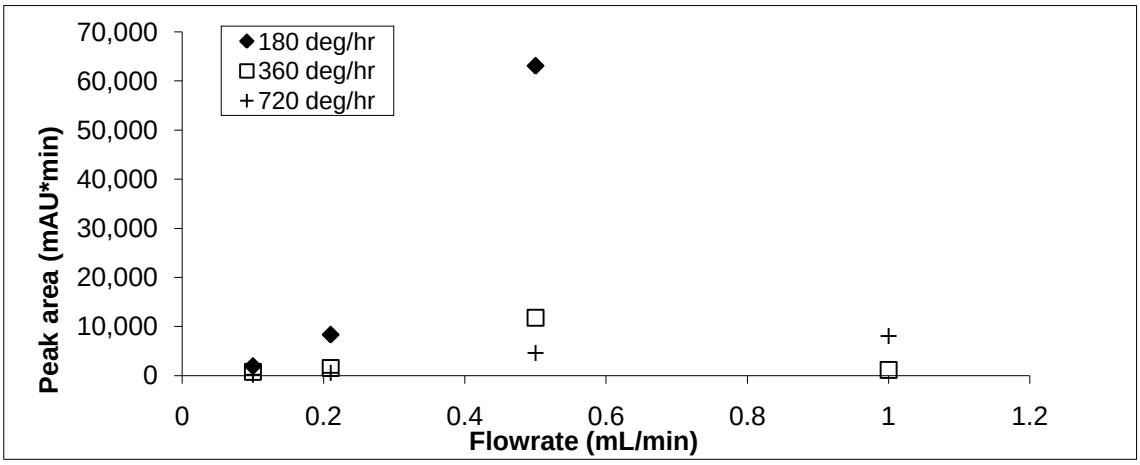

F.4.22 5 mg/mL BSA concentration, 1M NaCl concentration, Trial 4, 180-720 deg/hr rotation speed

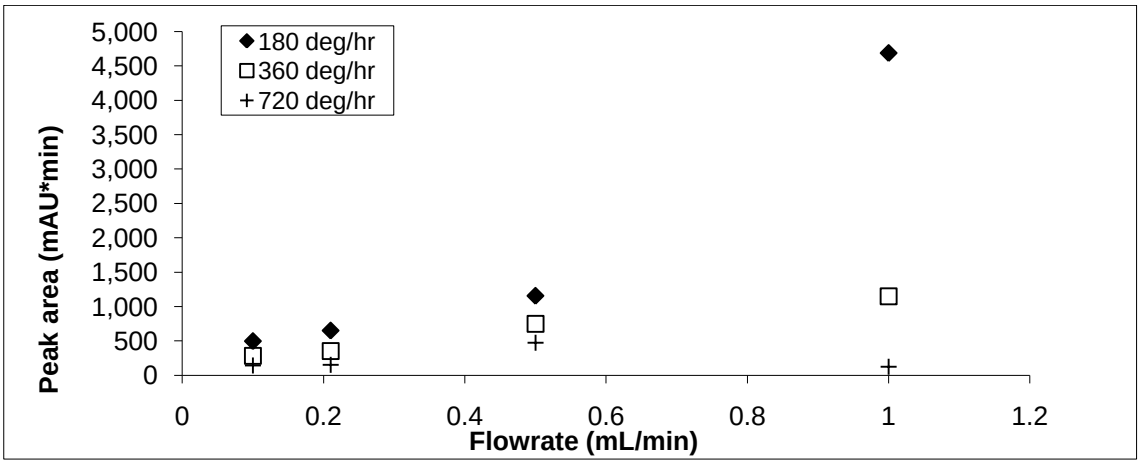

F.4.23 5 mg/mL BSA concentration, 1M NaCl concentration, Trial 5, 180-720 deg/hr rotation speed

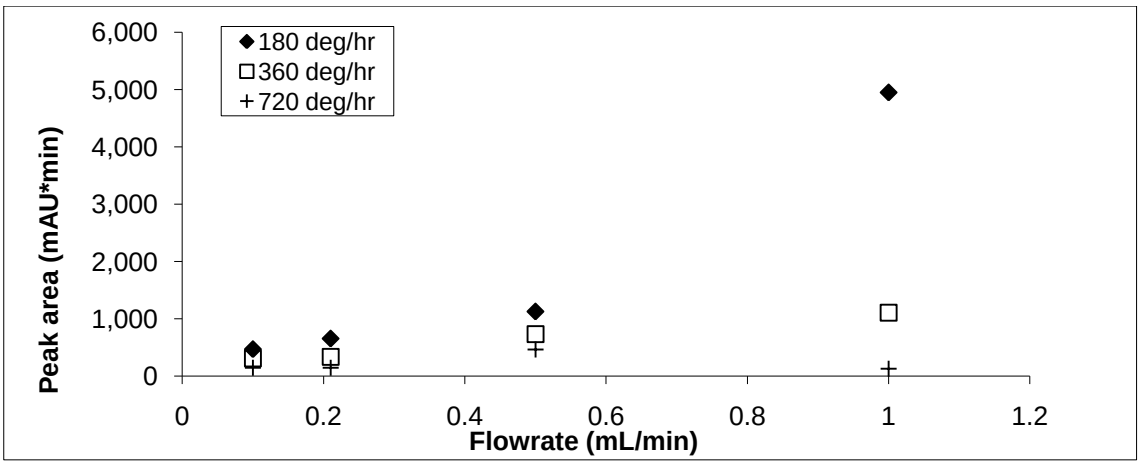

F.4.24 5 mg/mL BSA concentration, 1M NaCl concentration, Trial 6, 180-720 deg/hr rotation speed

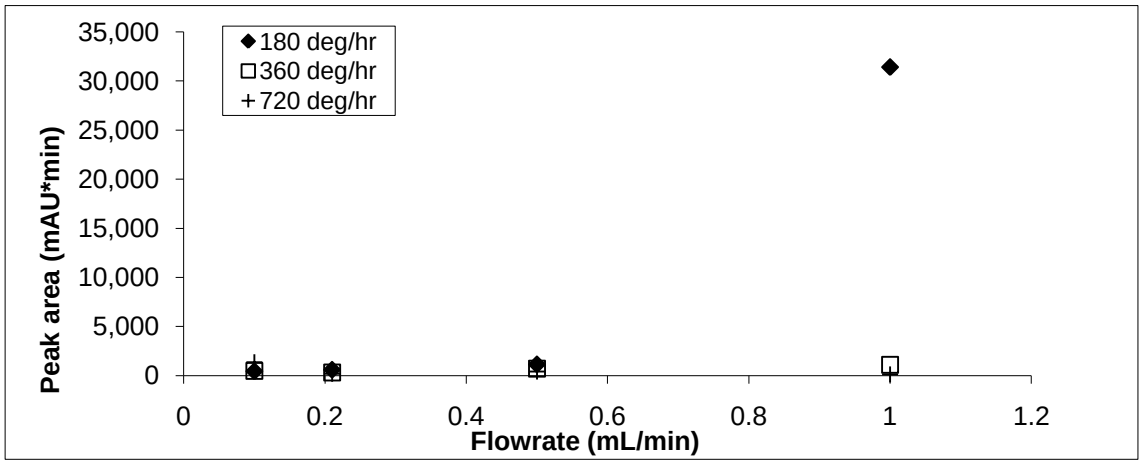

F.4.25 5 mg/mL BSA concentration, 1M NaCl concentration, Trial 7, 180-720 deg/hr rotation speed

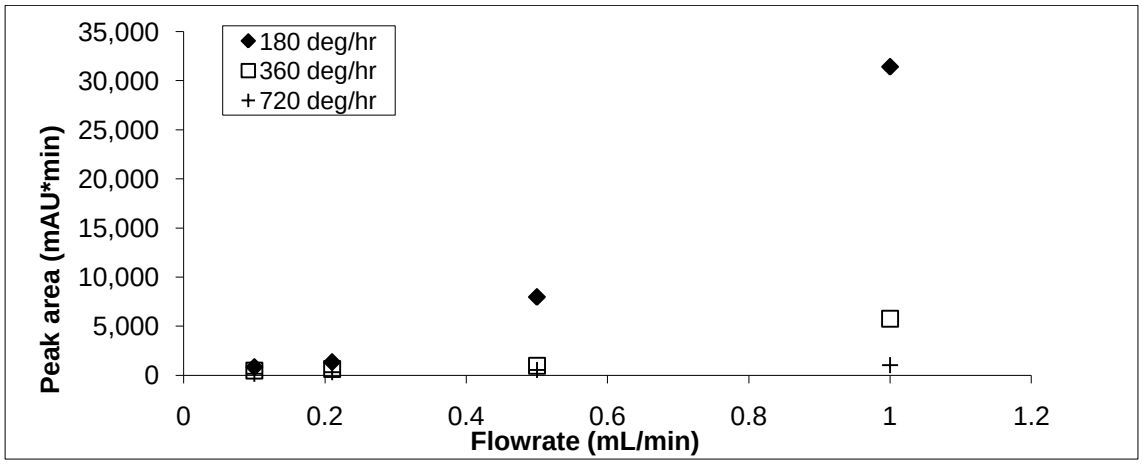

F.4.26 5 mg/mL BSA concentration, 1M NaCl concentration, Trial 8, 180-720 deg/hr rotation speed

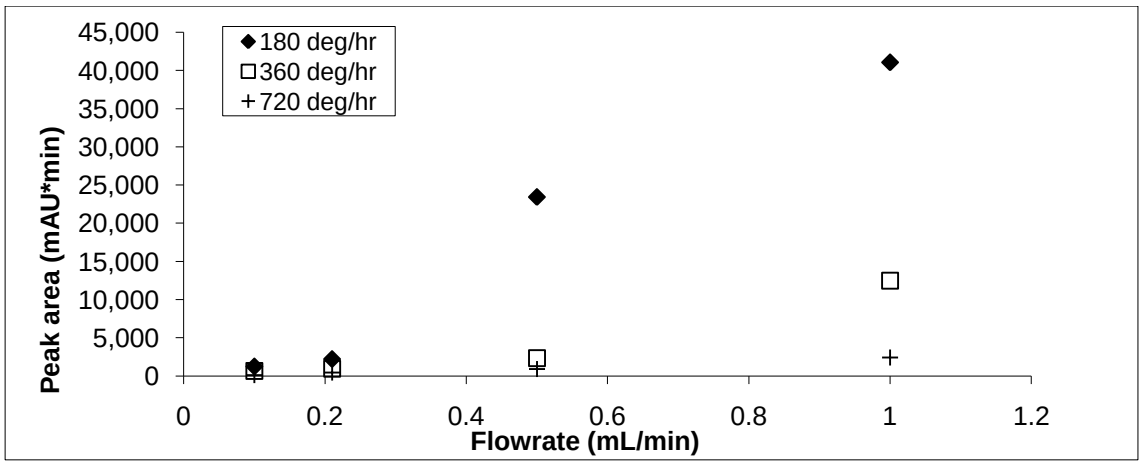

F.4.27 5 mg/mL BSA concentration, 1M NaCl concentration, Trial 9, 180-720 deg/hr rotation speed

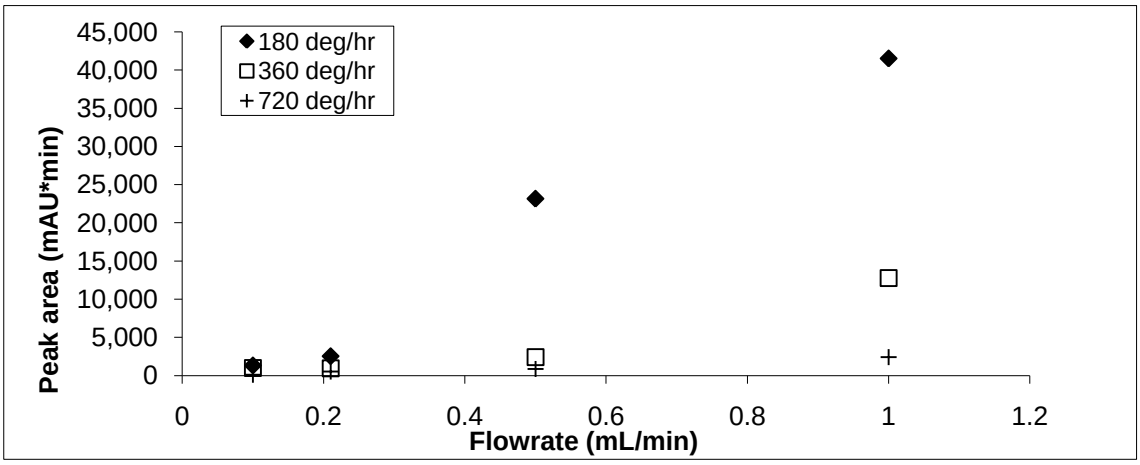

F.4.28 1.5 mg/mL BSA concentration, 2M NaCl concentration, Trial 1, 180-720 deg/hr rotation speed

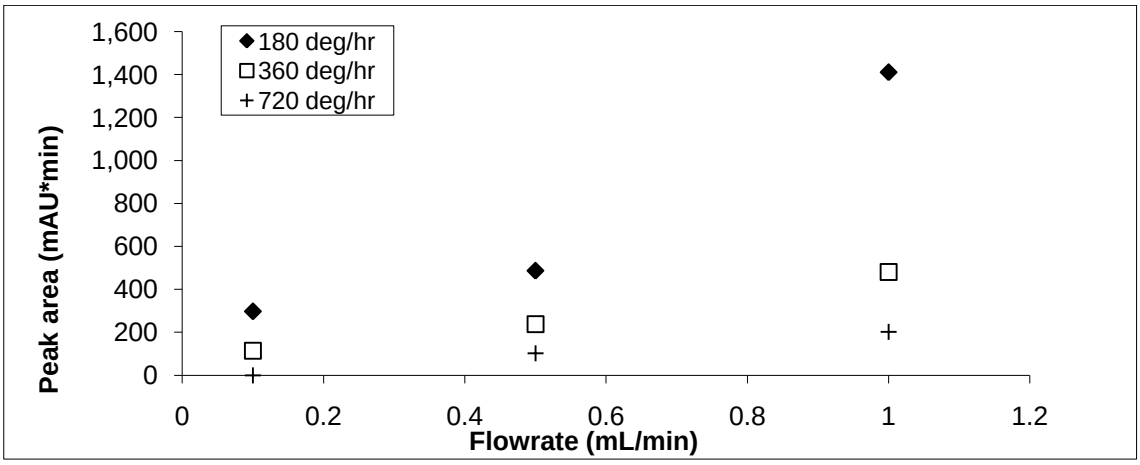

F.4.29 1.5 mg/mL BSA concentration, 2M NaCl concentration, Trial 2, 180-720 deg/hr rotation speed

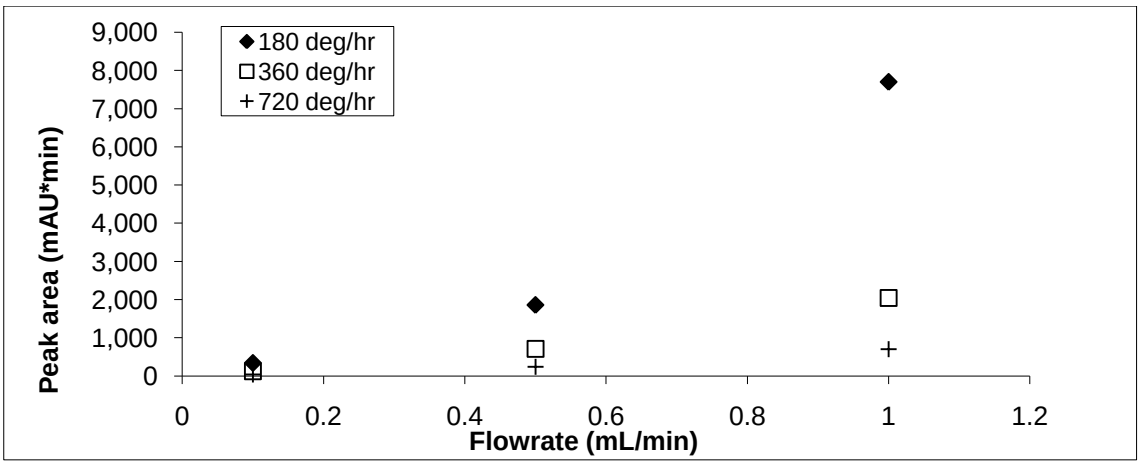

F.4.30 1.5 mg/mL BSA concentration, 2M NaCl concentration, Trial 3, 180-720 deg/hr rotation speed

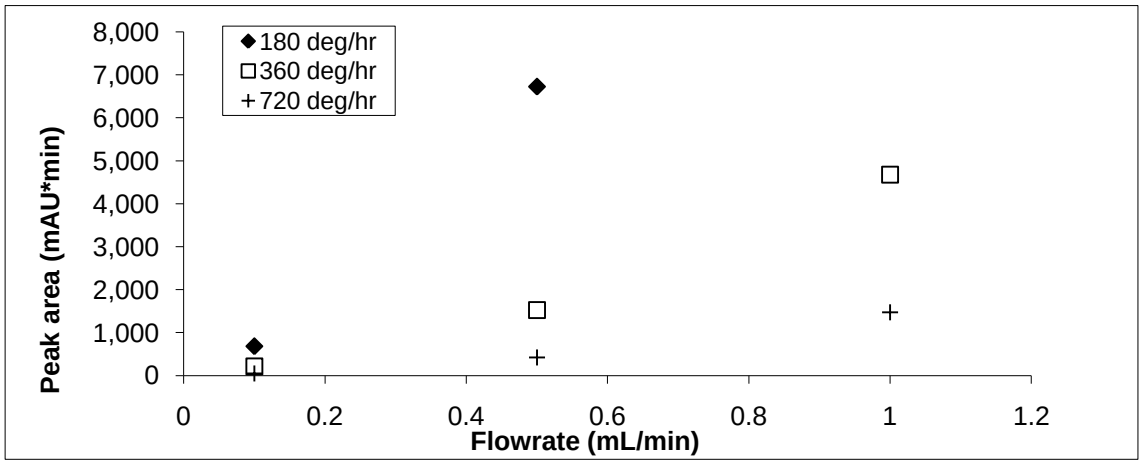

F.4.31 1.5 mg/mL BSA concentration, 2M NaCl concentration, Trial 4, 180-720 deg/hr rotation speed

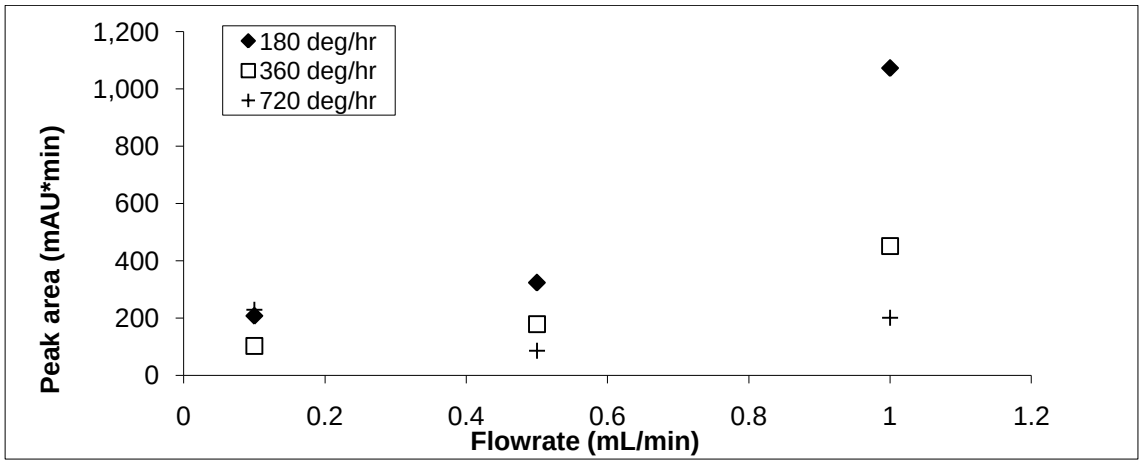

F.4.32 1.5 mg/mL BSA concentration, 2M NaCl concentration, Trial 5, 180-720 deg/hr rotation speed

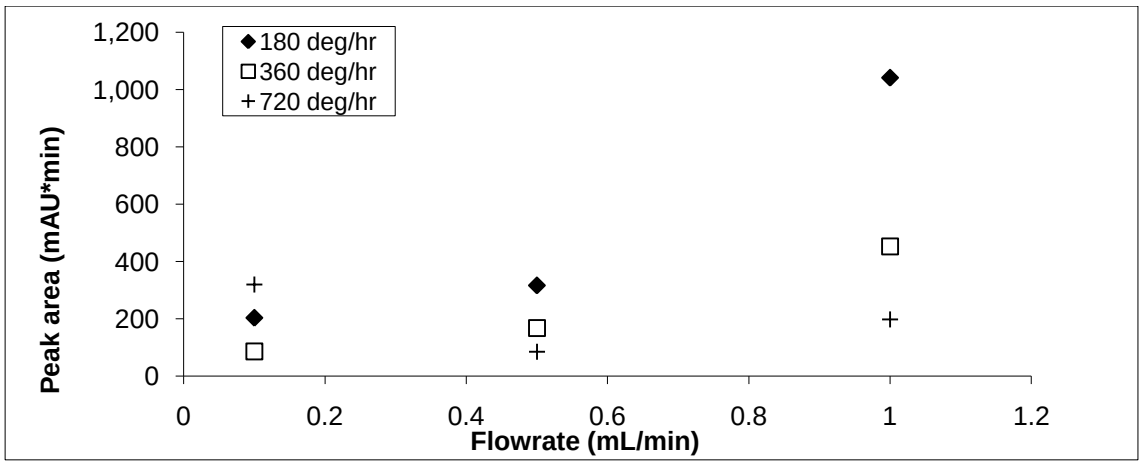

F.4.33 1.5 mg/mL BSA concentration, 2M NaCl concentration, Trial 6, 180-720 deg/hr rotation speed

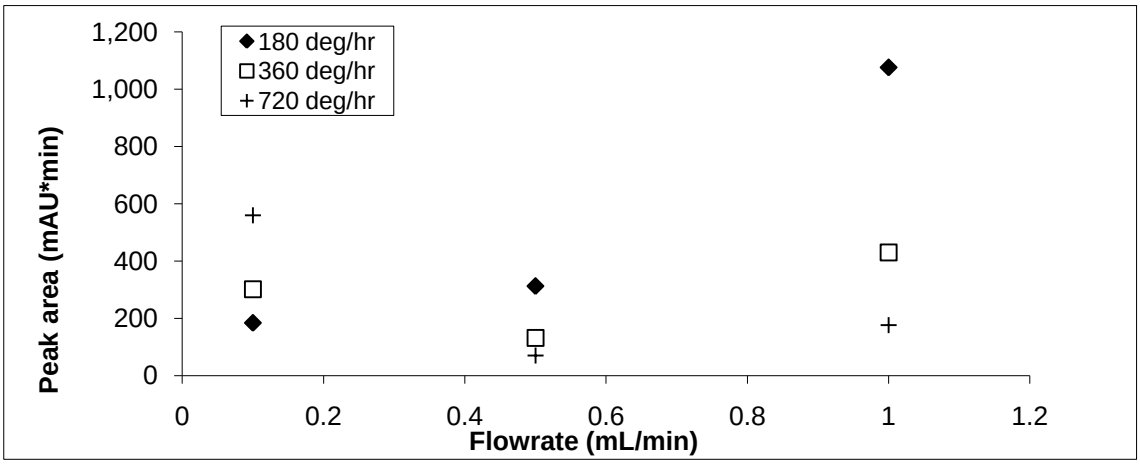

F.4.34 1.5 mg/mL BSA concentration, 2M NaCl concentration, Trial 7, 180-720 deg/hr rotation speed

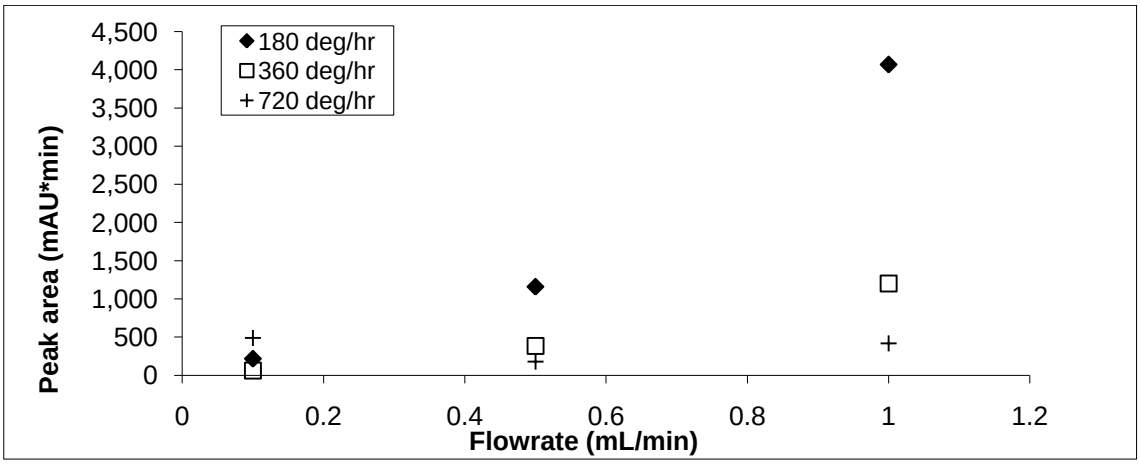

F.4.35 1.5 mg/mL BSA concentration, 2M NaCl concentration, Trial 8, 180-720 deg/hr rotation speed

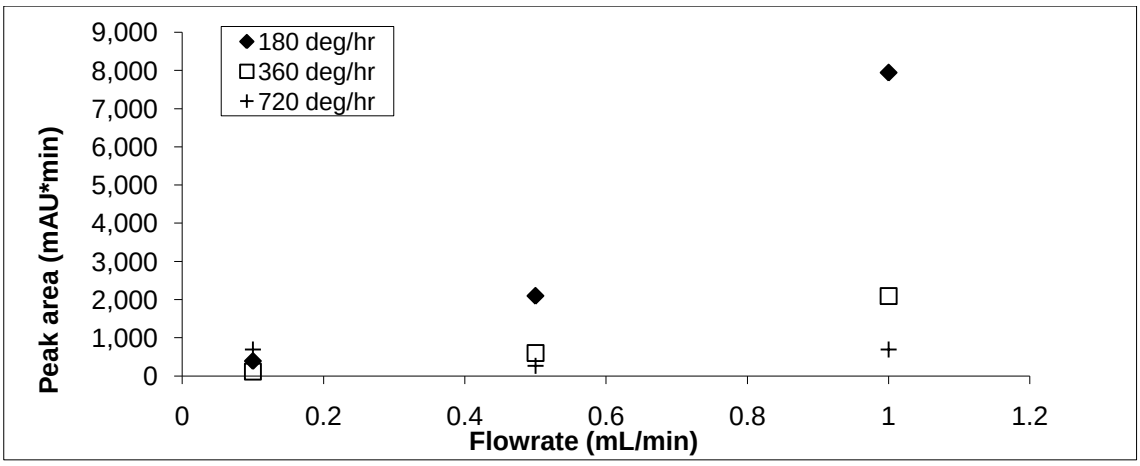

F.4.36 1.5 mg/mL BSA concentration, 2M NaCl concentration, Trial 9, 180-720 deg/hr rotation speed

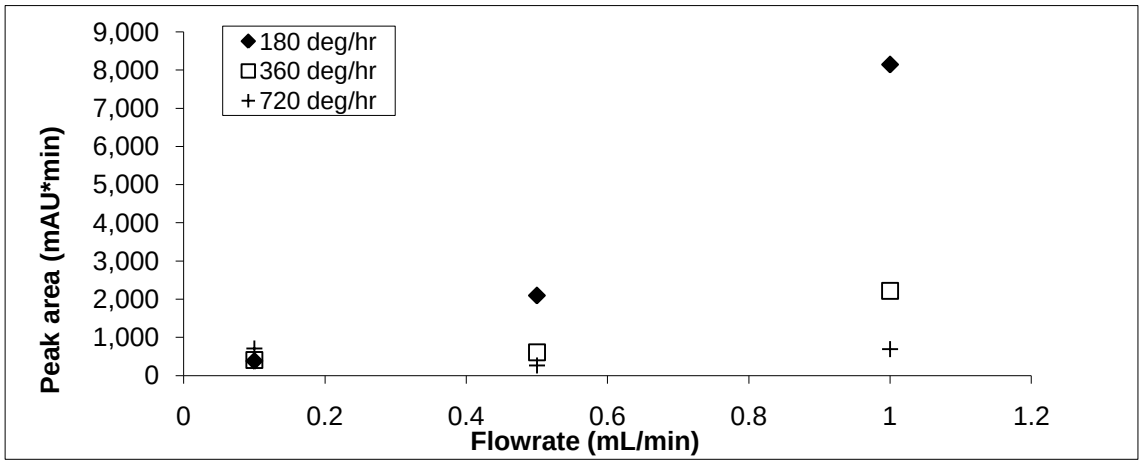

F.5 Feed concentration

F.5.1 180 deg/hr rotation speed, 1M NaCl concentration, Trial 1, 0.1-1.0 mL/min flow rate

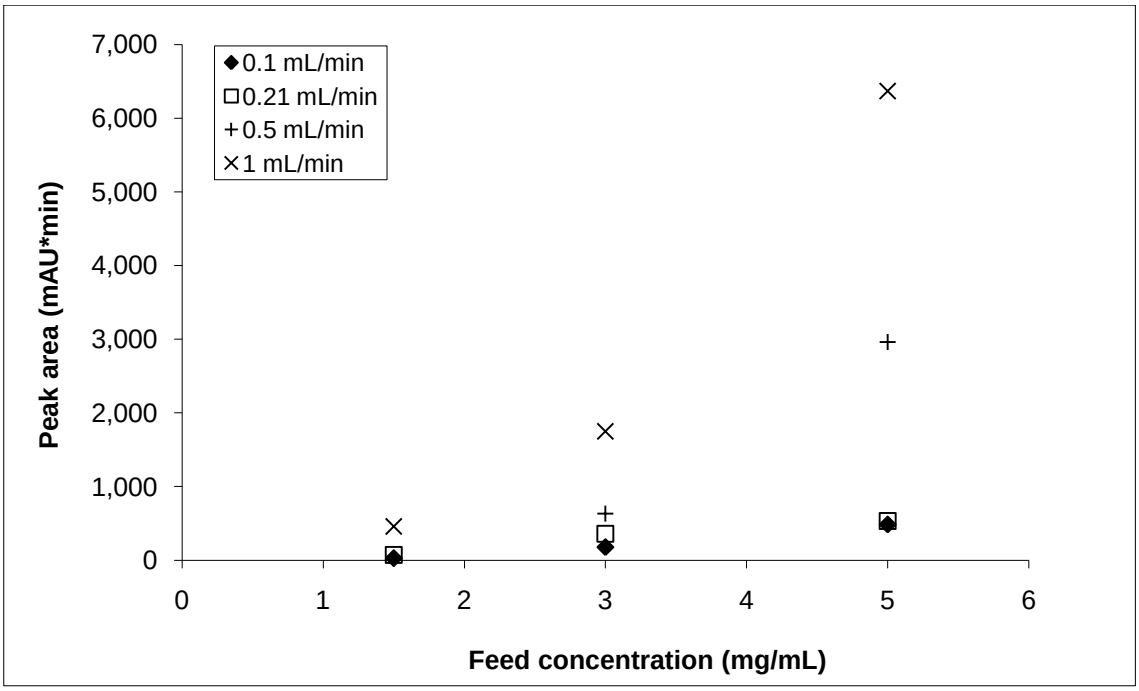

F.5.2 180 deg/hr rotation speed, 1M NaCl concentration, Trial 2, 0.1-1.0 mL/min flow rate

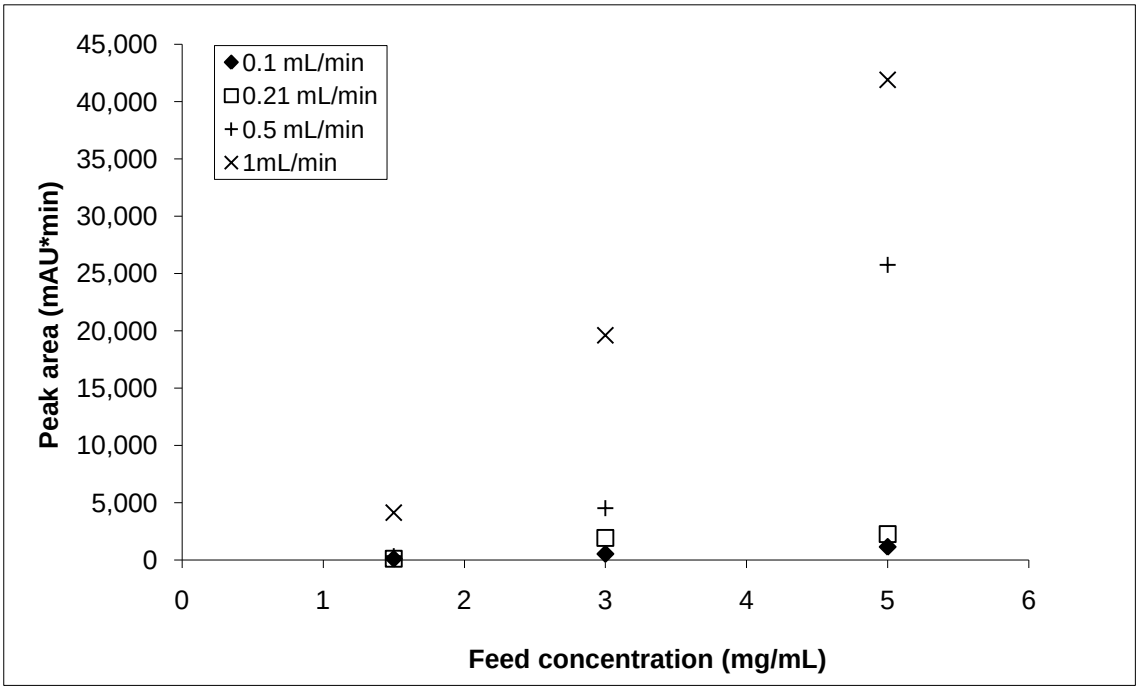

F.5.3 180 deg/hr rotation speed, 1M NaCl concentration, Trial 3, 0.1-1.0 mL/min flow rate

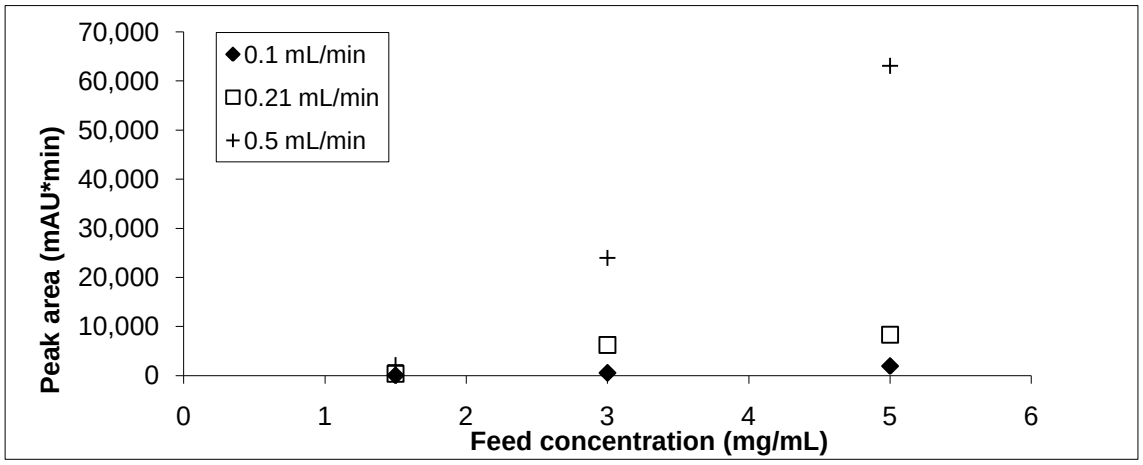

F.5.4 180 deg/hr rotation speed, 1M NaCl concentration, Trial 4, 0.1-1.0 mL/min flow rate

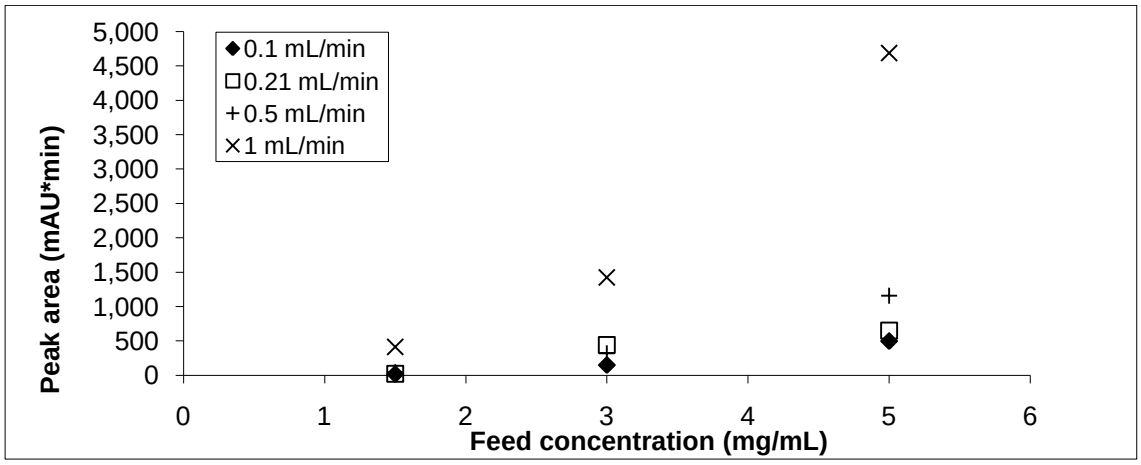

F.5.5 180 deg/hr rotation speed, 1M NaCl concentration, Trial 5, 0.1-1.0 mL/min flow rate

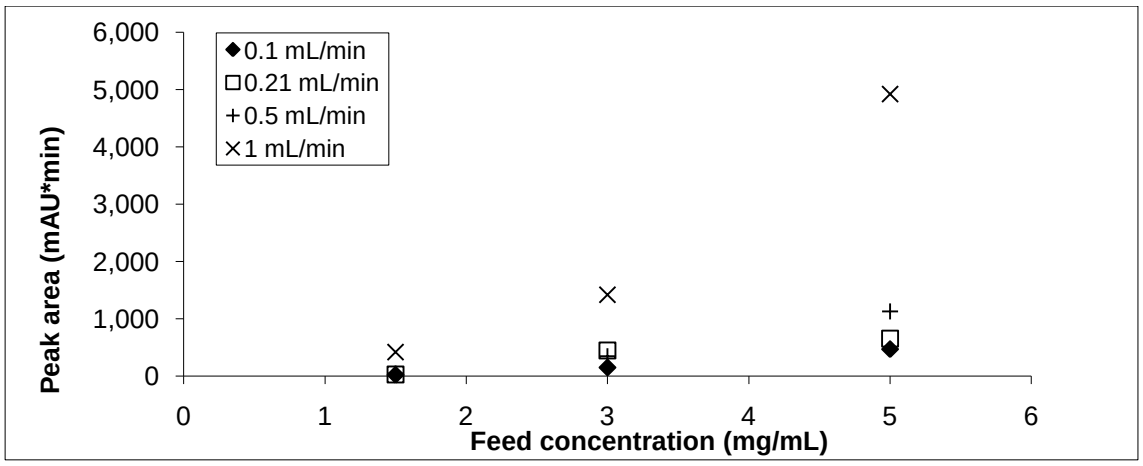

F.5.6 180 deg/hr rotation speed, 1M NaCl concentration, Trial 6, 0.1-1.0 mL/min flow rate

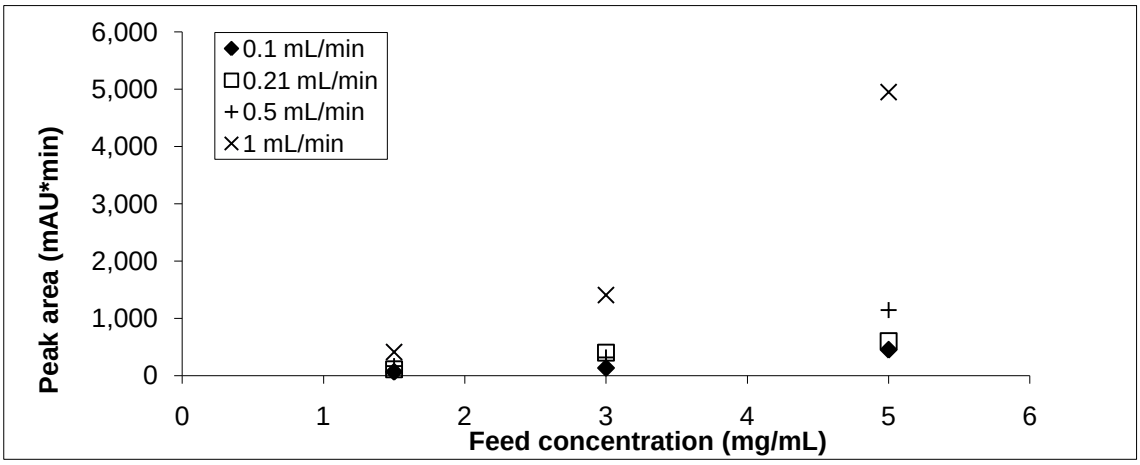

F.5.7 180 deg/hr rotation speed, 1M NaCl concentration, Trial 7, 0.1-1.0 mL/min flow rate

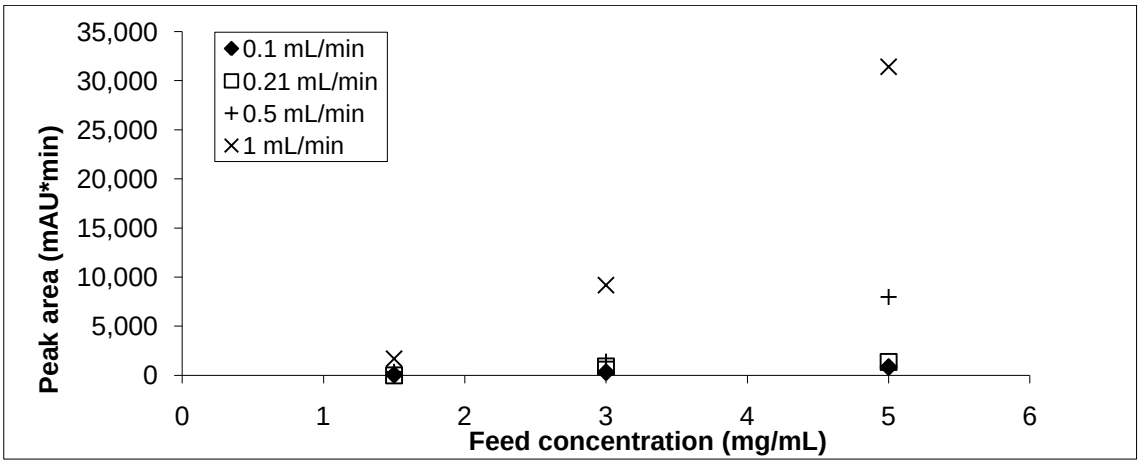

F.5.8 180 deg/hr rotation speed, 1M NaCl concentration, Trial 8, 0.1-1.0 mL/min flow rate

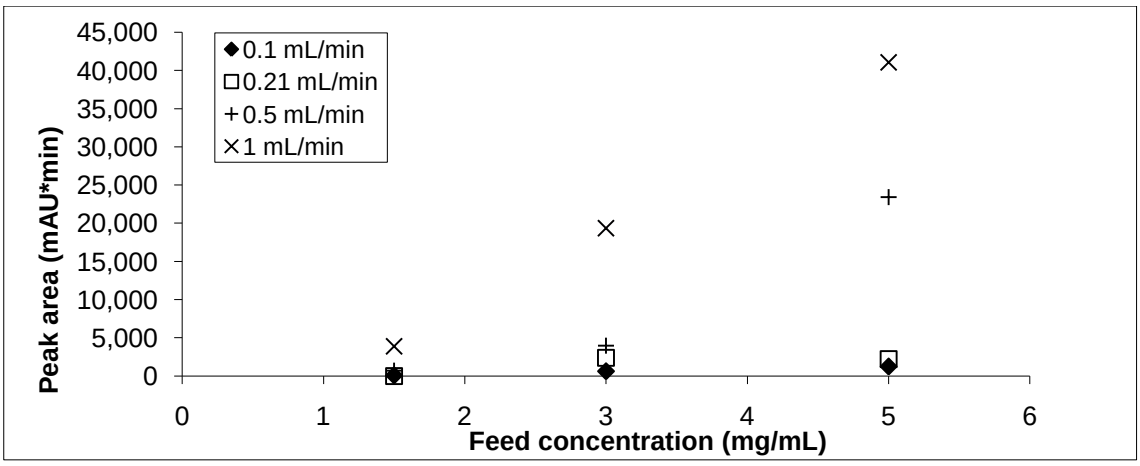

F.5.9 180 deg/hr rotation speed, 1M NaCl concentration, Trial 9, 0.1-1.0 mL/min flow rate

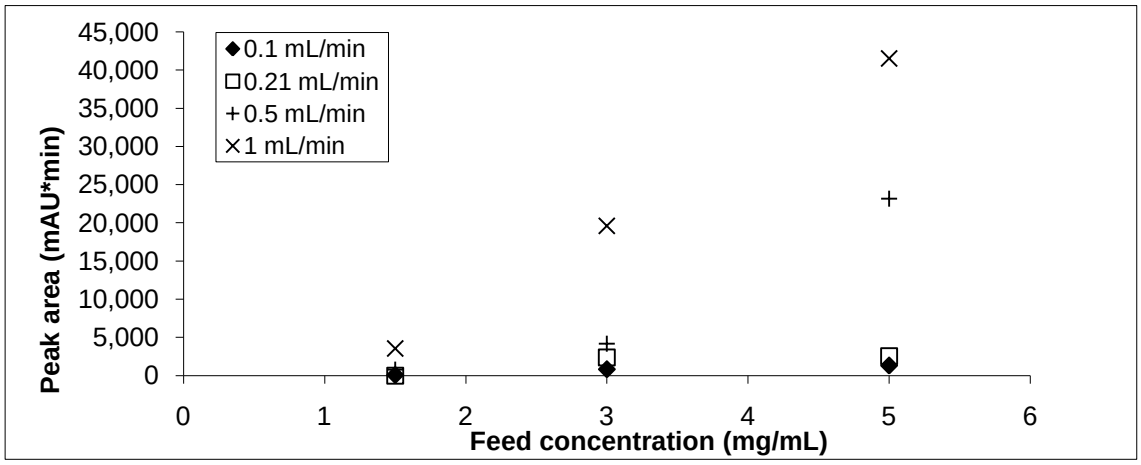

F.5.10 360 deg/hr rotation speed, 1M NaCl concentration, Trial 1, 0.1-1.0 mL/min flow rate

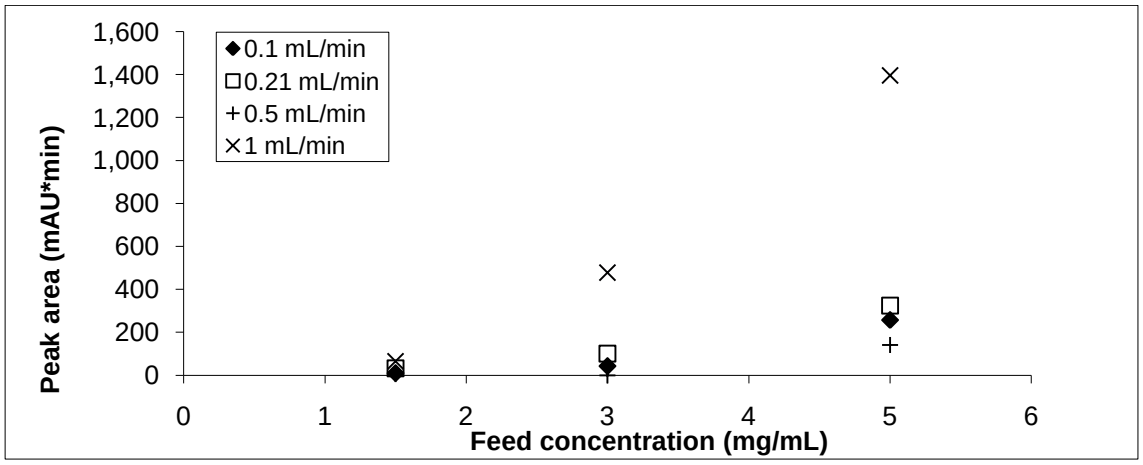

F.5.11 360 deg/hr rotation speed, 1M NaCl concentration, Trial 2, 0.1-1.0 mL/min flow rate

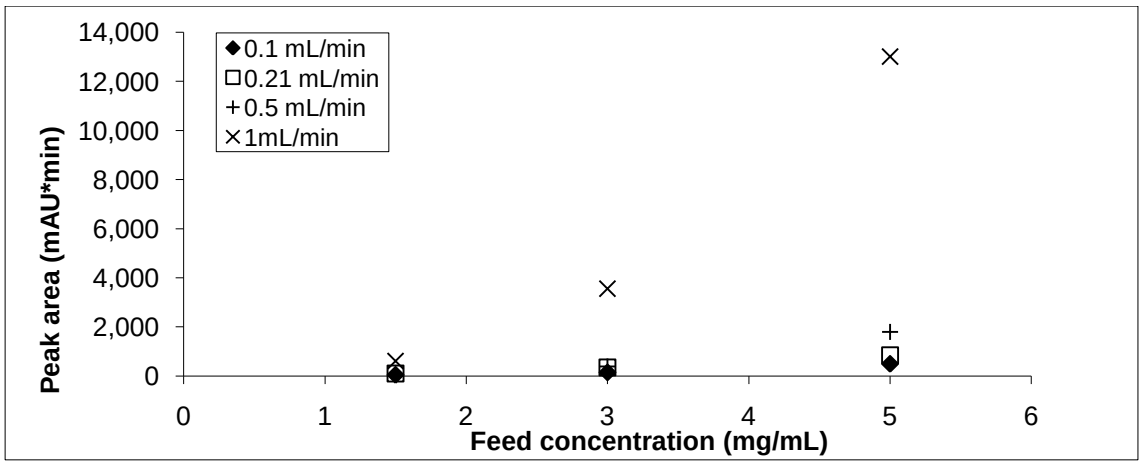

F.5.12 360 deg/hr rotation speed, 1M NaCl concentration, Trial 3, 0.1-1.0 mL/min flow rate

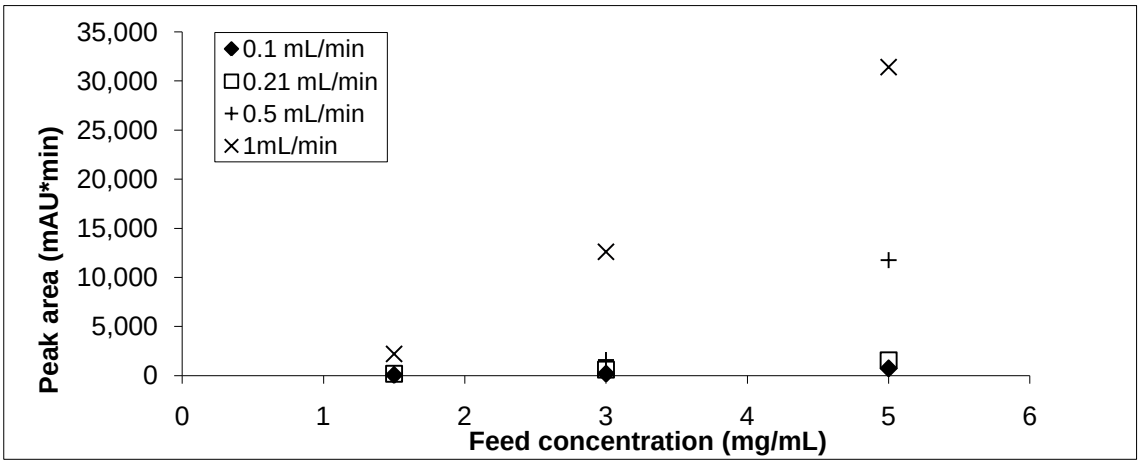

F.5.13 360 deg/hr rotation speed, 1M NaCl concentration, Trial 4, 0.1-1.0 mL/min flow rate

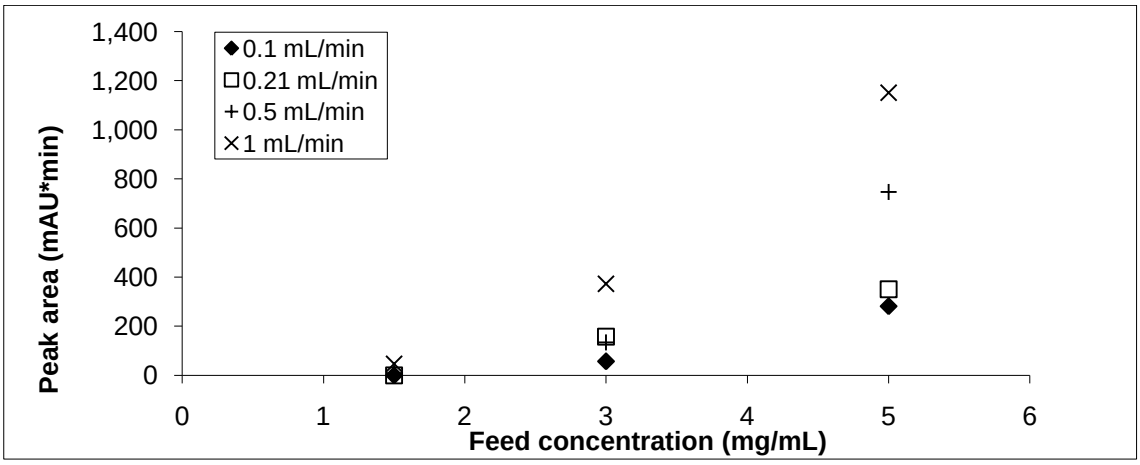

F.5.14 360 deg/hr rotation speed, 1M NaCl concentration, Trial 5, 0.1-1.0 mL/min flow rate

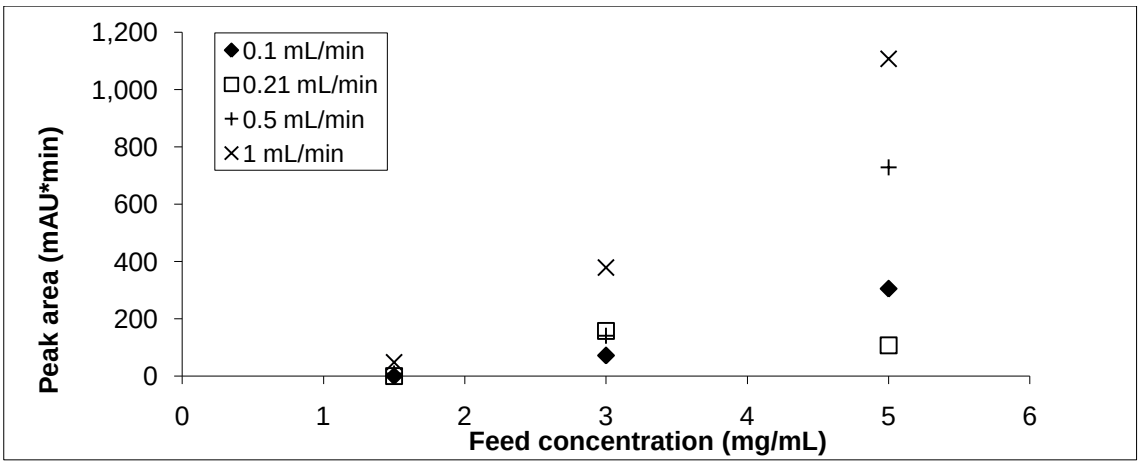

F.5.15 360 deg/hr rotation speed, 1M NaCl concentration, Trial 6, 0.1-1.0 mL/min flow rate

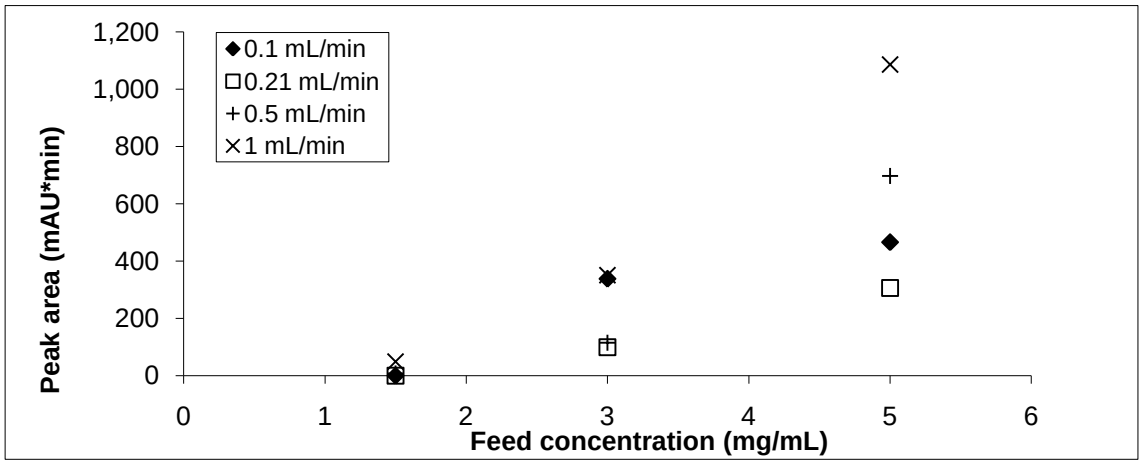

F.5.16 360 deg/hr rotation speed, 1M NaCl concentration, Trial 7, 0.1-1.0 mL/min flow rate

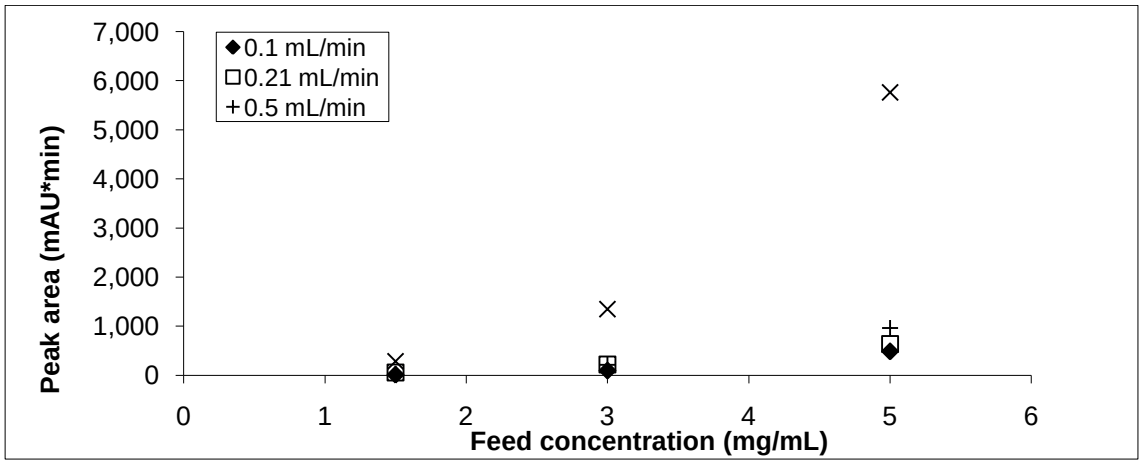

F.5.17 360 deg/hr rotation speed, 1M NaCl concentration, Trial 8, 0.1-1.0 mL/min flow rate

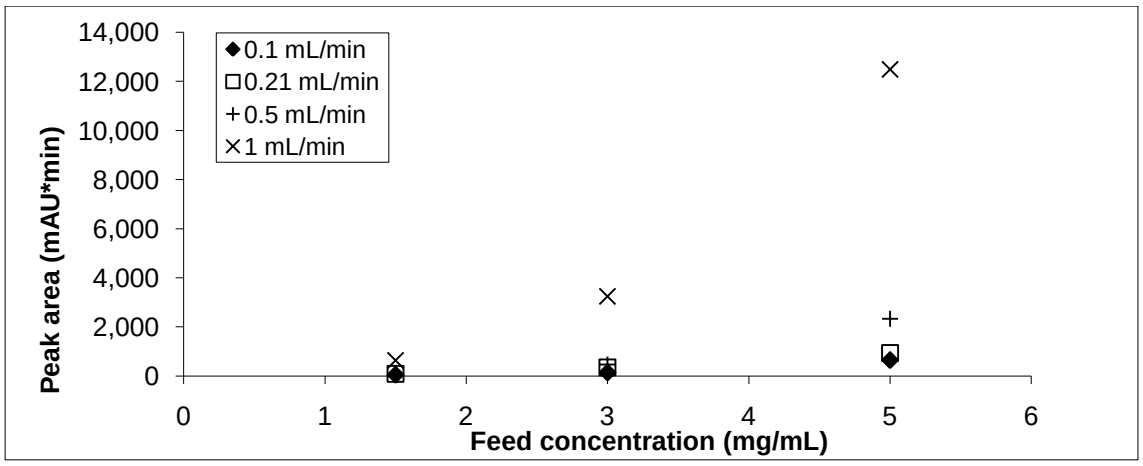

F.5.18 360 deg/hr rotation speed, 1M NaCl concentration, Trial 9, 0.1-1.0 mL/min flow rate

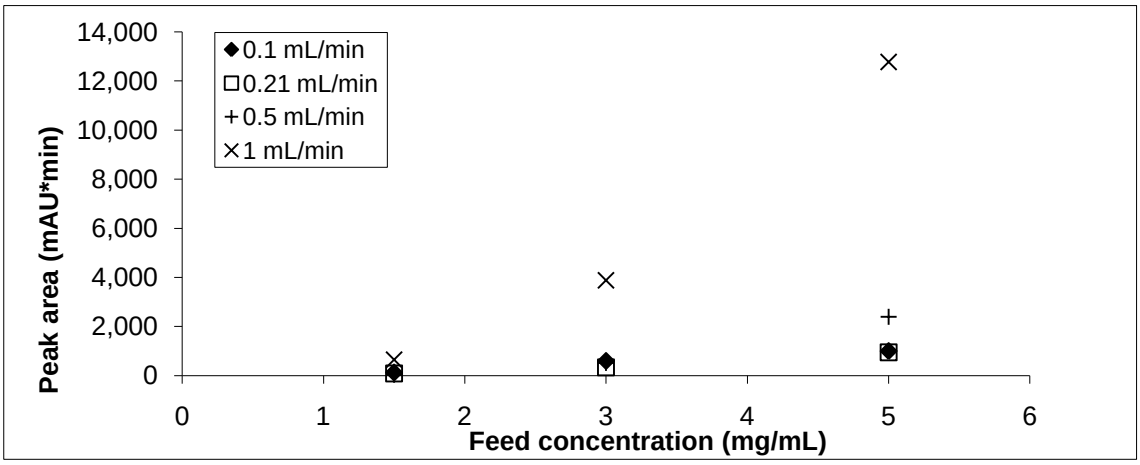

F.5.19 720 deg/hr rotation speed, 1M NaCl concentration, Trial 1, 0.1-1.0 mL/min flow rate

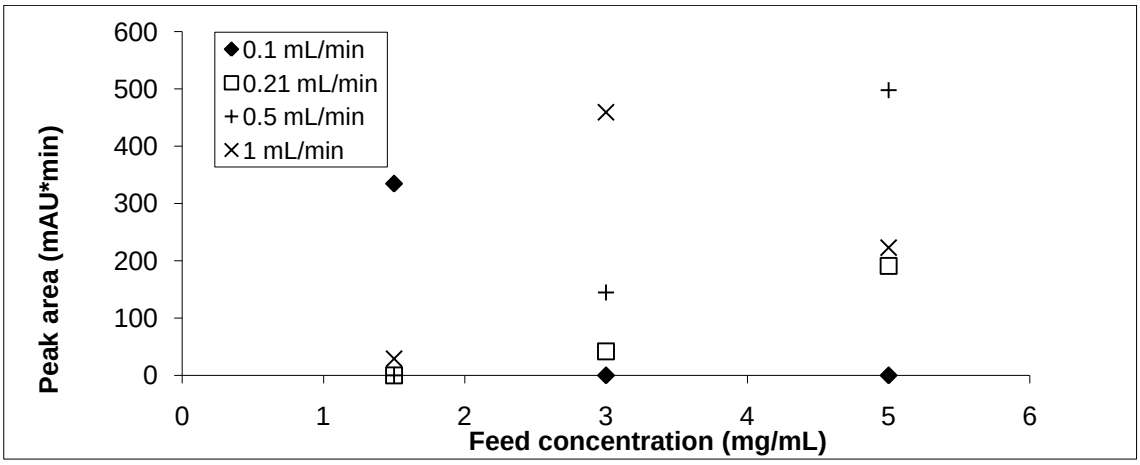

F.5.20 720 deg/hr rotation speed, 1M NaCl concentration, Trial 2, 0.1-1.0 mL/min flow rate

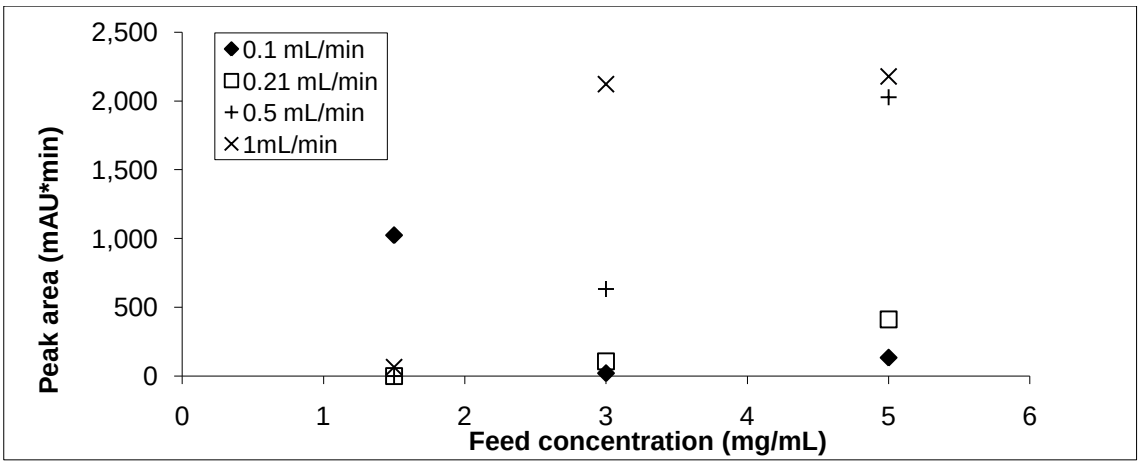

F.5.21 720 deg/hr rotation speed, 1M NaCl concentration, Trial 3, 0.1-1.0 mL/min flow rate

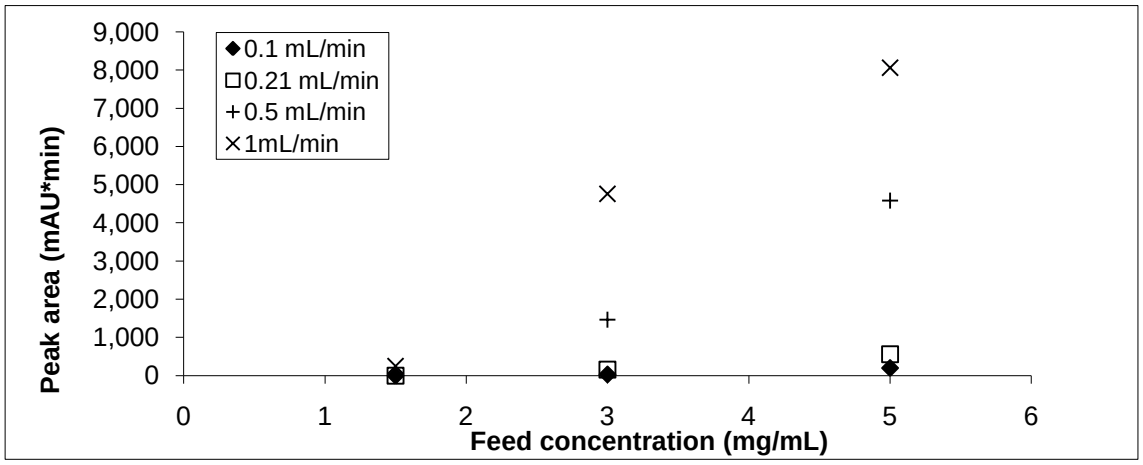

F.5.22 720 deg/hr rotation speed, 1M NaCl concentration, Trial 4, 0.1-1.0 mL/min flow rate

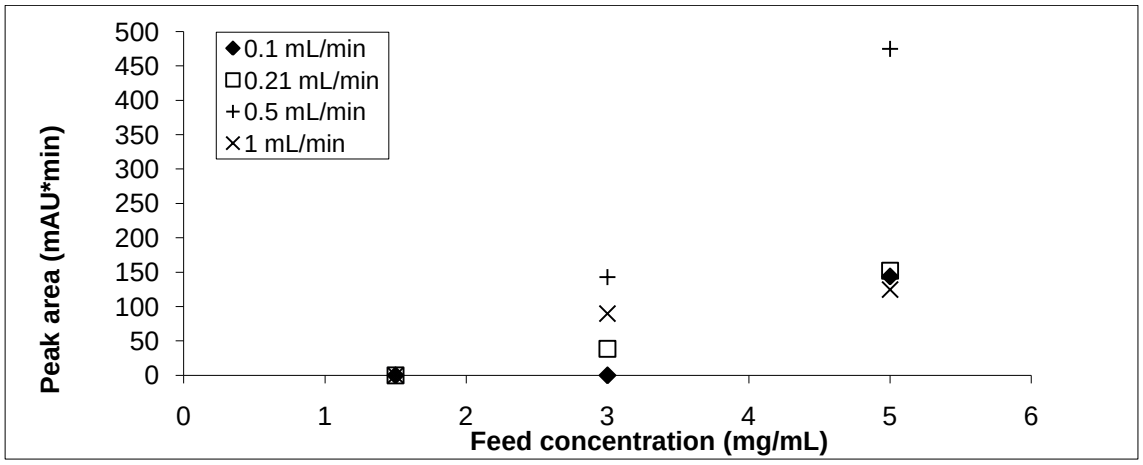

F.5.23 720 deg/hr rotation speed, 1M NaCl concentration, Trial 5, 0.1-1.0 mL/min flow rate

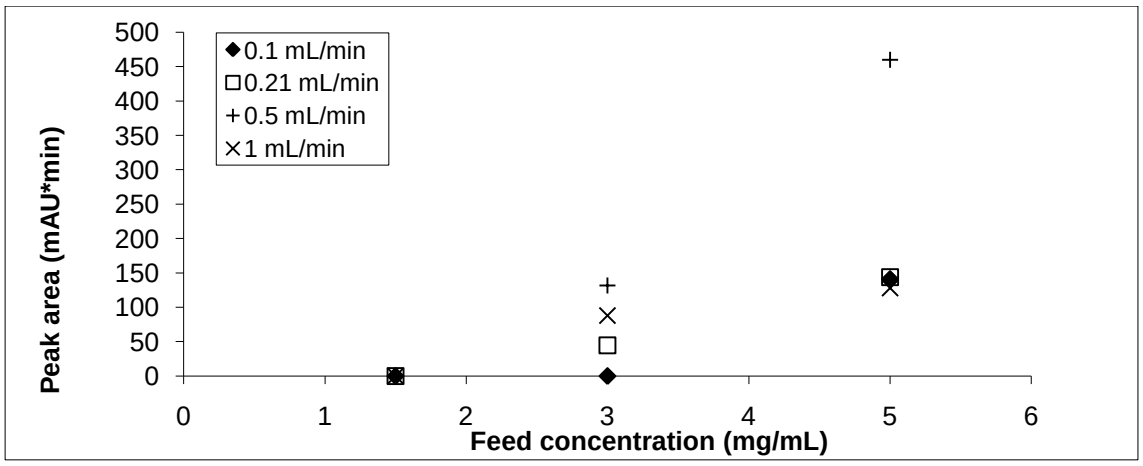

F.5.24 720 deg/hr rotation speed, 1M NaCl concentration, Trial 6, 0.1-1.0 mL/min flow rate

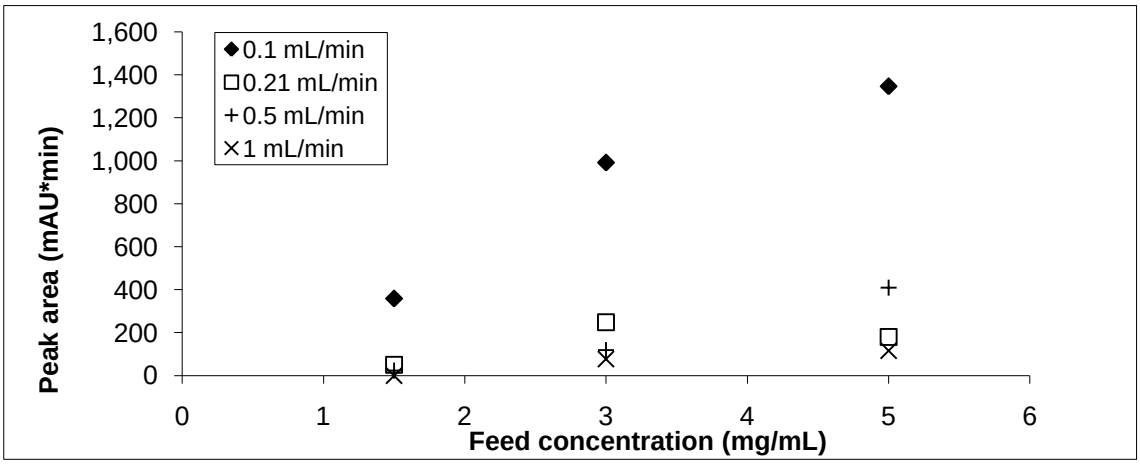

F.5.25 720 deg/hr rotation speed, 1M NaCl concentration, Trial 7, 0.1-1.0 mL/min flow rate

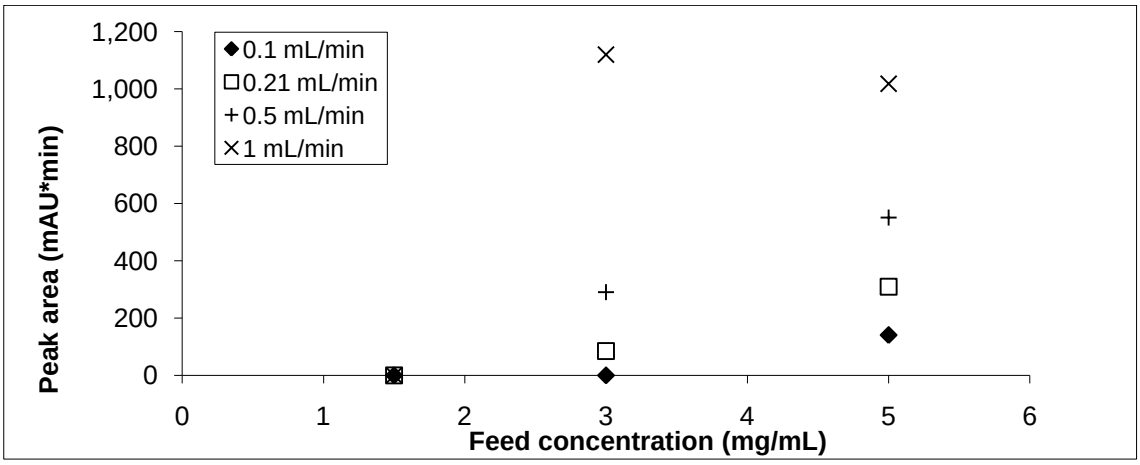

F.5.26 720 deg/hr rotation speed, 1M NaCl concentration, Trial 8, 0.1-1.0 mL/min flow rate

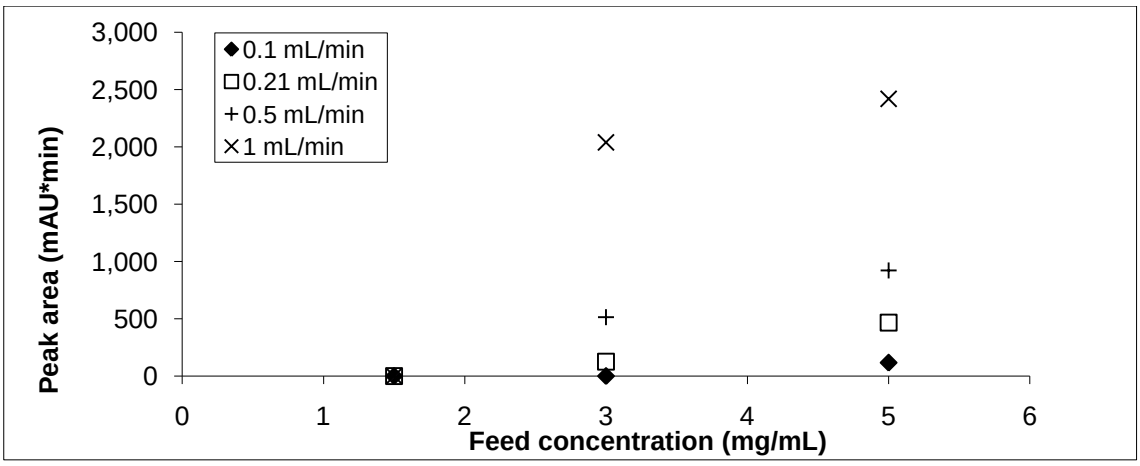

F.5.27 720 deg/hr rotation speed, 1M NaCl concentration, Trial 9, 0.1-1.0 mL/min flow rate

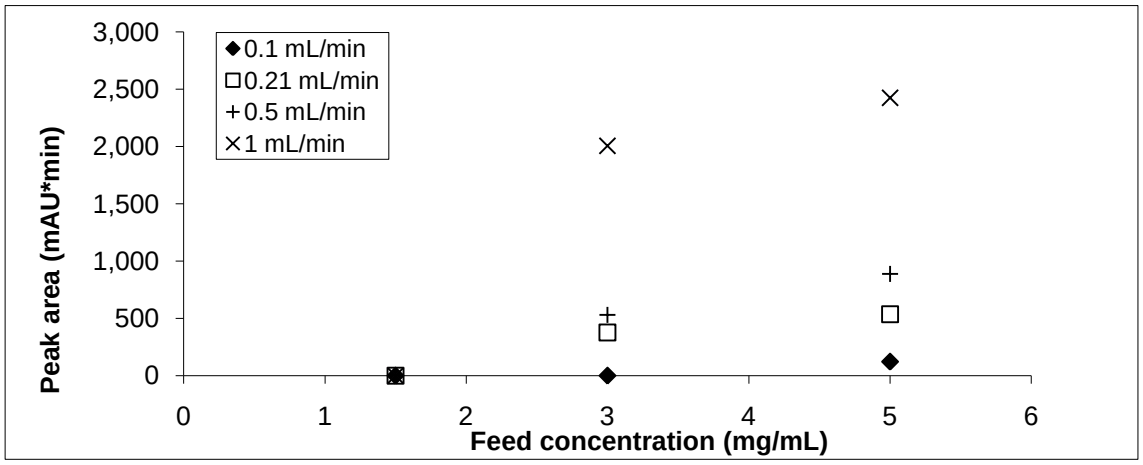

F.6 Elution buffer concentration

F.6.1 180 deg/hr rotation speed, 1.5 mg/mL BSA concentration, Trial 1, 0.1-1.0 mL/min flow rate

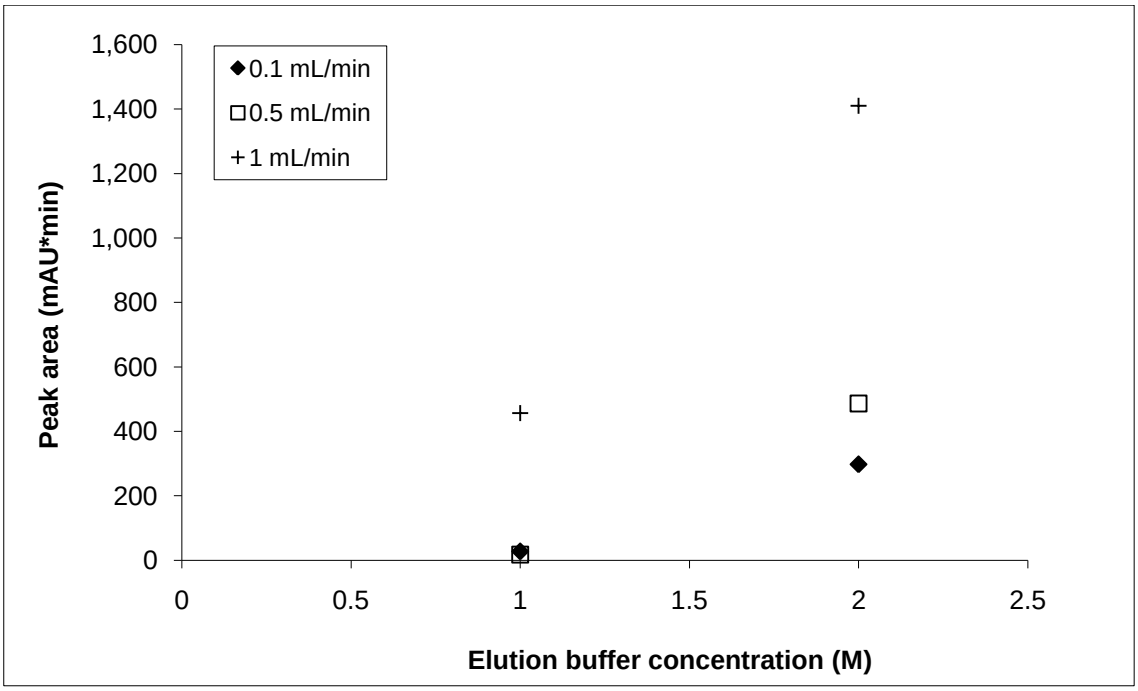

F.6.2 180 deg/hr rotation speed, 1.5 mg/mL BSA concentration, Trial 2, 0.1-1.0 mL/min flow rate

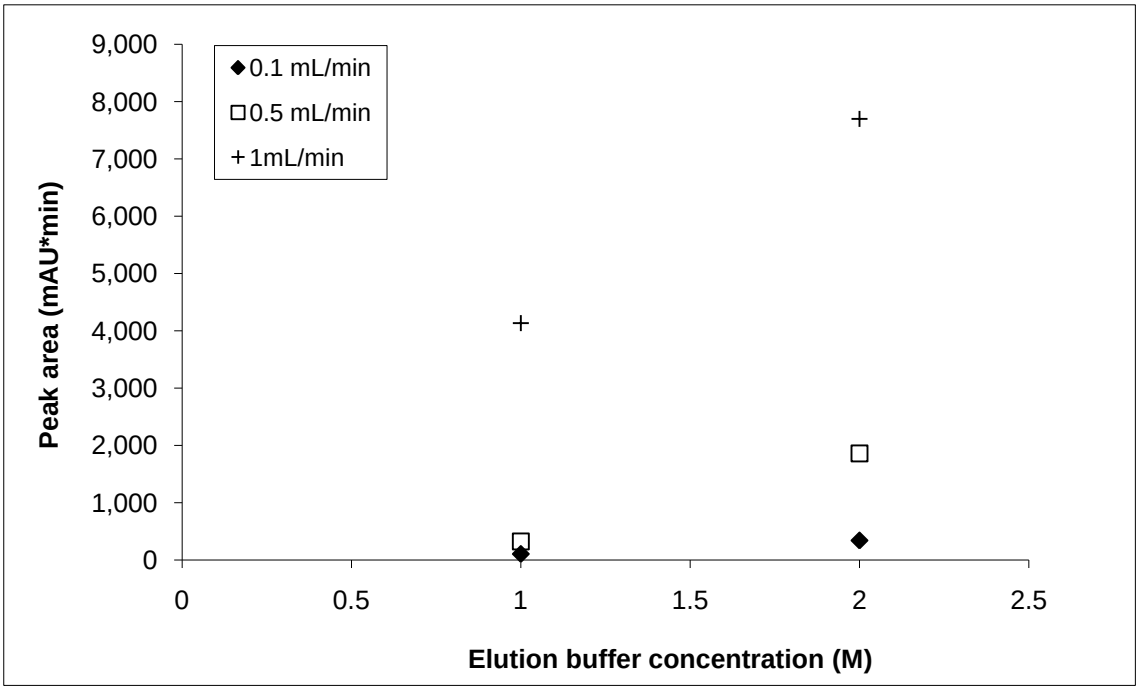

F.6.3 180 deg/hr rotation speed, 1.5 mg/mL BSA concentration, Trial 3, 0.1-1.0 mL/min flow rate

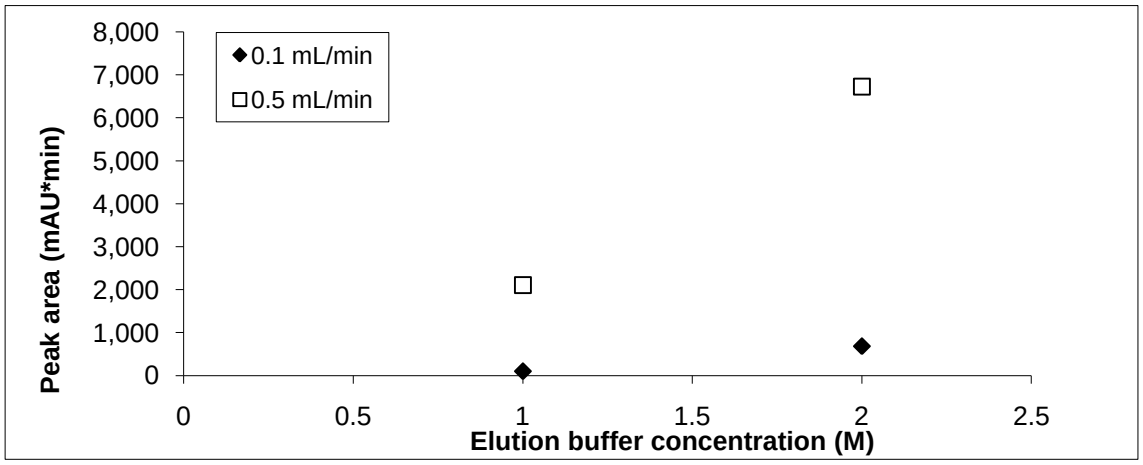

F.6.4 180 deg/hr rotation speed, 1.5 mg/mL BSA concentration, Trial 4, 0.1-1.0 mL/min flow rate

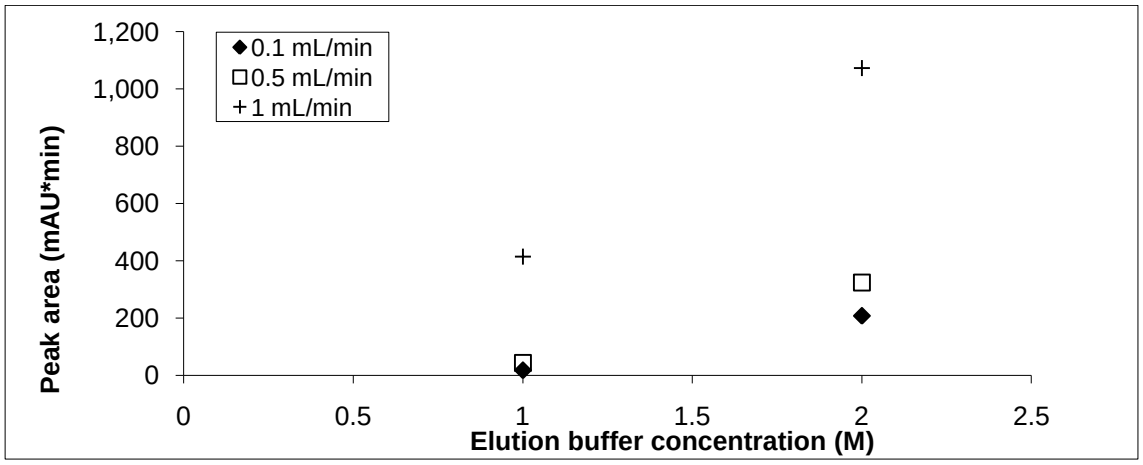

F.6.5 180 deg/hr rotation speed, 1.5 mg/mL BSA concentration, Trial 5, 0.1-1.0 mL/min flow rate

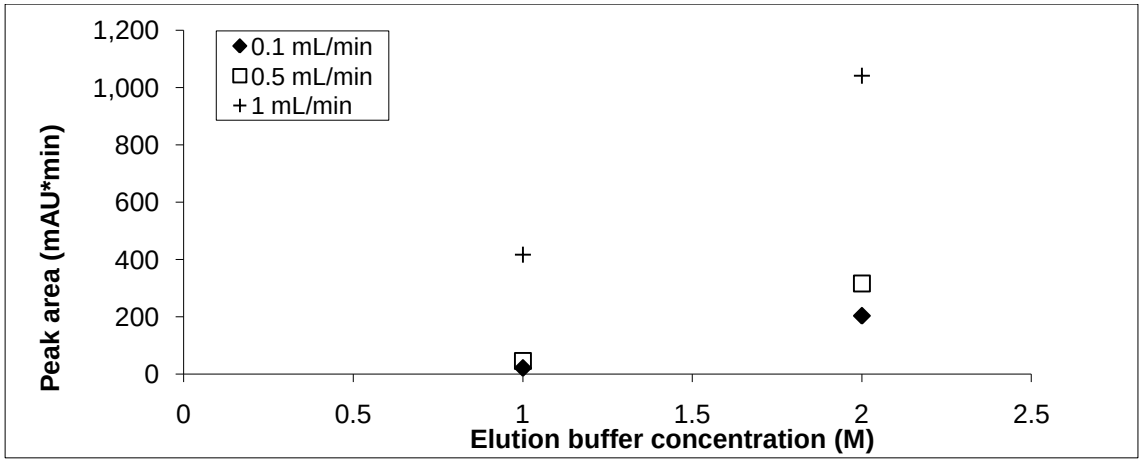

F.6.6 180 deg/hr rotation speed, 1.5 mg/mL BSA concentration, Trial 6, 0.1-1.0 mL/min flow rate

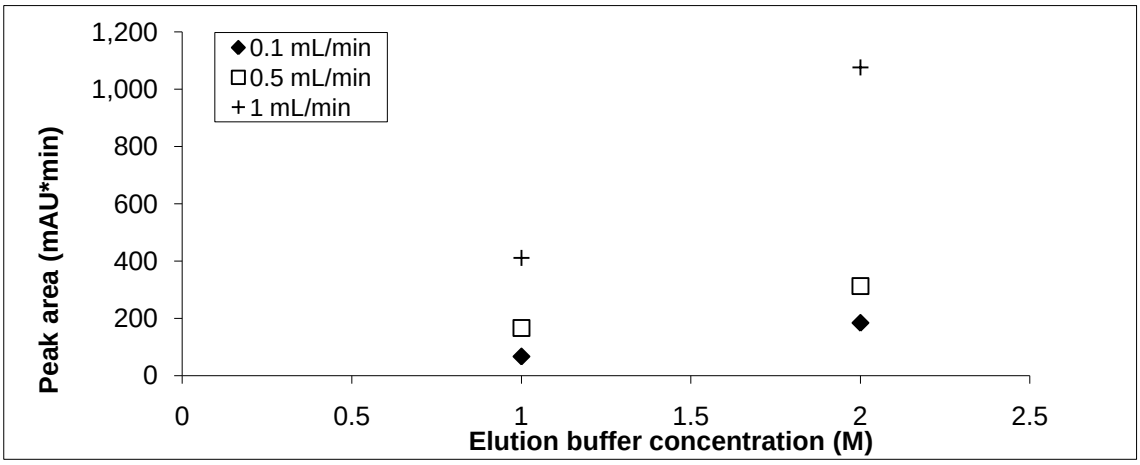

F.6.7 1. 180 deg/hr rotation speed, 1.5 mg/mL BSA concentration, Trial 7, 0.1-1.0 mL/min flow rate

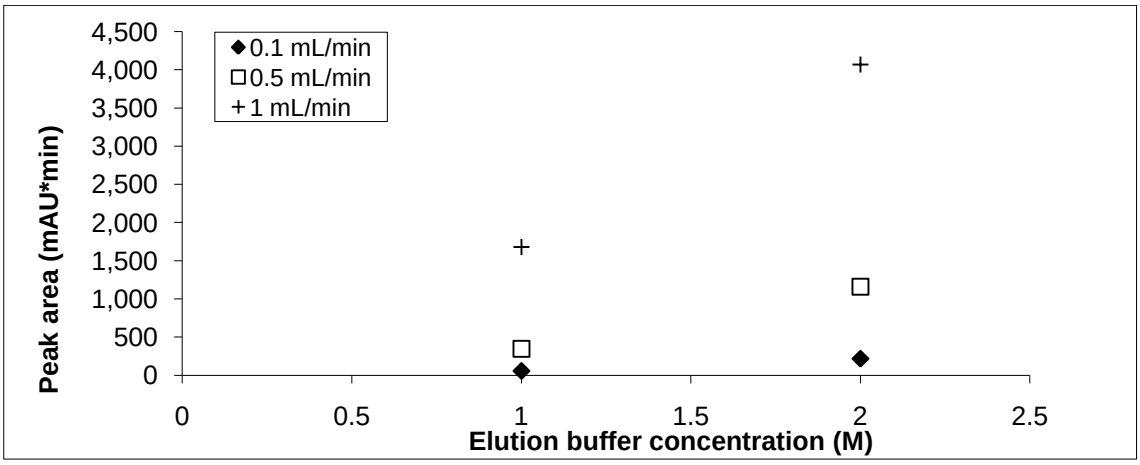

F.6.8 180 deg/hr rotation speed, 1.5 mg/mL BSA concentration, Trial 8, 0.1-1.0 mL/min flow rate

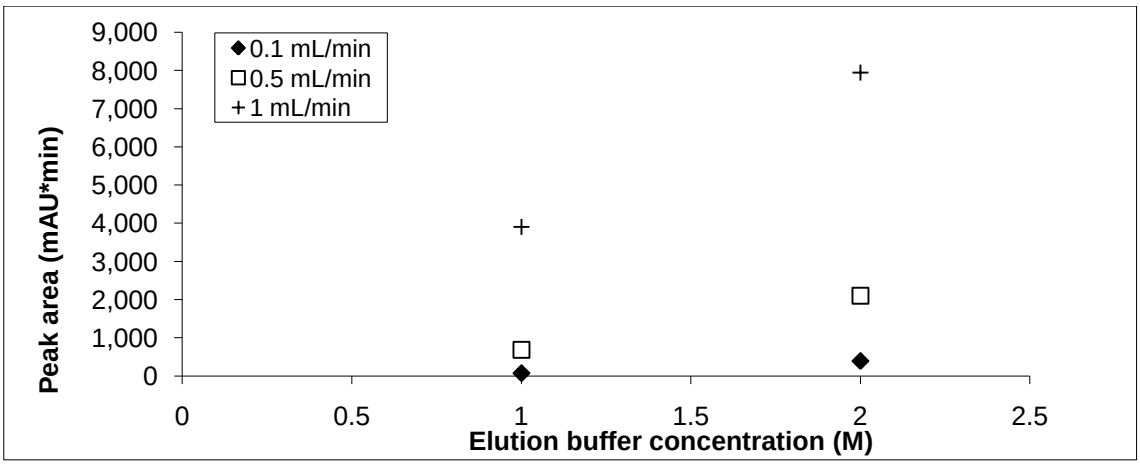

F.6.9 180 deg/hr rotation speed, 1.5 mg/mL BSA concentration, Trial 9, 0.1-1.0 mL/min flow rate

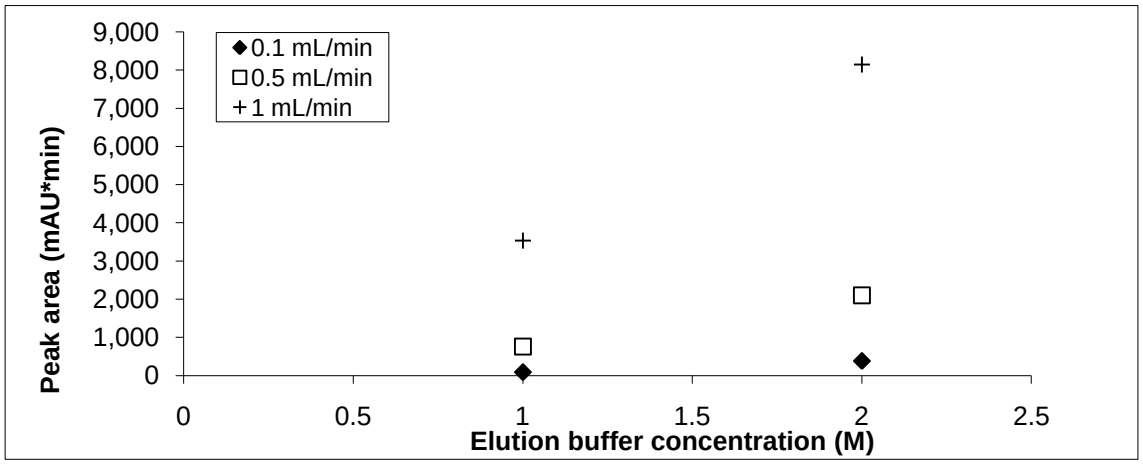

F.6.10 360 deg/hr rotation speed, 1.5 mg/mL BSA concentration, Trial 1, 0.1-1.0 mL/min flow rate

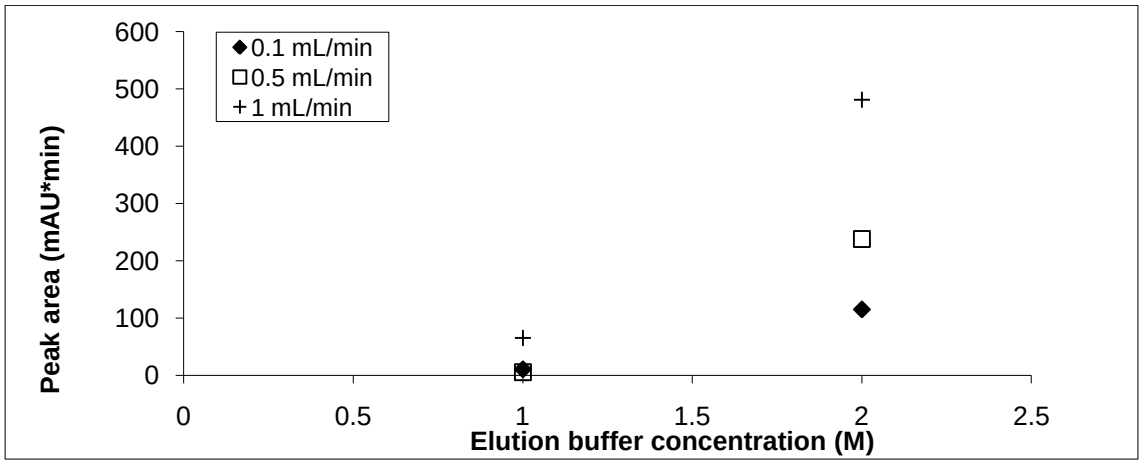

F.6.11 360 deg/hr rotation speed, 1.5 mg/mL BSA concentration, Trial 2, 0.1-1.0 mL/min flow rate

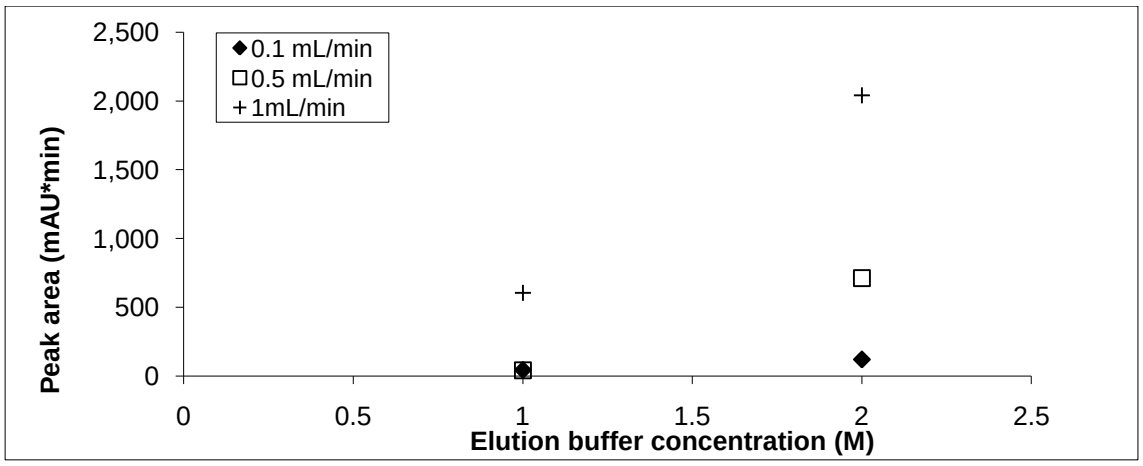

F.6.12 360 deg/hr rotation speed, 1.5 mg/mL BSA concentration, Trial 3, 0.1-1.0 mL/min flow rate

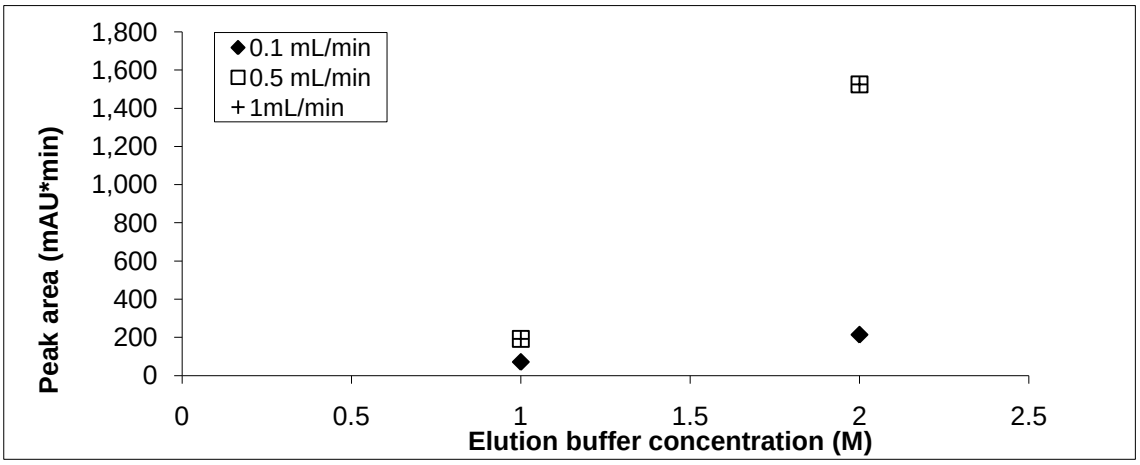

F.6.13 360 deg/hr rotation speed, 1.5 mg/mL BSA concentration, Trial 4, 0.1-1.0 mL/min flow rate

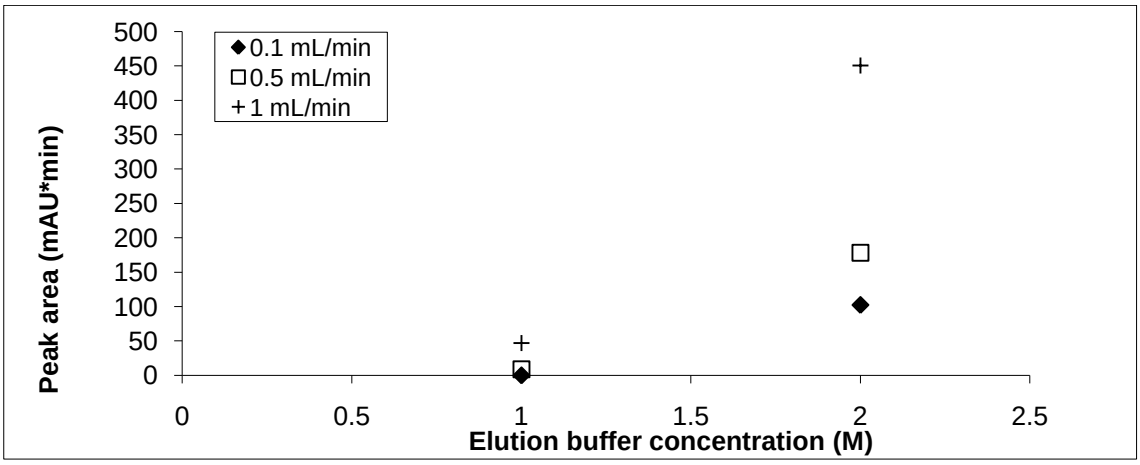

F.6.14 360 deg/hr rotation speed, 1.5 mg/mL BSA concentration, Trial 5, 0.1-1.0 mL/min flow rate

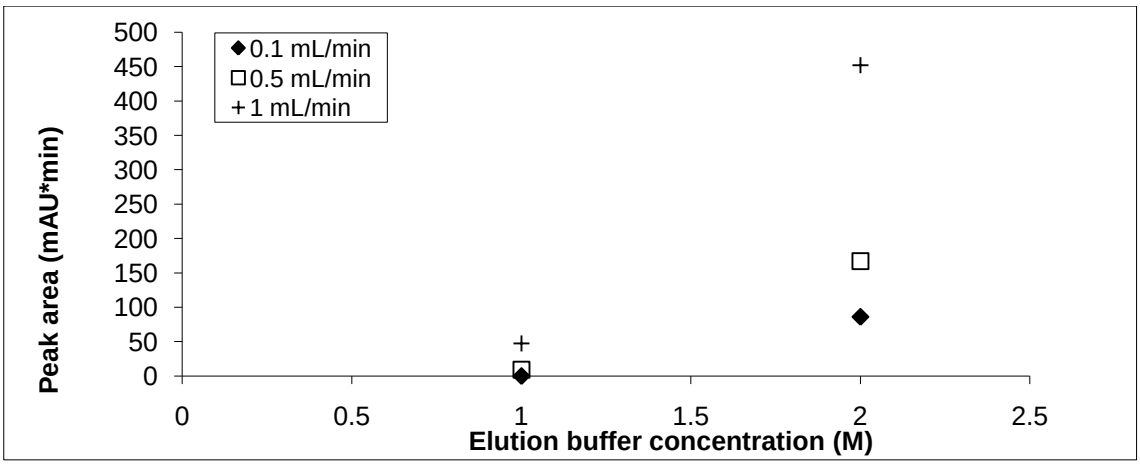

F.6.15 360 deg/hr rotation speed, 1.5 mg/mL BSA concentration, Trial 6, 0.1-1.0 mL/min flow rate

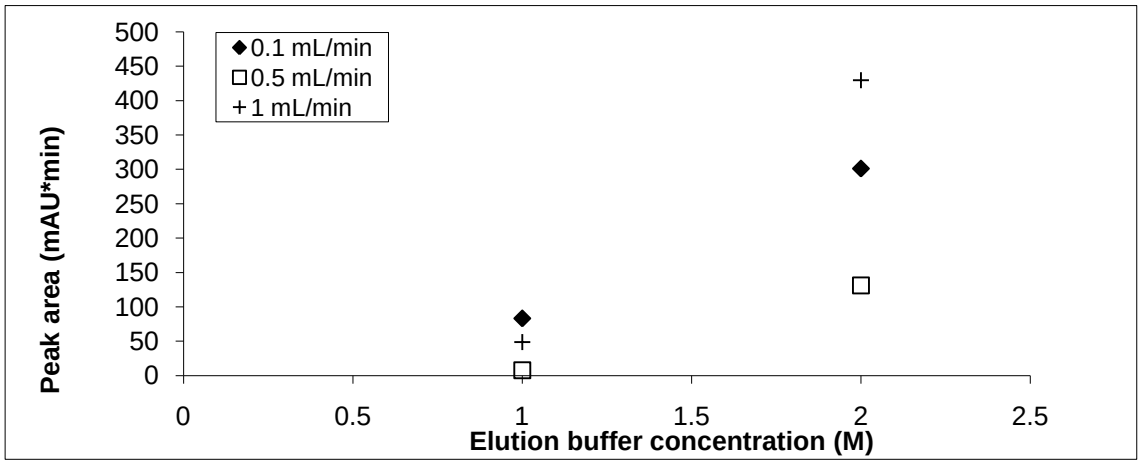

F.6.16 360 deg/hr rotation speed, 1.5 mg/mL BSA concentration, Trial 7, 0.1-1.0 mL/min flow rate

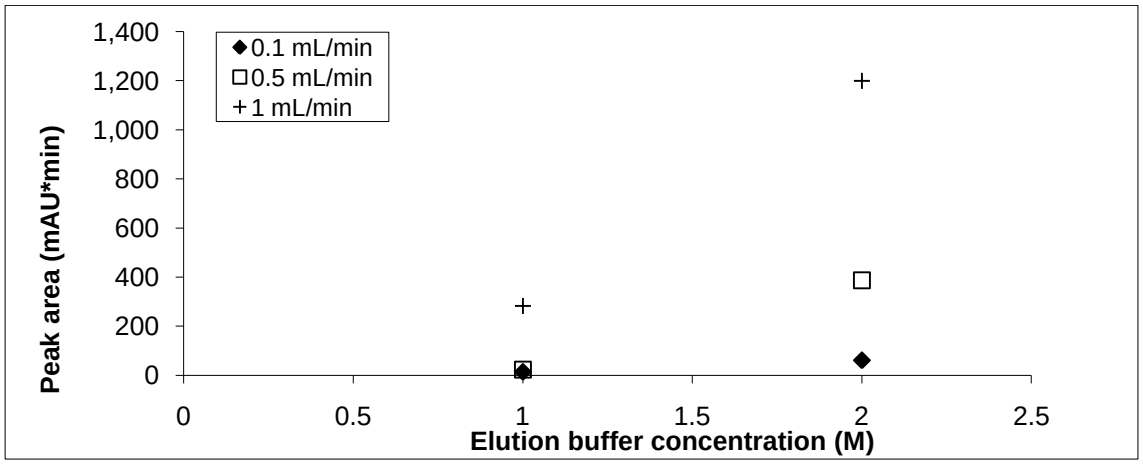

F.6.17 360 deg/hr rotation speed, 1.5 mg/mL BSA concentration, Trial 8, 0.1-1.0 mL/min flow rate

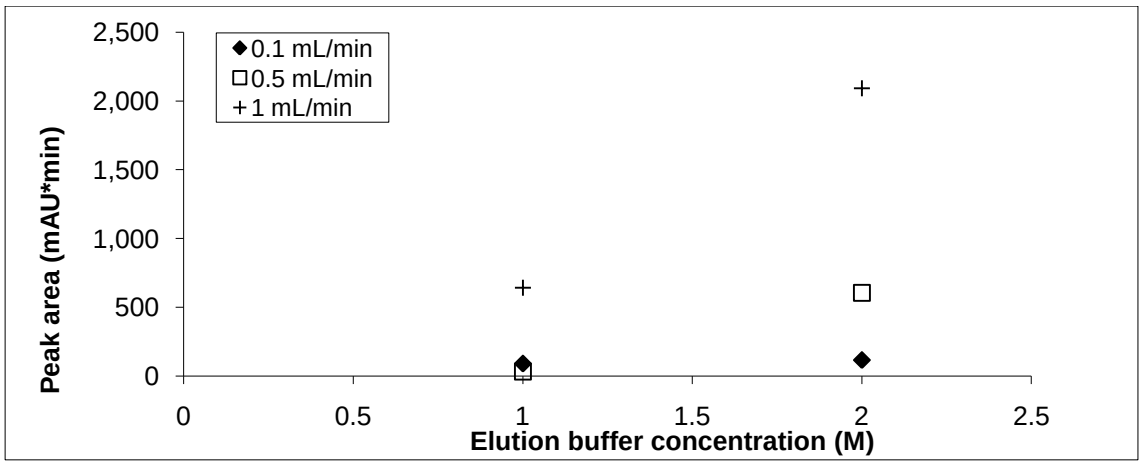

F.6.18 360 deg/hr rotation speed, 1.5 mg/mL BSA concentration, Trial 9, 0.1-1.0 mL/min flow rate

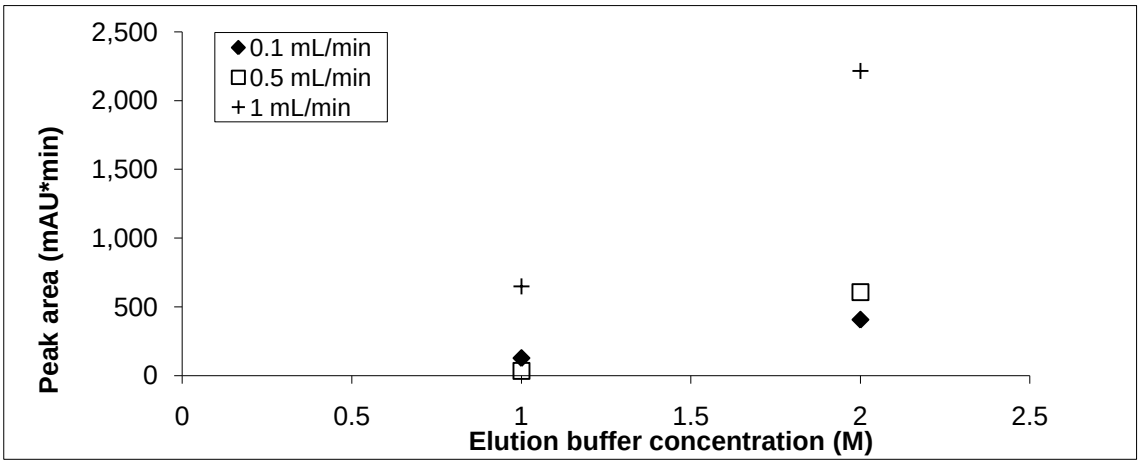

F.6.19 720 deg/hr rotation speed, 1.5 mg/mL BSA concentration, Trial 1, 0.1-1.0 mL/min flow rate

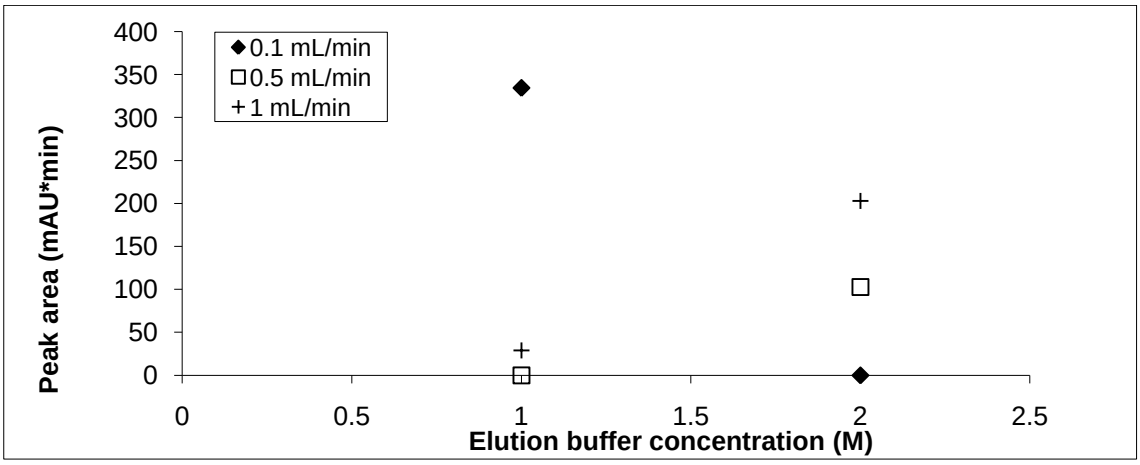

F.6.20 720 deg/hr rotation speed, 1.5 mg/mL BSA concentration, Trial 2, 0.1-1.0 mL/min flow rate

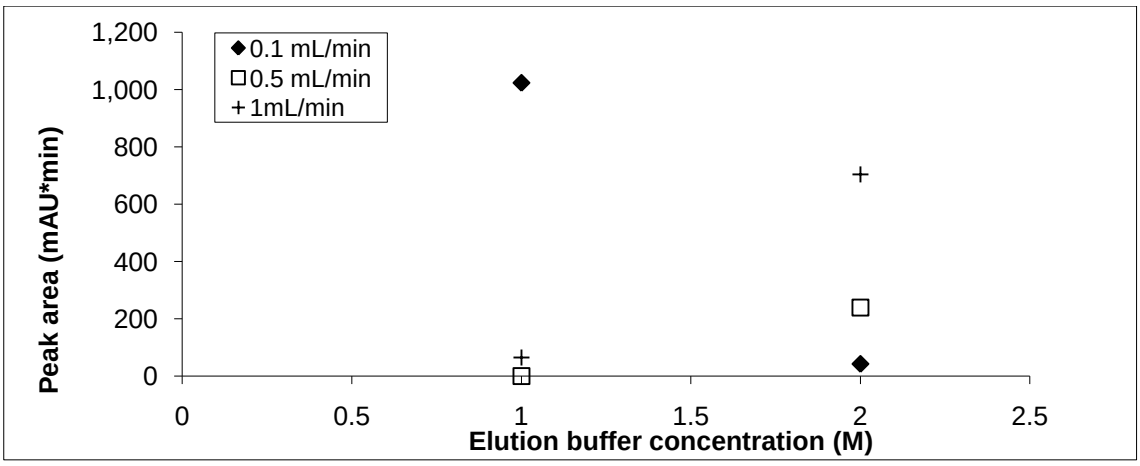

F.6.21 720 deg/hr rotation speed, 1.5 mg/mL BSA concentration, Trial 3, 0.1-1.0 mL/min flow rate

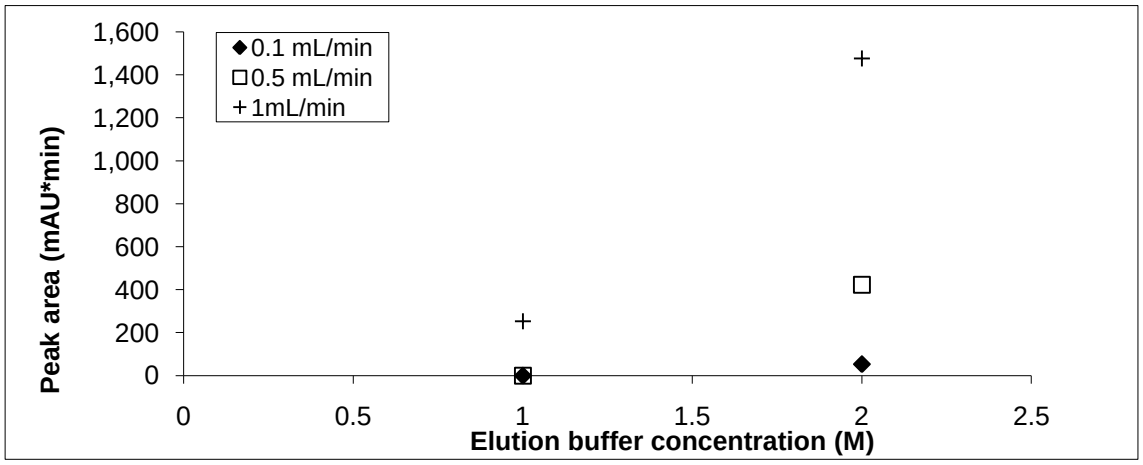

F.6.22 720 deg/hr rotation speed, 1.5 mg/mL BSA concentration, Trial 4, 0.1-1.0 mL/min flow rate

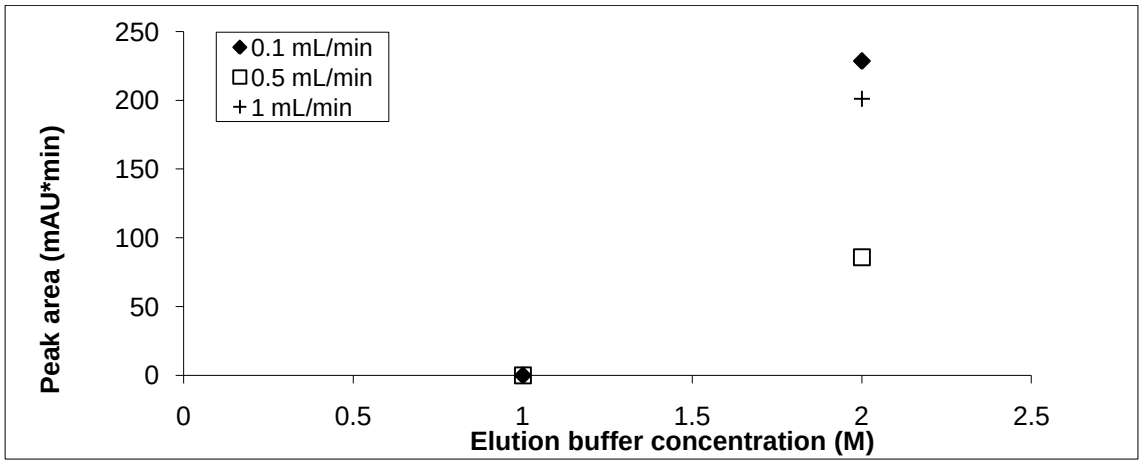

F.6.23 720 deg/hr rotation speed, 1.5 mg/mL BSA concentration, Trial 5, 0.1-1.0 mL/min flow rate

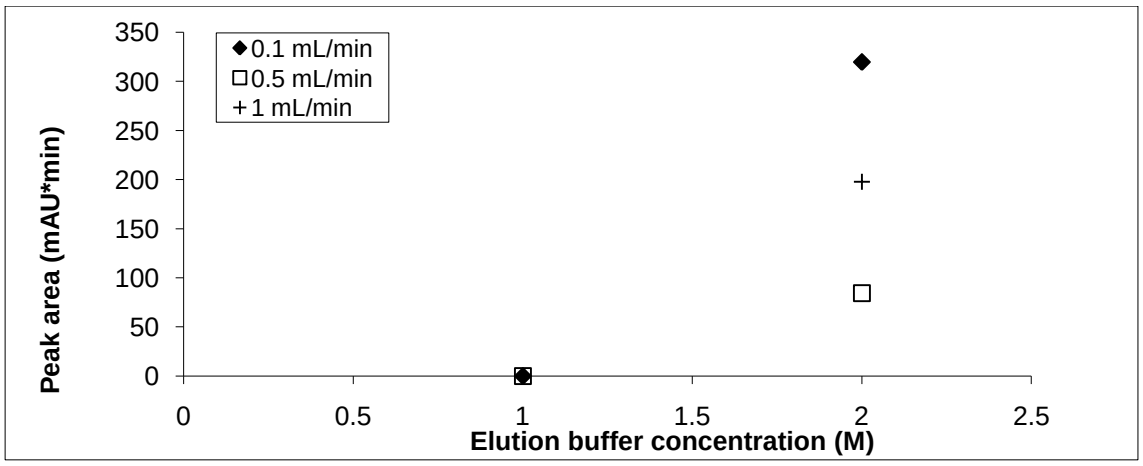

F.6.24 720 deg/hr rotation speed, 1.5 mg/mL BSA concentration, Trial 6, 0.1-1.0 mL/min flow rate

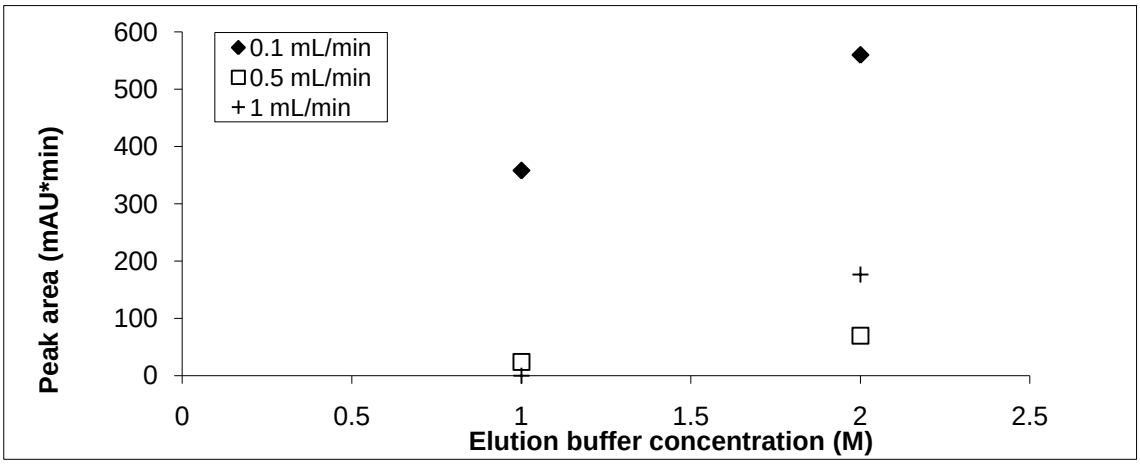

F.6.25 720 deg/hr rotation speed, 1.5 mg/mL BSA concentration, Trial 7, 0.1-1.0 mL/min flow rate

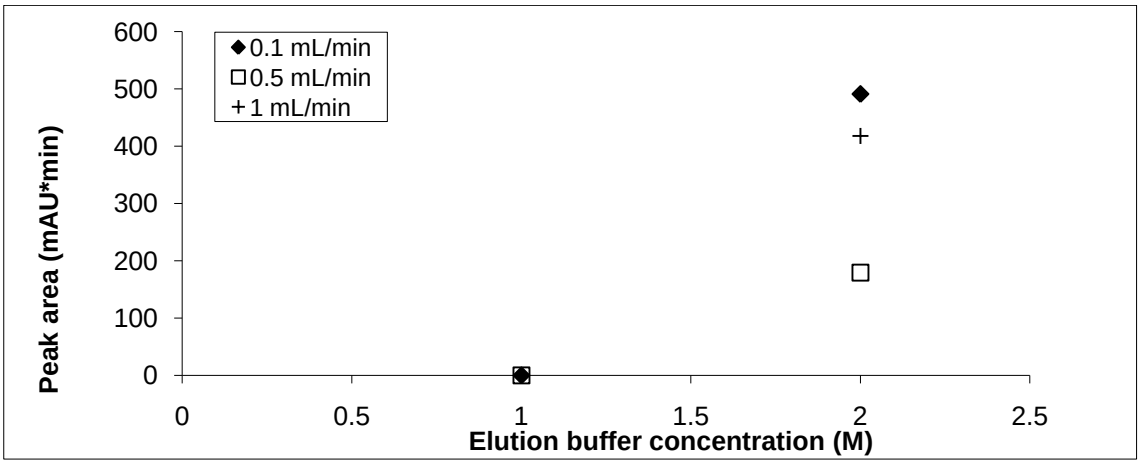

F.6.26 720 deg/hr rotation speed, 1.5 mg/mL BSA concentration, Trial 8, 0.1-1.0 mL/min flow rate

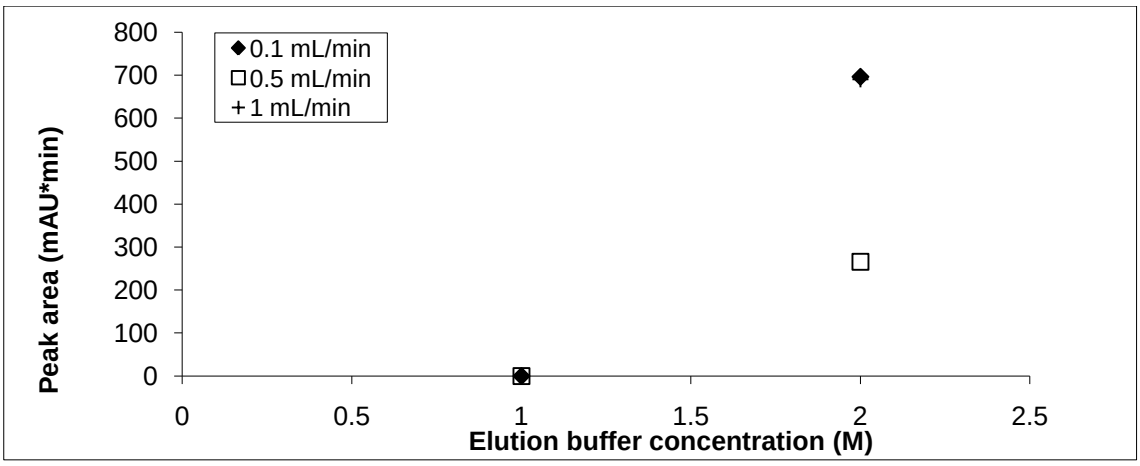

F.6.27 720 deg/hr rotation speed, 1.5 mg/mL BSA concentration, Trial 9, 0.1-1.0 mL/min flow rate

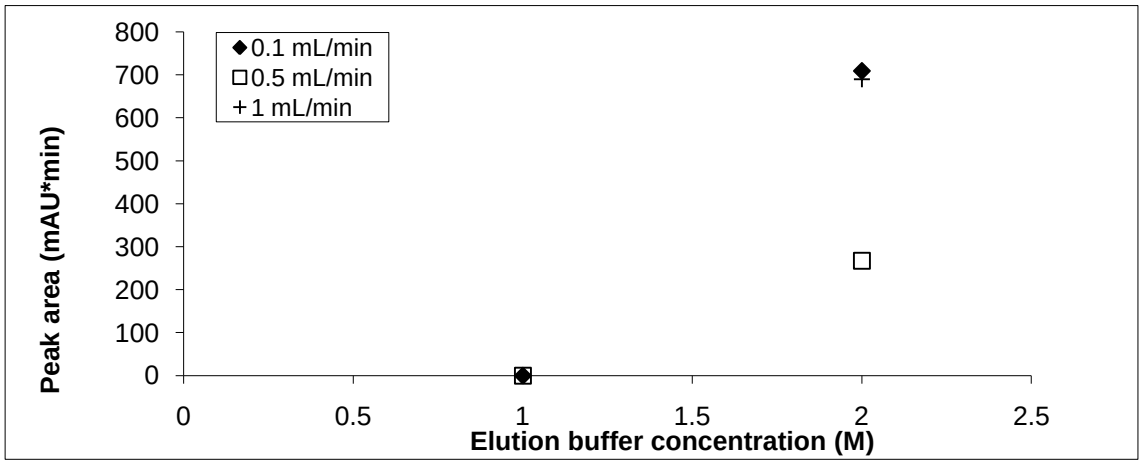

Appendix G Yield

G.1 Loading sections

G.1.1 1.5 mg/mL BSA concentration, 1M NaCl concentration, 180 deg/hr rotation speed, 0.1-1.0mL/min flow rate

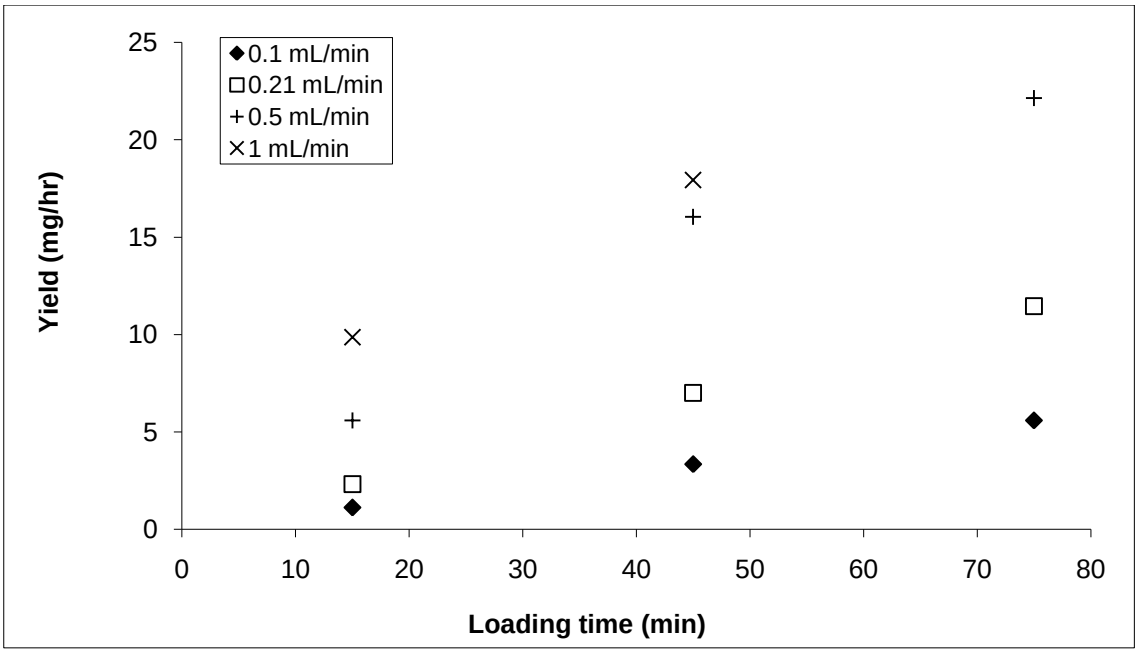

G.1.2 1.5 mg/mL BSA concentration, 1M NaCl concentration, 360 deg/hr rotation speed, 0.1-1.0mL/min flow rate

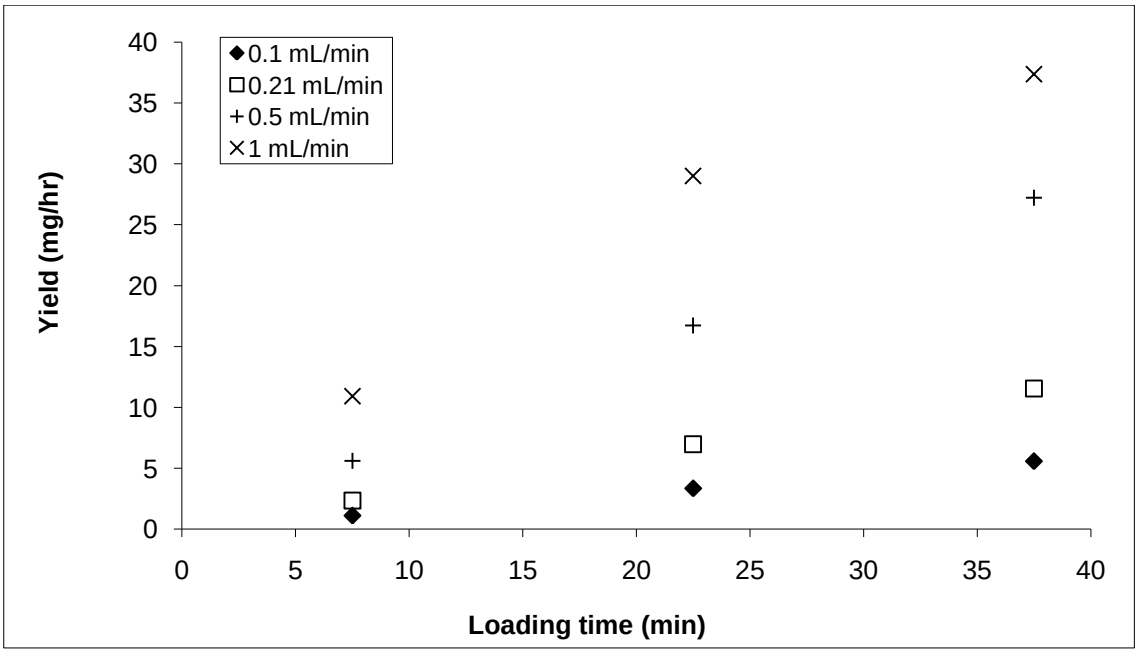

G.1.3 1.5 mg/mL BSA concentration, 1M NaCl concentration, 720 deg/hr rotation speed, 0.1-1.0mL/min flow rate

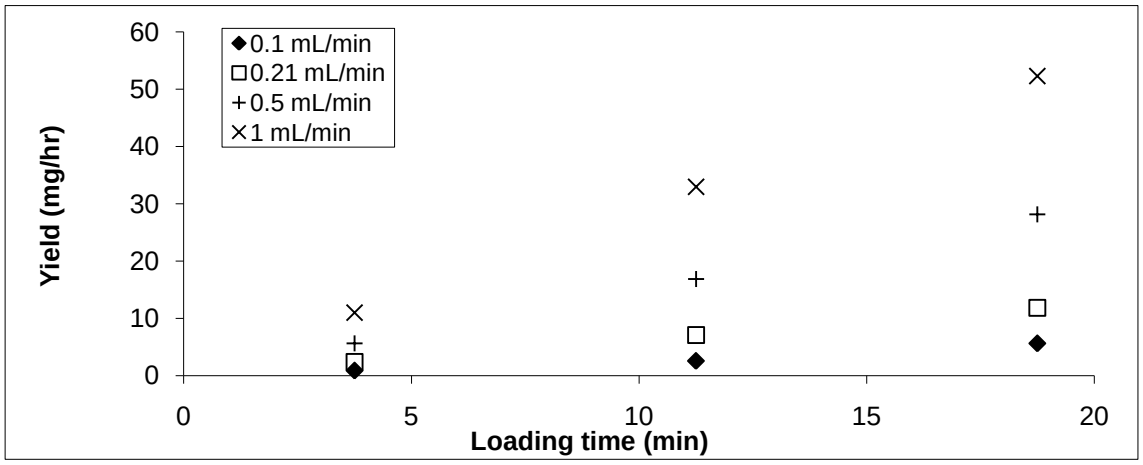

G.1.4 3 mg/mL BSA concentration, 1M NaCl concentration, 180 deg/hr rotation speed, 0.1-1.0mL/min flow rate

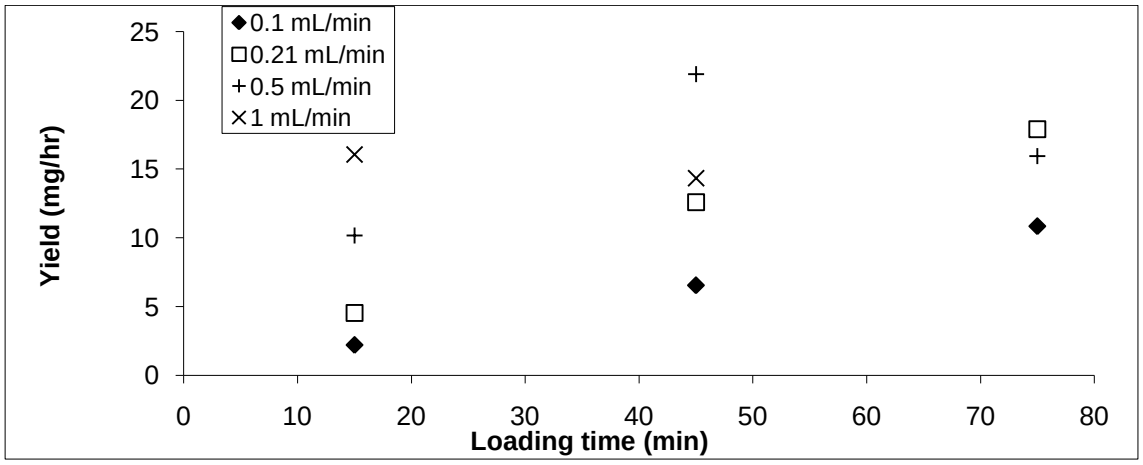

G.1.5 3 mg/mL BSA concentration, 1M NaCl concentration, 360 deg/hr rotation speed, 0.1-1.0mL/min flow rate

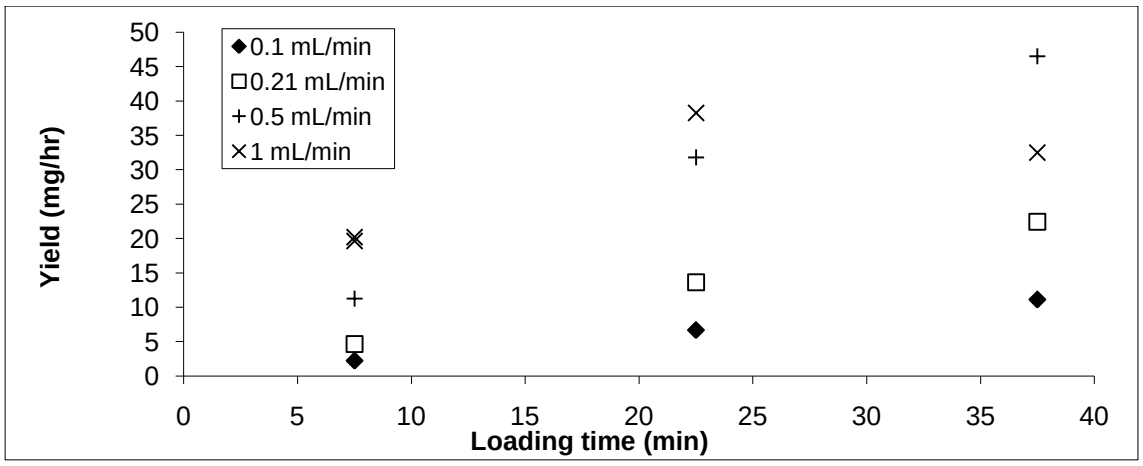

G.1.6 3 mg/mL BSA concentration, 1M NaCl concentration, 720 deg/hr rotation speed, 0.1-1.0mL/min flow rate

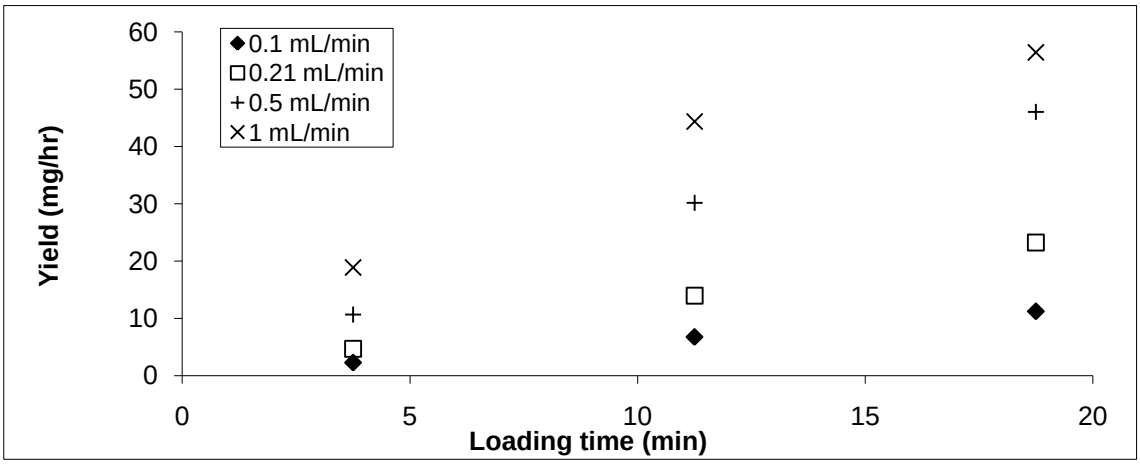

G.1.7 5 mg/mL BSA concentration, 1M NaCl concentration, 180 deg/hr rotation speed, 0.1-1.0mL/min flow rate

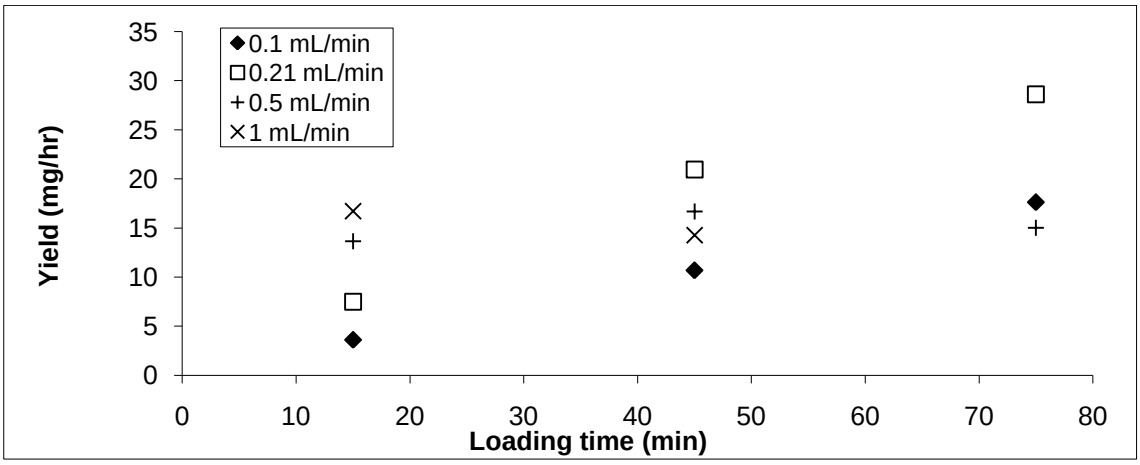

G.1.8 5 mg/mL BSA concentration, 1M NaCl concentration, 360 deg/hr rotation speed, 0.1-1.0mL/min flow rate

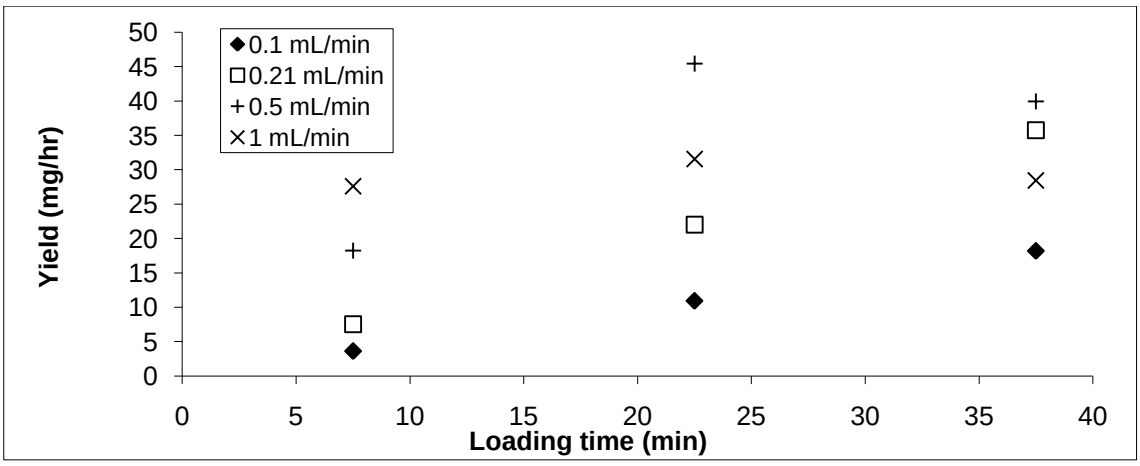

G.1.9 5 mg/mL BSA concentration, 1M NaCl concentration, 720 deg/hr rotation speed, 0.1-1.0mL/min flow rate

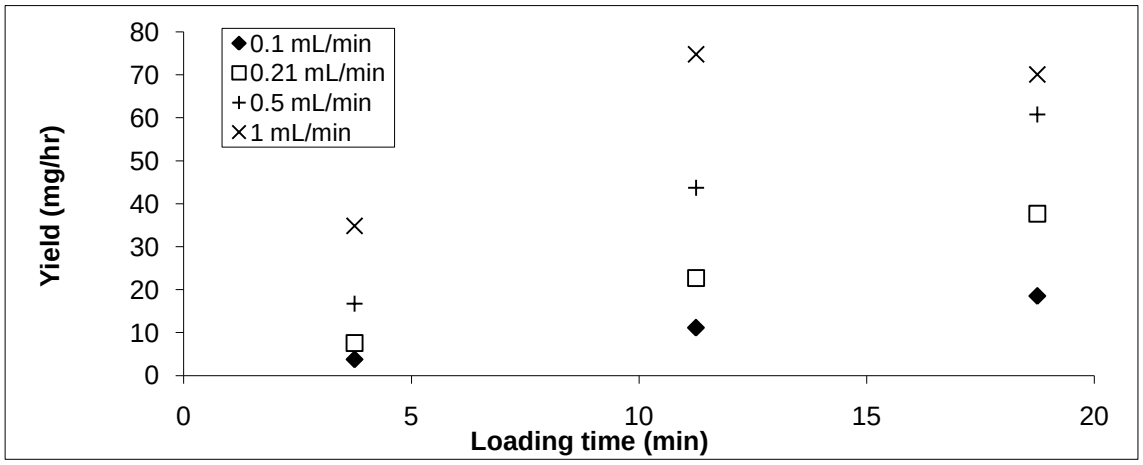

G.1.10 1.5 mg/mL BSA concentration, 2M NaCl concentration, 180 deg/hr rotation speed, 0.1-1.0mL/min flow rate

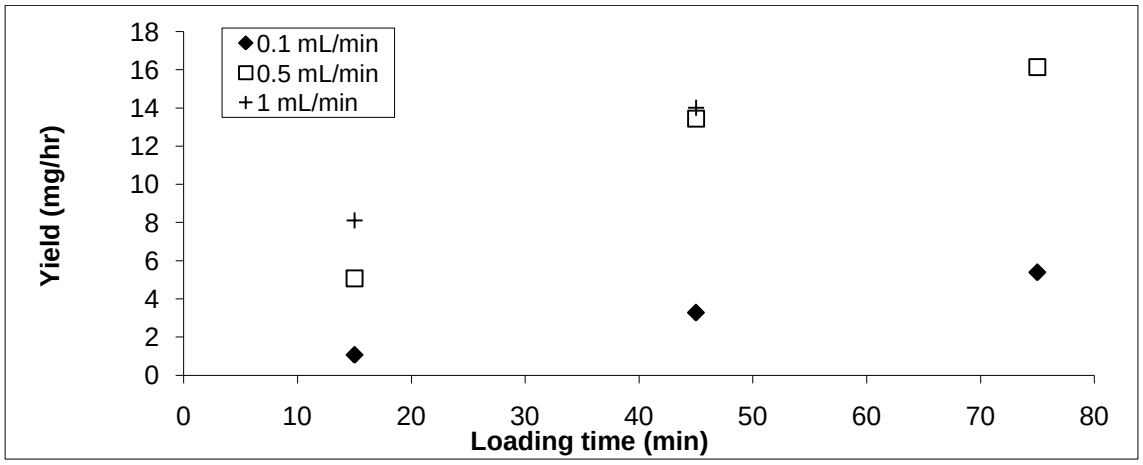

G.1.11 1.5 mg/mL BSA concentration, 2M NaCl concentration, 360 deg/hr rotation speed, 0.1-1.0mL/min flow rate

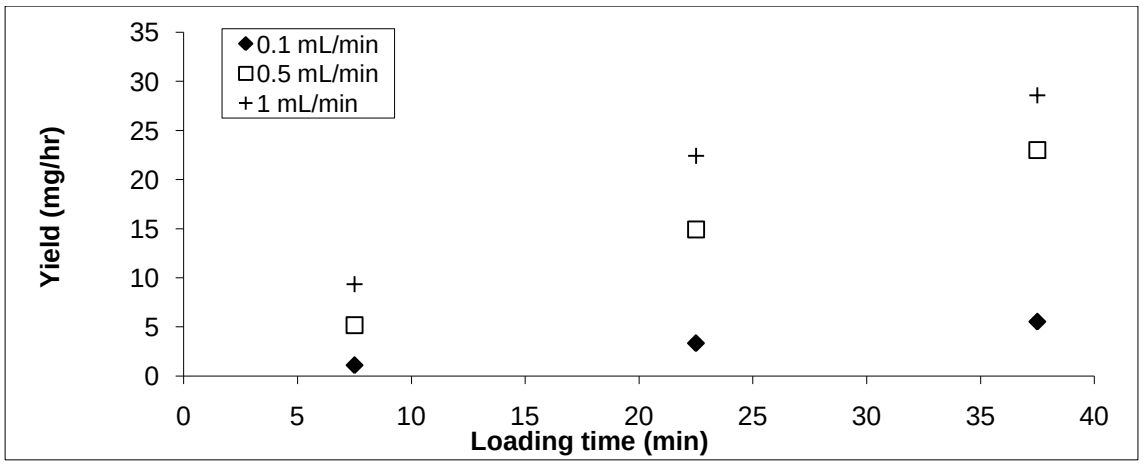

G.1.12 1.5 mg/mL BSA concentration, 2M NaCl concentration, 720 deg/hr rotation speed, 0.1-1.0mL/min flow rate

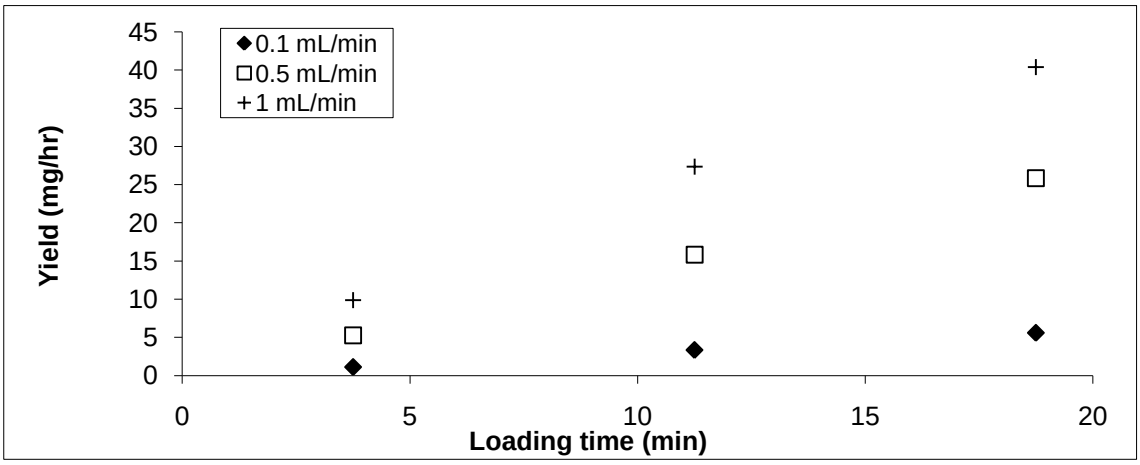

G.2 Elution sections

G.2.1 1.5 mg/mL BSA concentration, 1M NaCl concentration, 180 deg/hr rotation speed, 0.1-1.0mL/min flow rate

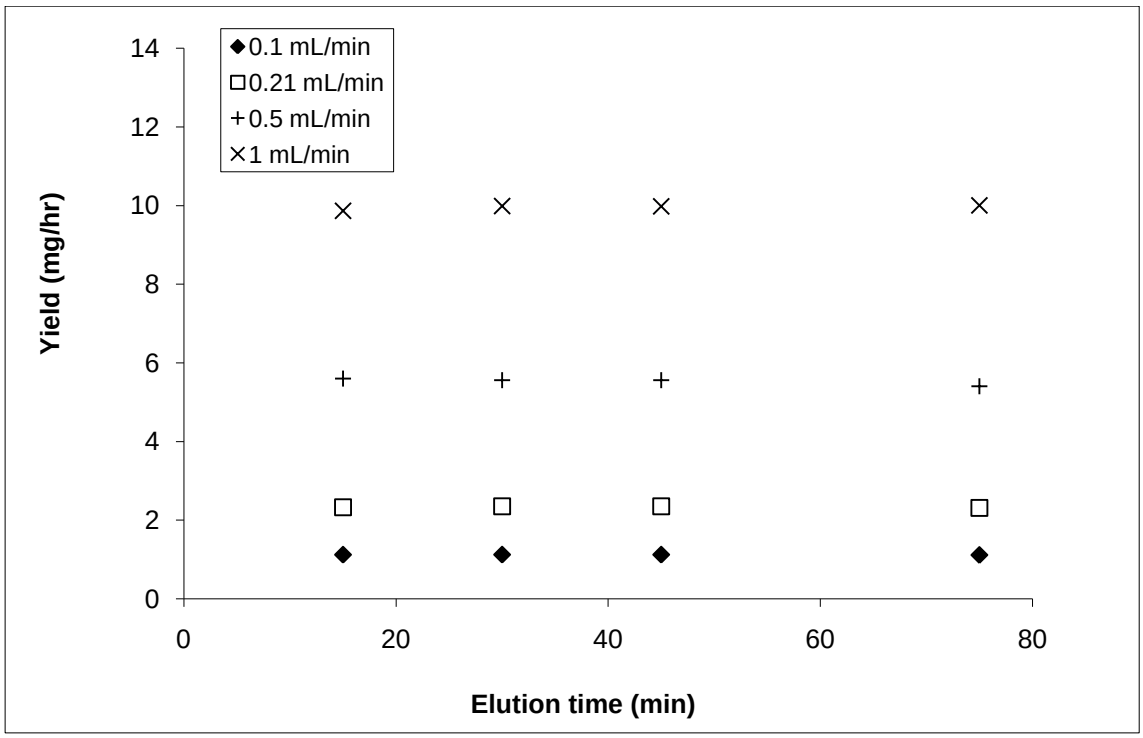

G.2.2 1.5 mg/mL BSA concentration, 1M NaCl concentration, 360 deg/hr rotation speed, 0.1-1.0mL/min flow rate

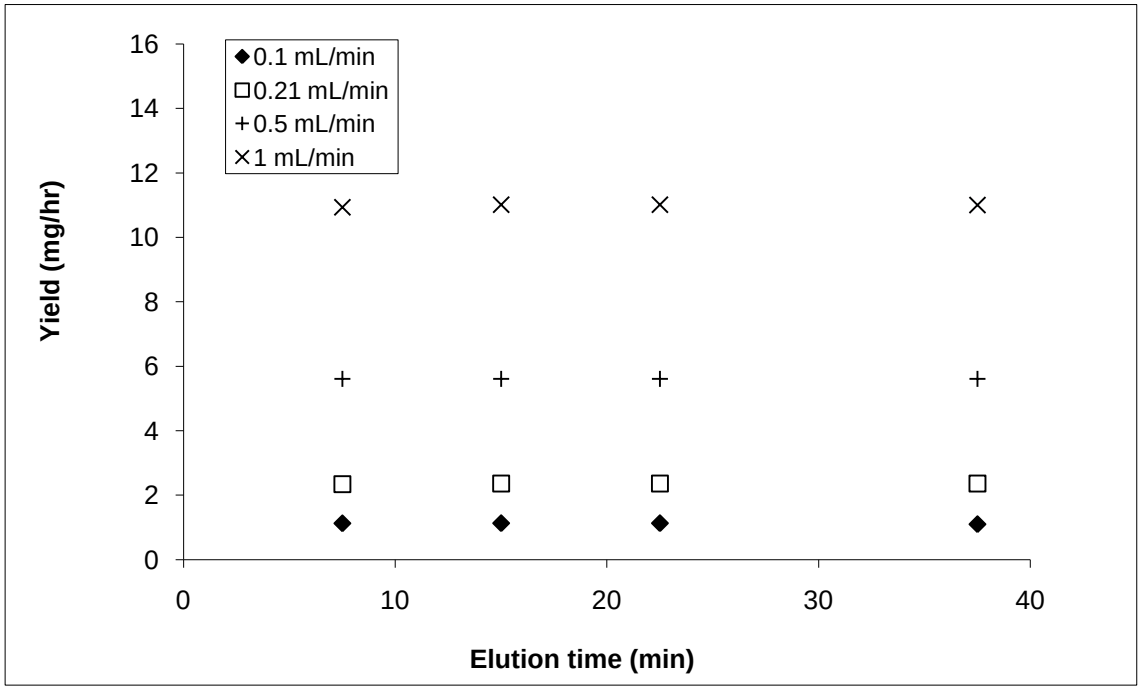

G.2.3 1.5 mg/mL BSA concentration, 1M NaCl concentration, 720 deg/hr rotation speed, 0.1-1.0mL/min flow rate

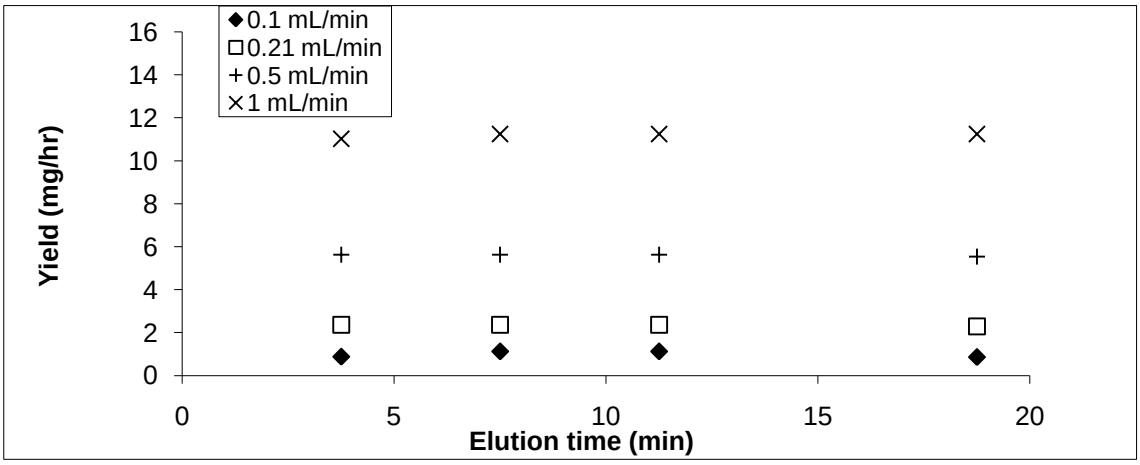

G.2.4 3 mg/mL BSA concentration, 1M NaCl concentration, 180 deg/hr rotation speed, 0.1-1.0mL/min flow rate

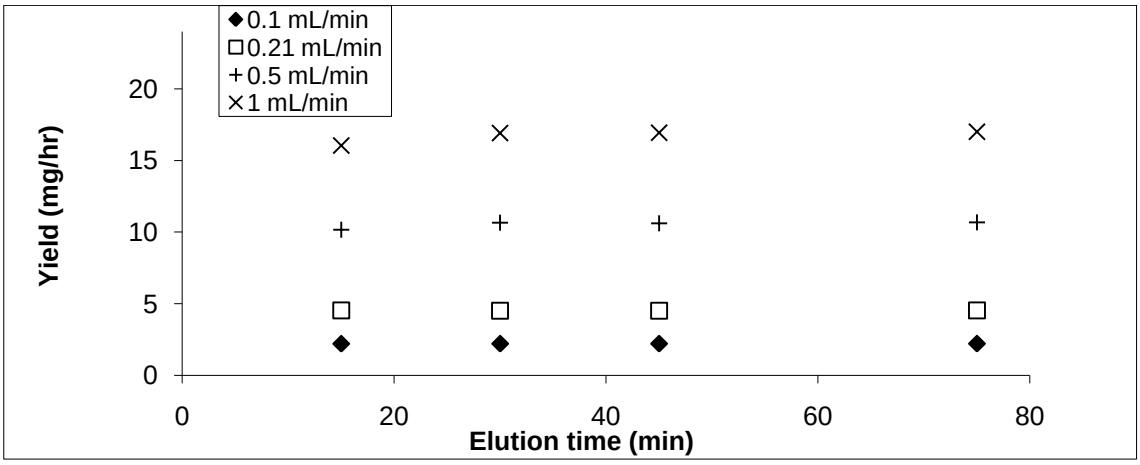

G.2.5 3 mg/mL BSA concentration, 1M NaCl concentration, 360 deg/hr rotation speed, 0.1-1.0mL/min flow rate

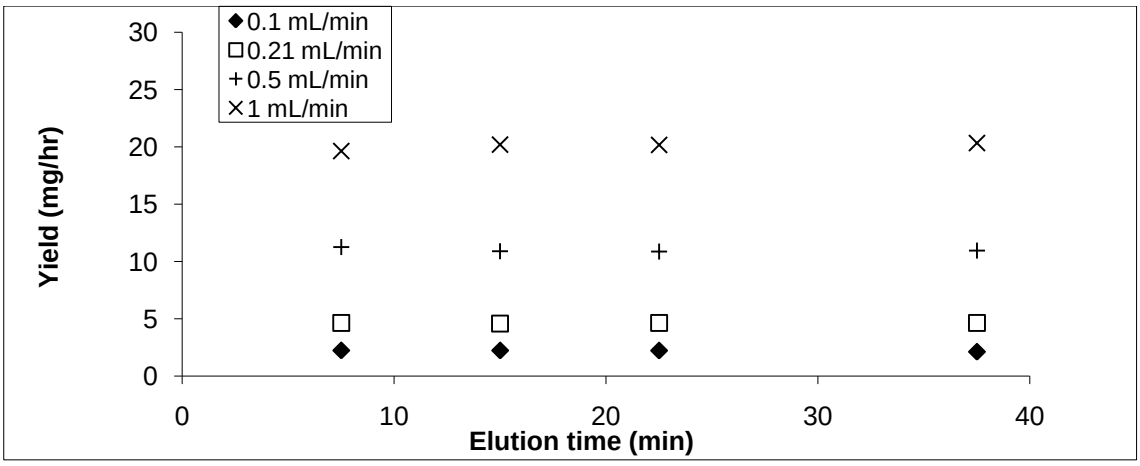

G.2.6 3 mg/mL BSA concentration, 1M NaCl concentration, 720 deg/hr rotation speed, 0.1-1.0mL/min flow rate

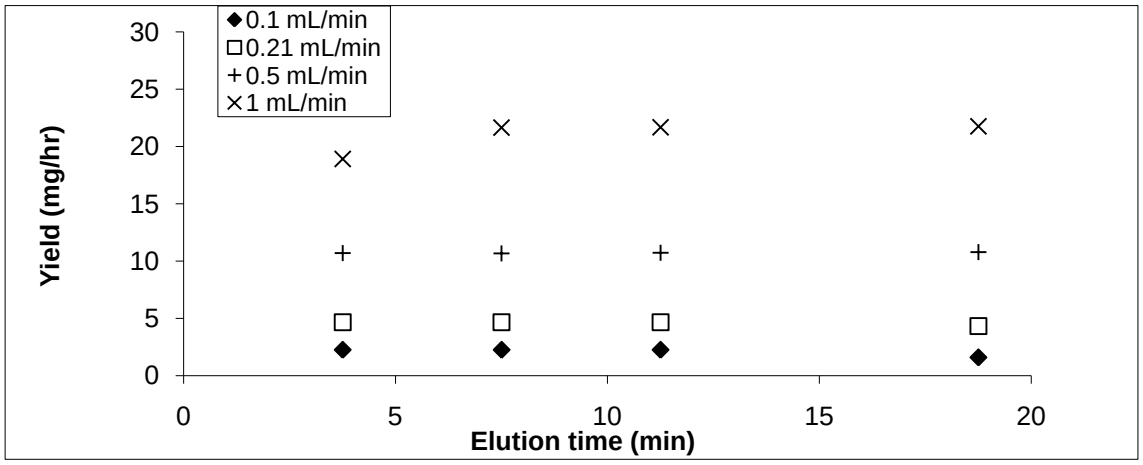

G.2.7 5 mg/mL BSA concentration, 1M NaCl concentration, 180 deg/hr rotation speed, 0.1-1.0mL/min flow rate

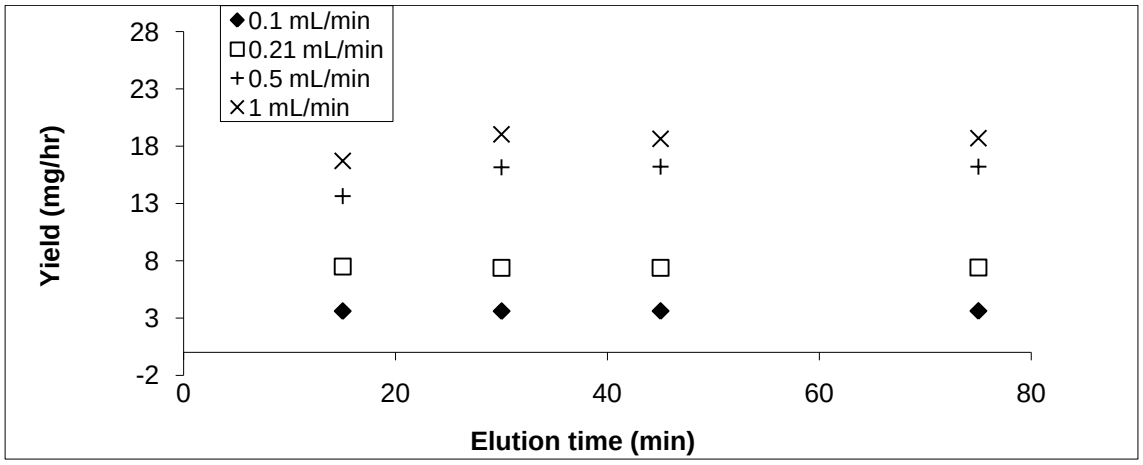

G.2.8 5 mg/mL BSA concentration, 1M NaCl concentration, 360 deg/hr rotation speed, 0.1-1.0mL/min flow rate

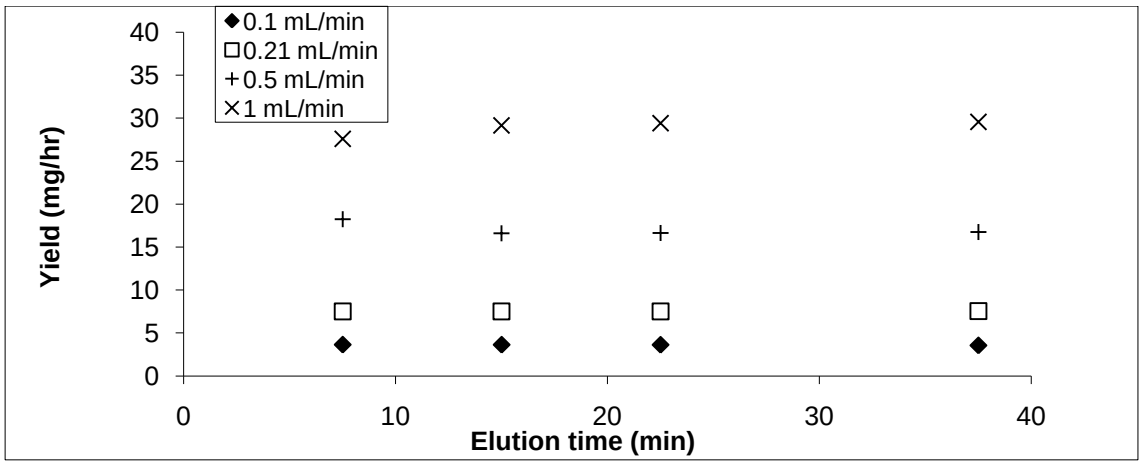

G.2.9 5 mg/mL BSA concentration, 1M NaCl concentration, 720 deg/hr rotation speed, 0.1-1.0mL/min flow rate

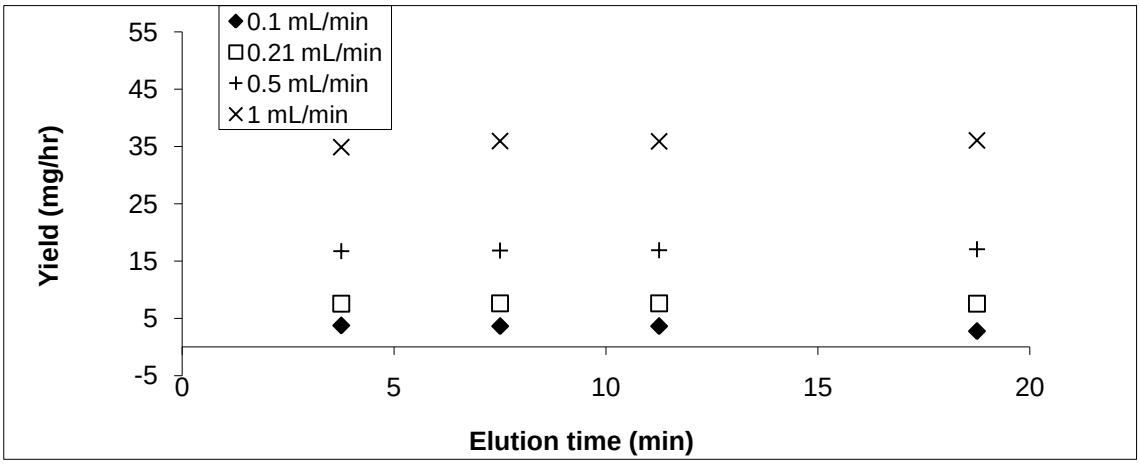

G.2.10 1.5 mg/mL BSA concentration, 2M NaCl concentration, 180 deg/hr rotation speed, 0.1-1.0mL/min flow rate

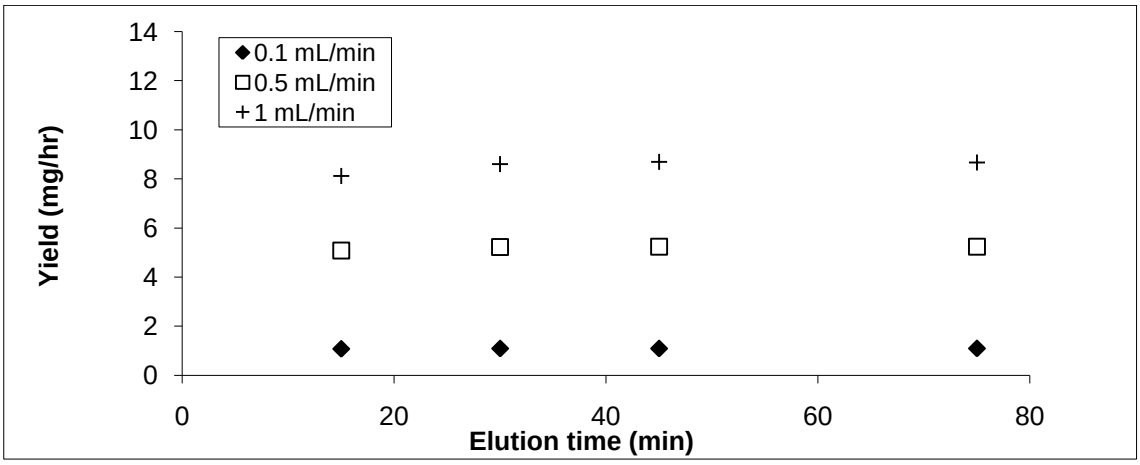

G.2.11 1.5 mg/mL BSA concentration, 2M NaCl concentration, 360 deg/hr rotation speed, 0.1-1.0mL/min flow rate

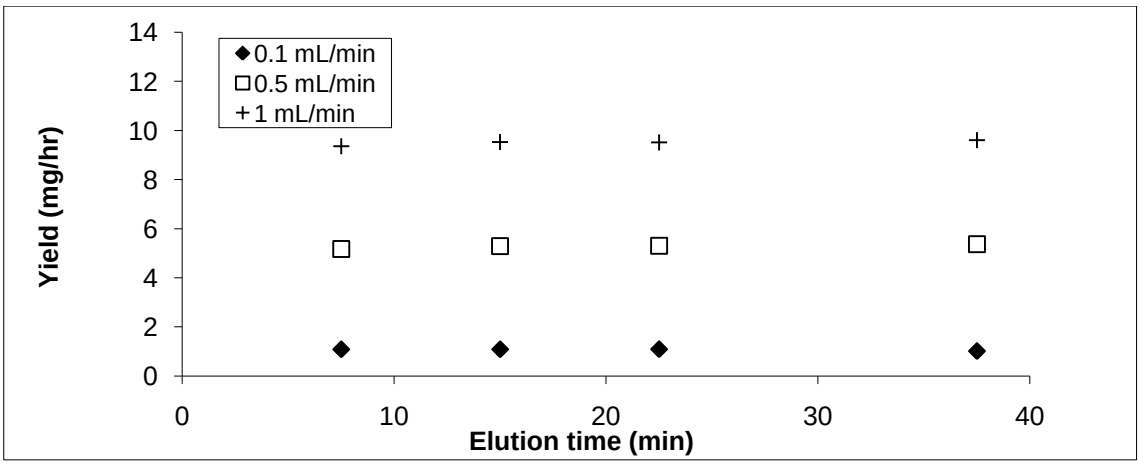

G.2.12 1.5 mg/mL BSA concentration, 2M NaCl concentration, 720 deg/hr rotation speed, 0.1-1.0mL/min flow rate

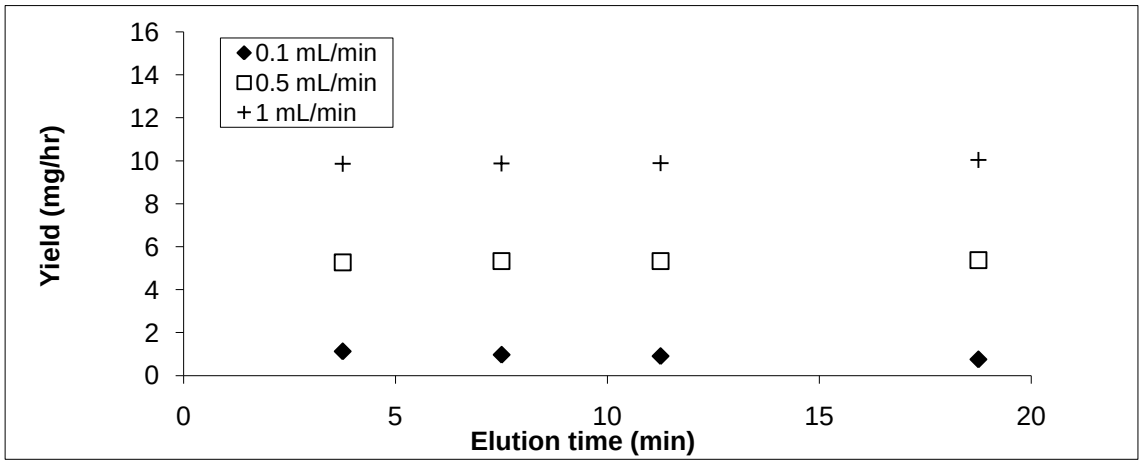

G.3 Rotation speed

G.3.1 1.5 mg/mL BSA concentration, 1M NaCl concentration, Trial 1, 0.1-1.0mL/min flow rate

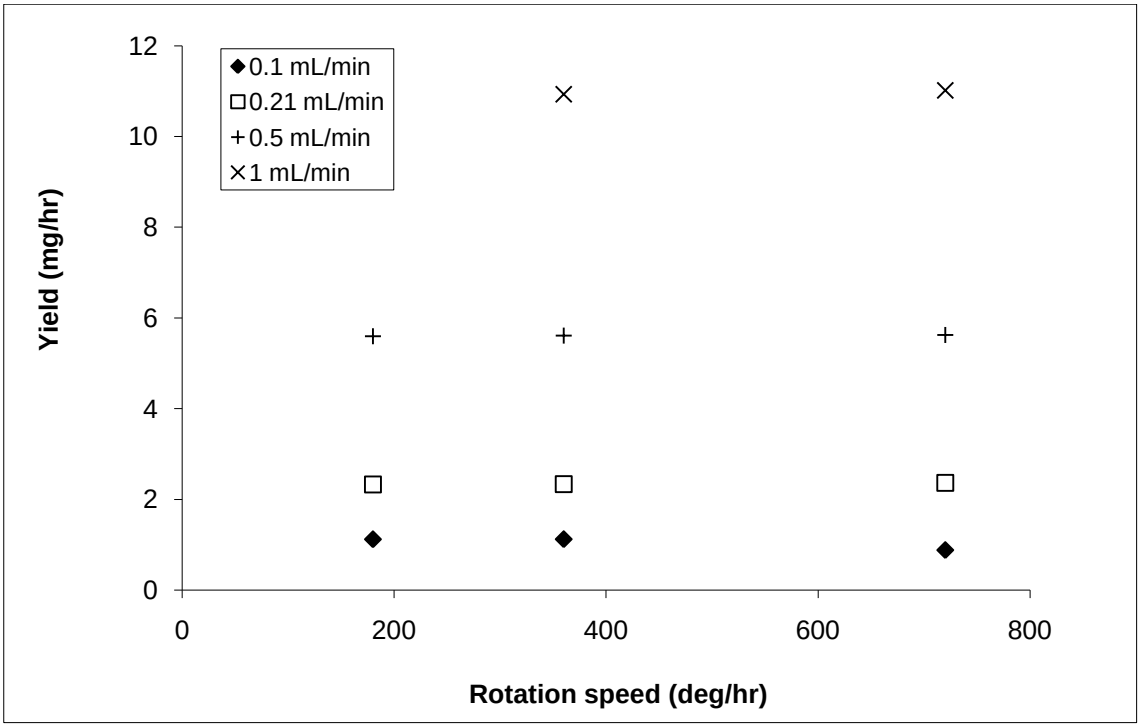

G.3.2 1.5 mg/mL BSA concentration, 1M NaCl concentration, Trial 2, 0.1-1.0mL/min flow rate

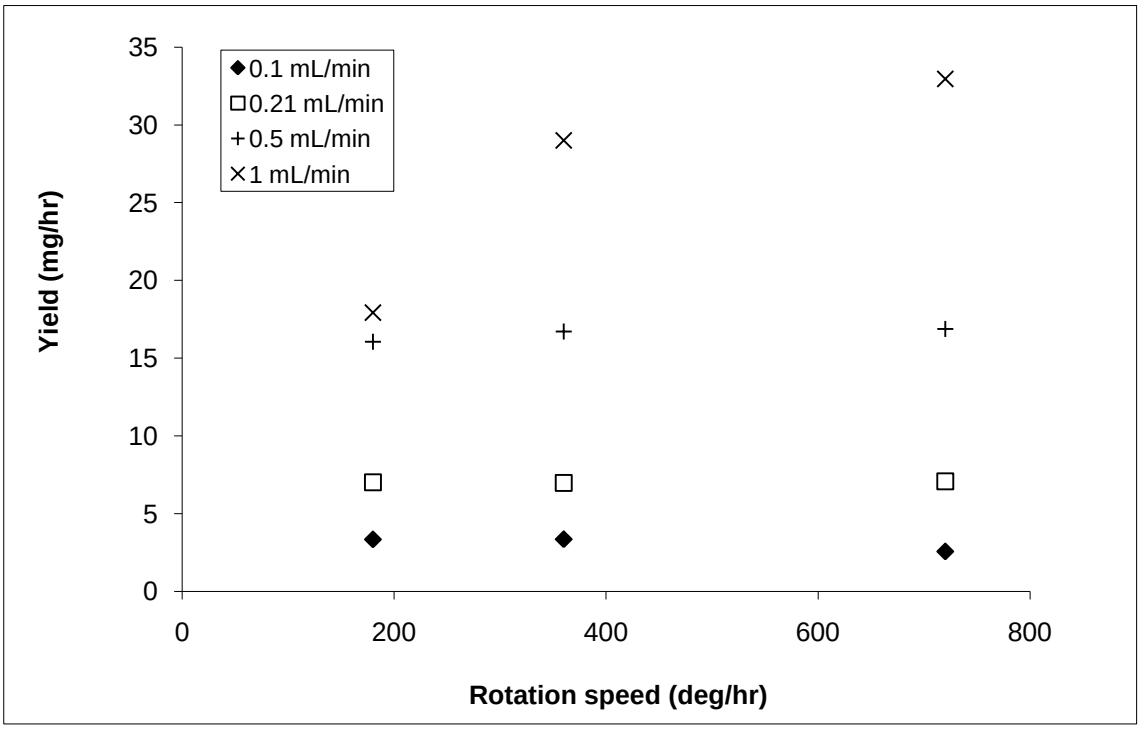

G.3.3 1.5 mg/mL BSA concentration, 1M NaCl concentration, Trial 3, 0.1-1.0mL/min flow rate

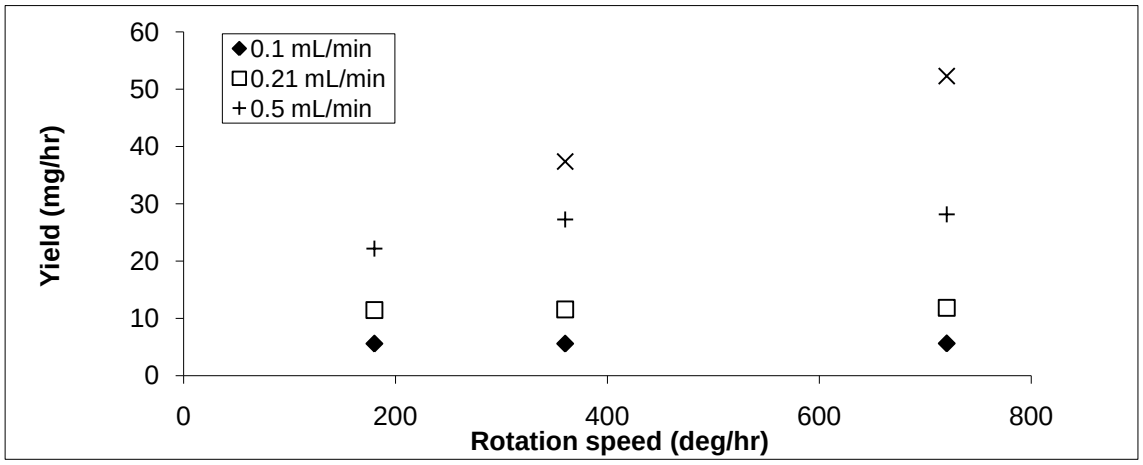

G.3.4 1.5 mg/mL BSA concentration, 1M NaCl concentration, Trial 4, 0.1-1.0mL/min flow rate

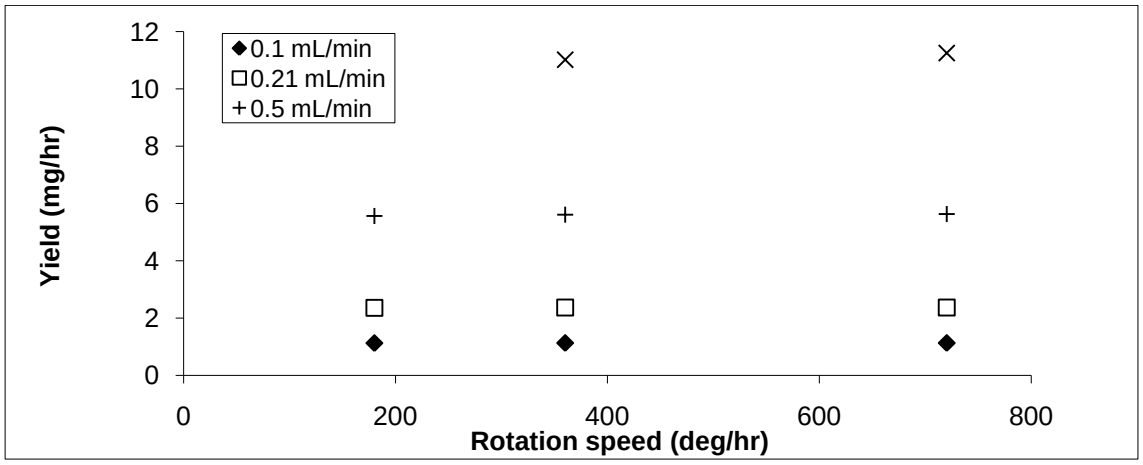

G.3.5 1.5 mg/mL BSA concentration, 1M NaCl concentration, Trial 5, 0.1-1.0mL/min flow rate

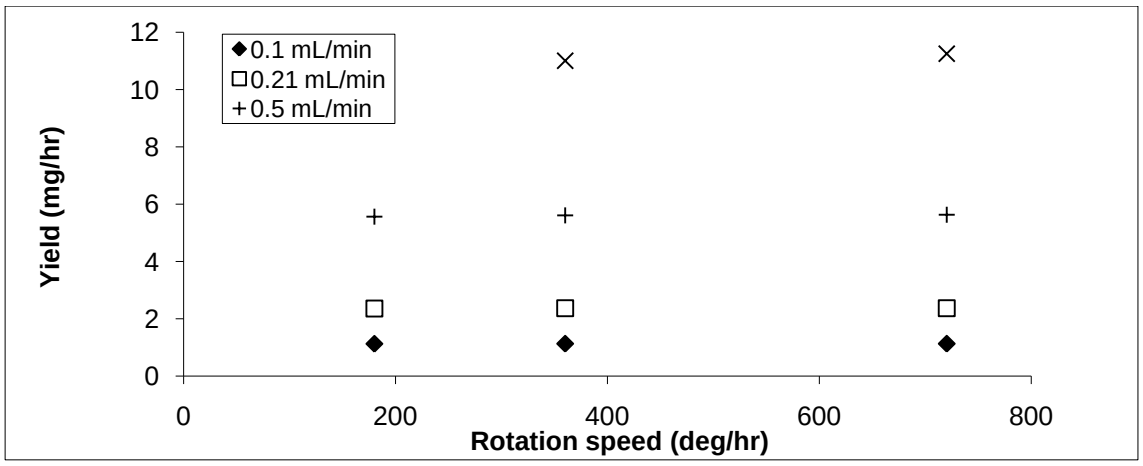

G.3.6 1.5 mg/mL BSA concentration, 1M NaCl concentration, Trial 6, 0.1-1.0mL/min flow rate

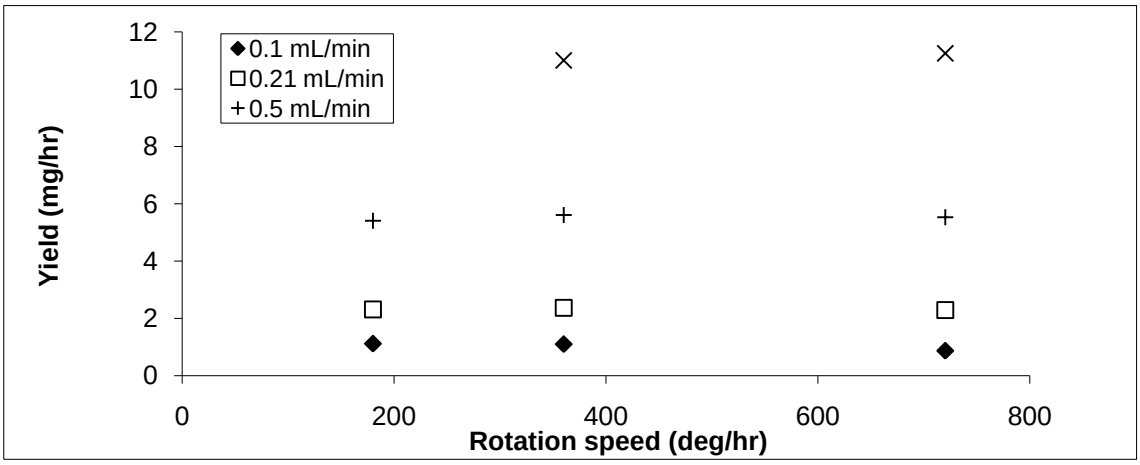

G.3.7 1.5 mg/mL BSA concentration, 1M NaCl concentration, Trial 7, 0.1-1.0mL/min flow rate

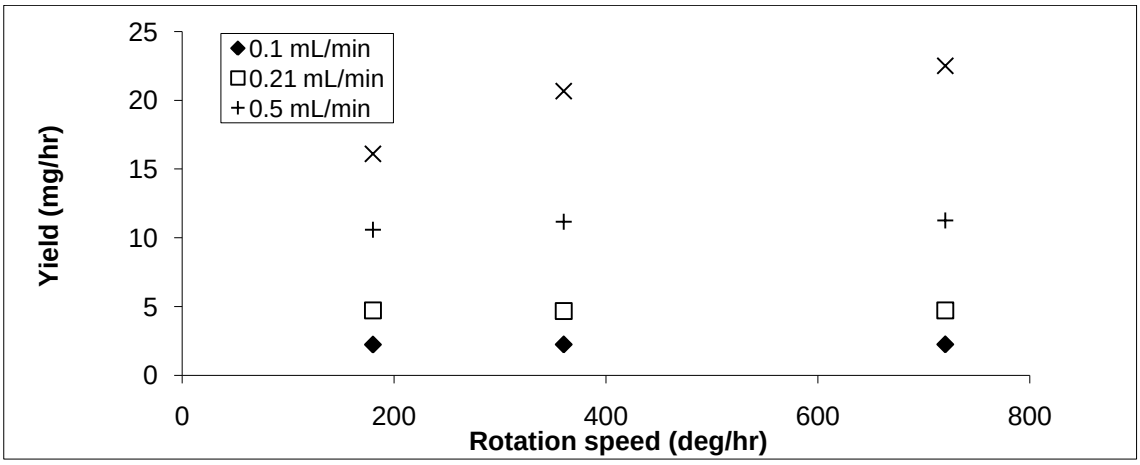

G.3.8 1.5 mg/mL BSA concentration, 1M NaCl concentration, Trial 8, 0.1-1.0mL/min flow rate

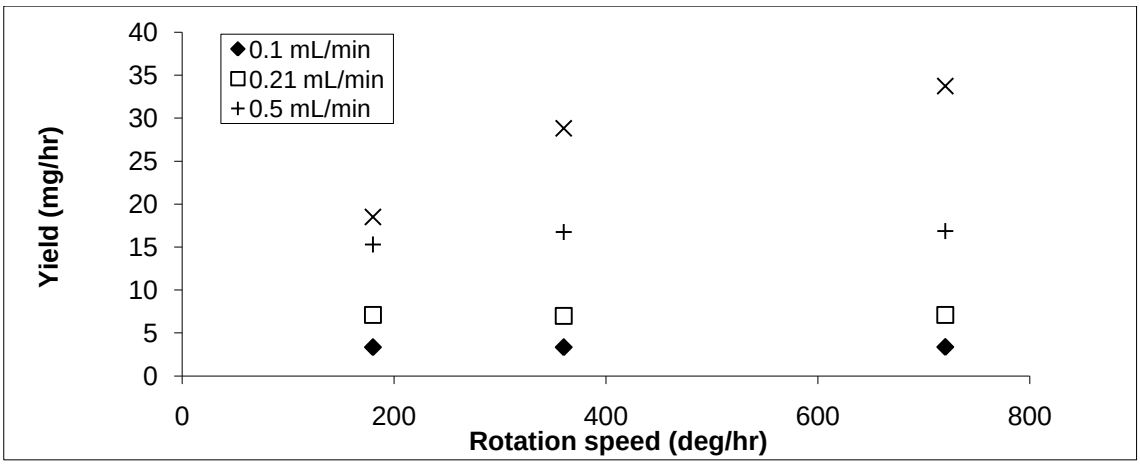

G.3.9 1.5 mg/mL BSA concentration, 1M NaCl concentration, Trial 9, 0.1-1.0mL/min flow rate

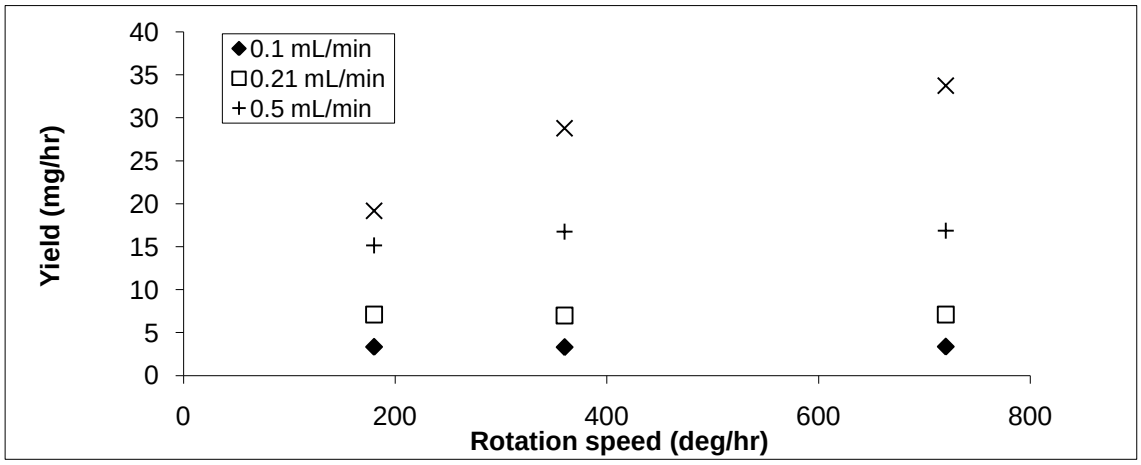

G.3.10 3 mg/mL BSA concentration, 1M NaCl concentration, Trial 1, 0.1-1.0mL/min flow rate

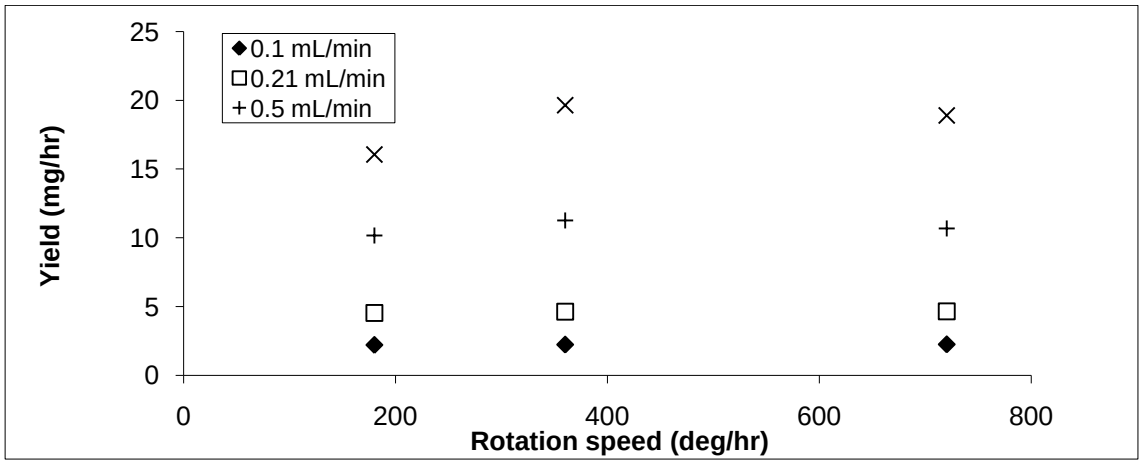

G.3.11 3 mg/mL BSA concentration, 1M NaCl concentration, Trial 2, 0.1-1.0mL/min flow rate

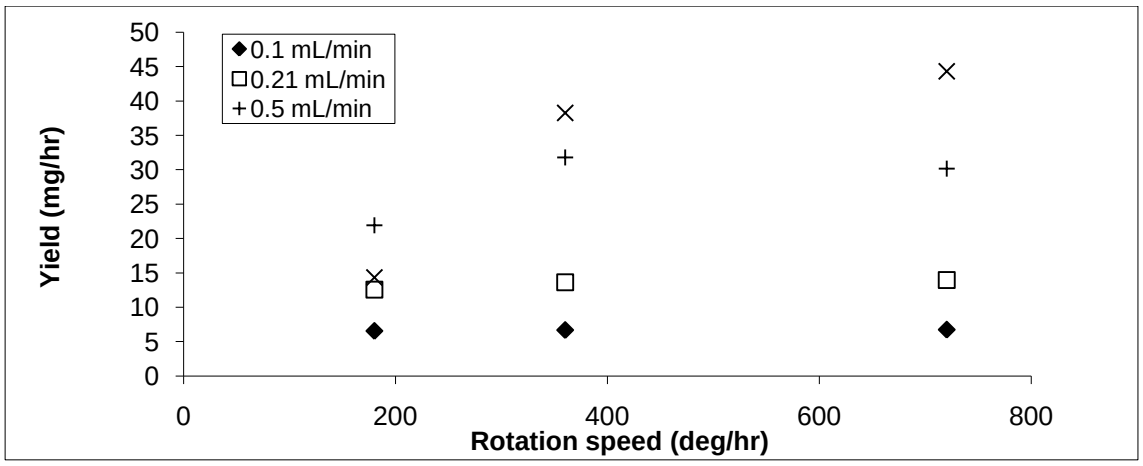

G.3.12 3 mg/mL BSA concentration, 1M NaCl concentration, Trial 3, 0.1-1.0mL/min flow rate

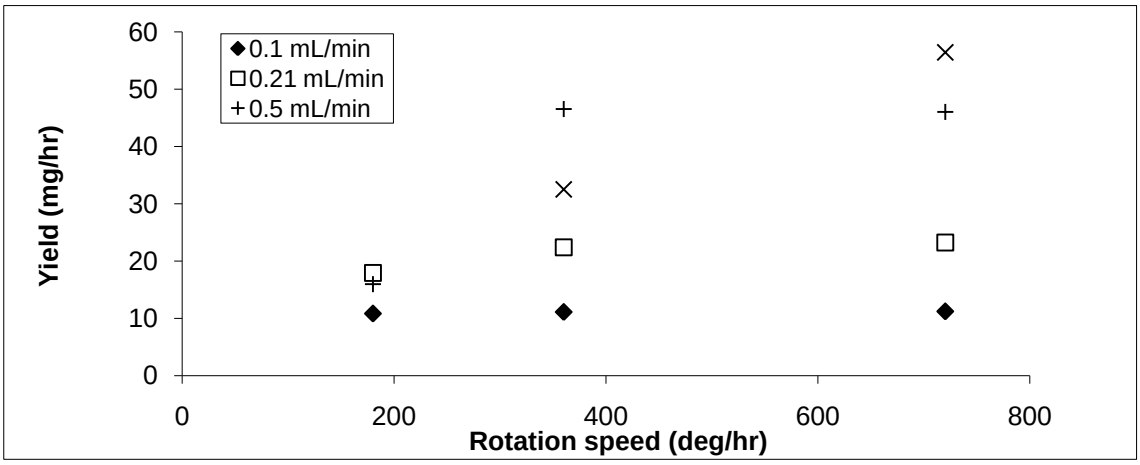

G.3.13 3 mg/mL BSA concentration, 1M NaCl concentration, Trial 4, 0.1-1.0mL/min flow rate

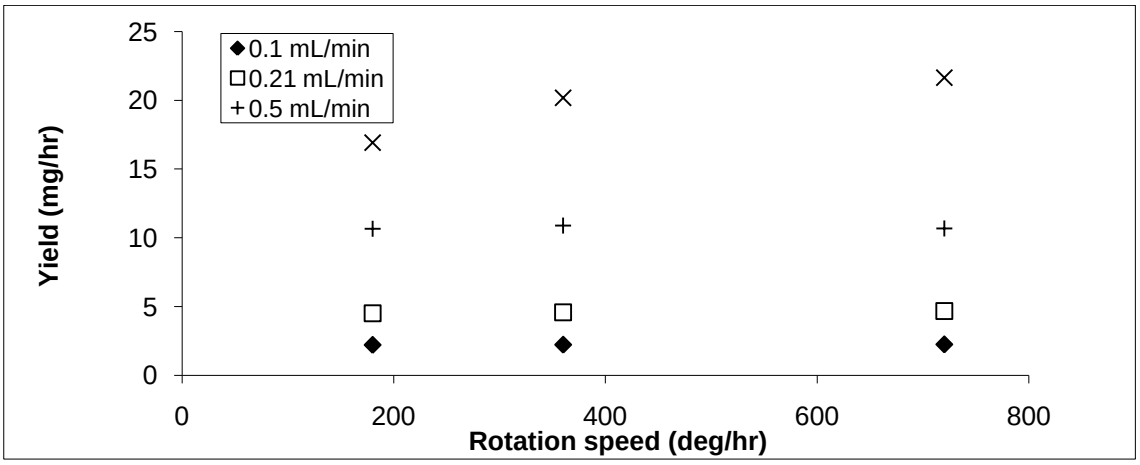

G.3.14 3 mg/mL BSA concentration, 1M NaCl concentration, Trial 5, 0.1-1.0mL/min flow rate

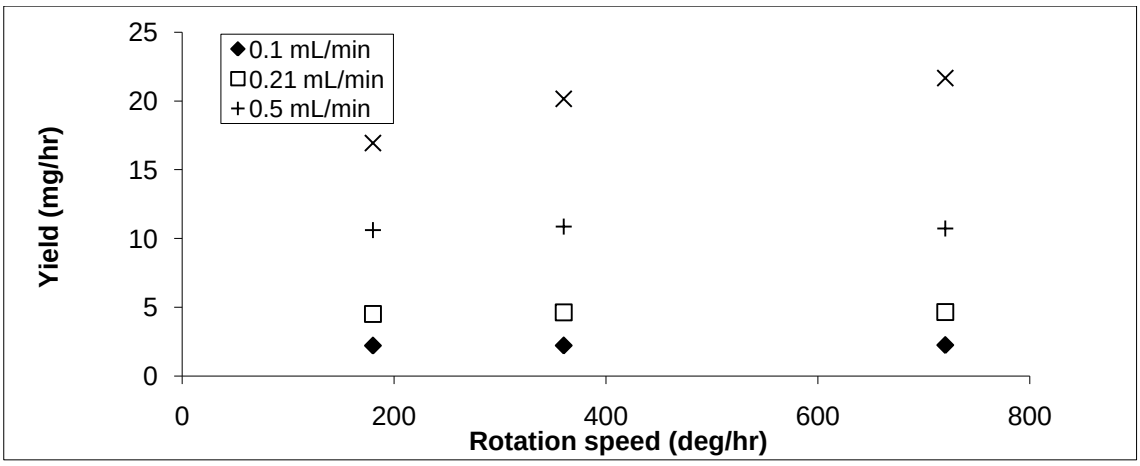

G.3.15 3 mg/mL BSA concentration, 1M NaCl concentration, Trial 6, 0.1-1.0mL/min flow rate

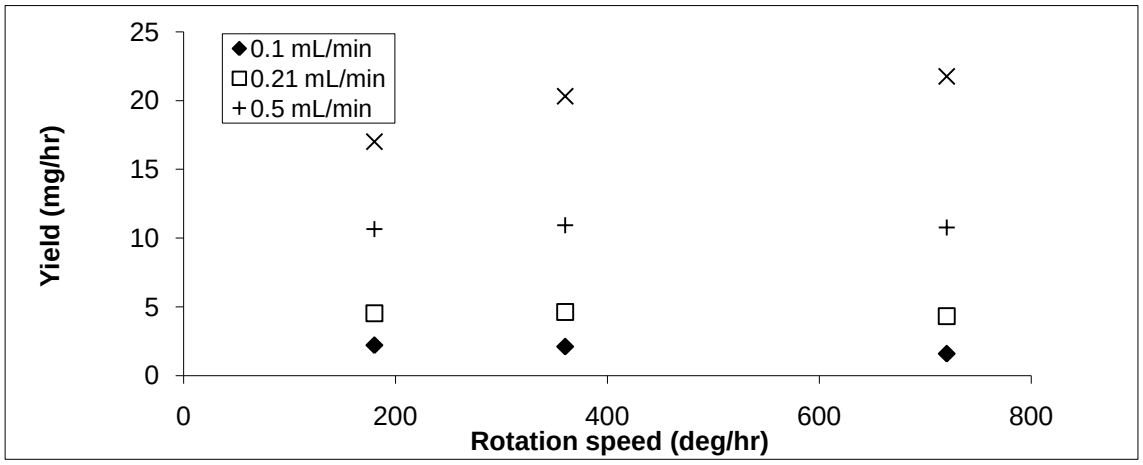

G.3.16 3 mg/mL BSA concentration, 1M NaCl concentration, Trial 7, 0.1-1.0mL/min flow rate

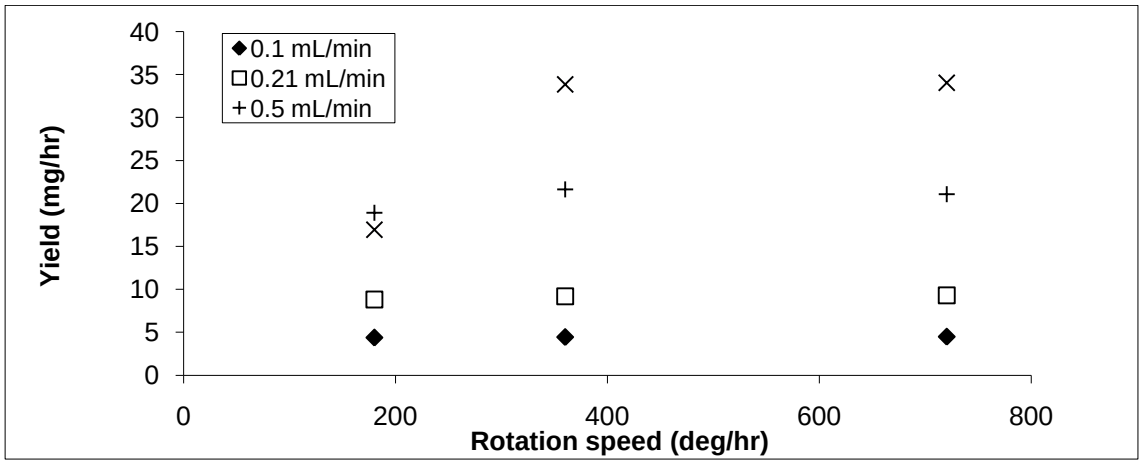

G.3.17 3 mg/mL BSA concentration, 1M NaCl concentration, Trial 8, 0.1-1.0mL/min flow rate

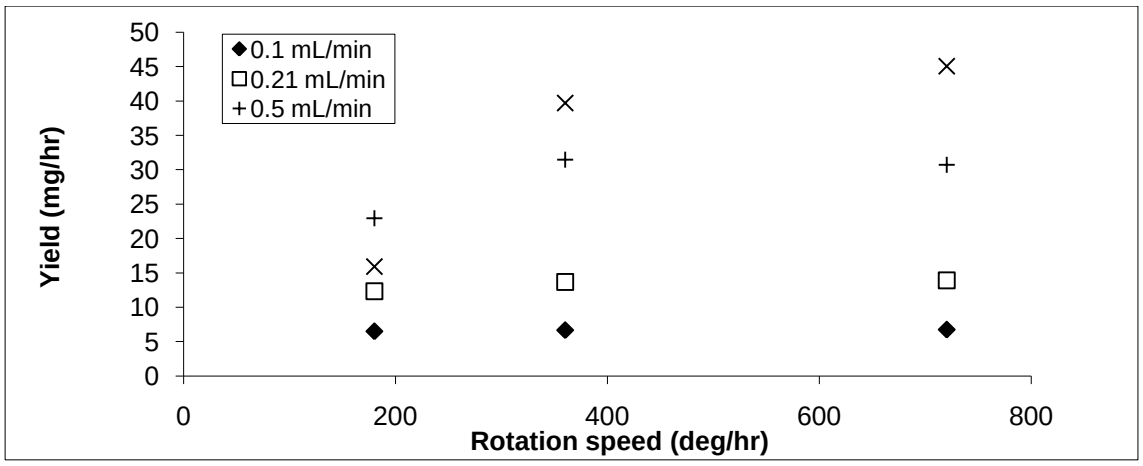

G.3.18 3 mg/mL BSA concentration, 1M NaCl concentration, Trial 9, 0.1-1.0mL/min flow rate

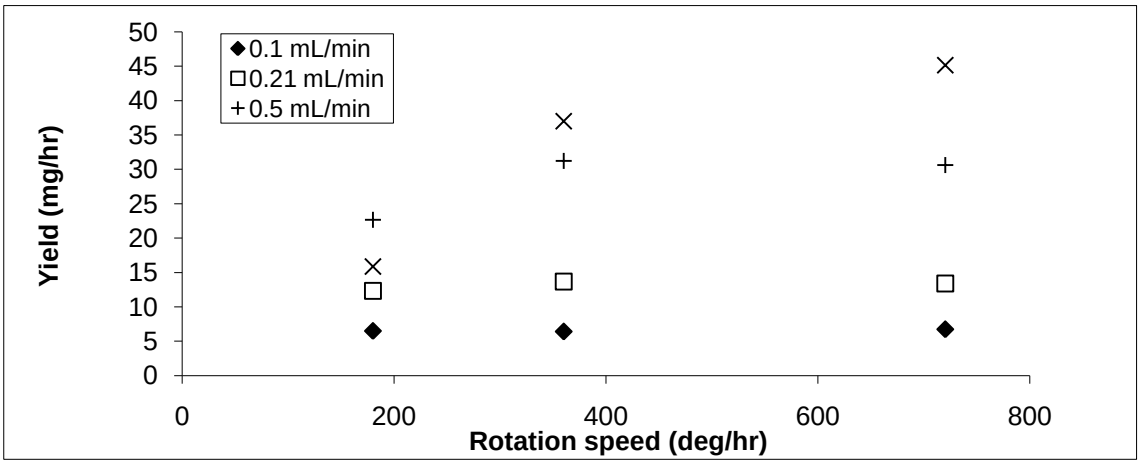

G.3.19 5 mg/mL BSA concentration, 1M NaCl concentration, Trial 1, 0.1-1.0mL/min flow rate

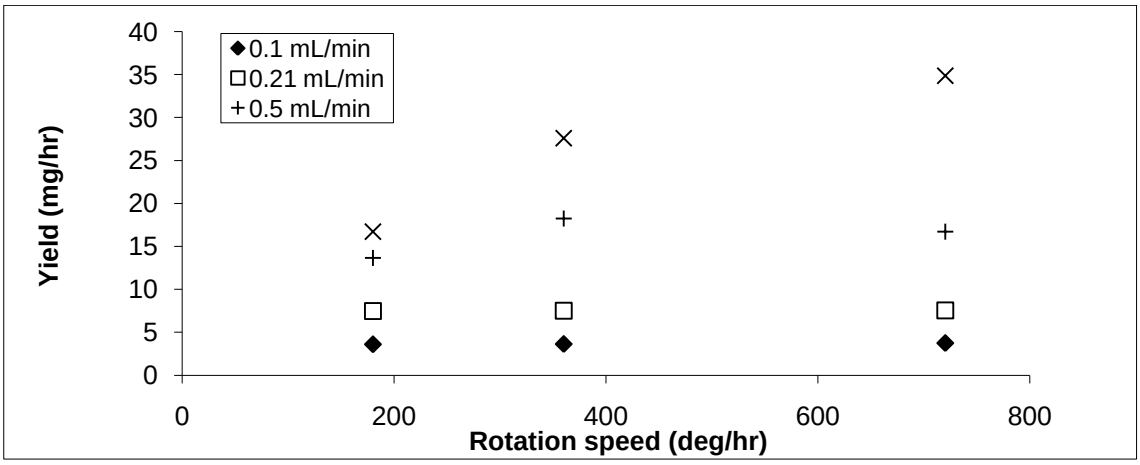

G.3.20 5 mg/mL BSA concentration, 1M NaCl concentration, Trial 2, 0.1-1.0mL/min flow rate

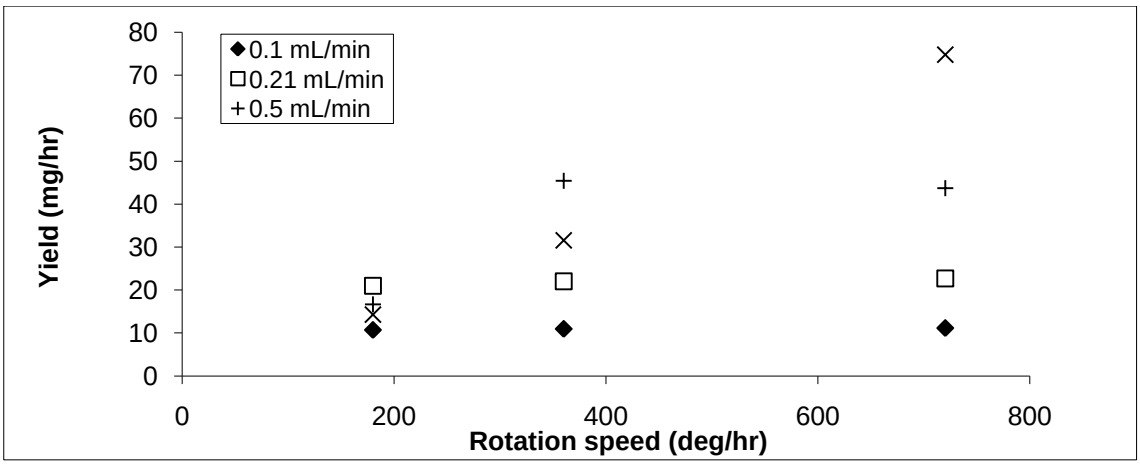

G.3.21 5 mg/mL BSA concentration, 1M NaCl concentration, Trial 3, 0.1-1.0mL/min flow rate

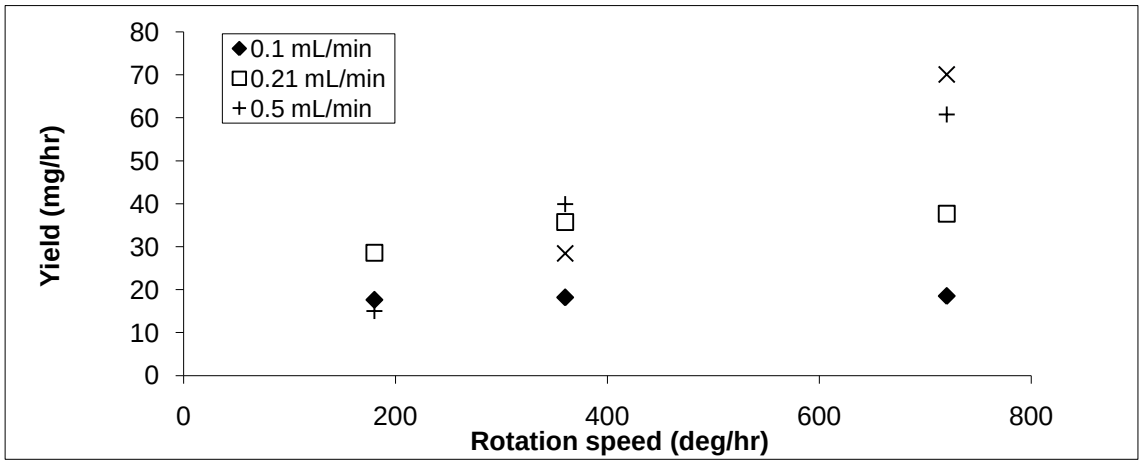

G.3.22 5 mg/mL BSA concentration, 1M NaCl concentration, Trial 4, 0.1-1.0mL/min flow rate

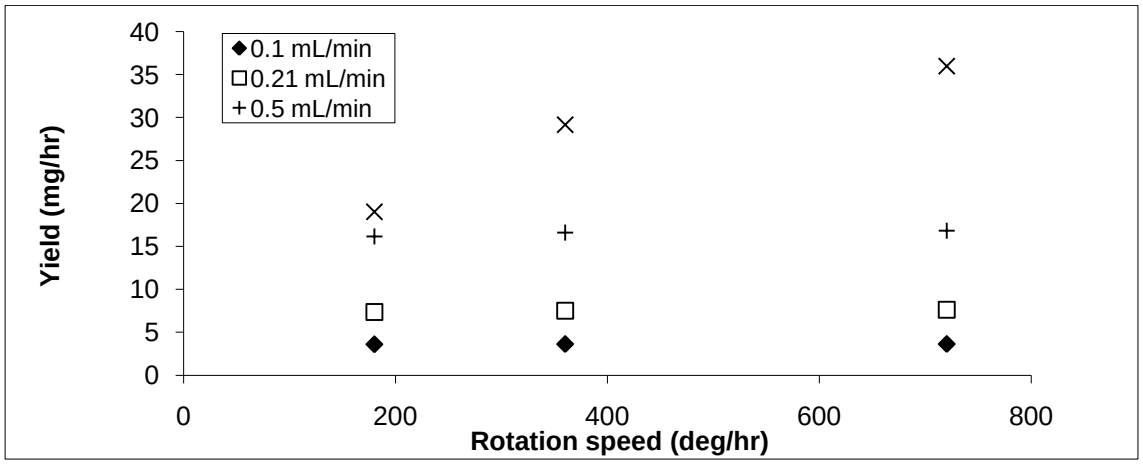

G.3.23 5 mg/mL BSA concentration, 1M NaCl concentration, Trial 5, 0.1-1.0mL/min flow rate

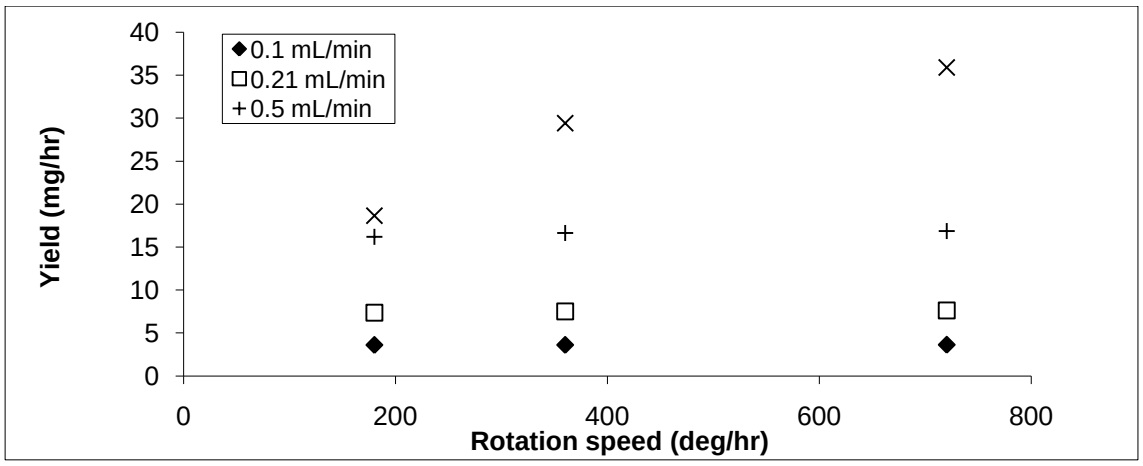

G.3.24 5 mg/mL BSA concentration, 1M NaCl concentration, Trial 6 0.1-1.0mL/min flow rate

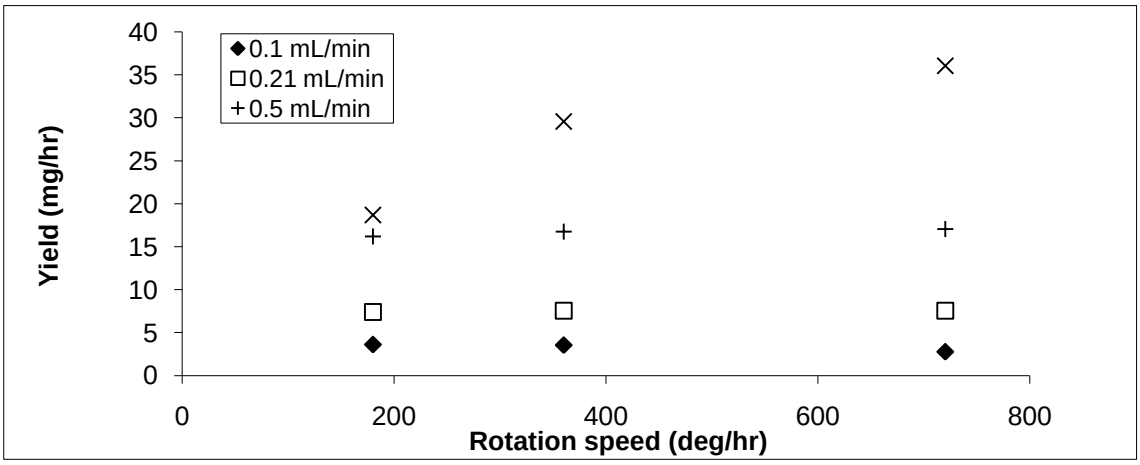

G.3.25 5 mg/mL BSA concentration, 1M NaCl concentration, Trial 7, 0.1-1.0mL/min flow rate

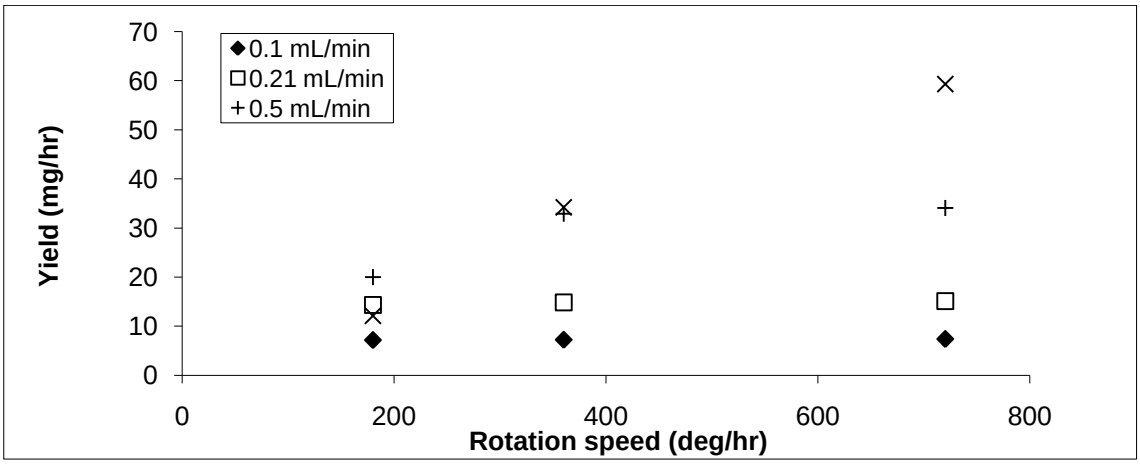

G.3.26 5 mg/mL BSA concentration, 1M NaCl concentration, Trial 8, 0.1-1.0mL/min flow rate

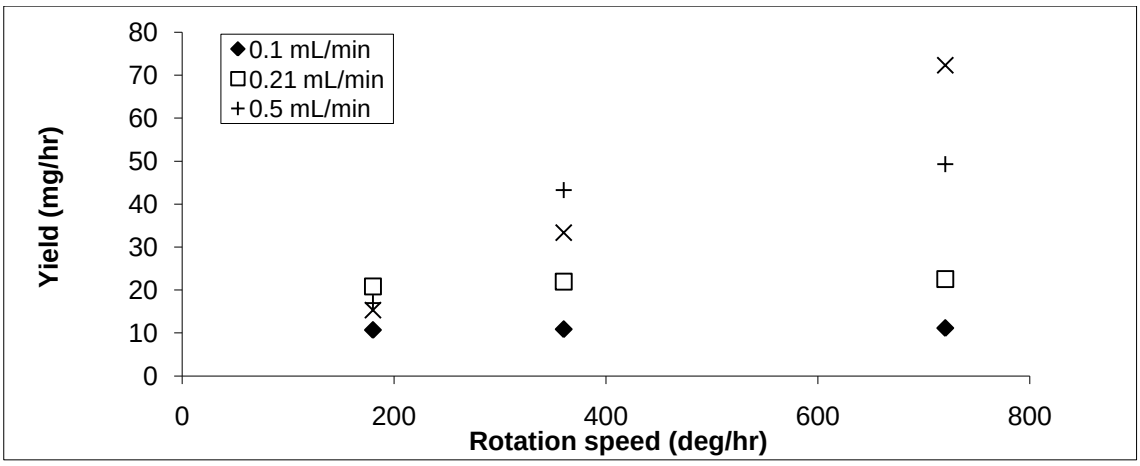

G.3.27 5 mg/mL BSA concentration, 1M NaCl concentration, Trial 9, 0.1-1.0mL/min flow rate

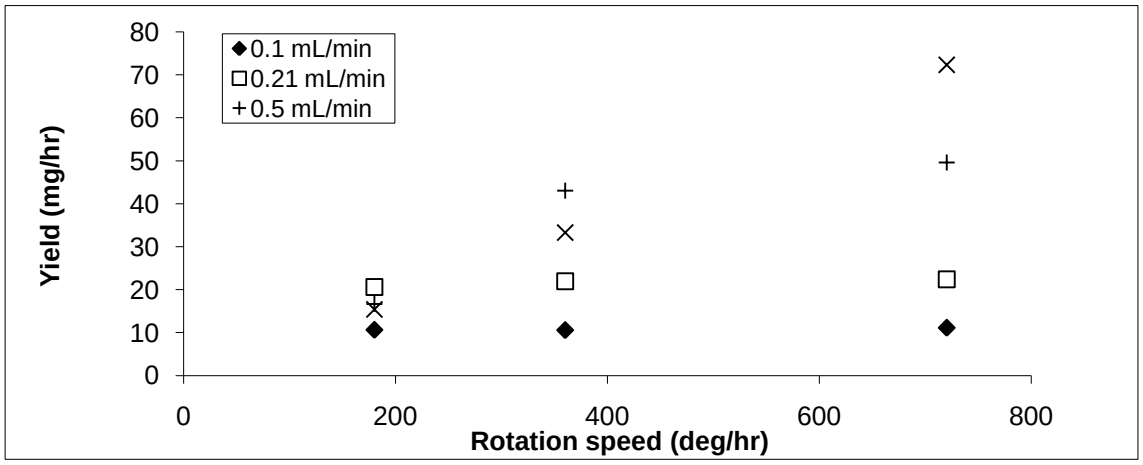

G.3.28 1.5 mg/mL BSA concentration, 2M NaCl concentration, Trial 1, 0.1-1.0mL/min flow rate

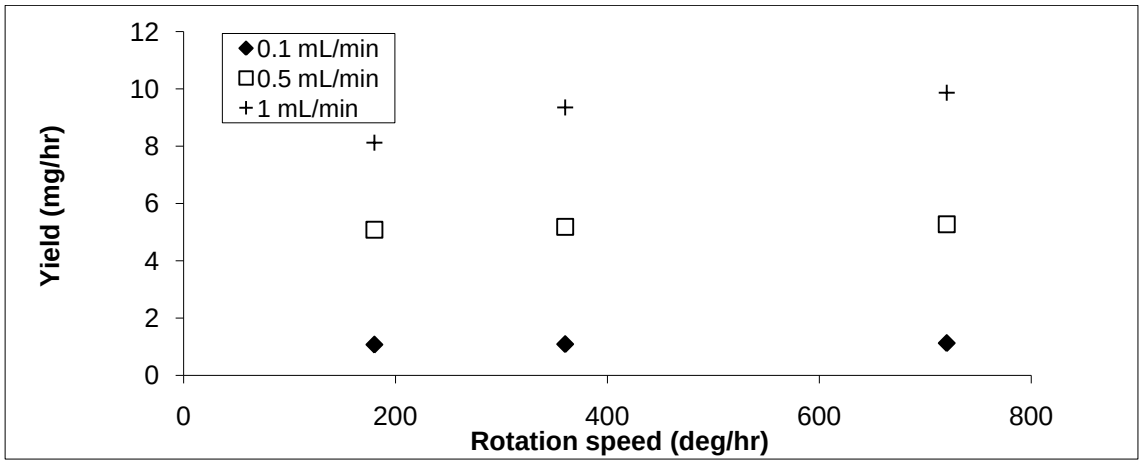

G.3.29 1.5 mg/mL BSA concentration, 2M NaCl concentration, Trial 2, 0.1-1.0mL/min flow rate

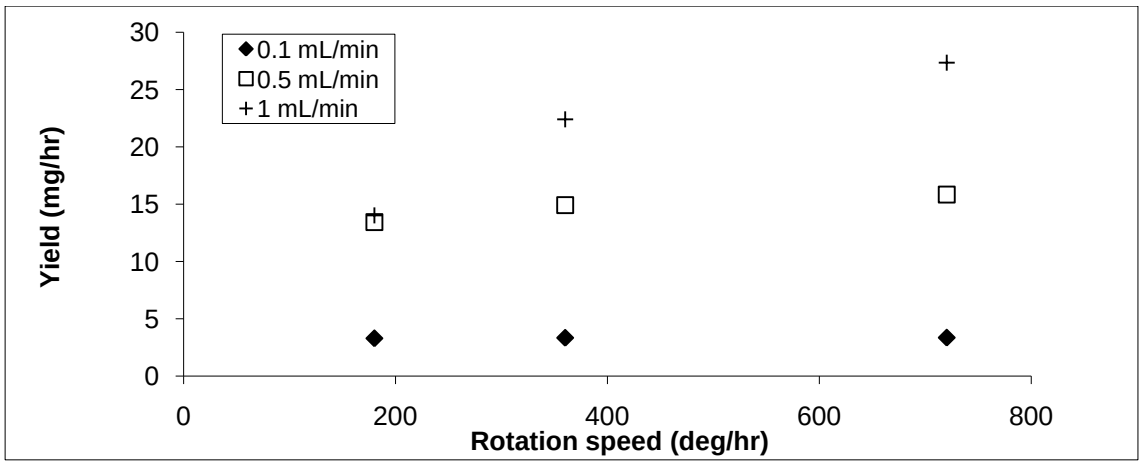

G.3.30 1.5 mg/mL BSA concentration, 2M NaCl concentration, Trial 3, 0.1-1.0mL/min flow rate

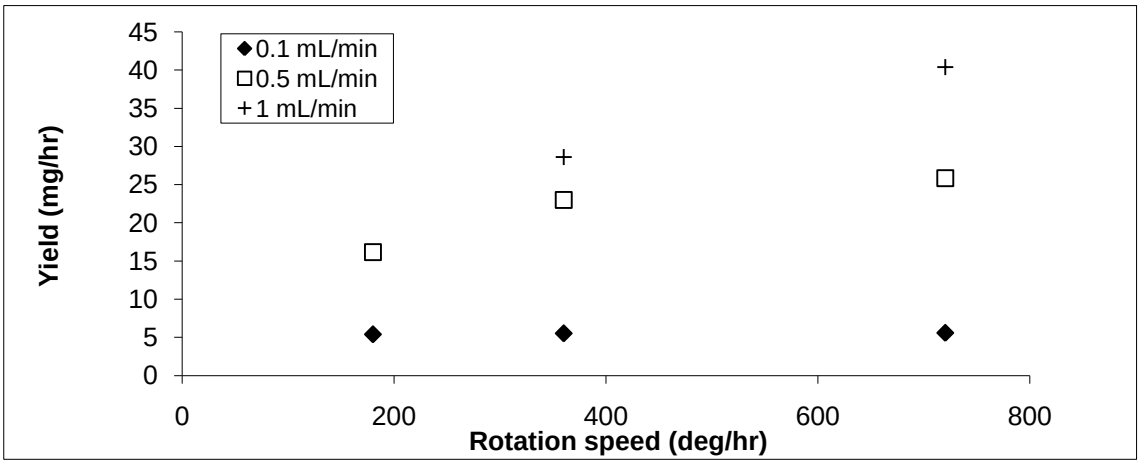

G.3.31 1.5 mg/mL BSA concentration, 2M NaCl concentration, Trial 4, 0.1-1.0mL/min flow rate

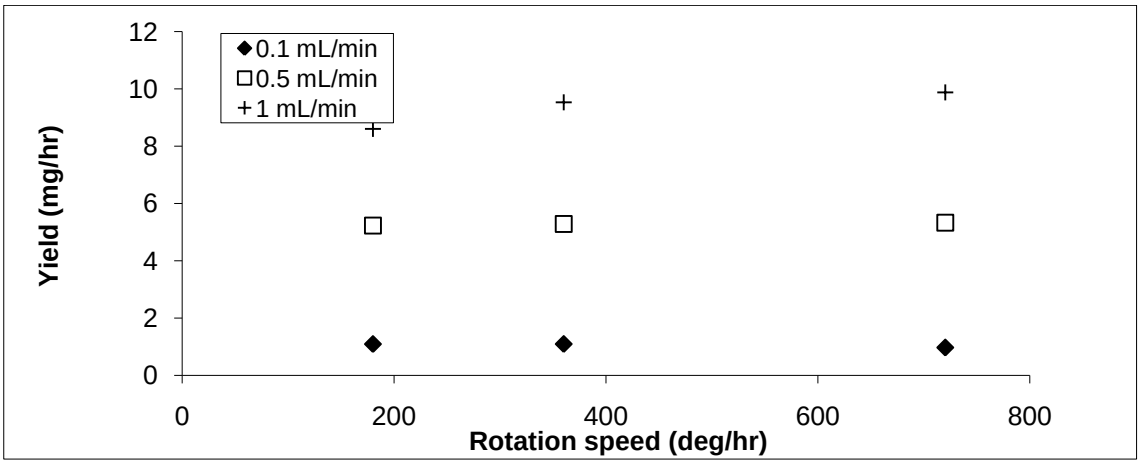

G.3.32 1.5 mg/mL BSA concentration, 2M NaCl concentration, Trial 5, 0.1-1.0mL/min flow rate

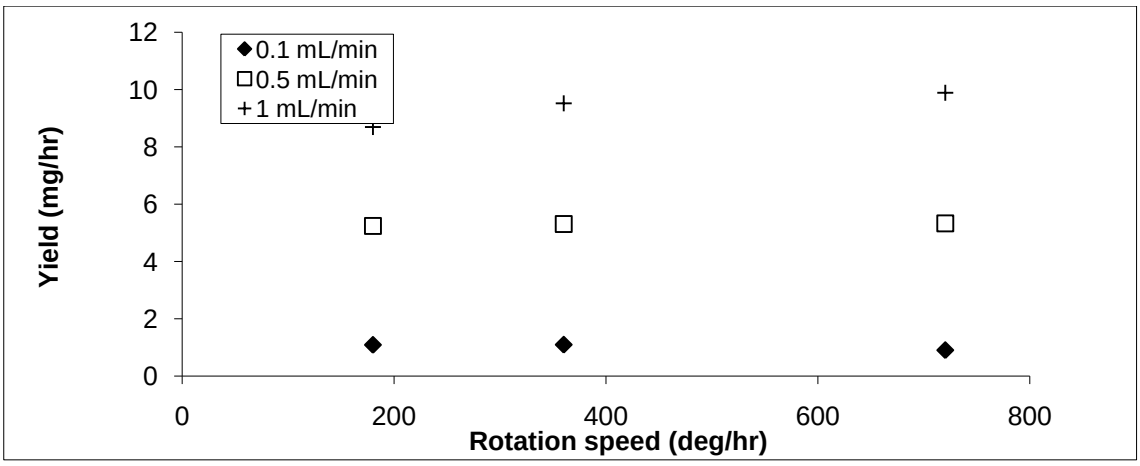

G.3.33 1.5 mg/mL BSA concentration, 2M NaCl concentration, Trial 6, 0.1-1.0mL/min flow rate

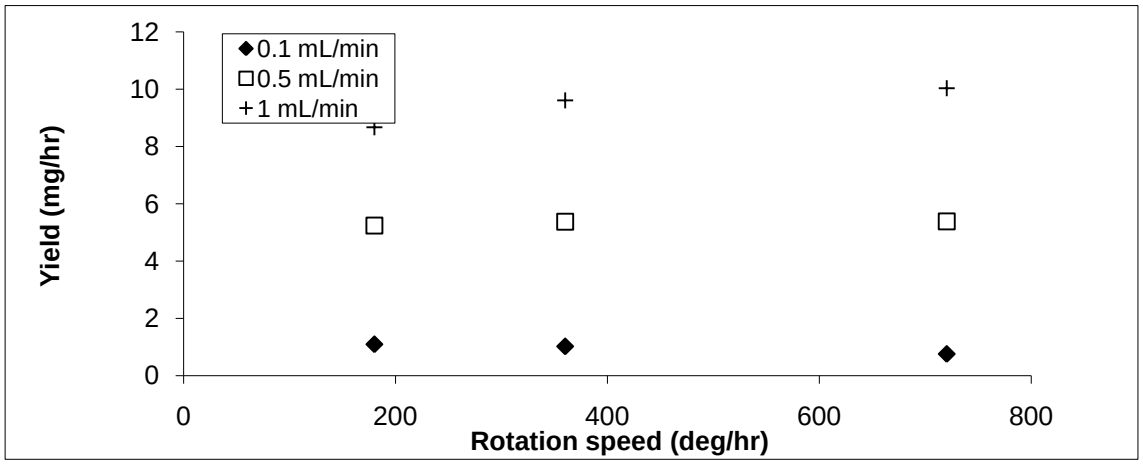

G.3.34 1.5 mg/mL BSA concentration, 2M NaCl concentration, Trial 7, 0.1-1.0mL/min flow rate

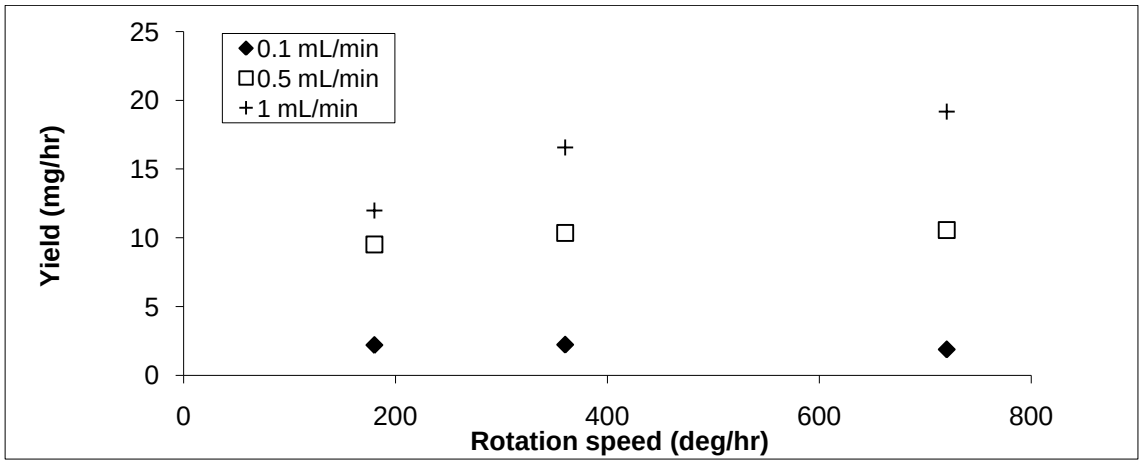

G.3.35 1.5 mg/mL BSA concentration, 2M NaCl concentration, Trial 8, 0.1-1.0mL/min flow rate

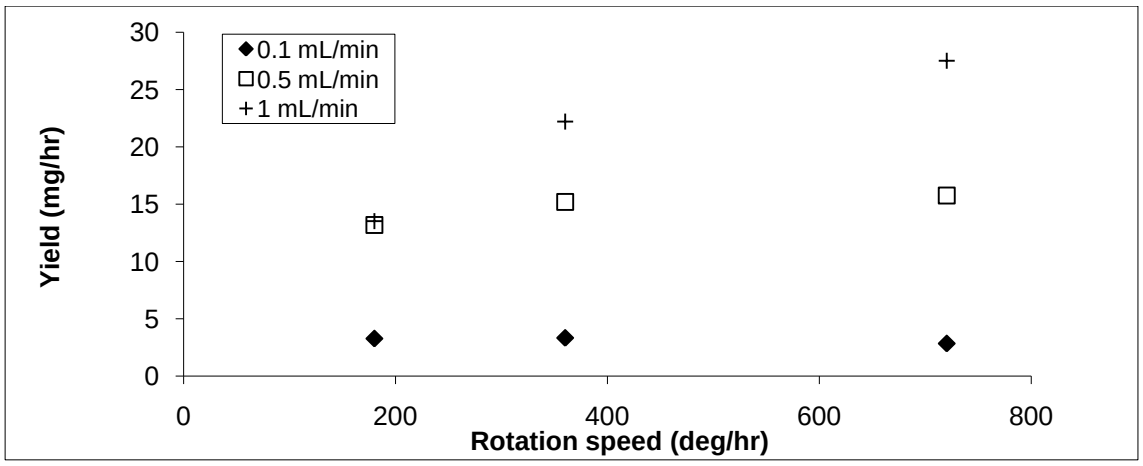

G.3.36 1.5 mg/mL BSA concentration, 2M NaCl concentration, Trial 9, 0.1-1.0mL/min flow rate

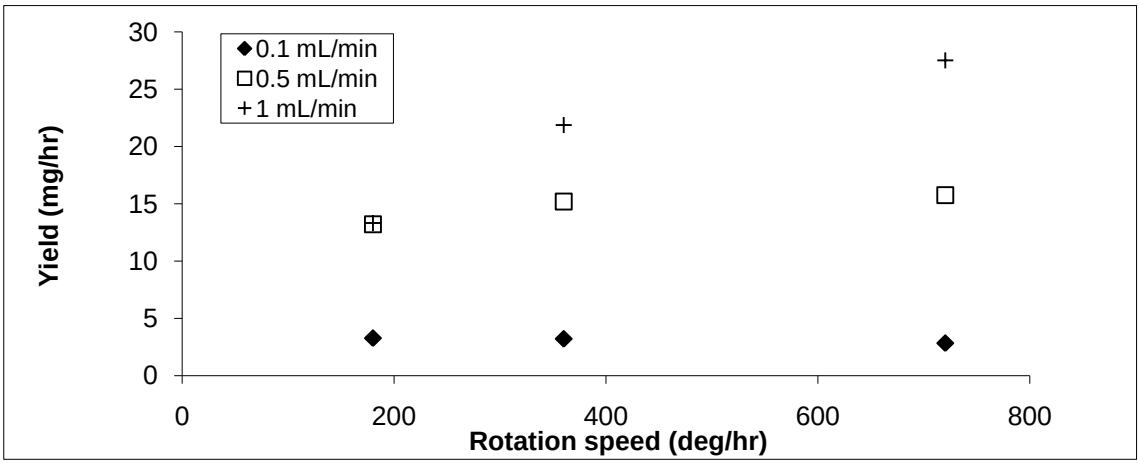

G.4 Flow rate

G.4.1 1.5 mg/mL BSA concentration, 1M NaCl concentration, Trial 1, 180-720 deg/hr rotation speed

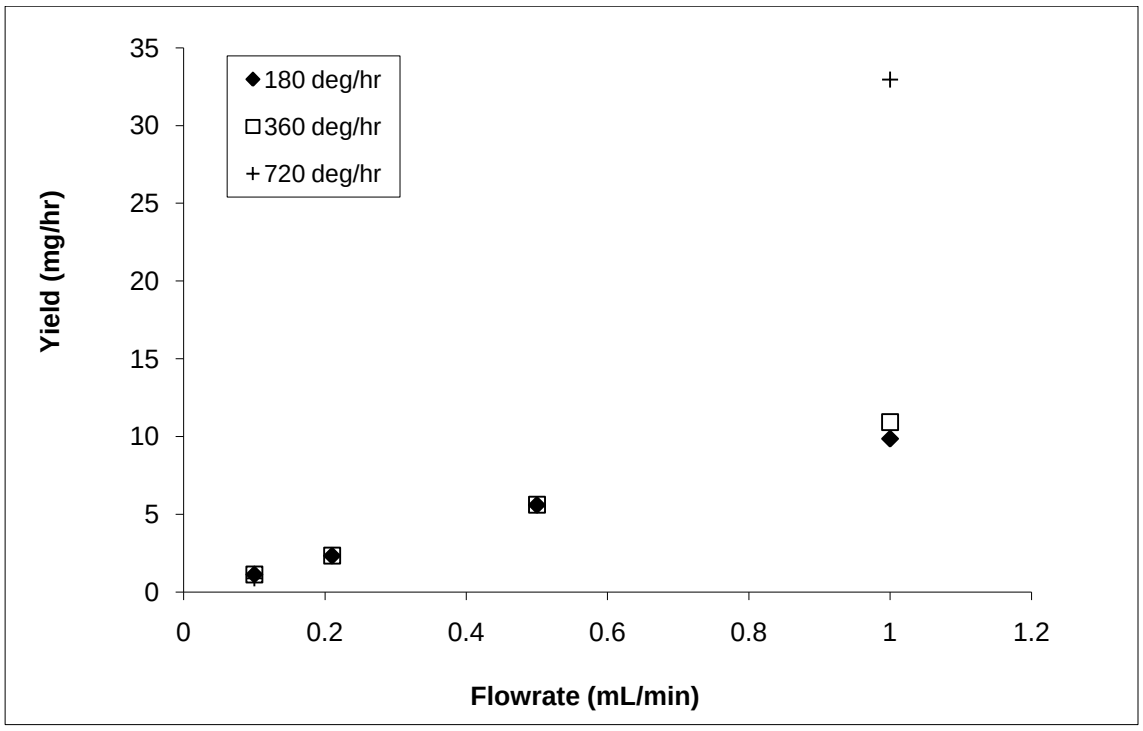

G.4.2 1.5 mg/mL BSA concentration, 1M NaCl concentration, Trial 2, 180-720 deg/hr rotation speed

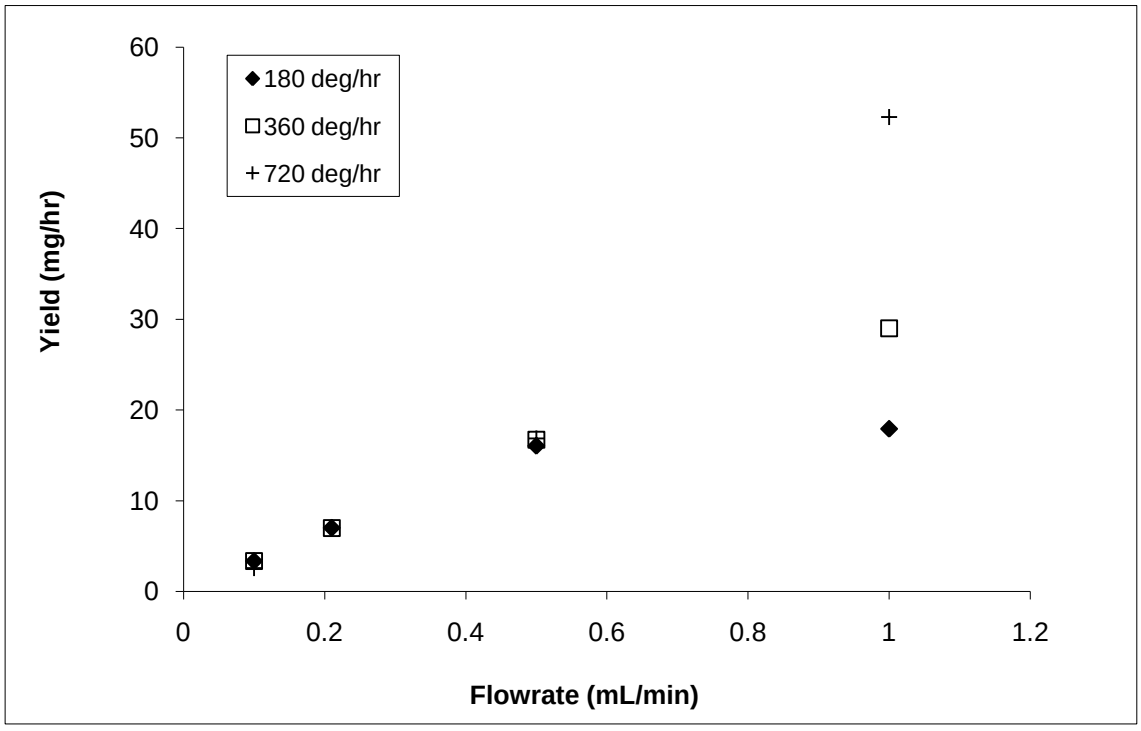

G.4.3 1.5 mg/mL BSA concentration, 1M NaCl concentration, Trial 3, 180-720 deg/hr rotation speed

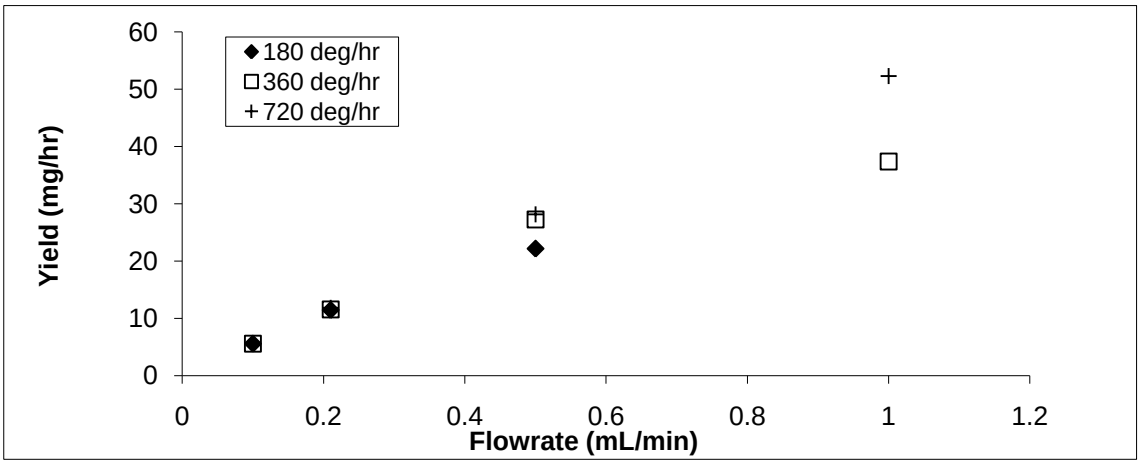

G.4.4 1.5 mg/mL BSA concentration, 1M NaCl concentration, Trial 4, 180-720 deg/hr rotation speed

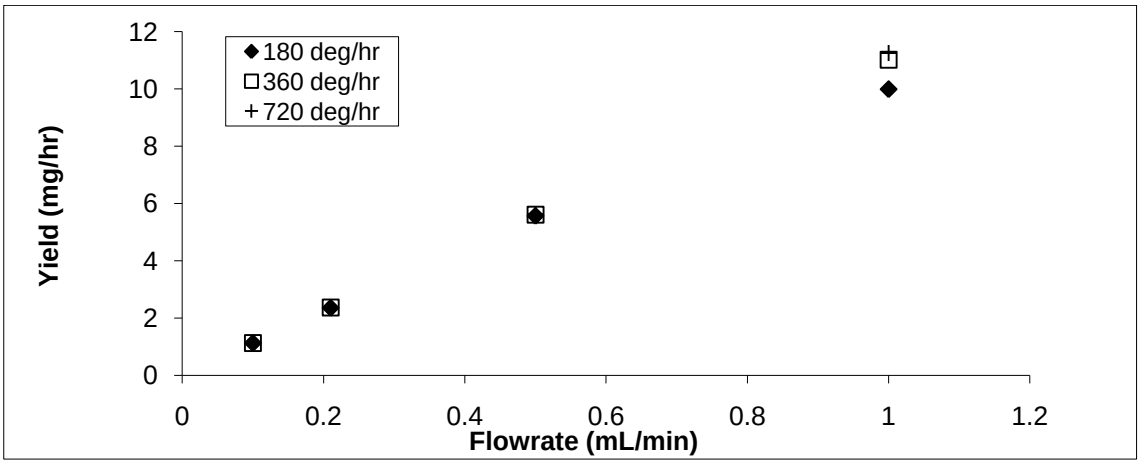

G.4.5 1.5 mg/mL BSA concentration, 1M NaCl concentration, Trial 5, 180-720 deg/hr rotation speed

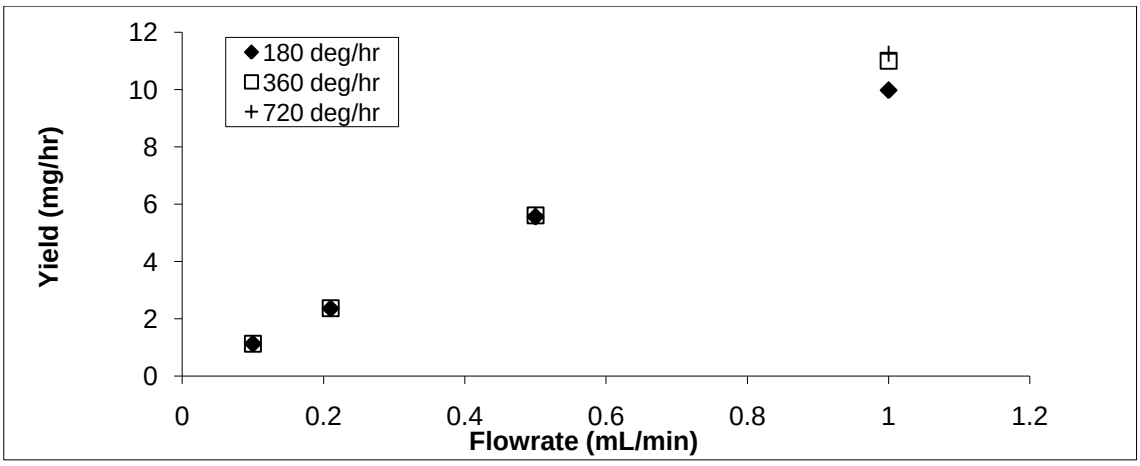

G.4.6 1.5 mg/mL BSA concentration, 1M NaCl concentration, Trial 6, 180-720 deg/hr rotation speed

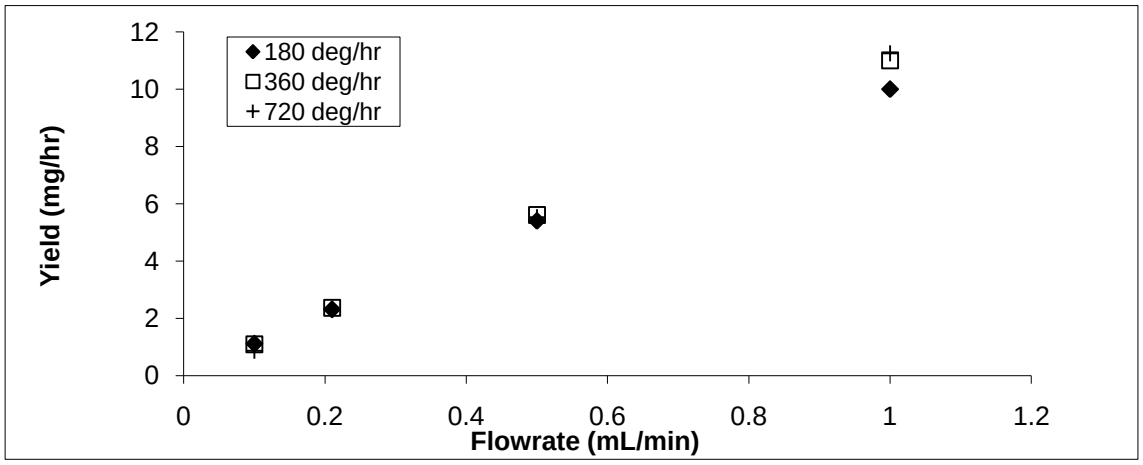

G.4.7 1.5 mg/mL BSA concentration, 1M NaCl concentration, Trial 7, 180-720 deg/hr rotation speed

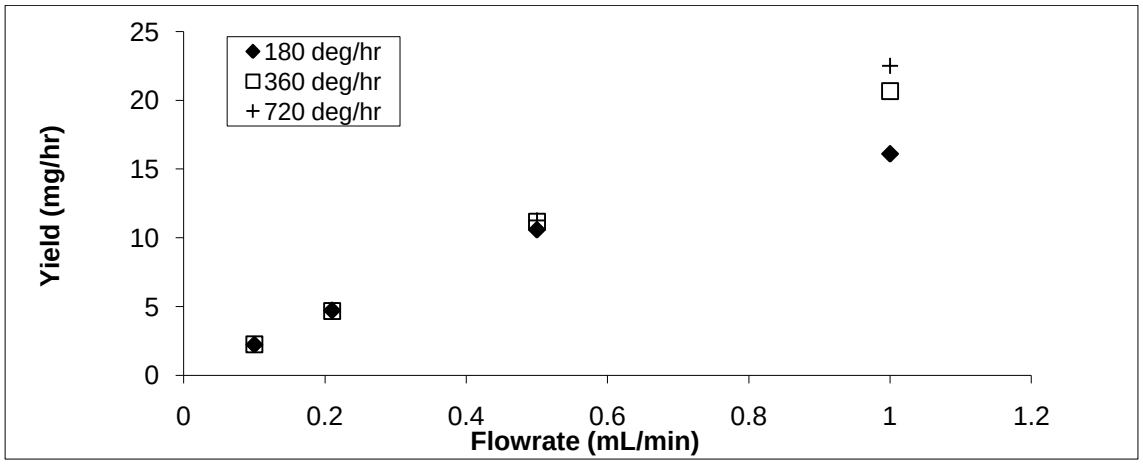

G.4.8 1.5 mg/mL BSA concentration, 1M NaCl concentration, Trial 8, 180-720 deg/hr rotation speed

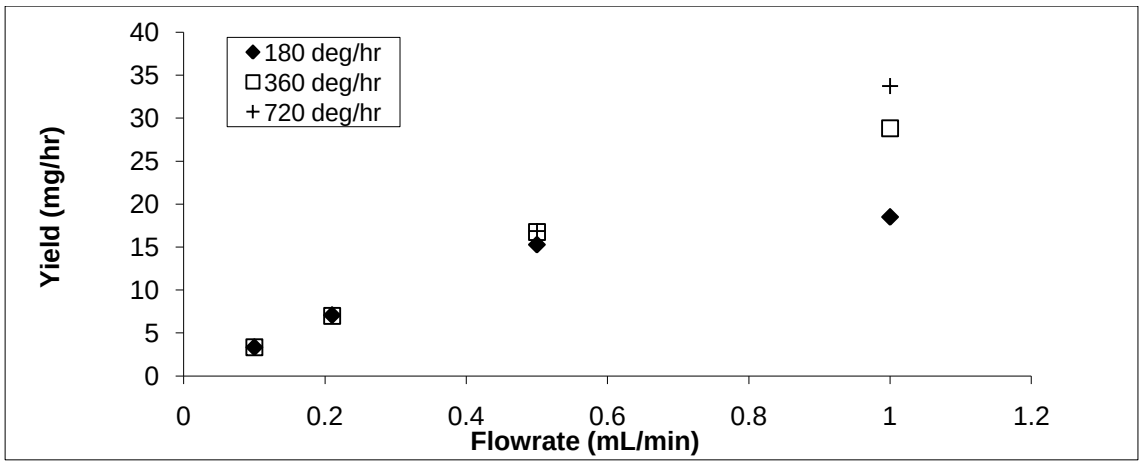

G.4.9 1.5 mg/mL BSA concentration, 1M NaCl concentration, Trial 9, 180-720 deg/hr rotation speed

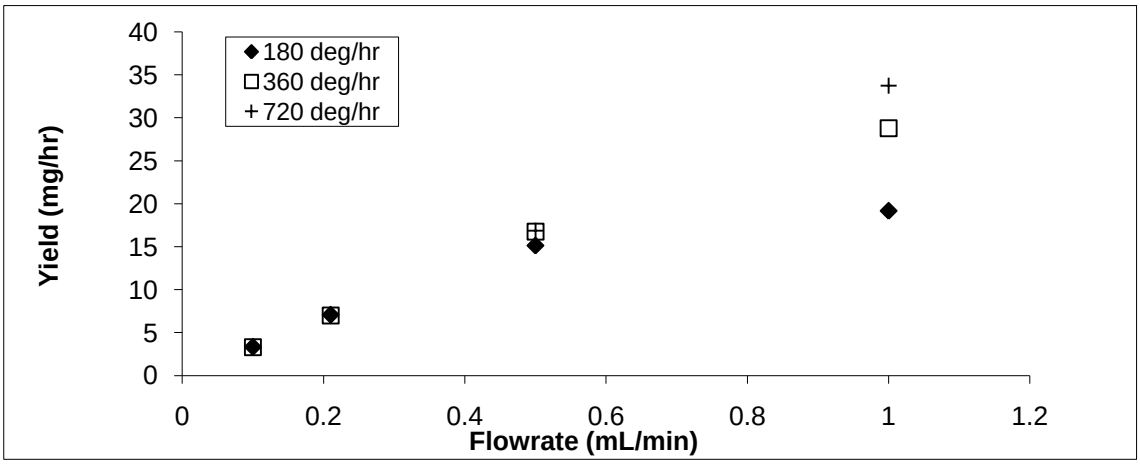

G.4.10 3 mg/mL BSA concentration, 1M NaCl concentration, Trial 1, 180-720 deg/hr rotation speed

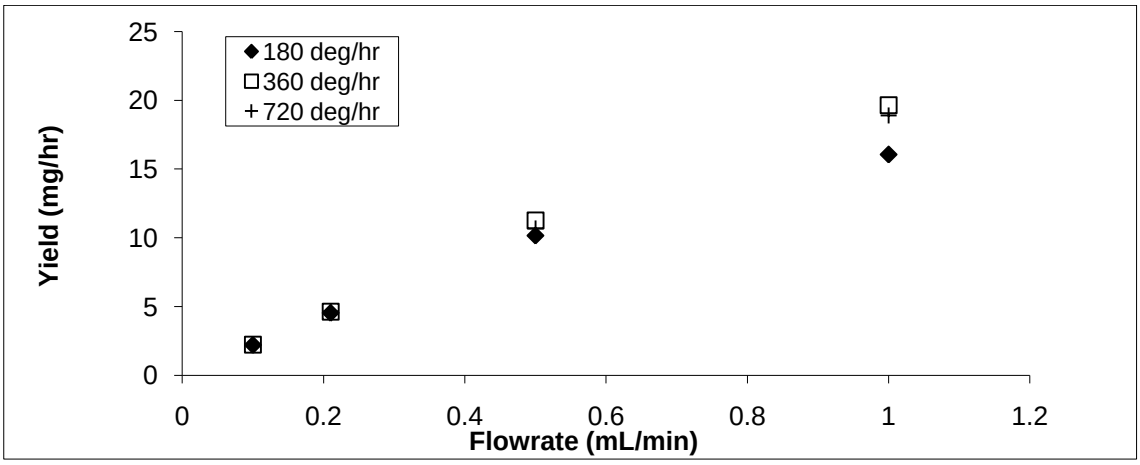

G.4.11 3 mg/mL BSA concentration, 1M NaCl concentration, Trial 2, 180-720 deg/hr rotation speed

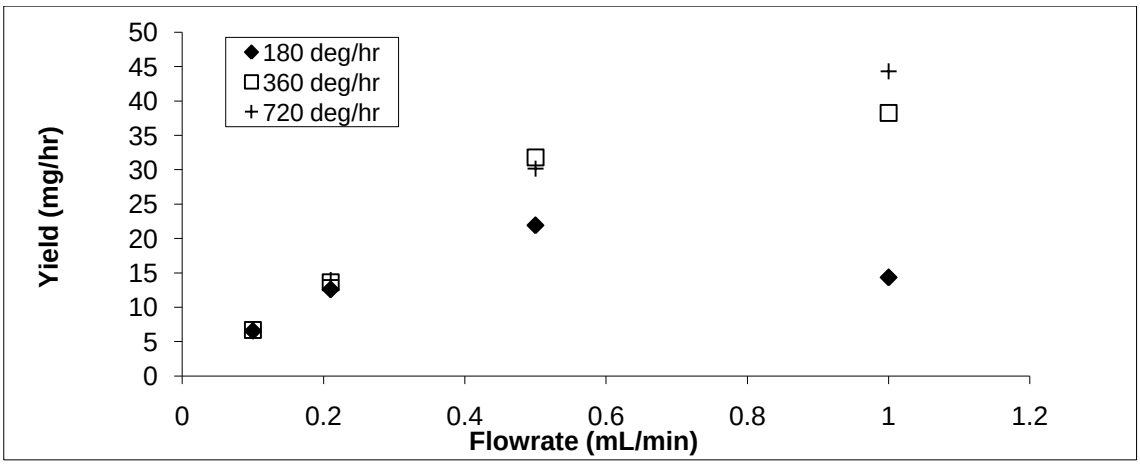

G.4.12 3 mg/mL BSA concentration, 1M NaCl concentration, Trial 3, 180-720 deg/hr rotation speed

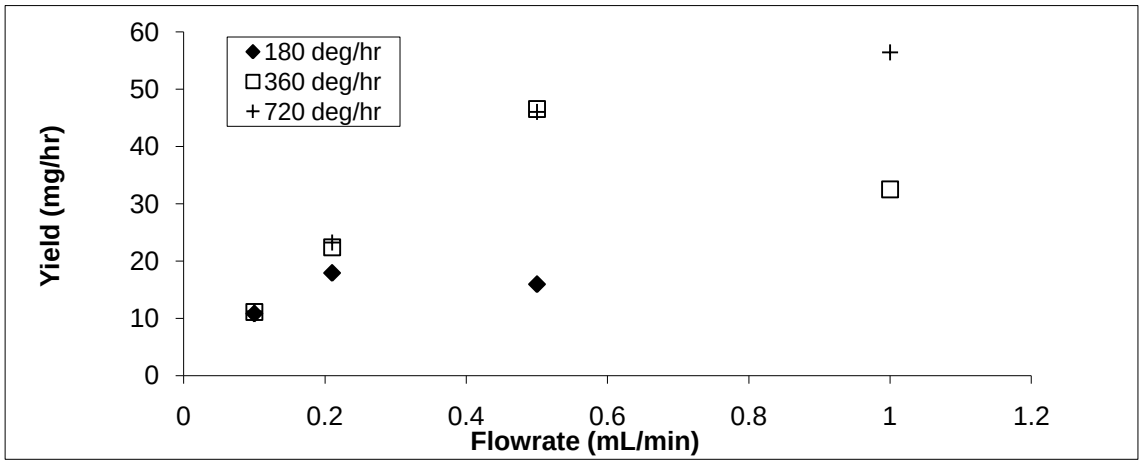

G.4.13 3 mg/mL BSA concentration, 1M NaCl concentration, Trial 4, 180-720 deg/hr rotation speed

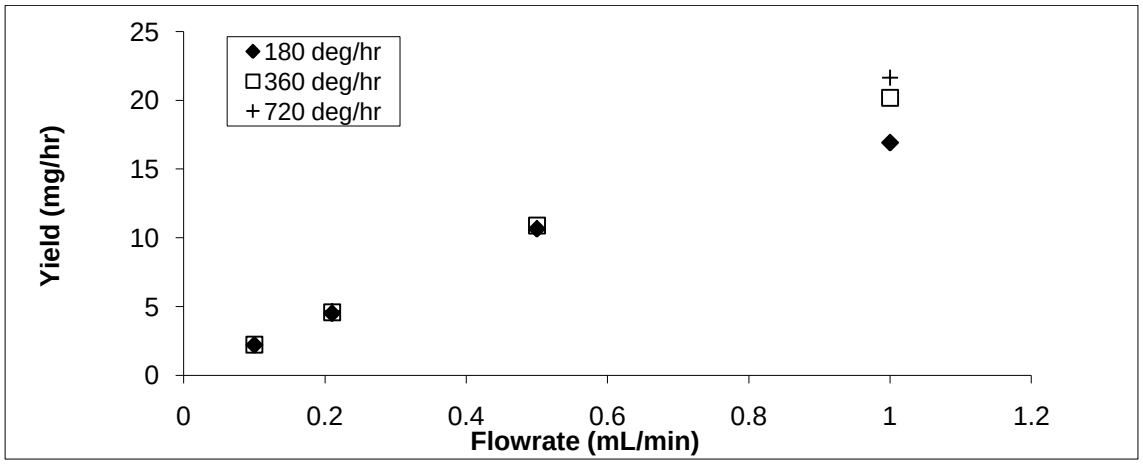

G.4.14 3 mg/mL BSA concentration, 1M NaCl concentration, Trial 5, 180-720 deg/hr rotation speed

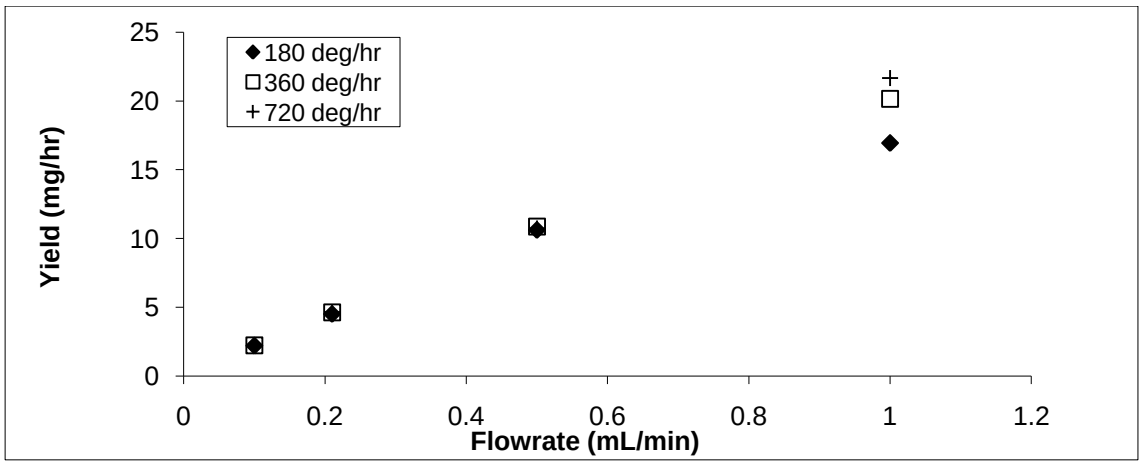

G.4.15 3 mg/mL BSA concentration, 1M NaCl concentration, Trial 6, 180-720 deg/hr rotation speed

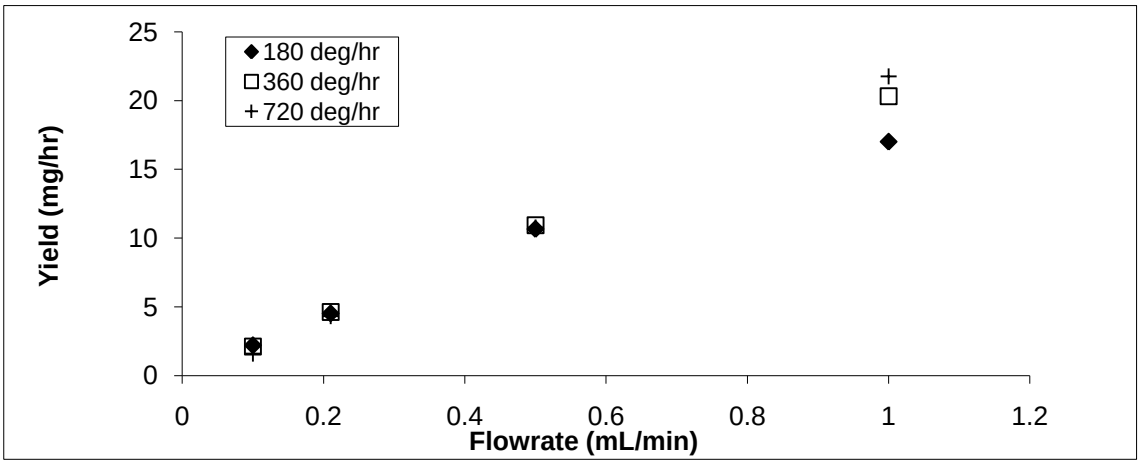

G.4.16 3 mg/mL BSA concentration, 1M NaCl concentration, Trial 7, 180-720 deg/hr rotation speed

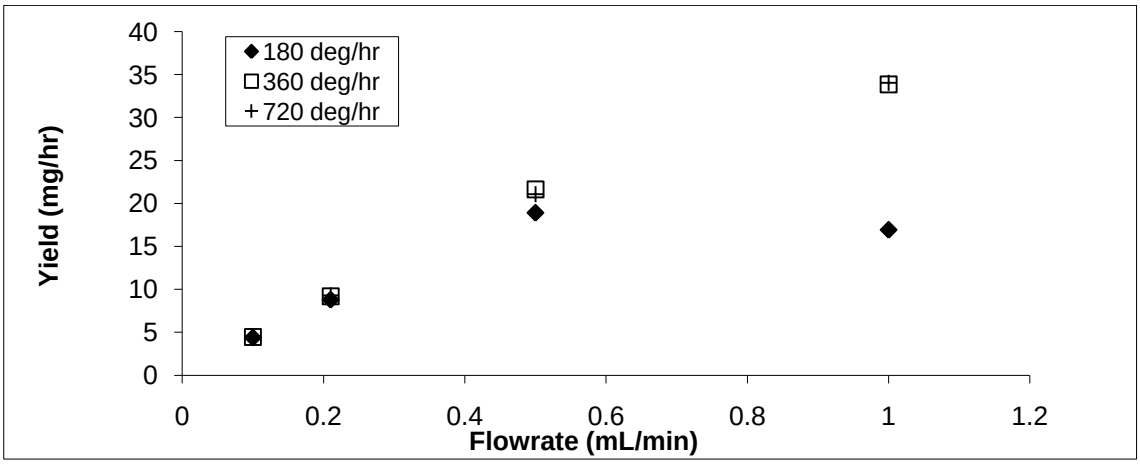

G.4.17 3 mg/mL BSA concentration, 1M NaCl concentration, Trial 8, 180-720 deg/hr rotation speed

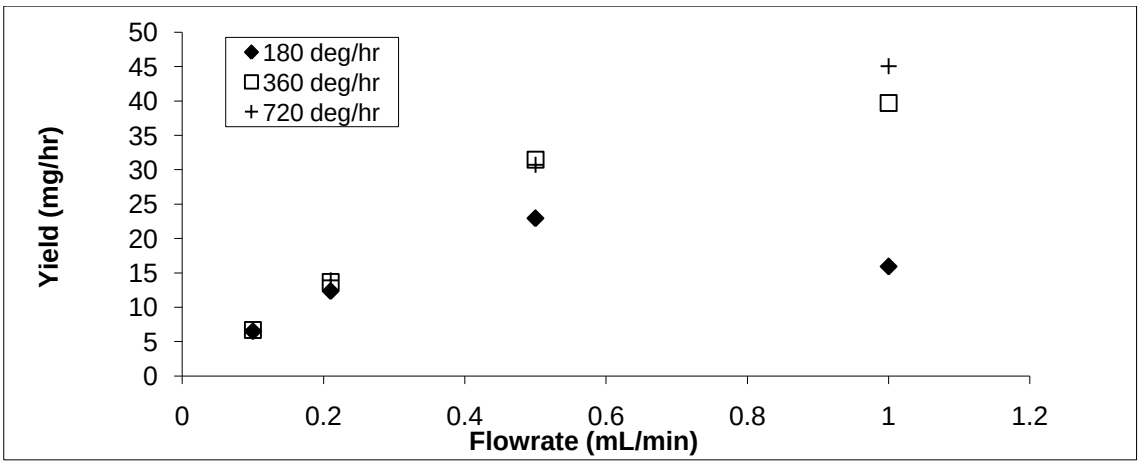

G.4.18 3 mg/mL BSA concentration, 1M NaCl concentration, Trial 9, 180-720 deg/hr rotation speed

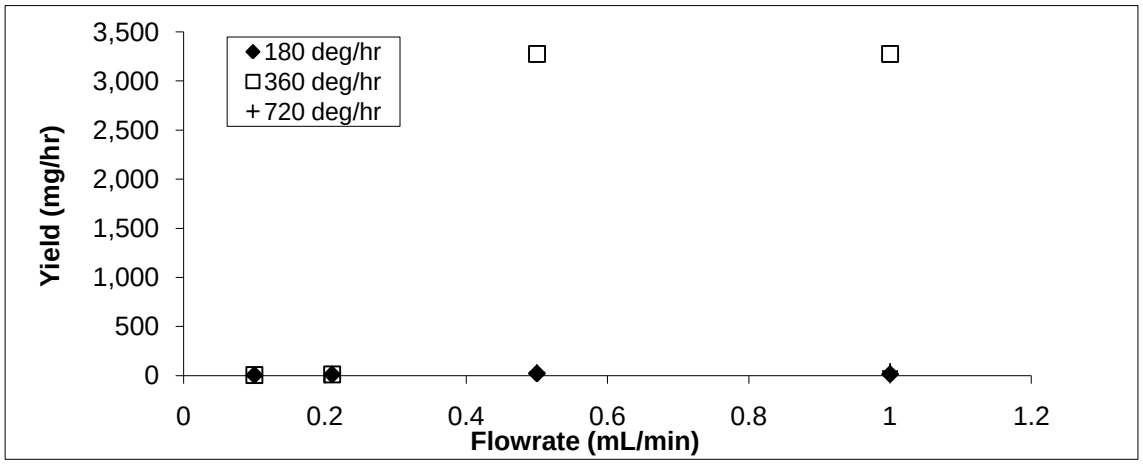

G.4.19 5 mg/mL BSA concentration, 1M NaCl concentration, Trial 1, 180-720 deg/hr rotation speed

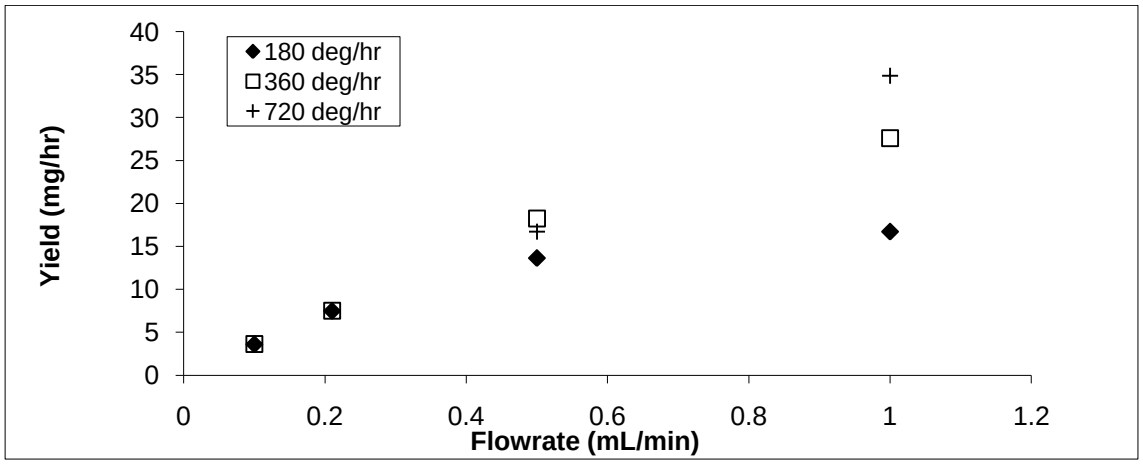

G.4.20 5 mg/mL BSA concentration, 1M NaCl concentration, Trial 2, 180-720 deg/hr rotation speed

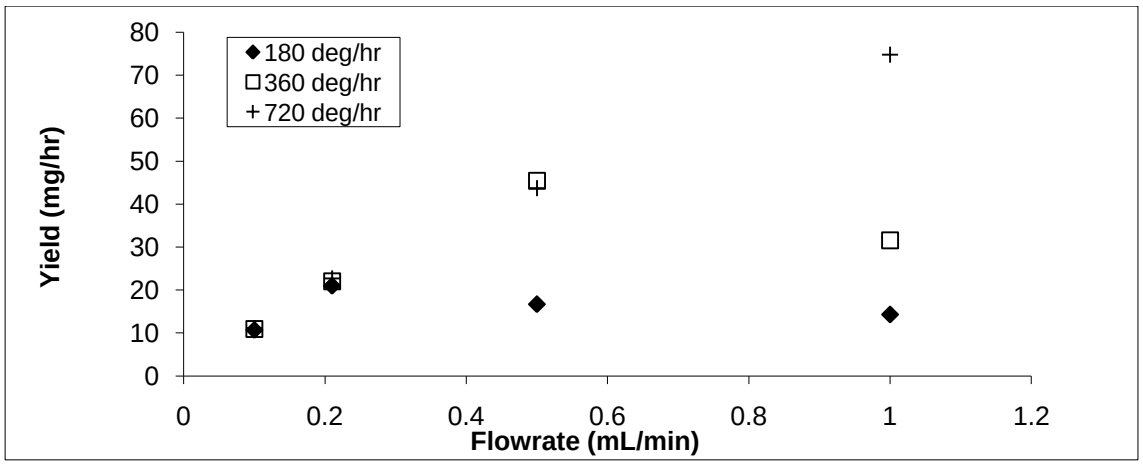

G.4.21 5 mg/mL BSA concentration, 1M NaCl concentration, Trial 3, 180-720 deg/hr rotation speed

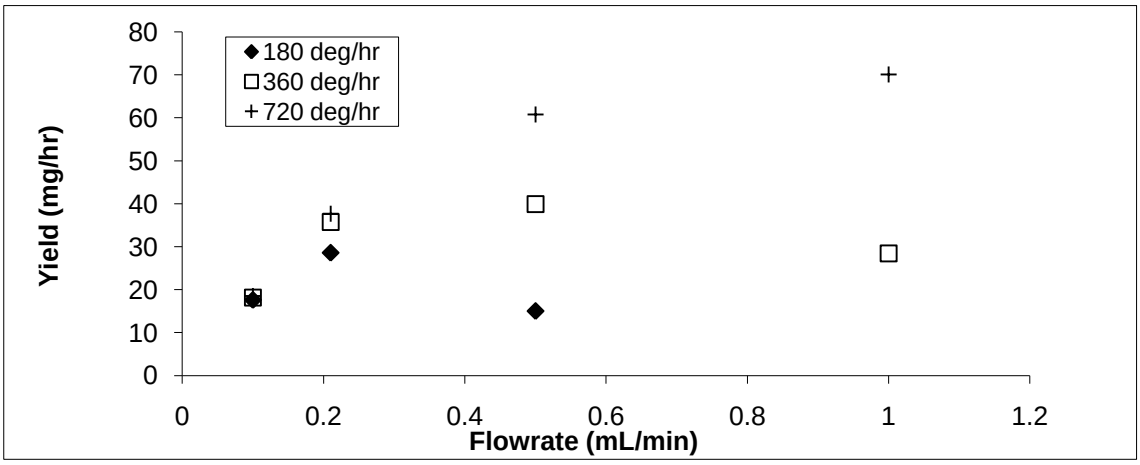

G.4.22 5 mg/mL BSA concentration, 1M NaCl concentration, Trial 4, 180-720 deg/hr rotation speed

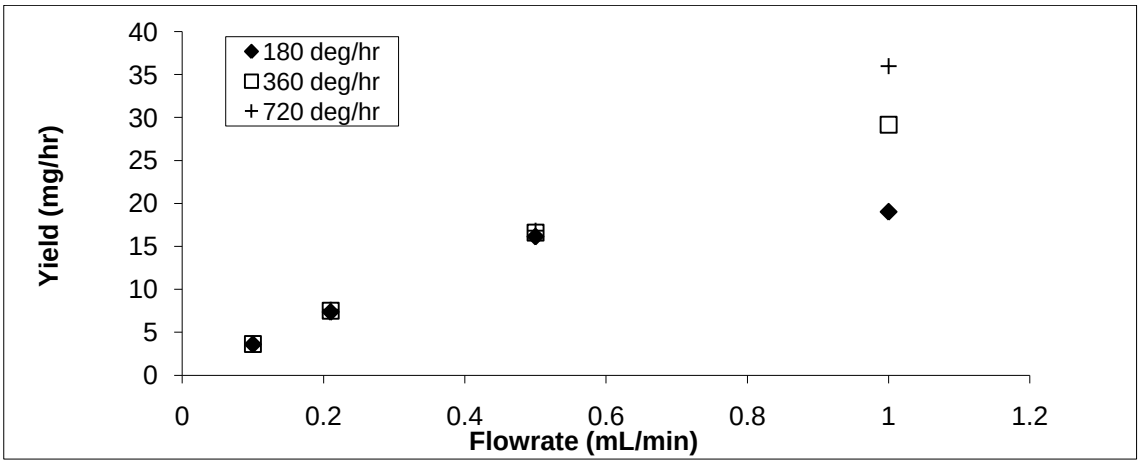

G.4.23 5 mg/mL BSA concentration, 1M NaCl concentration, Trial 5, 180-720 deg/hr rotation speed

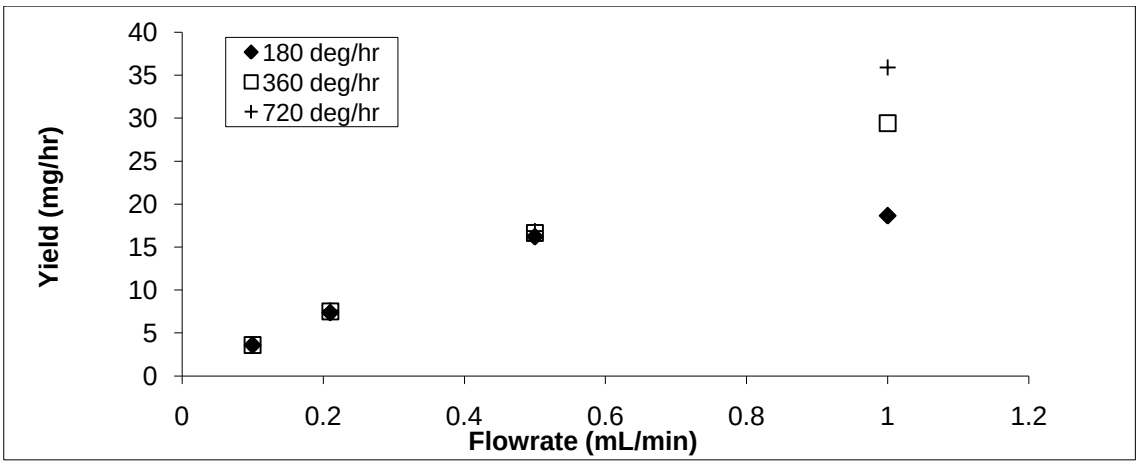

G.4.24 5 mg/mL BSA concentration, 1M NaCl concentration, Trial 6, 180-720 deg/hr rotation speed

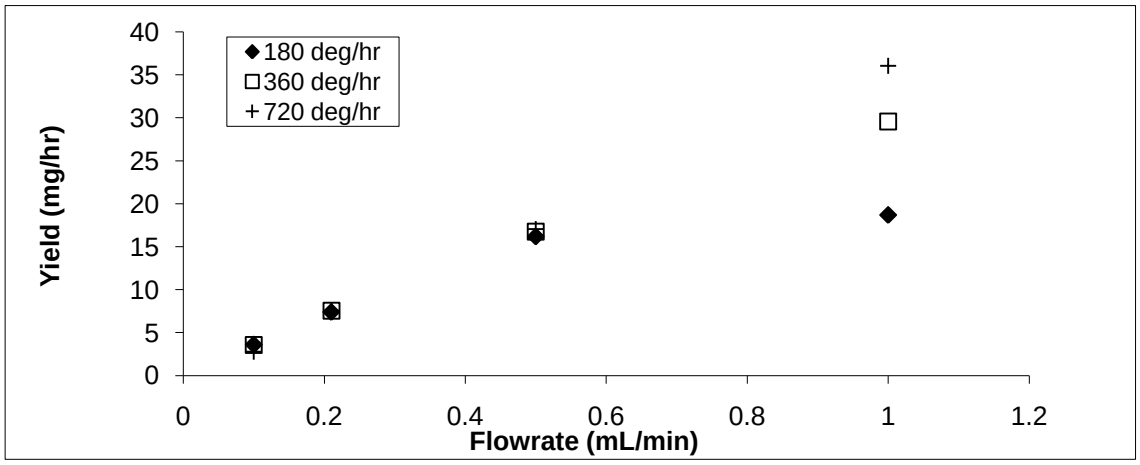

G.4.25 5 mg/mL BSA concentration, 1M NaCl concentration, Trial 7, 180-720 deg/hr rotation speed

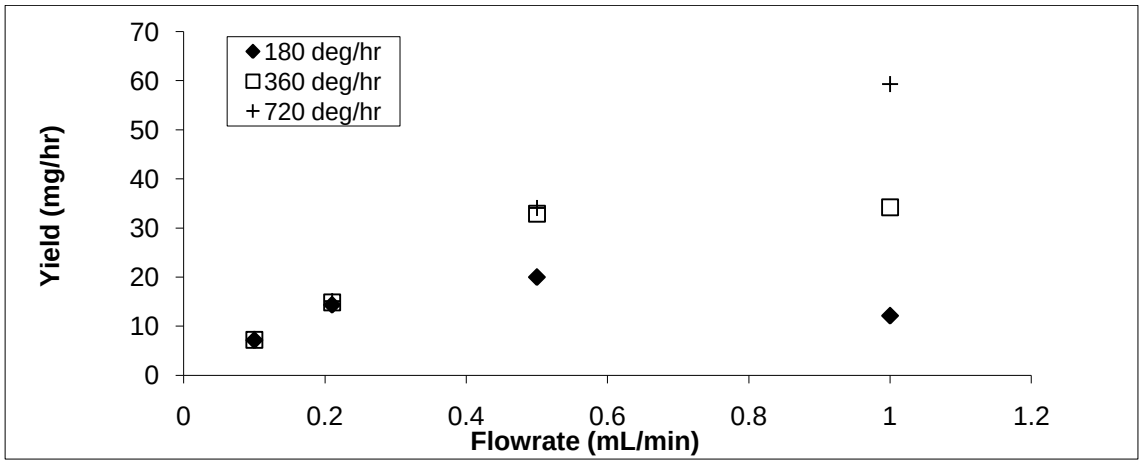

G.4.26 5 mg/mL BSA concentration, 1M NaCl concentration, Trial 8, 180-720 deg/hr rotation speed

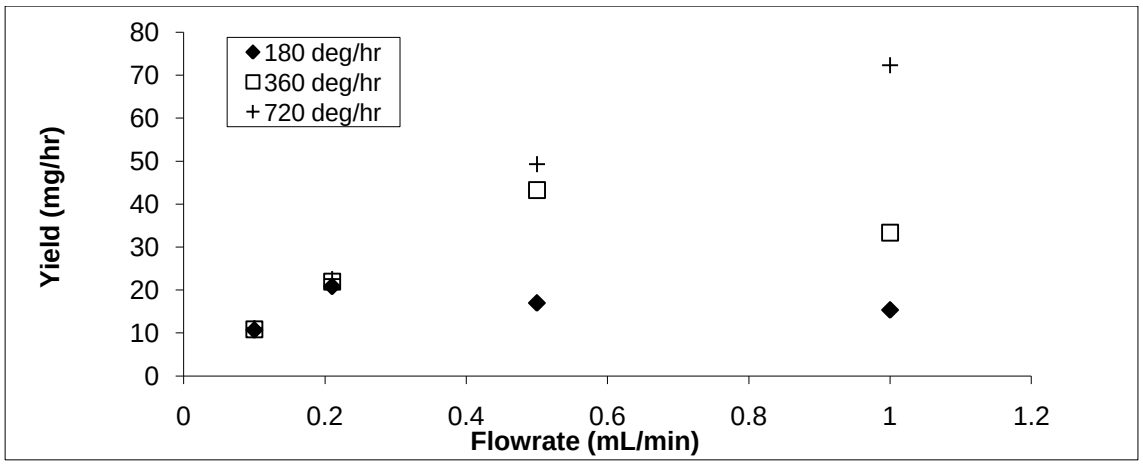

G.4.27 5 mg/mL BSA concentration, 1M NaCl concentration, Trial 9, 180-720 deg/hr rotation speed

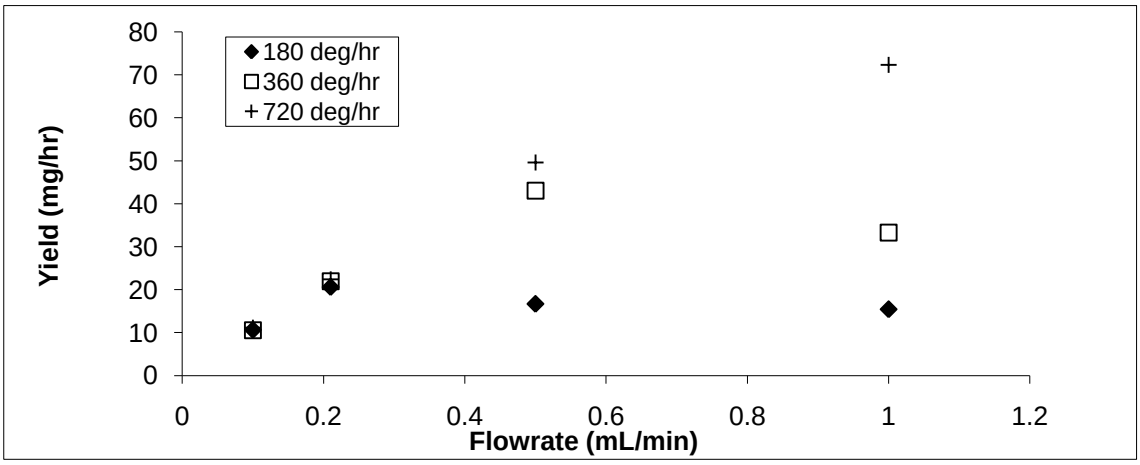

G.4.28 1.5 mg/mL BSA concentration, 2M NaCl concentration, Trial 1, 180-720 deg/hr rotation speed

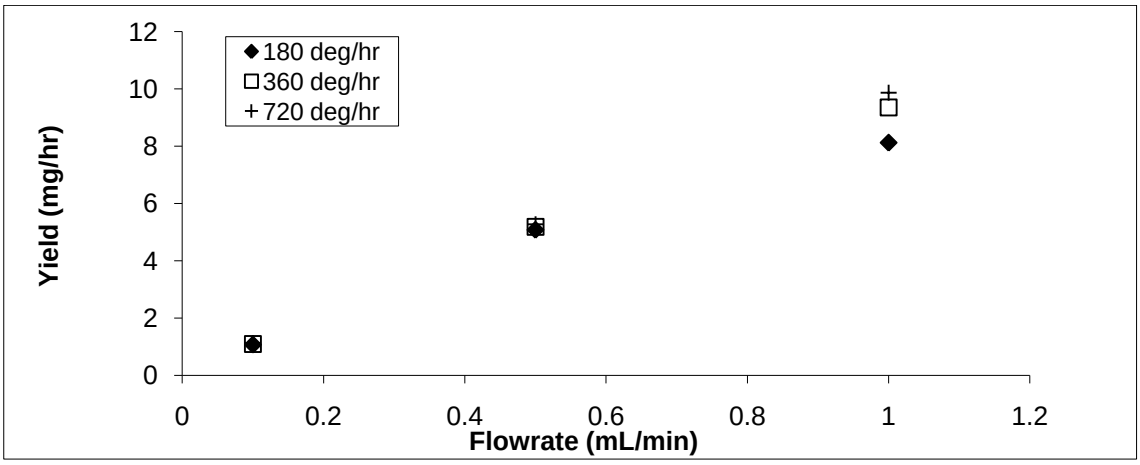

G.4.29 1.5 mg/mL BSA concentration, 2M NaCl concentration, Trial 2, 180-720 deg/hr rotation speed

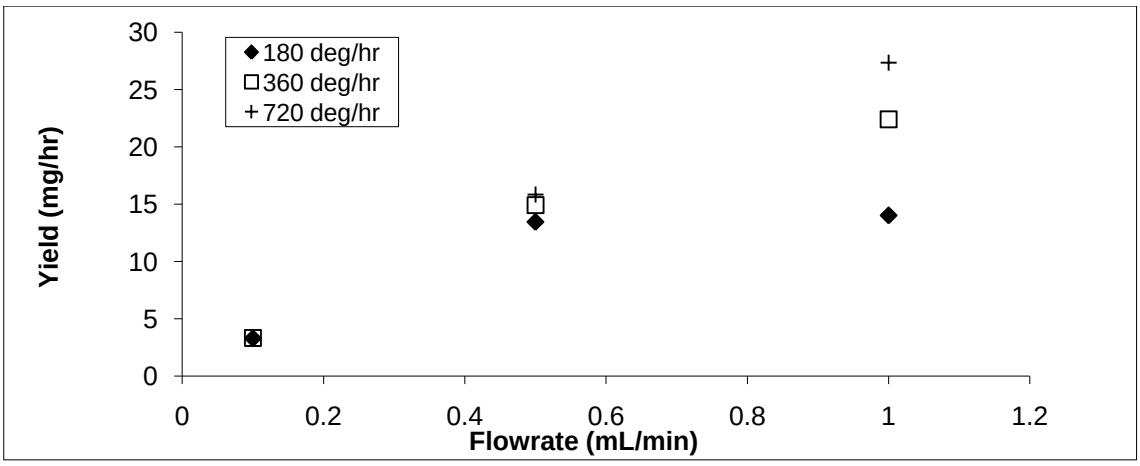

G.4.30 1.5 mg/mL BSA concentration, 2M NaCl concentration, Trial 3, 180-720 deg/hr rotation speed

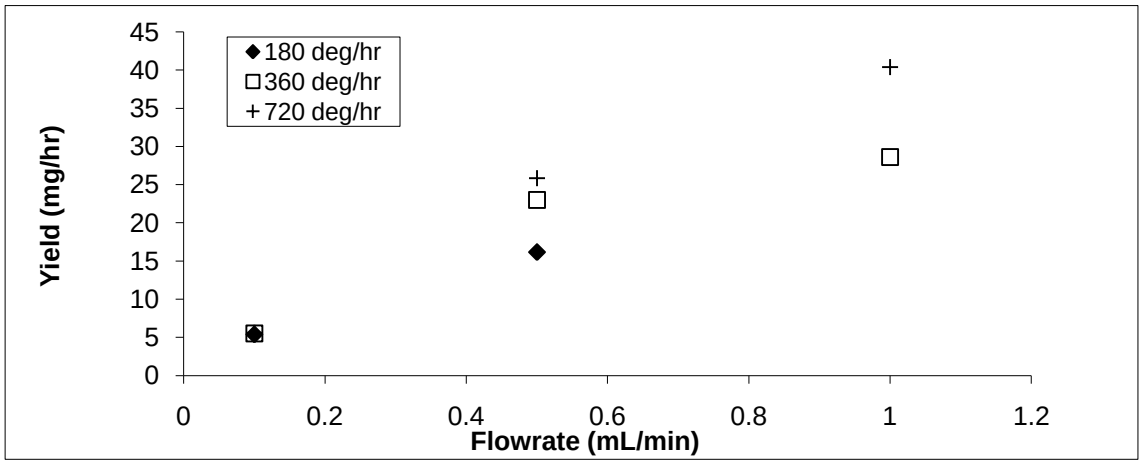

G.4.31 1.5 mg/mL BSA concentration, 2M NaCl concentration, Trial 4, 180-720 deg/hr rotation speed

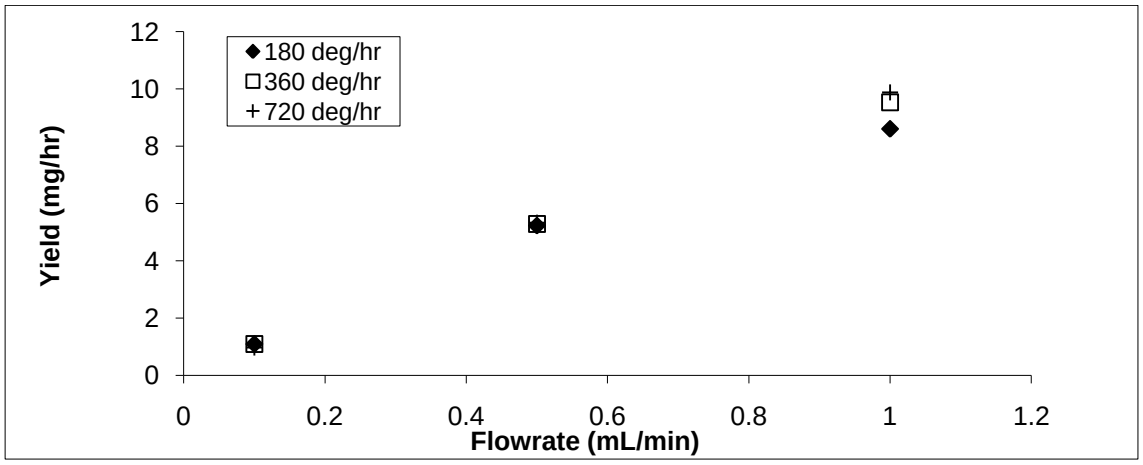

G.4.32 1.5 mg/mL BSA concentration, 2M NaCl concentration, Trial 5, 180-720 deg/hr rotation speed

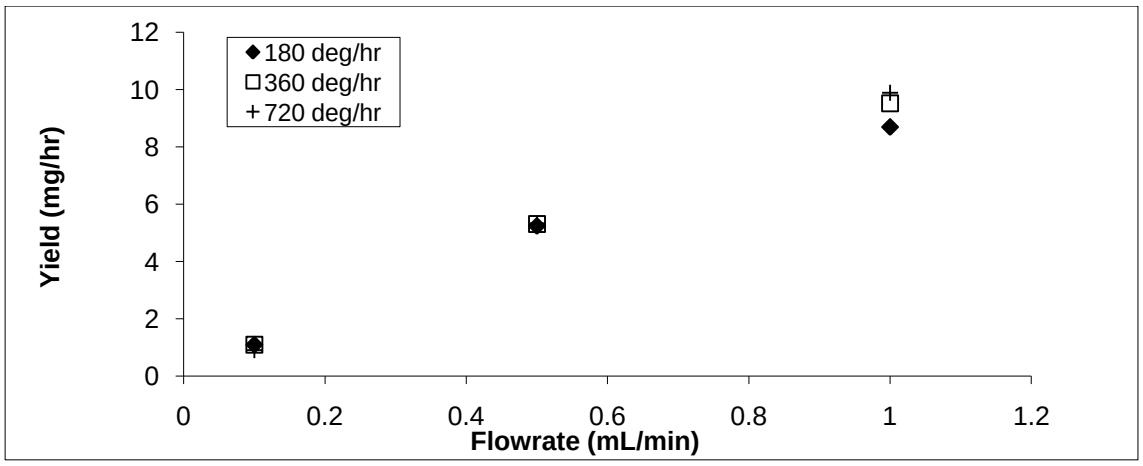

G.4.33 1.5 mg/mL BSA concentration, 2M NaCl concentration, Trial 6, 180-720 deg/hr rotation speed

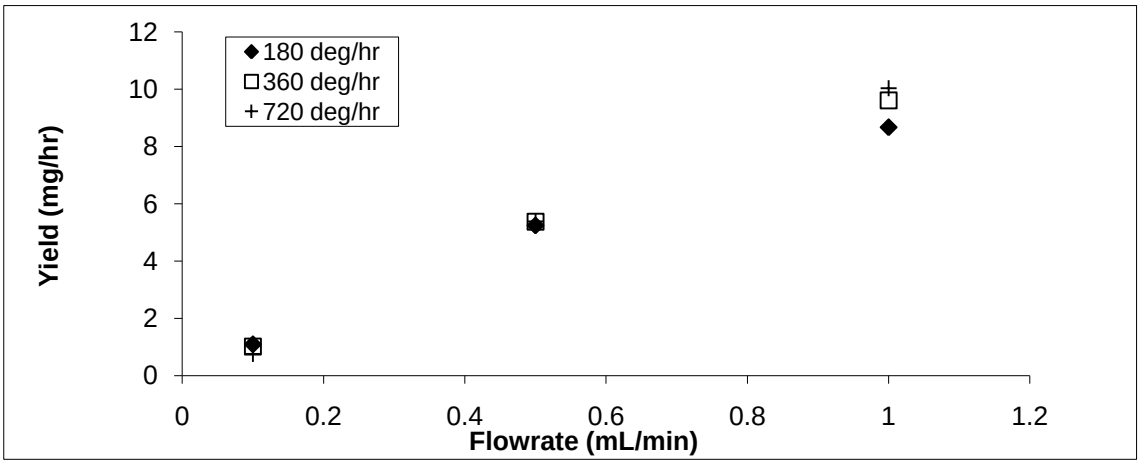

G.4.34 1.5 mg/mL BSA concentration, 2M NaCl concentration, Trial 7, 180-720 deg/hr rotation speed

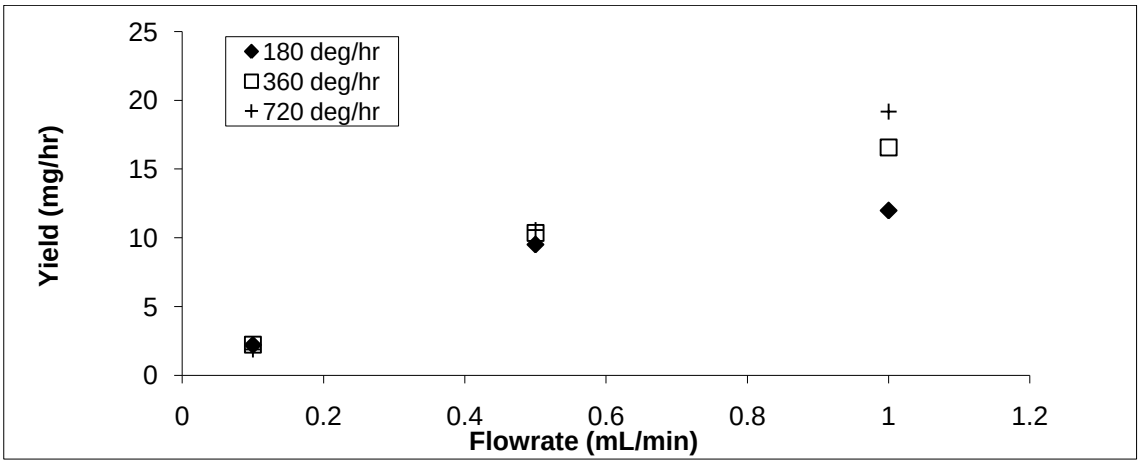

G.4.35 1.5 mg/mL BSA concentration, 2M NaCl concentration, Trial 8, 180-720 deg/hr rotation speed

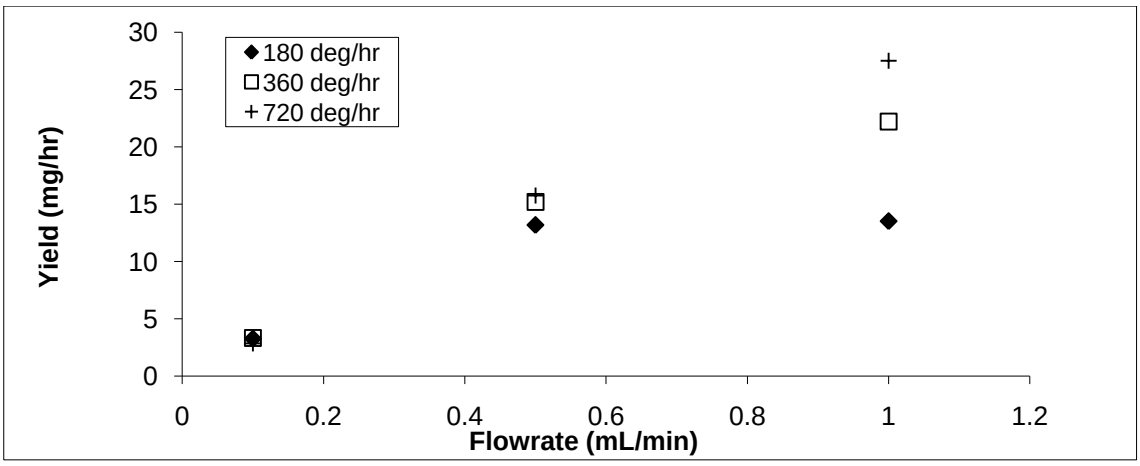

G.4.36 1.5 mg/mL BSA concentration, 2M NaCl concentration, Trial 9, 180-720 deg/hr rotation speed

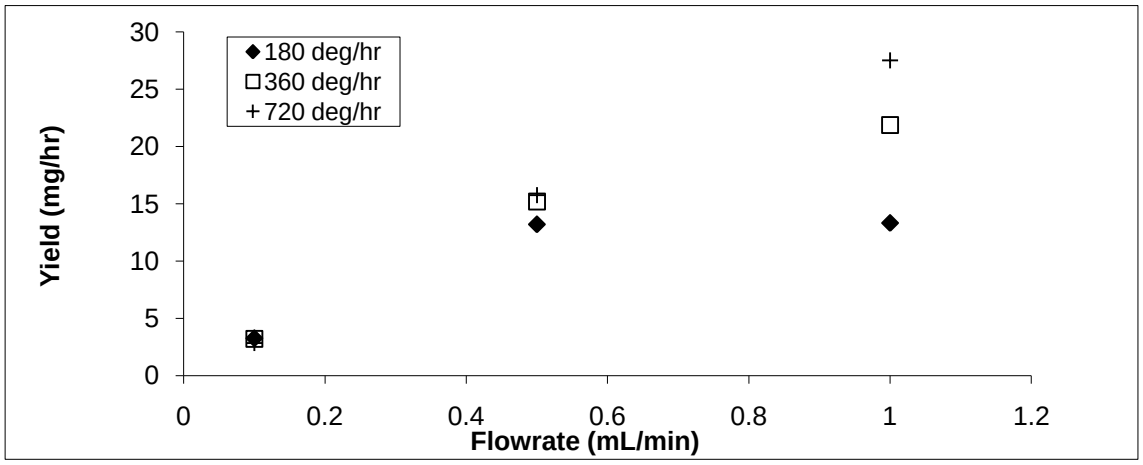

G.5 Feed concentration

G.5.1 180 deg/hr rotation speed, 1M NaCl concentration, Trial 1, 0.1-1.0 mL/min flow rate

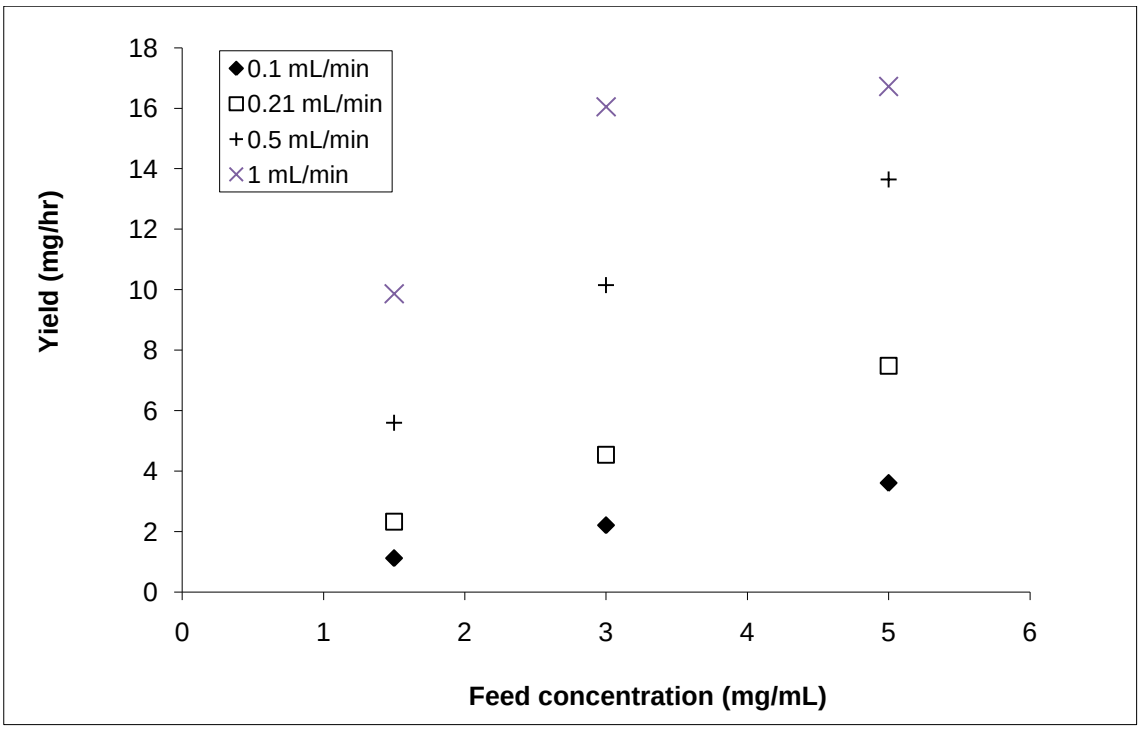

G.5.2 180 deg/hr rotation speed, 1M NaCl concentration, Trial 2, 0.1-1.0 mL/min flow rate

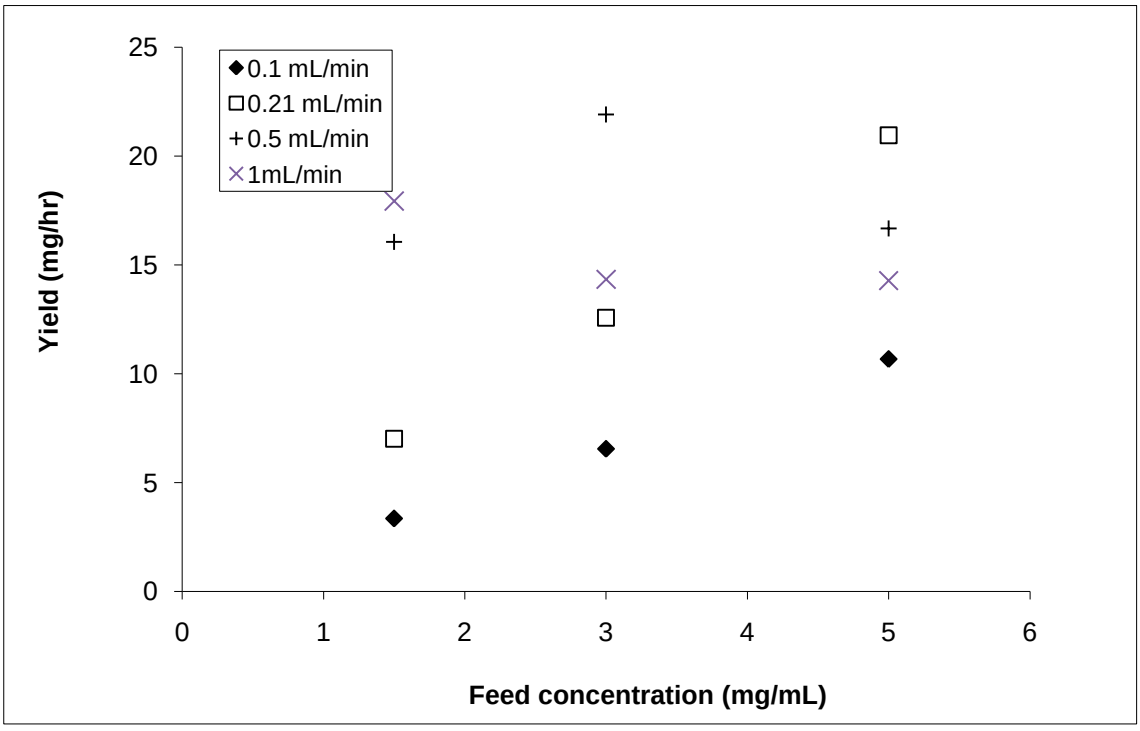

G.5.3 180 deg/hr rotation speed, 1M NaCl concentration, Trial 3, 0.1-0.5 mL/min flow rate

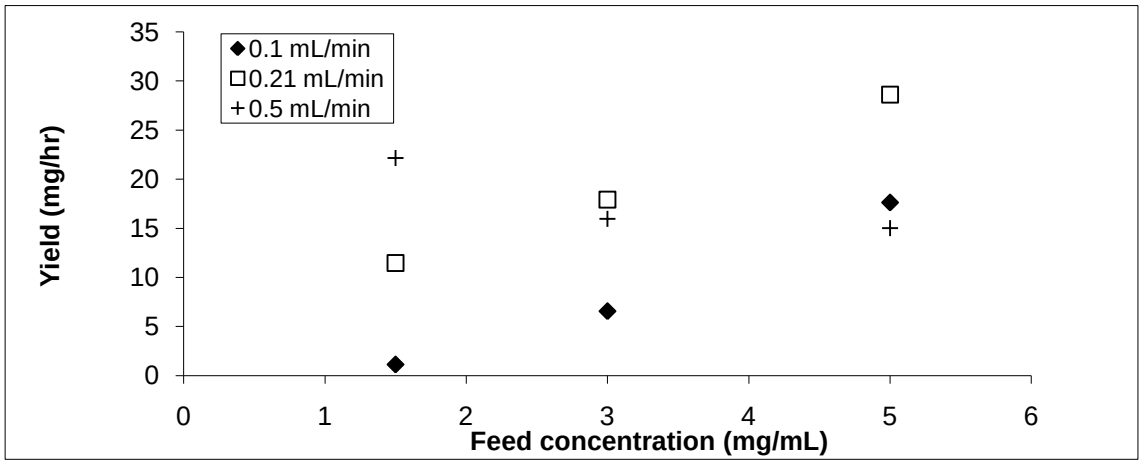

G.5.4 180 deg/hr rotation speed, 1M NaCl concentration, Trial 4, 0.1-1.0 mL/min flow rate

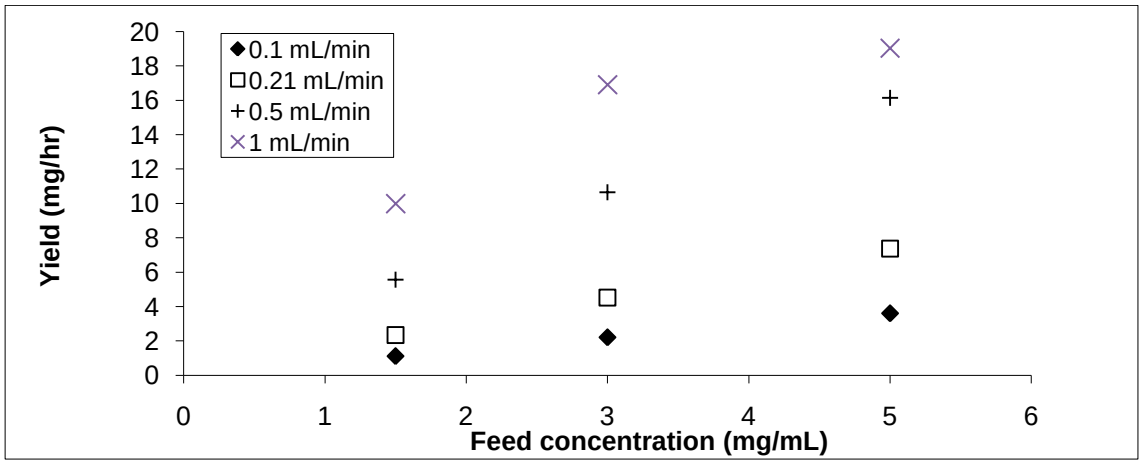

G.5.5 180 deg/hr rotation speed, 1M NaCl concentration, Trial 5, 0.1-1.0 mL/min flow rate

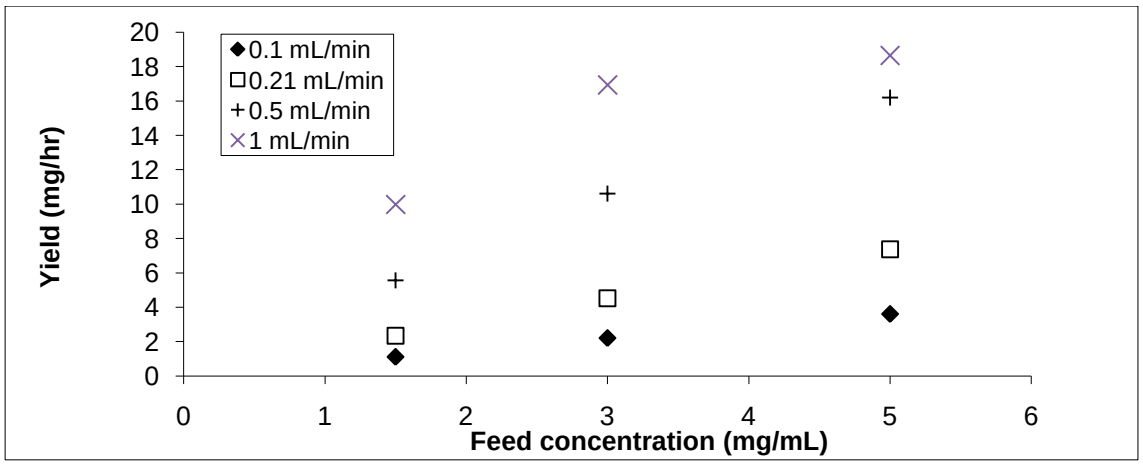

G.5.6 180 deg/hr rotation speed, 1M NaCl concentration, Trial 6, 0.1-1.0 mL/min flow rate

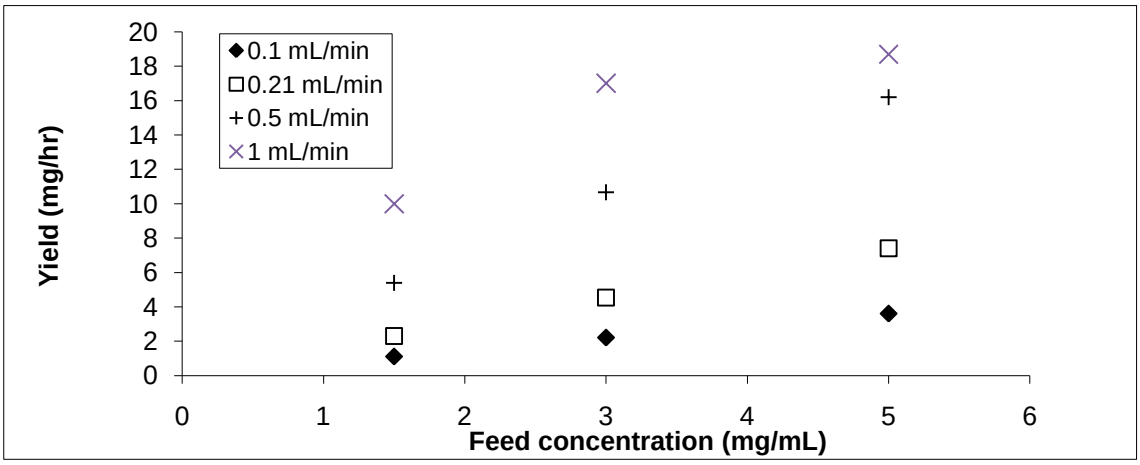

G.5.7 180 deg/hr rotation speed, 1M NaCl concentration, Trial 7, 0.1-1.0 mL/min flow rate

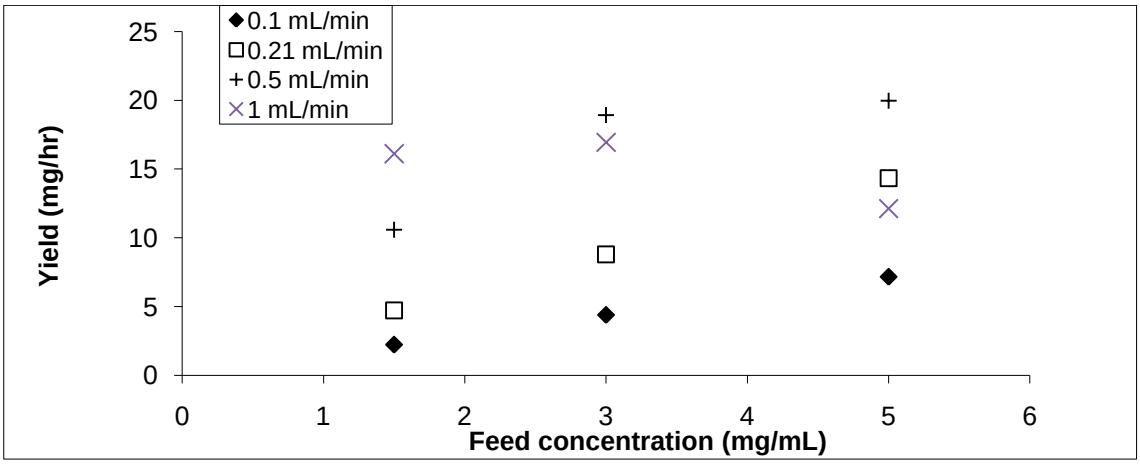

G.5.8 180 deg/hr rotation speed, 1M NaCl concentration, Trial 8, 0.1-1.0 mL/min flow rate

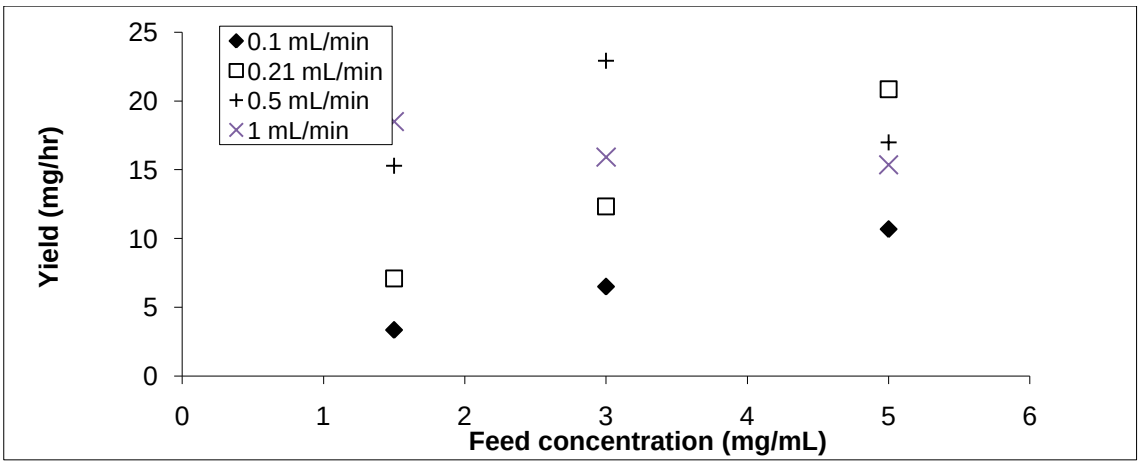

G.5.9 180 deg/hr rotation speed, 1M NaCl concentration, Trial 9, 0.1-1.0 mL/min flow rate

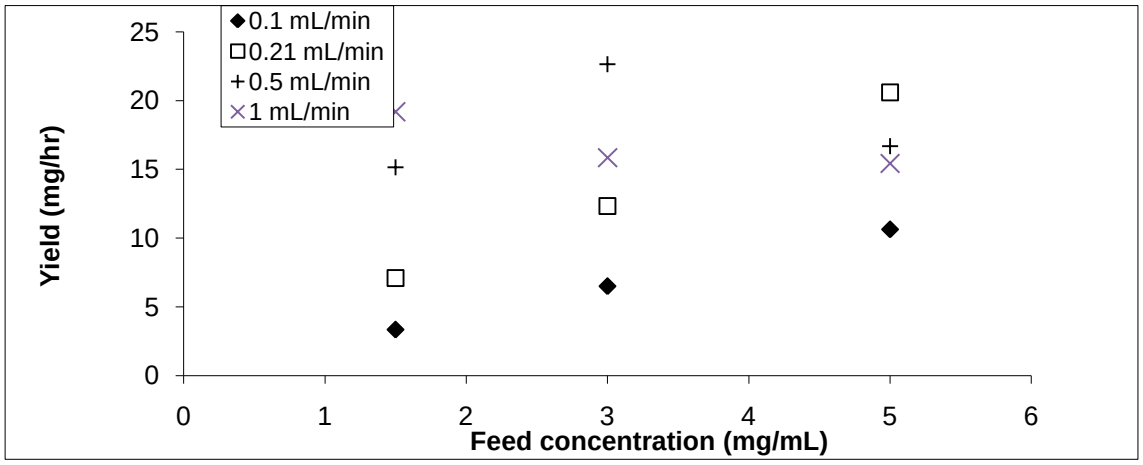

G.5.10 360 deg/hr rotation speed, 1M NaCl concentration, Trial 1, 0.1-1.0 mL/min flow rate

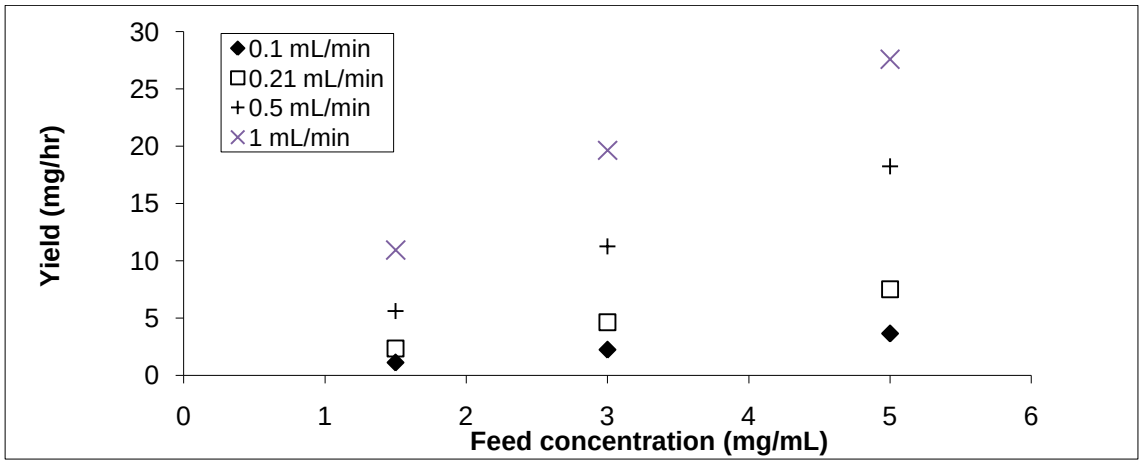

G.5.11 360 deg/hr rotation speed, 1M NaCl concentration, Trial 2, 0.1-1.0 mL/min flow rate

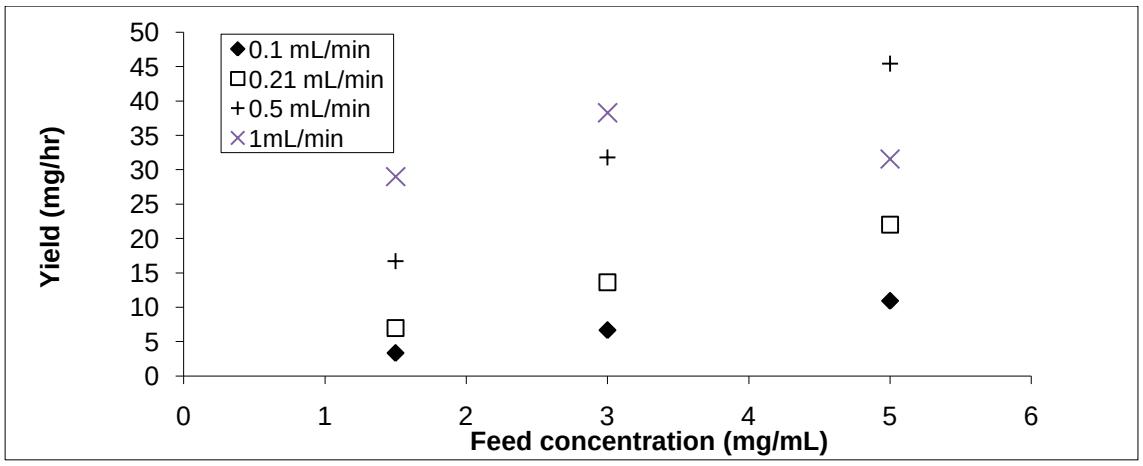

G.5.12 360 deg/hr rotation speed, 1M NaCl concentration, Trial 3, 0.1-1.0 mL/min flow rate

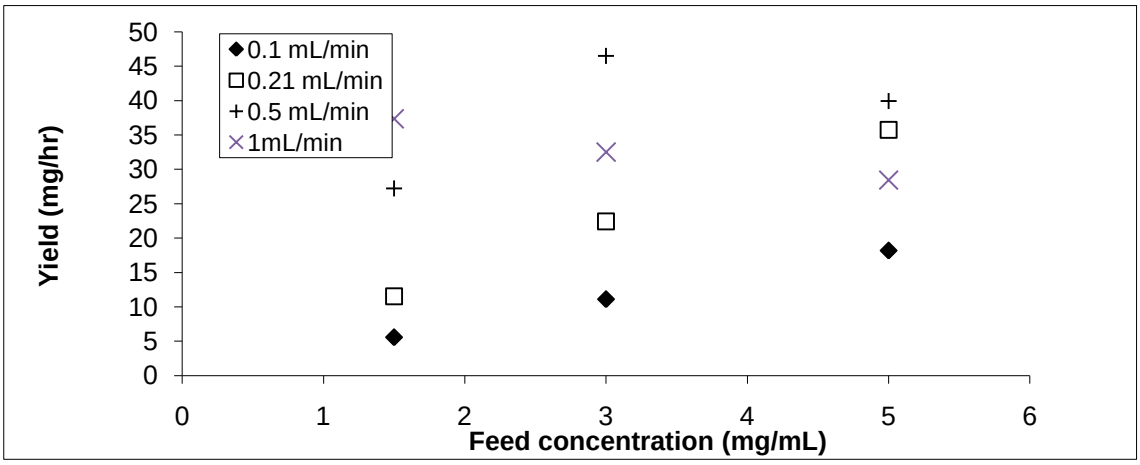

G.5.13 360 deg/hr rotation speed, 1M NaCl concentration, Trial 4, 0.1-1.0 mL/min flow rate

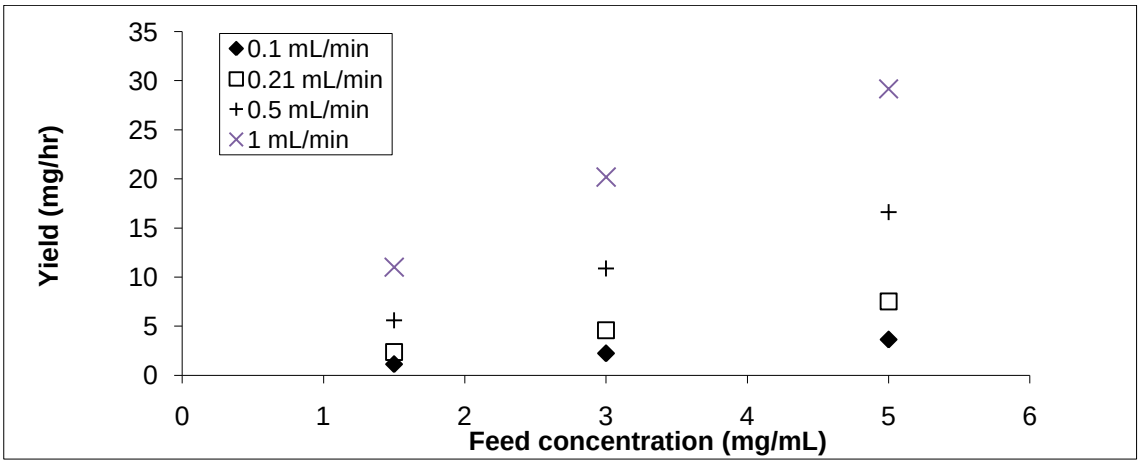

G.5.14 360 deg/hr rotation speed, 1M NaCl concentration, Trial 5, 0.1-1.0 mL/min flow rate

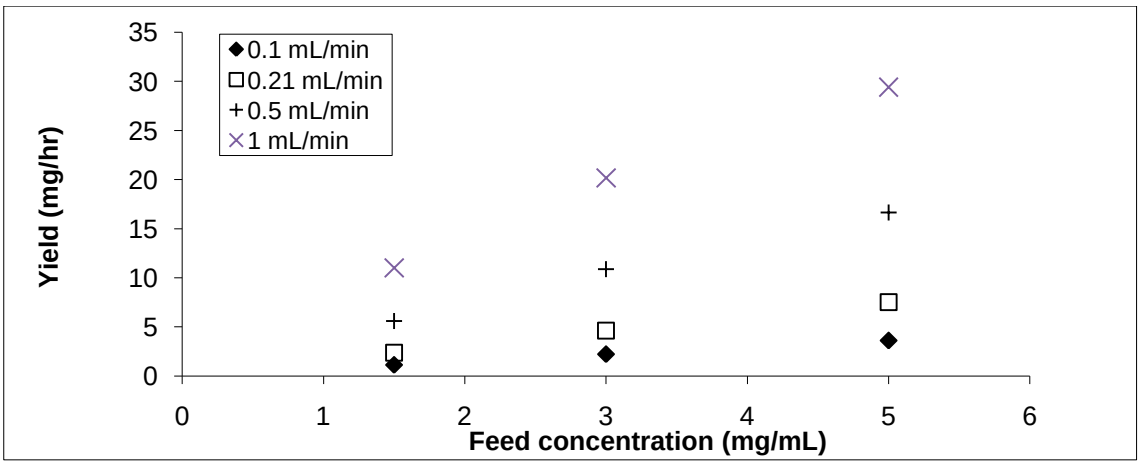

G.5.15 360 deg/hr rotation speed, 1M NaCl concentration, Trial 6, 0.1-1.0 mL/min flow rate

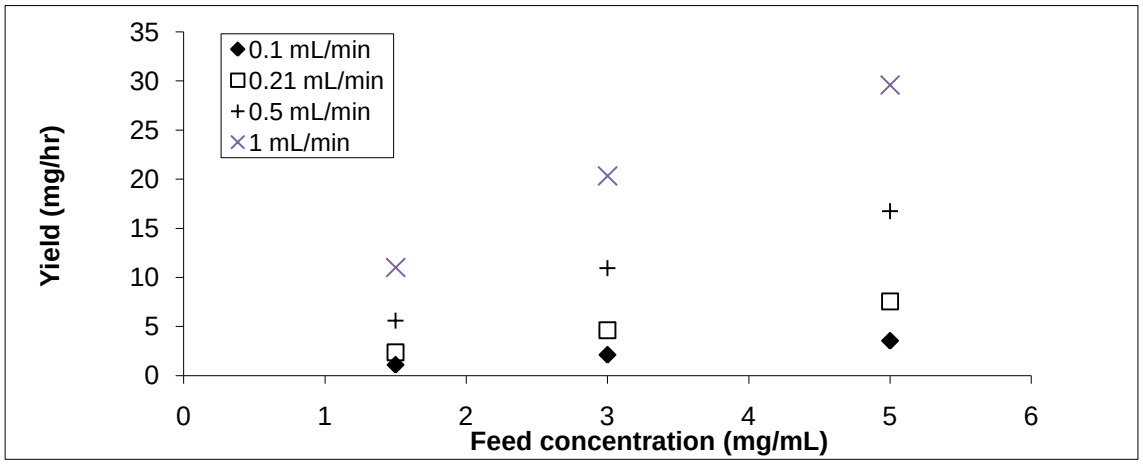

G.5.16 360 deg/hr rotation speed, 1M NaCl concentration, Trial 7, 0.1-1.0 mL/min flow rate

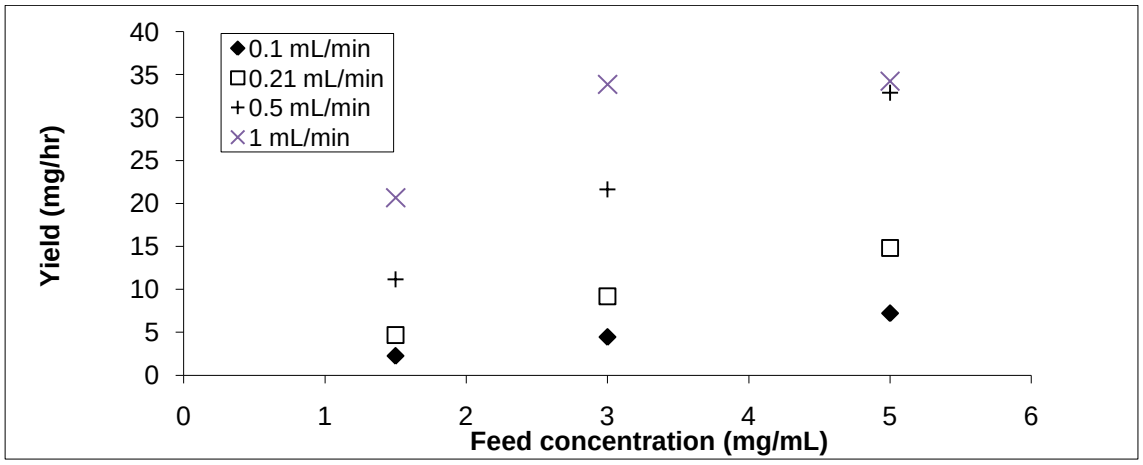

G.5.17 360 deg/hr rotation speed, 1M NaCl concentration, Trial 8, 0.1-1.0 mL/min flow rate

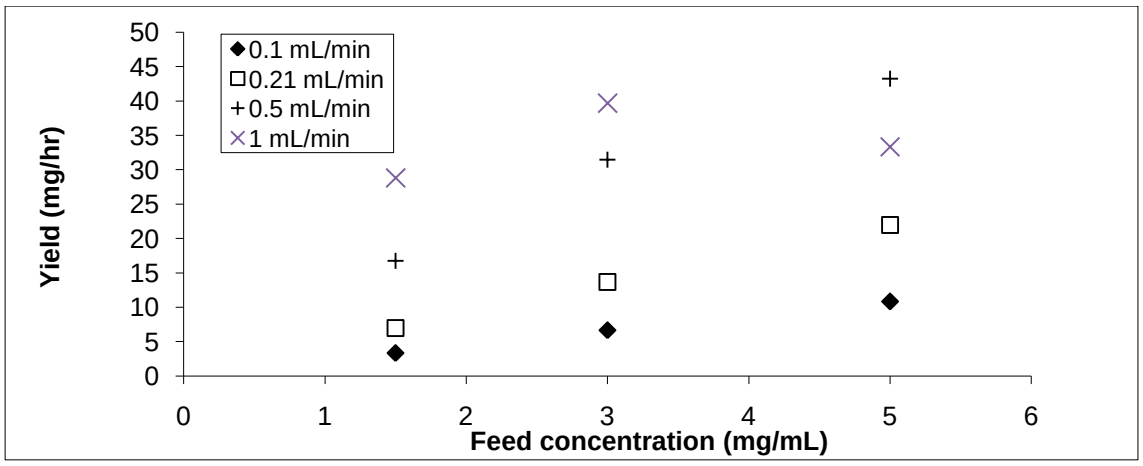

G.5.18 360 deg/hr rotation speed, 1M NaCl concentration, Trial 9, 0.1-1.0 mL/min flow rate

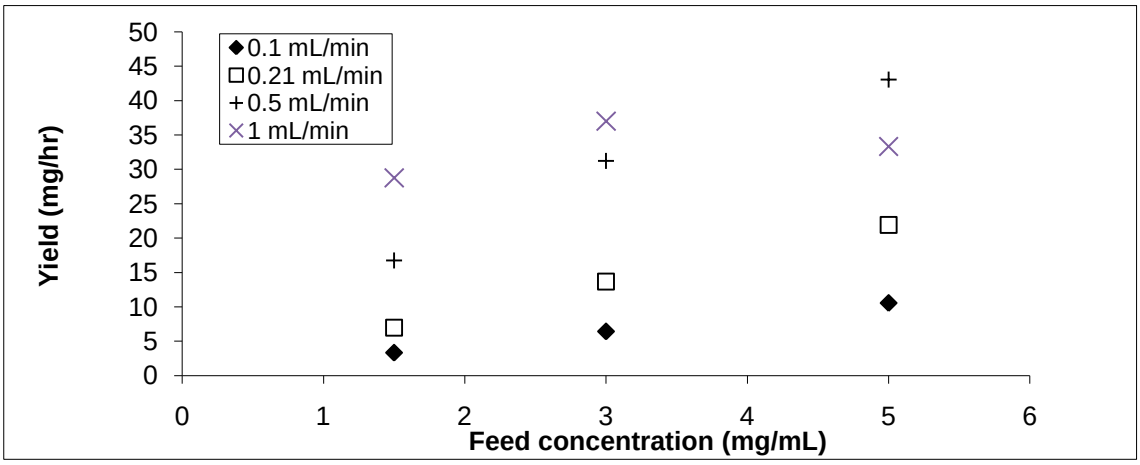

G.5.19 720 deg/hr rotation speed, 1M NaCl concentration, Trial 1, 0.1-1.0 mL/min flow rate

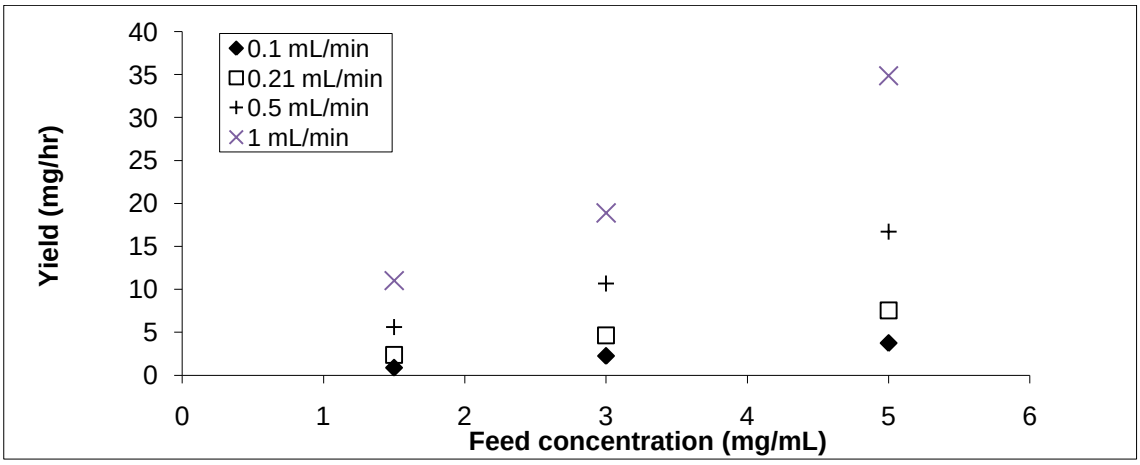

G.5.20 720 deg/hr rotation speed, 1M NaCl concentration, Trial 2, 0.1-1.0 mL/min flow rate

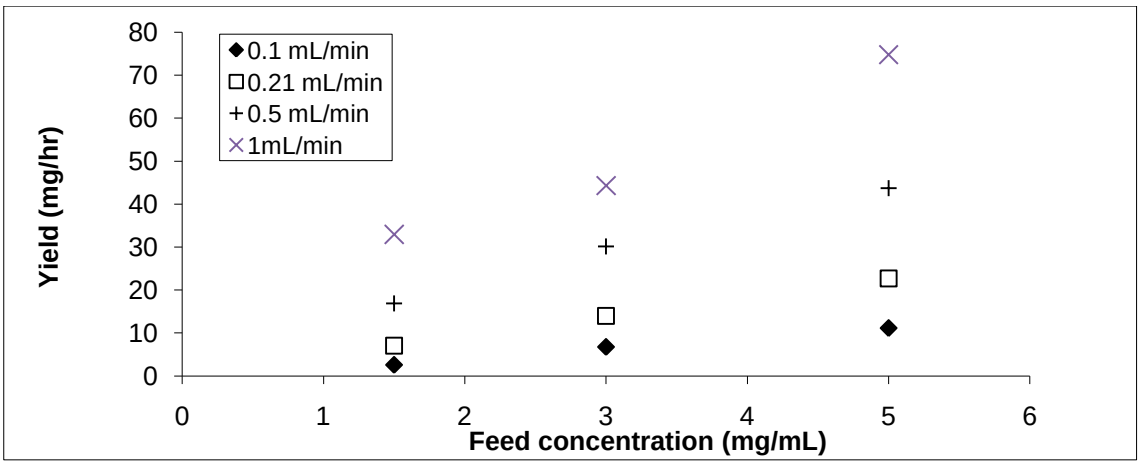

G.5.21 720 deg/hr rotation speed, 1M NaCl concentration, Trial 3, 0.1-1.0 mL/min flow rate

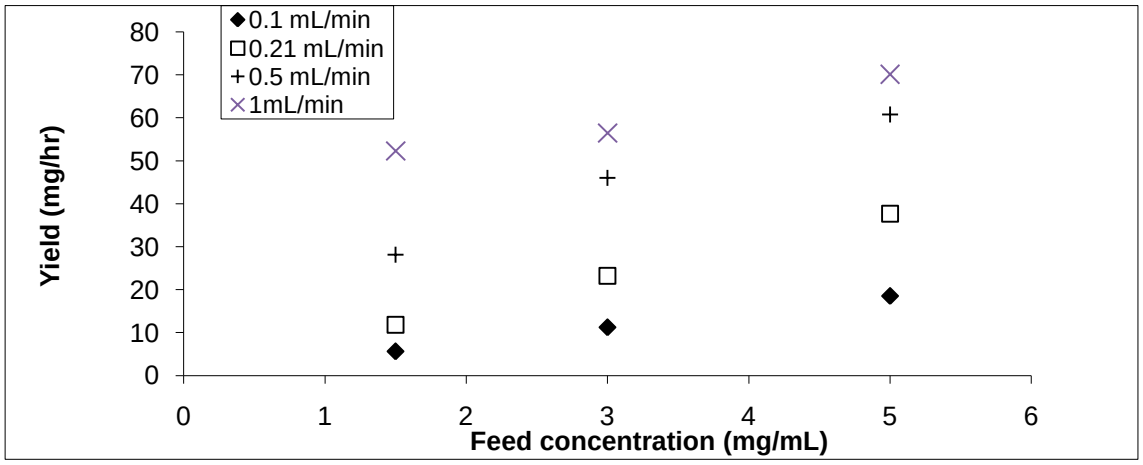

G.5.22 720 deg/hr rotation speed, 1M NaCl concentration, Trial 4, 0.1-1.0 mL/min flow rate

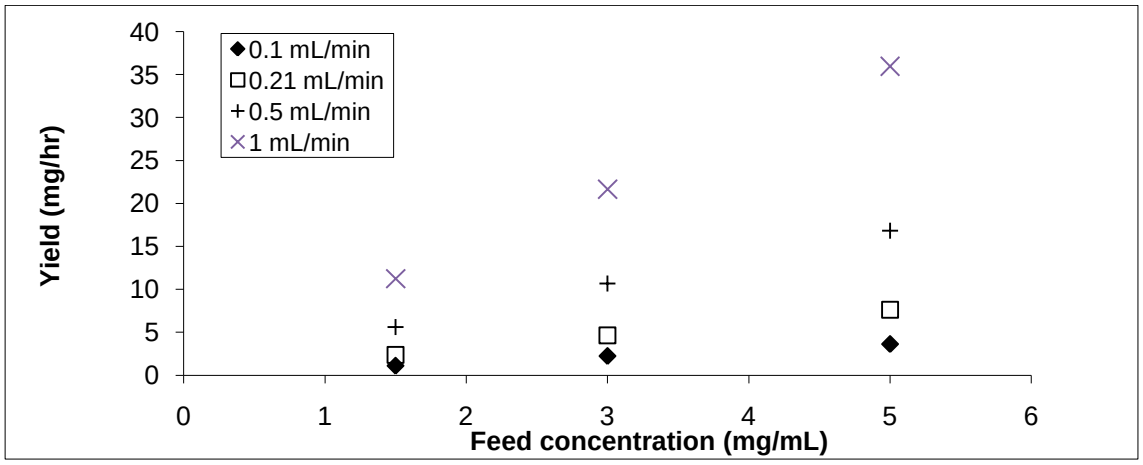

G.5.23 720 deg/hr rotation speed, 1M NaCl concentration, Trial 5, 0.1-1.0 mL/min flow rate

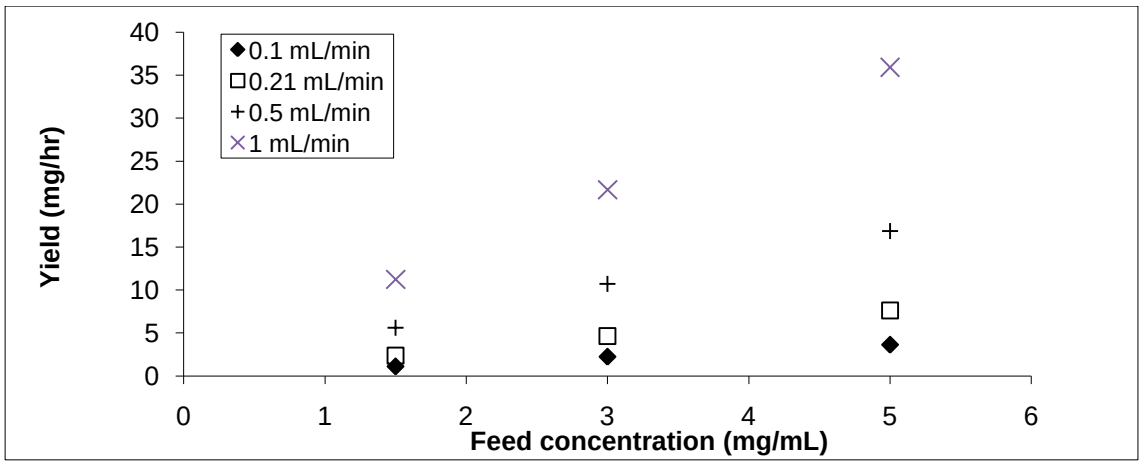

G.5.24 720 deg/hr rotation speed, 1M NaCl concentration, Trial 6, 0.1-1.0 mL/min flow rate

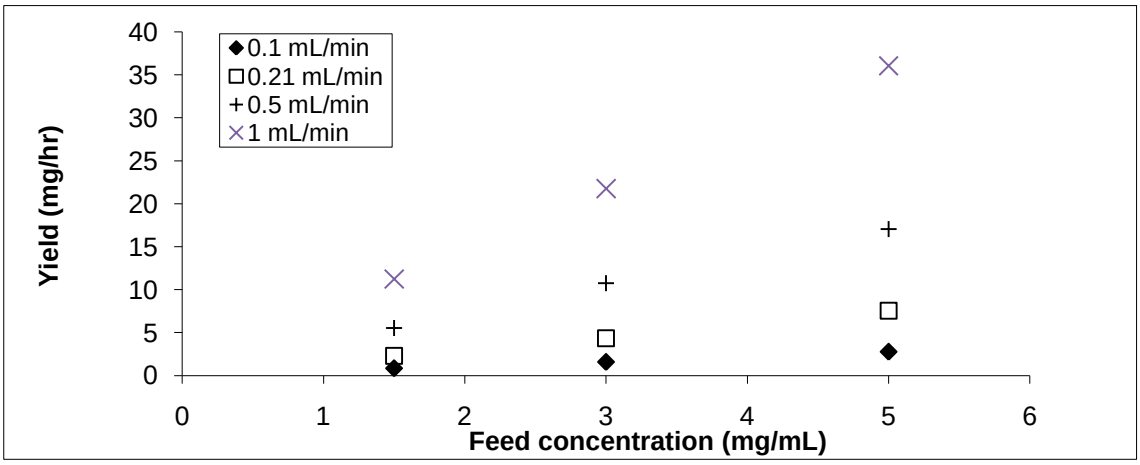

G.5.25 720 deg/hr rotation speed, 1M NaCl concentration, Trial 7, 0.1-1.0 mL/min flow rate

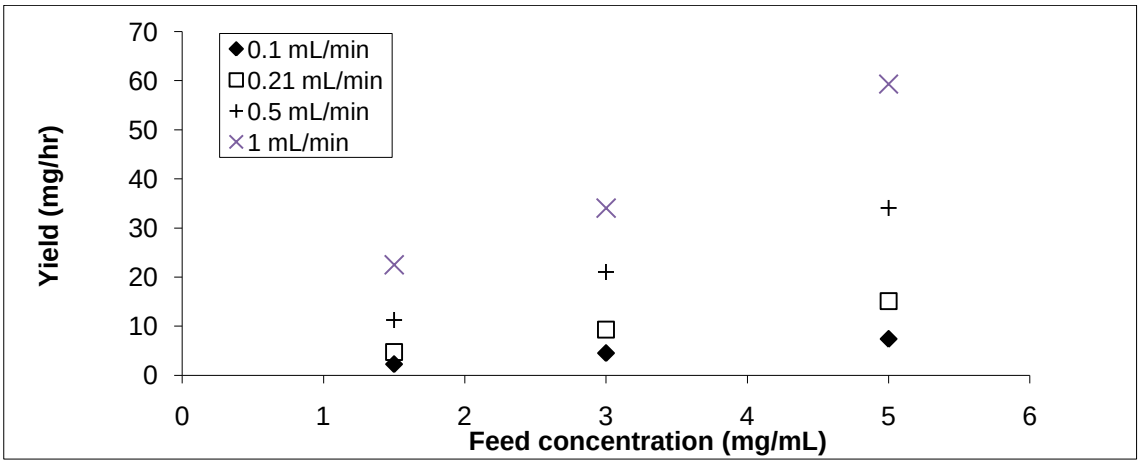

G.5.26 720 deg/hr rotation speed, 1M NaCl concentration, Trial 8, 0.1-1.0 mL/min flow rate

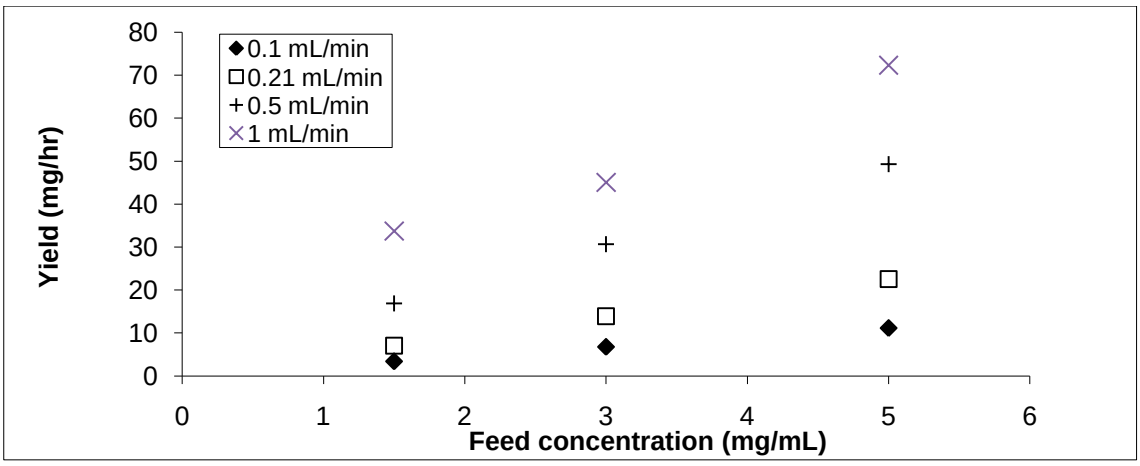

G.5.27 720 deg/hr rotation speed, 1M NaCl concentration, Trial 9, 0.1-1.0 mL/min flow rate

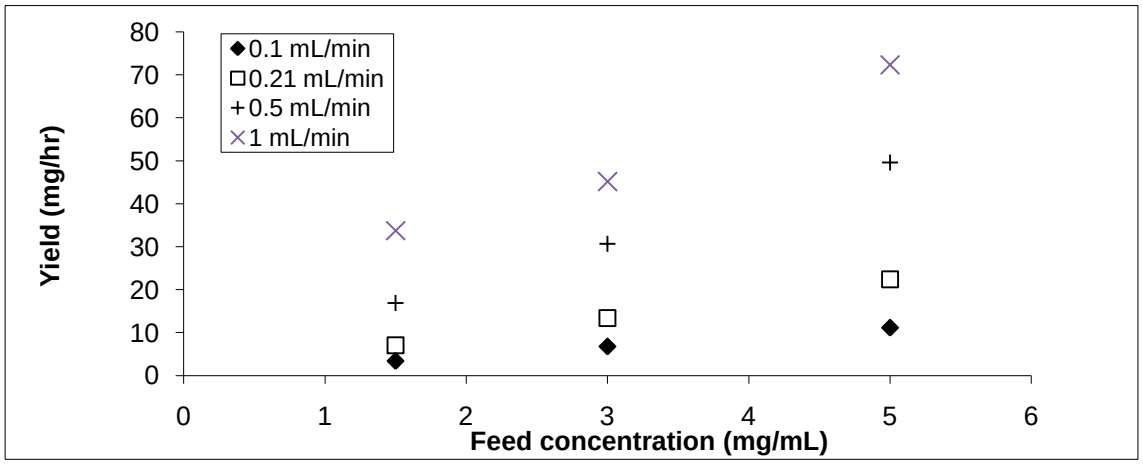

G.6 Elution buffer concentration

G.6.1 180 deg/hr rotation speed, 1.5 mg/mL BSA concentration, Trial 1, 0.1-1.0 mL/min flow rate

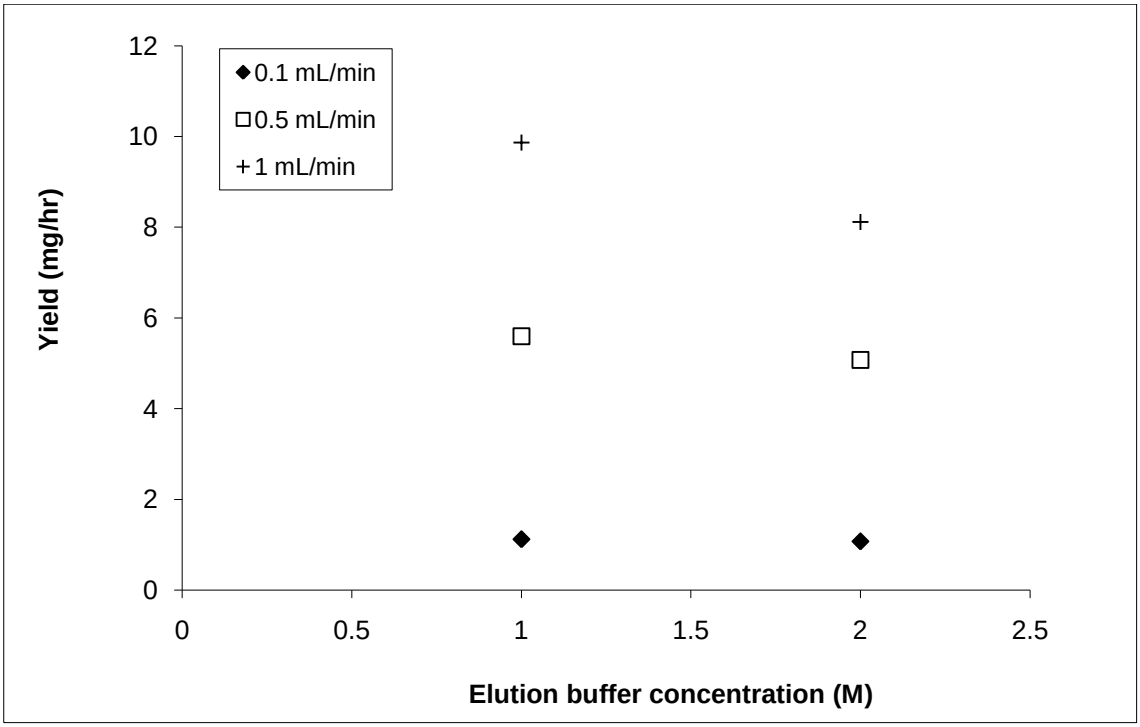

G.6.2 180 deg/hr rotation speed, 1.5 mg/mL BSA concentration, Trial 2, 0.1-1.0 mL/min flow rate

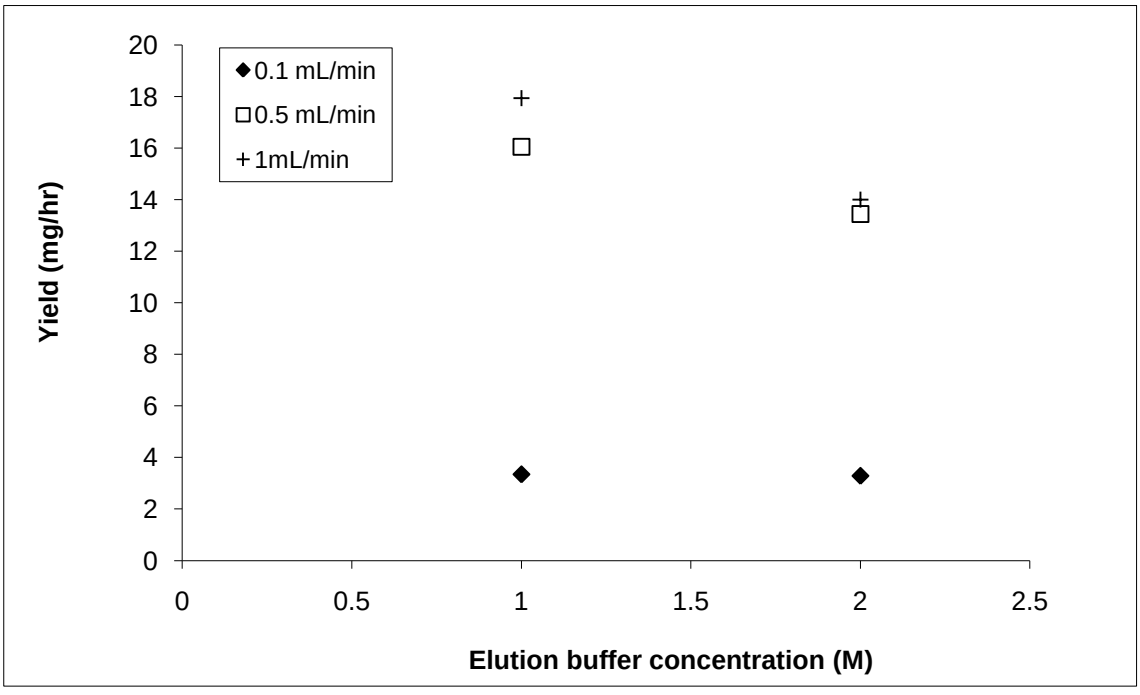

G.6.3 180 deg/hr rotation speed, 1.5 mg/mL BSA concentration, Trial 3, 0.1-0.5 mL/min flow rate

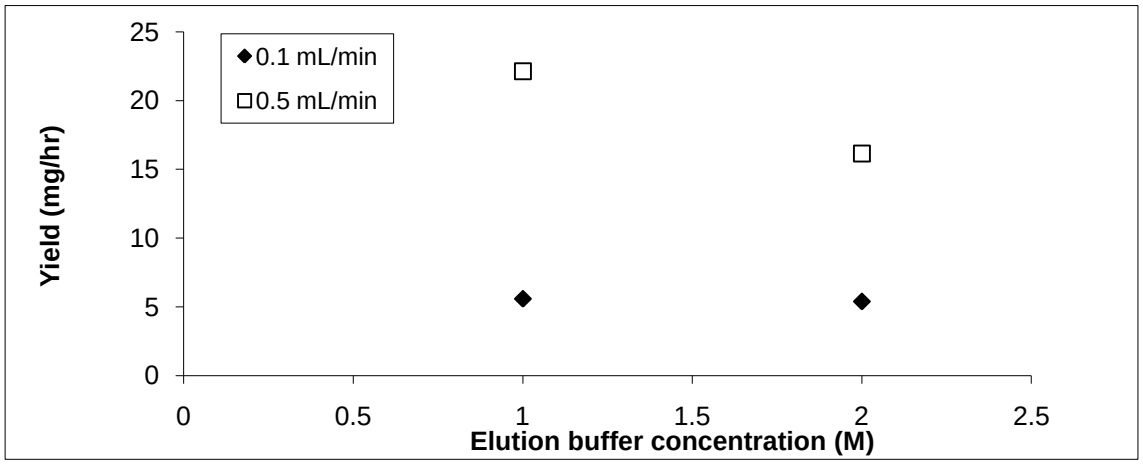

G.6.4 180 deg/hr rotation speed, 1.5 mg/mL BSA concentration, Trial 4, 0.1-1.0 mL/min flow rate

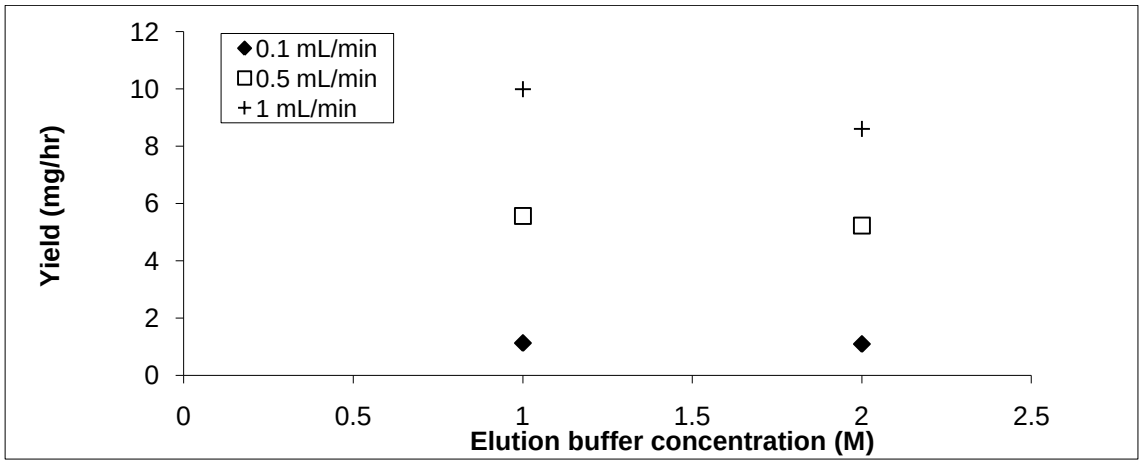

G.6.5 180 deg/hr rotation speed, 1.5 mg/mL BSA concentration, Trial 5, 0.1-1.0 mL/min flow rate

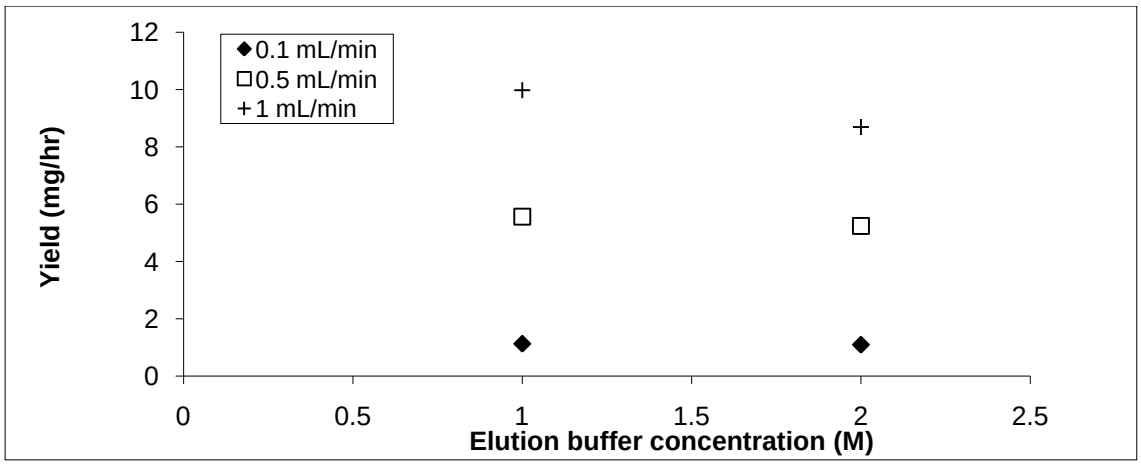

G.6.6 180 deg/hr rotation speed, 1.5 mg/mL BSA concentration, Trial 6, 0.1-1.0 mL/min flow rate

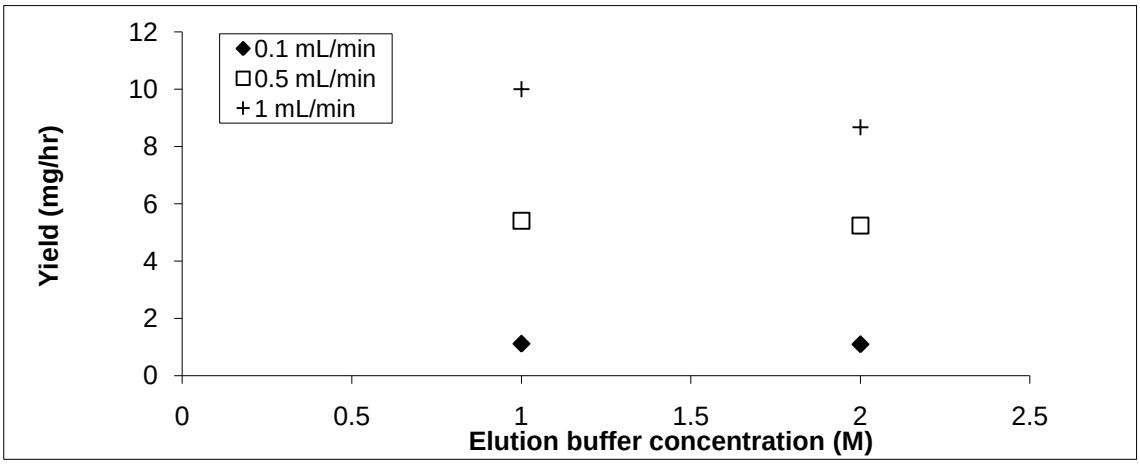

G.6.7 180 deg/hr rotation speed, 1.5 mg/mL BSA concentration, Trial 7, 0.1-1.0 mL/min flow rate

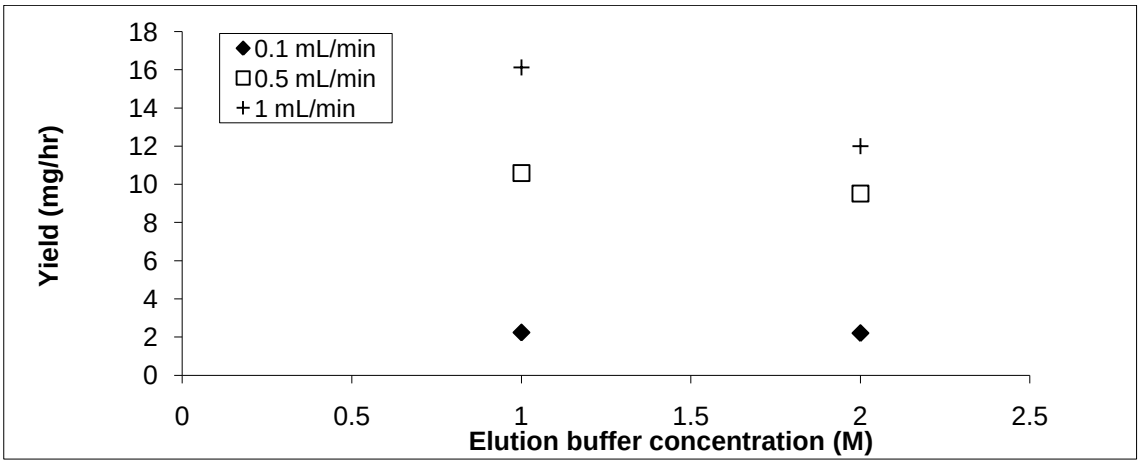

G.6.8 180 deg/hr rotation speed, 1.5 mg/mL BSA concentration, Trial 8, 0.1-1.0 mL/min flow rate

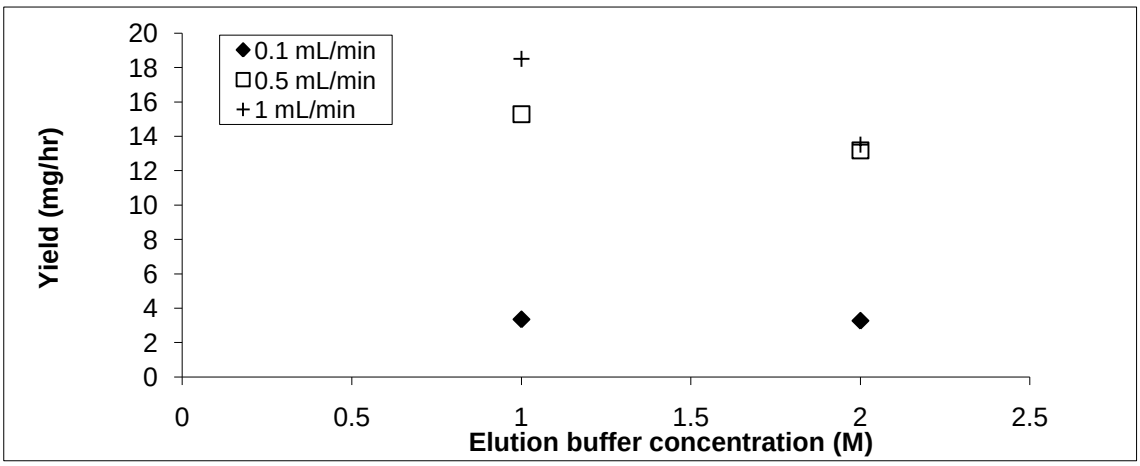

G.6.9 180 deg/hr rotation speed, 1.5 mg/mL BSA concentration, Trial 9, 0.1-1.0 mL/min flow rate

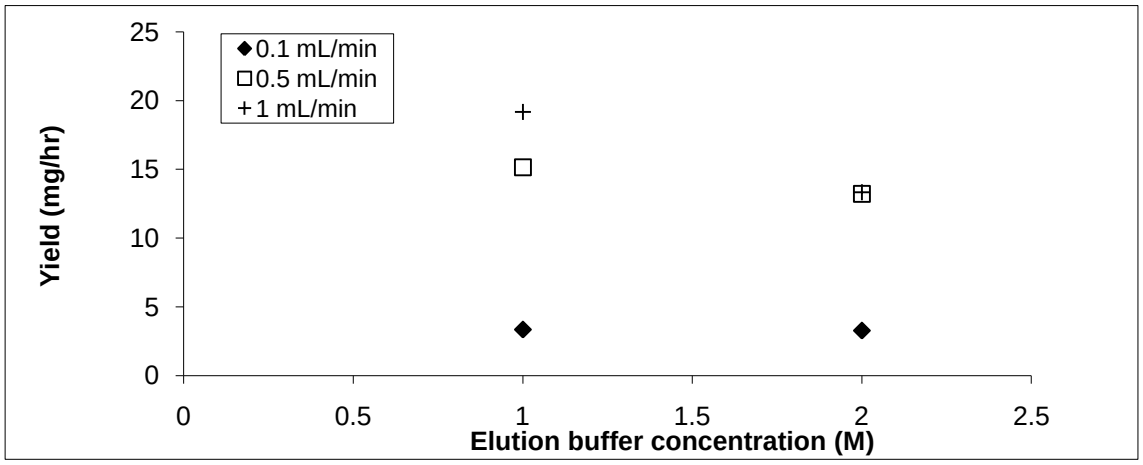

G.6.10 360 deg/hr rotation speed, 1.5 mg/mL BSA concentration, Trial 1, 0.1-1.0 mL/min flow rate

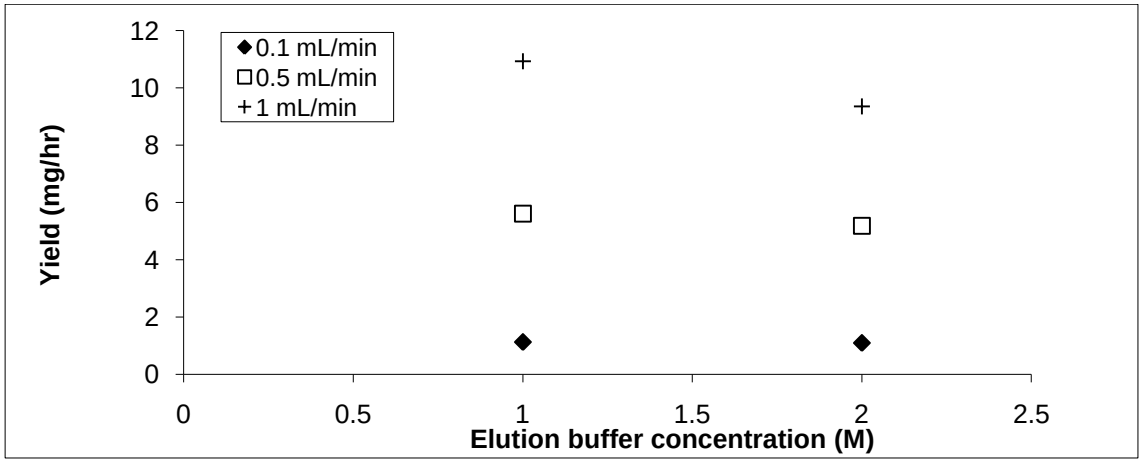

G.6.11 360 deg/hr rotation speed, 1.5 mg/mL BSA concentration, Trial 2, 0.1-1.0 mL/min flow rate

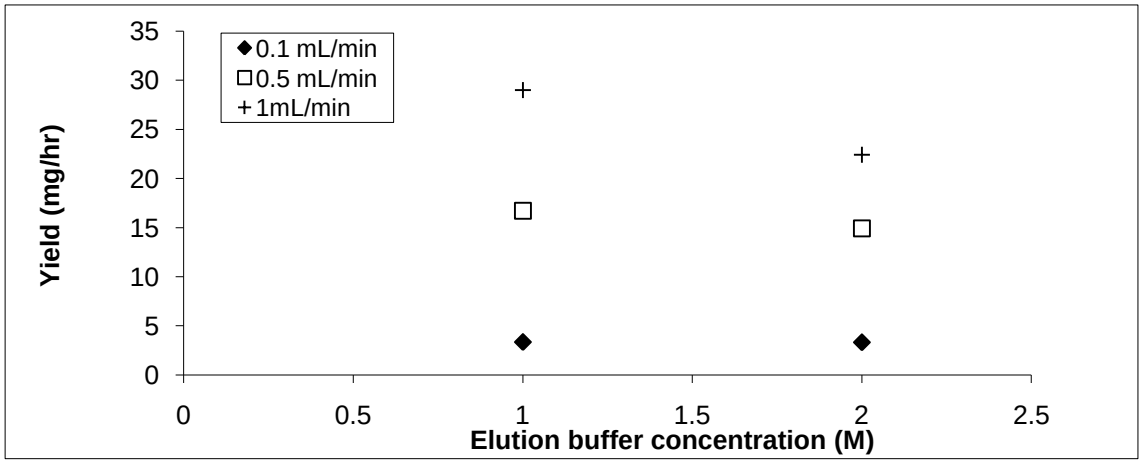

G.6.12 360 deg/hr rotation speed, 1.5 mg/mL BSA concentration, Trial 3, 0.1-1.0 mL/min flow rate

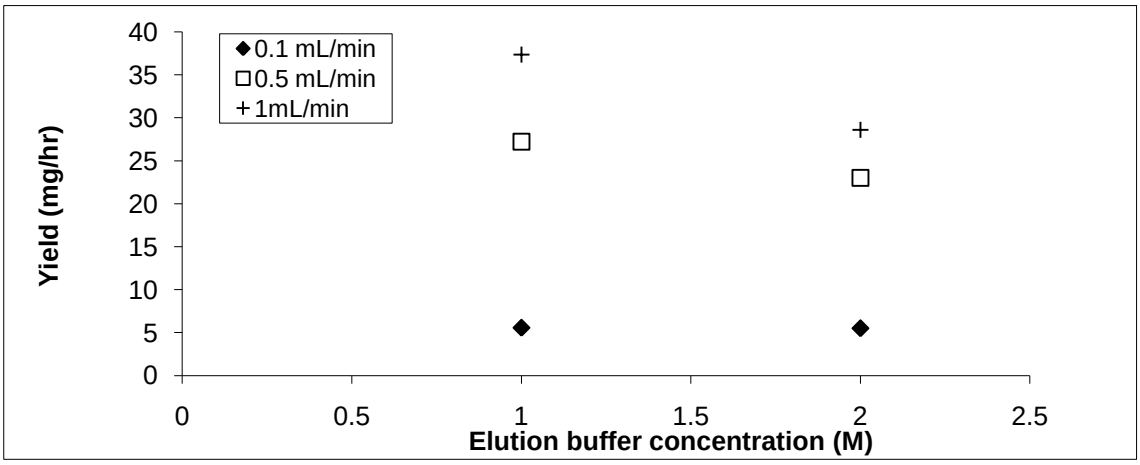

G.6.13 360 deg/hr rotation speed, 1.5 mg/mL BSA concentration, Trial 4, 0.1-1.0 mL/min flow rate

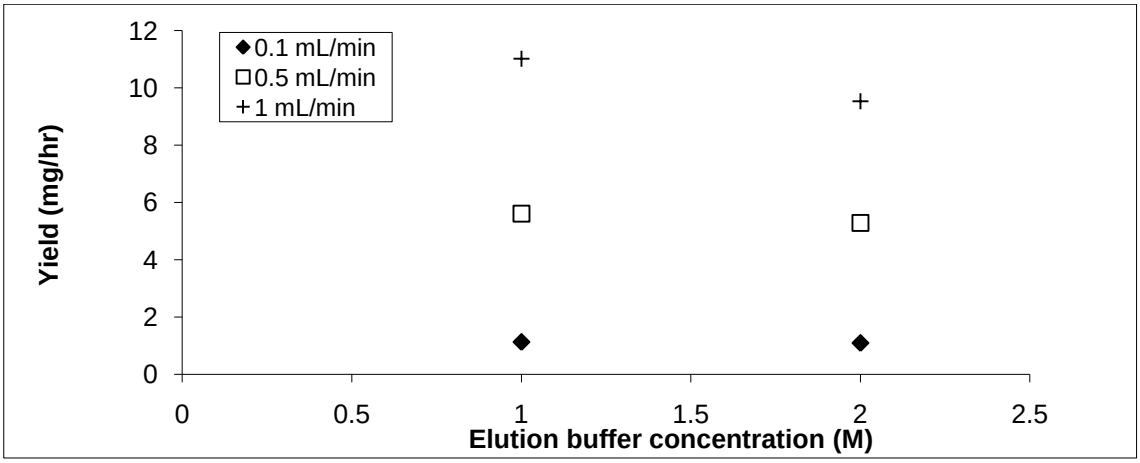

G.6.14 360 deg/hr rotation speed, 1.5 mg/mL BSA concentration, Trial 5, 0.1-1.0 mL/min flow rate

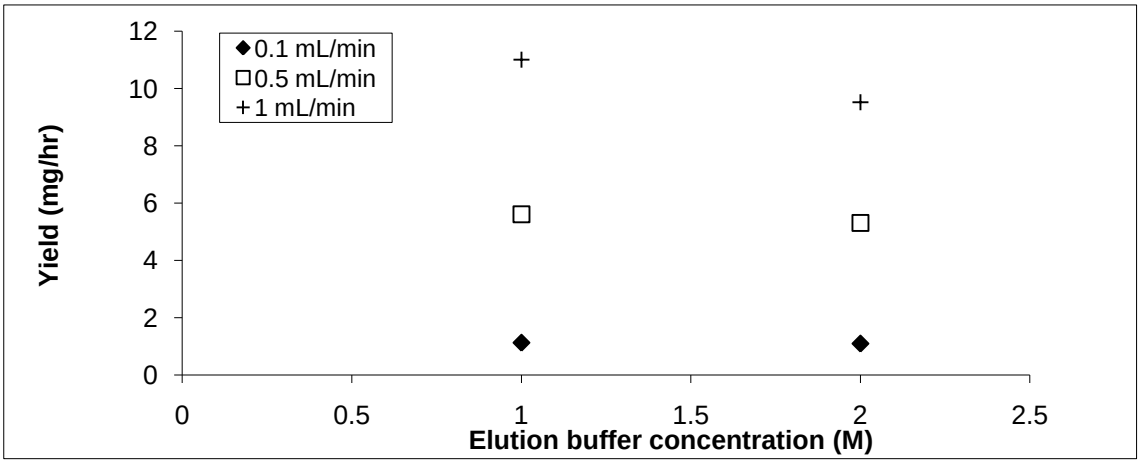

G.6.15 360 deg/hr rotation speed, 1.5 mg/mL BSA concentration, Trial 6, 0.1-1.0 mL/min flow rate

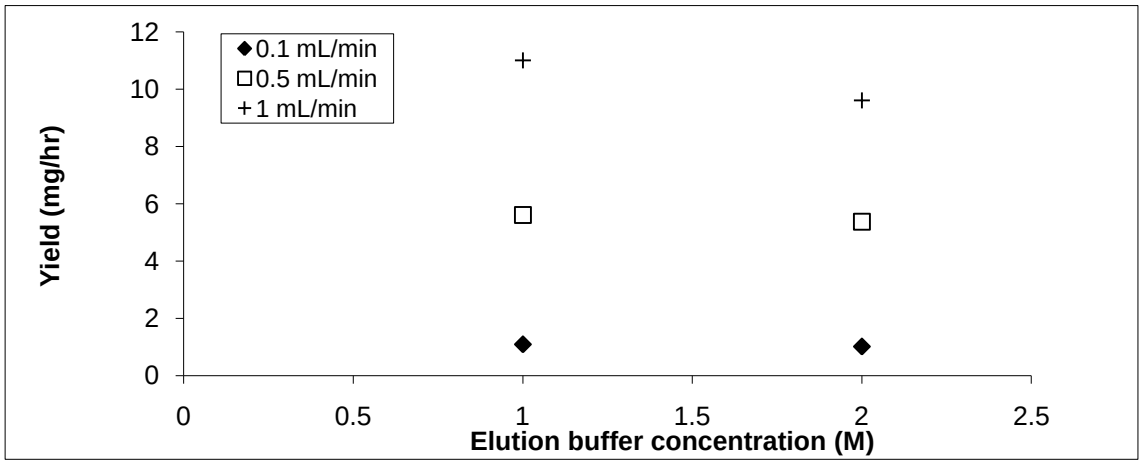

G.6.16 360 deg/hr rotation speed, 1.5 mg/mL BSA concentration, Trial 7, 0.1-1.0 mL/min flow rate

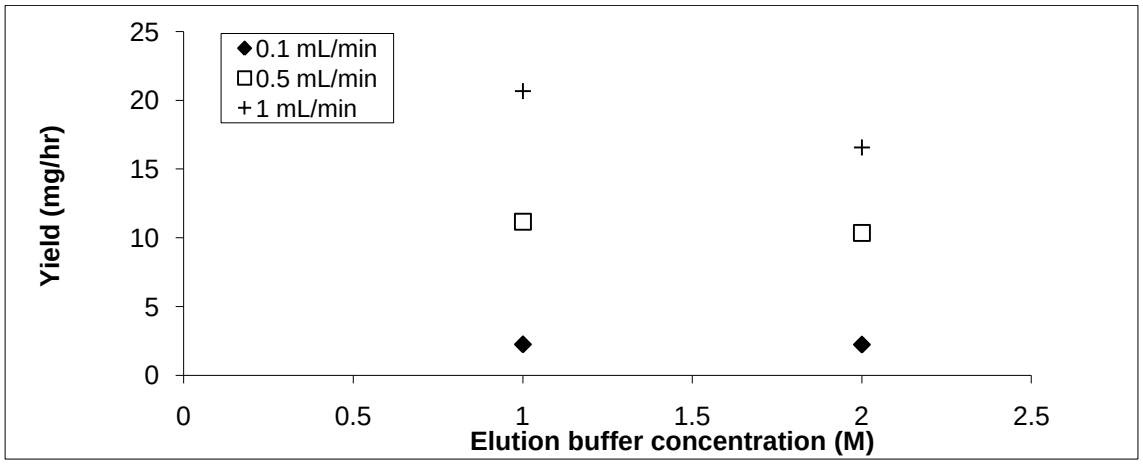

G.6.17 360 deg/hr rotation speed, 1.5 mg/mL BSA concentration, Trial 8, 0.1-1.0 mL/min flow rate

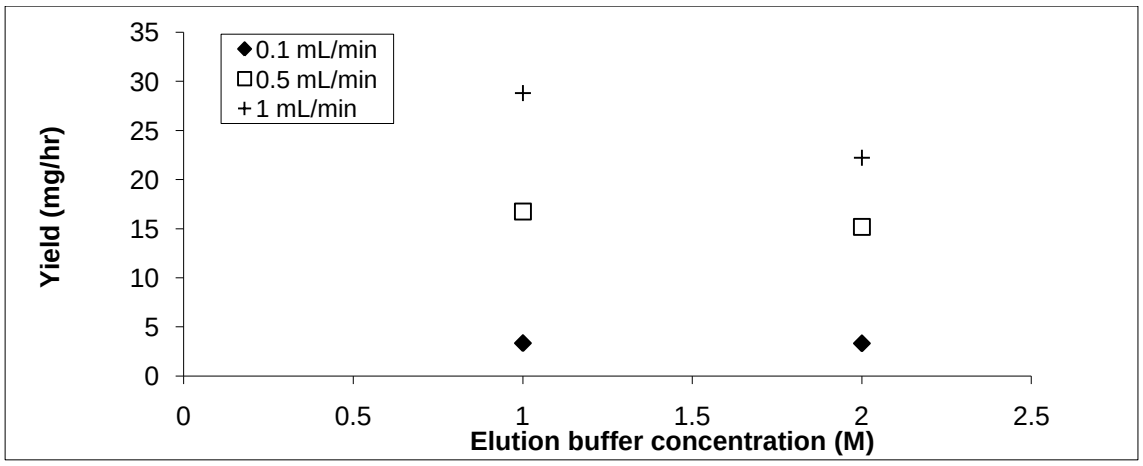

G.6.18 360 deg/hr rotation speed, 1.5 mg/mL BSA concentration, Trial 9, 0.1-1.0 mL/min flow rate

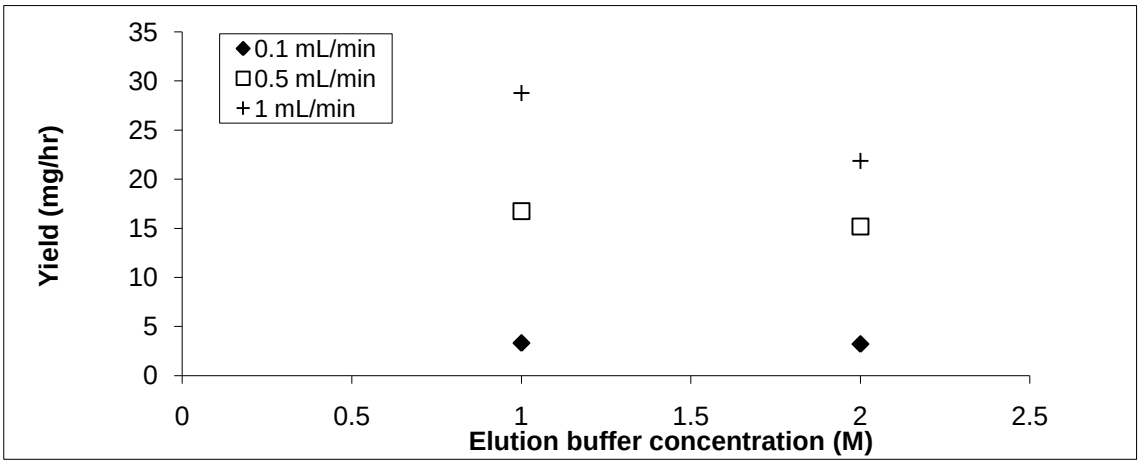

G.6.19 720 deg/hr rotation speed, 1.5 mg/mL BSA concentration, Trial 1, 0.1-1.0 mL/min flow rate

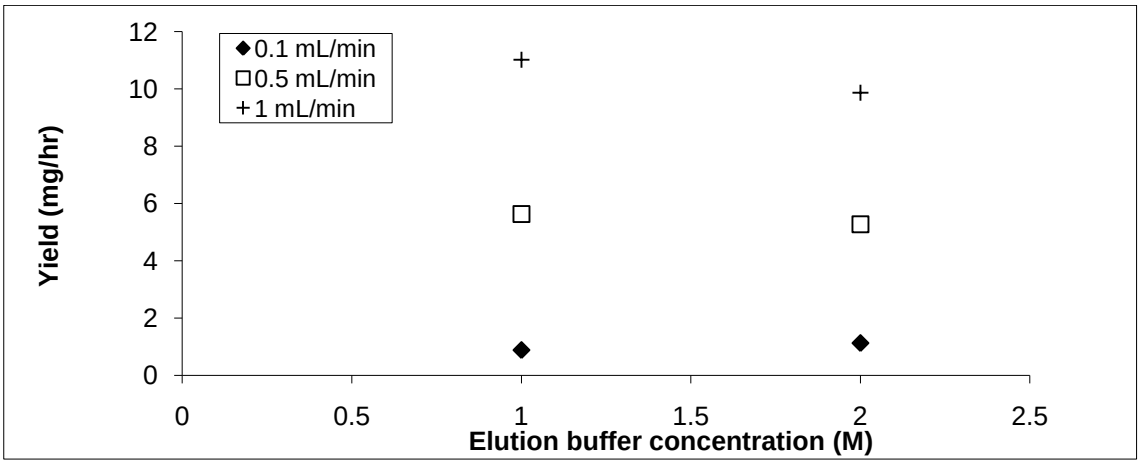

G.6.20 720 deg/hr rotation speed, 1.5 mg/mL BSA concentration, Trial 2, 0.1-1.0 mL/min flow rate

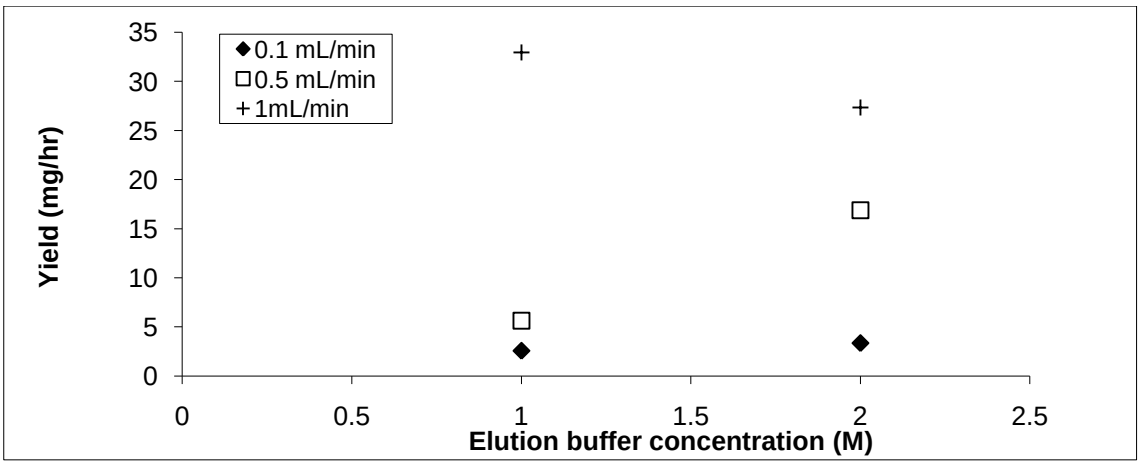

G.6.21 720 deg/hr rotation speed, 1.5 mg/mL BSA concentration, Trial 3, 0.1-1.0 mL/min flow rate

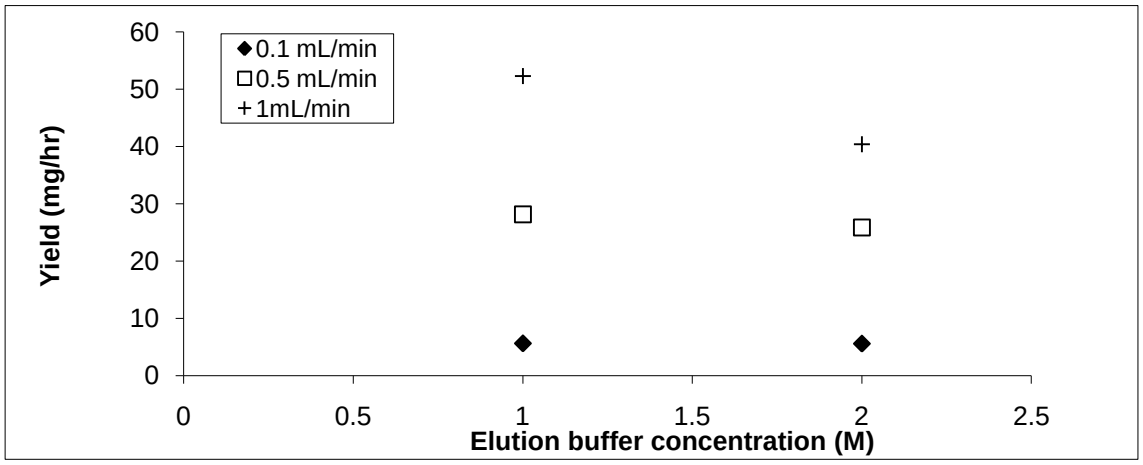

G.6.22 720 deg/hr rotation speed, 1.5 mg/mL BSA concentration, Trial 4, 0.1-1.0 mL/min flow rate

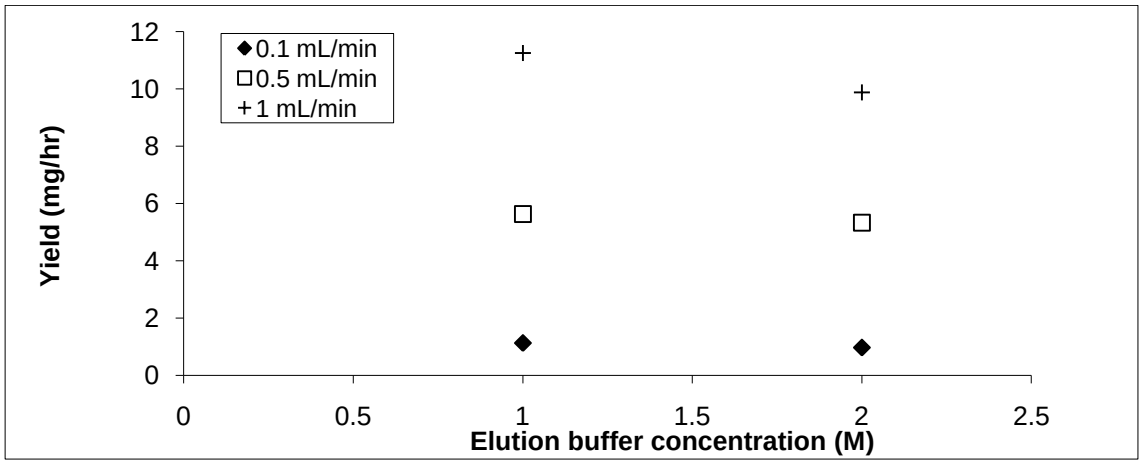

G.6.23 720 deg/hr rotation speed, 1.5 mg/mL BSA concentration, Trial 5, 0.1-1.0 mL/min flow rate

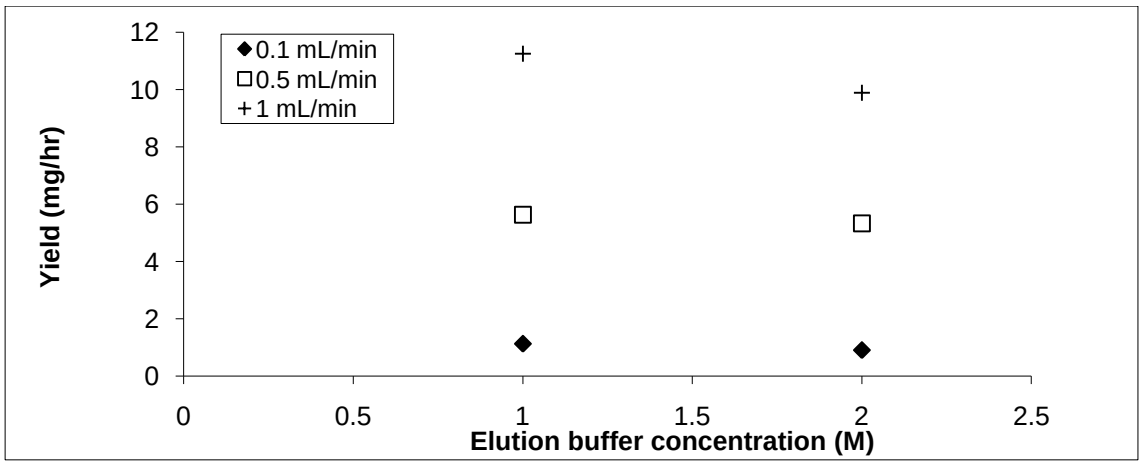

G.6.24 720 deg/hr rotation speed, 1.5 mg/mL BSA concentration, Trial 6, 0.1-1.0 mL/min flow rate

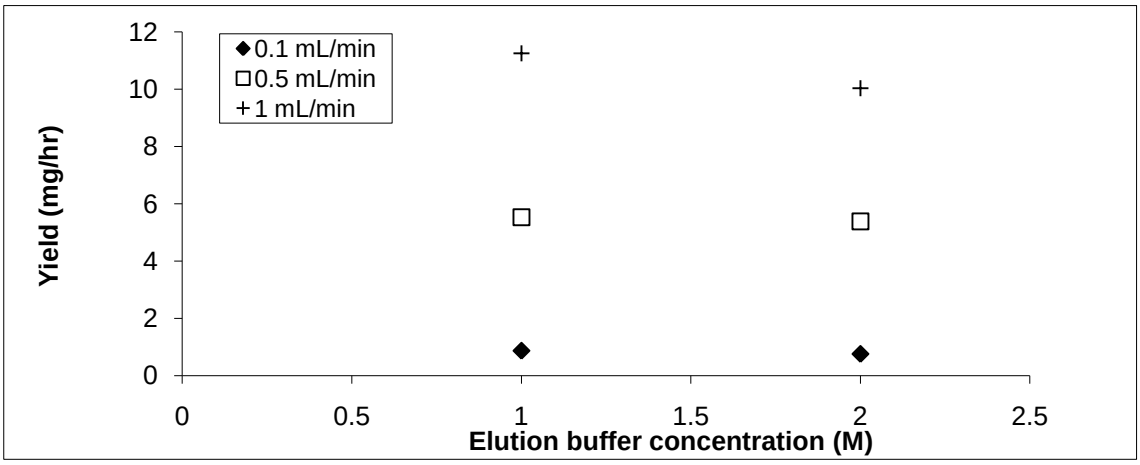

G.6.25 720 deg/hr rotation speed, 1.5 mg/mL BSA concentration, Trial 7, 0.1-1.0 mL/min flow rate

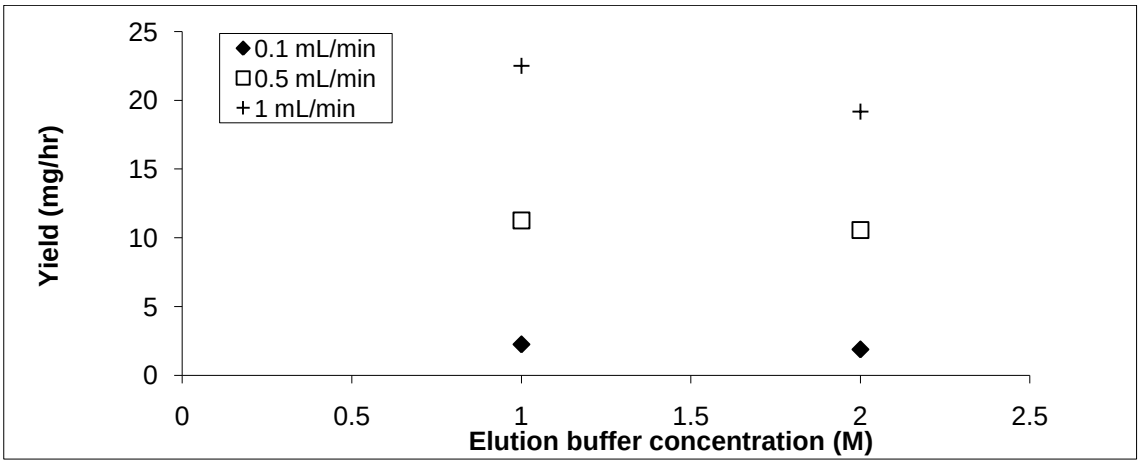

G.6.26 720 deg/hr rotation speed, 1.5 mg/mL BSA concentration, Trial 8, 0.1-1.0 mL/min flow rate

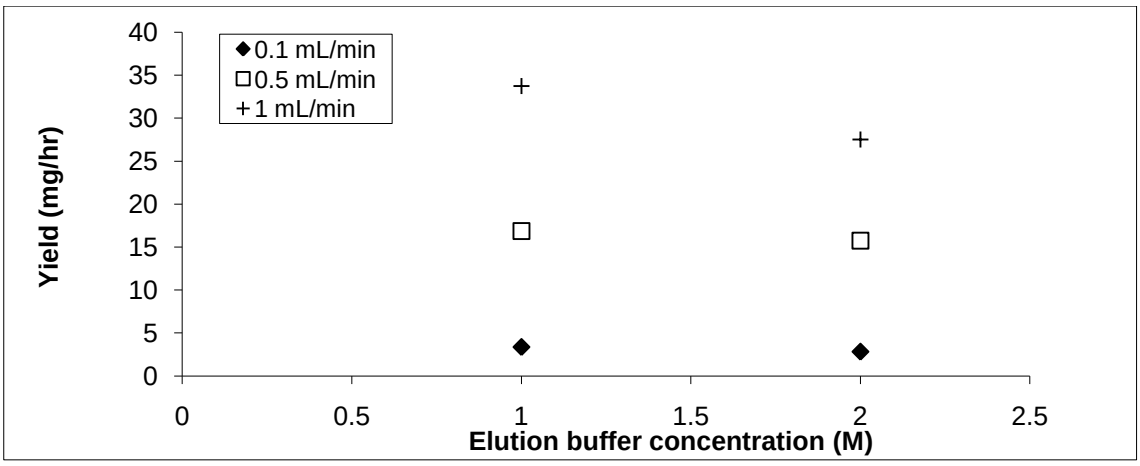

G.6.27 720 deg/hr rotation speed, 1.5 mg/mL BSA concentration, Trial 9, 0.1-1.0 mL/min flow rate

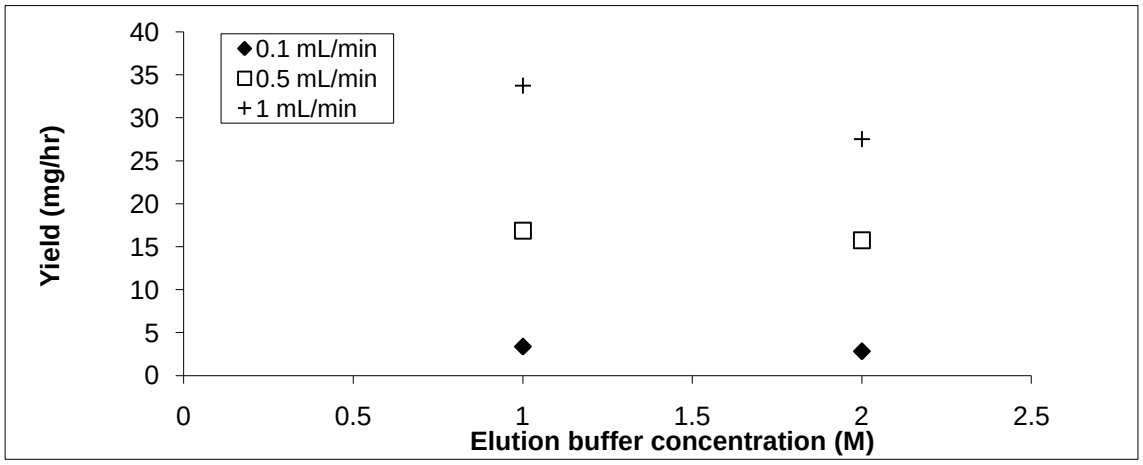

G.7 Yield data summary

Table 20. 1.5 mg/mL BSA, 1M NaCl, 180 deg/hr rotation speed.

Flow rate mL/min	Trial	Peak area captured mAU*min	Peak area loss mAU*min	BSA captured %	BSA loss %	Load per cycle mg	Throughput mg/hr	Yield mg/hr
0.1	1	5534	27	99.51	0.49	2.25	1.125	1.120
0.1	2	11013	104	99.06	0.94	6.75	3.375	3.343
0.1	3	15642	102	99.35	0.65	11.25	5.625	5.589
0.1	4	5492	18	99.68	0.32	2.25	1.125	1.121
0.1	5	5451	21	99.62	0.38	2.25	1.125	1.121
0.1	6	5671	67	98.84	1.16	2.25	1.125	1.112
0.1	7	8658	56	99.36	0.64	4.50	2.250	2.236
0.1	8	10930	74	99.33	0.67	6.75	3.375	3.352
0.1	9	10878	92	99.16	0.84	6.75	3.375	3.347
0.21	1	4550	71	98.46	1.54	4.73	2.363	2.326
0.21	2	8483	97	98.87	1.13	14.18	7.088	7.008
0.21	3	11832	371	96.96	3.04	23.63	11.813	11.453
0.21	4	4474	23	99.49	0.51	4.73	2.363	2.350
0.21	5	4527	25	99.46	0.54	4.73	2.363	2.350
0.21	6	4958	108	97.86	2.14	4.73	2.363	2.312
0.21	7	7289	0	100.00	0.00	9.45	4.725	4.725
0.21	8	8856	0	100.00	0.00	14.18	7.088	7.088
0.21	9	8674	0	100.00	0.00	14.18	7.088	7.088
0.5	1	3687	18	99.52	0.48	11.25	5.625	5.598
0.5	2	6209	319	95.11	4.89	33.75	16.875	16.051
0.5	3	7798	2106	78.73	21.27	56.25	28.125	22.144
0.5	4	3780	43	98.88	1.12	11.25	5.625	5.562
0.5	5	3767	45	98.81	1.19	11.25	5.625	5.558
0.5	6	4019	166	96.03	3.97	11.25	5.625	5.402
0.5	7	5554	346	94.13	5.87	22.50	11.250	10.590
0.5	8	6583	683	90.60	9.40	33.75	16.875	15.288
0.5	9	6688	764	89.75	10.25	33.75	16.875	15.145
1	1	3256	457	87.69	12.31	22.50	11.250	9.865
1	2	4683	4131	53.13	46.87	67.50	33.750	17.932
1	3	N/A	N/A	N/A	N/A	N/A	N/A	N/A
1	4	3265	414	88.75	11.25	22.50	11.250	9.984
1	5	3266	417	88.68	11.32	22.50	11.250	9.977
1	6	3293	411	88.91	11.09	22.50	11.250	10.002
1	7	4236	1678	71.62	28.38	45.00	22.500	16.115
1	8	4743	3906	54.83	45.17	67.50	33.750	18.507
1	9	4654	3532	56.85	43.15	67.50	33.750	19.188

Table 21. 1.5 mg/mL BSA, 1M NaCl, 360 deg/hr rotation speed.

Flow rate	Trial	Peak area		BSA		Load per cycle	Throughput	Yield
		captured	loss	captured	loss			
mL/min		mAU*min	mAU*min	%	%	mg	mg/hr	mg/hr
0.1	1	3022	10	99.66	0.34	1.13	1.125	1.1212
0.1	2	7426	44	99.42	0.58	3.38	3.375	3.3553
0.1	3	9977	71	99.29	0.71	5.63	5.625	5.5852
0.1	4	3178	0	100.00	0.00	1.13	1.125	1.1250
0.1	5	3056	0	100.00	0.00	1.13	1.125	1.1250
0.1	6	2922	83	97.23	2.77	1.13	1.125	1.0939
0.1	7	5553	14	99.75	0.25	2.25	2.250	2.2445
0.1	8	7186	55	99.24	0.76	3.38	3.375	3.3494
0.1	9	7172	128	98.25	1.75	3.38	3.375	3.3159
0.21	1	2859	32	98.91	1.09	2.36	2.363	2.3366
0.21	2	6286	98	98.46	1.54	7.09	7.088	6.9783
0.21	3	8454	191	97.79	2.21	11.81	11.813	11.5510
0.21	4	2858	0	100.00	0.00	2.36	2.363	2.3625
0.21	5	2859	0	100.00	0.00	2.36	2.363	2.3625
0.21	6	2858	0	100.00	0.00	2.36	2.363	2.3625
0.21	7	4832	59	98.79	1.21	4.73	4.725	4.6677
0.21	8	6244	90	98.57	1.43	7.09	7.088	6.9864
0.21	9	6274	90	98.59	1.41	7.09	7.088	6.9873
0.5	1	2435	6	99.77	0.23	5.63	5.625	5.6119
0.5	2	4570	42	99.09	0.91	16.88	16.875	16.7223
0.5	3	5840	192	96.82	3.18	28.13	28.125	27.2308
0.5	4	2391	9	99.63	0.37	5.63	5.625	5.6041
0.5	5	2386	9	99.62	0.38	5.63	5.625	5.6035
0.5	6	2382	8	99.67	0.33	5.63	5.625	5.6063
0.5	7	3617	23	99.36	0.64	11.25	11.250	11.1782
0.5	8	4463	33	99.27	0.73	16.88	16.875	16.7511
0.5	9	4503	35	99.24	0.76	16.88	16.875	16.7466
1	1	2226	65	97.14	2.86	11.25	11.250	10.9286
1	2	3688	604	85.92	14.08	33.75	33.750	28.9984
1	3	4358	2204	66.42	33.58	56.25	56.250	37.3591
1	4	2173	47	97.90	2.10	11.25	11.250	11.0132
1	5	2169	47	97.86	2.14	11.25	11.250	11.0098
1	6	2174	49	97.80	2.20	11.25	11.250	11.0025
1	7	3187	282	91.86	8.14	22.50	22.500	20.6685
1	8	3743	641	85.38	14.62	33.75	33.750	28.8145
1	9	3740	648	85.23	14.77	33.75	33.750	28.7661

Table 22. 1.5 mg/mL BSA, 1M NaCl, 720 deg/hr rotation speed.

Flow rate mL/min	Trial	Peak area captured mAU*min	Peak area loss mAU*min	BSA captured %	BSA loss %	Load per cycle mg	Throughput mg/hr	Yield mg/hr
0.1	1	1208	334	78.33	21.67	0.56	1.125	0.8812
0.1	2	3245	1023	76.02	23.98	1.69	3.375	2.5657
0.1	3	6519	0	100.00	0.00	2.81	5.625	5.6250
0.1	4	1522	0	100.00	0.00	0.56	1.125	1.1250
0.1	5	1458	0	100.00	0.00	0.56	1.125	1.1250
0.1	6	1180	358	76.73	23.27	0.56	1.125	0.8632
0.1	7	2999	0	100.00	0.00	1.13	2.250	2.2500
0.1	8	4330	0	100.00	0.00	1.69	3.375	3.3750
0.1	9	4349	0	100.00	0.00	1.69	3.375	3.3750
0.21	1	1514	0	100.00	0.00	1.18	2.363	2.3625
0.21	2	4203	0	100.00	0.00	3.54	7.088	7.0875
0.21	3	5410	0	100.00	0.00	5.91	11.813	11.8125
0.21	4	1545	0	100.00	0.00	1.18	2.363	2.3625
0.21	5	1488	0	100.00	0.00	1.18	2.363	2.3625
0.21	6	1467	51	96.64	3.36	1.18	2.363	2.2832
0.21	7	2875	0	100.00	0.00	2.36	4.725	4.7250
0.21	8	3855	0	100.00	0.00	3.54	7.088	7.0875
0.21	9	3819	0	100.00	0.00	3.54	7.088	7.0875
0.5	1	1427	0	100.00	0.00	2.81	5.625	5.6250
0.5	2	3131	0	100.00	0.00	8.44	16.875	16.8750
0.5	3	4136	0	100.00	0.00	14.06	28.125	28.1250
0.5	4	1466	0	100.00	0.00	2.81	5.625	5.6250
0.5	5	1438	0	100.00	0.00	2.81	5.625	5.6250
0.5	6	1436	24	98.37	1.63	2.81	5.625	5.5333
0.5	7	2443	0	100.00	0.00	5.63	11.250	11.2500
0.5	8	3147	0	100.00	0.00	8.44	16.875	16.8750
0.5	9	3150	0	100.00	0.00	8.44	16.875	16.8750
1	1	1359	29	97.92	2.08	5.63	11.250	11.0156
1	2	2658	65	97.62	2.38	16.88	33.750	32.9484
1	3	3339	252	92.98	7.02	28.13	56.250	52.2986
1	4	1378	0	100.00	0.00	5.63	11.250	11.2500
1	5	1379	0	100.00	0.00	5.63	11.250	11.2500
1	6	1367	0	100.00	0.00	5.63	11.250	11.2500
1	7	2100	0	100.00	0.00	11.25	22.500	22.5000
1	8	2630	0	100.00	0.00	16.88	33.750	33.7500
1	9	2643	0	100.00	0.00	16.88	33.750	33.7500

Table 23. 3 mg/mL BSA, 1M NaCl, 180 deg/hr rotation speed.

Flow rate mL/min	Trial	Peak area captured mAU*min	Peak area loss mAU*min	BSA captured %	BSA loss %	Load per cycle mg	Throughput mg/hr	Yield mg/hr
0.1	1	9214	177	98.12	1.88	4.50	2.250	2.2076
0.1	2	17008	528	96.99	3.01	13.50	6.750	6.5467
0.1	3	23379	881	96.37	3.63	22.50	11.250	10.8413
0.1	4	8849	150	98.34	1.66	4.50	2.250	2.2126
0.1	5	8885	148	98.36	1.64	4.50	2.250	2.2131
0.1	6	8876	134	98.51	1.49	4.50	2.250	2.2165
0.1	7	13284	313	97.70	2.30	9.00	4.500	4.3965
0.1	8	16172	613	96.35	3.65	13.50	6.750	6.5034
0.1	9	22212	831	96.39	3.61	13.50	6.750	6.5065
0.21	1	8782	359	96.08	3.92	9.45	4.725	4.5396
0.21	2	15149	1924	88.73	11.27	28.35	14.175	12.5774
0.21	3	19540	6240	75.80	24.20	47.25	23.625	17.9069
0.21	4	9380	443	95.49	4.51	9.45	4.725	4.5119
0.21	5	9425	443	95.51	4.49	9.45	4.725	4.5127
0.21	6	9476	401	95.94	4.06	9.45	4.725	4.5331
0.21	7	12519	918	93.17	6.83	18.90	9.450	8.8046
0.21	8	15871	2363	87.04	12.96	28.35	14.175	12.3381
0.21	9	15778	2360	86.99	13.01	28.35	14.175	12.3308
0.5	1	5863	631	90.28	9.72	22.50	11.250	10.1562
0.5	2	8360	4519	64.91	35.09	67.50	33.750	21.9079
0.5	3	9476	23950	28.35	71.65	112.50	56.250	15.9460
0.5	4	5653	320	94.64	5.36	22.50	11.250	10.6469
0.5	5	5726	344	94.33	5.67	22.50	11.250	10.6126
0.5	6	5768	316	94.81	5.19	22.50	11.250	10.6662
0.5	7	7304	1382	84.09	15.91	45.00	22.500	18.9210
0.5	8	8391	3962	67.93	32.07	67.50	33.750	22.9254
0.5	9	8491	4163	67.10	32.90	67.50	33.750	22.6460
1	1	4349	1747	71.34	28.66	45.00	22.500	16.0507
1	2	5286	19608	21.23	78.77	135.00	67.500	14.3319
1	3	N/A	N/A	N/A	N/A	N/A	N/A	N/A
1	4	4309	1425	75.15	24.85	45.00	22.500	16.9082
1	5	4320	1420	75.25	24.75	45.00	22.500	16.9323
1	6	4364	1408	75.60	24.40	45.00	22.500	17.0108
1	7	5548	9193	37.64	62.36	90.00	45.000	16.9361
1	8	5973	19356	23.58	76.42	135.00	67.500	15.9174
1	9	6011	19601	23.47	76.53	135.00	67.500	15.8423

Table 24. 3 mg/mL BSA, 1M NaCl, 360 deg/hr rotation speed.

Flow rate mL/min	Trial	Peak area captured mAU*min	Peak area loss mAU*min	BSA captured %	BSA loss %	Load per cycle mg	Throughput mg/hr	Yield mg/hr
0.1	1	5590	43	99.24	0.76	2.25	2.250	2.2328
0.1	2	12618	144	98.87	1.13	6.75	6.750	6.6737
0.1	3	15976	201	98.76	1.24	11.25	11.250	11.1104
0.1	4	5592	57	98.99	1.01	2.25	2.250	2.2273
0.1	5	5450	72	98.70	1.30	2.25	2.250	2.2207
0.1	6	5326	338	94.03	5.97	2.25	2.250	2.1156
0.1	7	9457	98	98.97	1.03	4.50	4.500	4.4538
0.1	8	11893	144	98.80	1.20	6.75	6.750	6.6690
0.1	9	11783	599	95.16	4.84	6.75	6.750	6.4235
0.21	1	4621	102	97.85	2.15	4.73	4.725	4.6234
0.21	2	8923	343	96.30	3.70	14.18	14.175	13.6508
0.21	3	11422	618	94.87	5.13	23.63	23.625	22.4121
0.21	4	4760	157	96.81	3.19	4.73	4.725	4.5742
0.21	5	4750	107	97.79	2.21	4.73	4.725	4.6205
0.21	6	4726	99	97.94	2.06	4.73	4.725	4.6278
0.21	7	7626	217	97.23	2.77	9.45	9.450	9.1883
0.21	8	9386	345	96.45	3.55	14.18	14.175	13.6725
0.21	9	9348	339	96.50	3.50	14.18	14.175	13.6793
0.5	1	3849	0	100.00	0.00	11.25	11.250	11.2500
0.5	2	6313	388	94.21	5.79	33.75	33.750	31.7965
0.5	3	7553	1580	82.70	17.30	56.25	56.250	46.5165
0.5	4	3952	134	96.72	3.28	11.25	11.250	10.8805
0.5	5	3962	140	96.58	3.42	11.25	11.250	10.8652
0.5	6	3994	115	97.20	2.80	11.25	11.250	10.9352
0.5	7	5426	216	96.17	3.83	22.50	22.500	21.6380
0.5	8	6379	468	93.17	6.83	33.75	33.750	31.4445
0.5	9	6445	519	92.55	7.45	33.75	33.750	31.2341
1	1	3276	478	87.26	12.74	22.50	22.500	19.6337
1	2	4656	3554	56.71	43.29	67.50	67.500	38.2804
1	3	5118	12592	28.90	71.10	112.50	112.500	32.5101
1	4	3245	372	89.71	10.29	22.50	22.500	20.1851
1	5	3264	378	89.61	10.39	22.50	22.500	20.1631
1	6	3282	351	90.34	9.66	22.50	22.500	20.3267
1	7	4091	1349	75.21	24.79	45.00	45.000	33.8434
1	8	4632	3246	58.80	41.20	67.50	67.500	39.6871
1	9	4714	3888	54.80	45.20	67.50	67.500	36.9915

Table 25. 3 mg/mL BSA, 1M NaCl, 720 deg/hr rotation speed.

Flow rate mL/min	Trial	Peak area captured mAU*min	Peak area loss mAU*min	BSA captured %	BSA loss %	Load per cycle mg	Throughput mg/hr	Yield mg/hr
0.1	1	3097	0	100.00	0.00	1.13	2.250	2.2500
0.1	2	7932	19	99.76	0.24	3.38	6.750	6.7335
0.1	3	10961	32	99.71	0.29	5.63	11.250	11.2171
0.1	4	3015	0	100.00	0.00	1.13	2.250	2.2500
0.1	5	2910	0	100.00	0.00	1.13	2.250	2.2500
0.1	6	2412	991	70.88	29.12	1.13	2.250	1.5948
0.1	7	5646	0	100.00	0.00	2.25	4.500	4.5000
0.1	8	7773	0	100.00	0.00	3.38	6.750	6.7500
0.1	9	7909	0	100.00	0.00	3.38	6.750	6.7500
0.21	1	2867	42	98.56	1.44	2.36	4.725	4.6570
0.21	2	6824	107	98.46	1.54	7.09	14.175	13.9564
0.21	3	8493	155	98.21	1.79	11.81	23.625	23.2017
0.21	4	2867	38	98.68	1.32	2.36	4.725	4.6627
0.21	5	2814	45	98.43	1.57	2.36	4.725	4.6510
0.21	6	2712	248	91.62	8.38	2.36	4.725	4.3292
0.21	7	4907	84	98.31	1.69	4.73	9.450	9.2905
0.21	8	6445	125	98.10	1.90	7.09	14.175	13.9053
0.21	9	6311	376	94.37	5.63	7.09	14.175	13.3771
0.5	1	2724	145	94.96	5.04	5.63	11.250	10.6829
0.5	2	5342	632	89.42	10.58	16.88	33.750	30.1788
0.5	3	6629	1468	81.87	18.13	28.13	56.250	46.0527
0.5	4	2668	143	94.92	5.08	5.63	11.250	10.6781
0.5	5	2665	132	95.30	4.70	5.63	11.250	10.7207
0.5	6	2676	119	95.73	4.27	5.63	11.250	10.7701
0.5	7	4235	290	93.59	6.41	11.25	22.500	21.0583
0.5	8	5191	514	90.98	9.02	16.88	33.750	30.7072
0.5	9	5215	530	90.78	9.22	16.88	33.750	30.6383
1	1	2407	459	83.98	16.02	11.25	22.500	18.8951
1	2	4062	2124	65.67	34.33	33.75	67.500	44.3258
1	3	4790	4759	50.16	49.84	56.25	112.500	56.4347
1	4	2267	90	96.20	3.80	11.25	22.500	21.6447
1	5	2258	88	96.26	3.74	11.25	22.500	21.6586
1	6	2257	77	96.70	3.30	11.25	22.500	21.7582
1	7	3477	1120	75.64	24.36	22.50	45.000	34.0384
1	8	4095	2039	66.76	33.24	33.75	67.500	45.0622
1	9	4051	2005	66.90	33.10	33.75	67.500	45.1566

Table 26. 5 mg/mL BSA, 1M NaCl, 180 deg/hr rotation speed.

Flow rate mL/min	Trial	Peak area captured mAU*min	Peak area loss mAU*min	BSA captured %	BSA loss %	Load per cycle mg	Throughput mg/hr	Yield mg/hr
0.1	1	12051	486	96.13	3.87	7.50	3.750	3.6047
0.1	2	21328	1144	94.91	5.09	22.50	11.250	10.6773
0.1	3	29544	1915	93.91	6.09	37.50	18.750	17.6087
0.1	4	12216	499	96.08	3.92	7.50	3.750	3.6029
0.1	5	12254	468	96.32	3.68	7.50	3.750	3.6120
0.1	6	12244	451	96.45	3.55	7.50	3.750	3.6167
0.1	7	18267	837	95.62	4.38	15.00	7.500	7.1713
0.1	8	22897	1230	94.90	5.10	22.50	11.250	10.6764
0.1	9	23010	1316	94.59	5.41	22.50	11.250	10.6414
0.21	1	10134	532	95.01	4.99	15.75	7.875	7.4821
0.21	2	17669	2249	88.71	11.29	47.25	23.625	20.9574
0.21	3	22119	8320	72.67	27.33	78.75	39.375	28.6122
0.21	4	9585	653	93.62	6.38	15.75	7.875	7.3730
0.21	5	9636	653	93.65	6.35	15.75	7.875	7.3749
0.21	6	9609	599	94.13	5.87	15.75	7.875	7.4127
0.21	7	13701	1345	91.06	8.94	31.50	15.750	14.3425
0.21	8	16563	2200	88.27	11.73	47.25	23.625	20.8545
0.21	9	17196	2527	87.19	12.81	47.25	23.625	20.5979
0.5	1	7909	2960	72.77	27.23	37.50	18.750	13.6440
0.5	2	10851	25753	29.64	70.36	112.50	56.250	16.6753
0.5	3	12035	63095	16.02	83.98	187.50	93.750	15.0179
0.5	4	7178	1157	86.12	13.88	37.50	18.750	16.1468
0.5	5	7157	1126	86.41	13.59	37.50	18.750	16.2018
0.5	6	7265	1145	86.39	13.61	37.50	18.750	16.1979
0.5	7	9085	7974	53.26	46.74	75.00	37.500	19.9715
0.5	8	10135	23432	30.19	69.81	112.50	56.250	16.9838
0.5	9	9763	23155	29.66	70.34	112.50	56.250	16.6832
1	1	5126	6370	44.59	55.41	75.00	37.500	16.7217
1	2	6088	41885	12.69	87.31	225.00	112.500	14.2761
1	3	N/A	N/A	N/A	N/A	N/A	N/A	N/A
1	4	4826	4686	50.74	49.26	75.00	37.500	19.0270
1	5	4865	4920	49.72	50.28	75.00	37.500	18.6455
1	6	4923	4950	49.86	50.14	75.00	37.500	18.6990
1	7	6061	31414	16.17	83.83	150.00	75.000	12.1301
1	8	6491	41075	13.65	86.35	225.00	112.500	15.3517
1	9	6603	41520	13.72	86.28	225.00	112.500	15.4354

Table 27. 5 mg/mL BSA, 1M NaCl, 360 deg/hr rotation speed.

Flow rate mL/min	Trial	Peak area captured mAU*min	Peak area loss mAU*min	BSA captured %	BSA loss %	Load per cycle mg	Throughput mg/hr	Yield mg/hr
0.1	1	8325	257	97.01	2.99	3.75	3.750	3.6379
0.1	2	16669	492	97.13	2.87	11.25	11.250	10.9275
0.1	3	23094	733	96.92	3.08	18.75	18.750	18.1728
0.1	4	8390	281	96.76	3.24	3.75	3.750	3.6284
0.1	5	8416	305	96.50	3.50	3.75	3.750	3.6189
0.1	6	8203	466	94.63	5.37	3.75	3.750	3.5484
0.1	7	13054	487	96.40	3.60	7.50	7.500	7.2300
0.1	8	17823	644	96.51	3.49	11.25	11.250	10.8577
0.1	9	15790	1003	94.03	5.97	11.25	11.250	10.5783
0.21	1	6724	325	95.39	4.61	7.88	7.875	7.5122
0.21	2	11682	848	93.23	6.77	23.63	23.625	22.0256
0.21	3	15267	1551	90.78	9.22	39.38	39.375	35.7434
0.21	4	7105	351	95.30	4.70	7.88	7.875	7.5047
0.21	5	7055	332	95.50	4.50	7.88	7.875	7.5208
0.21	6	7073	306	95.86	4.14	7.88	7.875	7.5487
0.21	7	10238	638	94.13	5.87	15.75	15.750	14.8259
0.21	8	12230	931	92.93	7.07	23.63	23.625	21.9539
0.21	9	12292	951	92.82	7.18	23.63	23.625	21.9280
0.5	1	5108	140	97.32	2.68	18.75	18.750	18.2482
0.5	2	7553	1800	80.76	19.24	56.25	56.250	45.4261
0.5	3	8730	11772	42.58	57.42	93.75	93.750	39.9206
0.5	4	5781	747	88.55	11.45	18.75	18.750	16.6041
0.5	5	5784	728	88.82	11.18	18.75	18.750	16.6541
0.5	6	5790	697	89.25	10.75	18.75	18.750	16.7346
0.5	7	6854	964	87.67	12.33	37.50	37.500	32.8751
0.5	8	7768	2336	76.88	23.12	56.25	56.250	43.2453
0.5	9	7819	2400	76.51	23.49	56.25	56.250	43.0381
1	1	3883	1396	73.55	26.45	37.50	37.500	27.5825
1	2	5069	13011	28.04	71.96	112.50	112.500	31.5408
1	3	5614	31418	15.16	84.84	187.50	187.500	28.4241
1	4	4029	1151	77.78	22.22	37.50	37.500	29.1664
1	5	4022	1107	78.42	21.58	37.50	37.500	29.4080
1	6	4057	1086	78.88	21.12	37.50	37.500	29.5797
1	7	4831	5759	45.62	54.38	75.00	75.000	34.2147
1	8	5260	12492	29.63	70.37	112.50	112.500	33.3333
1	9	5377	12779	29.61	70.39	112.50	112.500	33.3164

Table 28. 5 mg/mL BSA, 1M NaCl, 720 deg/hr rotation speed.

Flow rate mL/min	Trial	Peak area captured mAU*min	Peak area loss mAU*min	BSA captured %	BSA loss %	Load per cycle mg	Throughput mg/hr	Yield mg/hr
0.1	1	4509	0	100.00	0.00	1.88	3.750	3.7500
0.1	2	11187	133	98.83	1.17	5.63	11.250	11.1181
0.1	3	14606	201	98.64	1.36	9.38	18.750	18.4958
0.1	4	4556	144	96.95	3.05	1.88	3.750	3.6355
0.1	5	4561	141	97.00	3.00	1.88	3.750	3.6376
0.1	6	3816	1346	73.93	26.07	1.88	3.750	2.7722
0.1	7	9031	141	98.46	1.54	3.75	7.500	7.3847
0.1	8	10563	117	98.91	1.09	5.63	11.250	11.1272
0.1	9	10518	121	98.86	1.14	5.63	11.250	11.1220
0.21	1	4608	191	96.02	3.98	3.94	7.875	7.5614
0.21	2	9700	411	95.93	4.07	11.81	23.625	22.6646
0.21	3	12542	560	95.72	4.28	19.69	39.375	37.6907
0.21	4	4453	152	96.69	3.31	3.94	7.875	7.6145
0.21	5	4298	144	96.76	3.24	3.94	7.875	7.6200
0.21	6	4254	179	95.96	4.04	3.94	7.875	7.5565
0.21	7	7563	310	96.07	3.93	7.88	15.750	15.1306
0.21	8	9653	465	95.41	4.59	11.81	23.625	22.5399
0.21	9	9699	536	94.76	5.24	11.81	23.625	22.3881
0.5	1	4070	498	89.10	10.90	9.38	18.750	16.7062
0.5	2	7045	2027	77.66	22.34	28.13	56.250	43.6834
0.5	3	8424	4579	64.78	35.22	46.88	93.750	60.7341
0.5	4	4141	475	89.72	10.28	9.38	18.750	16.8218
0.5	5	4117	460	89.95	10.05	9.38	18.750	16.8656
0.5	6	4149	410	91.01	8.99	9.38	18.750	17.0652
0.5	7	5519	551	90.92	9.08	18.75	37.500	34.0963
0.5	8	6529	921	87.64	12.36	28.13	56.250	49.2986
0.5	9	6578	887	88.12	11.88	28.13	56.250	49.5685
1	1	2948	223	92.97	7.03	18.75	37.500	34.8637
1	2	4324	2179	66.49	33.51	56.25	112.500	74.7960
1	3	4812	8057	37.39	62.61	93.75	187.500	70.1092
1	4	2904	125	95.88	4.12	18.75	37.500	35.9566
1	5	2897	128	95.77	4.23	18.75	37.500	35.9123
1	6	2884	115	96.15	3.85	18.75	37.500	36.0569
1	7	3850	1017	79.10	20.90	37.50	75.000	59.3236
1	8	4349	2418	64.27	35.73	56.25	112.500	72.3077
1	9	4362	2423	64.29	35.71	56.25	112.500	72.3233

Table 29. 1.5 mg/mL BSA, 2M NaCl, 180 deg/hr rotation speed.

Flow rate mL/min	Trial	Peak area captured mAU*min	Peak area loss mAU*min	BSA captured %	BSA loss %	Load per cycle mg	Throughput mg/hr	Yield mg/hr
0.1	1	6154	298	95.39	4.61	2.25	1.125	1.0731
0.1	2	12341	340	97.32	2.68	6.75	3.375	3.2845
0.1	3	15942	685	95.88	4.12	11.25	5.625	5.3932
0.1	4	5976	208	96.64	3.36	2.25	1.125	1.0872
0.1	5	5933	203	96.69	3.31	2.25	1.125	1.0877
0.1	6	5919	184	96.98	3.02	2.25	1.125	1.0910
0.1	7	9771	216	97.84	2.16	4.50	2.250	2.2013
0.1	8	12293	392	96.91	3.09	6.75	3.375	3.2707
0.1	9	12426	384	97.00	3.00	6.75	3.375	3.2738
0.5	1	4508	487	90.26	9.74	11.25	5.625	5.0769
0.5	2	7264	1859	79.62	20.38	33.75	16.875	13.4363
0.5	3	9061	6723	57.40	42.60	56.25	28.125	16.1450
0.5	4	4219	324	92.87	7.13	11.25	5.625	5.2240
0.5	5	4225	316	93.04	6.96	11.25	5.625	5.2333
0.5	6	4251	313	93.15	6.85	11.25	5.625	5.2396
0.5	7	6354	1159	84.57	15.43	22.50	11.250	9.5143
0.5	8	7488	2099	78.11	21.89	33.75	16.875	13.1809
0.5	9	7557	2098	78.27	21.73	33.75	16.875	13.2078
1	1	3653	1410	72.15	27.85	22.50	11.250	8.1164
1	2	5463	7700	41.50	58.50	67.50	33.750	14.0069
1	3	N/A	N/A	N/A	N/A	N/A	N/A	N/A
1	4	3482	1072	76.46	23.54	22.50	11.250	8.6015
1	5	3532	1042	77.23	22.77	22.50	11.250	8.6882
1	6	3608	1076	77.03	22.97	22.50	11.250	8.6660
1	7	4643	4069	53.29	46.71	45.00	22.500	11.9904
1	8	5306	7944	40.04	59.96	67.50	33.750	13.5151
1	9	5315	8147	39.48	60.52	67.50	33.750	13.3258

Table 30. 1.5 mg/mL BSA, 2M NaCl, 360 deg/hr rotation speed.

Flow rate mL/min	Trial	Peak area captured mAU*min	Peak area loss mAU*min	BSA captured %	BSA loss %	Load per cycle mg	Throughput mg/hr	Yield mg/hr
0.1	1	3492	115	96.81	3.19	1.13	1.125	1.0891
0.1	2	8486	120	98.61	1.39	3.38	3.375	3.3281
0.1	3	11377	215	98.15	1.85	5.63	5.625	5.5208
0.1	4	3118	102	96.82	3.18	1.13	1.125	1.0893
0.1	5	3067	86	97.27	2.73	1.13	1.125	1.0943
0.1	6	2851	301	90.44	9.56	1.13	1.125	1.0175
0.1	7	6073	61	99.00	1.00	2.25	2.250	2.2276
0.1	8	8242	116	98.61	1.39	3.38	3.375	3.3282
0.1	9	8092	407	95.21	4.79	3.38	3.375	3.2135
0.5	1	2757	238	92.06	7.94	5.63	5.625	5.1783
0.5	2	5420	712	88.38	11.62	16.88	16.875	14.9147
0.5	3	6842	1525	81.77	18.23	28.13	28.125	22.9990
0.5	4	2766	178	93.95	6.05	5.63	5.625	5.2848
0.5	5	2739	167	94.25	5.75	5.63	5.625	5.3013
0.5	6	2743	131	95.43	4.57	5.63	5.625	5.3680
0.5	7	4434	386	91.99	8.01	11.25	11.250	10.3486
0.5	8	5448	604	90.02	9.98	16.88	16.875	15.1917
0.5	9	5442	606	89.98	10.02	16.88	16.875	15.1844
1	1	2370	481	83.13	16.87	11.25	11.250	9.3521
1	2	4033	2041	66.39	33.61	33.75	33.750	22.4072
1	3	4831	4674	50.83	49.17	56.25	56.250	28.5897
1	4	2487	451	84.66	15.34	11.25	11.250	9.5240
1	5	2486	452	84.62	15.38	11.25	11.250	9.5196
1	6	2509	430	85.38	14.62	11.25	11.250	9.6049
1	7	3360	1200	73.69	26.31	22.50	22.500	16.5796
1	8	4028	2092	65.81	34.19	33.75	33.750	22.2124
1	9	4078	2215	64.80	35.20	33.75	33.750	21.8714

Table 31. 1.5 mg/mL BSA, 2M NaCl, 720 deg/hr rotation speed.

Flow rate mL/min	Trial	Peak area captured mAU*min	Peak area loss mAU*min	BSA captured %	BSA loss %	Load per cycle mg	Throughput mg/hr	Yield mg/hr
0.1	1	1640	0	100.00	0.00	0.56	1.125	1.1250
0.1	2	4543	42	99.08	0.92	1.69	3.375	3.3440
0.1	3	7106	54	99.25	0.75	2.81	5.625	5.5830
0.1	4	1394	229	85.91	14.09	0.56	1.125	0.9665
0.1	5	1299	320	80.25	19.75	0.56	1.125	0.9029
0.1	6	1127	560	66.80	33.20	0.56	1.125	0.7515
0.1	7	2536	491	83.78	16.22	1.13	2.250	1.8849
0.1	8	3673	697	84.05	15.95	1.69	3.375	2.8368
0.1	9	3691	709	83.88	16.12	1.69	3.375	2.8311
0.5	1	1539	103	93.74	6.26	2.81	5.625	5.2728
0.5	2	3614	239	93.80	6.20	8.44	16.875	15.8287
0.5	3	4839	423	91.96	8.04	14.06	28.125	25.8650
0.5	4	1550	86	94.76	5.24	2.81	5.625	5.3300
0.5	5	1533	84	94.78	5.22	2.81	5.625	5.3316
0.5	6	1534	70	95.65	4.35	2.81	5.625	5.3801
0.5	7	2769	179	93.93	6.07	5.63	11.250	10.5669
0.5	8	3684	266	93.27	6.73	8.44	16.875	15.7391
0.5	9	3693	267	93.26	6.74	8.44	16.875	15.7376
1	1	1438	203	87.64	12.36	5.63	11.250	9.8597
1	2	3003	704	81.01	18.99	16.88	33.750	27.3410
1	3	3764	1476	71.83	28.17	28.13	56.250	40.4032
1	4	1447	201	87.79	12.21	5.63	11.250	9.8767
1	5	1429	198	87.85	12.15	5.63	11.250	9.8832
1	6	1452	176	89.17	10.83	5.63	11.250	10.0313
1	7	2414	418	85.24	14.76	11.25	22.500	19.1795
1	8	3040	690	81.49	18.51	16.88	33.750	27.5034
1	9	3047	690	81.53	18.47	16.88	33.750	27.5179

Appendix H Trial Ranking

H.1 Productivity ranking

H.1.1 Rotation speed

Trial	Number of sections				Flow rate	Feed concentration	Elution buffer concentration	Productivity rank for rotation speed		
	Loading	Equilibration	Elution	Equilibration	mL/min	mg/mL	M	180 deg/hr	360 deg/hr	720 deg/hr
A1	3	2	1	2	1	5	1	0.5734	0.9128	1.7630
A2	3	1	2	2	1	5	1	0.5945	0.9480	1.7141
A3	3	1	3	1	1	5	1	0.5962	0.9477	1.7144
A4	5	1	1	1	0.5	5	1	0.7059	1.4105	1.6044
A5	2	2	2	2	1	5	1	0.7670	1.2011	1.6946
A6	3	2	1	2	0.21	1.5	1	1.0932	1.0926	1.0948
A7	2	2	2	2	0.5	1.5	1	1.1374	1.1490	1.1504
A8	3	1	2	2	0.21	3	1	1.1534	1.1796	1.1842
A9	3	1	3	1	0.5	3	1	1.2385	1.4018	1.3901
A10	1	3	1	3	1	3	1	1.1741	1.2445	1.2300

H.1.2 Flow rate

Trial	Number of sections				Rotation speed deg/hr	Feed concentration mg/mL	Elution buffer concentration M	Productivity rank for flow rate			
	Loading	Equilibration	Elution	Equilibration				0.1 mL/min	0.21 mL/min	0.5 mL/min	1 mL/min
B1	3	2	1	2	360	3	1	1.0887	1.1792	1.4128	1.3281
B2	3	1	2	2	360	3	1	1.0887	1.1796	1.4059	1.3558
B3	3	1	3	1	360	3	1	1.0838	1.1798	1.4018	1.3028
B4	5	1	1	1	360	3	1	1.1477	1.2920	1.5607	0.9318
B5	2	2	2	2	360	3	1	1.0593	1.1212	1.2839	1.3823

H.1.3 Feed concentration

Trial	Number of sections				Rotation speed deg/hr	Flow rate mL/min	Elution buffer concentration M	Productivity rank for feed concentration		
	Loading	Equilibration	Elution	Equilibration				5 mg/mL	3 mg/mL	1.5 mg/mL
C1	3	2	1	2	180	1	1	0.5734	0.8574	1.1403
C2	3	1	2	2	180	1	1	0.5945	0.8885	1.1516
C3	3	1	3	1	180	1	1	0.5962	0.8871	1.1650
C4	5	1	1	1	180	0.5	1	0.7059	0.9598	1.2585
C5	2	2	2	2	180	1	1	0.7670	1.0500	1.1753
C6	3	2	1	2	360	1	1	0.9480	1.3281	1.3578
C7	3	1	2	2	360	1	1	0.9128	1.3558	1.3542
C8	3	1	3	1	360	1	1	0.9477	1.3028	1.3533
C9	5	1	1	1	360	0.5	1	1.1953	1.5607	1.3584
C10	2	2	2	2	360	1	1	1.2011	1.3823	1.2648
C11	3	2	1	2	720	1	1	1.7630	1.4469	1.4355
C12	3	1	2	2	720	1	1	1.7141	1.4614	1.4512
C13	3	1	3	1	720	1	1	1.7144	1.4633	1.4512

C14	5	1	1	1	720	0.5	1	1.6044	1.5516	1.3760
C15	2	2	2	2	720	1	1	1.6946	1.3862	1.3008

H.1.4 Loading sections

Trial	Rotation speed deg/hr	Flow rate mL/min	Feed concentration mg/mL	Elution buffer concentration M	Elution sections	Productivity rank for Loading sections		
						1	3	5
D1	180	0.21	3	1	1	1.0595	1.1581	1.2035
D2	360	0.21	3	1	1	1.0612	1.1792	1.2920
D3	720	0.21	3	1	1	1.0618	1.1852	1.3075
D4	360	0.21	1.5	1	1	1.0311	1.0926	1.1528
D5	360	0.21	5	1	1	1.0982	1.2844	1.4550
D6	180	1	3	1	1	1.1741	0.8574	N/A
D7	360	1	3	1	1	1.2445	1.3281	0.9318
D8	720	1	3	1	1	1.2300	1.4469	1.4021
D9	360	1	1.5	1	1	1.1441	1.3578	1.3807
D10	360	1	5	1	1	1.3064	0.9128	0.3800

H.1.5 Elution sections

Trial	Rotation speed deg/hr	Flow rate mL/min	Feed concentration mg/mL	Elution buffer concentration M	Loading sections	Productivity rank for elution sections			
						1	2	3	5
E1	180	0.21	3	1	1	1.0595	1.0590	1.0590	1.0594
E2	360	0.21	3	1	1	1.0612	1.0602	1.0611	1.0613
E3	720	0.21	3	1	1	1.0618	1.0619	1.0617	1.0554
E4	360	0.21	1.5	1	1	1.0311	1.0316	1.0316	1.0316
E5	360	0.21	5	1	1	1.0982	1.0980	1.0983	1.0989
E6	180	1	3	1	1	1.1741	1.1909	1.1914	1.1929
E7	360	1	3	1	1	1.2825	1.2553	1.2549	1.2581
E8	720	1	3	1	1	1.1741	1.2840	1.2843	1.2862
E9	360	1	1.5	1	1	1.2445	1.1458	1.1457	1.1455
E10	360	1	5	1	1	1.2300	1.3376	1.3423	1.3457

H.1.6 Elution buffer concentration

Feed solution M	Rotation speed deg/hr	Flow rate mL/min	Number of sections				Productivity rank for elution buffer concentration	
			Loading	Equil	Elution	Equil	1 M	2M
1	720	0.1	1	3	1	3	1.0102	1.0150
1	720	0.1	3	2	1	2	1.0292	1.0445
1	720	0.1	5	1	1	1	1.0752	1.0744
1	720	0.1	1	2	2	3	1.0150	1.0119
1	720	0.1	1	2	3	2	1.0150	1.0107
1	720	0.1	1	1	5	1	1.0099	1.0077
1	720	0.1	2	2	2	2	1.0301	1.0229
1	720	0.1	3	1	2	2	1.0451	1.0345
1	720	0.1	3	1	3	1	1.0451	1.0344
1	720	0.5	1	3	1	3	1.0752	1.0683
1	720	0.5	3	2	1	2	1.2256	1.2050
1	720	0.5	5	1	1	1	1.3760	1.3316
1	720	0.5	1	2	2	3	1.0752	1.0694
1	720	0.5	1	2	3	2	1.0752	1.0694
1	720	0.5	1	1	5	1	1.0734	1.0704
1	720	0.5	2	2	2	2	1.1504	1.1370
1	720	0.5	3	1	2	2	1.2256	1.2033
1	720	0.5	3	1	3	1	1.2256	1.2033
1	720	1	1	3	1	3	1.1458	1.1231
1	720	1	3	2	1	2	1.4355	1.3253
1	720	1	5	1	1	1	1.6744	1.4406
1	720	1	1	2	2	3	1.1504	1.1234
1	720	1	1	2	3	2	1.1504	1.1235
1	720	1	1	1	5	1	1.1504	1.1265
1	720	1	2	2	2	2	1.3008	1.2356
1	720	1	3	1	2	2	1.4512	1.3284
1	720	1	3	1	3	1	1.4512	1.3287

H.2 HTW ranking

H.2.1 Rotation speed

Trial	Number of sections				Flow rate	Feed concentration	Elution buffer concentration	HTW rank for rotation speed		
	Loading	Equilibration	Elution	Equilibration	mL/min	mg/mL	M	180 deg/hr	360 deg/hr	720 deg/hr
A1	1	3	1	3	0.5	1.5	1	0.4160	0.4026	0.3971
A2	1	2	3	2	0.5	1.5	1	0.3507	0.4306	0.4380
A3	2	2	2	2	0.5	1.5	1	0.1495	0.3515	0.3883
A4	3	2	1	2	0.5	1.5	1	0.2845	0.4693	0.5915
A5	3	1	3	1	0.5	1.5	1	0.1464	0.2468	0.5313
A6	1	3	1	3	0.1	3	1	0.1154	0.1983	0.0827
A7	1	2	3	2	0.1	5	1	0.0864	0.1040	0.0971
A8	2	2	2	2	0.21	3	1	0.1255	0.1971	0.2639
A9	3	2	1	2	1	3	1	0.3491	0.4498	0.6774
A10	3	1	3	1	1	5	1	0.1660	0.4008	0.6338

H.2.2 Flow rate

Trial	Number of sections				Rotation speed	Feed concentration	Elution buffer concentration	HTW rank for flow rate			
	Loading	Equilibration	Elution	Equilibration	deg/hr	mg/mL	M	0.1 mL/min	0.21 mL/min	0.5 mL/min	1 mL/min
B1	1	3	1	3	360	3	1	0.1983	0.2659	0.4088	0.4167
B2	1	2	3	2	360	3	1	0.0824	0.1287	0.2160	0.3908
B3	2	2	2	2	360	3	1	0.1371	0.1971	0.2622	0.3105
B4	3	2	1	2	360	3	1	0.1625	0.2818	0.3864	0.4498
B5	3	1	3	1	360	3	1	0.0892	0.1954	0.2418	0.2726

H6

H.2.3 Feed concentration

Trial	Number of sections					Rotation	Elution buffer concentration	HTW rank for feed concentration		
	Load	Equilibration	Elution	Equilibration			M	1.5 mg/mL	3 mg/mL	5 mg/mL
C1	1	3	1	3	0.1	180	1	0.1038	0.1154	0.1356
C2	1	2	3	2	0.5	180	1	0.3507	0.2023	0.1701
C3	2	2	2	2	0.5	180	1	0.1495	0.2314	0.2047
C4	3	2	1	2	1	180	1	0.3287	0.3491	0.3332
C5	3	1	3	1	1	180	1	0.2474	0.1725	0.1660
C6	1	3	1	3	0.1	360	1	0.0942	0.1983	0.1353
C7	1	2	3	2	0.5	360	1	0.4306	0.2160	0.2058
C8	2	2	2	2	0.5	360	1	0.3984	0.2622	0.3633
C9	3	2	1	2	1	360	1	0.5951	0.4498	0.6376
C10	3	1	3	1	1	360	1	0.4201	0.2726	0.4008
C11	1	3	1	3	0.1	720	1	0.0608	0.0827	0.0736
C12	1	2	3	2	0.5	720	1	0.4380	0.2580	0.2573
C13	2	2	2	2	0.5	720	1	0.3883	0.3830	0.4015
C14	3	2	1	2	1	720	1	1.0000	0.6774	0.9254
C15	3	1	3	1	1	720	1	0.9254	0.4282	0.6338

H.2.4 Loading section

Trial	Rotation speed deg/hr	Flow rate mL/min	Feed mg/mL	Elution buffer M	Elution sections	HTW rank for loading sections		
						1	3	5
D1	180	0.5	3	1	1	0.2646	0.2977	0.2856
D2	360	0.5	3	1	1	0.4088	0.3864	0.4097
D3	720	0.5	3	1	1	0.4376	0.5513	0.6329
D4	360	0.5	1.5	1	1	0.4026	0.4693	0.4380
D5	360	0.5	5	1	1	0.4689	0.4848	0.4784
D6	180	1	3	1	1	0.5011	0.3491	N/A
D7	360	1	3	1	1	0.4167	0.4498	0.4647
D8	720	1	3	1	1	0.5684	0.6774	0.6966
D9	360	1	1.5	1	1	0.5333	0.5951	0.6163
D10	360	1	5	1	1	0.6020	0.6376	0.6374

H.2.5 Elution sections

Trial	Rotation speed deg/hr	Flow rate mL/min	Feed concentration mg/mL	Elution buffer concentration M	Loading sections	HTW rank for elution sections			
						1	2	3	5
E1	180	0.5	3	1	1	0.2646	0.1885	0.2023	0.2240
E2	360	0.5	3	1	1	0.4088	0.3044	0.2160	0.2307
E3	720	0.5	3	1	1	0.4376	0.4599	0.2580	0.2834
E4	360	0.5	1.5	1	1	0.4026	0.3778	0.4306	0.4432
E5	360	0.5	5	1	1	0.4689	0.2496	0.2058	0.2597
E6	180	1	3	1	1	0.5011	0.4907	0.4483	0.4315
E7	360	1	3	1	1	0.4167	0.3911	0.3908	0.4173
E8	720	1	3	1	1	0.5684	0.1664	0.3954	0.3837
E9	360	1	1.5	1	1	0.5333	0.5551	0.5955	0.6627
E10	360	1	5	1	1	0.6020	0.3913	0.4448	0.4768
E11	180	0.5	3	1	3	0.297684	0.213392	0.207942	
E12	360	0.5	3	1	3	0.386429	0.29193	0.241792	
E13	720	0.5	3	1	3	0.551263	0.425945	0.35718	
E14	360	0.5	1.5	1	3	0.469255	0.351466	0.246817	
E15	360	0.5	5	1	3	0.484815	0.401103	0.345068	

H.2.6 Elution buffer concentration

Feed concentration M	Rotation speed deg/hr	Flow rate mL/min	Number of sections				Productivity rank for elution buffer concentration	
			Loading	Equilibration	Elution	Equilibration	1 M	2M
1	180	0.1	1	3	1	3	0.103753	0.089507
1	180	0.1	3	2	1	2	0.1473	0.13168
1	180	0.1	5	1	1	1	0.145437	0.145519
1	180	0.1	1	2	2	3	0.102217	0.066352
1	180	0.1	1	2	3	2	0.113732	0.065781
1	180	0.1	1	1	5	1	0.107597	0.069699
1	180	0.1	2	2	2	2	0.216531	0.109745
1	180	0.1	3	1	2	2	0.09641	0.133721
1	180	0.1	3	1	3	1	0.09751	0.093424
1	180	0.5	1	3	1	3	0.415991	0.277905
1	180	0.5	3	2	1	2	0.284492	0.319871
1	180	0.5	5	1	1	1	0.430807	0.43138
1	180	0.5	1	2	2	3	0.361533	0.217745
1	180	0.5	1	2	3	2	0.350681	0.213395
1	180	0.5	1	1	5	1	0.31545	0.219213
1	180	0.5	2	2	2	2	0.149544	0.206305
1	180	0.5	3	1	2	2	0.154616	0.296907
1	180	0.5	3	1	3	1	0.146447	0.313025
1	180	1	1	3	1	3	0.369138	0.408087
1	180	1	3	2	1	2	0.32866	0.378106
1	180	1	5	1	1	1	N/A	N/A
1	180	1	1	2	2	3	0.342459	0.334073
1	180	1	1	2	3	2	0.338968	0.375109
1	180	1	1	1	5	1	0.311799	0.389967
1	180	1	2	2	2	2	0.317107	0.467337

1	180	1	3	1	2	2	0.28333	0.387315
1	180	1	3	1	3	1	0.247402	0.371794
1	360	0.1	1	3	1	3	0.094204	0.054654
1	360	0.1	3	2	1	2	0.189107	0.145748
1	360	0.1	5	1	1	1	0.178855	0.149577
1	360	0.1	1	2	2	3	0.111228	0.042652
1	360	0.1	1	2	3	2	0.084694	0.035243
1	360	0.1	1	1	5	1	0.076005	0.041952
1	360	0.1	2	2	2	2	0.11524	0.083066
1	360	0.1	3	1	2	2	0.136801	0.109464
1	360	0.1	3	1	3	1	0.152619	0.119788
1	360	0.5	1	3	1	3	0.402603	0.241113
1	360	0.5	3	2	1	2	0.469255	0.319996
1	360	0.5	5	1	1	1	0.437977	0.337086
1	360	0.5	1	2	2	3	0.37777	0.21905
1	360	0.5	1	2	3	2	0.430553	0.21077
1	360	0.5	1	1	5	1	0.443211	0.200699
1	360	0.5	2	2	2	2	0.398371	0.312701
1	360	0.5	3	1	2	2	0.351466	0.290346
1	360	0.5	3	1	3	1	0.246817	0.277777
1	360	1	1	3	1	3	0.533262	0.313386
1	360	1	3	2	1	2	0.595055	0.40681
1	360	1	5	1	1	1	0.616284	0.404287
1	360	1	1	2	2	3	0.555113	0.293109
1	360	1	1	2	3	2	0.595544	0.287106
1	360	1	1	1	5	1	0.662664	0.30296
1	360	1	2	2	2	2	0.455058	0.439806
1	360	1	3	1	2	2	0.420843	0.429767
1	360	1	3	1	3	1	0.420072	0.421652

H12

	720	0.1	1	3	1	3	0.060839	0.04168
1	720	0.1	3	2	1	2	0.124658	0.102452
1	720	0.1	5	1	1	1	0.13699	0.13182
1	720	0.1	1	2	2	3	0.056001	0.032098
1	720	0.1	1	2	3	2	0.048268	0.021863
1	720	0.1	1	1	5	1	0.04909	0.030242
1	720	0.1	2	2	2	2	0.104956	0.062557
1	720	0.1	3	1	2	2	0.146671	0.091255
1	720	0.1	3	1	3	1	0.121689	0.073377
1	720	0.5	1	3	1	3	0.397149	0.19327
1	720	0.5	3	2	1	2	0.591481	0.390059
1	720	0.5	5	1	1	1	0.626438	0.513896
1	720	0.5	1	2	2	3	0.285017	0.203214
1	720	0.5	1	2	3	2	0.437969	0.162606
1	720	0.5	1	1	5	1	0.440472	0.1499
1	720	0.5	2	2	2	2	0.388338	0.250208
1	720	0.5	3	1	2	2	0.425249	0.300897
1	720	0.5	3	1	3	1	0.531264	0.338149
1	720	1	1	3	1	3	0.932441	0.400515
1	720	1	3	2	1	2	1	0.599774
1	720	1	5	1	1	1	0.990573	0.643051
1	720	1	1	2	2	3	0.838886	0.313448
1	720	1	1	2	3	2	0.929074	0.379685
1	720	1	1	1	5	1	0.928978	0.392306
1	720	1	2	2	2	2	0.934144	0.470752
1	720	1	3	1	2	2	0.859726	0.578186
1	720	1	3	1	3	1	0.925357	0.441717

H.2.7 Elution peak width in terms of angle

Feed (mg/mL)	Elution buffer (M)	Flow rate (mLmin)	Sections				Peak width with increasing rotation speeds		
			Loading	equilibration	Elution	Equilibration	(deg)	(deg)	(deg)
1.5	1	0.1	1	3	1	3	76.27	95.58	159.36
1.5	1	0.1	3	2	1	2	87.36	107.52	204.48
1.5	1	0.1	5	1	1	1	96.00	135.90	268.80
1.5	1	0.1	1	2	2	3	74.88	81.82	168.96
1.5	1	0.1	1	2	3	2	66.57	104.00	195.84
1.5	1	0.1	1	1	5	1	72.48	113.50	155.52
1.5	1	0.1	2	2	2	2	52.01	135.90	174.72
1.5	1	0.1	3	1	2	2	133.11	144.84	176.64
1.5	1	0.1	3	1	3	1	131.64	129.92	207.36
1.5	1	0.21	1	3	1	3	59.70	81.82	128.00
1.5	1	0.21	3	2	1	2	87.36	104.00	228.28
1.5	1	0.21	5	1	1	1	76.32	106.78	179.20
1.5	1	0.21	1	2	2	3	52.70	81.82	132.28
1.5	1	0.21	1	2	3	2	48.53	76.28	128.04
1.5	1	0.21	1	1	5	1	52.32	67.94	128.04
1.5	1	0.21	2	2	2	2	84.26	128.42	147.20
1.5	1	0.21	3	1	2	2	118.41	135.90	149.76
1.5	1	0.21	3	1	3	1	128.40	135.90	188.16
1.5	1	0.5	1	3	1	3	32.01	55.26	70.44
1.5	1	0.5	3	2	1	2	54.39	61.22	84.48
1.5	1	0.5	5	1	1	1	37.92	70.20	89.20
1.5	1	0.5	1	2	2	3	36.05	58.26	99.96
1.5	1	0.5	1	2	3	2	37.44	50.76	65.72
1.5	1	0.5	1	1	5	1	40.32	49.26	65.72
1.5	1	0.5	2	2	2	2	97.06	67.20	112.68
1.5	1	0.5	3	1	2	2	98.45	82.14	117.36

1.5	1	0.5	3	1	3	1	104.00	78.39	93.84
1.5	1	1	1	3	1	3	37.44	47.78	46.92
1.5	1	1	3	2	1	2	49.08	50.76	56.28
1.5	1	1	5	1	1	1		52.26	61.04
1.5	1	1	1	2	2	3	40.80	46.30	51.60
1.5	1	1	1	2	3	2	41.28	43.32	46.92
1.5	1	1	1	1	5	1	44.64	38.82	46.92
1.5	1	1	2	2	2	2	48.48	62.70	56.28
1.5	1	1	3	1	2	2	57.12	71.68	65.64
1.5	1	1	3	1	3	1	65.28	71.68	60.96

Feed	Elution buffer	Flow rate	Sections				Peak width with increasing rotation speeds		
			Loading	equilibration	Elution	Equilibration			
(mg/mL)	(M)	(mLmin)					(deg)	(deg)	(deg)
3	1	0.1	1	3	1	3	91.52	75.00	199.68
3	1	0.1	3	2	1	2	105.38	155.32	293.76
3	1	0.1	5	1	1	1	109.54	179.20	322.56
3	1	0.1	1	2	2	3	115.10	140.38	232.32
3	1	0.1	1	2	3	2	152.53	176.20	255.36
3	1	0.1	1	1	5	1	124.80	164.26	188.16
3	1	0.1	2	2	2	2	124.80	159.80	234.24
3	1	0.1	3	1	2	2	141.45	173.24	280.32
3	1	0.1	3	1	3	1	133.11	277.76	286.08
3	1	0.21	1	3	1	3	63.79	79.14	134.40
3	1	0.21	3	2	1	2	69.33	98.58	147.84
3	1	0.21	5	1	1	1	81.81	98.56	172.80
3	1	0.21	1	2	2	3	105.39	117.96	151.68
3	1	0.21	1	2	3	2	108.16	162.78	172.80
3	1	0.21	1	1	5	1	97.07	134.42	161.28
3	1	0.21	2	2	2	2	110.93	128.42	161.28

3	1	0.21	3	1	2	2	87.36	137.40	174.72
3	1	0.21	3	1	3	1	103.39	140.38	178.56
3	1	0.5	1	3	1	3	54.09	64.20	84.48
3	1	0.5	3	2	1	2	55.47	80.64	96.00
3	1	0.5	5	1	1	1	61.01	80.64	90.24
3	1	0.5	1	2	2	3	77.65	85.14	78.72
3	1	0.5	1	2	3	2	72.11	119.48	140.16
3	1	0.5	1	1	5	1	65.18	112.00	126.72
3	1	0.5	2	2	2	2	68.45	112.00	126.72
3	1	0.5	3	1	2	2	77.65	106.02	122.88
3	1	0.5	3	1	3	1	79.05	128.42	145.92
3	1	1	1	3	1	3	30.72	65.70	78.72
3	1	1	3	2	1	2	48.00	71.58	82.56
3	0	0	0	0	0	0	0.00	71.68	86.40
3	1	1	1	2	2	3	31.89	71.70	305.92
3	1	1	1	2	3	2	34.66	71.70	128.64
3	1	1	1	1	5	1	36.05	67.20	132.48
3	1	1	2	2	2	2	85.97	97.08	113.28
3	1	1	3	1	2	2	92.91	83.64	115.20
3	1	1	3	1	3	1	95.65	117.98	130.56

Feed	Elution buffer	Flow rate	Sections				Peak width with increasing rotation speeds		
			Loading	equilibration	Elution	Equilibration			
(mg/mL)	(M)	(mLmin)					(deg)	(deg)	(deg)
5	1	0.1	1	3	1	3	92.91	141.88	295.68
5	1	0.1	3	2	1	2	123.41	168.74	337.92
5	1	0.1	5	1	1	1	99.84	182.18	384.00
5	1	0.1	1	2	2	3	102.62	167.26	224.64
5	1	0.1	1	2	3	2	142.83	179.18	234.24
5	1	0.1	1	1	5	1	176.11	207.58	182.40

5	1	0.1	2	2	2	2	156.69	164.26	266.88
5	1	0.1	3	1	2	2	104.01	165.78	297.60
5	1	0.1	3	1	3	1	144.21	177.70	303.36
5	1	0.21	1	3	1	3	72.10	94.08	153.60
5	1	0.21	3	2	1	2	117.87	112.00	165.12
5	1	0.21	5	1	1	1	102.61	103.04	190.08
5	1	0.21	1	2	2	3	87.36	107.52	165.12
5	1	0.21	1	2	3	2	102.62	132.92	193.92
5	1	0.21	1	1	5	1	95.67	183.68	209.28
5	1	0.21	2	2	2	2	92.91	110.52	149.76
5	1	0.21	3	1	2	2	92.91	103.02	159.36
5	1	0.21	3	1	3	1	135.89	141.86	215.04
5	1	0.5	1	3	1	3	73.49	59.74	99.20
5	1	0.5	3	2	1	2	101.22	67.20	105.60
5	1	0.5	5	1	1	1	73.49	73.18	81.60
5	1	0.5	1	2	2	3	80.43	106.02	126.72
5	1	0.5	1	2	3	2	90.13	128.42	163.20
5	1	0.5	1	1	5	1	79.04	101.54	147.84
5	1	0.5	2	2	2	2	80.43	85.12	134.40
5	1	0.5	3	1	2	2	85.97	80.64	140.16
5	1	0.5	3	1	3	1	90.13	94.08	144.00
5	1	1	1	3	1	3	48.96	49.26	57.60
5	1	1	3	2	1	2	50.88	52.26	69.12
5	0	0	0	0	0	0	0.00	53.76	72.96
5	1	1	1	2	2	3	33.27	74.68	63.36
5	1	1	1	2	3	2	29.13	65.70	63.36
5	1	1	1	1	5	1	29.13	61.24	57.60
5	1	1	2	2	2	2	67.94	65.70	88.32
5	1	1	3	1	2	2	84.58	83.64	78.72
5	1	1	3	1	3	1	101.23	82.14	99.84

Feed	Elution buffer	Flow rate	Sections				Peak width with increasing rotation speeds		
			Loading	equilibration	Elution	Equilibration			
(mg/mL)	(M)	(mLmin)					(deg)	(deg)	(deg)
1.5	2	0.1	1	3	1	3	84.58	159.78	184.32
1.5	0	0.1	3	2	1	2	94.29	137.38	222.72
1.5	0	0.1	5	1	1	1	92.91	159.80	268.80
1.5	0	0.1	1	2	2	3	112.70	185.16	222.72
1.5	0	0.1	1	2	3	2	110.93	216.54	282.24
1.5	0	0.1	1	1	5	1	105.39	173.24	167.04
1.5	0	0.1	2	2	2	2	101.23	179.22	243.84
1.5	0	0.1	3	1	2	2	91.52	180.68	243.84
1.5	0	0.1	3	1	3	1	130.35	164.26	288.00
1.5	0	0.5	1	3	1	3	43.41	73.18	109.44
1.5	0	0.5	3	2	1	2	45.76	80.64	113.28
1.5	0	0.5	5	1	1	1	35.52	83.62	97.92
1.5	0	0.5	1	2	2	3	54.09	85.14	103.68
1.5	0	0.5	1	2	3	2	55.47	88.10	128.64
1.5	0	0.5	1	1	5	1	54.09	92.58	138.24
1.5	0	0.5	2	2	2	2	65.87	76.16	144.00
1.5	0	0.5	3	1	2	2	48.96	89.58	145.92
1.5	0	0.5	3	1	3	1	46.08	94.08	130.56
1.5	0	1	1	3	1	3	31.68	70.20	78.72
1.5	0	1	3	2	1	2	40.32	68.70	82.56
1.5	0	0	0	0	0	0	0.00	74.66	84.48
1.5	0	1	1	2	2	3	38.83	77.64	99.84
1.5	0	1	1	2	3	2	34.66	79.14	80.64
1.5	0	1	1	1	5	1	33.27	74.66	78.72
1.5	0	1	2	2	2	2	30.51	58.26	96.00
1.5	0	1	3	1	2	2	38.83	64.20	86.40

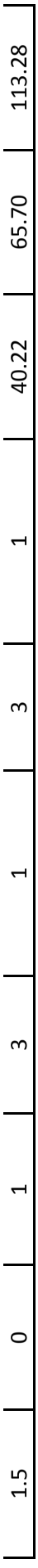
113.28
65.70
40.22
1
3
1
3
1
0
1.5

H.3 Overall ranking

H.3.1 Rotation speed

Trial	Number of sections				Flow rate	Feed concentration	Elution buffer concentration	Overall rank for rotation speed		
	Loading	Equilibration	Elution	Equilibration	mL/min	mg/mL	M	180 deg/hr	360 deg/hr	720 deg/hr
A1	3	1	3	1	1	5	1	0.7621	1.3484	2.3482
A2	3	1	2	2	1	5	1	0.7918	1.3440	2.5191
A3	3	2	1	2	1	5	1	0.9067	1.5504	2.6884
A4	5	1	1	1	0.5	5	1	0.9341	1.6738	2.0911
A5	2	2	2	2	1	5	1	1.0077	1.6906	2.3722
A6	3	2	1	2	0.1	1.5	1	1.1918	1.1814	1.1539
A7	2	2	2	2	0.1	3	1	1.1645	1.1963	1.4648
A8	3	1	2	2	0.21	3	1	1.3191	1.3801	1.4648
A9	3	1	3	1	0.5	1.5	1	1.3381	1.4699	1.7569
A10	1	3	1	3	0.5	3	1	1.3935	1.5592	1.5769

H.3.2 Flow rate

Trial	Number of sections				Rotation speed	Feed concentration	Elution buffer concentration	Overall rank for flow rate			
	Loading	Equilibration	Elution	Equilibration	deg/hr	mg/mL	M	0.1 mL/min	0.21 mL/min	0.5 mL/min	1 mL/min
B1	1	3	1	3	360	3	1	1.2280	1.3271	1.5592	1.6612
B2	1	2	3	2	360	3	1	1.2512	1.4610	1.7993	1.7779
B3	2	2	2	2	360	3	1	1.3041	1.5997	1.9704	1.3965
B4	3	2	1	2	360	3	1	1.1119	1.1898	1.3589	1.6457
B5	3	1	3	1	360	3	1	1.1151	1.2164	1.3749	1.6754
B6	1	3	1	3	180	1.5	1	1.1187	1.2199	1.4907	1.4923
B7	1	2	3	2	720	5	1	1.1450	1.2585	1.4709	2.3335
B8	2	2	2	2	720	1.5	1	1.1350	1.2924	1.5387	2.2350
B9	3	2	1	2	180	3	1	1.2193	1.3691	1.5161	1.2065
B10	3	1	3	1	180	5	1	1.2440	1.3782	1.1658	0.7621

H.3.3 Feed concentration

Trial	Number of sections				Rotation speed	Flow rate	Elution buffer concentration	Overall rank for feed concentration		
	Loading	Equilibration	Elution	Equilibration	deg/hr	mL/min	M	5 mg/mL	3 mg/mL	1.5 mg/mL
C1	3	2	1	2	180	1	1	0.9067	1.2065	1.4690
C2	3	1	2	2	180	1	1	0.7918	1.0671	1.4349
C3	3	1	3	1	180	1	1	0.7621	1.0595	1.4124
C4	5	1	1	1	180	0.5	1	0.9341	1.2454	1.6893
C5	2	2	2	2	180	1	1	1.0077	1.2361	1.4924
C6	3	2	1	2	360	1	1	1.5504	1.7779	1.9529
C7	3	1	2	2	360	1	1	1.3440	1.7371	1.7751
C8	3	1	3	1	360	1	1	1.3484	1.5754	1.7733
C9	5	1	1	1	360	0.5	1	1.6738	1.9704	1.7964
C10	2	2	2	2	360	1	1	1.6906	1.6929	1.7199
C11	3	2	1	2	720	1	1	2.6884	2.1243	2.4355
C12	3	1	2	2	720	1	1	2.5191	1.9451	2.3110
C13	3	1	3	1	720	1	1	2.3482	1.8915	2.3766
C14	5	1	1	1	720	0.5	1	2.0911	2.1845	2.0025
C15	2	2	2	2	720	1	1	2.3722	1.8481	2.2350

H.3.4 Loading sections

Trial	Rotation speed deg/hr	Flow rate mL/min	Feed concentration mg/mL	Elution buffer concentration M	Elution sections	Overall rank for loading sections		
						1	3	5
D1	180	0.5	3	1	1	1.3935	1.5161	1.2454
D2	360	0.5	3	1	1	1.5592	1.7993	1.9704
D3	720	0.5	3	1	1	1.5769	1.9323	2.1845
D4	360	0.5	1.5	1	1	1.4775	1.6919	1.7964
D5	360	0.5	5	1	1	1.7097	2.0241	1.6738
D6	180	1	3	1	1	1.6751	1.2065	N/A
D7	360	1	3	1	1	1.6612	1.7779	1.3965
D8	720	1	3	1	1	1.7984	2.1243	2.0987
D9	360	1	1.5	1	1	1.6774	1.9529	1.9970
D10	360	1	5	1	1	1.9084	1.5504	1.0174

H.3.5 Elution sections

Trial	Rotation speed deg/hr	Flow rate mL/min	Feed concentration mg/mL	Elution buffer concentration M	Loading sections	Overall rank for elution sections			
						1	2	3	5
E1	180	0.5	3	1	1	1.3935	1.3270	1.3402	1.3630
E2	360	0.5	3	1	1	1.5592	1.4475	1.3589	1.3749
E3	720	0.5	3	1	1	1.5769	1.5990	1.3980	1.4244
E4	360	0.5	1.5	1	1	1.4775	1.4526	1.5053	1.5180
E5	360	0.5	5	1	1	1.7097	1.4581	1.4152	1.4707
E6	180	1	3	1	1	1.6751	1.6816	1.6396	1.6244
E7	360	1	3	1	1	1.6612	1.6464	1.6457	1.6754
E8	720	1	3	1	1	1.7984	1.4504	1.6797	1.6700
E9	360	1	1.5	1	1	1.6774	1.7009	1.7412	1.8082
E10	360	1	5	1	1	1.9084	1.7288	1.7871	1.8225
E11	180	0.5	3	1	3	1.206515	1.067066	1.059543	
E12	360	0.5	3	1	3	1.799259	1.697839	1.643566	
E13	720	0.5	3	1	3	1.932294	1.817363	1.747244	
E14	360	0.5	1.5	1	3	1.952885	1.775059	1.773335	
E15	360	0.5	5	1	3	2.024105	1.897528	1.837419	

H.3.6 Elution buffer concentration

Feed concentration M	Rotation speed deg/hr	Flow-rate mL/min	Number of sections				Overall rank for elution buffer concentration	
			Loading	Equilibration	Elution	Equilibration	1 M	2M
1	180	0.1	1	3	1	3	1.118686	1.103528
1	180	0.1	3	2	1	2	1.191802	1.175023
1	180	0.1	5	1	1	1	1.219928	1.216166
1	180	0.1	1	2	2	3	1.117187	1.080649
1	180	0.1	1	2	3	2	1.12869	1.080089
1	180	0.1	1	1	5	1	1.122381	1.084072
1	180	0.1	2	2	2	2	1.246328	1.13887
1	180	0.1	3	1	2	2	1.141089	1.176793
1	180	0.1	3	1	3	1	1.142078	1.136557
1	180	0.5	1	3	1	3	1.490667	1.342336
1	180	0.5	3	2	1	2	1.493899	1.477894
1	180	0.5	5	1	1	1	1.689263	1.571925
1	180	0.5	1	2	2	3	1.435495	1.285067
1	180	0.5	1	2	3	2	1.424567	1.2809
1	180	0.5	1	1	5	1	1.386263	1.286843
1	180	0.5	2	2	2	2	1.286971	1.322598
1	180	0.5	3	1	2	2	1.349041	1.449909
1	180	0.5	3	1	3	1	1.338059	1.466556
1	180	1	1	3	1	3	1.492331	1.496902
1	180	1	3	2	1	2	1.468965	1.441263
1	180	1	5	1	1	1	0	0
1	180	1	1	2	2	3	1.467986	1.432422
1	180	1	1	2	3	2	1.464346	1.475162
1	180	1	1	1	5	1	1.437681	1.489585
1	180	1	2	2	2	2	1.492427	1.561578
1	180	1	3	1	2	2	1.434937	1.440805
1	180	1	3	1	3	1	1.412397	1.421562
1	360	0.1	1	3	1	3	1.109169	1.06899
1	360	0.1	3	2	1	2	1.233843	1.189949
1	360	0.1	5	1	1	1	1.253277	1.222734
1	360	0.1	1	2	2	3	1.126269	1.05699
1	360	0.1	1	2	3	2	1.099735	1.04968
1	360	0.1	1	1	5	1	1.090434	1.05488
1	360	0.1	2	2	2	2	1.145213	1.112707
1	360	0.1	3	1	2	2	1.18142	1.153666
1	360	0.1	3	1	3	1	1.196579	1.161736
1	360	0.5	1	3	1	3	1.47755	1.307538
1	360	0.5	3	2	1	2	1.691867	1.507079
1	360	0.5	5	1	1	1	1.796422	1.612352
1	360	0.5	1	2	2	3	1.452564	1.287568
1	360	0.5	1	2	3	2	1.505334	1.279612
1	360	0.5	1	1	5	1	1.518049	1.270852
1	360	0.5	2	2	2	2	1.547369	1.445392

1	360	0.5	3	1	2	2	1.574643	1.482872
1	360	0.5	3	1	3	1	1.469907	1.470161
1	360	1	1	3	1	3	1.677353	1.426491
1	360	1	3	2	1	2	1.952885	1.635084
1	360	1	5	1	1	1	1.997009	1.612642
1	360	1	1	2	2	3	1.700867	1.409593
1	360	1	1	2	3	2	1.741232	1.403502
1	360	1	1	1	5	1	1.808208	1.421033
1	360	1	2	2	2	2	1.719876	1.624252
1	360	1	3	1	2	2	1.775059	1.654211
1	360	1	3	1	3	1	1.773335	1.639394
1	720	0.1	1	3	1	3	1.071087	1.056721
1	720	0.1	3	2	1	2	1.153874	1.146966
1	720	0.1	5	1	1	1	1.212194	1.206198
1	720	0.1	1	2	2	3	1.071042	1.044024
1	720	0.1	1	2	3	2	1.063309	1.032537
1	720	0.1	1	1	5	1	1.058984	1.037942
1	720	0.1	2	2	2	2	1.135038	1.085463
1	720	0.1	3	1	2	2	1.191794	1.1258
1	720	0.1	3	1	3	1	1.166812	1.107808
1	720	0.5	1	3	1	3	1.472354	1.261552
1	720	0.5	3	2	1	2	1.817094	1.595107
1	720	0.5	5	1	1	1	2.002461	1.845496
1	720	0.5	1	2	2	3	1.360221	1.272619
1	720	0.5	1	2	3	2	1.513173	1.232043
1	720	0.5	1	1	5	1	1.513874	1.220291
1	720	0.5	2	2	2	2	1.538747	1.387189
1	720	0.5	3	1	2	2	1.650862	1.504183
1	720	0.5	3	1	3	1	1.756877	1.541405
1	720	1	1	3	1	3	2.078242	1.523597
1	720	1	3	2	1	2	2.435471	1.925027
1	720	1	5	1	1	1	2.66495	2.083611
1	720	1	1	2	2	3	1.989295	1.436864
1	720	1	1	2	3	2	2.079483	1.503228
1	720	1	1	1	5	1	2.079388	1.518761
1	720	1	2	2	2	2	2.234962	1.706302
1	720	1	3	1	2	2	2.310953	1.90663
1	720	1	3	1	3	1	2.376584	1.770446

Appendix I Simulated and Experimental Data

I.1 5 mg/mL BSA concentration, 720 rotation speed, 1 mL/min flow rate, 1M NaCl concentration, 11.25 min loading, 7.5 min equilibration, 3.75 min elution and 7.5 min reequilibration.

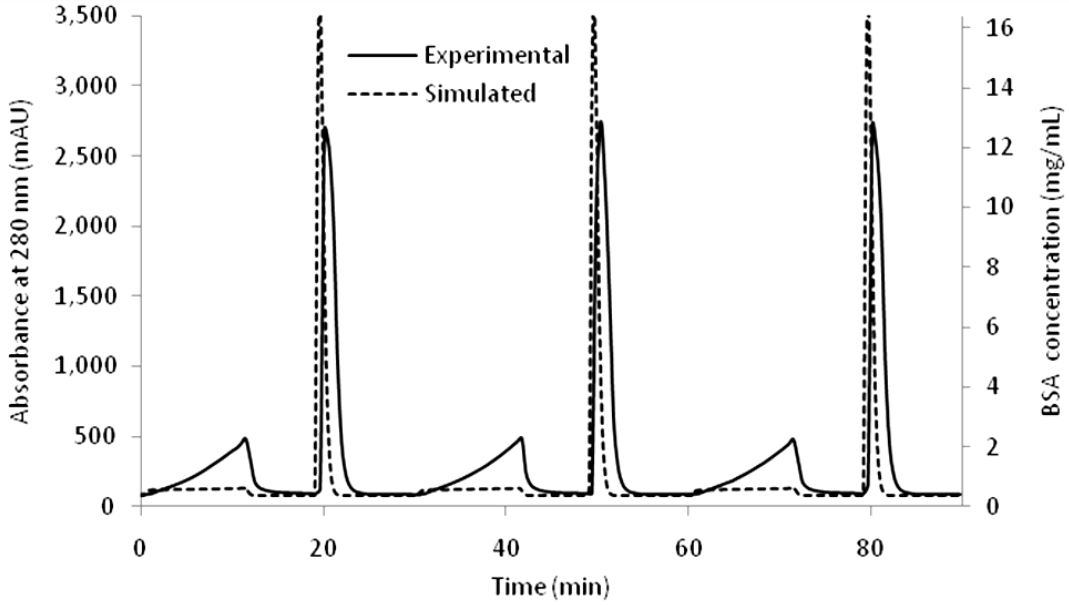

I.2 5 mg/mL BSA concentration, 720 rotation speed, 1 mL/min flow rate, 1M NaCl concentration, 11.25 min loading, 3.75 min equilibration, 7.5 min elution and 7.5 min reequilibration.

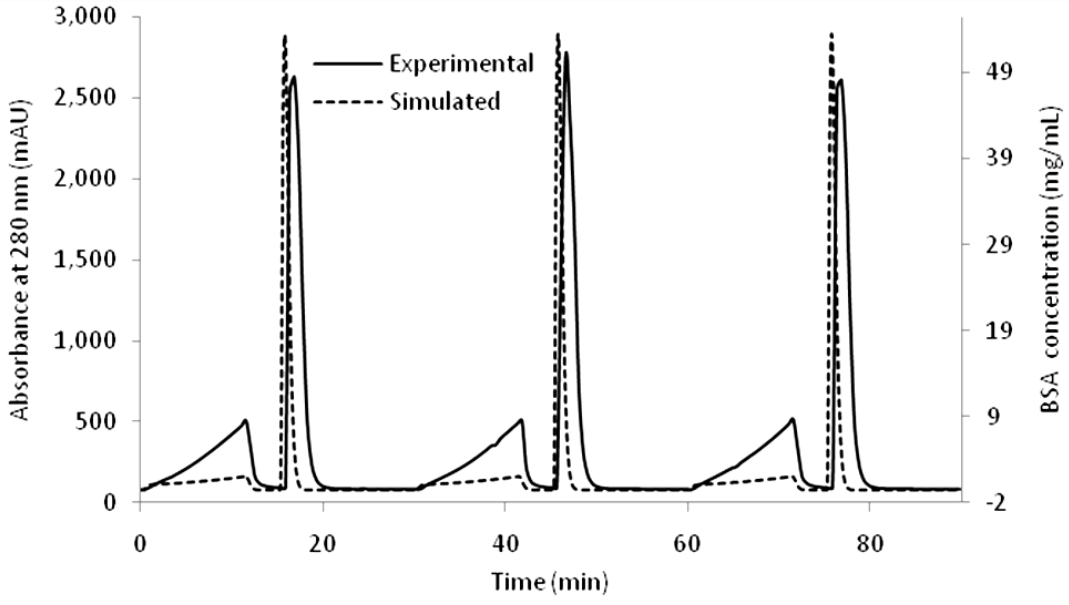

I.3 5 mg/mL BSA concentration, 720 rotation speed, 1 mL/min flow rate, 1M NaCl concentration, 3.75 min loading, 3.75 min equilibration, 18.75 min elution and 3.75 min reequilibration.

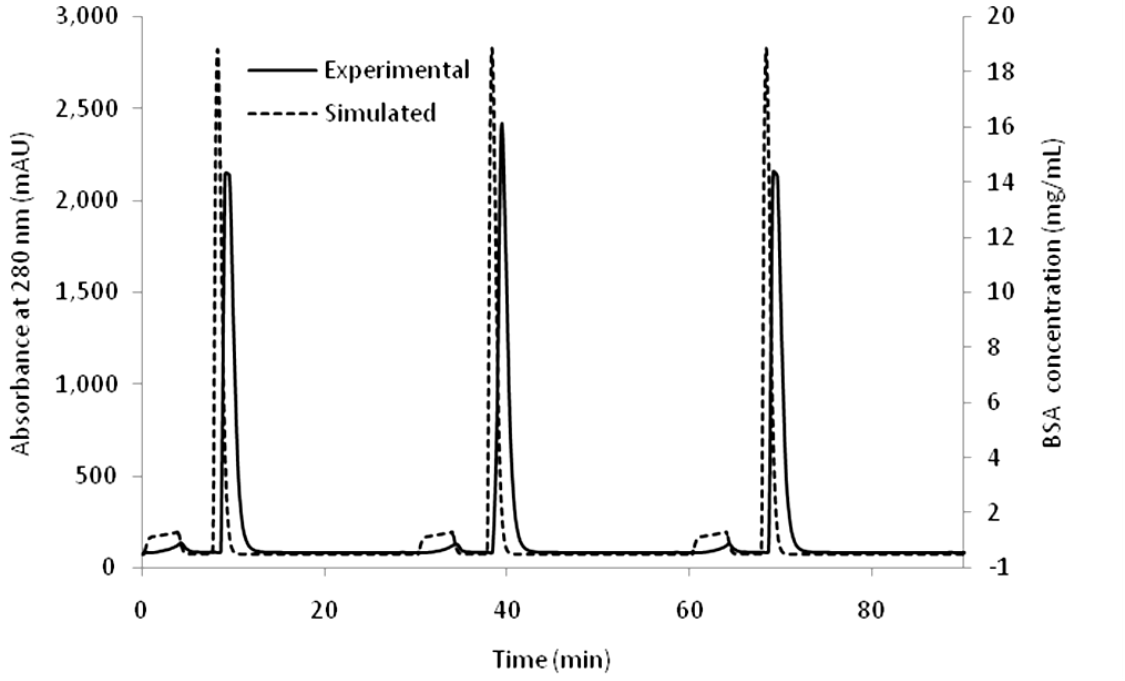

I.4 5 mg/mL BSA concentration, 720 rotation speed, 1 mL/min flow rate, 1M NaCl concentration, 3.75 min loading, 11.25 min equilibration, 3.75 min elution and 11.25 min reequilibration.

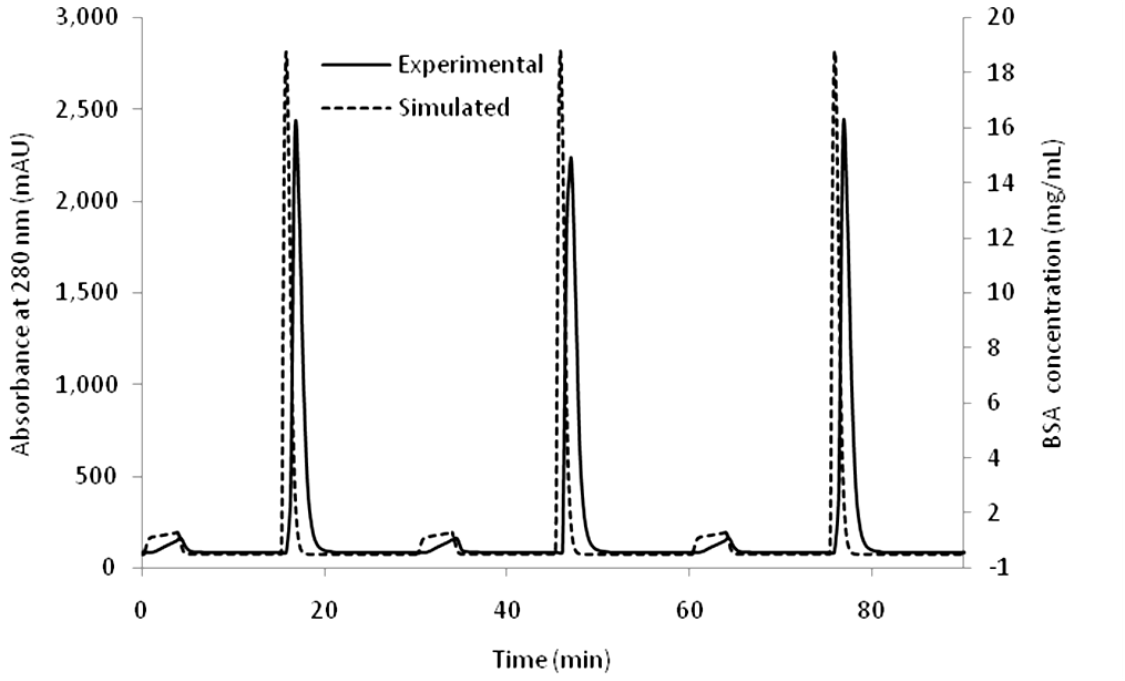

I.5 5 mg/mL BSA concentration, 720 rotation speed, 1 mL/min flow rate, 1M NaCl concentration, 11.25 min loading, 3.75 min equilibration, 11.25 min elution and 3.75 min reequilibration.

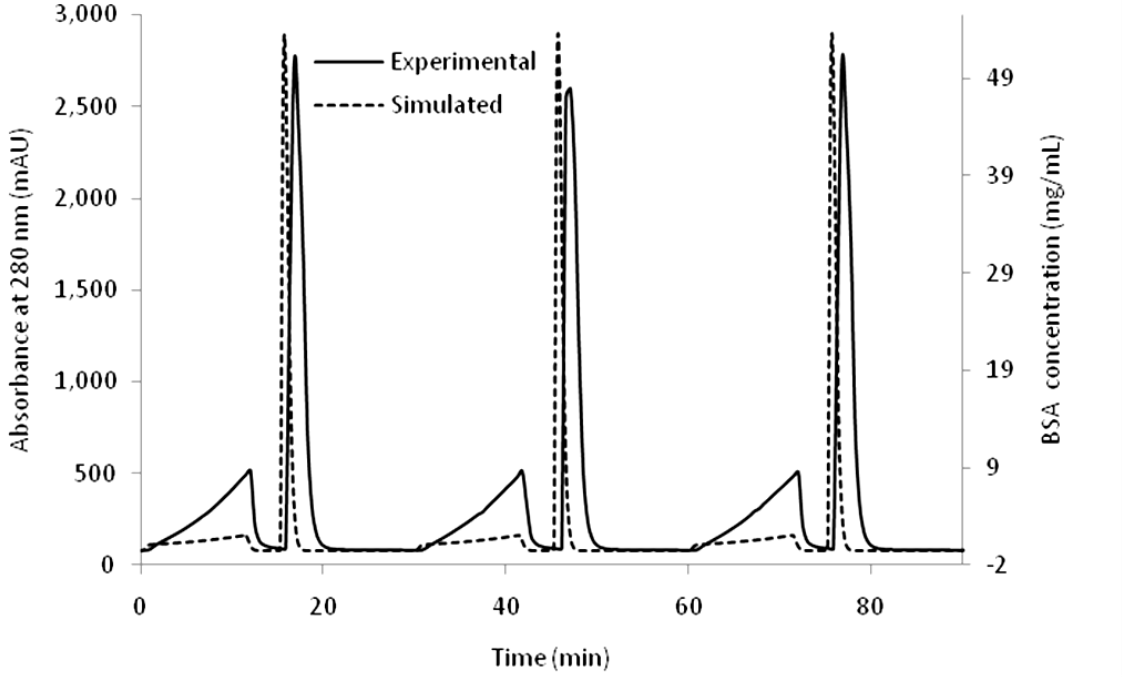

I.6 5 mg/mL BSA concentration, 720 rotation speed, 1 mL/min flow rate, 1M NaCl concentration, 7.5 min loading, 7.5 min equilibration, 7.5 min elution and 7.5 min reequilibration.

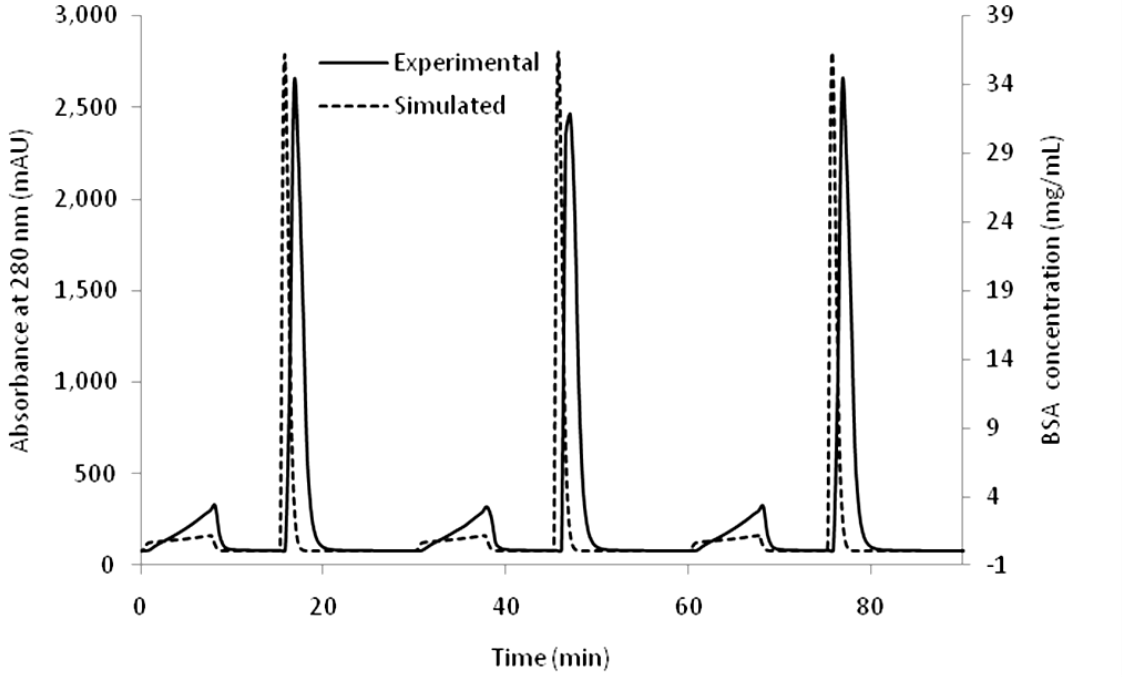

I.7 5 mg/mL BSA concentration, 720 rotation speed, 1 mL/min flow rate, 1M NaCl concentration, 3.75 min loading, 7.5 min equilibration, 7.5 min elution and 11.25 min reequilibration.

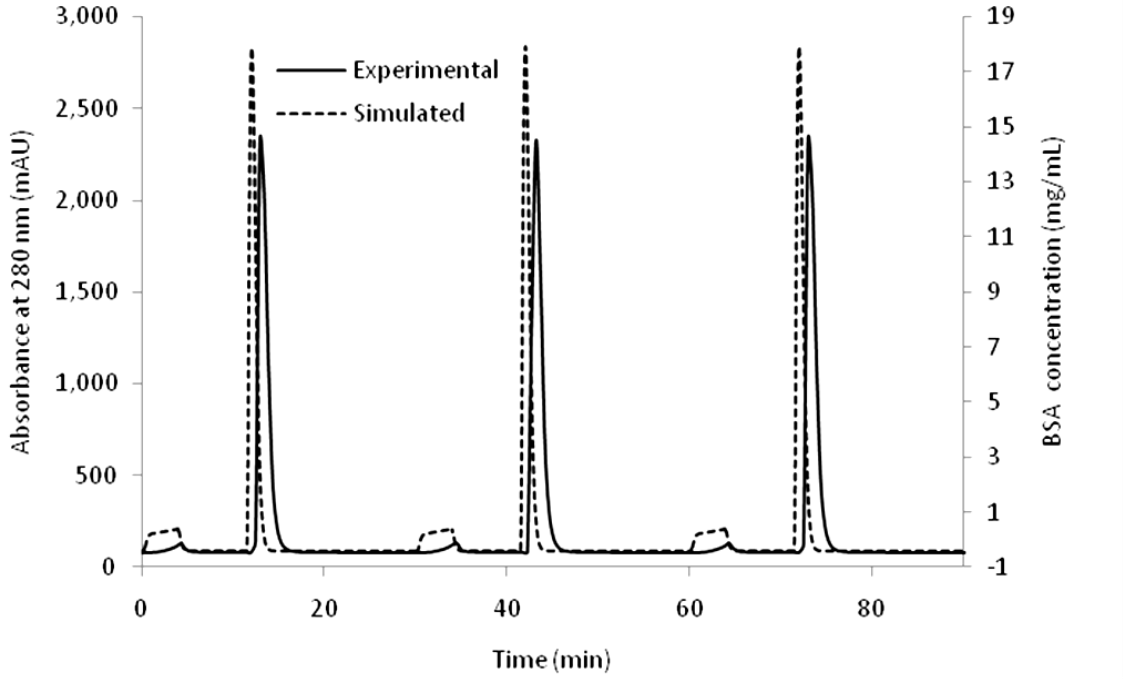

I.8 1.5 mg/mL BSA concentration, 720 rotation speed, 1 mL/min flow rate, 1M NaCl concentration, 18.75 min loading, 3.75 min equilibration, 3.75 min elution and 3.75 min reequilibration.

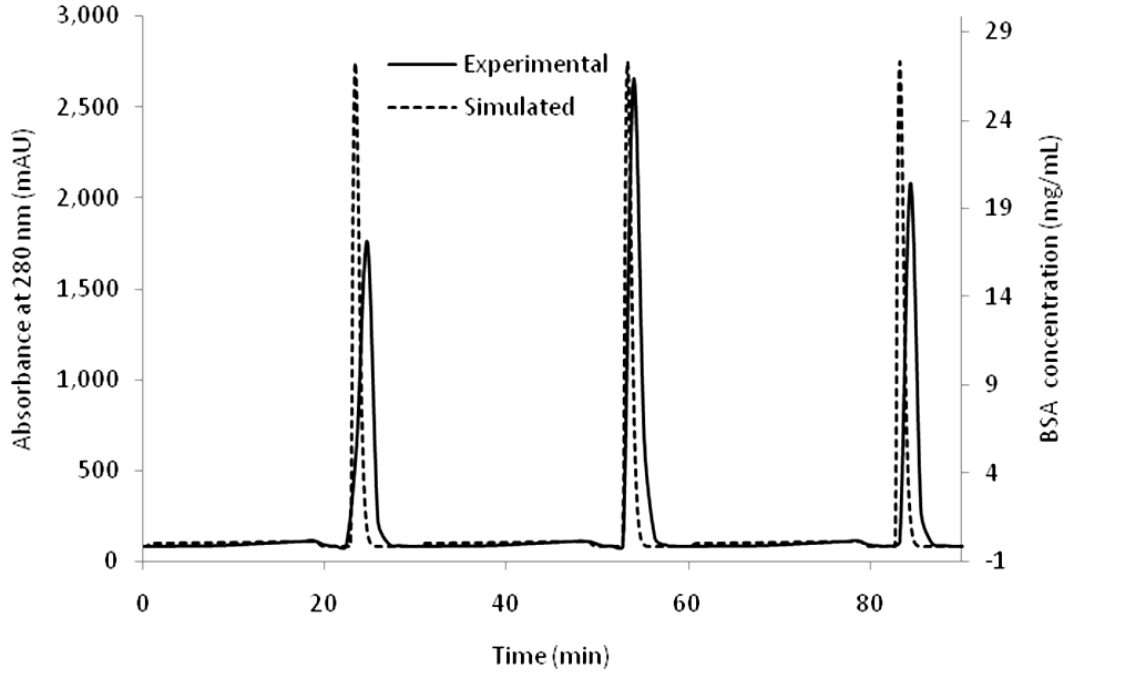

I.9 1.5 mg/mL BSA concentration, 720 rotation speed, 1 mL/min flow rate, 1M NaCl concentration, 11.25 min loading, 7.5 min equilibration, 3.75 min elution and 7.5 min reequilibration.

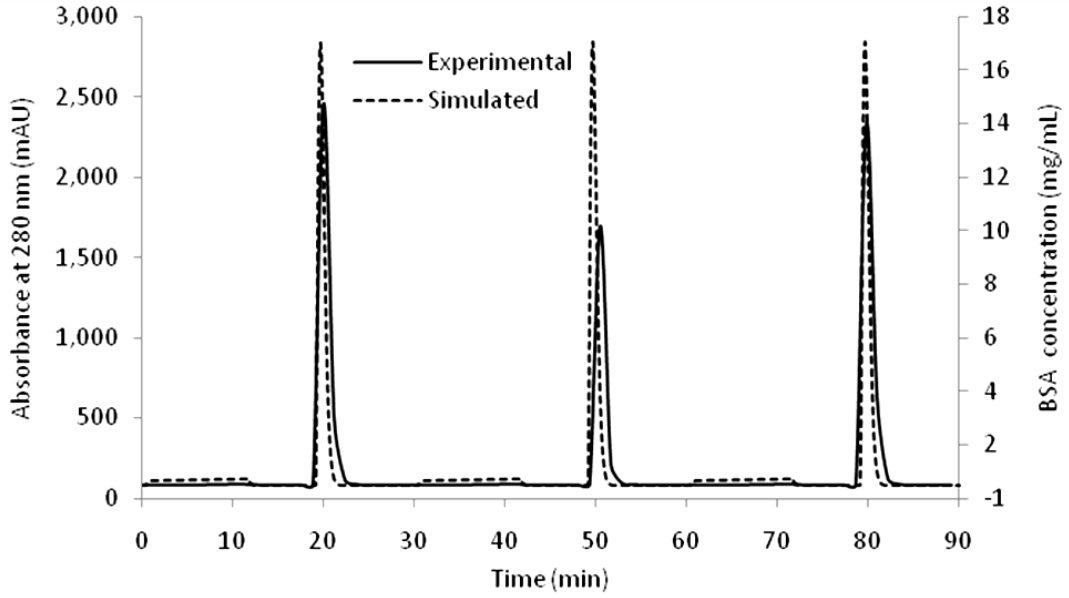

I.10 1.5 mg/mL BSA concentration, 720 rotation speed, 1 mL/min flow rate, 1M NaCl concentration, 11.25 min loading, 3.75 min equilibration, 11.25 min elution and 3.75 min reequilibration.

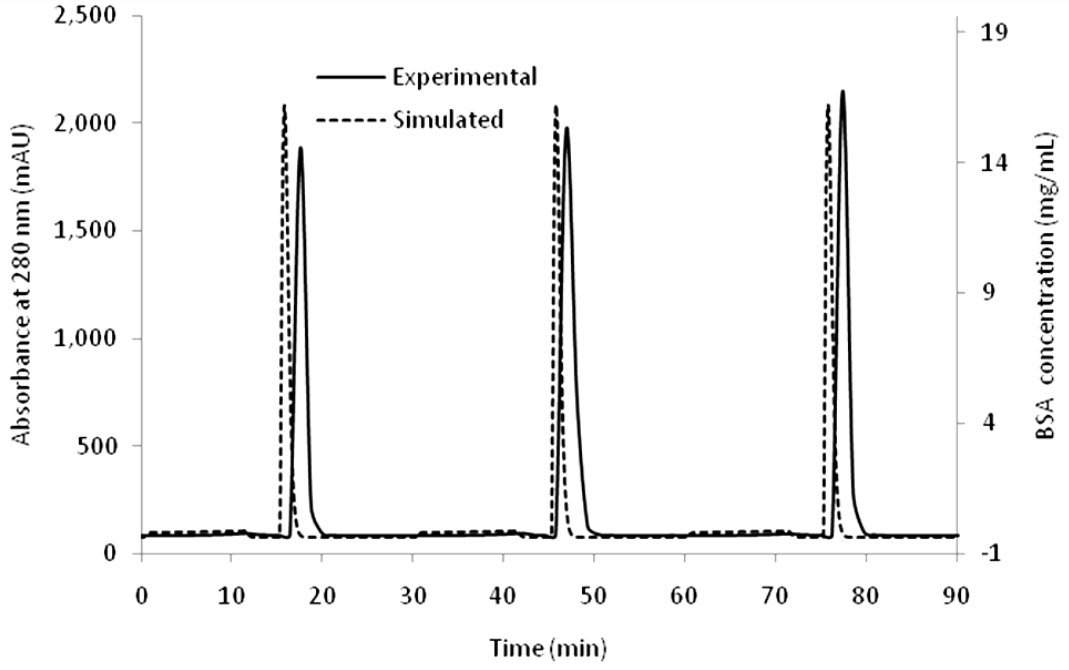

Appendix J Matlab Model

J.1 Continuous BSA purification with an axial column

```
%Column properties
H=3;%Column height (cm)
D=0.7;%Column diameter (cm)
V=(pi().*D.*D./4).*H;%Column volume (cm3)

%Resin properties
Dp=0.01;%Particle diameter (cm)
Er=0.33;%Void fraction (-)
Ep=0.7;%Pore fraction (-)

%Protein properties
cstart=1.5;%Sarting concentration ( mg/mL)
kf=0.003;%Film diffusion coefficient (cm/s)
Kp=47;%Langmuir coefficient (mL/ mg)
k1=0.001;%adsorption rate (mL/ mg.s)
k2=k1./Kp;%desorption rate (1/s)
crpmax=100;%Loading capacity for protein ( mg/mL resin)

%Salt properties
csstart=56;%Starting concentration ( mg/mL)
kfs=0.0001;%Film diffusion coefficient (cm/s)
Kps=1500;%Langmuir coefficient (mL/ mg)
k1s=0.001;%adsorption rate (mL/ mg.s)
k2s=k1s./Kps;%desorption rate (1/s)
crsmax=1.5;%Loading capacity for salt ( mg/mL resin)

Qmin=1.0;%Flow rate (mL/min)
Qsec=Qmin./60;%Flow rate (mL/s)

%Model properties
Ns=ceil(H./(Dp.*30));%Number of stages
Hs=H./Ns;%Stage height
Vs=V./Ns;%Stage volume
tres=Vs./Qsec;%Residence time (s)
J=5;%Dividing factor for delt
delt=tres./J;%Change in time (s)
trun=90;%Run time (min)
tcycle=30;
tloadstart=0;
tloadfin=18.75;
tsaltstart=22.5;
tsaltfin=26.25;
ts=ceil(trun.*60./delt)+1;%Total time step

%Preallocation
c=zeros(ts+1,Ns+1);
```

```
cp=zeros(ts+1,Ns+1);
cr=zeros(ts+1,Ns+1);
cs=zeros(ts+1,Ns+1);
cps=zeros(ts+1,Ns+1);
crs=zeros(ts+1,Ns+1);
tx=zeros(ts+1);
txc=zeros(ts+1);
time=zeros(ts+1);
vol=zeros(ts+1);

%Boundary conditions
for t=2:ts+1;
        tx(t)=(t-1).*delt./60;%Time(min)
        txc(t)=tcycle.*(0.5+atan(tan(((tx(t)./tcycle).*pi)+(pi./2))).*(1./pi()));
        time(t)=(t-1).*delt./60;%Time (min)
        vol(t)=(t-1).*delt.*Qsec;%Volume (mL)
    for n=1;
        if txc(t)>tloadstart && txc(t)<tloadfin;
            c(t,n)=cstart;
        end

        if txc(t)>tsaltstart && txc(t)<tsaltfin;
            cs(t,n)=csstart;
        end
    end
   for n=2:Ns+1;
        %Protein
        c(t,n)=c(t-1,n)+(((c(t-1,n-1)-c(t-1,n)).*Qsec.*delt)./(Vs.*Er))-((3.*kf.*(c(t-1,n)-cp(t-
1,n)).*(1-Er).*delt)./((Dp./2).*Er));
        cp(t,n)=cp(t-1,n)+((((3.*kf.*(c(t-1,n)-cp(t-1,n))./((Dp./2).*Ep)).*delt))-(k1.*cp(t-
1,n).*(crpmax-cr(t-1,n)).*delt)+(k2.*(1+(Kps.*cps(t-1,n))).*cr(t-1,n).*delt);
        cr(t,n)=cr(t-1,n)+(k1.*cp(t-1,n).*(crpmax-cr(t-1,n)).*delt.*Ep)-(k2.*(1+(Kps.*cps(t-
1,n))).*cr(t-1,n).*delt.*Ep);

        %Salt
        cs(t,n)=cs(t-1,n)+(((cs(t-1,n-1)-cs(t-1,n)).*Qsec.*delt)./(Vs.*Er))-((3.*kfs.*(cs(t-1,n)-
cps(t-1,n)).*(1-Er).*delt)./((Dp./2).*Er));
        cps(t,n)=cps(t-1,n)+((((3.*kfs.*(cs(t-1,n)-cps(t-1,n))./((Dp./2).*Ep)).*delt))-(k1s.*cps(t-
1,n).*(crsmax-crs(t-1,n)).*delt)+(k2s.*crs(t-1,n).*delt);
        crs(t,n)=crs(t-1,n)+(k1s.*cps(t-1,n).*(crsmax-crs(t-1,n)).*delt.*Ep)-(k2s.*crs(t-
1,n).*delt.*Ep);
    end
end

%Plot data
X=time(1:ts);
A=c(1:ts,Ns+1);
B=cs(1:ts,Ns+1)./csstart;

figure;
plot(X,A,'-',X,B,':');
ylabel('Concentration ( mg/ml)');
xlabel('Time (min)');
title('Elution curve');
```